THE SKIN IMMUNE RESPONSE TO INFECTIOUS AGENTS

EDITED BY: Fatima Conceição-Silva, Fernanda Nazaré Morgado, Fabienne Tacchini-Cottier and Roberta Olmo Pinheiro

PUBLISHED IN: Frontiers in Immunology and Frontiers in Microbiology

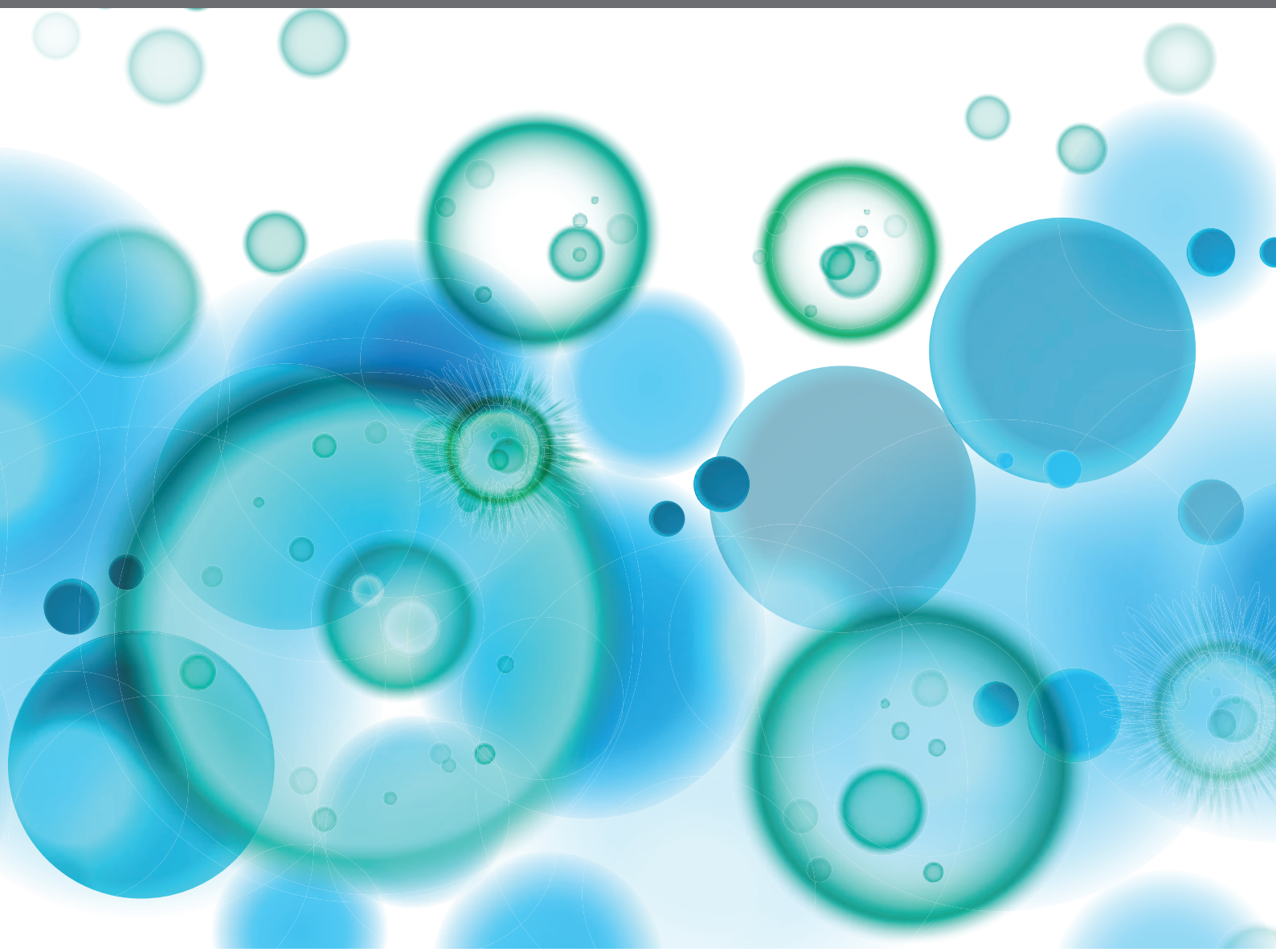

frontiers Research Topics

frontiers

ISSN 1664-8714
ISBN 978-2-88971-492-6
DOI 10.3389/978-2-88971-492-6

About Frontiers

Frontiers is more than just an open-access publisher of scholarly articles: it is a pioneering approach to the world of academia, radically improving the way scholarly research is managed. The grand vision of Frontiers is a world where all people have an equal opportunity to seek, share and generate knowledge. Frontiers provides immediate and permanent online open access to all its publications, but this alone is not enough to realize our grand goals.

Frontiers Journal Series

The Frontiers Journal Series is a multi-tier and interdisciplinary set of open-access, online journals, promising a paradigm shift from the current review, selection and dissemination processes in academic publishing. All Frontiers journals are driven by researchers for researchers; therefore, they constitute a service to the scholarly community. At the same time, the Frontiers Journal Series operates on a revolutionary invention, the tiered publishing system, initially addressing specific communities of scholars, and gradually climbing up to broader public understanding, thus serving the interests of the lay society, too.

Dedication to Quality

Each Frontiers article is a landmark of the highest quality, thanks to genuinely collaborative interactions between authors and review editors, who include some of the world's best academicians. Research must be certified by peers before entering a stream of knowledge that may eventually reach the public - and shape society; therefore, Frontiers only applies the most rigorous and unbiased reviews.
Frontiers revolutionizes research publishing by freely delivering the most outstanding research, evaluated with no bias from both the academic and social point of view. By applying the most advanced information technologies, Frontiers is catapulting scholarly publishing into a new generation.

What are Frontiers Research Topics?

Frontiers Research Topics are very popular trademarks of the Frontiers Journals Series: they are collections of at least ten articles, all centered on a particular subject. With their unique mix of varied contributions from Original Research to Review Articles, Frontiers Research Topics unify the most influential researchers, the latest key findings and historical advances in a hot research area! Find out more on how to host your own Frontiers Research Topic or contribute to one as an author by contacting the Frontiers Editorial Office: frontiersin.org/about/contact

THE SKIN IMMUNE RESPONSE TO INFECTIOUS AGENTS

Topic Editors:
Fatima Conceição-Silva, Oswaldo Cruz Foundation, Brazil
Fernanda Nazaré Morgado, Oswaldo Cruz Institute, Brazil
Fabienne Tacchini-Cottier, University of Lausanne, Switzerland
Roberta Olmo Pinheiro, Fundação Oswaldo Cruz (Fiocruz), Brazil

Citation: Conceição-Silva, F., Morgado, F. N., Tacchini-Cottier, F., Pinheiro, R. O., eds. (2021). The Skin Immune Response to Infectious Agents. Lausanne: Frontiers Media SA. doi: 10.3389/978-2-88971-492-6

Table of Contents

frontiers in Immunology

EDITORIAL
published: 12 January 2022
doi: 10.3389/fimmu.2021.810059

Editorial: The Skin Immune Response to Infectious Agents

Fatima Conceição-Silva[1]*, *Fernanda N. Morgado*[1], *Roberta O. Pinheiro*[2] *and Fabienne Tacchini-Cottier*[3]

[1] Immunoparasitology Laboratory, Oswaldo Cruz Institute, Fundação Oswaldo Cruz, Rio de Janeiro, Brazil, [2] Leprosy Laboratory, Oswaldo Cruz Institute, Fundação Oswaldo Cruz, Rio de Janeiro, Brazil, [3] Biochemistry Department, University of Lausanne, Lausanne, Switzerland

Keywords: skin, immune response, infectious diseases, skin immune system, skin-associated lymphoid tissues (SALT)

Editorial on the Research Topic

The Skin Immune Response to Infectious Agents

This Research Topic highlights different mechanisms associated with the skin immune response against infectious agents. The skin was originally defined as a tissue that covers the body, protecting internal tissues and organs from external physical, chemical, and biological aggressions. A greater understanding of the particularities of the skin immune response began with the identification of skin-associated lymphoid tissues (SALT) (1, 2), and the description of the dermal perivascular units (PVU) comprising layers of CD4 and CD8 T cells around capillaries in the dermis (3). SALT and PVU represent examples of the skin immune response organization (4, 5). Thereafter, the skin immune system (SIS) was defined based on work delineating the presence and function of immune cells at this site (6–10). The identification of SIS, SALT, and other skin immune compartments, such as the immune system of the hair follicle (11), helped to change the definition of the skin from a tissue to a linear organ. Due to its size and total weight (approximately $2m^2$ and about 16% of body weight) it is considered one of the largest organs in the human body. In parallel, the idea of compartmentalization of the immune response with this organ has gained strength *via* the demonstration of decisive events in the control or development of skin diseases and through studies on the *in situ* immune response, particularly for infectious skin diseases. The understanding of the dynamics of immune response to different pathogens that penetrate and multiply in the skin has markedly increased. However, much is still unknown about events related to the encounter between the pathogen and the local immune responses and thus this area still requires further investigation. This is the central idea behind this Research Topic and papers within this collection have assessed the impact of the interaction of SIS with different pathogens.

In this context, the skin immune response during leishmaniasis is described in five articles of this Research Topic. Leishmaniasis is a vector-borne disease caused by protozoans of the genus *Leishmania*, most of which result in tegumentary lesions of affected individuals in endemic areas around the world. The host immune response is considered essential for the progression and control of the disease (12), and different cells and molecules contribute to the inflammatory reaction to *Leishmania* parasites. Although macrophages have been extensively studied, the function of neutrophils is pivotal in the skin immune response against *Leishmania*, as they are rapidly recruited to the infected site. In this context, Passelli et al. review the role of neutrophils in recruiting inflammatory cells to the infected dermis. *Leishmania* spp. are intracellular parasites,

OPEN ACCESS

Edited and reviewed by:
Ian Marriott,
University of North Carolina at Charlotte, United States

***Correspondence:**
Fatima Conceição-Silva
fconcei@ioc.fiocruz.br

Specialty section:
This article was submitted to Microbial Immunology, a section of the journal Frontiers in Immunology

Received: *05 November 2021*
Accepted: *23 December 2021*
Published: *12 January 2022*

Citation:
Conceição-Silva F, Morgado FN, Pinheiro RO and Tacchini-Cottier F (2022) Editorial: The Skin Immune Response to Infectious Agents. Front. Immunol. 12:810059. doi: 10.3389/fimmu.2021.810059

mainly residing within mononuclear phagocytic cells, but $CD4^+$ and $CD8^+$ T-cells play an important role in controlling infection by both cytokine production and direct cytotoxicity. In this context, a new function of $CD8^+$ T cells is presented by Koh et al., who demonstrate for the first time the production of lymphocyte extracellular traps (LETs) by $CD8^+$ T cells, both *in vitro* and *in vivo* (human tegumentary lesions), suggesting a role of LETs in disease progression. Current therapies targeting programmed cell death (PD)-1 receptor and its ligand (PD-L1) restore T cell activity. In this Research Topic, two articles by Moura et al. and Fonseca-Martins et al. discuss the role of PD-1 and PD-L1 in leishmaniasis. PD-L1 expressed in both macrophages and neutrophils may have suppressive activity and the blockade of PD-L1 may contribute to a reduction in cutaneous pathology. As such, these articles present potential new mechanisms of protection focusing on the PD-1/PD-L1 pathway. Collectively, all the studies mentioned in this topic are relevant to the development of new therapies. Among them, this pathway and so these host-directed therapies represent a promising approach in the treatment of infectious diseases and Novais et al. discuss these perspectives in the field of cutaneous leishmaniasis.

Leprosy is another infection of worldwide importance that affects the skin and nerves. The disease ranges from self-limited to severe forms that can lead to loss of tissue and function when not treated and four manuscripts discuss the skin immune response during leprosy. Although historically the Th1-Th2 dichotomy has been associated with leprosy polarity, an *in vitro* model of *Mycobacterium leprae* infection generated by Leal-Calvo et al. demonstrates that macrophages also have a central role. In addition, the effect of immunosenescence in the skin immune response against the bacilli and the mechanisms in which age-related changes in T cell subsets may influence the onset of leprosy is also discussed by Silva et al. Existence of relapse, resistance to drugs used in the multidrug therapy (MDT), and the low bactericidal activity of rifampicin have previously been described. Even after MDT, multibacillary patients may present high bacillary loads, thus it is important to clarify the mechanisms underlying this phenomenon. In this context, Ferreira et al. demonstrate that a reduction in the bacillary index in the slit-skin smear of patients is associated with higher levels of CXCL10 (IP-10) and IFN-γ and so this. This could be helpful in monitoring the treatment efficacy in leprosy patients (Ferreira et al). Furthermore, CXCL10/IP-10 and IFN-γ are associated with a reduction in the bacillary load by inducing autophagy in host cells. Role of autophagy in the pathogenesis of skin diseases caused by mycobacteria is reviewed by Bittencourt et al. and they discuss the potential for repurposing drugs to target host cells for mycobacterial control.

Other bacteria can produce skin infections and one of the most common is *Staphylococcus aureus*, which can be found as part of the skin's microbiome, but, in certain circumstances, it can become more aggressive, causing localized or disseminated skin lesions and endogenous disease. Two studies in this collection focus on the relationship between *S. aureus* and the skin immune response. Hamid et al. focus on the neutrophil-*S. aureus* interactions after mouse infection with planktonic or biofilm forms of *S. aureus*. Both bacterial forms induce an early and considerable pro-inflammatory cytokine profile in the lesion together with a predominance of neutrophils. However, some differences in the dynamics of recruitment and functional properties of phagocytes against biofilms are described and the authors discuss their role in promoting an adaptative immune response against *S. aureus*. Another study by Hendriks et al. suggests the importance of $CD4^+$ T cells as a barrier to the primary entry site of *S. aureus*.

Another bacterium, *Haemophilus ducreyi*, can induce skin lesions, mainly in children, as well as sexually transmitted genital ulcers in adults. Brothwell et al. review the current literature related to the host-pathogen interaction network, including the adaptation of this organism to its metabolic surroundings and the use of new technologies to better understand *H. ducreyi* pathogenesis.

Many pathogens can colonize and/or invade the skin, producing infections with different grades of severity. In this Research Topic, skin interactions with viruses and fungi are also discussed. Lei et al. review the virus-host immune response interface and discuss both host immune responses and virus immune evasion mechanisms.

Regarding skin immune responses to fungi, different species are able to produce skin infection. Skin mycoses can affect the keratinous layer as well as the epithelial and dermal layers. Depending on the fungus causing the infection, it can produce disease in immunocompetent individuals or hosts with some degree of immunosuppression. One of the most common skin mycoses is caused by a group of fungi known as dermatophytes, which produce a superficial mycosis with a worldwide distribution. In this context, Burstein et al. present an innovative experimental model of dermatophytosis to explore its pathogenesis and further understand the mechanisms of fungal virulence, evasion, as well as immune responses elicited during infection, including the role of C- type lectin receptors and cytokines such as IL-17 and IFN-γ.

Purpureocillum lilacinum is considered an emerging pathogen for humans, mainly in immunosuppressed patients, being one of the causal agents of hyalohyphomycosis. Corrêa-Moreira et al. demonstrate a decrease in the number of macrophages and neutrophils as well as in the amount of IL-1β and nitric oxide (NO) in immunosuppressed mice when compared with immunocompetent animals. The authors discuss these results that contribute to a greater understanding of this, as yet, scarcely studied infection.

A plethora of cell types, cytokines, and other molecules are involved in the SIS and the predominance of each one can be stimulated by different pathogens. In this context, Langerhans cells are pivotal to mounting the specific immune response. Oulee et al. identify and evaluate 31 genes that encode proteins that are involved in antimicrobial activity. Based on their results, authors discuss the potential role of Langerhans cells in orchestrating skin immune responses.

The skin is an important organ of the human body, functioning as a homeostatic organ and a mechanical barrier

to the external environment, but it is also capable of mounting specific immune responses to different infectious agents such as protozoa, viruses, bacteria, and fungi. The SIS is organized to respond to different stimuli, and disease progression or control can be influenced by the skin immune response (6–10). The articles presented here demonstrate that the skin immune mechanisms related to protection against infectious diseases involve both innate and adaptive immune cells, as well as host characteristics like ageing and metabolic status. A better understanding of the pathways associated with the immunopathogenesis of skin infectious diseases may contribute to the development of new therapeutic and prophylactic strategies. While the present collection provides important new information, many questions remain unanswered. We hope that readers will find this Research Topic a useful reference to understand the complex mechanisms associated with the immune response against pathogens that infect the skin.

AUTHOR CONTRIBUTIONS

All authors have written, reviewed, and approved the final version of the manuscript.

FUNDING

This work was supported by PAEF-Fiocruz e Programa Jovem Cientista do Nosso Estado - Faperj (E-26/202.760/2019).

REFERENCES

1. Streilein JW. Skin-Associated Lymphoid Tissues (SALT): Origins and Functions. *J Invest Dermatol* (1983) 80:12s–6s. doi: 10.1111/1523-1747.ep12536743
2. Streilein JW. Circuits and Signals of the Skin-Associated Lymphoid Tissues (SALT). *J Invest Dermatol* (1985) 85:10s–3s. doi: 10.1111/1523-1747.ep12275413
3. Bos JD, Kapsenberg ML. The Skin Immune System: Progress in Cutaneous Biology. *Immunol Today* (1993) 14:75–8. doi: 10.1016/0167-5699(93)90062-P
4. Bos JD, Kapsenberg ML. The Skin Immune System Its Cellular Constituents and Their Interactions. *Immunol Today* (1986) 7:235–40. doi: 10.1016/0167-5699(86)90111-8
5. Bos JD, Zonneveld I, Das PK, Krieg SR, van der Loos CM, Kapsenberg ML. The Skin Immune System (SIS): Distribution and Immunophenotype of Lymphocyte Subpopulations in Normal Human Skin. *J Invest Dermatol* (1987) 88:569–73. doi: 10.1111/1523-1747.ep12470172
6. Spellberg B. The Cutaneous Citadel: A Holistic View of Skin and Immunity. *Life Sci* (2000) 67:477–502. doi: 10.1016/S0024-3205(00)00653-6
7. Jarrett R, Ogg G. Lipid-Specific T Cells and the Skin. *Br J Dermatol* (2016) 175:19–25. doi: 10.1111/bjd.14908
8. Abdallah F, Mijouin L, Pichon C. Skin Immune Landscape: Inside and Outside the Organism. *Mediators Inflammation* (2017) 2017:5095293. doi: 10.1155/2017/5095293
9. Matejuk A. Skin Immunity. *Arch Immunol Ther Exp (Warsz)* (2018) 66:45–54. doi: 10.1007/s00005-017-0477-3
10. Noske K. Secreted Immunoregulatory Proteins in the Skin. *J Dermatol Sci* (2018) 89:3–10. doi: 10.1016/j.jdermsci.2017.10.008
11. Paus R, Nickoloff BJ, Ito T. A "Hairy" Privilege. *Trends Immunol* (2005) 26:32–40. doi: 10.1016/j.it.2004.09.014
12. Conceição-Silva F, Morgado FN. Leishmania Spp-Host Interaction: There Is Always an Onset, But Is There an End? *Front Cell Infect Microbiol* (2019) 9:1308. doi: 10.3389/fcimb.2019.00330

Conflict of Interest: The authors declare that the research was conducted in the absence of any commercial or financial relationships that could be construed as a potential conflict of interest.

frontiers in Immunology

ORIGINAL RESEARCH
published: 08 October 2020
doi: 10.3389/fimmu.2020.594581

Human CD8+ T Cells Release Extracellular Traps Co-Localized With Cytotoxic Vesicles That Are Associated With Lesion Progression and Severity in Human Leishmaniasis

*Carolina Cattoni Koh[1], Amanda B. Wardini[1], Millene Vieira[1], Livia S. A. Passos[1], Patrícia Massara Martinelli[2], Eula Graciele A. Neves[1], Lis Riberido do Vale Antonelli[3], Daniela Faria Barbosa[1], Teresiama Velikkakam[1], Eduardo Gutseit[1], Gustavo B. Menezes[4], Rodolfo Cordeiro Giunchetti[1], Paulo Roberto Lima Machado[5,6], Edgar M. Carvalho[5,6], Kenneth J. Gollob[6,7] and Walderez Ornelas Dutra[1,6]**

[1] Laboratório de Biologia das Interações Celulares, Departamento de Morfologia, Instituto de Ciências Biológicas, Universidade Federal de Minas Gerais, Belo Horizonte, Brazil, [2] Laboratório Profa. Conceição Machado, Departamento de Morfologia, Instituto de Ciências Biológicas, Universidade Federal de Minas Gerais, Belo Horizonte, Brazil, [3] Laboratório de Biologia e Imunologia de Doenças Infecciosas e Parasitárias, Instituto René Rachou, FIOCRUZ-MG, Belo Horizonte, Brazil, [4] Center for Gastrointestinal Biology, Departamento de Morfologia, Instituto de Ciências Biológicas, Universidade Federal de Minas Gerais, Belo Horizonte, Brazil, [5] Serviço de Imunologia, Universidade Federal da Bahia, Salvador, Brazil, [6] Instituto Nacional de Ciência e Tecnologia em Doenças Tropicais, INCT-DT, Salvador, Brazil, [7] International Research Center, A.C. Camargo Cancer Center, São Paulo, Brazil

OPEN ACCESS

Edited by:
Roberta Olmo Pinheiro,
Oswaldo Cruz Foundation, Brazil

Reviewed by:
David Sacks,
National Institutes of Health (NIH), United States
Claudia Ida Brodskyn,
Gonçalo Moniz Institute (IGM), Brazil

***Correspondence:**
Walderez Ornelas Dutra
waldutra@gmail.com;
waldutra@icb.ufmg.br

Specialty section:
This article was submitted to Microbial Immunology, a section of the journal Frontiers in Immunology

Received: 13 August 2020
Accepted: 22 September 2020
Published: 08 October 2020

Citation:
Koh CC, Wardini AB, Vieira M, Passos LSA, Martinelli PM, Neves EGA, Antonelli LRdV, Barbosa DF, Velikkakam T, Gutseit E, Menezes GB, Giunchetti RC, Machado PRL, Carvalho EM, Gollob KJ and Dutra WO (2020) Human CD8+ T Cells Release Extracellular Traps Co-Localized With Cytotoxic Vesicles That Are Associated With Lesion Progression and Severity in Human Leishmaniasis. Front. Immunol. 11:594581. doi: 10.3389/fimmu.2020.594581

Cell death plays a fundamental role in mounting protective and pathogenic immunity. Etosis is a cell death mechanism defined by the release of extracellular traps (ETs), which can foster inflammation and exert microbicidal activity. While etosis is often associated with innate cells, recent studies showed that B cells and CD4+ T cells can release ETs. Here we investigate whether CD8+ T cells can also release ETs, which might be related to cytotoxicity and tissue pathology. To these ends, we first employed an in vitro system stimulating human CD8+ T cells isolated from healthy volunteers with anti-CD3/anti-CD28. Using time-frame video, confocal and electron microscopy, we demonstrate that human CD8+ T cells release ETs upon stimulation (herein LETs – lymphocyte extracellular traps), which display unique morphology and functional characteristics. CD8+ T cell-derived LETs form long strands that co-localize with CD107a, a marker of vesicles containing cytotoxic granules. In addition, these structures connect the LET-releasing cell to other neighboring cells, often resulting in cell death. After demonstrating the release of LETs by human CD8+ T cells in vitro, we went on to study the occurrence of CD8-derived LETs in a human disease setting. Thus, we evaluated the occurrence of CD8-derived LETs in lesions from patients with human tegumentary leishmaniasis, where CD8+ T cells play a key role in mediating pathology. In addition, we evaluated the association of these structures with the intensity of the inflammatory infiltrate in early and late cutaneous, as well as in mucosal leishmaniasis lesions. We demonstrated that progression and severity of debilitating and mutilating forms of human tegumentary leishmaniasis are associated

with the frequency of CD8+ T cells in etosis, as well as the occurrence of CD8-derived LETs carrying CD107a+ vesicles in the lesions. We propose that CD8+ T cell derived LETs may serve as a tool for delivering cytotoxic vesicles to distant target cells, providing insights into mechanisms of CD8+ T cell mediated pathology.

Keywords: extracellular traps, CD8+ T cells, etosis, cytotoxicity, pathology, leishmaniasis

INTRODUCTION

T cell activation and function is dependent on mechanisms that involve direct cell-cell interaction, as well as autocrine, paracrine and endocrine responses to soluble factors produced by a variety of cells. While CD4+ T cells are major orchestrators of the immune response by producing cytokines and mediating B cell activation, CD8+ T cells are classically associated with cytotoxic functions. Cytotoxicity involves the coordinated activity of a series of enzymes, which are delivered by lytic granules containing lysosomal-associated membrane proteins (LAMP), including CD107a (LAMP-1) (1). The mechanisms of cytotoxic granule delivery described to date involve an intimate proximity between the cytotoxic cell and its target (2–4). This delivery triggers cell death via both apoptotic-mediated mechanisms, and those independent on apoptosis (1, 3, 5).

Apoptosis, necrosis and etosis are distinct cell death mechanisms that occur under physiological and pathological circumstances and are critical for maintaining cell and tissue homeostasis. While apoptosis is the result of a misbalance between pro- and anti-apoptotic factors and caspase activation, leading to biochemical and morphological changes such as membrane asymmetry, chromatin fragmentation, and release of intracellular contents in apoptotic bodies (6–8), necrosis is characterized by massive disintegration of organelles, accumulation of intracellular water, and subsequent release of intracellular content in a disorderly manner (9). Etosis is an event in which cells release extracellular nets or traps (ETs, hence the name etosis), usually leading to cell death in a mechanism distinct from apoptosis and necrosis (10, 11). ETs are mainly composed of DNA and histones, but cytoskeletal proteins may also be present (12). Innate immune cells release ETs in response to bacterial and parasite components, as well as following in vitro stimulation with PMA and LPS (10, 13–17).

Neutrophil derived ETs play an important role in the control of infections, since they are capable of physically retaining and eliminating pathogens (18–20). One such example is the protozoan parasite *Leishmania*, which is susceptible to neutrophil-derived ETs (21, 22). Despite exerting a potentially protective role against pathogens, ETs can also amplify inflammatory responses, which may be detrimental if not controlled (23). Human infection with *Leishmania* leads to a spectrum of debilitating, mutilating and potentially deadly diseases. The cutaneous and mucosal manifestations of tegumentary leishmaniasis have been associated with exacerbated inflammatory and cytotoxic responses (24, 25), in which CD8+ T cells play a fundamental role (26–28).

While etosis is mostly related to innate immune cells, it was recently shown that B cells can release ETs in response to CpG stimulation (29), and that CD4+ T cells can also release ETs (16, 30). Thus, we hypothesized that CD8+ T cells can also release ETs, and that these ETs might be associated with CD8-mediated cytotoxic function and play a role in tissue pathology in human diseases. Thus, we performed a series of studies to determine if CD8+ T cells can release ETs and if they are associated with severity in human leishmaniasis, a devastating disease that affects millions worldwide and is a well-established example of CD8-mediated pathology. Here we unequivocally demonstrate that human CD8+ T cells release ETs that display a unique morphology upon activation (herein referred to as LETs - lymphocyte-derived ETs). Importantly, we show that CD8-derived LETs connect the LET-releasing cell with target cells, and co-localize with CD107a, a marker of cytotoxic granules. In addition, we show that progression and severity of human tegumentary leishmaniasis is associated with the release of CD107a+ LETs by CD8+ T cells. Our findings suggest that delivery of CD107a+ vesicles by CD8-derived LETs may provide an alternative mechanism of CD8-mediated cytotoxicity, with implications for disease pathology, and on the design of new therapeutic interventions.

PATIENTS, MATERIALS, AND METHODS

Patients With Leishmaniasis and Healthy Donors

Fifteen healthy volunteers were enrolled in this study for the various experiments of T cell activation to detect etosis, apoptosis, cell activation, as well as cytotoxic molecule and cytokine expression. All in vitro experiments were performed using cells from healthy donors.

A total of twenty-one leishmaniasis patients from the endemic area of Corte de Pedra, state of Bahia, Brazil were also enrolled in the study. We evaluated the presence of extracellular DNA (LETs), as well as determined the frequency of CD8+CD107+ LETs in lesions from cutaneous and mucosal leishmaniasis patients. Patients' medical care, evaluation, and characterization were under the responsibility of Drs EC e PM. Diagnosis for leishmaniasis was performed based on clinical and laboratorial criteria. Detection of suggestive skin or mucosal lesions was associated to positive skin Montenegro test, parasite isolation and/or histopathological analysis to confirm diagnosis of CL or ML. For all CL and ML cases parasite species were typed to confirm that disease was due to *L. braziliensis*

infection. Cutaneous patients enrolled in this study (total n=14) presented with a single ulcerated lesion and had not been previously diagnosed or treated for leishmaniasis. CL patients were classified as early-stage cutaneous leishmaniasis (Early-CL – approximately 15 days of illness, non-ulcerated palpular lesion) or late-stage cutaneous leishmaniasis (Late-CL – approximately 60 days of illness, classical ulcerated lesion), as previously established by us (26, 31). Mucosal patients (total n=7) presented with nasal lesions and, at the time of biopsy collection, and did not display concomitant cutaneous disease. Skin and mucosal biopsies were obtained from the edges of the active lesions with a 4-mm punch or scalpel, after the application of local anesthetic, processed and stored as previously done by us (24, 26). Samples were collected before treatment, which was offered to all patients as needed, despite their enrollment in this project. The ethics committees of the Federal Universities of Bahia and Minas Gerais approved all the procedures involved in this study and all individuals signed an informed consent.

Histological and Immunofluorescence Staining in Tissues

Biopsies were used to obtain sections of 4 to 5 μm were placed on polarized slides and fixed for 10 min in acetone at -20°C or 15 min in 4% paraformaldehyde at room temperature. Slides were incubated with phosphate buffered saline (PBS) for 15 min and stained with hematoxylin-eosin or submitted to immunofluorescence. Immunofluorescence reactions were done using fluorescein isothiocyanate (FITC) - conjugated to monoclonal antibodies directed to surface receptors (CD4, CD8, CD68, CD107, Biolegend, San Diego, CA, USA) or anti-histone (Invitrogen, San Diego, CA, USA). Sections were incubated with antibody mixtures overnight at 4°C, followed by extensive wash with PBS. Samples were permeabilized for 1 h with 0.01% Triton X-100 prior to anti-histone and anti-CD107 stainings. Preparations stained with anti-histone were subsequently incubated with a Donkey anti-mouse IgG (H + L) secondary antibody labeled with Alexa Fluor 488 for 1 h. Finally, all slides were stained with 4',6'-diamidino-2-phenylindole (DAPI, Molecular Probes, Eugene, OR, USA) and mounted using Vectashield® (Burlingame, CA, USA) mounting medium. Slides were kept at 4°C, protected from light, until they were acquired in a laser scanning confocal microscope (Zeiss 5 Live or Zeiss LSM 880), using an oil immersion objective (40×, 1.3 Oil). A water-cooled argon UV laser (488 nm) or a krypton/argon laser was used to excite the preparation. Images were analyzed using ImageJ 1.48v software. Isotype controls were used to confirm the lack of nonspecific staining. Frequency of cell subpopulations were determined by histological staining (mononuclear and polymorphonuclear) or by immunofluorescence (using fluorescence labeled anti-CD4, anti-CD8, anti-CD68, anti-CD107 monoclonal antibodies), and were performed by counting the total number of cells in a minimum of three acquired fields/slide, which was used to calculate the mean number of positive cells/section for each patient. Intensity of the inflammatory infiltrate was determined by counting the number of DAPI+ cells within the connective tissue and calculating the number of cells/field.

Separation, Plating, and Culture of Human Peripheral Blood Mononuclear Cells (PBMC)

Purification of peripheral blood mononuclear cells (PBMC) was performed as previously done by us (32). Briefly, heparinized blood was applied over a Ficoll-Hypaque (GE Healthcare Life Sciences) gradient, centrifuged at 600*g* for 40 min, at room temperature, and PBMC were collected at the interface between the plasma and Ficoll. Cells were washed 3 times by centrifugation with PBS and resuspended in RPMI supplemented with antibiotic (penicillin 200 U/ml and streptomycin 0.1 mg/ml; Sigma, St. Louis, MO, USA) and l-glutamine (1 mM; Sigma, St. Louis, MO, USA) to a concentration of 10^7 cells/ml. Lymphocyte-enriched fraction (LEF) was obtained by collecting non-adherent cells, after a 1-h incubation at 37°C in 6 flat-bottom well plates, using an initial concentration of 4×10^6 cells/well. LEF were placed in 13-mm glass coverslips pretreated with poly-L-lysine (0.01%), at a concentration of 5×10^5 cells/coverslip for electron microscopy, or 1×10^5 cells/coverslip for immunofluorescence. LEF were stimulated with anti-CD3 and anti-CD28 monoclonal antibodies (2 μg and 1 μg/ml, respectively – Biolegend, San Diego, CA, USA), or incubated with media only for 24 h. In addition, cells were induced to lysis (1 h at -80°C) or necrosis (1 h at 56°C), as positive controls of DNA release and cell death. Samples were also submitted to treatment with DNAse (Ambion™ DNase I RNase-free, Invitrogen, Carlsbad, CA, USA) using 2 U/μl, by incubation at 37°C for 6 h.

LEF were also incubated in a polypropylene tube under the same conditions described above and used for flow cytometry analysis to determine cell death and expression of TNF. Supernatant from stimulated cultures, treated or not with DNAse, were collected for DNA and lactate dehydrogenase (LDH) measurement.

Purification and Stimulation of Sorted CD8+ and CD4+ T Lymphocytes

CD8+ and CD4+ T lymphocytes were purified from the LEF (obtained as described above), using a FACS Aria II flow cytometer (Becton Dickinson, San Jose, CA, USA). Briefly, LEF were incubated with anti-CD8 and anti-CD4 monoclonal antibodies for 30 min at 4°C, washed twice with PBS, and resuspended at the concentration of 1×10^6 cells/ml. Cells were submitted to the sorting procedures, as previously done (33), and yielded a purity of over 95%, as determined by flow cytometry. For some assays (as indicated in the text), purified lymphocytes were labeled with 5 mM carboxyfluorescein succinimidyl ester (CFSE, Sigma, St. Louis, MO, USA) by incubation for 10 min at room temperature, washed with PBS, plated in coverslips and stimulated or not with anti-CD3 and anti-CD28, as described above, for 24 h. Preparations were then processed for immunofluorescence and electron microscopy analysis.

Immunofluorescence Reactions in Cell Monolayers and Confocal Microscopy Analysis

For immunofluorescence labeling, coverslips containing stimulated and non-stimulated cells were fixed with 2%

paraformaldehyde by incubation for 15 min at room temperature. Cells were permeabilized with 0.01% Triton X-100 for 3 min, and the coverslips were incubated with a blocking solution of 1% bovine serum albumin (BSA) + 0.1% tween 20 for 1 h. Coverslips were incubated overnight with monoclonal antibodies directed to the different molecules (anti-histone, anti-CD8-Pe-Cy5, anti-CD107a-FITC – Biolegend, San Diego, CA, USA). Subsequently, samples were washed with PBS exhaustively. For the anti-histone staining, samples were incubated with the Donkey anti-mouse IgG (H + L) secondary antibody labeled with Alexa Fluor 488 for 1 h, and then washed with PBS. To stain with Alexa Fluor 594-phalloidin, cells were permeabilized, incubated for 20 min, and washed.

Finally, DNA of all samples was stained with DAPI (1:500) and/or with propidium iodide (PI) for 15 min at room temperature. Slides were extensively washed with PBS, coverslips were mounted with Vectashield® (Abcam, San Francisco, CA, USA), and remained at 4°C protected from light until acquisition in a laser confocal microscope.

Imaging was performed with a Zeiss 5 LIVE or Zeiss LSM 880 (software ZEN 2009), using an oil immersion objective (40×, 1.3 Oil). A water-cooled argon UV laser (488 nm) or a krypton/argon laser were used to excite the preparation (through its 363 nm line, 488 nm line or 568 nm line), and light emitted was selected with band pass filters (515-565 for FITC, 445/50 for DAPI and 575-640 for PI). Images were analyzed using ImageJ 1.48v software. ETs were analyzed by observing extracellular structures stained with DAPI and/or PI and/or histone.

To quantify the frequency of ETs and number of cells releasing ETs in each preparation, we counted the number of extracellular structures that were positive for DAPI and/or PI, as well as the number of cells that were associated with these structures, respectively. Results were expressed as ratio of the stimulated culture over the media control.

Transmission and Scanning Electron Microscopy (EM)

Coverslips containing different cell preparations were fixed in 2.5% glutaraldehyde in 0.1 M cacodylate buffer for 2 h at room temperature. For transmission EM, the cells were post-fixed in 2% OsO_4 (Sigma, St. Louis, MO, USA) in 0.1 M buffer and then counterstained with aqueous 2% uranyl acetate. Dehydration was performed in a graded ethanol series followed by acetone. Monolayers of cells were flat embedded in Epon resin (Sigma, St. Louis, MO, USA) and ultrathin sections were stained with lead citrate. Images were collected using a transmission electron microscope Tecnai G2-12 - SpiritBiotwin FEI - 120 kV.

For scanning EM, coverslips were post-fixed by the OTO (osmium - tanic acid – osmium - Sigma, St. Louis, MO, USA) method, dehydrated in graded ethanol series and dried at critical point under CO_2. The samples were coated with 3 nm of gold and the images were acquired in the scanning electron microscope (FEG - Quanta 200 FEI).

DNA and LDH Quantification

DNA was quantified in the supernatants of the cultures, under the different conditions, using the PicoGreen dsDNA kit (Invitrogen, San Jose, CA, USA) according to manufacturer's instructions.

To quantify LHD in culture supernatants, we used the LDH UV kit (kindly offered by Bioclin, Belo Horizonte, MG, Brazil), according to manufacturer's instructions.

Flow Cytometry Analysis of PBMC

Staining was performed as routinely done by us (32). Briefly, wells were harvested, plated at 2×10^5 cells/well, incubated with a 40-µl mix of monoclonal antibodies CD4-Percp-Cy5.5, anti-CD8-APCCy7 or anti-CD69-PE for 15 min at 4°C, washed with PBS, and fixed for 20 min with 2% formaldehyde/PBS. Then cells were washed twice, permeabilized by incubation for 15 min with 0.5% saponin solution, washed, and subjected to intracellular staining with anti-TNF-APC, anti-CD107a-FITC monoclonal antibodies for 20 min at room temperature. Samples were washed twice with 0.5% saponin solution, resuspended in PBS and read on a flow cytometer. To stain with annexin V and propidium iodide (PI), culture cells were washed with PBS and incubated for 15 min with annexin V. After washing, PI was added just prior to acquisition on the flow cytometer. Samples were acquired on the FACS CANTO II and analyzed using FlowJo software (Tree Star, Ashland, OR, USA). All antibodies were from BioLegend (San Diego, CA, USA).

Time Series for Visualizing CD8-Derived Extracellular Traps and Cell Death

To produce the movies (Time-series), CD8+ T lymphocytes were purified as described above. Non-CD8 cells, leftover from the purification of CD8+ cells, were stained with CFSE as described above, and used as target cells. A proportion of 1:4 CD8+ cells (8×10^4 cells) to 20% non-CD8 cells used as targets (2×10^4 cells) were plated in 24-well plates pretreated with poly-L-lysine and stimulated with anti-CD3/CD28. After 14 h of incubation, ethidium homodimer (EthD-1) (final concentration of 4 µM - LIVE/DEAD ® Viability/Cytotoxicity Kit for mammalian cells - Molecular Probes. Eugene, Oregon, USA) and ionomycin (final concentration of 500 ng/ml; Sigma Aldrich, San Luis, Missouri, USA) were added. A Zeiss 5 Live confocal was used and images were captured every 10 s with CFSE (ex/em ~ 495 nm/~ 515 nm) and EthD-1 (ex/em ~ 532 nm/~ 635 nm) filters. The latter can enter cells with damaged membranes and undergoes a 40-fold increase in fluorescence when binding to nucleic acids, producing a bright fluorescence. The movies were produced using the *Free Microscope Software ZEN blue edition from ZEISS Microscopy* at a rate of 30 frames per second.

Statistical Analysis

The paired t-test was used to verify differences between Gaussian-distributed data and comparing the same samples under different experimental conditions. Unpaired T test was used to compare amongst different groups. Differences that returned values of $p \leq 0.05$ were considered statistically

significant. Results were presented as mean+/-standard errors, as samples fell into the normal distribution using Kolmogorov-Smirnov test. All correlation analyses were performed using the Spearman test.

RESULTS

Human T Lymphocytes Release Extracellular DNA via Etosis

We stimulated lymphocyte-enriched PBMC (~72% CD4+ and CD8+ T cells) from healthy individuals with anti-CD3 and anti-CD28 antibodies. This antibody combination provides a T cell specific stimulation that does not directly stimulate other cells in the culture (34, 35). Following 24 h of stimulation, extracellular DNA was detected by staining with DAPI and PI and analyzed by confocal microscopy. **Figure 1A** (top panels) display representative images of unstimulated preparations, as well as preparations in which necrosis was induced by heat, showing that DNA staining (DAPI+ and PI+) was focused inside the cells in both cases. **Figure 1A** (bottom panels) demonstrates that cultures stimulated with anti-CD3/anti-CD28 released extracellular DNA strands associated with cells as seen by co-staining with DAPI and PI (arrows). Quantification of the extracellular DNA strands (extracellular traps – ETs) showed that ETs appear more frequently in anti-CD3/anti-CD28-stimulated cultures, as compared to cultures in which necrosis was induced ($p < 0.05$) (**Figure 1B**). In addition, the number of cells involved in ETs formation was also higher in anti-CD3/anti-CD28-stimulated cultures (**Figure 1C**), as compared to necrotic preparations ($p < 0.05$). Interestingly, stimulation with anti-CD3/anti-CD28 increases the number of CD8+ cells associated with formation of ETs (the sum of %CD8/DAPI plus %CD8/CD8 increases from 40.5% to 56%) (**Figure 1D**).

To quantify the amount of DNA released by lymphocyte-enriched preparations stimulated with anti-CD3/anti-CD28, we measured the DNA in culture supernatants using the PicoGreen dsDNA kit, as described in Materials and Methods. While all preparations released DNA in the supernatant, the release by anti-CD3/anti-CD28-stimulated cells was two-fold higher than that seen from the necrosis group (**Figure 1E**). Lysed cells (positive control) had the highest DNA titers (**Figure 1E**). The DNA signal was abolished by treatment with DNAse in all preparations, as expected (**Figure 1E**).

We measured the release of lactate dehydrogenase (LDH), an important molecule classically associated with necrosis (36). The necrosis cultures presented greater release of LDH than the anti-CD3/anti-CD28-stimulated cultures (**Figure 1F**). Cell lysis was used as a positive control, showing high release of LDH. Thus, DNA release was higher in anti-CD3/anti-CD28 stimulated cultures as compared to necrosis, whereas LDH release was higher in the group where necrosis was induced, showing an important difference between the two processes.

We also evaluated the occurrence of apoptosis and total cell death in the cultures by staining with Annexin V and/or propidium iodide (PI) using flow cytometry. The frequency of total lymphocyte death was determined within the lymphocyte gate and corresponded to the sum of total PI+ cells and total Annexin V+ cells. Non-stimulated and anti-CD3/anti-CD28-stimulated cultures had a low occurrence of cell death as compared to necrosis and staurosporin-treated cultures (**Supplementary Figure 1A**). Occurrence of apoptosis, as measured by the frequency of Annexin V+ PI- cells, was low in all cultures (except for the staurosporin control), although also higher in the necrosis group as compared to media and anti-CD3/CD28 (**Supplementary Figure 1B**). Occurrence of necrosis (as measured by $AnnexinV^{low}$ PI+ cells) was low in all cultures, except for the necrosis-induced cultures (**Supplementary Figure 1C**).

Electron Microscopy Shows Ultrastructural Characteristics Suggestive of Etosis in Anti-CD3/Anti-CD28 Stimulated Cells

We performed scanning (SEM) and transmission electron microscopy (TEM) to visualize the DNA-composed structures and cell morphology in lymphocyte-enriched cultures stimulated with anti-CD3/anti-CD28 or induced to necrosis. **Figures 2A–C** show the presence of fine structures that seem to connect one cell to another, as indicated by arrows, observed in SEM. The observed structures were clearly more evident in anti-CD3/anti-CD28-stimulated cultures (**Figure 2B**). **Figures 2D–F** show that treatment with DNAse abolished the presence of such structures. **Figure 2G** shows the detail of a DNA-formed structure derived from an anti-CD3/anti-CD28-stimulated culture. The average thickness of each filament that formed the structures was 14.7 nm, consistent with a DNA filament. **Figures 2H–J** show the morphology of typical lymphocytes observed in non-stimulated cultures, anti-CD3/anti-CD28-stimulated cultures and necrosis induced cultures, respectively.

TEM images of unstimulated cells showed aspects of typical resting lymphocytes with an intact nuclear envelope and organelles homogeneously dispersed in the cytoplasm (**Figure 2K**). In contrast, cells from anti-CD3/anti-CD28-stimulated cultures displayed a dramatically different morphology consistent with etosis (11), showing a lack of nuclear envelope and accumulation of organelles on one side of the cell (**Figure 2L**). These data clearly show the presence of DNA filament structures released by stimulated T cells with ultra-structural aspects compatible with the occurrence of etosis.

Extracellular DNA-Containing Structures Co-Stain With Anti-Histone Monoclonal Antibodies, but Not With Phalloidin, an Actin Marker

The presence of histones is a hallmark of ETs (10, 11). Thus, we performed a staining combining DAPI and anti-histone monoclonal antibodies. These two markers clearly co-localized on the extracellular structures in anti-CD3/anti-CD28 stimulated cultures, demonstrating the presence of ETs (**Figure 3A** in immunocytochemistry, and **Figure 3C**-in fluorescence

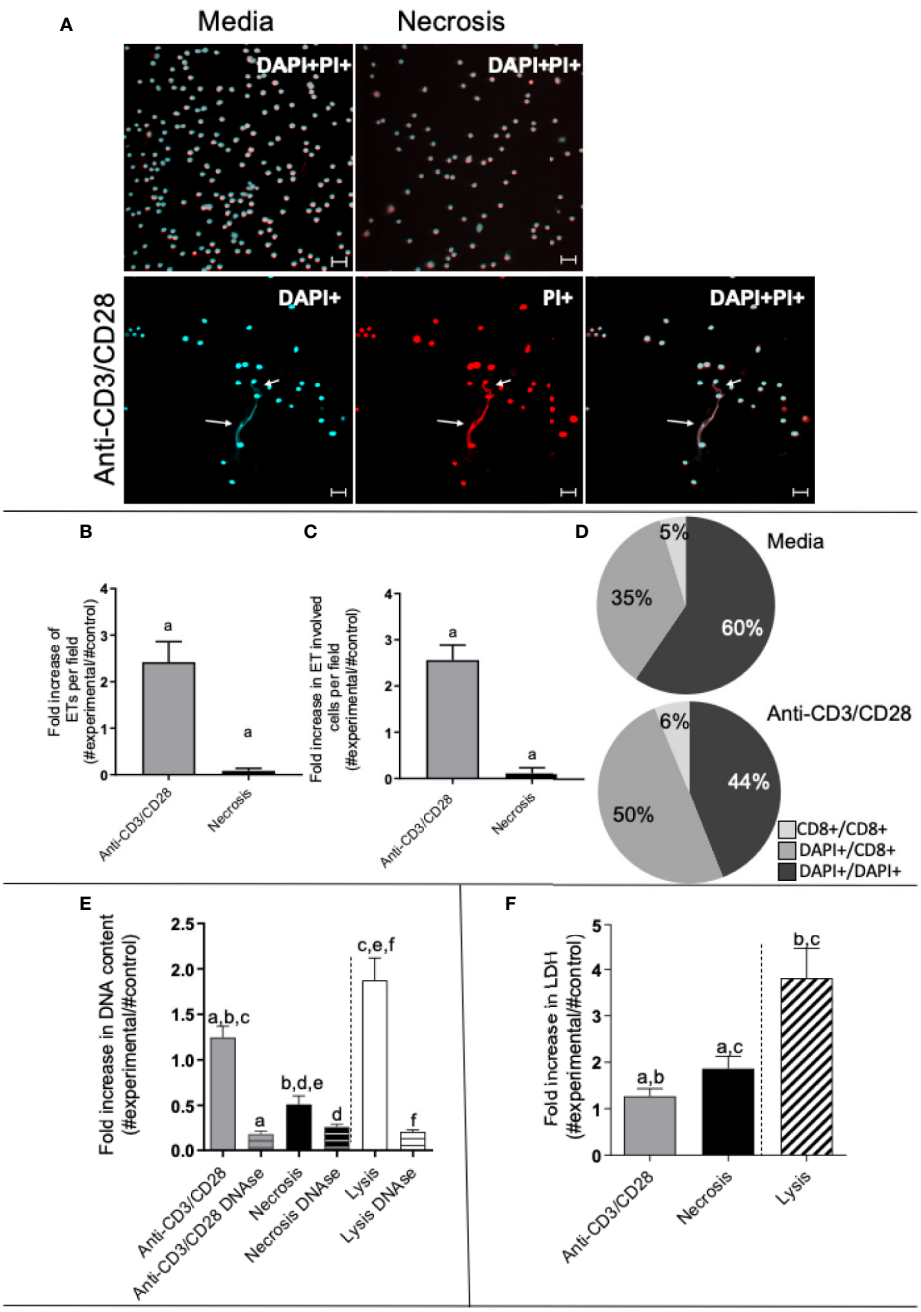

FIGURE 1 | Anti-CD3/anti-CD28 stimulation leads to the release of extracellular traps by T-lymphocyte enriched cultures. **(A)** Representative confocal image of non-stimulated culture (media), necrosis-induced culture (necrosis) and culture stimulated with anti-CD3/anti-CD28 stained with DAPI (light blue) and propidium iodide (PI - red). Arrows highlight extracellular DNA (extracellular traps – ETs) observed in the stimulated cultures. Bars = 20 μm. **(B)** Quantification of ETs after stimulation or induction of necrosis. **(C)** Quantification of the number of cells participating in the ETs in each group. **(D)** Determination of the frequency of ETs connecting DAPI+ cells to DAPI+ cells (DAPI+/DAPI+), any DAPI+ cells to CD8+ cells (DAPI+/CD8+) and CD8+ cells to CD8+ cells (CD8+/CD8+), as indicated, in non-stimulated and anti-CD3/anti-CD28 stimulated cultures. **(E)** Double-stranded DNA was quantified in the culture supernatant using the PicoGreen dsDNA kit (Invitrogen), according to the manufacturer's instructions. **(F)** Evaluation of necrosis by quantification of LDH release. The release of LDH into the culture supernatant was assessed by spectrophotometry (340 nm) using a commercial kit (Bioclin), according to the manufacturer's instructions. Data is presented as average per group ± standard error of the mean. Same letters in different bars represents statistically significant differences between them.

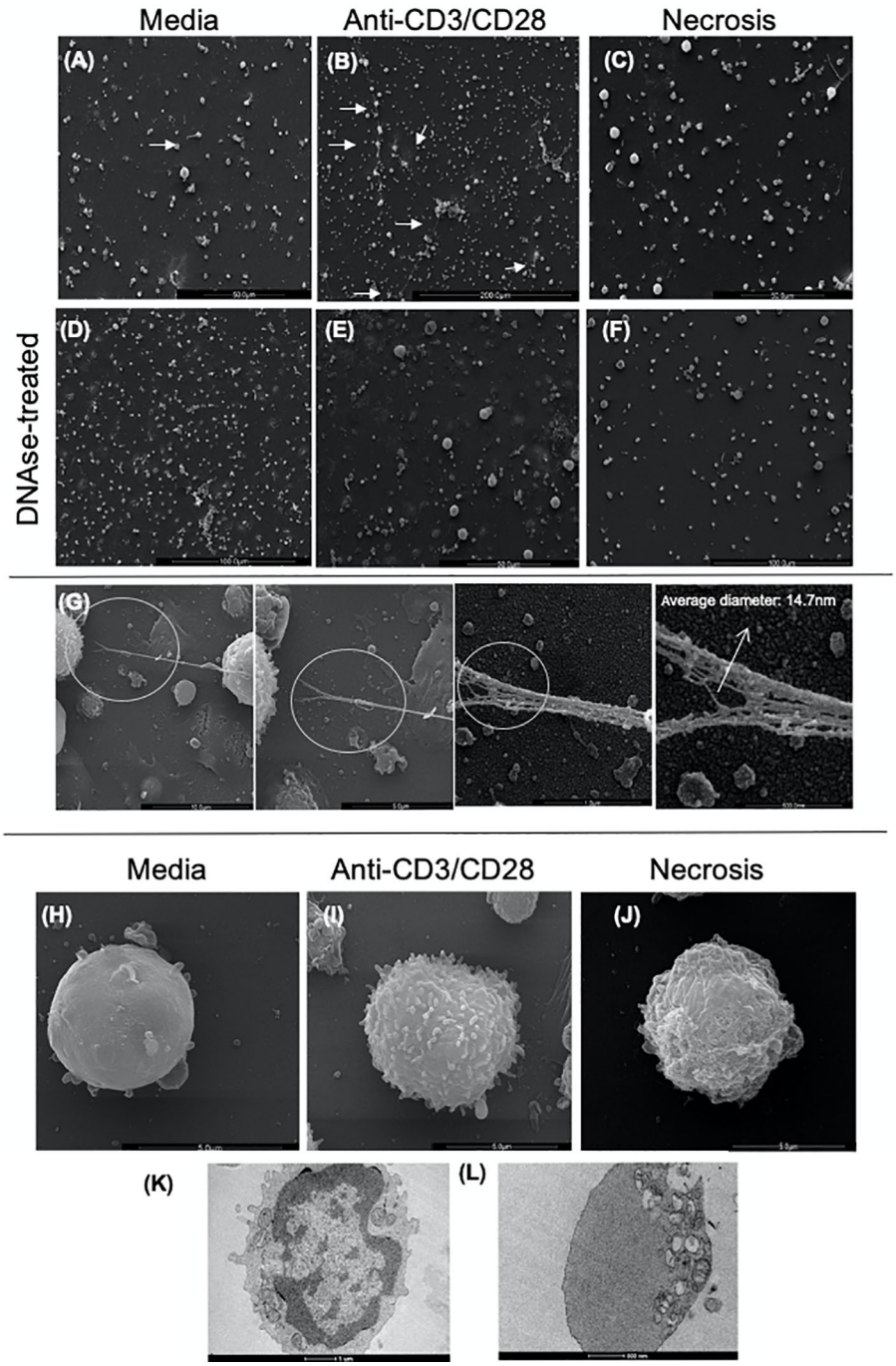

FIGURE 2 | Scanning and transmission electron microscopy of cultures enriched in T lymphocytes show the presence of extracellular traps (ETs). Representative scanning electron microscopy images of **(A)** Non-stimulated culture (media), **(B)** Culture stimulated with anti-CD3/anti-CD28, **(C)** Necrosis-induced culture (necrosis). In the **(A–C)** images, the arrows indicate structures compatible with extracellular traps (arrows). **(D)** Non-stimulated culture treated with DNAse (DNAse-treated media), **(E)** Culture stimulated with anti-CD3/anti-CD28 treated with DNAse, **(F)** Culture of cells induced to necrosis treated with DNAse (DNAse-treated necrosis). **(G)** Detail of an ET (extracellular DNA) present in a culture enriched with T lymphocytes after anti-CD3/anti-CD28 stimulation. High-resolution SEM analysis of ETs that consist of fibers with an average diameter of 14.7 nm, arrow. Scanning electron microscopy images of cell topography under different conditions, showing the distinction amongst them: media **(H)**, anti-CD3/anti-CD28 **(I)**, and necrotic **(J)**. Transmission electron microscopy of **(K)** unstimulated T cell; **(L)** cell in etosis present in culture stimulated with anti-CD3/anti-CD28.

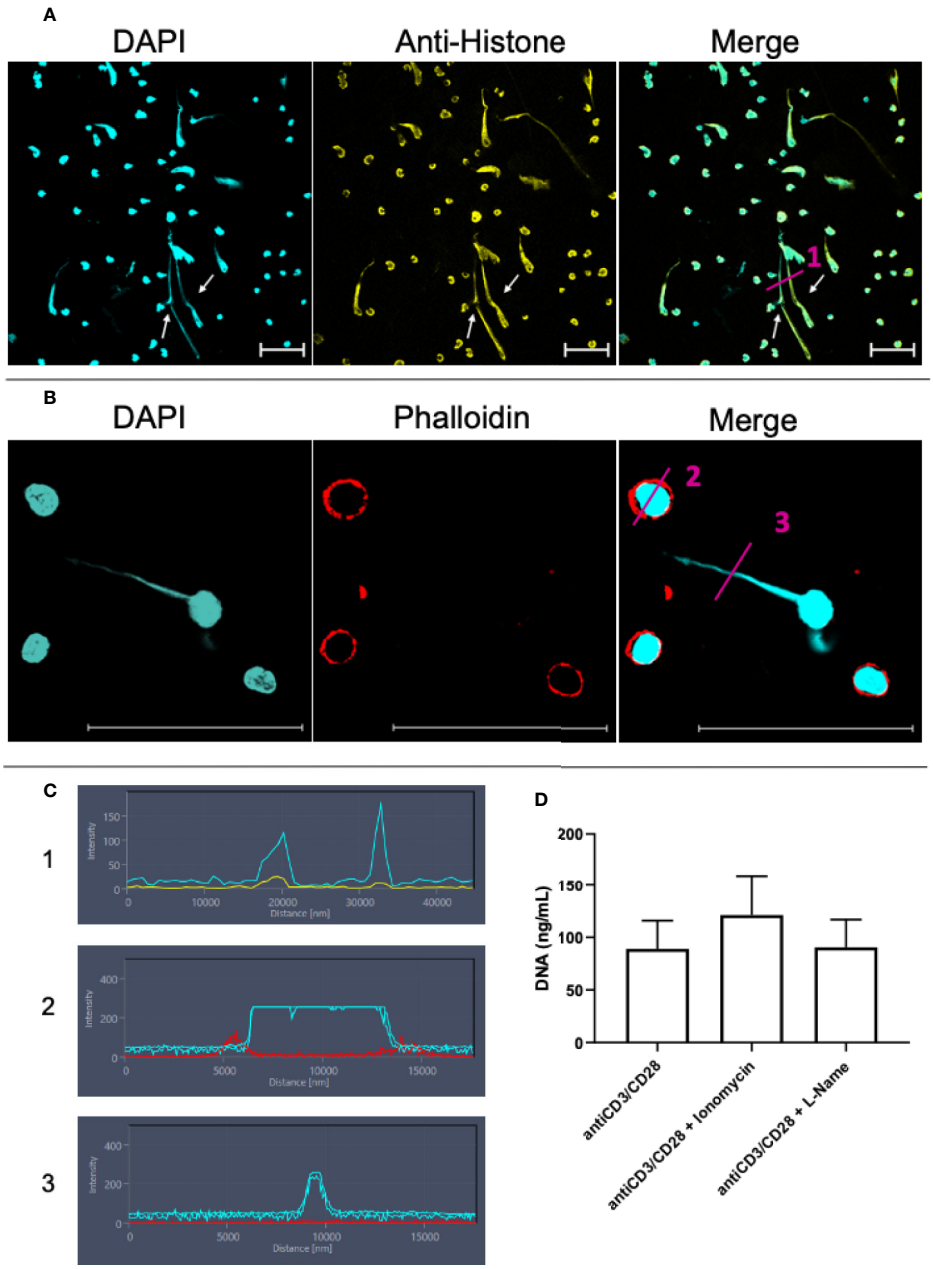

FIGURE 3 | Lymphocytes are able to release extracellular traps (ETs) composed of DNA and histones. T lymphocyte-enriched preparations were plated on poly-L-lysine coverslips, stimulated or not with anti-CD3/anti-CD28 and maintained in culture for 24 h. The preparations were stained with DAPI (light blue) and/or anti-histone (yellow), and/or phalloidin (red - actin evidence). Bars = 50 µm. **(A)** Representative confocal image of culture stimulated with anti-CD3/anti-CD28 and labeled with DAPI (light blue)/anti-histone (yellow). Arrows highlighted extracellular traps observed in the stimulated cultures. **(B)** Samples were stained with DAPI (light blue)/phalloidin (red). **(C)** shows histograms derived from the details marked with (1), (2) and (3) in panels **(A, B)**, showing the co-localization of DAPI and histones (1) and the lack of co-localization of DAPI and actin in the cell body (2) and in the extracellular DNA-structure (3). **(D)** shows the effect of ionomycin and L-NAME in the release of extracellular DNA by anti-CD3/anti-CD28 stimulated cultures.

histogram 1). The histogram shows that DAPI (blue line) and histone (yellow line) co-localize.

In order to exclude the possibility that the long DNA-containing structures were tunneling nanotubes or cytonemes, structures involved in cell communication that contains DNA and actin (37–39), we co-stained the samples with phalloidin, an actin-detecting molecule, and DAPI. **Figure 3B** clearly shows that the extracellular DAPI+ DNA structures do not co-stain for phalloidin, thereby excluding the presence of actin in the structures, and ruling out the possibility that they are

tunneling nanotubes or cytonemes. This result is also observed in histograms 2 and 3 in **Figure 3C**. The histograms show that phalloidin (red) and DAPI (blue) staining do not overlap.

Arginine deaminases 4 (PAD4) is fundamental for the occurrence of etosis in neutrophils and is responsible for DNA unfolding (40, 41). PAD4 activity is increased by intracellular Ca^{++}, which is elevated by the calcium ionophore ionomycin (42). iNOS activity has also been correlated with ET release by neutrophils (40). **Figure 3D** shows that ionomycin treatment in lymphocyte-enriched cultures increases DNA release by 36% ($p= 0.07$, as compared to anti-CD3/CD28 stimulated cultures), suggesting that Ca^{++} is also associated to DNA release by lymphocytes. On the other hand, blocking of iNOS activity by L-N^G-Nitro arginine methyl ester (L-NAME) does not alter the release of ETs in lymphocyte-enriched cultures (**Figure 3D**).

Human CD8+ T Cells Release Extracellular Traps That Are Morphologically Distinct From the Ones Released by CD4+ T Cells

We then focused on studying whether CD8+ T cells can release ETs. CD8+ T cells were purified using a cell sorter, stimulated with anti-CD3/anti-CD28, and analyzed using confocal and electron microscopy. As a comparison, CD4+ cells were also purified and submitted to the same culture conditions. **Figure 4A** (top panels) show that stimulated CD8+ T cells release ETs as filaments connecting neighboring cells (arrows). In contrast, CD4+ T cells release ETs with a diffuse pattern around the cells (**Figure 4A**, bottom panels, arrows). **Figure 4B** shows that both CD8+ and CD4+ derived ETs are composed mainly of DNA (DAPI+, blue intensity curve), but also contain some cytoplasm proteins (CFSE+, pink intensity curve). Scanning microscopy analysis confirmed that activated CD8+ T cells released long and thin structures, often connecting one cell to another (**Figure 4C**, arrow in top panels, **Figure 4D**, and **Supplementary Video 1**). In contrast, CD4+ T cells release DNA around the cell, forming a halo (**Figure 4C**, bottom panels). CD4+ T cells appeared to have a disintegrated membrane, suggesting cell death.

To investigate the activation state of the stimulated cells, as well as the occurrence of apoptosis in the different cultures, we evaluated the expression of CD69 and TNF as indicators of activation, and AnnexinV/PI as indicators of apoptosis.

Figure 5A shows the selection of lymphocyte subpopulations to be analyzed in scatter plots (granularity x CD4+ or granularity x CD8+) obtained by flow cytometry. **Figure 5B** shows the isotype controls. **Figures 5C**, **E** show representative histograms of CD69 and TNF-alpha, respectively. After 24 h of stimulation, we observed that both CD4+ and CD8+ T cells had a higher expression of CD69 when compared to media control (**Figure 5D**). Interestingly, activated CD4+ T cell cultures exhibit a much greater frequency of TNF-alpha+ cells as compared to non-stimulated cultures, than CD8+ T cell cultures (**Figure 5F**). The overall frequency of cell death for CD4+ and CD8+ T cells (**Figures 5G, J**, respectively), as well as necrosis (**Figures 5I, L**, respectively), was low in stimulated cultures. While the frequency of cells in apoptosis was also low, it was higher in CD4+ T cell stimulated cultures, as compared to non-stimulated ones (**Figure 5H**). This statistically significant difference was not observed in cultures of CD8+ T cells (**Figure 5K**). This suggests that the higher production of TNF observed in CD4+ T cells may be associated with the higher apoptosis observed in CD4+ T cells, as this cytokine may induce apoptosis.

Release of Extracellular DNA by CD8+ T Cells Is Followed by Death of Target Cells

To confirm the dynamics of LET release by CD8+ T cells in real-time, we performed time-frame videos (**Figure 6A** as a static figure and **Supplementary Video 2**). CD8+ T cells were purified and cultured with CFSE-stained target cells at a ratio of 1:4, as described in *Methods*. **Figure 6A** shows a CD8+ T cell-derived extracellular DNA filament forming (chevron, last frame of first row), toward a CFSE-labeled live cell (pink), and its subsequent death (thin arrow fifth frame in second row from top shows the cell transitioning from pink to blue; the following frame shows the cell in blue). Arrows in last row show the extracellular DNA connecting both cells. **Figure 6B** shows the histogram for the fluorescence of ethidium homodimer (EthD-1) obtained from image in first row, which is positive in cell 1 (CD8+ T cell, blue) indicating loss of membrane integrity, and negative in cell 2 (target cell, still alive), which is stained with CFSE (pink). **Figure 6C** shows the histogram for the extracellular DNA released from cell 1, and also shows that cell 2 is now positive for EthD-1, depicting its loss of membrane integrity after contact with the CD8+ T cell-derived LET. This sequence can be visualized in **Supplementary Video 2** and shows that the release of extracellular DNA by CD8+ T cells is followed by the death of the neighboring cell.

CD8+ T Cell-Derived LETs Carry CD107a+ Vesicles

Next, we sought to determine if the LETs could carry cytotoxic signals by examining the physical association of cytolytic vesicles expressing CD107a with CD8+ T cell-derived LETs. We observed that the expression of CD107a (**Figure 6D**, pink, in square) colocalized with DAPI-stained LETs (**Figure 6D**, blue, in square) coming from CD8+ T cells (**Figure 6D**, yellow), and being delivered to a distant cell (**Figure 6E**, arrow). Interestingly, the CD8+ T cell releasing the LET also exhibits a dramatic polarization of the CD8 molecule on the opposite pole from where the LET is released (**Figure 6E**). Co-localization of CD107a and LET is also seen in the histogram insert relative to the section highlighted by the square in **Figure 6D**. Ultrastructural analysis shows that one of the cells connected to the extracellular DNA displays the telltale topology of an apoptotic cell (**Figures 6F, G**), with membrane blebs (blue arrow in **Figure 6G**). Together, these data suggest that the delivery of CD107a+ vesicles by the launched CD8+ T cell-derived LETs may be involved in the observed cell death.

LETs Are Associated With Increased Tissue Pathology in Human Leishmaniasis

After demonstrating that CD8+ T cells can release LETs, we sought to investigate if this phenomenon was associated with the

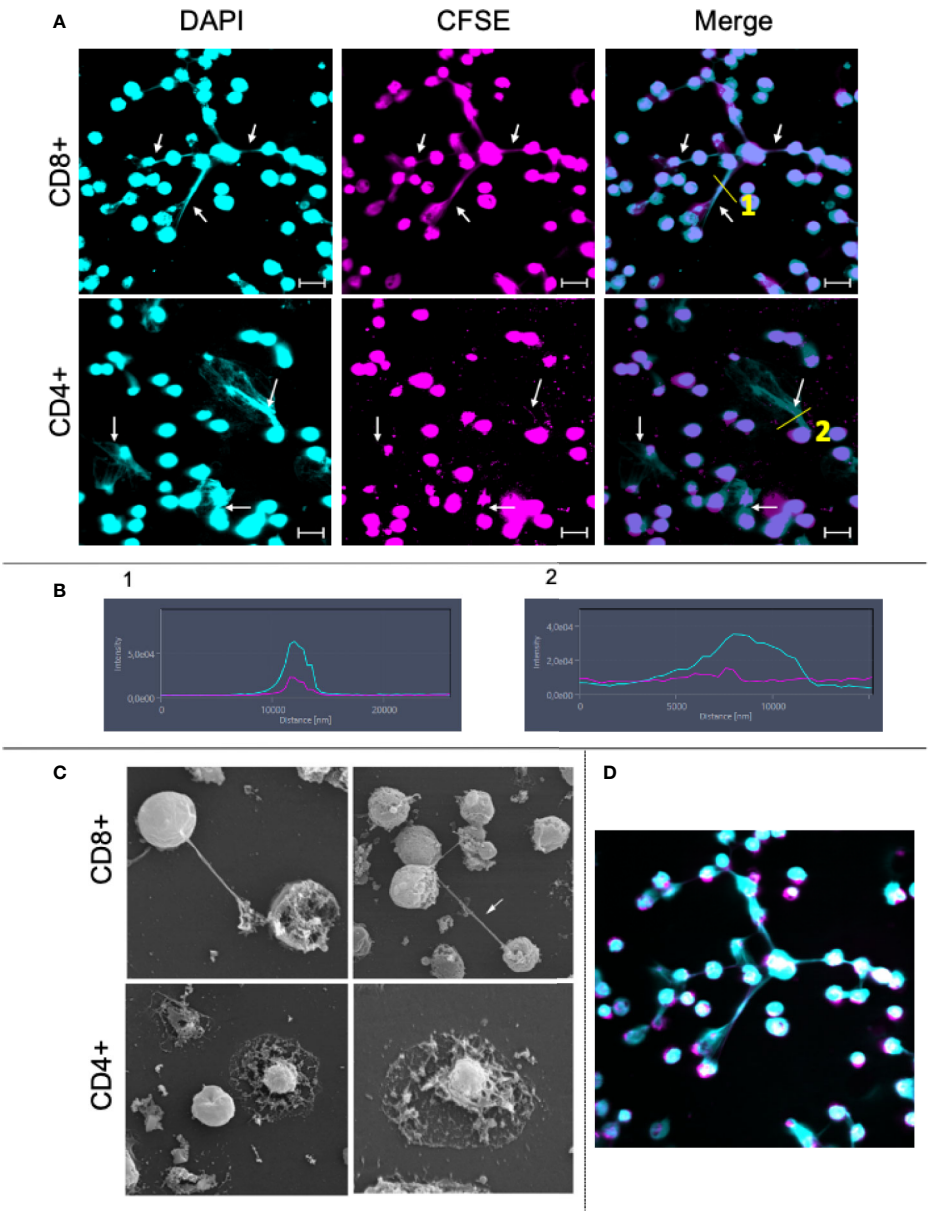

FIGURE 4 | Purified CD8+ and CD4+ T lymphocytes release extracellular traps (ETs) upon stimulation. Purification of CD8+ and CD4+ T lymphocytes was done by sorting as described in Material and Methods. **(A)** CD8+ and CD4+ lymphocytes were stained with CFSE, plated on poly-L-lysine coverslips and stimulated with anti-CD3/anti-CD28 for 24 h. After incubation the cells were stained with DAPI as described in the Materials and Methods. Representative images from confocal microscopy analyses for show the DAPI+ (light blue) cells, CFSE+ (pink) cells and for both. Arrows highlight the extracellular traps. Bars = 20 μm. **(B)** shows histograms derived from the details marked with (1) and (2) in panels **(A)**, demonstrating the co-localization of DAPI and CFSE in CD8-derived and CD4-derived ETs, respectively. **(C)** CD8+ and CD4+ cells were stimulated and processed for SEM analysis, as described. Lymphocytes cells were plated on poly-L-lysine coverslips, stimulated with anti-CD3/anti-CD28 and maintained in culture for 48 h. The left CD8+ and CD4+ images have a magnification of 3,000× while the right ones, 5,000×. Arrow: structure connecting cells. **(D)** Confocal image obtained by staining with CFSE (pink) and DAPI (blue, as above) showing CD8+ T cell-derived DNA filament connecting cells.

pathology of human tegumentary leishmaniasis, a disease in which CD8+ T cells play a key role in pathology. Thus, we focused our study on LETs derived from CD8+ T cells in cutaneous and mucosal forms of leishmaniasis.

Previous studies have shown that skin lesions from individuals infected with Leishmania displayed neutrophil-derived ETs (14, 22). In addition, we have demonstrated that CD8+ T cells play a key role in the development of cutaneous leishmaniasis (CL) lesions (24, 26, 27), and transcriptome analysis from patient lesions has supported the existence of an inflammatory CD8+ cytolytic T cell response in lesion microenvironment (43, 44). While further investigating cellular

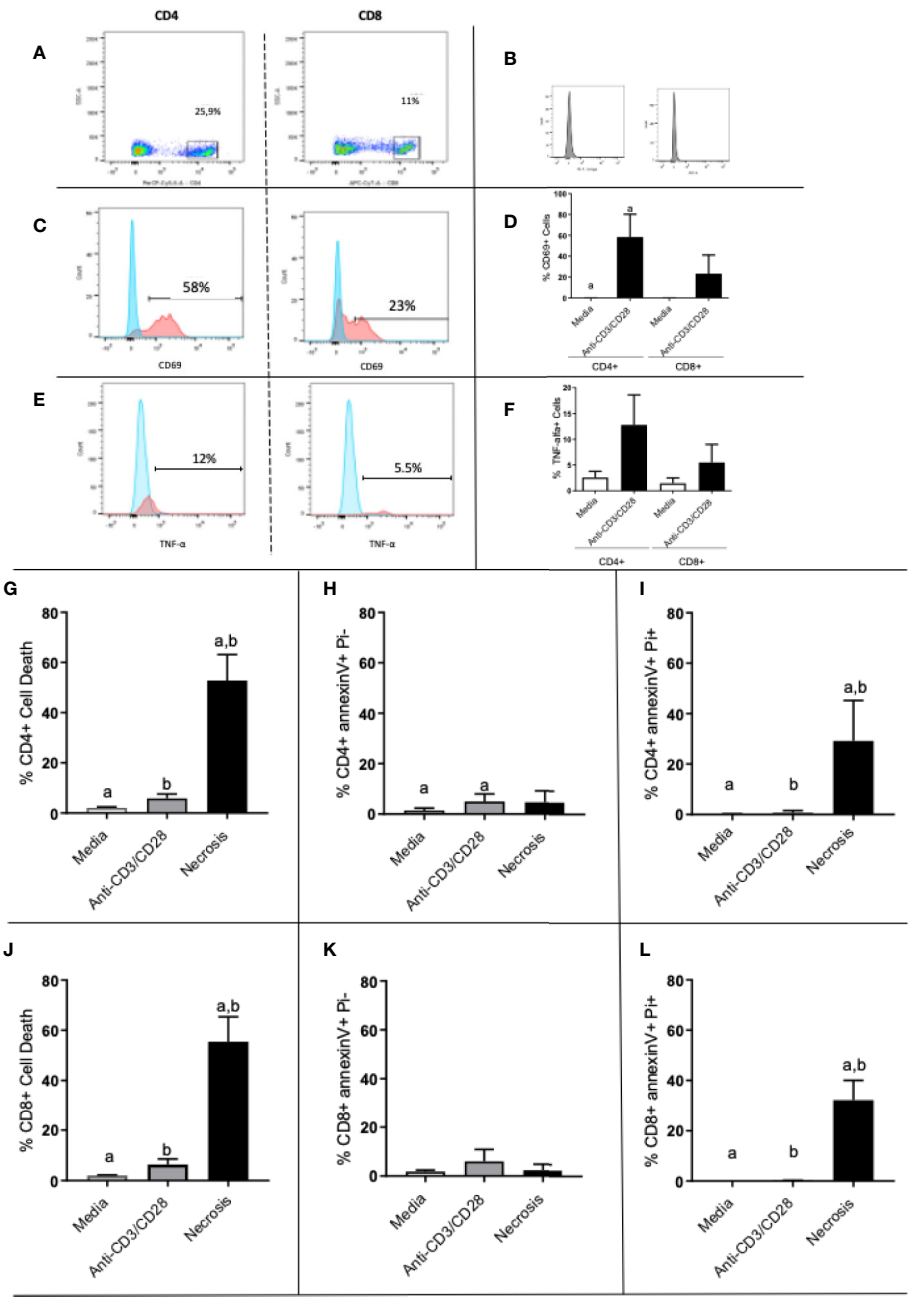

FIGURE 5 | Evaluation of activation and death of CD4+ and CD8+ T cells. **(A)** Gate selection for CD4+ and CD8+ analysis; **(B)** isotype controls; **(C, E)** representative histograms for CD69 and TNF analysis, respectively, in CD4 and CD8 cells, as indicated. Expression of CD69 and **(D)** TNF **(F)** by CD4+ and CD8+ T lymphocytes before and after stimulation with anti-CD3/anti-CD28. **(G–I)** show total death, early apoptosis and late apoptosis of CD4+ T cells, respectively. **(J, L)** show total death, early apoptosis and late apoptosis of CD8+ T cells, respectively. Data is presented as average per group ± standard error of the mean and presence of the same letters in different bars represents statistically significant differences between them ($p<0.05$).

mechanisms of tissue destruction in leishmaniasis, we observed, using confocal microscopy, that lesions from CL patients infected with *L. braziliensis* were dense with what appeared to be DNA filaments as evidenced by DAPI staining (**Figure 7A**, arrows). We further stained the lesions with DAPI and anti-histone antibodies concomitantly, and observed the co-localization of extracellular DNA and histones, suggesting that the observed structures were indeed ETs (**Figure 7B**, overall and arrows). Importantly, we also determined that the inflammatory infiltrate of those lesions was predominantly composed of mononuclear cells, with a very low frequency of polymorphonuclear cells (**Figure 7C**), and that over 60% of the

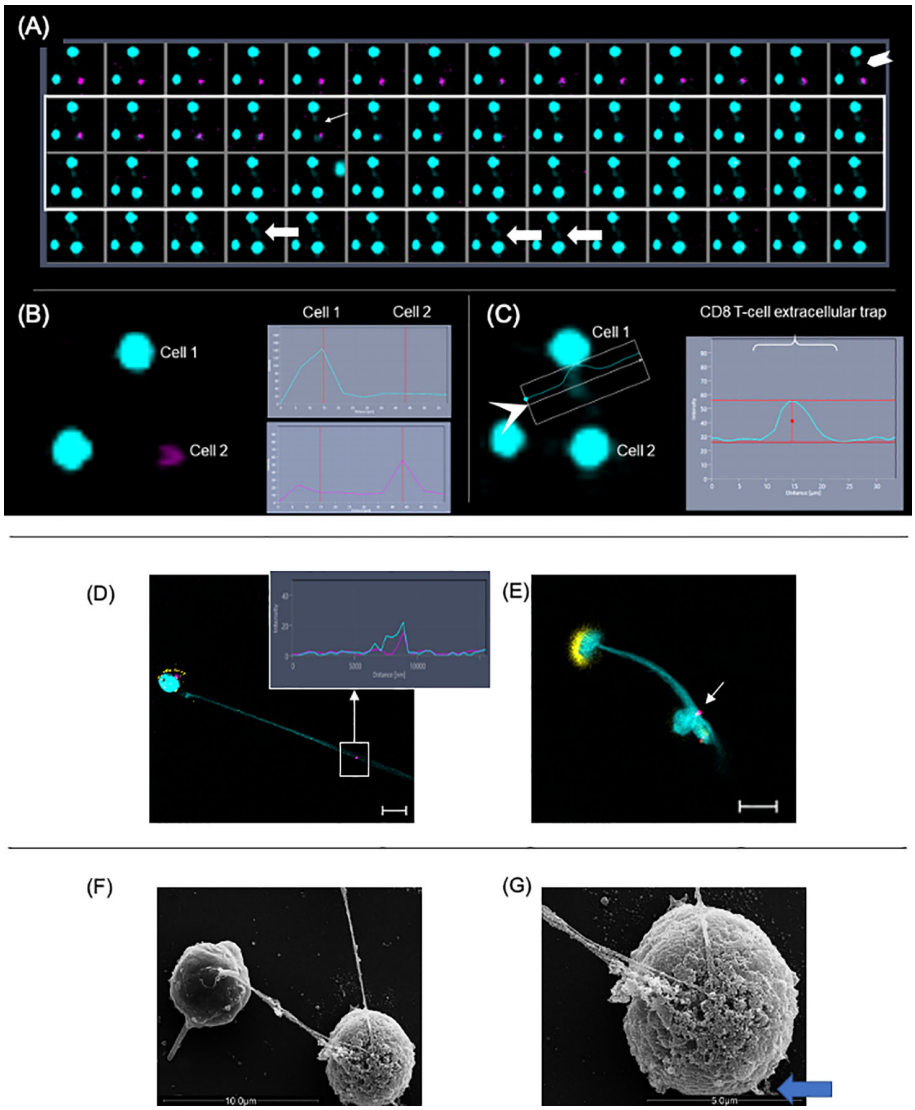

FIGURE 6 | Extracellular DNA from CD8+ T cells induces death of neighboring cells. Purified CD8+ T cells were cultured with CFSE-labeled targets (pink) at a ratio of 1:4. Cultures were stimulated with anti-CD3/anti-CD28+ionomycin and stained with live-dead marker (EthD-1). Images were obtained in 10-s intervals using excitation/emission capture of 495/515 nm for CFSE and 532/635 for EthD-1, on a Zeiss 5-live microscope. **(A)** Static images showing the moment in which the liberation of extracellular DNA by a CD8+ T cell (chevron, last frame in first row) is followed by the conversion of a pink cell (target) into a blue cell (light arrow at frame 5, second row), indicating death. **(B)** Fluorescence histograms showing cell 1 (EthD-1- blue) and cell 2 (CFSE-pink) before the release of extracellular DNA by cell 1. **(C)** Fluorescence histogram showing extracellular DNA from cell 1. In this detail, it is possible to see the DNA strand extruding toward cell 2. This can also be observed in **(A)** in frames 4, 8 and 9 from last row (fat arrows). **(D, E)** Representative immunofluorescence image of T-lymphocyte enriched cultures stained with anti-CD8 (yellow), anti-CD107a (pink), DAPI (light blue). Arrow indicates that CD107a+ vesicles co-localized with the extracellular trap (DAPI+). Bars = 10 μm. Detail shows histogram demonstrating the co-localization of CD107a+ and DAPI+ staining. **(F)** Scanning electron microscopy image showing two cells connected by a DNA filament. **(G)** The SEM detail shows the telltale morphology of an apoptotic cell with a ruffled and blebbed membrane (blue arrow).

inflammatory infiltrate was composed of CD4+ and CD8+ cells (**Figure 7C**). Thus, the presence of DNA+histone+ structures outside the cells, our in vitro findings demonstrating CD8+ T cell produced LETs, together with T cell dominant lesions from *L. braziliensis*-infected individuals in the virtual absence of neutrophils (our own study, as well as a lack of transcriptome profiles consistent with neutrophils – *44*), led us to investigate whether T cell released LETs in cutaneous leishmaniasis lesions, and if they were related to disease progression and severity.

The intensity of the inflammatory infiltrate present in lesions from patients with CL and ML is a measure of pathology severity in these diseases (24–26). As expected, our analysis of this cohort confirmed that disease progression from early to late in CL and the more severe ML form displays a more intense inflammatory

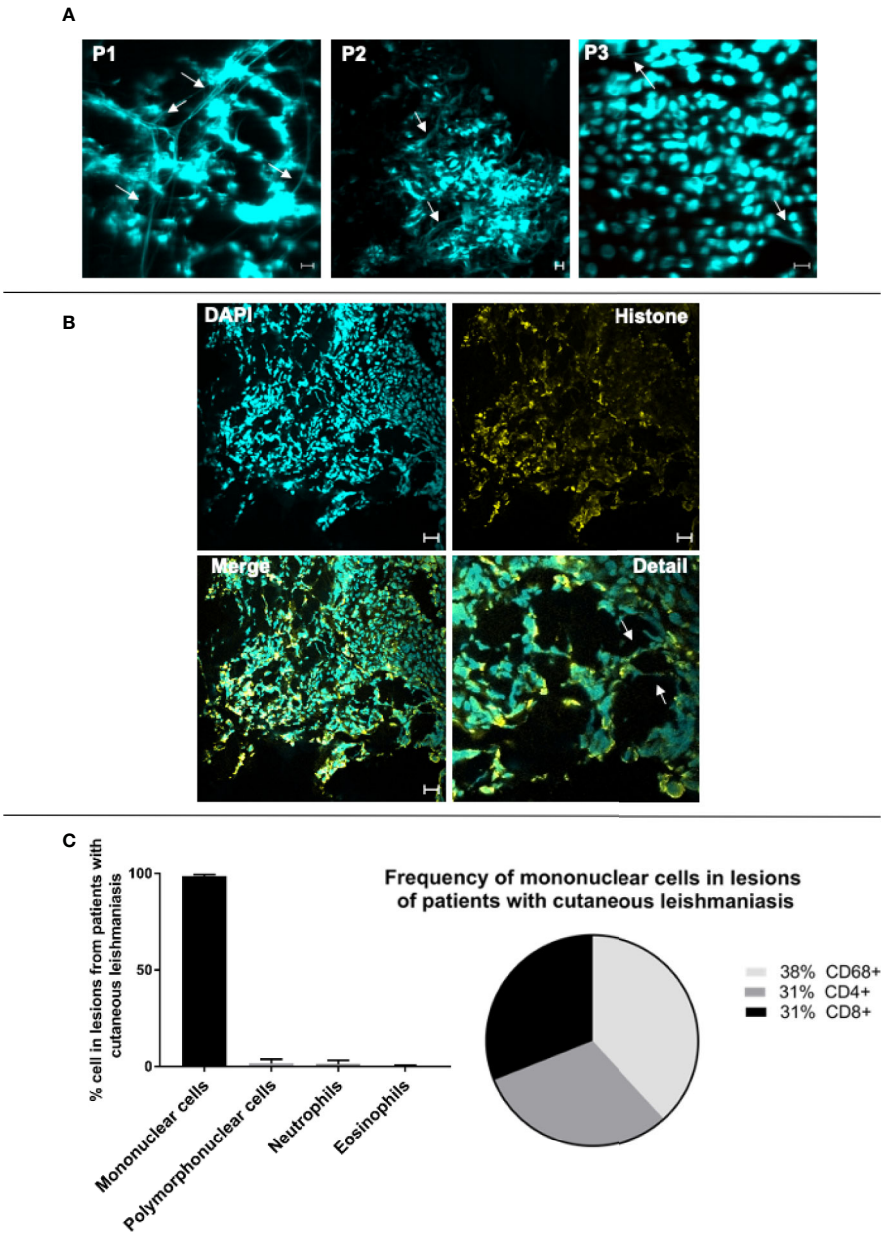

FIGURE 7 | Lesions of patients with cutaneous leishmaniasis display extracellular DNA. Tissue sections were stained with DAPI or Alexa 488-labeled anti-histone monoclonal antibodies as described in *Materials and Methods*. **(A)** Representative confocal images of lesions from patients with cutaneous leishmaniasis stained with DAPI alone (P1, P2 and P3 represent three different patients), showing the occurrence of extracellular DNA structures. The bars = 10 μm. **(B)** Representative lesion from a cutaneous leishmaniasis patient stained with DAPI and anti-histone monoclonal antibody. In detail, colocalization of the DAPI (light blue) and histone (yellow). Arrows show extracellular DNA co-stained with DAPI and anti-histone monoclonal antibody. Bars = 20 μm. **(C)** Evaluation of cellular composition of lesions from cutaneous leishmaniasis patients (n=14) through histopathology analysis using hematoxylin/eosin stain (graph), and confocal microscopy using anti-CD4, anti-CD8 and anti-CD68 monoclonal antibodies (pie chart), as described in *Materials and Methods*.

infiltrate (**Supplementary Figure 2A**). We show here that the number of CD8+ cells (**Supplementary Figure 2B**), as well as the number of CD8+CD107+ cells (**Supplementary Figure 2C**) display a positive correlation with the intensity of the inflammatory infiltrate in the evaluated TL disease forms.

In order to investigate the association between the presence of LETs with the progression and severity of tegumentary leishmaniasis (TL), we compared the number of DNA strands in lesions from patients with early versus late CL lesions, and of CL versus mucosal (ML) lesions. We also evaluated the participation of CD8+ T cells, as well as CD8+CD107a+ cells in the release of LETs in these lesions. **Figure 8A** shows representative staining with DAPI, CD8 and CD107a in lesions from patients with different stages of CL or with ML, clearly

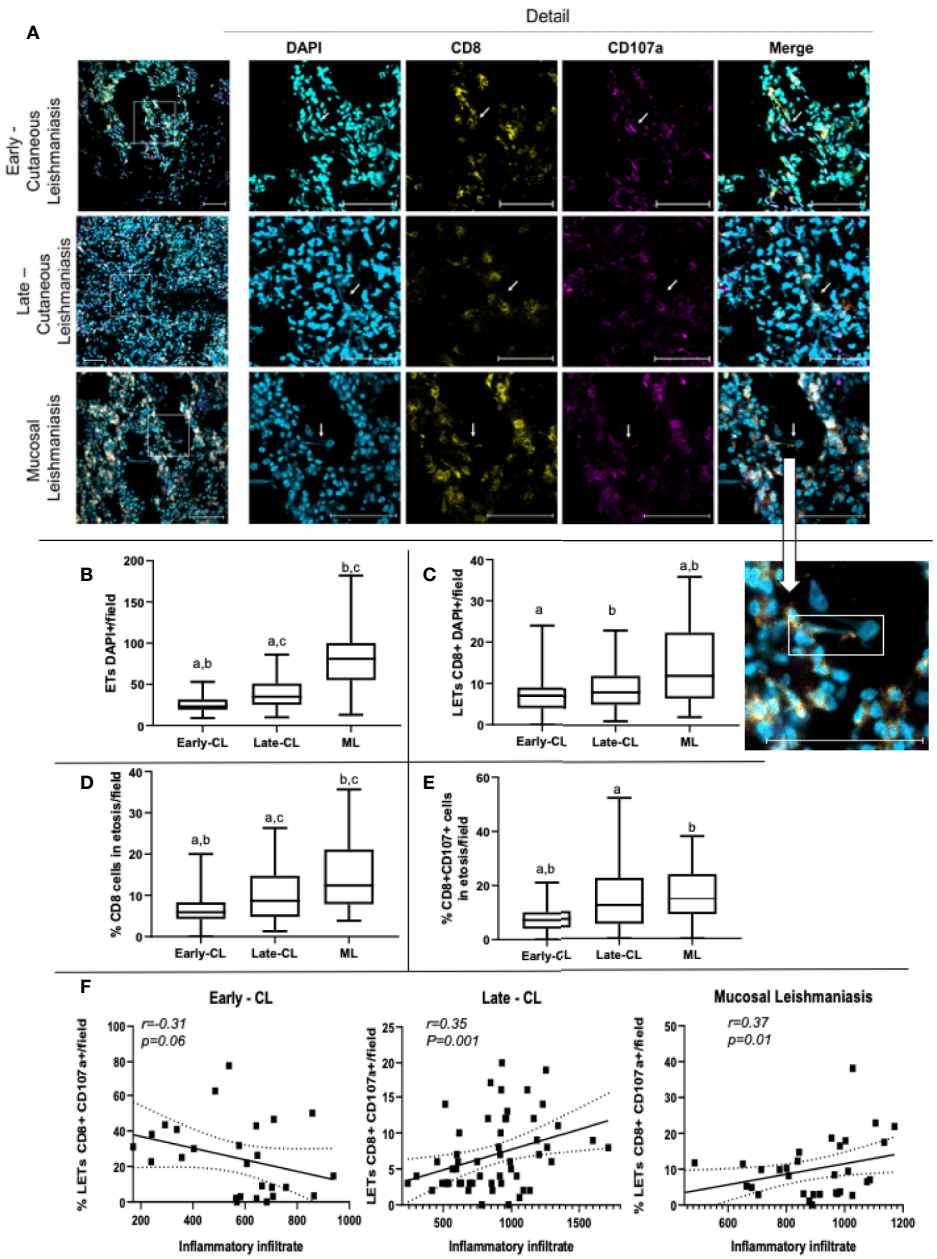

FIGURE 8 | Lesions of patients with early and late cutaneous, as well as mucosal leishmaniasis, display extracellular DNA, CD8+ cells and CD107a expression. Tissue sections were stained with DAPI, anti-CD8-PE and anti-CD107a-FITC monoclonal antibodies as described in Materials and Methods. **(A)** Representative confocal images of lesions from patients with early (n=2; 27 fields) and late cutaneous leishmaniasis (n=4; 43 fields), and mucosal leishmaniasis (n=2; 28 fields) stained with DAPI alone, anti-CD8 alone, anti-CD107 alone and a merged image of the three stainings (right panels). The detail image shows extracellular DNA co-localized with CD107a+ vesicle, connected to a cell. The bars = 50 µm. **(B)** number of total ETs; **(C)** number of CD8+ cells connected to LETs; **(D)** percentage of CD8+ cells in etosis within the total CD8+ population; **(E)** percentage of CD8+CD107a+ cells in etosis within the total CD8+CD107a+ sub-population. Data is presented as average per group ± standard error of the mean and presence of the same letters in different bars represents statistically significant differences between them ($p<0.05$). **(F)** Correlation analysis between the number of inflammatory cells/lesion field and the frequency of CD8+CD107+LETs/field for each clinical form.

showing the existence of CD8-associated LETs, colocalizing DNA strands and CD107a. We observed that progression from early to late CL lesions was accompanied by an increase in the number of overall ETs, and that the same was observed when comparing both stages of CL versus the more severe form, ML (**Figure 8B**). Examining the number of CD8 cells involved in the release of LETs, we observed similar numbers comparing early and late CL lesions, but greater numbers when comparing more severe ML to CL lesions (**Figure 8C**). The percentage of CD8 cells undergoing etosis was related to the progression from early

to late, as well as when comparing CL to the more severe ML (**Figure 8D**). A significant increase in the percentage of CD8 +CD107a+ cells in etosis was observed with lesion progression and severity (**Figure 8E**).

In order to determine if LETs are also associated with the in situ inflammatory pathology in the different clinical forms, we performed a correlation between the number of cells present in the inflammatory infiltrate, as a measure of the intensity of the inflammation, versus the frequency of CD8+CD107+ cells releasing LETs. Interestingly, we observed that while the frequency of CD8+CD107+ cells in etosis was not correlated with the inflammatory infiltrate in early stages of CL, the frequency of CD8+CD107+ cells in etosis was correlated with the intensity of the inflammatory infiltrate as CL progressed (late CL), and also with the severe ML form (**Figure 8F**), clearly associating release of LETs by CD8+CD107+ cells with disease progression and severity.

DISCUSSION

Our study demonstrates for the first time that human CD8+ T lymphocytes release extracellular traps (LETs) upon stimulation, and that these LETs are morphologically distinct from the ones released by CD4+ T cells. Importantly, ETs derived from CD8+ T cells form long DNA filaments connecting one cell to another, contain CD107a+ vesicles, and induce death in cells that enter in contact with it. This suggests that release of ETs by CD8+ T lymphocytes may represent a mechanism of delivering cytotoxic vesicles to distant targets.

Brinkmann et al. (10) first demonstrated that ETs were composed mainly of DNA and histones. Other authors also characterized ETs produced by different cells as containing mainly DNA (13, 15, 45). Here we demonstrated that the structures released by anti-CD3/anti-CD28 stimulated lymphocytes are also composed principally of DNA since: (1) they have a structure and diameter similar to a DNA filament as shown by SEM, (2) treatment with DNAse eliminates the structures observed in SEM, (3) they stain with DAPI, PI and anti-histone antibodies, and (4) supernatants from stimulated cultures contain DNA. Together, these data allow us to conclude that lymphocyte-derived ETs (LETs) are also composed of DNA as described for ETs derived from neutrophils and other cell types. While previous work has suggested that lymphocytes can release extracellular DNA (16), our work brings a more in-depth characterization of these structures.

Given necrosis can also lead to DNA release (46, 47), it was critical to demonstrate that the observed LETs were not related to necrosis. To test this possibility, we first demonstrated that cell death, particularly necrosis, was extremely low in the stimulated cultures. In addition, the release of the enzyme lactate dehydrogenase (LDH), which is characteristic of necrosis (36), was significantly lower in the supernatant of anti-CD3/anti-CD28-stimulated cultures as compared to the necrosis-induced, and positive control groups (lysed cells). We also observed that anti-CD3/anti-CD28-stimulated cultures led to a greater DNA release than the cultures induced to necrosis. Moreover, DNAse I treatment decreased DNA quantification in the supernatants from anti-CD3/anti-CD28-stimulated cultures, confirming that the DNA collected in the culture supernatant was double-stranded DNA, as previously shown in other models of etosis (14, 48). Necrosis activates intracellular DNAse to cleave DNA, which explains the low quantification of DNA released in necrosis (49). The presence of LETs was detected using DAPI and PI, which is a DNA intercalating agent, used in other studies to show the presence of DNA in ETs (46). In addition, co-localization of extracellular DNA and histones by immunofluorescence (10, 13) in cells from the stimulated cultures confirmed the occurrence of LETs, formed by nuclear DNA.

Previous studies have demonstrated that Ca^{++} mobilization and production of reactive oxygen species (ROS) are associated with the release of ETs by neutrophils (21, 41, 50). Here we showed that the release of LETs is associated with the increase of Ca^{++}, as the use of a Ca^{++} ionophore (ionomycin) increased the release of LETs. On the other hand, inhibition of nitric oxide synthase, important in the generation of ROS, did not alter the release of LETs. It is possible that NOS activation is related to the release of ETs by innate cells, but not particularly important in lymphocytes, as the expression of this enzyme is greater in innate cells. These analyses demonstrate that the mechanisms involved in the release of LETs share some common and distinct pathways regarding the release of ETs by other cell types.

Quantitative analysis of extracellular DNA demonstrated that anti-CD3/anti-CD28 stimulation induced a greater release of LETs and involved a greater number of cells releasing LETs, as compared to the necrosis group. While anti-CD3/anti-CD28 stimulates all T cells, not all cells in the cultures release ETs. The characteristics of ET-releasing T cells remain to be determined. It is possible that these structures are only released by pre-activated T cells, or by a subset of memory or effector cells. Identification of such sub-populations are beyond the scope of this paper but studies to further characterize ET-releasing T cells are underway in our lab. Given the use of anti-CD3-anti-CD28 does not directly involve MHC-peptide/TCR interaction, we were unable to determine here if antigen-specific interaction triggers the release of LETs. Further studies using antigen-specific responses are necessary to clarify the role of class I-mediated antigen presentation in the process of LET formation.

Cultures stimulated with anti-CD3/anti-CD28 present a greater number of extracellular strands connecting one cell to another, as observed by scanning electron microscopy (SEM). Importantly, DNAse treatment eliminated the strands at the ultrastructural level, thereby confirming their DNA composition. SEM showed morphology consistent with resting, activated and necrotic cells from non-stimulated, anti-CD3/anti-CD28 stimulated and necrosis cultures, respectively. This shows clear differences amongst stimulated and necrosis cultures: the necrosis group had cells with a degraded cell membrane, typical of necrotic cells (51), whereas the activated cells had a ruffled membrane typical of healthy activated cells (51, 52). Also, using SEM, the thickness of the filaments was determined to be

14.7 nm in diameter, compatible with DNA strands (10, 40). Internal morphology analysis, as evaluated by transmission electron microscopy (TEM), showed that resting cells displayed intact plasma and nuclear membranes, with typical heterochromatin, and organelles homogeneously dispersed in the cytoplasm, whereas cells from the activated cultures, in which LETs were observed, displayed morphology similar to that observed in cells in etosis (11), without a visible nuclear membrane and organelles polarized towards one side of the cell.

Tunneling nanotubes (TNTs) and cytonemes, are actin-based structures described as involved in cell-cell communication (37–39). Analysis of actin detection clearly showed that there was no co-localization of actin and DNA staining, excluding the possibility that the structures we observed were TNTs or cytonemes.

Confocal microscopy analysis of cultures using purified CD8+ T cells showed that they released DAPI+ LETs upon stimulation with anti-CD3/anti-CD28. LETs are mainly composed of DNA, but also contain cytoplasmic proteins, as evidenced by CFSE labeling, and as described for ETs from neutrophils and monocytes (10, 15, 53). Interestingly, SEM analysis of the stimulated purified cells showed that the morphology of CD8-derived LETs was dramatically distinct from the ones derived from CD4+ T cells. While CD8-derived LETs were composed of DNA filaments connecting two distant cells, CD4-derived LETs appeared as a "cloud" around the cells. In addition, the CD4+ T cells appeared to have a disintegrated membrane, suggesting cell death. While the overall cell death in cultures was low, the frequency of CD4+ T cells undergoing apoptosis in the stimulated cultures was higher than in non-stimulated ones. In addition, stimulated CD4 cultures produced high levels of TNF, which has been associated with cell death (54). Interestingly, recent work demonstrated that NETs can carry miRNA associated with the regulation of TNF function (55).

CD8+ T cell effector function is associated with cytolytic activity, which involves the delivery of granules containing cytotoxic molecules to the target cells (1). Cytotoxic granules contain cytolytic enzymes, and classically express lysosomal markers, such as LAMP-1 (CD107a) (1, 3, 56). The mechanisms of delivery of cytotoxic granules described to date demonstrate that this process involves cell-to-cell interaction (57). However, the morphological appearance of the CD8-derived LETs connecting one cell to another led us to hypothesize that these LETs could be involved in the delivery of cytotoxic granules to distant cells. To test this, we evaluated the expression of CD107a in cultures of CD8+ T cells stimulated with anti-CD3/anti-CD28, using confocal microscopy. Our data showed a clear co-localization of CD107a with the DAPI+ LETs released by CD8+ T cells. In addition, SEM also showed cells connected to CD8 LETs displaying morphology consistent with that of dying cells. This mechanism of death delivery has implications for CD8 mediated immunoregulation and immunopathology in highly activated inflammatory microenvironments. Not only could CD8+ T cells deliver death to a distant cell, but the release of LETs could trigger a stronger inflammatory cascade, similar to that seen by neutrophil released ETs (14, 58).

After demonstrating in vitro that CD8+ T cells can release LETs, we moved our approach to test if this phenomenon was associated with pathology in a human disease setting. ETs derived primarily from neutrophils have been associated with the pathogenesis of several autoimmune diseases, as well as cancer and diabetes-associated vasculopathy (59–61). In addition, NETs have been associated with leishmaniasis (14, 22). Thus, In order to also verify the relevance of CD8-derived LETs in a disease setting, we studies the occurrence of these structures in human tegumentary leishmaniasis (TL), given previous studies had shown that CD8+ T cell cytotoxicity was associated with tissue pathology in leishmaniasis caused by *L. braziliensis* infection (24–28). Thus, we evaluated if the progression and severity of lesions caused by *L. braziliensis* were associated with occurrence of CD8+ T cell derived LETs. We first performed a double staining using DAPI and anti-histone monoclonal antibodies in lesions from TL patients and observed that DAPI+ and anti-histone+ structures co-localized inside cells (nucleus), as well as outside in strands, suggesting the presence of ETs in lesions from patients infected with *L. braziliensis*. Histopathological analysis of the lesions did not show extensive necrosis as found by others (62), suggesting that extracellular DNA was not derived from necrosis. While previous study showed the presence of NETs in leishmaniasis lesions from individuals from Rio de Janeiro state, other studies had shown that lesions from patients infected with *L. braziliensis* from Corte de Pedra (the same endemic region we studied here) display low frequencies of neutrophils (26). This was confirmed by our data, showing that CD4+ and CD8+ T cells compose the great majority of cellular infiltrate present in the analyzed lesions. In addition, transcriptome studies from lesions of patients from Corte de Pedra showed a lack of neutrophil associated transcripts (43).

Our further analysis using anti-CD8, anti-CD107a and DAPI co-staining showed that the frequency of CD8+ T cells releasing LETs is clearly associated with the progression from the early to the late, ulcerated, phase of cutaneous leishmaniasis (CL), as well as with disease severity, since the lesions obtained from patients with the mutilating mucosal form (ML) also display more CD8-derived LETs. In addition, the percentage of CD8+ cells expressing the cytotoxic marker CD107a in etosis increased with the progression from early to late CL, as well as with the establishment of ML. Importantly, CD8+CD107+ cells releasing LETs were positively correlated with the intensity of the inflammatory infiltrate in late CL and in ML lesions, which shows a clear association of this process with progression and severity of local tissue pathology. The use of inflammatory infiltrate intensity as surrogate of pathology was chosen as it is not possible to measure the size lesions in early CL, as lesions are not yet ulcerated, and the measure of size of ML lesions is quite uncertain due to their location (mainly internal regions of nose and throat). These data emphasize the role of CD8 T cells in mediating tissue destruction in human leishmaniasis, suggesting that the release of LETs carrying cytotoxic vesicles by these cells may be one important mechanism by which CD8+ T cells induce tissue pathology. The use of molecules that inhibit the release of

ETs has been proposed as therapeutic alternatives in inflammatory diseases were ETs play a role (63). Thus, it is possible that CD8-derived LETs may also be a therapeutic target in human TL, bettering the lives of millions.

Whether CD8+ T cell derived LETs induce pathology by amplifying inflammation or directly by causing death of tissue cells cannot be responded based on the tissue analysis we performed. In fact, these activities may not exclude one another. Yet, another possible function of CD8+ T cell-derived LETs is the elimination of *Leishmania*-infected cells. In addition, other cell types present in the lesions may also be able to release LETs and contribute to tissue destruction and/or parasite control. Finally, comparing the role of LET-associated cytotoxicity versus other classic mechanisms of cytotoxicity will bring valuable information regarding disease pathology. These are important points that, while not the focus of the current work, are under investigation in our lab.

Our results suggest that the release of LETs by CD8+ T cells may present a novel mechanism of cell-cell communication, likely associated with the delivery of CD107a+ cytotoxic vesicles to distant cells. These findings bring new insights to the understanding of CD8-mediated cytotoxicity and have critical implications in physiologic and pathologic mechanisms where CD8-induced cell death plays a critical role such as in infections by intracellular pathogens and cancer.

DATA AVAILABILITY STATEMENT

All datasets presented in this study are included in the article/ **Supplementary Material**.

ETHICS STATEMENT

The studies involving human participants were reviewed and approved by COEP—Federal University of Bahia. The patients/ participants provided their written informed consent to participate in this study.

AUTHOR CONTRIBUTIONS

CK, AW, MV, LP, EN, TV, and EG performed the confocal, EM, FACS analysis. CK and AW also contributed to study design and analysis. PRLM and EC were responsible for care and material collection from leishmaniasis patients. DF performed the stainings and analysis of leishmania lesions. PMM overlooked all EM experiments and analysis. LA and RG contributed to the sorting experiments. GM contributed to study design and provided anti-histone antibodies. KG and WD designed the studies and overlooked all experiments and data analysis. All authors contributed to the article and approved the submitted version.

FUNDING

This work was supported by FAPEMIG (#Universal 2014), CNPq (#Universal 2015), INCT-DT. CK, EG, LP, LA, GM, RG, PRLM, EC, KG, and WD are CNPq fellows and EGAN was a FAPEMIG fellow.

ACKNOWLEDGMENTS

We would like to thank Dr Luciana Andrade for generous donation of phalloidin, Dr Leda Quercia Vieira and Leonardo Vaz for providing L-NAME, as well as Bioclin for providing the LDH-measuring kit.

SUPPLEMENTARY MATERIAL

The Supplementary Material for this article can be found online at: https://www.frontiersin.org/articles/10.3389/fimmu.2020.594581/full#supplementary-material

SUPPLEMENTARY FIGURE 1 | Anti-CD3/anti-CD28-stimulated cell cultures display low cell death. Cell death was assessed by annexin V and propidium iodide (Pi) staining using flow cytometry. Cultures treated with staurosporine were used as a positive control for apoptosis. **(A)** shows total cell death, **(B)** shows occurrence of early apoptosis and **(C)** shows frequency of necrosis. Data is presented as average per group ± standard error of the mean. The presence of the same letters in different bars represents statistically significant differences between them ($p < 0.05$). Bottom panels show representative FACS plots of annexinV and PI staining for each condition.

SUPPLEMENTARY FIGURE 2 | Lesions of patients with different forms of tegumentary leishmaniasis display extracellular DNA associated with tissue pathology. Frozen tissue sections were stained with DAPI, PE-labeled anti-CD8 and FITC-labeled anti-CD107a monoclonal antibodies as described in Materials and Methods. Inflammatory infiltrate, and frequency of CD8+ and CD8+CD107+ cells were determined as described in Material and Methods. **(A)** Inflammatory infiltrate in lesions of patients with the different clinical forms. Results are presented as boxplots with the median for all fields counted for each clinical form (Early-CL n=2, 27 fields; late-CL n=4, 43 fields; ML n=2, 28 fields). **(B)** Correlation analysis between the number of CD8+ cells and number of cells in the inflammatory infiltrate for each clinical form. **(C)** Correlation analysis between the number of CD8+CD107+ cells and number of cells in the inflammatory infiltrate for each clinical form.

SUPPLEMENTARY VIDEO 1 | Video showing 3D image of CD8+ T cells after stimulation with anti-CD3/anti-CD28. Purification of CD8 T lymphocytes was done by sorting, as described in Material and Methods. TCD8+ lymphocytes were stained with CFSE, plated on poly-L-lysine coverslips and stimulated with anti-CD3/ anti-CD28 for 24 h. After incubation the cells were stained with DAPI as described in the Materials and Methods and analyzed in a confocal microscope.

SUPPLEMENTARY VIDEO 2 | Extracellular DNA from CD8+ T cells induce death of neighboring cells. Purified CD8 T cells were cultured with CFSE-labeled targets (pink) at a ratio of 1:4. Cultures were stimulated with anti-CD3/ anti-CD28+ionomycin and stained with live-dead marker (EthD-1), as described in Materials and Methods. Images were obtained in 10-s intervals using excitation/emission captures of 495/515 nm for CFSE and 532/635 for EthD-1, on a Zeiss 5-live microscope. In (a), the movie shows the release of extracellular traps by a CD8+ T cell (light blue) and non-CD8 target cells stained in CFSE (pink) (arrow). Following, upon release of the LET, the pink cell dies after contact with the LET, becoming stained in light blue. In (b), the sequence

of static frames, highlighting the box with the occurrence of etosis and death of the cell previously stained in pink (described in figure 3). In (c), there is an image of a cell in light blue (cell 1, CD8+ T cell stained with EthD-1) and one in pink (cell 2, target stained with CFSE), followed by intensity fluorescence histograms for each cell. The light blue curve represents the staining with EthD-1 and the pink curve represents the staining with CFSE. (d) Shows an image after the death of the pink cell by LETs. In addition, the profiles and the fluorescence intensities of EthD-1 (light blue) for the LETs are shown in the box. The video was recorded at a rate of 30 frames per second and corresponds from 14 h 16 min to 14 h 30 min of culture.

REFERENCES

1. Peters PJ, Borst J, Oorschot V, Fukuda M, Krähenbühl O, Tschopp J, et al. Cytotoxic T lymphocyte granules are secretory lysosomes, containing both perforin and granzymes. *J Exp Med* (1991) 173:1099–109. doi: 10.1084/jem.173.5.1099
2. Gertner-Dardenne J, Poupot M, Gray B, Fournié JJ. Lipophilic fluorochrome trackers of membrane transfers between immune cells. *Immunol Invest* (2007) 36:665–85. doi: 10.1080/08820130701674646
3. Flesch IE, Hollett NA, Wong YC, Tscharke DC. Linear fidelity in quantification of anti-viral CD8+ T cells. *PloS One* (2012) 7(6):e39533. doi: 10.1371/journal.pone.0039533
4. de la Roche M, Asano Y, Griffiths GM. Origins of the cytolytic synapse. *Nat Rev Immunol* (2016) 16:421–32. doi: 10.1038/nri.2016.54
5. Martínez-Lostao L, Anel A, Pardo J. How do cytotoxic lymphocytes kill cancer cells? *Clin Cancer Res* (2015) 21:5047–56. doi: 10.1158/1078-0432.CCR-15-0685
6. Fadok VA, Voelker DR, Campbell PA, Cohen JJ, Bratton DL, Henson PM. Exposure of phosphatidylserine on the surface of apoptotic lymphocytes triggers specific recognition and removal by macrophages. *J Immunol* (1992) 148:2207–16.
7. Minko T, Kopecková P, Kopeček J. Preliminary evaluation of caspases-dependent apoptosis signaling pathways of free and HPMA copolymer-bound doxorubicin in human ovarian carcinoma cells. *J Control Release* (2001) 71:227–37. doi: 10.1016/S0168-3659(01)00220-6
8. Fadeel B, Orrenius S. Apoptosis: a basic biological phenomenon with wide-ranging implications in human disease. *J Intern Med* (2005) 258:479–517. doi: 10.1111/j.1365-2796.2005.01570.x
9. Majno G, La Gattuta M, Thompson TE. Cellular death and necrosis: chemical, physical and morphologic changes in rat liver. *Virchows Arch Pathol Anat Physiol Klin Med* (1960) 333:421–65. doi: 10.1007/BF00955327
10. Brinkmann V, Reichard U, Goosmann C, Fauler B, Uhlemann Y, Weiss DS, et al. Neutrophil extracellular traps kill bacteria. *Science* (2004) 303:1532–5. doi: 10.1126/science.1092385
11. Fuchs TA, Abed U, Goosmann C, Hurwitz R, Schulze I, Wahn V, et al. Novel cell death program leads to neutrophil extracellular traps. *J Cell Biol* (2007) 176:231–41. doi: 10.1083/jcb.200606027
12. Urban CF, Ermert D, Schmid M, Abu-Abed U, Goosmann C, Nacken W, et al. Neutrophil extracellular traps contain calprotectin, a cytosolic protein complex involved in host defense against *Candida albicans*. *PloS Pathog* (2009) 5:e1000639. doi: 10.1371/journal.ppat.1000639
13. Yousefi S, Gold JA, Andina N, Lee JJ, Kelly AM, Kozlowski E, et al. Catapult-like release of mitochondrial DNA by eosinophils contributes to antibacterial defense. *Nat Med* (2008) 14:949–53. doi: 10.1038/nm.1855
14. Guimarães-Costa AB, Nascimento MT, Froment GS, Soares RP, Morgado FN, Conceição-Silva F, et al. *Leishmania amazonensis* promastigotes induce and are killed by neutrophil extracellular traps. *Proc Natl Acad Sci USA* (2009) 106:6748–53. doi: 10.1073/pnas.0900226106
15. Chow OA, von Köckritz-Blickwede M, Bright AT, Hensler ME, Zinkernagel AS, Cogen AL, et al. Statins enhance formation of phagocyte extracellular traps. *Cell Host Microbe* (2010) 8:445–54. doi: 10.1016/j.chom.2010.10.005
16. Rocha Arrieta YC, Rojas M, Vasquez G, Lopez J. The Lymphocytes Stimulation Induced DNA Release, a Phenomenon Similar to NETosis. *Scand J Immunol* (2017) 86:229–38. doi: 10.1111/sji.12592
17. Muniz VS, Silva JC, Braga YA, Melo RC, Ueki S, Takeda M, et al. Eosinophils release extracellular DNA traps in response to *Aspergillus fumigatus*. *J Allergy Clin Immunol* (2018) 141:571–85.e7. doi: 10.1016/j.jaci.2017.07.048
18. Urban C, Zychlinsky A. Netting bacteria in sepsis. *Nat Med* (2007) 13:403–4. doi: 10.1038/nm0407-403
19. Bartneck M, Keul HA, Zwadlo-Klarwasser G, Groll J. Phagocytosis independent extracellular nanoparticle clearance by human immune cells. *Nano Lett* (2010) 10:59–63. doi: 10.1021/nl902830x
20. Guimarães-Costa AB, Nascimento MT, Wardini AB, Pinto-da-Silva LH, Saraiva EM. ETosis: A Microbicidal Mechanism beyond Cell Death. *J Parasitol Res* (2012) 2012:929743. doi: 10.1155/2012/929743
21. DeSouza-Vieira T, Guimarães-Costa A, Rochael NC, Lira MN, Nascimento MT, Lima-Gomez PS, et al. Neutrophil extracellular traps release induced by Leishmania: role of PI3Kγ, ERK, PI3Kσ, PKC, and [Ca2+] [Ca2+]. *J Leukoc Biol* (2016) 100:801–10. doi: 10.1189/jlb.4A0615-261RR
22. Morgado FN, Nascimento MT, Saraiva EM, Oliveira-Ribeiro CD, Madeira MDF, Costa-Santos MD, et al. Are Neutrophil Extracellular Traps Playing a Role in the Parasite Control in Active American Tegumentary Leishmaniasis Lesions? *PloS One* (2015) 10:e0133063. doi: 10.1371/journal.pone.0133063
23. Papayannopoulos V. Neutrophil extracellular traps in immunity and disease. *Nat Rev Immunol* (2018) 18:134–47. doi: 10.1038/nri.2017.105
24. Faria DR, Gollob KJ, Barbosa JJr, Schriefer A, Machado PR, Lessa H, et al. Decreased in situ expression of interleukin-10 receptor is correlated with the exacerbated inflammatory and cytotoxic responses observed in mucosal leishmaniasis. *Infect Immun* (2005) 73:7853–9. doi: 10.1128/IAI.73.12.7853-7859.2005
25. Campos TM, Costa R, Passos S, Carvalho LP. Cytotoxic activity in cutaneous leishmaniasis. *Mem Inst Oswaldo Cruz* (2017) 112:733–40. doi: 10.1590/0074-02760170109
26. Faria DR, Souza PE, Durães FV, Carvalho EM, Gollob KJ, Machado PR, et al. Recruitment of CD8(+) T cells expressing granzyme A is associated with lesion progression in human cutaneous leishmaniasis. *Parasite Immunol* (2009) 31:432–9. doi: 10.1111/j.1365-3024.2009.01125.x
27. Cardoso TM, Machado Á, Costa DL, Carvalho LP, Queiroz A, Machado P, et al. Protective and pathological functions of CD8+ T cells in *Leishmania braziliensis* infection. *Infect Immun* (2015) 83:898–906. doi: 10.1128/IAI.02404-14
28. Novais FO, Wong AC, Villareal DO, Beiting DP, Scott P. CD8 $^{+}$ T cells lack local signals to produce IFN-γ in the skin during Leishmania infection. *J Immunol* (2018) 200:1737–45. doi: 10.4049/jimmunol.1701597
29. Ingelsson B, Söderberg D, Strid T, Söderberg A, Bergh AC, Loitto V, et al. Lymphocytes eject interferogenic mitochondrial DNA webs in response to CpG and non-CpG oligodeoxynucleotides of class C. *Proc Natl Acad Sci USA* (2018) 115:E478–87. doi: 10.1073/pnas.1711950115
30. Costanza M, Poliani PL, Portararo P, Cappetti B, Musio S, Pagani F, et al. DNA threads released by activated CD4^{+} T lymphocytes provide autocrine costimulation. *Proc Natl Acad Sci USA* (2019) 116:8985–94. doi: 10.1073/pnas.1822013116
31. Machado P, Araújo C, Da Silva AT, Almeida RP, D'Oliveira AJr, Bittencourt A, et al. Failure of early treatment of cutaneous leishmaniasis in preventing the development of an ulcer. *Clin Infect Dis* (2002) 34:E69–73. doi: 10.1086/340526
32. Souza PE, Rocha MO, Rocha-Vieira E, Menezes CA, Chaves AC, Gollob KJ, et al. Monocytes from patients with indeterminate and cardiac forms of Chagas' disease display distinct phenotypic and functional characteristics associated with morbidity. *Infect Immun* (2004) 72:5283–91. doi: 10.1128/IAI.72.9.5283-5291.2004
33. Figueiredo MM, Costa PA, Diniz SQ, Henriques PM, Kano FS, Tada MS, et al. T follicular helper cells regulate the activation of B lymphocytes and antibody production during *Plasmodium vivax* infection. *PloS Pathog* (2017) 13: e1006484. doi: 10.1371/journal.ppat.1006484
34. Azuma M, Ito D, Yagita H, Okumura K, Phillips JH, Lanier LL, et al. B70 antigen is a second ligand for CTLA-4 and CD28. *Nature* (1993) 366:76–9. doi: 10.1038/366076a0
35. Bour-Jordan H, Bluestone JA. Regulating the regulators: costimulatory signals control the homeostasis and function of regulatory T cells. *Immunol Rev* (2009) 229:41–66. doi: 10.1111/j.1600-065X.2009.00775.x
36. Chan FK, Moriwaki K, De Rosa MJ. Detection of necrosis by release of lactate dehydrogenase activity. *Methods Mol Biol* (2013) 979:65–70. doi: 10.1007/978-1-62703-290-2_7

37. Rustom A, Saffrich R, Markovic I, Walther P, Gerdes HH. Nanotubular highways for intercellular organelle transport. *Science* (2004) 303:1007–10. doi: 10.1126/science.1093133
38. Onfelt B, Nedvetzki S, Benninger RK, Purbhoo MA, Sowinski S, Hume AN, et al. Structurally distinct membrane nanotubes between human macrophages support long-distance vesicular traffic or surfing of bacteria. *J Immunol* (2006) 177:8476–83. doi: 10.4049/jimmunol.177.12.8476
39. Stanganello E, Scholpp S. Role of cytonemes in Wnt transport. *J Cell Sci* (2016) 129:665–72. doi: 10.1242/jcs.182469
40. Brinkmann V, Zychlinsky A. Neutrophil extracellular traps: is immunity the second function of chromatin? *J Cell Biol* (2012) 198:773 783. doi: 10.1083/jcb.201203170
41. Muraro SP, De Souza GF, Gallo SW, Da Silva BK, De Oliveira SD, Vinolo MA, et al. Respiratory Syncytial Virus induces the classical ROS-dependent NETosis through PAD-4 and necroptosis pathways activation. *Sci Rep* (2018) 8:14166. doi: 10.1038/s41598-018-32576-y
42. Mondal S, Thompson PR. Protein Arginine Deiminases (PADs): biochemistry and chemical biology of protein citrullination. *Acc Chem Res* (2019) 52:818–32. doi: 10.1021/acs.accounts.9b00024
43. Novais FO, Carvalho LP, Passos S, Roos DS, Carvalho EM, Scott P, et al. Genomic profiling of human *Leishmania braziliensis* lesions identifies transcriptional modules associated with cutaneous immunopathology. *J Invest Dermatol* (2015) 135:94–101. doi: 10.1038/jid.2014.305
44. Christensen SM, Dillon LA, Carvalho LP, Passos S, Novais FO, Hughitt VK, et al. Meta-transcriptome profiling of the human-*Leishmania braziliensis* cutaneous lesion. *PloS Negl Trop Dis* (2016) 10(9):e0004992. doi: 10.1371/journal.pntd.0004992
45. von Köckritz-Blickwede M, Goldmann O, Thulin P, Heinemann K, Norrby-Teglund A, Rohde M, et al. Phagocytosis-independent antimicrobial activity of mast cells by means of extracellular trap formation. *Blood* (2008) 111:3070–80. doi: 10.1182/blood-2007-07-104018
46. Hoppenbrouwers T, Autar AS, Sultan AR, Abraham TE, van Cappellen WA, Houtsmuller AB, et al. In vitro induction of NETosis: comprehensive live imaging comparison and systematic review. *PloS One* (2017) 12:e0176472. doi: 10.1371/journal.pone.0176472
47. Jorgensen I, Rayamajhi M, Miao EA. Programmed cell death as a defence against infection. *Nat Rev Immunol* (2017) 17:151–64. doi: 10.1038/nri.2016.147
48. Schorn C, Janko C, Krenn V, Zhao Y, Munoz LE, Schett G, et al. Bonding the foe - NETting neutrophils immobilize the pro-inflammatory monosodium urate crystals. *Front Immunol* (2012) 3:376. doi: 10.3389/fimmu.2012.00376
49. Koyama R, Arai T, Kijima M, Sato S, Miura S, Yuasa M, et al. DNase γ, DNase I and caspase-activated DNase cooperate to degrade dead cells. *Genes Cells* (2016) 21:1150–63. doi: 10.1111/gtc.12433
50. Muñoz LE, Boeltz S, Bilyy R, Schauer C, Mahajan A, Widulin N, et al. Neutrophil Extracellular Traps Initiate Gallstone Formation. *Immunity* (2019) 51:443–50.e4. doi: 10.1016/j.immuni.2019.07.002
51. Padanilam BJ. Cell death induced by acute renal injury: a perspective on the contributions of apoptosis and necrosis. *Am J Physiol Renal Physiol* (2003) 284:F608–27. doi: 10.1152/ajprenal.00284.2002
52. Zhang C, Xu Y, Gu J, Schlossman SF. A cell surface receptor defined by a mAb mediates a unique type of cell death similar to oncosis. *Proc Natl Acad Sci USA* (1998) 95:6290–5. doi: 10.1073/pnas.95.11.6290
53. Doster RS, Rogers LM, Gaddy JA, Aronoff DM. Macrophage Extracellular Traps: A Scoping Review. *J Innate Immun* (2018) 10:3–13. doi: 10.1159/000480373
54. Kim JJ, Lee SB, Park JK, Yoo YD. TNF-α-induced ROS production triggering apoptosis is directly linked to Romo1 and Bcl-X(L). *Cell Death Differ* (2010) 17:1420–34. doi: 10.1038/cdd.2010.19
55. Linhares-Lacerda L, Temerozo JR, Ribeiro-Alves M, Azevedo EP, Mojoli A, Nascimento MTC, et al. Neutrophil extracellular trap-enriched supernatants carry microRNAs able to modulate TNF-α production by macrophages. *Sci Rep* (2020) 10:2715. doi: 10.1038/s41598-020-59486-2
56. Giraldo NA, Bolaños NI, Cuellar A, Guzman F, Uribe AM, Bedoya A, et al. Increased CD4+/CD8+ double-positive T cells in chronic Chagasic patients. *PloS Negl Trop Dis* (2011) 5:e1294. doi: 10.1371/journal.pntd.0001294
57. Anikeeva N, Sykulev Y. Mechanisms controlling granule-mediated cytolytic activity of cytotoxic T lymphocytes. *Immunol Res* (2011) 51:183–94. doi: 10.1007/s12026-011-8252-8
58. de Buhr N, Bonilla MC, Jimenez-Soto M, von Köckritz-Blickwede M, Dolz G. Extracellular trap formation in response to *Trypanosoma cruzi* infection in granulocytes isolated from dogs and common opossums, natural reservoir hosts. *Front Microbiol* (2018) 9:966. doi: 10.3389/fmicb.2018.00966
59. Romero V, Fert-Bober J, Nigrovic PA, Darrah E, Haque UJ, Lee DM, et al. Immune-mediated pore-forming pathways induce cellular hypercitrullination and generate citrullinated autoantigens in rheumatoid arthritis. *Sci Transl Med* (2013) 5:209–150. doi: 10.1126/scitranslmed.3006869
60. Berezin A. Neutrophil extracellular traps: the core player in vascular complications of diabetes mellitus. *Diabetes Metab Syndr* (2019) 13:3017–23. doi: 10.1016/j.dsx.2018.07.010
61. Kim TY, Gu JY, Jung HS, Koh Y, Kim I, Kim HK. Elevated extracellular trap formation and contact system activation in acute leukemia. *J Thromb Thrombol* (2018) 46:379–85. doi: 10.1007/s11239-018-1713-3
62. Saldanha MG, Queiroz A, Machado PR, de Carvalho LP, Scott P, de Carvalho Filho EM, et al. Characterization of the histopathologic features in patients in the early and late phases of cutaneous leishmaniasis. *Am J Trop Med Hyg* (2017) 96:645–52. doi: 10.4269/ajtmh.16-0539
63. Okubo K, Kamiya M, Urano Y, Nishi H, Herter JM, Mayadas T, et al. Lactoferrin Suppresses Neutrophil Extracellular Traps Release in Inflammation. *EBioMedicine* (2016) 10:204–15. doi: 10.1016/j.ebiom.2016.07.012

Conflict of Interest: The authors declare that the research was conducted in the absence of any commercial or financial relationships that could be construed as a potential conflict of interest.

frontiers in Immunology

REVIEW
published: 06 November 2020
doi: 10.3389/fimmu.2020.593901

Skin Viral Infections: Host Antiviral Innate Immunity and Viral Immune Evasion

Vivian Lei[1,2], *Amy J. Petty*[2], *Amber R. Atwater*[1], *Sarah A. Wolfe*[1] *and Amanda S. MacLeod*[1,3,4,5*]

[1] Department of Dermatology, Duke University, Durham, NC, United States, [2] School of Medicine, Duke University, Durham, NC, United States, [3] Department of Immunology, Duke University, Durham, NC, United States, [4] Pinnell Center for Investigative Dermatology, Duke University, Durham, NC, United States, [5] Department of Molecular Genetics and Microbiology, Duke University, Durham, NC, United States

The skin is an active immune organ that functions as the first and largest site of defense to the outside environment. Serving as the primary interface between host and pathogen, the skin's early immune responses to viral invaders often determine the course and severity of infection. We review the current literature pertaining to the mechanisms of cutaneous viral invasion for classical skin-tropic, oncogenic, and vector-borne skin viruses. We discuss the skin's evolved mechanisms for innate immune viral defense against these invading pathogens, as well as unique strategies utilized by the viruses to escape immune detection. We additionally explore the roles that demographic and environmental factors, such as age, biological sex, and the cutaneous microbiome, play in altering the host immune response to viral threats.

Keywords: cutaneous innate immunity, skin viruses, antiviral proteins, skin antiviral response, cutaneous microbiome, skin aging

OPEN ACCESS

Edited by:
Fabienne Tacchini-Cottier, University of Lausanne, Switzerland

Reviewed by:
Irah L. King, McGill University, Canada
Walderez Ornelas Dutra, Federal University of Minas Gerais, Brazil

****Correspondence:***
Amanda S. MacLeod
amanda.macleod@duke.edu

Specialty section:
This article was submitted to Microbial Immunology, a section of the journal Frontiers in Immunology

Received: *11 August 2020*
Accepted: *06 October 2020*
Published: *06 November 2020*

Citation:
Lei V, Petty AJ, Atwater AR, Wolfe SA and MacLeod AS (2020) Skin Viral Infections: Host Antiviral Innate Immunity and Viral Immune Evasion. Front. Immunol. 11:593901. doi: 10.3389/fimmu.2020.593901

INTRODUCTION

The skin is a dynamic barrier organ that establishes a clear boundary between the host and the outside world. As an immune organ, the skin actively surveils the surrounding environment and establishes an appropriate barrier and immune response to commensal microbiota including bacteria, fungi, and viruses. However, upon disruption of the skin barrier, the skin must orchestrate complex immune signals to protect against infiltration and attack by pathogenic invaders. Importantly, responses by the cutaneous innate immune system and its effectors play essential roles in early destruction of pathogens as well as establishment of an immune barrier to prevent systemic infection. This is accomplished *via* phagocytic cells (*i.e.* macrophages, neutrophils, and dendritic cells), leukocytes (*i.e.* natural killer (NK) cells, mast cells, basophils, and eosinophils), as well as epidermal keratinocytes. The introduction of pathogens activates these innate immune cells' pathogen recognition receptors (PRRs), including toll-like receptors (TLRs), nucleotide-binding oligomerization domain (NOD)-like receptors, retinoic acid-inducible gene 1 (RIG-I)-like helicase receptors, and c-type lectin receptors. PRRs recognize different pathogen-associated molecular patterns (PAMPs) on microbes and damage-associated molecular patterns (DAMPs) that arise from damaged host cells, which subsequently leads to the induction of pro-inflammatory

cytokines, such as tumor necrosis factor (TNF)-α and interferon (IFN)-γ, as well as chemokines that recruit phagocytic cells. Keratinocytes and infiltrating immune cells further the hostile environment to pathogens by generating peptides and proteins with distinct antibacterial, antifungal, antiviral capabilities (1).

Cutaneous viral infection presents a unique challenge to the skin's immune system, as viruses have the ability to hijack host machinery to advance viral replication. As such, early abrogation of viral pathogenicity by the innate immune response establishes a protective antiviral state and limits the potential for systemic spread. Here, we provide an overview of viral entry mechanisms by various viruses with differing infection propensities, *i.e.* classically skin-tropic and oncogenic skin viruses, as well as vector-introduced skin viruses. We review how these viruses uniquely interact with different aspects of the cutaneous innate immune system, and we further explore some evolved viral mechanisms that directly interfere with the host innate immune response. Lastly, we provide insights on how demographic and environmental factors, such as host age, biological sex, and the commensal microbiome, contribute to various aspects of innate antiviral immunity in the skin (**Figure 1**, **Table 1**).

CLASSICAL SKIN-TROPIC VIRUSES

Herpes Simplex Virus (HSV)

Herpes simplex virus (HSV) type-1 and 2, of the *Herpesviridae* family, are enveloped double-stranded DNA viruses that are notable for their neurotropism to the dorsal root ganglia and trigeminal ganglia after primary infection at a mucocutaneous site (2). Primary and reactivated infections are marked by tender grouped erythematous vesicles with varying presentations and degrees of severity (3). HSV-1 is typically characterized by oro-facial lesions with primary infection most often occurring in childhood, whereas HSV-2 is traditionally known as a sexually transmitted infection producing genital lesions, although both types can be found at either site (4). In immunocompromised and neonatal patients, HSV has the potential to disseminate and cause severe morbidity and mortality (3).

In both primary and reactivated infections, viral entry and replication largely occur in the epidermis, where keratinocytes are the predominant cell type. Host cell entry is coordinated by seven HSV glycoproteins; however, four glycoproteins (gB, gD, gH, and gL) are necessary and sufficient for complete viral fusion (5). Viral entry steps start with initial attachment to heparan sulfate proteoglycans (HSPGs) on keratinocytes *via* gB and gC. Subsequent fusion of the viral envelope with the plasma membrane is mediated by gB and heterodimer gH/gL (6, 7). Envelope glycoprotein gD additionally interacts with cell surface receptors nectin-1, nectin-2, and herpesvirus entry mediator (HVEM) to aid in viral envelope fusion with the plasma membrane (8, 9). After fusion, HSV viral spread relies on the trans-Golgi network for delivery of viral glycoproteins and particles with resultant infection of nearby cells *via* cell–cell junctions (10, 11).

At the cell surface, Toll-like receptor (TLR) 2 senses viral gB and gH/gL and activates the nuclear factor κB (NF-κB) pathway to induce expression of pro-inflammatory cytokines (*e.g.* tumor necrosis factor (TNF)-α, interleukin (IL)-6 and IL-12) and chemokines (*e.g.* CC chemokine ligand 2 (CCL2)) (12–15).

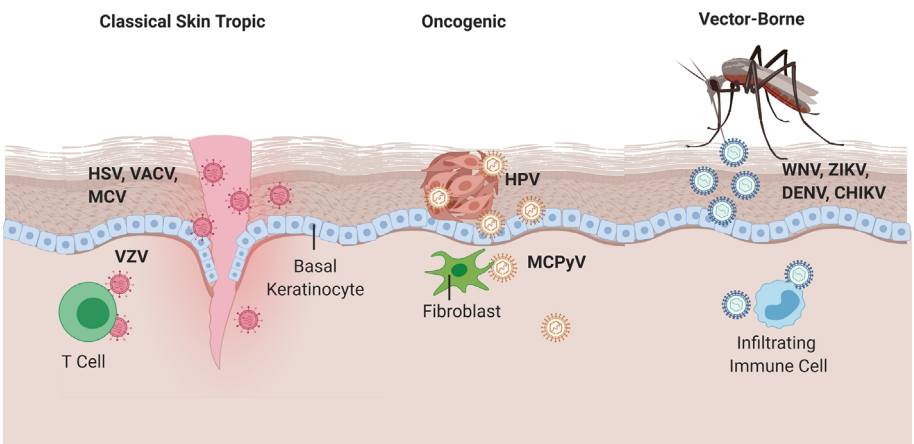

FIGURE 1 | Viral entry of classical skin tropic, oncogenic, and vector-borne viruses. Classical skin tropic viruses such as herpes simplex virus (HSV), vaccinia virus (VACV), molluscum contagiosum virus (MCV), and varicella zoster virus (VZV) have tropism to skin epidermis where keratinocytes are the predominant cell type. HSV and MCV can enter the skin *via* defects in the skin barrier, which provide viruses with direct contact to the basal epidermal layers. VACV is introduced iatrogenically *via* vaccination needles. VZV inoculation occurs in the respiratory epithelia and hematogenously spreads to epidermis *via* infected T cells. Oncogenic viruses such as human papillomaviruses (HPV) and merkel cell polyomavirus (MCPyV) commonly take on their neoplastic potential in immunocompromised patients where the barrier to overcome immune defenses are significantly lower. HPV enters *via* micro-lesions and replicates in keratinocytes, whereas MCPyV has proclivities toward replication in dermal fibroblasts and $CD4^+$ T cells, respectively. West Nile, Zika, Dengue, and Chikungunya viruses are introduced into the skin *via* mosquito vectors and cause a local inflammatory response that homes immune cells to the skin infection site, which allows for subsequent infection of migratory immune cells and potential for systemic spread.

TABLE 1 | Summary of cutaneous viruses, their cell tropism, their innate immune sensors and evasion targets, and populations vulnerable to viral infection.

Virus	Cell Tropism	Innate Immune Sensors	Immune Evasion Targets	Vulnerable Populations
Classical Skin-Tropic Viruses				
Herpes Simplex Virus (HSV)	Epidermal keratinocytes	• Toll-like Receptors (TLR): TLR2, TLR3, TLR9 • NOD-like receptors • Melanoma differentiation-associated gene 5 (MDA5) • Interferon-inducible protein 16 (IFI16) • Helicases: Ku70, DHX9, DHX36, DDX60	• Macrophage receptor with collagenous structure (MARCO) • Cyclic guanosin monophosphate synthase (cGAS)/Stimulator of interferon genes (STING)-mediated interferon production • Absent in melanoma 2 (AIM2)	• Neonatal • Immunocompromised • Males – HSV-1 • Females – HSV-2
Vaccinia Virus (VACV)	Dendritic cells, macrophages, monocytes	Not yet identified	Not yet identified	Patients with history of atopic dermatitis
Molluscum Contagiosum Virus (MCV)	Epidermal keratinocytes	• TLR3, TLR9	Dermal immune cells	Children
Varicella Zoster Virus (VZV)	Primary infection at upper respiratory epithelium, hematologic transport to skin keratinocytes *via* infected T cells	• TLR9 • cGAS	Not yet identified	• Children • Elderly (Herpes Zoster) • Immunocompromised • Males
Oncogenic Viruses				
Human Papillomavirus (HPV)	Basal keratinocytes	• TLR3, TLR7, TLR8, TLR9 • AIM2 • Interferon-gamma inducible protein 16 (IFI16)	• Interferon regulatory transcription factors: IRF1, IRF3 • C-C motif chemokine ligand 20 (CCL20)	• Immunocompromised
Merkel Cell Polyomavirus (MCPyV)	Keratinocytes, dermal fibroblasts	TLR9	• Nuclear factor-γB • Major histocompatibility complex class I (MHC-I)	• Immunocompromised • Females
Vector-borne Viruses				
Flaviviruses – Zika (ZIKV), West Nile (WNV),	• Dendritic cells – ZIKV, DENV	• TLR3	• Pathogen recognition receptors – WNV	• Females – DENV
Dengue (DENV)	• Keratinocytes – WNV	• MDA5	• Nuclear factor-κB – ZIKV	• Elderly – WNV
Chikungunya Virus (CHIKV)	Dermal fibroblasts	• Retinoic acid-inducible gene I (RIG-I)		

Once within the cell, HSV nucleic acids activate TLR3 and TLR9 in the endosomes, while a slew of PRRs (*i.e.* NOD-like receptors, melanoma differentiation-associated gene 5 (MDA5), interferon-inducible protein 16 (IFI16), and several helicases (Ku70, DHX9, DHX36, DDX60)) sense HSV DNA and RNA in the cytoplasm (16). Together, PRR activation confers type I and III interferon signaling in both human keratinocytes and infiltrating monocyte-lineage cells (17–21). Several induced interferon stimulated gene (ISG) products, such as myxovirus (Mx) A and double-stranded RNA-activated protein kinase (PKR), have direct antiviral properties against HSV, such as limiting viral replication and initiating autophagy to limit cell–cell spread (22). The importance of these many facets of the innate immune antiviral response are highlighted in observations that patients with tyrosine kinase 2 (TYK2) deficiency, who have impaired type I IFN, IL-6, and IL-12 responses, have increased frequency of recurrent HSV infections (23).

Additional innate host defense regulators acting prior to the canonical IFN signaling pathways have also been discovered to play roles in the battle against HSV. For example, promyelocytic leukemia nuclear bodies associate with histone chaperones to capture viral DNA and block HSV replication (24, 25). Keratinocytes were also found to release IL-1α and IL-36 to bolster the antiviral state by acting as early alarm signals for leukocyte recruitment and increasing cellular sensitivity to type I IFN signaling, respectively (26, 27).

Recent discoveries have also identified novel potential roles of NK cells to contribute directly to innate protection against HSV infection. A 2003 study in mice identified that NK cells provided a critical source of early IFNs to control HSV-2 infection and that mice deficient in NK cells had enhanced susceptibility to HSV (28). Corroborating these observations is a case report in 2004 of two individuals with NK cell deficiency who were observed to have severe disseminated HSV-2 infection (29). Absence of NK cells resulted in a diminished $CD4^+$ and $CD8^+$ T cell responses, and the presence of NK cells alone were identified to be able to rescue dysmorphic $CD8^+$ T cells to mount an effective $CD8^+$ T cell response even in the absence of $CD4^+$ T helper cells (30). These findings propose a potential role of NK cells to mediate and bridge innate and adaptive immune responses. Further investigations can be conducted to elucidate the specific mechanisms utilized by NK cells to enhance T cell responses and determine whether NK cells exposed to HSV confer a 'memory' response to more readily bolster both innate and adaptive immune functions upon HSV reactivation. These discoveries may present NK cells as attractive targets to enhance both arms of the immune response against HSV infection. The role of innate lymphoid cells (ILCs) has been additionally studied in the context of HSV infection, though *in vivo* mouse studies showed that ILC-deficiency showed no difference in survival or disease severity (31).

Despite the many innate immune players against HSV, the virus has evolved mechanisms to usurp host machinery and enhance infectivity. For example, HSV was discovered to use scavenger receptors to increase affinity of surface protein interactions (32), inhibit intracellular viral DNA sensing (33, 34), dampen pro-inflammatory cytokine production and inflammasome formation (35), and directly abrogate type I IFN signaling (36). These mechanisms have rendered HSV to be one of the most successful viruses capable of infecting other cell types, including fibroblasts, lymphocytes, and leukocytes (8). Unsurprisingly, HSV's ability to counteract multiple facets of the early, innate cutaneous immune response helps to explain its capacity to successfully infect beyond the initial infection site and cause latent disease. Given the plethora of studies of viral mechanisms and viral targets for immune evasion, HSV is primed as a viable target to study ways to strengthen innate antiviral immune responses, both IFN-dependent and IFN-independent, to provide different avenues of attenuating disease severity.

Vaccinia Virus

Vaccinia viruses are large, enveloped double-stranded DNA viruses of the *Poxviridae* family. Due to highly conserved structural proteins across orthopoxviruses, VACV is often used to immunize against smallpox caused by variola virus (37). All human orthopoxvirus infections are zoonoses and typically present as localized or disseminated papules, vesicles, or scabs that may be accompanied by fever, lymphadenopathy, malaise, and myalgia (38).

VACV replication preferentially occurs in cutaneous sites with compromised barrier function (39), where there is increased access to the basolateral membrane (40). Viral entry begins with attachment of four viral proteins (A26, A27, D8 and H3) of the mature virion to cell surface glycosaminoglycans (GAGs), extracellular matrix proteins, and, at lipid rafts, integrin membrane receptors (41, 42). Following attachment is an intricate synchrony of twelve entry proteins that compose the fusion complex, which introduces viral DNA into the cell (reviewed in 43).

Infection with VACV is uncommon when exposure occurs in a healthy cutaneous environment where innate immune responses effectively suppress viral pathogenicity. In fact, a study by Rice and colleagues showed that enhancement of early pro-inflammatory signals using a scarification model of viral delivery significantly decreased lethality of VACV. The group proposed that scarification allowed keratinocytes to actively produce an antiviral state through secretion of chemokines and cytokines (44). These findings are corroborated by discoveries that TNF-receptor knockout and IL-1 receptor type 1 knockout mice had larger cutaneous lesions and higher viral copies compared to their wild type counterparts (45, 46). *In vitro*, VACV viral infection of epidermal Langerhans cells (LC) and plasmacytoid dendritic cells (pDCs) resulted in inhibition of their ability to elicit cytokine production, including IFN-α and IFN-γ (47, 48). Activated NK cells also secrete necessary IFN-γ to attenuate early infection and promote VACV clearance (49–51). Together, these findings suggest a key role in early innate immune signaling in preventing viral lethality; these signals are essential for VACV vaccine efficacy.

Though typically regarded as safe, VACV vaccination has the potential to cause eczema vaccinatum or progressive vaccinia,

both severe and potentially lethal complications (52, 53). Occurring mostly in individuals with a history of atopic dermatitis (AD), a disease that is distinguished by barrier defects resulting from disrupted terminal epidermal differentiation, disseminated VACV includes a generalized vesiculopustular eruption that can progress to large non-healing lesions and predispose individuals to sepsis (54, 55). Viral progression is theorized to be due to reduced capability of AD skin's innate immune mechanisms to subvert viral attack. With VACV's preferential infection of dendritic cells, macrophages, and monocytes (56), infection of epidermal antigen-presenting LCs at the early stage impairs release of pro-inflammatory cytokines and IFNs (48). Next, attempts to limit viral spread *via* programmed cell death are offset by AD skin's hyper-proliferative state, which presents the virus with many new targets (57). Moreover, the skew towards Th2 responses in AD, with increased IL-4 and IL-13 expression in particular, further decreases antiviral cytokines and type I and II IFNs (58, 59). Consequently, this results in reduced expression of antimicrobial proteins such as human β-defensin (hBD) 3 and human cathelicidin LL-37, which have been shown to directly deter VACV pathogenicity (60, 61). Together, the compromised immune landscape in AD skin provides fertile ground for VACV spread. Given the strong association between VACV (and also HSV) dissemination and AD, future studies are warranted regarding how alterations in terminal epidermal differentiation affect innate antiviral immune signatures at homeostasis as well as upon viral challenge.

Molluscum Contagiosum Virus

Molluscum contagiosum virus, an enveloped linear double-stranded DNA virus of the *Poxviridae* family, is introduced *via* direct contact with infected skin or fomites (62). Although MCV infection is common, specific studies on viral entry mechanisms have been limited due to lack of working *in vivo* and *in vitro* models. Early electron microscopy of MCV showed preferential infection of keratinocytes in the basal layers at the outset of primary infection (63, 64). Similar to other viruses with tropism to the basal layer, micro-abrasions in the skin provide MCV a direct pathway of entry, and it has been well documented that individuals with skin barrier defects have increased susceptibility (65, 66). Viral proliferation then continues in mitotically active keratinocytes and expands apically, giving rise to distinct dome-shaped papules called molluscum bodies. Viral dissemination occurs as viral particles exit *via* a keratinized tunnel at the umbilicated center of the lesion (67).

MCV is notable for its ability to evade immune detection as it replicates within epidermal keratinocytes; it forms enclosed molluscum bodies that effectively evade dermal immune detection (68, 69). Interestingly, reports that physical manipulation of molluscum bodies results in local inflammation and ultimate resolution of the infection posit the notion of viral clearance by nearby dermal immune cells (70, 71). Although studies of specific innate immune responses to MCV are limited, one study suggests that MCV activates TLR3 and TLR9 in epidermal keratinocytes. They additionally observed upregulation of IFN-β and TNF-α in the environment surrounding molluscum bodies (72). Work by Vermi et al. further identified plasmacytoid and type I IFN-induced dendritic cells as key effectors in spontaneous regression of MCV in the aforementioned inflammatory setting (73). While MCV's preference toward epidermal replication allows it to escape dermal immune detection, it remains unclear whether and how epidermal Langerhans cells contribute to immune responses to MCV infection and whether MCV has evolved mechanisms to silence LC contributions to immune surveillance.

Varicella Zoster Virus

Varicella zoster virus is another neurotropic enveloped, double-stranded DNA virus of the *Herpesviridae* family with primary infection consisting of a generalized pruritic vesicular eruption along with fever, headache and malaise (74). Unlike the previously discussed skin-tropic viruses, infection of epidermal keratinocytes is introduced *via* hematologic transport of infected T cells after primary inoculation in the upper respiratory epithelium (75, 76). VZV utilizes gB and heterodimer gH/gL, conserved fusion machinery of herpesviruses, for attachment and entry into keratinocytes. Within the skin, cell–cell fusion generates multinucleated infected cells that reside within the vesicular skin lesions. Studies show that VZV fusion protein gB possesses components on both its ecto- and cytoplasmic domains that are essential for infectivity: gB drives VZV's replication, cell–cell fusion, and characteristic syncytial formation (77, 78). However, additional studies suggest that VZV virulence requires careful regulation of gB, as gain-of-function mutations in gB have been shown to limit viral spread in human skin (79).

Given the poor outcomes in VZV-infected individuals with adaptive immune deficiencies, early establishment of an antiviral state in the skin is vital. These responses work effectively to limit disease severity and activate cell-mediated immunity. Cytosolic sensing activates stimulator of interferon genes (STING)-mediated IFN-γ production to upregulate antiviral genes, like *MxA* and *OAS*. TLR9 dependent sensing of VZV is also noted to trigger massive IFN-α release by pDCs (80, 81). Exogenous treatment with IFN-α has been shown to abrogate VZV severity through inhibition of viral replication *via* interferon regulator factor (IRF) protein 9 (82, 83). However, IFN-α signaling was not sufficient to completely terminate VZV transmission due to down-regulation of this pathway by viral gene products (75). Natural killer cells also prevent viral spread by killing infected cells, and their absence has been linked to severe infection (84, 85). Given the discoveries of the important role of NK cells during innate immune signaling and priming adaptive responses in other skin viruses, studies of the specific functions of NK cells in the context of VZV can provide promising avenues of discovery into establishment of an early antiviral state.

ONCOGENIC VIRUSES

Human Papillomavirus

Human papillomaviruses are non-enveloped double-stranded DNA viruses that can be transmitted through direct skin-to-skin

contact (86). There are more than 200 described HPV types. The alpha HPVs (*i.e.* HPV16, 18, 31, 33, 35, 39, 45, 51, 52, 56, 58 and 59) are considered high risk or carcinogenic and have been identified as etiologic agents of a multitude of cancers, including cervical, oropharyngeal, vaginal, vulvar, penile, and anal cancers (87, 88). Beta and gamma types are considered possibly carcinogenic or non-carcinogenic. Several studies have identified potential contributory roles of beta HPVs to non-melanoma skin cancer when associated with ultraviolet radiation (89). The low risk non-carcinogenic HPVs are known to cause benign lesions such as anogenital, palmar, and plantar warts (90).

Viral penetration into the epidermis is facilitated *via* microlesions and HPV's replication cycle starts at the mitotically active basal layer (91). Once within the basal layer, viruses gain entry into the cells through endocytosis, which are enabled by viral proteins L1 and L2 that help the virus interact with the cell surface. Molecules such as HSPGs and syndecan-1 are putative targets of HPV that enable viral trafficking into the host cell (92). After internalization, HPV virions reach the nucleus through the clathrin-mediated endocytic pathway (93, 94).

Within the basal layers, HPV DNA copy number is low and viral replication is slow. As viral replication speeds up and the virus leaves the basal layer to reach the upper layers of the epidermis, innate and adaptive immune responses become more important in surveilling and controlling viral spread (95). HPV DNA within a host cell is recognized by innate pathogen sensors, including absence in melanoma 2 (AIM2), interferon-gamma inducible protein 16 (IFI16), and cyclic guanosine monophosphate-adenosine monophosphate synthase (cGAS) (96–98). AIM2 inflammasome activation results in maturation of caspase-1 and IL-1β in HPV16-infected keratinocytes (99). TLR activation in keratinocytes by HPV also results in release of pro-inflammatory cytokines such as TNF-α, IL-8, C-X-C motif chemokine ligand 9 (CXCL9), and type I interferon (IFN-α and -β) (100). In fact, higher expression of TLRs was found to be correlative with clearance of initial HPV16 infection in women (101).

HPV-infected keratinocytes additionally recruit macrophages, Langerhans cells (LCs), natural killer (NK) cells, and T lymphocytes in the initial antiviral response. TLR activation in macrophages and LCs through NF-γB and interferon response factor (IRF)-3 further promotes the release of TNF-α, IFN-γ, IL-1β, IL-12 and IL-18, which can in turn activate other inflammatory cells through paracrine signaling. IL-1 and TNF-α have also been shown to downregulate the transcription of viral oncoproteins E6 and E7 (100). Though there is limited evidence on the role NK cells play in controlling HPV infections, it was reported that patients with functional NK deficiencies were more susceptible to HPV infection and HPV-associated cancer (102). Together, these studies highlight the importance of host innate immunity during the initial antiviral responses against HPV in cutaneous tissues.

Many studies provide evidence that HPV has evolved mechanisms to counter host immune responses. HPV-infected cells can reprogram the local immune milieu to promote chronic inflammation and subsequently carcinogenesis. HPV E6 protein can directly target IRF3 while E7 protein interferes with the antiviral and pro-apoptotic functions of IRF1 *via* protein–protein interactions, leading to suppressed IFN signaling and downstream responses (103–105). Additionally, HPV infection was found to interfere with LC homeostasis due to the suppression of C-C motif chemokine ligand 20 (CCL20), a chemokine critical for the repopulation of $CD1a^+$ LC precursor cells in the epidermis (106). It was shown that viral E7 protein abrogates the binding of CCAAT/enhancer-binding protein beta (C/EBPβ) in the promoter region of CCL20. As a result, CCL20-directed migration of LCs and subsequent antigen-presentation in the epithelium is suppressed, allowing for viral persistence (106). In summary, HPV modulates several host cellular pathways to evade immune responses, leading to virus-mediated immunosuppression and neoplastic development. However, given the diversity of HPV types and their various neoplastic or benign propensities, further investigations are needed to identify differential mechanisms utilized by the host to respond to various HPV types, as well as how certain specific HPVs are able to subvert host immune signaling to impart immunosuppression and impart neoplastic potential.

Merkel Cell Polyomavirus

Merkel cell polyomavirus belongs to the *Polyomaviridae* family which consists of non-enveloped, double-stranded DNA viruses that have infectious and tumorigenic potential (107). Since the initial identification in Merkel cell carcinoma (MCC) in 2008, many reports have provided additional evidence of the causal relationship between MCPyV and MCC (108–112). MCC is an aggressive cancer that is characterized by a rapidly expanding, asymptomatic, erythematous dome-shaped tumor that presents often on sun-exposed areas of the skin (113).

It remains under debate which cutaneous cell type(s) MCPyV primarily infects due to poor replication of MCPyV in *in vitro* cultures (114). Keratinocytes were thought to be the primary target due to chronic cutaneous shedding of MCPyV (115). However, a recent report showed that MCPyV preferentially infects human dermal fibroblasts (116). Viral attachment relies on recognition of sulfated GAGs and interaction with sialylated oligosaccharides containing the Neu5Acα2-3Gal linear motif by viral capsid protein, VP1 (117, 118). MCPyV eventually enters target cells through caveolar/lipid raft-mediated endocytosis (119).

Many recent reports suggest the important role the host immune system plays in MCPyV infection and MCC development. First of all, immunocompromised patients are more likely to develop MCC (120). Secondly, high intratumoral $CD8^+$ T cell counts and immune transcripts are associated with more favorable outcomes in MCC patients (121, 122). Innate immune responses were thought to play a critical role in the initial sensing and clearance of MCPyV virions. Shadzad et al. reported that TLR9, a critical sensor for viral and bacterial dsDNA, is downregulated by MCPyV large T antigen during infection (123). Additionally, MCPyV small T antigen negatively regulates NF-γB-mediated inflammatory signaling by inhibiting IKKα/IKKβ-induced IγB

phosphorylation, further dampening host antiviral responses (124). Lastly, MCPyV-positive MCC tumors were discovered to have lower expression of major histocompatibility complex class I (MHC-I) compared to MCPyV-negative MCC samples, suggesting another potential mechanism by which MCPyV-infection cells escape immune destruction (125). However, precise interactions between MCPyV and the host immune system are largely unknown. Further work is needed to elucidate the various mechanisms by which MCPyV subverts host immune surveillance to establish persistence.

VECTOR-BORNE SKIN VIRUSES

Mosquitos infect hundreds of millions of people around the world annually, introducing individuals to pathogenic bacteria, parasites, and viruses that have the potential to cause severe systemic illness in the host and, with Zika virus, their offspring (126, 127). Despite the prevalence of mosquito-borne illnesses and their threat to global human health, little is known about the early stages of cutaneous infection.

Zika virus (ZIKV), West Nile virus (WNV), and Dengue virus (DENV) belong to the *Flaviviridae* family and are enveloped RNA viruses. ZIKV and DENV have a predisposition to infect cutaneous dendritic cells, whose migratory characteristic allows for rapid dissemination and viremia (128, 129). WNV has been shown to preferentially infect keratinocytes, though it is capable of infecting dendritic cells as well (130, 131). Flaviviral envelope (E) glycoprotein is key to initial viral entry *via* low-affinity attachment to GAGs on the target cell surface (132, 133). More specific attachment to a wide array of entry receptors that help facilitate internalization into dendritic cells has been identified, including C-type lectin receptors, $\alpha v\beta 3$ integrins, T-cell immunoglobulin and mucin domain (TIM) and TYRO3, AXL and MER (TAM) receptors (134). Clathrin-dependent endocytosis then allows for viral fusion into the target cell (135).

Chikungunya virus (CHIKV) is also an enveloped RNA virus but belongs to the *Togaviridae* family with tropism to dermal fibroblasts (136). CHIKV viral glycoprotein E2 interaction with cell surface GAGs, TIM family receptors, and prohibitins has been shown to assist with early interactions of CHIKV with the target cell, although CHIKV is able to infect in the absence of these proteins (137). Similar to flaviviruses, CHIKV utilizes clathrin-dependent endocytosis to generate a low pH environment to cause conformational changes in glyocoprotein E1 and permit fusion (138).

Once in the skin, ZIKV, WNV, DENV, and CHIKV all trigger PRRs retinoic acid-inducible gene I (RIG-I), TLR3, and melanoma differentiation associated gene-5 (MDA-5). Next, pro-inflammatory cytokine and chemokine signaling is coupled with activation of IFN-β and antiviral proteins, including members of the OAS, Mx, interferon stimulated gene (ISG), and interferon induced proteins with tetratricopeptide repeats (IFIT) families, in keratinocytes and dermal myeloid cells (81, 129, 139–142). Specific to ZIKV, our group recently identified a novel IFN-independent pathway of antiviral protein induction *via* IL-27. Uniquely, signal transducer and activator of transcription (STAT) 1- and interferon regulatory factor (IRF) 3-dependent IL-27 signaling was able to induce antiviral proteins OAS1, OAS2, OASL2, and MX1 in keratinocytes and reduce ZIKV pathogenicity when the virus was introduced *via* a cutaneous, and not intravenous, route (143). These results suggest a potential avenue to distinctly upregulate cutaneous antiviral proteins independent of interferon signaling, although whether this pathway confers similar resistance to other vector-borne viruses remains to be discovered.

Given arboviruses' predilection to infect immune cells, the recruitment of distal immune cells to the dermis may not be as advantageous to the host as is the case for many other pathogens. After an early infection in the epidermis, a second round occurs when the immune response homes arbovirus-susceptible monocytes and monocyte-derived dendritic cells to the site (144). These infected immune cells then travel to the draining lymph nodes to continue systemic spread. This begs the question of whether pathogenicity can be reduced or limited to the epidermis by dampening inflammatory signaling. One group observed a 75–90% reduction in infection of LCs, macrophages, and dermal dendritic cells when cytokine IL-1β expression was inhibited (128).

An additional non-viral factor also contributes to the immune picture. Intriguingly, mosquito saliva has been shown to significantly alter the early innate signatures to enhance viral spread. Mosquito saliva protein D7 inhibits DENV virions and envelope proteins (145). ZIKV-activated NF-κB signaling is inhibited by salival protein LTRIN (146). In CHIKV, mosquito saliva suppresses Th1 cytokine (IFN-γ and IL-2), TLR3, and chemokine expression while simultaneously pushing toward a Th2 polarity—which, as we have discussed, is a less advantageous antiviral profile from the host perspective (147, 148). Decreases in expression of PRRs and antiviral proteins with specific targeting of flaviviruses (OAS1, MX1, and ISG20) were also observed in WNV-infected keratinocytes (149, 150).

The unique mode of inoculation of vector-borne viruses at the skin presents an alluring rationale to study potential methods of undermining viral pathogenicity when the infection is still local and while innate immune responses predominate. However, the frequency of mosquito bites and the lack of urgency to seek medical attention prior to systemic infection may pose a conceivable difficulty for translation into clinical practice.

DEMOGRAPHIC AND ENVIRONMENTAL CONTRIBUTORS TO HOST ANTIVIRAL RESPONSES

As a frontline organ of defense against the outside world, maintaining integrity of the skin barrier and function is critical to the organ's success in combating potential invaders. However, increasing studies show that, like other regenerating organs, the skin is constantly adapting in response to a multitude of environmental factors (**Figure 2**).

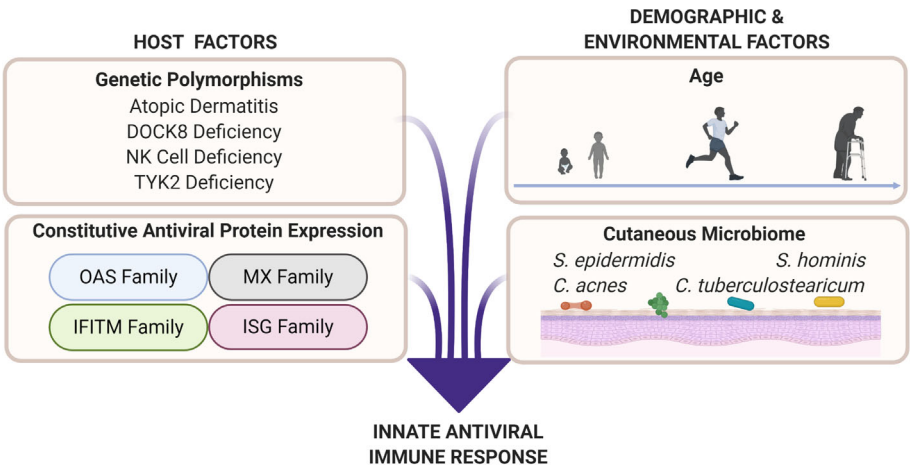

FIGURE 2 | Cutaneous antiviral immune responses are influenced by host as well as demographic and environmental factors. Genetic polymorphisms that result in atopic dermatitis, dedicator of cytokinesis 8 (DOCK8) deficiency, natural killer (NK) cell deficiency, and tyrosine kinase 2 (TYK2) deficiency produce unique immune profiles that are disadvantageous for viral protection. Professional antiviral proteins such as those in the oligoadenylate synthetase (OAS), myxovirus resistance (MX), interferon-induced transmembrane (IFITM), and interferon-stimulated gene (ISG) families are part of the innate antiviral response. These proteins exert their antiviral abilities by inhibiting various parts of the viral replication cycle (151). Factors such as age (see **Figure 3**), biological sex, and cutaneous microbiome have potential to deter or enhance innate antiviral responses. Microbial interactions, such as bacteria–viral, viral–viral, and fungal–viral, can possibly produce antiviral effectors or influence host antiviral responses.

Age

Given the skin's constant contact with potential pathogens, the susceptibility of certain patient populations to skin viruses is an interesting area of investigation. Notably, age appears to play a role in the host immune defenses against viral invaders (**Figure 3**). Some trends are more obvious: MCV and VACV show increased incidence and more severe effects in children as prevalence of AD is highest in this age group, and as previously discussed, the AD

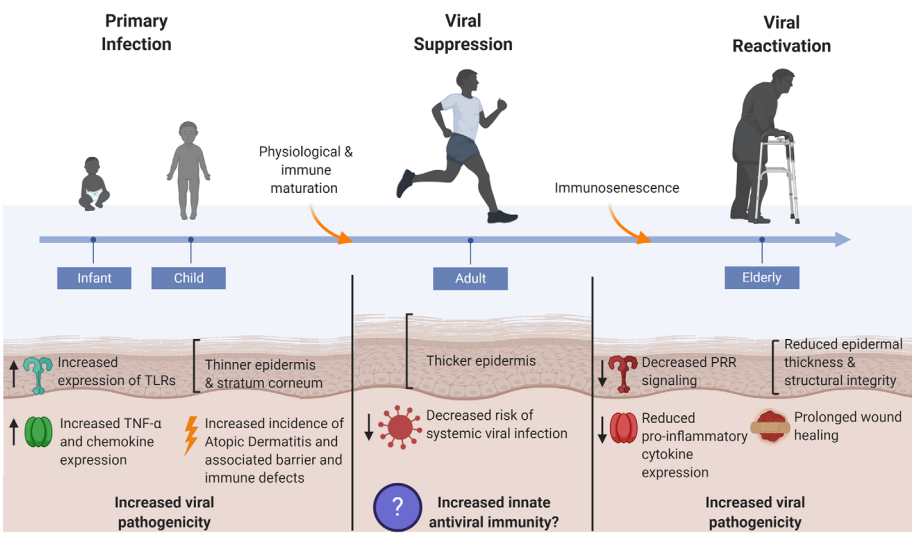

FIGURE 3 | Skin's antiviral protection changes throughout age. Systemic viral infections are most prevalent at the young and elderly ages where factors such as epidermal thickness and cutaneous innate immunity are markedly different from healthy adult human skin. Thin skin leads to increased susceptibility to micro-injuries and abrasions, thereby providing direct avenues for viral entry. Dysregulated innate immune signaling, consequent to immunological immaturity or immunosenescence in the young and elderly, respectively, furthers the risk of systemic viral infection as immune defenses cannot adequately control early viral propagation. The young and elderly are also at increased risk for viral pathogen exposure due to compromises in skin barrier integrity that manifest in the form of atopic dermatitis in the young and chronic non-healing wounds in the elderly.

milieu contributes to increased viral pathogenicity and impaired antiviral responses (152–154). However, there is less clarity on why certain age groups are more afflicted with other cutaneous viral infections. Intriguingly, prenatal, neonatal, and elderly populations have demonstrated increased susceptibility to systemic malaise and higher risk of mortality compared to young and mature adults. For example, whereas only mild symptoms would typically result from primary HSV infection in children and adults, preterm and neonatal infants, if untreated, only have a 40% chance of survival (155). Similarly, in the elderly population, reports have emerged suggesting that HSV increases the risk for development of neurological diseases like Alzheimer's and may be a direct infectious etiology (156). Moreover, while VZV dissemination occurs most commonly in children due to primary infection, suppression of the virus is maintained throughout adulthood. However, reactivation, which only occurs after VZV overthrows immune safeguards and presents in the form of herpes zoster, occurs most frequently in elderly individuals or upon immunosuppresion (157).

One potential explanation for these observations is alteration in the skin's physical barrier with aging. Preterm and neonatal infants have a thinner epidermis and stratum corneum, and a similar observation applies to the elderly population where cutaneous structural integrity deteriorates and skin thickness is once again reduced (158, 159). Such changes to skin integrity may render it more susceptible to micro-injuries and therefore subsequent pathogen exposure and infection. Functional studies on whether the rate of viral infectivity is enhanced in the setting of thin, fragile skin barriers are limited. Theoretically, decreased epidermal thickness may provide for earlier access to deeper skin layers, which could potentially lessen the time the virus spends replicating at the initial infection site prior to systemic spread, and therefore limit the time available for propagation of early innate immune responses as well as initiation of adaptive immune responses. Additional concerns are warranted in the elderly where the skin's wound healing capabilities are also reduced, thereby allowing for increased pathogen exposure (159).

Age also has profound effects on certain aspects of the skin's innate antiviral defenses. For example, in WNV infection, which usually afflicts individuals >60 years of age, worse outcomes were identified in mice with dysregulated TLR7 and STING signaling, both with critical roles in initiating antiviral signaling cascades (160, 161). Generally, older individuals exemplified decreased PRR signaling and decreased induction of pro-inflammatory cytokines and chemokines in several cutaneous compartments, including sebaceous glands, sweat glands, and epidermis (162). Surprisingly, prenatal skin actually exhibited higher levels of TLRs (1–5) compared to adults, and neonatal keratinocytes demonstrated greater secretion of TNF-α and several chemokines when stimulated with poly (I:C), a synthetic dsRNA used to mimic viral nucleic acids (163). It is unclear how this dichotomy corresponds to viral preference and susceptibility at different age groups, although similar outcomes of greater morbidity and mortality in both age groups highlight the importance of better understanding the regulators and effectors of innate antiviral immunity.

Studies have additionally identified discrepancies in the expression levels of cutaneous antimicrobial peptides and proteins at the extremes of age. For example, neonatal skin was observed to express increased levels of antimicrobial peptides LL-37 and hBD2 compared to adults in both mice and humans (164). Contrastingly, reduced levels of antimicrobial peptides were observed in aged skin compared to adult skin (165). While these studies begin to point toward differing antimicrobial signatures across age groups, investigations specifically looking at antiviral proteins and their functional implications are currently lacking.

Biological Sex

Biological sex poses another important variable when considering immune defenses against viral pathogens. Sex differences in innate and adaptive immunity have been well characterized in humans; known to us is that infant and adult males mount weaker innate and adaptive immune responses to pathogens compared to females and are, therefore, theorized to be more susceptible to viral infections. Particularly in the context of innate immunity, varied responses to pathogens can be explained by differential expression in TLR and type I IFN signaling between sexes, wherein females exhibit higher basal and inducible expression levels of TLR7, TLR9, IRF5, and IFN-α (166, 167). The sex differential expression of these pathways confers greater pro-inflammatory responses in peripheral blood mononuclear cells (PBMCs), neutrophils, and macrophages in males, whereas higher anti-inflammatory and cytokine signaling for type I IFN responses are seen in females (168, 169). Further, studies in rodents have shown that expression of signaling molecules associated with antiviral sensing and immunity (Myd88, IRF7, IFN-β, IFNAR1, JAK2, and STAT3) as well as antiviral protein Mx is higher in females compared to males (169). These dimorphic effects are posited to be mediated by gonadal hormones, with possible androgen- and estrogen-specific response elements driving different effector cells' signaling and expression.

Despite these findings, studies directly looking at the sex differential contribution to viral susceptibility and disease outcome in humans are complicated by various behavioral and environmental differences associated with biological sex as well as gender. Several of the previously discussed viruses show preferential responses between females *versus* males, though whether biological differences are the cause of these observations is more difficult to tease out. Studies show that males have higher relative incidence of more serious illness and susceptibility to VZV and HSV-1, which may be explained by the aforementioned weakened immune response and pro-inflammatory cytokine profile (170, 171). However, interestingly, epidemiological studies show that females infected with Dengue virus in endemic areas have the same susceptibility to infection though exhibit more severe symptoms, such as hemorrhagic fever, compared to male

counterparts (172). Females with Merkel cell carcinomas also have higher prevalence of MCPyV-positive tumors than male patients (173, 174). Additionally, HSV-2 shows a higher prevalence in females compared to males in humans (175, 176). These observations may appear to contradict immunological findings that females show a greater anti-inflammatory signature as well as an enhanced innate and adaptive immune profile compared to males. However, particularly in human studies, direct correlations of biological sex and viral susceptibility and disease outcome not only have to take into account sex hormones and chromosomal/genetic differences, they must also consider the differential effects that arise as a result of behaviors associated with gender and host environment, which may have direct consequences of increasing risk and susceptibility to certain viral pathogens. Murine studies have attempted to control for these confounding factors, although findings do not directly translate to humans. For example, increased progesterone levels are theorized to reduce immune-protective effects and therefore increase HSV-2 susceptibility in females. Female mice that underwent ovariectomy and had estradiol hormone injected showed reduced pathology compared to counterparts injected with progesterone or placebo (177). However, HSV-2 infection is increased in *ex vivo* human endometrial epithelial cells treated with estradiol (178). These divergent discoveries highlight the immense difficulty of using biological sex as a method of predicting viral susceptibility as well as disease outcome, although knowledge of sexual preferences of pathogens can be utilized to focus clinical efforts to provide better care to at-risk populations.

Cutaneous Microbiome

The skin is home to a highly diverse collection of commensal bacteria, fungi and viruses that form the cutaneous microbiome. The makeup of these colonizers varies across individuals, skin compartments (*e.g.* hair follicle *versus* sebaceous gland), body location (*e.g.* axillary *versus* facial skin), and even age (179–181). This diversity is mirrored in the varying relationships between host skin and commensal microbiota, ranging from opportunistic to mutualistic interactions. For example, the *Cutibacteria* family (formerly known as *Propionibacteria)* of bacteria is a major component of normal skin flora that colonizes preferentially to skin sites that are rich in sebaceous glands. The presence of cutibacteria has been observed to impart protective benefits to the host in common skin pathologies including atopic dermatitis and psoriasis (182, 183). Conversely, *Cutibacterium acnes* often causes opportunistic infections and is a common etiologic agent in diseases such as acne vulgaris (184). These disparate consequences imply a necessity for the skin to maintain a healthy balance between itself and its surrounding microbiome. Furthermore, the predisposition for viral infection in populations with dysbiosis, such as those with atopic dermatitis, proposes the question of how microbial interactions influence skin responses to viral challenges (185).

Recent studies have begun to identify various antimicrobial roles of skin microbiota. Skin bacterial commensal *Staphylococcus epidermidis* was observed to produce peptides called bacteriocins that have direct antimicrobial properties against *Staphylococcus aureus* and Group A *Streptococcus* (186). Additionally, *S. epidermidis* was noted to augment the antimicrobial actions of cathelicidin LL-37 (187). *C. acnes* is also reported to secrete bacteriocins with bactericidal properties toward other cutibacteria (188). This work indicates that commensal bacteria actively participate in maintaining cutaneous microbial homeostasis; however, there is a current lack of understanding of antifungal and antiviral contributions from the cutaneous resident microbiota, including fungi and viruses.

Evidence of how the skin microbiome directly influences cutaneous antiviral immunity is also limited, although studies in patients with primary immunodeficiency, such as dedicator of cytokinesis 8 (DOCK8) deficiency who have altered cutaneous microbiomes compared to healthy patients, reveal that changes in the cutaneous virome lead to increased colonization of DNA viruses like HPVs, HSVs, polyomaviruses, and MCV (189). Inferences can additionally be drawn from studies in other barrier organs and their commensal microbiome. For instance, germ-free mice, *i.e.* lacking intestinal commensal microbiota, were observed to be more susceptible to influenza A virus, coxsackie B virus, Friend leukemia virus, and murine cytomegalovirus (190, 191). In the respiratory epithelium, *S. epidermidis* produced an extracellular matrix-binding protein that exhibited anti-influenza activity (192). Further, probiotic colonization of resident *Corynebacteria* improved resistance to respiratory syncytial virus (193). At the vaginal surface, lack of *Lactobacillus* bacteria, a dominant colonizer of the vaginal mucosa, led to increased susceptibility of HSV-2 due to abrogated IFN-γ signaling (194). Together, these findings suggest that commensal microbiota contribute directly to antiviral immunity *via* secretion of antiviral effectors and through enhancement of host immune signaling at their resident sites.

CONCLUSION

The skin is an active immune organ with immune capabilities that are constantly challenged by friendly commensal and pathogenic microorganisms. Consequently, it has evolved effective defense strategies to combat a wide range of threats, ranging from overpopulation of opportunistic commensal bacteria to pathogenic viruses. Particularly in the scenario of viral infection, the skin's complex multi-layered defense strategies, even within the innate immune system alone, are highlighted as different viruses' attempt to hijack and suppress various aspects of its immune machinery. Given the severity of primary infections to many cutaneously introduced viruses, early antiviral responses are critical in the attempt to prevent further viral propagation and to allow time for adaptive immune

responses to take effect. Recent advances in understanding specific viral targets of innate immunity begin to provide opportunities for further exploration into bolstering areas of vulnerability, including weaknesses that arise throughout age and between females and males. Additionally, insights to antiviral contributions from the commensal microbiome obtained from studies in other barrier organs suggest potential for future study in the skin.

AUTHOR CONTRIBUTIONS

VL and AM contributed to conception and design of the review. VL and AP performed initial literature search and wrote the first draft of the manuscript. AM supervised all aspects of the review and manuscript writing and is the corresponding author. All authors contributed to the article and approved the submitted version.

FUNDING

VL is supported by the Burroughs-Wellcome and Poindexter Medical Student Research Fellowships. AM is supported by R01AI139207 and received a Duke Physician-Scientist Strong Start Award. AM is also supported by a Silab company partnership. The funding sources did not have any control over the content nor results of the review. The funders had no role in study design, data collection and analysis, decision to publish, or preparation of the manuscript.

REFERENCES

1. Coates M, Blanchard S, MacLeod AS. Innate antimicrobial immunity in the skin: A protective barrier against bacteria, viruses, and fungi. *PLoS Pathog* (2018) 14(12):e1007353. doi: 10.1371/journal.ppat.1007353
2. Davison AJ. Herpesvirus systematics. *Vet Microbiol* (2010) 143(1):52–69. doi: 10.1016/j.vetmic.2010.02.014
3. Cunningham AL, Diefenbach RJ, Miranda-Saksena M, Bosnjak L, Kim M, Jones C, et al. The cycle of human herpes simplex virus infection: virus transport and immune control. *J Infect Dis* (2006) 194(Suppl 1):S11–8. doi: 10.1086/505359
4. Smith JS, Robinson NJ. Age-specific prevalence of infection with herpes simplex virus types 2 and 1: a global review. *J Infect Dis* (2002) 186(Suppl 1): S3–S28. doi: 10.1086/343739
5. Karasneh GA, Shukla D. Herpes simplex virus infects most cell types in vitro: clues to its success. *Virol J* (2011) 8:481. doi: 10.1186/1743-422X-8-481
6. Shukla D, Spear PG. Herpesviruses and heparan sulfate: an intimate relationship in aid of viral entry. *J Clin Invest* (2001) Aug108(4):503–10. doi: 10.1172/JCI200113799
7. Connolly SA, Jackson JO, Jardetzky TS, Longnecker R. Fusing structure and function: a structural view of the herpesvirus entry machinery. *Nat Rev Microbiol* (2011) 9(5):369–81. doi: 10.1038/nrmicro2548
8. Spear PG. Herpes simplex virus: receptors and ligands for cell entry. *Cell Microbiol* (2004) 6(5):401–10. doi: 10.1111/j.1462-5822.2004.00389.x
9. Petermann P, Rahn E, Their K, Hsu MJ, Rixon FJ, Kopp SJ, et al. Role of nectin-1 and herpesvirus entry mediator as cellular erceptors for herpes simplex virus 1 on primary murine dermal fibroblasts. *J Virol* (2015) 89 (18):9407–16. doi: 10.1128/JVI.01415-15
10. Farnsworth A, Johnson DC. Herpes simplex virus gE/gI must accumulate in the trans-Golgi network at early times and then redistribute to cell junctions to promote cell-cell spread. *J Virol* (2006) 80(7):3167–79. doi: 10.1128/JVI.80.7.3167-3179.2006
11. Akhtar J, Shukla D. Viral entry mechanisms: cellular and viral mediators of herpes simplex virus entry. *FEBS J* (2009) 276(24):7228–36. doi: 10.1111/j.1742-4658.2009.07402.x
12. Sato A, Linehan MM, Iwasaki A. Dual recognition of herpes simplex viruses by TLR2 and TLR9 in dendritic cells. *Proc Natl Acad Sci U S A* (2006) 103 (46):17343–8. doi: 10.1073/pnas.0605102103
13. Ma Y, He B. Recognition of herpes simplex viruses: toll-like receptors and beyond. *J Mol Biol* (2014) 426(6):1133–47. doi: 10.1016/j.jmb.2013.11.012
14. Gianni T, Leoni V, Campadelli-Fiume G. Type I interferon and NF-κB activation elicited by herpes simplex virus gH/gL via αvβ3 integrin in epithelial and neuronal cell lines. *J Virol* (2013) 87(24):13911–6. doi: 10.1128/JVI.01894-13
15. Kurt-Jones EA, Chan M, Zhou S, Wang J, Reed G, Bronson R, et al. Herpes simplex virus 1 interaction with Toll-like receptor 2 contributes to lethal encephalitis. *Proc Natl Acad Sci U S A* (2004) 101(5):1315–20. doi: 10.1073/pnas.0308057100
16. Melchjorsen J. Sensing herpes: more than toll. *Rev Med Virol* (2012) 22 (2):106–21. doi: 10.1002/rmv.716
17. Zhou L, Li JL, Zhou Y, Liu JB, Zhuang K, Gao JF, et al. Induction of interferon-λ contributes to TLR3 and RIG-I activation-mediated inhibition of herpes simplex virus type 2 replication in human cervical epithelial cells. *Mol Hum Reprod* (2015) 21(12):917–29. doi: 10.1093/molehr/gav058
18. Donaghy H, Bosnjak L, Harman AN, Marsden V, Tyring SK, Meng TC, et al. Role for plasmacytoid dendritic cells in the immune control of recurrent human herpes simplex virus infection. *J Virol* (2009) 83(4):1952–61. doi: 10.1128/JVI.01578-08
19. Ank N, West H, Bartholdy C, Eriksson K, Thomsen AR, Paludan SR. Lambda interferon (IFN-lambda), a type III IFN, is induced by viruses and IFNs and displays potent antiviral activity against select virus infections in vivo. *J Virol* (2006) 80(9):4501–9. doi: 10.1128/JVI.80.9.4501-4509.2006
20. Lund J, Sato A, Akira S, Medzhitov R, Iwasaki A. Toll-like receptor 9-mediated recognition of Herpes simplex virus-2 by plasmacytoid dendritic cells. *J Exp Med* (2003) 198(3):513–20. doi: 10.1084/jem.20030162
21. Paludan SR, Bowie AG, Horan KA, Fitzgerald KA. Recognition of herpesviruses by the innate immune system. *Nat Rev Immunol* (2011) 11 (2):143–54. doi: 10.1038/nri2937
22. Handfield C, Kwock J, MacLeod AS. Innate Antiviral Immunity in the Skin. *Trends Immunol* (2018) 39(4):328–40. doi: 10.1016/j.it.2018.02.003
23. Kreins AY, Ciancanelli MJ, Okada S, Kong XF, Ramirez-Alejo N, Kilic SS, et al. Human TYK2 deficiency: Mycobacterial and viral infections without hyper-IgE syndrome. *J Exp Med* (2015) 212(10):1641–62. doi: 10.1084/jem.20140280
24. Alandijany T, Roberts APE, Conn KL, Loney C, McFarlane S, Orr A, et al. Distinct temporal roles for the promyelocytic leukaemia (PML) protein in the sequential regulation of intracellular host immunity to HSV-1 infection. *PLoS Pathog* (2018) 14(1):e1006769. doi: 10.1371/journal.ppat.1006769. [published correction appears in PLoS Pathog. 2018;14 (2):e1006927].
25. McFarlane S, Orr A, Roberts APE, Conn KL, Iliev V, Loney C, et al. The histone chaperone HIRA promotes the induction of host innate immune defences in response to HSV-1 infection. *PLoS Pathog* (2019) 15(3): e1007667. doi: 10.1371/journal.ppat.1007667
26. Milora KA, Miller SL, Sanmiguel JC, Jensen LE. Interleukin-1α released from HSV-1-infected keratinocytes acts as a functional alarmin in the skin. *Nat Commun* (2014) 5:5230. doi: 10.1038/ncomms6230
27. Wang P, Gamero AM, Jensen LE. IL-36 promotes anti-viral immunity by boosting sensitivity to IFN-α/β in IRF1 dependent and independent manners. *Nat Commun* (2019) 10(1):4700. doi: 10.1038/s41467-019-12318-y
28. Ashkar AA, Rosenthal KL. Interleukin-15 and natural killer and NKT cells play a critical role in innate protection against genital herpes simplex virus type 2 infection. *J Virol* (2003) 77(18):10168–71. doi: 10.1128/jvi.77.18.10168-10171.2003

29. Dalloul A, Oksenhendler E, Chosidow O, Ribaud P, Carcelain G, Louvet S, et al. Severe herpes virus (HSV-2) infection in two patients with myelodysplasia and undetectable NK cells and plasmacytoid dendritic cells in the blood. *J Clin Virol* (2004) 30(4):329–36. doi: 10.1016/j.jcv.2003.11.014
30. Nandakumar S, Woolard SN, Yuan D, Rouse BT, Kumaraguru U. Natural killer cells as novel helpers in anti-herpes simplex virus immune response. *J Virol* (2008) 82(21):10820–31. doi: 10.1128/JVI.00365-08
31. Hirose S, Wang S, Tormanen K, Wang Y, Tang J, Akbari O, et al. Roles of Type 1, 2, and 3 Innate Lymphoid Cells in Herpes Simplex Virus 1 Infection In Vitro and In Vivo. *J Virol* (2019) 93(13):e00523–19. doi: 10.1128/JVI.00523-19
32. MacLeod DT, Nakatsuji T, Yamasaki K, Kobzik L, Gallo RL. HSV-1 exploits the innate immune scavenger receptor MARCO to enhance epithelial adsorption and infection. *Nat Commun* (2013) 4:1963. doi: 10.1038/ncomms2963
33. Huang J, You H, Su C, Li Y, Chen S, Zheng C. Herpes Simplex Virus 1 Tegument Protein VP22 Abrogates cGAS/STING-Mediated Antiviral Innate Immunity. *J Virol* (2018) 92(15):e00841–18. doi: 10.1128/JVI.00841-18
34. Pan S, Liu X, Ma Y, Cao Y, He B. Herpes Simplex Virus 1 $\gamma_1$34.5 Protein Inhibits STING Activation That Restricts Viral Replication. *J Virol* (2018) 92 (20):e01015–18. doi: 10.1128/JVI.01015-18
35. Maruzuru Y, Ichinohe T, Sato R, Miyake K, Okano T, Suzuki T, et al. Herpes Simplex Virus 1 VP22 Inhibits AIM2-Dependent Inflammasome Activation to Enable Efficient Viral Replication. *Cell Host Microbe* (2018) 23(2):254–265.e7. doi: 10.1016/j.chom.2017.12.014
36. Yuan H, You J, You H, Zheng C. Herpes Simplex Virus 1 UL36USP Antagonizes Type I Interferon-Mediated Antiviral Innate Immunity. *J Virol* (2018) 92(19): e01161–18. doi: 10.1128/JVI.01161-18
37. Jacobs BL, Langland JO, Kibler KV, Denzler KL, White SD, Holechek SA, et al. Vaccinia virus vaccines: past, present and future. *Antiviral Res* (2009) 84(1):1–13. doi: 10.1016/j.antiviral.2009.06.006
38. Moss B. Smallpox vaccines: targets of protective immunity. *Immunol Rev* (2011) 239(1):8–26. doi: 10.1111/j.1600-065X.2010.00975.x
39. Oyoshi MK, Beaupré J, Venturelli N, Lewis CN, Iwakura Y, Geha RS. Filaggrin deficiency promotes the dissemination of cutaneously inoculated vaccinia virus. *J Allergy Clin Immunol* (2015) 135(6):1511–8. doi: 10.1016/j.jaci.2014.12.1923
40. Vermeer PD, McHugh J, Rokhlina T, Vermeer DW, Zabner J, Welsh MJ. Vaccinia virus entry, exit, and interaction with differentiated human airway epithelia. *J Virol* (2007) 81(18):9891–9. doi: 10.1128/JVI.00601-07. [published correction appears in J Virol. 2007 Dec;81(23):13278].
41. Izmailyan R, Hsao JC, Chung CS, Chen CH, Hsu PWC, Liao CL, et al. Integrin β1 mediates vaccinia virus entry through activation of PI3K/Akt signaling. *J Virol* (2012) 86(12):6677–87. doi: 10.1128/JVI.06860-11
42. White JM, Delos SE, Brecher M, Schornberg K. Structures and mechanisms of viral membrane fusion proteins: multiple variations on a common theme. *Crit Rev Biochem Mol Biol* (2008) 43(3):189–219. doi: 10.1080/10409230802058320. [published correction appears in Crit Rev Biochem Mol Biol. 2008 Jul-Aug;43(4):287-8].
43. Moss B. Poxvirus cell entry: how many proteins does it take? *Viruses* (2012) 4(5):688–707. doi: 10.3390/v4050688
44. Rice AD, Adams MM, Lindsey SF, Swetnam DM, Manning BR, Smith AJ, et al. Protective properties of vaccinia virus-based vaccines: skin scarification promotes a nonspecific immune response that protects against orthopoxvirus disease. *J Virol* (2014) 88(14):7753–63. doi: 10.1128/JVI.00185-14
45. Tian T, Dubin K, Jin Q, Qureshi A, King SL, Liu L, et al. Disruption of TNF-α/TNFR1 function in resident skin cells impairs host immune response against cutaneous vaccinia virus infection. *J Invest Dermatol* (2012) 132 (5):1425–34. doi: 10.1038/jid.2011.489
46. Tian T, Jin MQ, Dubin K, et al. IL-1R Type 1-Deficient Mice Demonstrate an Impaired Host Immune Response against Cutaneous Vaccinia Virus Infection. *J Immunol* (2017) 198(11):4341–51. doi: 10.4049/jimmunol.1500106
47. Cao H, Dai P, Wang W, Li H, Yuan J, Wang F, et al. Innate immune response of human plasmacytoid dendritic cells to poxvirus infection is subverted by vaccinia E3 via its Z-DNA/RNA binding domain. *PLoS One* (2012) 7(5): e36823. doi: 10.1371/journal.pone.0036823
48. Deng L, Dai P, Ding W, Granstein RD, Shuman S. Vaccinia virus infection attenuates innate immune responses and antigen presentation by epidermal dendritic cells. *J Virol* (2006) 80(20):9977–87. doi: 10.1128/JVI.00354-06
49. Abboud G, Tahiliani V, Desai P, Varkoly K, Driver J, Hutchinson TE, et al. Natural Killer Cells and Innate Interferon Gamma Participate in the Host Defense against Respiratory Vaccinia Virus Infection. *J Virol* (2015) 90 (1):129–41. doi: 10.1128/JVI.01894-15
50. Martinez J, Huang X, Yang Y. Direct action of type I IFN on NK cells is required for their activation in response to vaccinia viral infection in vivo. *J Immunol* (2008) 180(3):1592–7. doi: 10.4049/jimmunol.180.3.1592
51. Borst K, Flindt S, Blank P, Larsen PK, Chhatbar C, Skerra J, et al. Selective reconstitution of IFN−γ gene function in Ncr1+ NK cells is sufficient to control systemic vaccinia virus infection. *PLoS Pathog* (2020) 16(2): e1008279. doi: 10.1371/journal.ppat.1008279
52. Lane JM, Goldstein J. Adverse events occurring after smallpox vaccination. *Semin Pediatr Infect Dis* (2003) 14(3):189–95. doi: 10.1016/s1045-1870(03)00032-3
53. Vellozzi C, Lane JM, Averhoff F, Maure T, Norton S, Damon I, et al. Generalized vaccinia, progressive vaccinia, and eczema vaccinatum are rare following smallpox (vaccinia) vaccination: United States surveillance 2003. *Clin Infect Dis* (2005) 41(5):689–97. doi: 10.1086/432584
54. Czarnowicki T, Krueger JG, Guttman-Yassky E. Skin barrier and immune dysregulation in atopic dermatitis: an evolving story with important clinical implications. *J Allergy Clin Immunol Pract* (2014) 2(4):371–81. doi: 10.1016/j.jaip.2014.03.006
55. Vellozzi C, Lane JM, Averhoff F, Maurer T, Norton S, Damon I, et al. Generalized vaccinia, progressive vaccinia, and eczema vaccinatum are rare following smallpox (vaccinia) vaccination: United States surveillance, 2003. *Clin Infect Dis* (2005) 41(5):689–97. doi: 10.1086/432584
56. Yu Q, Jones B, Hu N, Chang H, Ahmad S, Liu J, et al. Comparative analysis of tropism between canarypox (ALVAC) and vaccinia viruses reveals a more restricted and preferential tropism of ALVAC for human cells of the monocytic lineage. *Vaccine* (2006) 24(40-41):6376–91. doi: 10.1016/j.vaccine.2006.06.011
57. He Y, Fisher R, Chowdhury S, Sultana I, Pereira CP, Bray M, et al. Vaccinia virus induces rapid necrosis in keratinocytes by a STAT3-dependent mechanism. *PLoS One* (2014) 9(11):e113690. doi: 10.1371/journal.pone.0113690
58. Freyschmidt EJ, Mathias CB, Diaz N, MacArthur DH, Laouar A, Manjunath N, et al. Skin inflammation arising from cutaneous regulatory T cell deficiency leads to impaired viral immune responses. *J Immunol* (2010) 185(2):1295–302. doi: 10.4049/jimmunol.0903144
59. Ong PY, Ohtake T, Brandt C, Strickland I, Boguniewicz M, Ganz T, et al. Endogenous antimicrobial peptides and skin infections in atopic dermatitis. *N Engl J Med* (2002) 347(15):1151–60. doi: 10.1056/NEJMoa021481
60. Howell MD, Jones JF, Kisich KO, Streib JE, Gallo RL, Leung DY. Selective killing of vaccinia virus by LL-37: implications for eczema vaccinatum. *J Immunol* (2004) 172(3):1763–7. doi: 10.4049/jimmunol.172.3.1763
61. Grigoryev DN, Howell MD, Watkins TN, Chen YC, Cheadle C, Boguniewicz M, et al. Vaccinia virus-specific molecular signature in atopic dermatitis skin. *J Allergy Clin Immunol* (2010) 125(1):153–159.e28. doi: 10.1016/j.jaci.2009.10.024
62. Senkevich TG, Koonin EV, Bugert JJ, Darai G, Moss B. The genome of molluscum contagiosum virus: analysis and comparison with other poxviruses. *Virology* (1997) 233(1):19–42. doi: 10.1006/viro.1997.8607
63. Dourmashkin R, Bernhard W. A study with the electron microscope of the skin tumour of molluscum contagiosum. *J Ultrastruct Res* (1959) 3:11–38. doi: 10.1016/S0022-5320(59)80011-3
64. Vreeswijk J, Leene W, Kalsbeek GL. Early interactions of the virus Molluscum contagiosum with its host cell. Virus-induced alterations in the basal and suprabasal layers of the epidermis. *J Ultrastruct Res* (1976) 54 (1):37–52. doi: 10.1016/s0022-5320(76)80006-8
65. Manti S, Amorini M, Cuppari C, Sapietro A, Procino F, Leonardi S, et al. Filaggrin mutations and Molluscum contagiosum skin infection in patients with atopic dermatitis. *Ann Allergy Asthma Immunol* (2017) 119(5):446–51. doi: 10.1016/j.anai.2017.07.019
66. Olsen JR, Piguet V, Gallacher J, Francis NA. Molluscum contagiosum and associations with atopic eczema in children: a retrospective longitudinal study in primary care. *Br J Gen Pract* (2016) 66(642):e53–8. doi: 10.3399/bjgp15X688093
67. Almeida HLJr, Abuchaim MO, Schneide MA, Marques L, Castro LA. Scanning electron microscopy of molluscum contagiosum. *Bras Dermatol* (2013) 88(1):90–3. doi: 10.1590/s0365-05962013000100011

68. Bhawan J, Dayal Y, Bhan AK. Langerhans cells in molluscum contagiosum, verruca vulgaris, plantar wart, and condyloma acuminatum. *J Am Acad Dermatol* (1986) 15(4 Pt 1):645–9. doi: 10.1016/s0190-9622(86)70219-3
69. Yamauchi-Yamada A, Yamamoto T, Nakayama Y, Ikedo K, Miyao T, Yamaguchi M, et al. Immune escape phenomenon in molluscum contagiosum and the induction of apoptosis. *J Dermatol* (2014) 41 (12):1058–64. doi: 10.1111/1346-8138.12695
70. Epstein WL. Molluscum contagiosum. *Semin Dermatol* (1992) 11(3):184–9.
71. Steffen C, Markman JA. Spontaneous disappearance of molluscum contagiosum. Report of a case. *Arch Dermatol* (1980) 116(8):923–4. doi: 10.1001/archderm.116.8.923
72. Ku JK, Kwon HJ, Kim MY, Kang H, Song PI, Armstrong CA, et al. Expression of Toll-like receptors in verruca and molluscum contagiosum. *J Korean Med Sci* (2008) 23(2):307–14. doi: 10.3346/jkms.2008.23.2.307
73. Vermi W, Fisogni S, Salogni L, Schärer L, Kutzner H, Sozzani S, et al. Spontaneous regression of highly immunogenic Molluscum contagiosum virus (MCV)-induced skin lesions is associated with plasmacytoid dendritic cells and IFN-DC infiltration. *J Invest Dermatol* (2011) 131(2):426–34. doi: 10.1038/jid.2010.256
74. Cohen JI. The varicella-zoster virus genome. *Curr Top Microbiol Immunol* (2010) 342:1–14. doi: 10.1007/82_2010_10
75. Ku CC, Zerboni L, Ito H, Graham BS, Wallace M, Arvin AM. Varicella-zoster virus transfer to skin by T Cells and modulation of viral replication by epidermal cell interferon-alpha. *J Exp Med* (2004) 200(7):917–25. doi: 10.1084/jem.20040634
76. Moffat JF, Stein MD, Kaneshima H, Arvin AM. Tropism of varicella-zoster virus for human CD4+ and CD8+ T lymphocytes and epidermal cells in SCID-hu mice. *J Virol* (1995) 69(9):5236–42. doi: 10.1128/JVI.69.9.5236-5242.1995
77. Vleck SE, Oliver SL, Brady JJ, Blau HM, Rajamani J, Sommer MH, et al. Structure-function analysis of varicella-zoster virus glycoprotein H identifies domain-specific roles for fusion and skin tropism. *Proc Natl Acad Sci U S A* (2011) 108(45):18412–7. doi: 10.1073/pnas.1111333108
78. Yang E, Arvin AM, Oliver SL. The Glycoprotein B Cytoplasmic Domain Lysine Cluster Is Critical for Varicella-Zoster Virus Cell-Cell Fusion Regulation and Infection. *J Virol* (2016) 91(1):e01707–16. doi: 10.1128/JVI.01707-16
79. Oliver SL, Brady JJ, Sommer MH, Richelt M, Sung P, Blau HM, et al. An immunoreceptor tyrosine-based inhibition motif in varicella-zoster virus glycoprotein B regulates cell fusion and skin pathogenesis. *Proc Natl Acad Sci U S A* (2013) 110(5):1911–6. doi: 10.1073/pnas.1216985110
80. Yu HR, Huang HC, Kuo HC, Sheen JM, Ou CY, Hsu TY, et al. IFN-α production by human mononuclear cells infected with varicella-zoster virus through TLR9-dependent and -independent pathways. *Cell Mol Immunol* (2011) 8(2):181–8. doi: 10.1038/cmi.2010.84
81. Kim JA, Park SK, Seo SW, Lee CH, Shin OS. STING Is Involved in Antiviral Immune Response against VZV Infection via the Induction of Type I and III IFN Pathways. *J Invest Dermatol* (2017) 137(10):2101–9. doi: 10.1016/j.jid.2017.03.041
82. Arvin AM, Kushner JH, Feldman S, Baehner RL, Hammond D, Merigan TC. Human leukocyte interferon for treatment of varicella in children with cancer. *N Engl J Med* (1982) 306:761–7. doi: 10.1056/NEJM198204013061301
83. Sen N, Sung P, Panda A, Arvin AM. Distinctive Roles for Type I and Type II Interferons and Interferon Regulatory Factors in the Host Cell Defense against Varicella-Zoster Virus. *J Virol* (2018) 92(21):e01151–18. doi: 10.1128/JVI.01151-18
84. Erdemli N, Ünal Ş, Okur H, Seçmeer G, Kara A, Gürgey A. Transient depletion of innate immunity in varicella infections in otherwise healthy children. *Turk J Haematol* (2009) 26(1):12–6.
85. Notarangelo LD, Mazzolari E. Natural killer cell deficiencies and severe varicella infection. *J Pediatr* (2006) 148(4):563–4. doi: 10.1016/j.jpeds.2005.06.028
86. Smola S. Immunopathogenesis of HPV-Associated Cancers and Prospects for Immunotherapy. *Viruses* (2017) 9(9):254. doi: 10.3390/v9090254
87. Tampa M, Mitran CI, Mitran MI, Ilinca N, Dumitru A, Matei C, et al. The Role of Beta HPV Types and HPV-Associated Inflammatory Processes in Cutaneous Squamous Cell Carcinoma. *J Immunol Res* (2020) 2020:5701639. doi: 10.1155/2020/5701639
88. Brianti P, De Flammineis E, Mercuri SR. Review of HPV-related diseases and cancers. *New Microbiol* (2017) 40(2):80–5.
89. Tommasino M. HPV and skin carcinogenesis. *Papillomavirus Res* (2019) 7:129–31. doi: 10.1016/j.pvr.2019.04.003
90. Gheit T. Mucosal and Cutaneous Human Papillomavirus Infections and Cancer Biology. *Front Oncol* (2019) 9:355. doi: 10.3389/fonc.2019.00355
91. Pyeon D, Pearce SM, Lank SM, Ahlquist P, Lambert PF. Establishment of human papillomavirus infection requires cell cycle progression. *PLoS Pathog* (2009) 5(2):e1000318. doi: 10.1371/journal.ppat.1000318
92. Giroglou T, Florin L, Schäfer F, Streeck RE, Sapp M. Human papillomavirus infection requires cell surface heparan sulfate. *J Virol* (2001) 75(3):1565–70. doi: 10.1128/JVI.75.3.1565-1570.2001
93. Florin L, Sapp M, Spoden GA. Host-cell factors involved in papillomavirus entry. *Med Microbiol Immunol* (2012) 201(4):437–48. doi: 10.1007/s00430-012-0270-1
94. Sapp M, Bienkowska-Haba M. Viral entry mechanisms: human papillomavirus and a long journey from extracellular matrix to the nucleus. *FEBS J* (2009) 276 (24):7206–16. doi: 10.1111/j.1742-4658.2009.07400.x
95. Paaso A, Jaakola A, Syrjänen S, Louvanto K. From HPV Infection to Lesion Progression: The Role of HLA Alleles and Host Immunity. *Acta Cytol* (2019) 63(2):148–58. doi: 10.1159/000494985
96. Hornung V, Ablasser A, Charrel-Dennis M, Bauernfeind F, Horvath G, Caffrey DR, et al. AIM2 recognizes cytosolic dsDNA and forms a caspase-1-activating inflammasome with ASC. *Nature* (2009) 458(7237):514–8. doi: 10.1038/nature07725
97. Li X, Shu C, Yi G, Chaton CT, Shelton CL, Diao J, et al. Cyclic GMP-AMP synthase is activated by double-stranded DNA-induced oligomerization. *Immunity* (2013) 39(6):1019–31. doi: 10.1016/j.immuni.2013.10.019
98. Unterholzner L, Keating SE, Baran M, Horan KA, Jensen SB, Sharma S, et al. IFI16 is an innate immune sensor for intracellular DNA. *Nat Immunol* (2010) 11(11):997–1004. doi: 10.1038/ni.1932
99. Reinholz M, Kawakami Y, Salzer S, Kreter A, Dombrowski Y, Koglin S, et al. HPV16 activates the AIM2 inflammasome in keratinocytes. *Arch Dermatol Res* (2013) 305(8):723–32. doi: 10.1007/s00403-013-1375-0
100. Moerman-Herzog A, Nakagawa M. Early Defensive Mechanisms against Human Papillomavirus Infection. *Clin Vaccine Immunol* (2015) 22(8):850–7. doi: 10.1128/CVI.00223-15
101. Daud II, Scott ME, Ma Y, Shiboski S, Farhat S, Moscicki AB. Association between toll-like receptor expression and human papillomavirus type 16 persistence. *Int J Cancer* (2011) 128(4):879–86. doi: 10.1002/ijc.25400
102. Orange JS. Natural killer cell deficiency. *J Allergy Clin Immunol* (2013) 132 (3):515–25. doi: 10.1016/j.jaci.2013.07.020
103. Zhou F, Chen J, Zhao KN. Human papillomavirus 16-encoded E7 protein inhibits IFN-γ-mediated MHC class I antigen presentation and CTL-induced lysis by blocking IRF-1 expression in mouse keratinocytes. *J Gen Virol* (2013) 94(Pt 11):2504–14. doi: 10.1099/vir.0.054486-0
104. Um SJ, Rhyu JW, Kim EJ, Jeon KC, Hwang ES, Park JS. Abrogation of IRF-1 response by high-risk HPV E7 protein in vivo. *Cancer Lett* (2002) 179 (2):205–12. doi: 10.1016/s0304-3835(01)00871-0
105. Ronco LV, Karpova AY, Vidal M, Howley PM. Human papillomavirus 16 E6 oncoprotein binds to interferon regulatory factor-3 and inhibits its transcriptional activity. *Genes Dev* (1998) 12(13):2061–72. doi: 10.1101/gad.12.13.2061
106. Sperling T, Ołdak M, Walch-Rückheim B, Wickenhauser C, Doorbar J, Pfister H, et al. Human papillomavirus type 8 interferes with a novel C/EBPβ-mediated mechanism of keratinocyte CCL20 chemokine expression and Langerhans cell migration. *PLoS Pathog* (2012) 8(7):e1002833. doi: 10.1371/journal.ppat.1002833
107. Chang Y, Moore PS. Merkel cell carcinoma: a virus-induced human cancer. *Annu Rev Pathol* (2012) 7:123–44. doi: 10.1146/annurev-pathol-011110-130227
108. Feng H, Shuda M, Chang Y, Moore PS. Clonal integration of a polyomavirus in human Merkel cell carcinoma. *Science* (2008) 319(5866):1096–100. doi: 10.1126/science.1152586
109. Shuda M, Kwun HJ, Feng H, Chang Y, Moore PS. Human Merkel cell polyomavirus small T antigen is an oncoprotein targeting the 4E-BP1

translation regulator. *J Clin Invest* (2011) 121(9):3623–34. doi: 10.1172/JCI46323
110. Andres C, Puchta U, Sander CA, Ruzicka T, Flaig MJ. Prevalence of Merkel cell polyomavirus DNA in cutaneous lymphomas, pseudolymphomas, and inflammatory skin diseases. *Am J Dermatopathol* (2010) 32(6):593–8. doi: 10.1097/DAD.0b013e3181ce8beb
111. Kassem A, Schöpflin A, Diaz C, Weyers W, Stickeler E, Werner M, et al. Frequent detection of Merkel cell polyomavirus in human Merkel cell carcinomas and identification of a unique deletion in the VP1 gene. *Cancer Res* (2008) 68(13):5009–13. doi: 10.1158/0008-5472.CAN-08-0949
112. Laude HC, Jonchère B, Maubec E, Carlotti A, Marinho E, Couturaud B, et al. Distinct merkel cell polyomavirus molecular features in tumour and non tumour specimens from patients with merkel cell carcinoma. *PLoS Pathog* (2010) 6(8):e1001076. doi: 10.1371/journal.ppat.1001076
113. Becker JC, Stang A, DeCaprio JA, DeCaprio JA, Cerroni L, Lebbé C, et al. Merkel cell carcinoma. *Nat Rev Dis Primers* (2017) 3:17077. doi: 10.1038/nrdp.2017.77
114. Liu W, MacDonald M, You J. Merkel cell polyomavirus infection and Merkel cell carcinoma. *Curr Opin Virol* (2016a) 20:20–7. doi: 10.1016/j.coviro.2016.07.011
115. Schowalter RM, Pastrana DV, Pumphrey KA, Moyer AL, Buck CB. Merkel cell polyomavirus and two previously unknown polyomaviruses are chronically shed from human skin. *Cell Host Microbe* (2010) 7(6):509–15. doi: 10.1016/j.chom.2010.05.006
116. Liu W, Yang R, Payne AS, Schowalter RM, Spurgeon ME, Lambert PF, et al. Identifying the Target Cells and Mechanisms of Merkel Cell Polyomavirus Infection. *Cell Host Microbe* (2016b) 19(6):775–87. doi: 10.1016/j.chom.2016.04.024
117. Schowalter RM, Pastrana DV, Buck CB. Glycosaminoglycans and sialylated glycans sequentially facilitate Merkel cell polyomavirus infectious entry. *PLoS Pathog* (2011) 7(7):e1002161. doi: 10.1371/journal.ppat.1002161
118. Neu U, Hengel H, Blaum BS, Schowalter RM, Macejak D, Gilbert M, et al. Structures of Merkel cell polyomavirus VP1 complexes define a sialic acid binding site required for infection. *PLoS Pathog* (2012) 8(7):e1002738. doi: 10.1371/journal.ppat.1002738
119. Becker M, Dominguez M, Greune L, Soria-Martinez L, Pfleiderer MM, Schowalter R, et al. Infectious Entry of Merkel Cell Polyomavirus. *J Virol* (2019) 93(6):e02004–18. doi: 10.1128/JVI.02004-18
120. Ma JE, Brewer JD. Merkel cell carcinoma in immunosuppressed patients. *Cancers (Basel)* (2014) 6(3):1328–50. doi: 10.3390/cancers6031328
121. Sihto H, Böhling T, Kavola H, Koljonen V, Salmi M, Jalkanen S, et al. Tumor infiltrating immune cells and outcome of Merkel cell carcinoma: a population-based study. *Clin Cancer Res* (2012) 18(10):2872–81. doi: 10.1158/1078-0432.CCR-11-3020
122. Paulson KG, Iyer JG, Tegeder AR, Thibodeau R, Schelter J, Koba S, et al. Transcriptome-wide studies of merkel cell carcinoma and validation of intratumoral CD8+ lymphocyte invasion as an independent predictor of survival. *J Clin Oncol* (2011) 29(12):1539–46. doi: 10.1200/JCO.2010.30.6308
123. Shahzad N, Shuda M, Gheit T, Kwun HJ, Cornet I, Saidj D, et al. The T antigen locus of Merkel cell polyomavirus downregulates human Toll-like receptor 9 expression. *J Virol* (2013) 87(23):13009–19. doi: 10.1128/JVI.01786-13
124. Griffiths DA, Abdul-Sada H, Knight LM, Jackson BR, Richards K, Prescott EL, et al. Merkel cell polyomavirus small T antigen targets the NEMO adaptor protein to disrupt inflammatory signaling. *J Virol* (2013) 87(24):13853–67. doi: 10.1128/JVI.02159-13
125. Paulson KG, Tegeder A, Willmes C, Iyer JG, Afanasiev OK, Schrama D, et al. Downregulation of MHC-I expression is prevalent but reversible in Merkel cell carcinoma. *Cancer Immunol Res* (2014) 2(11):1071–9. doi: 10.1158/2326-6066.CIR-14-0005
126. Caraballo H, King K. Emergency department management of mosquito-borne illness: malaria, dengue, and West Nile virus. *Emerg Med Pract* (2014) 16(5):1–24.
127. Chibueze EC, Tirado V, Lopes KD, Balogun OO, Takemoto Y, Swa T, et al. Zika virus infection in pregnancy: a systematic review of disease course and complications. *Reprod Health* (2017) 14(1):28. doi: 10.1186/s12978-017-0285-6
128. Duangkhae P, Erdos G, Ryman KD, Watkins SC, Falo LDJr, Marques ETAJr, et al. Interplay between Keratinocytes and Myeloid Cells Drives Dengue Virus Spread in Human Skin. *J Invest Dermatol* (2018) 138(3):618–26. doi: 10.1016/j.jid.2017.10.018
129. Hamel R, Dejarnac O, Wichit S, Ekchariyawat P, Neyret A, Luplertlop N, et al. Biology of Zika Virus Infection in Human Skin Cells. *J Virol* (2015) 89(17):8880–96. doi: 10.1128/JVI.00354-15
130. Lim PY, Behr MJ, Chadwick CM, Shi PY, Bernard KA. Keratinocytes are cell targets of West Nile virus in vivo. *J Virol* (2011) 85(10):5197–201. doi: 10.1128/JVI.02692-10
131. Kovats S, Turner S, Simmons A, Powe T, Chakravarty E, Alberola-Ila J. West Nile virus-infected human dendritic cells fail to fully activate invariant natural killer T cells. *Clin Exp Immunol* (2016) 186(2):214–26. doi: 10.1111/cei.12850
132. Chen Y, Maguire T, Hileman RE, Fromm JR, Esko JD, Linhardt J, et al. Dengue virus infectivity depends on envelope protein binding to target cell heparan sulfate. *Nat Med* (1997) 3(8):866–71. doi: 10.1038/nm0897-866
133. Stiasny K, Fritz R, Pangerl K, Heinz FX. Molecular mechanisms of flavivirus membrane fusion. *Amino Acids* (2011) 41(5):1159–63. doi: 10.1007/s00726-009-0370-4
134. Laureti M, Narayanan D, Rodriguez-Andres J, Fazakerley JK, Kedzierski L. Flavivirus Receptors: Diversity, Identity, and Cell Entry. *Front Immunol* (2018) 9:2180. doi: 10.3389/fimmu.2018.02180
135. Hackett BA, Cherry S. Flavivirus internalization is regulated by a size-dependent endocytic pathway. *Proc Natl Acad Sci U S A* (2018) 115(16):4246–51. doi: 10.1073/pnas.1720032115
136. Matusali G, Colavita F, Bordi L, Lalle E, Ippolito G, Capobianchi MR, et al. Tropism of the Chikungunya VirusPublished 2019 Feb 20. *Viruses* (2019) 11(2):175. doi: 10.3390/v11020175
137. van Duijl-Richter MK, Hoornweg TE, Rodenhuis-Zybert IA, Smit JM. Early Events in Chikungunya Virus Infection-From Virus Cell Binding to Membrane Fusion. *Viruses* (2015) 7(7):3647–74. doi: 10.3390/v7072792
138. Selvarajah S, Sexton NR, Kahle KM, Fong RH, Mattia KA, Gardner J, et al. A neutralizing monoclonal antibody targeting the acid-sensitive region in chikungunya virus E2 protects from disease. *PLoS Negl Trop Dis* (2013) 7(9):e2423. doi: 10.1371/journal.pntd.0002423
139. Nasirudeen AM, Wong HH, Thien P, Xu S, Lam KP, Liu DX. RIG-I, MDA5 and TLR3 synergistically play an important role in restriction of dengue virus infection. *PLoS Negl Trop Dis* (2011) 5(1):e926. doi: 10.1371/journal.pntd.0000926
140. Ekchariyawat P, Hamel R, Bernard E, Wichit S, Surasombatpattana P, Talignani L, et al. Inflammasome signaling pathways exert antiviral effect against Chikungunya virus in human dermal fibroblasts. *Infect Genet Evol* (2015) 32:401–8. doi: 10.1016/j.meegid.2015.03.025
141. Priya R, Patro IK, Parida MM. TLR3 mediated innate immune response in mice brain following infection with Chikungunya virus. *Virus Res* (2014) 189:194–205. doi: 10.1016/j.virusres.2014.05.010
142. Wichit S, Hamel R, Yainoy S, Gumpangseth N, Panich S, Phuadraksa T, et al. Interferon-inducible protein (IFI) 16 regulates Chikungunya and Zika virus infection in human skin fibroblasts. *EXCLI J* (2019) 18:467–76. doi: 10.17179/excli2019-1271
143. Kwock JT, Handfield C, Suwanpradid J, Hoang P, McFadden MJ, Labagnara KF, et al. IL-27 signaling activates skin cells to induce innate antiviral proteins and protects against Zika virus infection. *Sci Adv* (2020) 6(14):eaay3245. doi: 10.1126/sciadv.aay3245
144. Schmid MA, Harris E. Monocyte recruitment to the dermis and differentiation to dendritic cells increases the targets for dengue virus replication. *PLoS Pathog* (2014) 10(12):e1004541. doi: 10.1371/journal.ppat.1004541
145. Conway MJ, Londono-Renteria B, Troupin A, Watson AM, Klimstra WB, Fikrig E, et al. Aedes aegypti D7 Saliva Protein Inhibits Dengue Virus Infection. *PLoS Negl Trop Dis* (2016) 10(9):e0004941. doi: 10.1371/journal.pntd.0004941
146. Jin L, Guo X, Shen C, Hao X, Sun P, Li P, et al. Salivary factor LTRIN from Aedes aegypti facilitates the transmission of Zika virus by interfering with the lymphotoxin-β receptor. *Nat Immunol* (2018) 19(4):342–53. doi: 10.1038/s41590-018-0063-9
147. Thangamani S, Higgs S, Ziegler S, Vanlandingham D, Tesh R, Wikel S. Host immune response to mosquito-transmitted chikungunya virus differs from

that elicited by needle inoculated virus. *PLoS One* (2010) 5(8):e12137. doi: 10.1371/journal.pone.0012137
148. Puiprom O, Morales Vargas RE, Potiwat R, Chaichana P, Ikuta K, Ramasoota P, et al. Characterization of chikungunya virus infection of a human keratinocyte cell line: role of mosquito salivary gland protein in suppressing the host immune response. *Infect Genet Evol* (2013) 17:210–5. doi: 10.1016/j.meegid.2013.04.005
149. Schneider BS, Soong L, Coffey LL, Stevenson HL, McGee CE, Higgs S. Aedes aegypti saliva alters leukocyte recruitment and cytokine signaling by antigen-presenting cells during West Nile virus infection. *PLoS One* (2010) 5(7): e11704. doi: 10.1371/journal.pone.0011704
150. Garcia M, Alout H, Diop F, Damour A, Bengue M, Weill M, et al. Innate Immune Response of Primary Human Keratinocytes to West Nile Virus Infection and Its Modulation by Mosquito Saliva. *Front Cell Infect Microbiol* (2018) 8:387. doi: 10.3389/fcimb.2018.00387
151. Metz P, Reuter A, Bender S, Bartenschlager R. Interferon-stimulated genes and their role in controlling hepatitis C virus. *J Hepatol* (2013) 59(6):1331–41. doi: 10.1016/j.jhep.2013.07.033
152. Olsen JR, Gallacher J, Piguet V, Francis NA. Epidemiology of molluscum contagiosum in children: a systematic review. *Fam Pract* (2014) 31(2):130–6. doi: 10.1093/fampra/cmt075
153. Walsh SR, Dolin R. Vaccinia viruses: vaccines against smallpox and vectors against infectious diseases and tumors. *Expert Rev Vaccines* (2011) 10 (8):1221–40. doi: 10.1586/erv.11.79
154. Eichenfield LF, Ellis CN, Mancini AJ, Paller AS, Simpson EL. Atopic dermatitis: epidemiology and pathogenesis update. *Semin Cutan Med Surg* (2012) 31(3 Suppl):S3–5. doi: 10.1016/j.sder.2012.07.002
155. Corey L, Wald A. Maternal and neonatal herpes simplex virus infections. *N Engl J Med* (2009) 361(14):1376–85. doi: 10.1056/NEJMra0807633. [published correction appears in N Engl J Med. 2009 Dec 31;361(27):2681].
156. Itzhaki RF. Corroboration of a Major Role for Herpes Simplex Virus Type 1 in Alzheimer's Disease. *Front Aging Neurosci* (2018) 10:324. doi: 10.3389/fnagi.2018.00324
157. John AR, Canaday DH. Herpes Zoster in the Older Adult. *Infect Dis Clin North Am* (2017) 31(4):811–26. doi: 10.1016/j.idc.2017.07.016
158. Stamatas GN, Nikolovski J, Luedtke MA, Kollias N, Wiegand BC. Infant skin microstructure assessed in vivo differs from adult skin in organization and at the cellular level. *Pediatr Dermatol* (2010) 27(2):125–31. doi: 10.1111/j.1525-1470.2009.00973.x
159. Farage MA, Miller KW, Elsner P, Maibach HI. Characteristics of the Aging Skin. *Adv Wound Care (N Rochelle)* (2013) 2(1):5–10. doi: 10.1089/wound.2011.0356
160. Xie G, Luo H, Pang L, Peng BH, Winkelmann E, McGruder B, et al. Dysregulation of Toll-Like Receptor 7 Compromises Innate and Adaptive T Cell Responses and Host Resistance to an Attenuated West Nile Virus Infection in Old Mice. *J Virol* (2016) 90(3):1333–44. doi: 10.1128/JVI.02488-15
161. McGuckin Wuertz K, Treuting PM, Hemann EA, Esser-Nobis K, Snyder AG, Graham JB, et al. STING is required for host defense against neuropathological West Nile virus infection. *PLoS Pathog* (2019) 15(8): e1007899. doi: 10.1371/journal.ppat.1007899
162. Elewa RM, Abdallah MA, Zouboulis CC. Age-associated skin changes in innate immunity markers reflect a complex interaction between aging mechanisms in the sebaceous gland. *J Dermatol* (2015) 42(5):467–76. doi: 10.1111/1346-8138.12793
163. Iram N, Mildner M, Prior M, Petzelbauer P, Fiala C, Hacker S, et al. Age-related changes in expression and function of Toll-like receptors in human skin. *Development* (2012) 139(22):4210–9. doi: 10.1242/dev.083477
164. Dorschner RA, Lin KH, Murakami M, Gallo RL. Neonatal skin in mice and humans expresses increased levels of antimicrobial peptides: innate immunity during development of the adaptive response. *Pediatr Res* (2003) 53(4):566–72. doi: 10.1203/01.PDR.0000057205.64451.B7
165. Zhang LJ, Chen SX, Guerrero-Juarez CF, Li F, Yong Y, Liang Y, et al. Age-Related Loss of Innate Immune Antimicrobial Function of Dermal Fat Is Mediated by Transforming Growth Factor Beta. *Immunity* (2019) 50(1):121–136.e5. doi: 10.1016/j.immuni.2018.11.003
166. Klein SL, Flanagan KL. Sex differences in immune responses. *Nat Rev Immunol* (2016) 16(10):626–38. doi: 10.1038/nri.2016.90
167. Giefing-Kroll C, Berger P, Lepperdinger G, Grubeck-Loebenstein B. How sex and age affect immune responses, susceptibility to infections, and response to vaccination. *Aging Cell* (2015) 14:309–21. doi: 10.1111/acel.12326
168. Berghofer B, Frommer T, Haley G, Fink L, Bein G, Hackstein H. TLR7 ligands induce higher IFN-alpha production in females. *J Immunol* (2006) 177(4):2088–96. doi: 10.4.4049/jimmunol.177.4.2088
169. Hannah MF, Bajic VB, Kelin SL. Sex differences in the recognition of and innate antiviral responses to Seoul virus in Norway rats. *Brain Behav Immun* (2008) 22(4):503–16. doi: 10.1016/j.bbi.2007.10.005
170. Puchhammer-Stöckl E, Aberle SW, Heinzl H. Association of age and gender with alphaherpesvirus infections of the central nervous system in the immunocompetent host. *J Clin Virol* (2012) 53(4):356–9. doi: 10.1016/j.jcv.2011.12.015
171. McClelland EE, Smith JM. Gender specific differences in the immune response to infection. *Arch Immunol Ther Exp (Warsz)* (2011) 59(3):203–13. doi: 10.1007/x00005-11-0124-3
172. Kabra SK, Jain Y, Pandey RM, Madhulika, Singhal T, Tripathi P, et al. Dengue haemorrhagic fever in children in the 1996 Delhi epidemic. *Trans R Soc Trop Med Hyg* (1999) 93(3):294–8. doi: 10.1016/s0035-9203(99)90027-5
173. Schrama D, Peitsch WK, Zapatka M, Kneitz H, Houben R, Eib S, et al. Merkel cell polyomavirus status is not associated with clinical course of Merkel cell carcinoma. *J Invest Dermatol* (2011) 131(8):1631–8. doi: 10.1038/jid.2011.115
174. Wang L, Harms PW, Palanisamy N, Carskadon S, Cao X, Siddiqui J, et al. Age and Gender Associations of Virus Positivity in Merkel Cell Carcinoma Characterized Using a Novel RNA In Situ Hybridization Assay. *Clin Cancer Res* (2017) 23(18):5622–30. doi: 10.1158/1078-0432.CCR-17-0299
175. Rabenau HF, Buxbaum S, Preiser W, Weber B, Doerr HW. Seroprevalence of herpes simplex virus types 1 and type 2 in the Frankfurt am Main area, Germany. *Med Microbiol Immunol* (2002) 190(4):153–60. doi: 10.1007/s00430-001-0102-1
176. Glynn JR, Crampin AC, Ngwira BM, Ndhlovu R, Mwanyongo O, Fine PE. Herpes simplex virus type 2 trends in relation to the HIV epidemic in northern Malawi. *Sex Transm Infect* (2008) 84(5):356–60. doi: 10.1136/sti.2008.030056
177. Bhavanam S, Snider DP, Kaushic C. Intranasal and subcutaneous immunization under the effect of estradiol leads to better protection against genital HSV-2 challenge compared to progesterone. *Vaccine* (2008) 26(48):6165–72. doi: 10.1016/j.vaccine.2008.08.045
178. MacDonald EM, Savoy A, Gillgrass A, Fernandez S, Smieja M, Rosenthal KL, et al. Susceptibility of human female primary genital epithelial cells to herpes simplex virus, type-2 and the effect of TLR3 ligand and sex hormones on infection. *Biol Reprod* (2007) 77(6):1049–59. doi: 10.1095/biolreprod.107.063933.jmb.2013.11.012
179. Grice EA, Kong HH, Conlan S, Deming CB, David J, Young AC, et al. Topographical and temporal diversity of the human skin microbiome. *Science* (2009) 324(5931):1190–2. doi: 10.1126/science.1171700
180. Younge NE, Araújo-Pérez F, Brandon D, Seed PC. Early-life skin microbiota in hospitalized preterm and full-term infants. *Microbiome* (2018) 6(1):98. doi: 10.1186/s40168-018-0486-4
181. Naik S, Bouladoux N, Wilhelm C, Molloy MJ, Salcedo R, Kastenmuller W, et al. Compartmentalized control of skin immunity by resident commensals. *Science* (2012) 337(6098):1115–9. doi: 10.1126/science.1225152
182. Kong HH, Oh J, Deming C, Conlan S, Grice EA, Beatson MA, et al. Temporal shifts in the skin microbiome associated with disease flares and treatment in children with atopic dermatitis. *Genome Res* (2012) 22(5):850–9. doi: 10.1101/gr.131029.111
183. Wang WM, Jin HZ. Skin Microbiome: An Actor in the Pathogenesis of Psoriasis. *Chin Med J (Engl)* (2018) 131(1):95–8. doi: 10.4103/0366-6999.221269
184. Beylot C, Auffret N, Poli F, Claudel JP, Leccia MT, Del Giudice P, et al. Propionibacterium acnes: an update on its role in the pathogenesis of acne. *J Eur Acad Dermatol Venereol* (2014) 28(3):271–8. doi: 10.1111/jdv.12224
185. Paller AS, Kong HH, Seed P, Naik S, Scharschmidt TC, Gallo RL, et al. The microbiome in patients with atopic dermatitis. *J Allergy Clin Immunol* (2019) 143(1):26–35. doi: 10.1016/j.jaci.2018.11.015. [published correction appears in J Allergy Clin Immunol. 2019 Apr;143(4):1660].
186. Bastos MC, Ceotto H, Coelho ML, Nascimento JS. Staphylococcal antimicrobial peptides: relevant properties and potential biotechnological

applications. *Curr Pharm Biotechnol* (2009) 10(1):38–61. doi: 10.2174/138920109787048580

187. Cogen AL, Yamasaki K, Sanchez KM, Dorschner RA, Lai Y, MacLeod DT, et al. Selective antimicrobial action is provided by phenol-soluble modulins derived from Staphylococcus epidermidis, a normal resident of the skin. *J Invest Dermatol* (2010) 130(1):192–200. doi: 10.1038/jid.2009.243
188. Faye T, Holo H, Langsrud T, Nes IF, Brede DA. The unconventional antimicrobial peptides of the classical propionibacteria. *Appl Microbiol Biotechnol* (2011) 89(3):549–54. doi: 10.1007/s00253-010-2967-7
189. Tirosh O, Conlan S, Deming C, Lee-lin SQ, Huang X, Su HC, et al. Expanded skin virome in DOCK8-deficient patients. *Nat Med* (2018) 24(12):1815–21. doi: 10.1038/s41591-018-0211-7
190. Pfeiffer JK, Sonnenburg JL. The intestinal microbiota and viral susceptibility. *Front Microbiol* (2011) 2:92. doi: 10.3389/fmicb.2011.00092
191. Tanaka K, Sawamura S, Satoh T, Kobayashi K, Noda S. Role of the indigenous microbiota in maintaining the virus-specific CD8 memory T cells in the lung of mice infected with murine cytomegalovirus. *J Immunol* (2007) 178(8):5209–16. doi: 10.4049/jimmunol.178.8.5209
192. Chen HW, Liu PF, Liu YT, Kuo S, Zhang XQ, Schooley RT, et al. Nasal commensal Staphylococcus epidermidis counteracts influenza virus. *Sci Rep* (2016) 6:27870. doi: 10.1038/srep27870
193. Kanmani P, Clua P, Vizoso-Pinto MG, Rodriguez C, Alvarez S, Melnikov V, et al. Respiratory Commensal Bacteria *Corynebacterium pseudodiphtheriticum* Improves Resistance of Infant Mice to Respiratory Syncytial Virus and *Streptococcus pneumoniae* Superinfection. *Front Microbiol* (2017) 8:1613. doi: 10.3389/fmicb.2017.01613
194. Oh JE, Kim BC, Chang DH, Kwon M, Lee SY, Kang D, et al. Dysbiosis-induced IL-33 contributes to impaired antiviral immunity in the genital mucosa. *Proc Natl Acad Sci U S A* (2016) 113(6):E762–71. doi: 10.1073/pnas.1518589113

Conflict of Interest: AM consults for Silab and is on the scientific evaluation committee of the LEO Foundation and receives honoraria. AM's spouse is employed by Precision BioSiences and holds stock and stock options. AA received the Pfizer Independent Grant for Learning and Change and has consulted for Henkel.

The remaining authors declare that the research was conducted in the absence of any commercial or financial relationships that could be construed as a potential conflict of interest.

frontiers in Immunology

REVIEW
published: 02 December 2020
doi: 10.3389/fimmu.2020.605644

Skin Immunity to Dermatophytes: From Experimental Infection Models to Human Disease

Verónica L. Burstein[1,2], *Ignacio Beccacece*[1,2], *Lorena Guasconi*[1,2], *Cristian J. Mena*[1,2], *Laura Cervi*[1,2] *and Laura S. Chiapello*[1,2]*

[1] Laboratorio de Parasitología y Micología Experimental. Departamento de Bioquímica Clínica, Facultad de Ciencias Químicas, Universidad Nacional de Córdoba, Córdoba, Argentina, [2] Centro de Investigaciones en Bioquímica Clínica e Inmunología (CIBICI), Consejo Nacional de Investigaciones Científicas y Técnicas (CONICET), Córdoba, Argentina

Dermatophytoses (ringworms) are among the most frequent skin infections and are a highly prevalent cause of human disease worldwide. Despite the incidence of these superficial mycoses in healthy people and the compelling evidence on chronic and deep infections in immunocompromised individuals, the mechanisms controlling dermatophyte invasion in the skin are scarcely known. In the last years, the association between certain primary immunodeficiencies and the susceptibility to severe dermatophytosis as well as the evidence provided by novel experimental models mimicking human disease have significantly contributed to deciphering the basic immunological mechanisms against dermatophytes. In this review, we outline the current knowledge on fungal virulence factors involved in the pathogenesis of dermatophytoses and recent evidence from human infections and experimental models that shed light on the cells and molecules involved in the antifungal cutaneous immune response. The latest highlights emphasize the contribution of C-type lectin receptors signaling and the cellular immune response mediated by IL-17 and IFN-γ in the anti-dermatophytic defense and skin inflammation control.

Keywords: skin immunity, mycoses, antifungal immunity, fungal pathogenesis, interleukin-17

OPEN ACCESS

Edited by:
Fatima Conceição-Silva, Oswaldo Cruz Foundation, Brazil

Reviewed by:
Agostinho Carvalho, University of Minho, Portugal
Nalu Teixeira De Aguiar Peres, Federal University of Minas Gerais, Brazil

***Correspondence:**
Laura S. Chiapello
laura.chiapello@unc.edu.ar

Specialty section:
This article was submitted to Microbial Immunology, a section of the journal Frontiers in Immunology

Received: *12 September 2020*
Accepted: *03 November 2020*
Published: *02 December 2020*

Citation:
Burstein VL, Beccacece I, Guasconi L, Mena CJ, Cervi L and Chiapello LS (2020) Skin Immunity to Dermatophytes: From Experimental Infection Models to Human Disease. Front. Immunol. 11:605644. doi: 10.3389/fimmu.2020.605644

INTRODUCTION

The skin is the most extensive organ of the body, is an ecological niche for microbiota and the first barrier against aggression from environmental noxa and pathogenic microorganisms. Not only is a physical barrier but also a dynamic system constituted by the skin resident immune system that is crucial to control an infection, resolve damage, or maintain tissue homeostasis. Among the most frequent human skin infections, dermatophytoses (ringworms) represent the fourth cause of disease with a global incidence estimated in 20 to 25% within the healthy population (1–3). These infections are caused by filamentous fungi, ancestrally digesters of soil keratin, that have adapted to the keratinized tissue of mammals, and became parasitic microorganisms to animals and humans. Therefore, dermatophytoses are characterized by hyphae superficial invasion into the skin, hair, and nails causing subacute or chronic infections with different inflammation degrees among immunocompetent individuals (**Figure 1**). Recent taxonomic changes classify dermatophytes into five genera: *Epidermophyton*, *Trichophyton*,

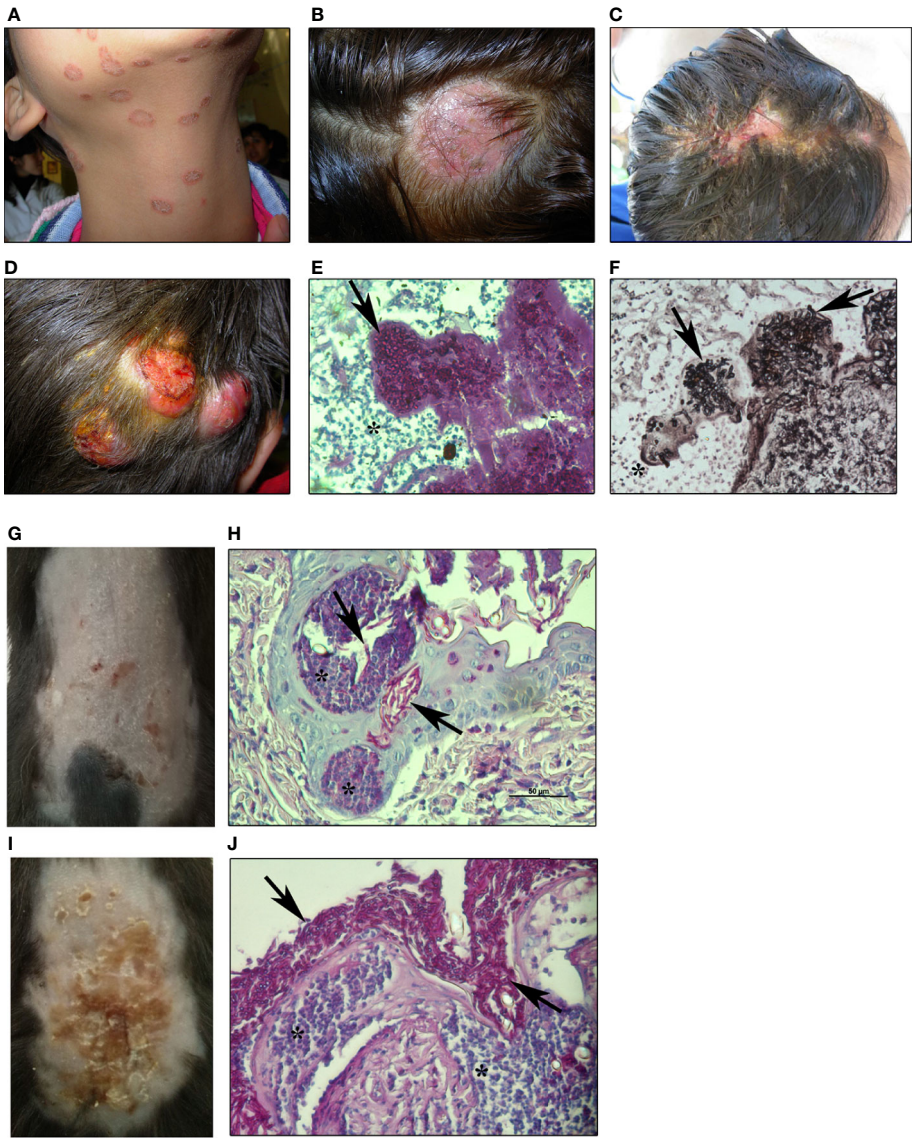

FIGURE 1 | Human and experimental dermatophytosis **(A, B)**. Superficial mild inflammatory infections in humans by *M. canis* **(A)** *tinea corporis* and **(B)** *tinea capitis* by *M. canis* **(C–F)**. Inflammatory human dermatophytosis **(C)**: inflammatory *tinea capitis* (*Kerion de Celsi*) by *T. mentagrophytes* and **(D)** deep infection of the scalp by *M. canis* (ref. 106) showing hyphae in dermis **(E)** stained with PAS-hematoxylin or **(F)** Grocott-Gomori's methenamine silver (GMS) staining (200x magnification) **(G–J)**. Experimental dermatophytosis after epicutaneous infection of **(G, H)** wild-type (WT) or **(I, J)** IL-17RA-deficient C57BL/6 mice with *M. canis* (8 days post-infection) (ref. 51) **(G)**. Mild inflammatory lesions and **(H)** histopathology showing PAS-positive hyphae invading the *stratum corneum* and hair follicles in WT **(I)**. Highly inflammatory lesions and **(J)** histopathology showing extensive superficial fungal proliferation in IL-17RA-deficient mice. Arrows: *M. canis* hyphae. Asterix: inflammatory reaction (400x magnification). All images are property of Chiapello's lab.

Microsporum, Arthroderma, and *Nannizzia* (4) and, among them, there are different species adapted to particular ecological niches and hosts which led to the classification in geophilic, zoophilic and anthropophilic fungi. Anthropophilic species (*Trichophyton rubrum, Epidermophyton floccosum*) are well adapted to humans and often cause chronic infections with mild clinical symptoms. In contrast, dermatophytes from animals (*Microsporum canis, Trichophyton/Arthroderma benhamiae, Trichophyton mentagrophytes*, etc.) or soil (*Nannizzia gypsea/Microsporum gypseum*) are frequently isolated from patients suffering from mild to highly inflammatory dermatophytosis but with lesions that are prone to spontaneous resolution (5) (**Figure 1**). In contrast, the immunosuppressed population (especially cell-mediated immunity deficiency settings such as HIV-AIDS, transplant, neoplasia, diabetes, or corticosteroid therapy) is particularly susceptible to these infections showing extensive superficial lesions that are often unresponsive to conventional antifungal treatment (3, 6, 7). This was recently observed in India where there was a significant increase

in treatment-recalcitrant, recurrent and chronic dermatophytosis probably due to indiscriminate use of antibiotics and corticosteroid drug combination (8).

Despite the high incidence of dermatophytosis in healthy people as well as the complications of these infections in immunocompromised individuals, the immune mechanisms that control dermatophyte invasion are less known and studied than those involved in other fungal diseases. In the last years, the identification of genetic mutations in patients with primary immunodeficiencies associated with severe deep or widespread dermatophytosis and the development of experimental models that mimic human infection have contributed to deciphering the basic mechanisms of cutaneous immunity against dermatophytes. Taking into account the recent evidence from human infections and experimental models, in this review we discuss the latest advances in the knowledge and state-of-the-art of innate and adaptive mechanisms of the immune response against dermatophyte fungi.

DERMATOPHYTE VIRULENCE FACTORS

In order to degrade keratin, dermatophytes secrete an arsenal of hydrolytic enzymes (proteases) which are assumed to be the main virulence factors in live tissue infection (9). It is known that the pathogenesis of dermatophytosis includes several stages (i.e. fungal adhesion, germination, invasion, penetration) associated with the secretion of enzymes to degrade skin components (10–12) (**Table 1**). Although there is a common understanding that dermatophyte keratinases are of major relevance for pathogenicity, the entire process of host adaptation during infection seems to be quite complex (15).

The colonization by anthropophilic species in humans or zoophilic species in animals usually causes asymptomatic infections or, eventually, chronic infections with minimal inflammation response suggesting a specific adaptation to the host probably in favor of survival and transmission. On the contrary, human infections with geophilic or zoophilic dermatophytes occur with inflammatory-associated symptoms and, generally, self-resolve (**Figure 1**). Therefore, depending on the host and the infective species, dermatophytes might differentially express virulence factors and activate, or suppress, particular immune receptors and signaling pathways that eventually would determine their own persistence or elimination. Comparative genome studies in various dermatophyte species have revealed that there are few differences in gene regulation and post-transcriptional mechanisms among them, but whether those differences might be responsible for the host-specific adaptation remains largely unknown (26).

Several dermatophyte enzymes and proteins participate in the keratin degradation and keratinolytic proteases activity culminates in the onset and maintenance of the infection process (9, 26). However, the virulence factors that are particularly related to pathogenicity degree and host adaptation have not been precisely identified yet. In the process of keratin degradation by dermatophytes, Graser et al. (12) have described three consecutive steps: first, the sulfitolysis stage [e.g., mediated by cysteine dioxygenases (20)], that liberates sulfites that reduce cysteine disulfuric bridges of the compact keratin in the stratum corneum should be in cursive to produce polypeptidic soluble chains that can be sliced by endoproteases. Second, endoproteases activity (subtilisins, deuterolysins, and fungalysins) liberates long peptides that are substrate to exoproteases (nonspecific amino- or carboxypeptidase, and prolyl peptidases) which, finally, transform

TABLE 1 | Virulence factors of dermatophytes.

Virulence factor	Description and function	References
Subtilisin-like proteases (Sub)	Endoprotease activity in keratin digestion. Reported as allergens and involved in immune response induction.	Woodfolk et al. (13). Gao and Takashima (14). Burmester et al. (15). Eymann et al. (16). Karami Robati et al. (17). Mehul et al. (18). Reviewed in Mercer and Stewart (9).
Fungalysin-like Metalloproteases (Mep)	Endoprotease activity in keratin digestion.	Burmester et al. (15). Eymann et al. (16).
Leucinaminopeptidases (Lap)	Exoprotease activity in keratin digestion.	Burmester et al. (15). Eymann et al. (16).
Dipeptidyl peptidases (Dpp)	Exoprotease activity in keratin digestion.	Burmester et al. (15). Eymann et al. (16).
Secondary metabolite production-associated enzymes	Polyketide synthase and non-ribosomal peptide synthetase.	Burmester et al. (15). Martínez et al. (19).
Cysteine dioxygenases	Sulfitolysis of keratin. Involved in triggering humoral immune response during infection.	Grumbt et al. (20). Eymann et al. (16). Reviewed in Mercer and Stewart (9).
Hydrophobins	Hydrophobin rodlet layer on conidial surface. Related to avoiding immune recognition by neutrophils.	Heddergott et al. (21). Eymann et al. (16).
Extracellular vesicles	Unknown cargo, probably virulence factors. Related with modulation of the host response.	Bitencourt et al. (22)
LysM proteins	Protein domains related to binding to skin glycoproteins. Possibly involved in immune evasion.	Martinez et al. (19). Kar et al. (23)
Heat shock proteins	Hsp 30, Hsp60, Hsp70. Associated with adaptation to human temperature, keratin digestion.	Reviewed in Martinez-Rossi et al. (24).
Other hydrolases and cell wall remodeling-associated enzymes.	Lipases, glucanases, chitinases, betaglusidases, mannosyl transferases. Many involved in triggering humoral immune response during infection.	Burmester et al. (15). Martínez et al. (19). Eymann et al. (16). Martins et al. (25).

long peptides into amino acids and short peptides that can be effectively assimilated by hyphae. Supporting this, Burmester et al. (15) analyzed the secretome of *Arthroderma benhamiae* after *in vitro* growth on keratin and revealed that about 75% of secreted proteins were proteases (subtilisin-like serine proteases: Sub3, Sub4, and Sub7; fungalysine-type metalloproteases: Mep1, Mep3, and Mep4; leucine aminopeptidases: Lap1 and Lap2; dipeptidyl-peptidases: DppIV and DppV) with the remaining formed by hydrolases and proteins involved in carbohydrate metabolism. Consistently, subtilisin proteases genes expression was detected on 93% of dermatophytes isolated from human patients (17) and, in particular, subtilisin 6 (Sub6) has been reported as the main protease secreted by *Trichophyton mentagrophytes* during guinea pig infection and human onychomycosis (14, 18). Also, Sub6 was detected in clinical samples infected with *Trichophyton rubrum* and it was one of the main allergens that produce an IgE-mediated response in susceptible hosts (5, 13). In this regard, exoproteome analysis of three *Trichophyton* species more frequently isolated from patients (*T. rubrum, T. interdigitale and A. benhamiae*) showed that, at least, 31 proteases (peptidases, oxide-reductases and beta-glucosidases) were recognized by antibodies in patients' sera, indicating that these proteins are antigens involved in triggering humoral immune response during infection (14, 16) (**Table 1**).

The ability of fungal-derived proteases to interfere with the host immune response has been demonstrated for other human pathogens. For instance, a metalloprotease released from *A. fumigatus* conidia facilitates early fungal immune evasion by cleaving complement proteins in the human host (27). Moreover, *Candida albicans* secretes aspartic proteases, that cleave pro-interleukin (IL)-1β to its biologically active form IL-1β (27) and promote inflammation, as well as candidalysin, a peptide toxin that damages epithelial membranes and triggers a danger response signaling pathway (28). Whether similar phenomena are also mediated by dermatophytes proteases is currently unknown.

On the other hand, the experimental evidence also suggests that dermatophyte pathogenesis involves mechanisms beyond the fungal machinery used for keratin degradation, including virulence factors like cell wall components and secreted products (**Table 1**). In this regard, the transcriptome profile analysis of *A. benhamiae* after *in vitro* interaction with human keratinocytes revealed that not only proteases were found to be differentially regulated but also genes associated with the synthesis of secondary metabolism molecules (polyketide synthase and non-ribosomal peptide synthetase), lipases and hydrophobin (hypA) (15). In a similar way to RodA hydrophobin of *Aspergillus fumigatus* (29), the hypA protein of *A. benhamiae* forms a hydrophobic rodlet layer that enables conidia to avoid recognition by immune cells at an early stage of infection (21). Furthermore, other genes associated to the host-fungi interaction, mainly through genomic and/or transcriptomic analysis, were proposed: genes related to heat shock proteins (24), other enzymes that participate in keratin degradation (hydrolases, glucanases, chitinases, mannosyl transferases) (25), ergosterol metabolism and reproduction, and LysM domain proteins (19, 23). Strikingly, various of these virulence factors might be transported to the extracellular space by extracellular vesicles (EVs), as it was demonstrated that *T. interdigitale* produces these structures *in vitro* (22).

Therefore, the dermatophyte molecules that drive skin invasion, trigger inflammation, or facilitate evasion during the infection process still remain poorly understood. Further comprehensive research on dermatophyte virulence factors is necessary to identify the main microbial mechanisms that mediate difficult-to-treat chronic infections or overly inflammatory responses.

DERMATOPHYTE RECOGNITION AND ACTIVATION OF THE INNATE IMMUNE SYSTEM

Immune and non-immune cells sense fungi through their cell wall components (i.e. polysaccharides, glycoproteins), secreted extracellular molecules (i.e. peptide toxins) or intracellular content (i.e. DNA) through different pattern recognition receptors (PRR) which, upon ligation, transduce intracellular signals that promote fungal phagocytosis, respiratory burst, cytokines and chemokines release, phagocyte lysis, among others, and thereby shape immune responses (30, 31). PRR can be classified based on their structure and function: C-type Lectin Receptors (CLR), Toll-like Receptors (TLR), Nucleotide-binding and Oligomerization Domain (NOD)-like receptors (NLR), and Retinoic acid Inducible Gene (RIG)-like receptors (RLR). Until now, signaling pathways mediated by CLR, TLR and NLR have been described in the interaction with dermatophytes and are key modulators of host antifungal immunity.

C-Type Lectin Receptors

C-type Lectin Receptors (CLR) comprise a superfamily of soluble and membrane-bound proteins characterized by the presence of, at least, one C-type lectin domain (CTLD), some of which act as a carbohydrate recognition domain (CRD). The fungal cell wall contains numerous structures like glycans, glycolipids and glycoproteins that are recognized by several CLR (30) including Dectin-1 (CLEC7a), Dectin-2 (CLEC6a), Dectin-3 (CLEC4d), MINCLE (CLEC4e), Mannose Receptor (CD206), DC-SIGN (CD209), etc (32, 33). Dectin-1 recognizes β-glucans in the cell wall of diverse pathogenic fungi and is the best-characterized receptor involved in antifungal immunity. Dectin-1 signaling involves an immunoreceptor tyrosine-based activation motif (ITAM)-containing cytoplasmic domain that is phosphorylated by a Src family kinase that allows Syk kinase recruitment. Dectin-2 recognizes α-mannans and transduces its signal through association with the ITAM-containing Fc receptor gamma (FcRγ) chain (34). In most CLR signaling, the Syk pathway activates a molecular scaffold composed by CARD9, Bcl10 and MALT1, which culminates in the recruitment of several transcription factors including NF-κB and MAP kinases. Additional intracellular pathways are also induced and include the Raf-1 kinase pathway and the canonical (NLRP3/caspase-1) and non-canonical (MALT1/caspase-8) inflammasome activation pathways (30, 33).

By using CLR soluble fusion proteins, Sato et al. (35) demonstrated that Dectin-1 and Dectin-2 bind to *Microsporum audouinii* and *Trichophyton rubrum* while Dectin-2 particularly recognizes high mannose structures or oligo-manosid residues in the hyphae cell wall. This seminal work described that Dectin-2 couples FcRγ chain in RAW cells (human macrophage cell line) to trigger innate immunity after ligation by fungal hyphae. The activation of myeloid cells *via* CLR was further observed *in vivo* after *T. rubrum* intraperitoneal infection of C57BL/6 mice (36, 37). In this setting, WT mice controlled systemic infection at 14 days showing a significant decrease in spleen fungal burden whereas mice deficient in Dectin-1 or Dectin-2 (Dectin-1 or Dectin-2 knock-out) and double knock-out (KO) counterparts were unable to do the same. In addition, other studies showed that soluble α-mannans (33) and mannose receptor (CD206) blocking antibody (38) inhibited *T. rubrum* conidia engulfment by macrophages *in vitro*.

In a human disease context, Ferwerda et al. (39) first reported a family with defective surface expression of mutated Dectin-1 and susceptibility to chronic vulvovaginal candidiasis and persistent onychomycosis by *T. rubrum*. In these patients, peripheral blood mononuclear cells poorly expressed Dectin-1 and were deficient in producing tumor necrosis factor (TNF), IL-6, and IL-17, after stimulation with β-glucans or *Candida albicans*. According to this, individuals with inherited deficiencies in CARD9, the CLR downstream adaptor molecule, are also susceptible to severe deep dermatophytosis (40).

C-type lectin receptors expression, and its downstream Syk-CARD9 signaling, is primarily restricted to myeloid cells like monocytes, macrophages, neutrophils and dendritic cells (30), but it has also been described in epithelial cells (41) and keratinocytes (42). Nevertheless, few studies have investigated the role of CLR-expressing cell populations in the skin during dermatophytosis. In a mouse model of dermatophyte antigen-induced contact hypersensitivity (CHS), the percutaneous application of trichophytin (a soluble antigen from *T. mentagrophytes*) upregulated Dectin-1 mRNA (messenger RNA) expression in skin tissue and Dectin-1-expressing cells were involved in trichophytin-induced CHS (39, 40). Furthermore, Dectin-1 mRNA expression was up-regulated in HaCaT cells (a human keratinocyte cell line) co-cultured with supernatant from *T. rubrum* culture (43). In contrast, Brasch et al. (44) studied Dectin-2 expression by immunohistochemistry in patients with dermatophytosis (*tinea corporis*) and did not observe significant differences in Dectin-2 expression in the skin tissue between patients and healthy control individuals.

Therefore, the current knowledge strongly suggests that Dectin-1, Dectin-2 and Mannose Receptor expressed on myeloid cells play a role in triggering the anti-dermatophytic defense. Nonetheless, the function of particular CLR on skin cellular subsets driving antifungal response has not been defined in the context of cutaneous infection yet.

NLRP3 Inflammasome and IL-1β Production in Fungal Infections

IL-1β is a potent inflammatory cytokine mainly produced by macrophages and neutrophils that promotes cytokine production, phagocytosis, oxidative burst and neutrophil degranulation. IL-1β is a cytokine produced as an inactive intracellular precursor triggered by PPR recognition of microbial pathogen-associated (PAMPs) or damage-associated (DAMPs) molecular patterns and later activated into the biologically active form by caspase-dependent cleavage after inflammasome assembly (45). The core of the majority of the inflammasomes is the NOD-like receptor (NLR) and the NLR family pyrin domain-containing 3 (NLRP3) is the most studied in fungal infections (46). IL-1β production *via* the inflammasome canonically requires two signals: the first is NF-κB-dependent activation provided by microbial binding to CLR or TLR that induces pro-IL-1β synthesis and NLRP3 transduction. The second signal is given by K^+ efflux, extracellular ATP (adenosine triphosphate), reactive oxygen species (ROS), fungal toxins, or particulate matter, etc (31). Consequently, the second signal promotes NLRP3 activation by triggering the assembly of a multiprotein complex composed of NLRP3, the adapter protein ASC and the caspase-1 pro-form. This complex serves as a platform for pro-caspase-1 activation and, thereby, facilitates proteolytic pro-IL-1β processing to mature IL-1β (31, 46).

Microsporum canis and *Trichophyton schoenleinii* hyphae have been demonstrated to induce IL-1β production by THP-1 cells (a human monocytic cell line) and murine dendritic cells in a NLRP3 dependent-manner (47, 48). In addition, Dectin-1-Syk-CARD9 signaling was critical for pro-IL-1β transcription induced by *M. canis*, suggesting that dermatophyte glycan recognition by CLR provides the first signal for NLRP3 and IL-1β synthesis. Importantly, *M. canis* also triggered IL-1β production *in vivo*, after intraperitoneal infection of WT mice, but IL-1β release was completely abolished in NLRP3- or ASC-deficient mice (47). In line with these studies, *T. rubrum* conidia phagocytosis also induced IL-1β *via* Dectin-1 and Dectin-2, in a NLRP3-ASC-caspase-1 dependent-manner (36) and IL-1 signaling in macrophages restricted *T. rubrum* conidia germination and hyphae growth (37). The second signal proposed for NLRP3 activation and IL-1β release by *M. canis* or *T. schoenleinii* was found to be dependent on cathepsin B activity, K^+ efflux and ROS production. Nevertheless, the dermatophyte-derived molecules that trigger this second signal remain unknown and, the only evidence, so far, is that it can be mediated by heat-sensitive molecules (47, 48). In this sense, dermatophyte heat-sensitive proteases might play a similar role as the secreted aspartic proteases (SAPs) from *C. albicans* which activate NLRP3 after its internalization *via* a clathrin-dependent mechanism with intracellular induction of K^+ efflux and ROS production (49).

Taken together, dermatophyte activation of NLRP3 inflammasome *via* CLR on myeloid cells represents a key event for triggering innate immunity. Experimental skin infection with *Arthroderma benhamiae, A. vanbreuseghemii* (50) or *M. canis* (51) elicited IL-1β production by epidermal cells, however, the role of inflammasome-dependent antifungal immunity during skin dermatophyte infection is currently unknown.

Toll-Like Receptors

Toll-like receptors (TLR) are membrane glycoproteins that were first described by their ability to control fungal infections in

Drosophila and later were found to mediate mammalian host response against microbial pathogens. Upon ligand binding, TLR intracellular signaling is mediated by myeloid differentiation primary response 88 (MyD88) and TIR domain-containing adapter-inducer interferon-β (TRIF) to trigger the inflammatory response. Fungal ligands that bind to TLR are not completely defined, however, experimental evidence suggests that TLR cross-signal together with CLR and modulate the antifungal defense (30). In this regard, it has been demonstrated that TLR-2 increases its ligand-binding spectrum by heterodimerization with Dectin-1 for β-glucan recognition (52).

The studies concerning the role of TLR in the anti-dermatophyte immune response have produced results showing pro-inflammatory as well as anti-inflammatory effects that need further elucidation. Myeloid cells, keratinocytes and fibroblasts increase TLR-2 and TLR-4 mRNA expression upon interaction with dermatophytes (43, 53). *In vitro* studies with feline neutrophils showed an increase in TLR-2 and TLR-4 mRNA levels after stimulation with live and heat-killed *M. canis* arthroconidia (54). Recently, Celestrino et al. (55) reported that TLR-2 is important for *T. rubrum* conidia phagocytosis and pro-inflammatory cytokines production by human monocytes. Additionally, considering that TLR-2 is not a phagocytic receptor, these authors suggested that TLR-2 enhances CLR-mediated phagocytic activity.

Interestingly, extracellular vesicles (EVs) produced by *Trichophyton interdigitale* have been demonstrated to induce proinflammatory mediators by bone marrow-derived macrophages and keratinocytes in a TLR-2-dependent manner (22). The EVs are spherical structures composed of a lipid-bilayer membrane produced by different microorganisms and play a role in the secretion of virulence factors. Therefore, this study showed that dermatophytes can modulate the host innate immune response by producing EVs loaded with still undefined dermatophyte virulence factors that interact with TLR.

On the other hand, published data using a deep dermatophytosis model in TLR-2 deficient mice subcutaneously infected with *T. mentagrophytes* demonstrated that fungal interaction with TLR-2 suppresses the inflammatory response of peritoneal macrophages and the production of IL-17, IL-10 and IFN-γ (interferon-gamma) by splenocytes (56). Coincidentally, we observed a lower fungal burden in the skin of TLR-2 deficient mice compared to WT using an epicutaneous model of *M. canis* infection (Beccacece I., unpublished data). According to this, Netea et al. (57) observed that TLR-2 deficient mice were more resistant to disseminated candidiasis than WT, as there was increased chemotaxis and enhanced candidacidal capacity of TLR-2$^{-/-}$ macrophages due to a more robust Dectin-1-mediated immune response in the absence of TLR-2. Furthermore, TLR-2 expression apparently suppresses Dectin-1-dependent production of CXCL8 (IL-8) against fungal β-glucans (52, 58). CXCL8 is a member of the CXCL chemokine family primarily involved in neutrophil recruitment and activation in response to tissue damage or infection (59) and can be directly induced in human keratinocytes by dermatophytes (53, 60).

In patients with dermatophytosis, TLR-2 and TLR-4 immunohistochemical staining was observed in lower epidermis from infected skin (44). Accordingly, a recent study demonstrated that *T. benhamiae* induced *in vitro* TLR-2 expression in human keratinocytes and dermal fibroblasts (53). Thus, so far, there is no clear evidence on the fungal molecules and mechanisms involved in TLR-dermatophyte interactions but, as many intracellular signaling molecules are shared between PRR pathways, it seems that a functionally important cross-talk with CLR might be crucial for the antifungal response outcome. The *in vivo* studies suggest a role of TLR-2 in downmodulating inflammation during dermatophytosis.

DERMATOPHYTE INTERACTION WITH SKIN CELLS IN THE CONTEXT OF INFECTION

The *stratum corneum*, the outer layer of the skin, is composed of dead keratinocytes, keratin and hydrophobic lipids along with antimicrobial peptides (AMP), and function as a barrier against the environment and potential pathogens. In the epidermis, keratinocytes are essential to initiate the cutaneous immune response since they express various innate receptors (TLR, CLR, NLR, etc.) that detect pathogens and induce cytokine, chemokine, and antimicrobial peptide synthesis to locally modulate the recruitment and function of inducers and effectors cells from immunity. Furthermore, keratinocytes express cytokine receptors (such as IL-17R, IL-22R and TNFR) that potentiate this response. In between these cells, there are immune cell subsets strategically located to tissue immunosurveillance like Langerhans cells (LC) and resident memory CD8$^+$ T cells; while in the dermis, there is a great variety of cell populations: different subsets of dermal dendritic cells (DC), macrophages, mast cells, innate lymphoid cells (ILC), γδ T cells and memory-resident and regulatory T cells (CD4$^+$ and CD8$^+$). Furthermore, there are nervous terminals that innervate the skin and lymphoid vessels from where immune cells migrate to lymphoid organs (61) (**Figure 2**).

Dermatophyte invasion is mostly restricted to keratinized tissues such as skin, hair, and nails but with the potential to cause extensive chronic superficial infections or even invasive systemic disease in immunocompromised patients. Widespread chronic or extracutaneous invasive infections have been largely related to patients with keratinization disorders or cell-mediated immunity deficiencies such as those observed in HIV, bone marrow and solid organ transplant recipients, or corticosteroid therapy (3, 5). In the last decade, inherited mutations in key signaling innate immunity pathways have been related to dermatophytosis susceptibility as well (40, 62, 63). Considering that our immune system exhibits tissue-specific restrictions (64) and the majority of results were obtained using myeloid cell populations, we scarcely understand the cellular and molecular mechanisms involved in the skin immune response to dermatophytes (**Figure 2**).

Keratinocytes: Active Initiators of Cutaneous Immunity Response

The first epidermal cells encountered during the dermatophyte infection process are keratinocytes (60, 65, 66). Upon exposure to

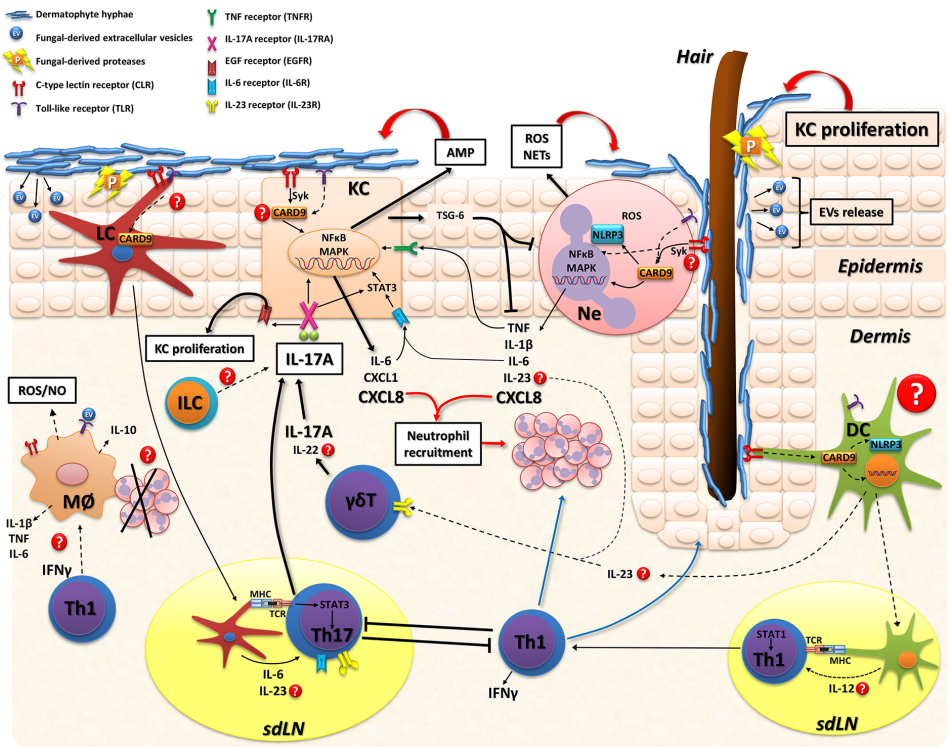

FIGURE 2 | Model of skin immune response in dermatophytosis. Dermatophyte fungi invade the *stratum corneum* and release proteases (P) that degrade keratin for fungal growth and facilitate tissue invasion. Extracellular vesicles (EV) loaded with fungal virulence factors might be also released during infection. Host recognition of dermatophytes is mainly through CLR and TLR on myeloid cells and keratinocytes. The adapter protein CARD9 is a key molecule in fungal sensing that signals downstream various CLR and mediates cross-signaling of other innate receptors (TLR and NLR). Keratinocytes (KC) sense fungal hyphae and consequently release: 1) antimicrobial peptides (AMP; including cathelicidin and β-defensin) that are effector molecules promoting fungal clearance, 2) proinflammatory mediators (IL-6, CXCL8, TNF) that further stimulate inflammation and neutrophil recruitment or 3) immunosuppressive proteins, such as TSG-6, particularly in human infections with anthropophilic dermatophytes. Also, IL-6, IL-17, and IL-22 further stimulate KC activation. Neutrophils recognize fungi and trigger the intracellular activation of MAPK and NFκB pathways leading to proinflammatory cytokines/chemokines release that also enhance KC activation, recruit more inflammatory leukocytes and, probably, promote IL-17 producing-lymphocytes through IL-23 release. Neutrophils also secrete reactive oxygen species (ROS) and neutrophil extracellular traps (NETs) that kill dermatophytes. The role of macrophages has not been directly evaluated during skin infections but these cells might also kill dermatophytes by IFN-γ-induced ROS and nitric oxide (NO) production or even resolve inflammation through phagocytosis of apoptotic neutrophils with production of anti-inflammatory cytokines (e.g.: IL-10). As for adaptive immunity, Langerhans cells (LC) are located in the epidermis and sense dermatophytes, migrate to skin draining lymph nodes and promote Th17 differentiation (ref. 51). Whereas in the dermis, different subsets of dendritic cells (DC) are probably involved in sensing fungal molecules and producing cytokines that drive IL-17- or IFN-γ- mediated immunity. IL-17A produced by adaptive Th17 cells and innate lymphocytes (γδT or ILC) boosts KC activation/proliferation and inhibits superficial fungal growth. Upon binding to IL-17RA/IL-17RC in KC, IL-17A activates Act1-TRAF6-NFkB/MAPK or STAT-3 intracellular pathways and induce cytokines/chemokines and AMP production. Furthermore, the IL-17/IL-17RA pathway transactivates epidermal growth factor receptor (EGFR) which promotes KC proliferation. During mild superficial experimental infection with *M. canis*, type 17 immunity restricts both fungal growth and an exacerbated type 1 (IFN-γ mediated) inflammation (ref. 51). Conversely, IFN-γ mediated-response suppresses cytokines related to the IL-17 pathway leading to an increased fungal burden. During *T. benhamiae* experimental infection both Th1 and Th17 phenotypes are induced and control the cutaneous mycoses (ref. 120). Dotted lines and question marks refer to mechanisms not directly demonstrated in the context of skin dermatophytosis. CARD9 signaling might be involved in various skin cells populations of the antifungal defense. KC, keratinocyte; LC, Langerhans cell; DC, dendritic cell; Ne, neutrophil; ILC, innate lymphoid cell; Mø, macrophages; sdLN, skin draining lymph node; CLR, C-type lectin receptor; TLR, Toll-like receptor; NLR, nucleotide-binding oligomerization domain (NOD)-like receptor; IL-17RA/IL-17RC, interleukin 17 receptor A/C; TCR, T cell receptor; MHC, major histocompatibility complex; AMP, antimicrobial peptides; ROS, reactive oxygen species; NO, nitric oxide; NETs, neutrophil extracellular traps; P, proteases; EV, extracellular vesicles.

dermatophytes, keratinocytes release pro-inflammatory mediators such as IL-6, CXCL8, TNF, and AMP including cathelicidin and β-defensins (53, 66, 67). Tani et al. (60) demonstrated that CXCL8 was detected in supernatants of 24 h co-culture of normal human epidermal keratinocytes (NHEKs) with microconidia from *T. mentagrophytes*, *T. rubrum*, or *T. tonsurans*. Cytokine production was strongly enhanced with the zoophilic *T. mentagrophytes*, whereas lower levels were seen with the other anthropophilic species. Moreover, only *T. mentagrophytes* induced TNF and granulocyte-macrophage colony-stimulating factor (GM-CSF) production by NHEKs. These results support clinical evidence from human dermatophytosis showing that zoophilic dermatophytes induce more severe inflammatory responses than anthropophilic species. As described above for NLRP3 activation in myeloid cells, heat-killed fungi were unable to induce cytokine production by NHEKs, suggesting that metabolic activity or products secreted by dermatophytes are necessary to trigger

the inflammatory response. Similar findings were recently reported by Faway et al. (66) using reconstructed human epidermis (RHE), an *in vitro* three-dimensional model of human skin. After infection with *T. rubrum* arthroconidia, hyphae invaded the *stratum corneum* and located in the whole intercellular space altering the epidermal barrier integrity and activating keratinocyte response with mRNA expression and release of CXCL8, TNF-stimulated gene 6 protein (TSG-6), AMP (human β-defensin-2 and -3 and S100A7) and, in a lesser extent, IL-1α, IL-1β, TNF, thymic stromal lymphopoietin (TSLP), and granulocyte colony-stimulating factor (G-CSF). In line with these data, Hesse-Macabata et al. (53) have recently described that *T. benhamiae* promotes expression and secretion of pro-inflammatory cytokines/chemokines as well as expression of various AMP, TLR-2 and proliferation marker Ki67 after infection of human keratinocytes and dermal fibroblast.

Taken together, these *in vitro* models demonstrate that, in the absence of immune cells, keratinocytes not only form a physical barrier against dermatophyte invasion but also actively confer an early antifungal defense by triggering a skin-specific immune response (**Figure 2**). It is worthy to notice that experiments using reconstructed human epidermis (RHE) also produced high levels of the immunosuppressive protein TSG-6 after *T. rubrum* infection (66), indicating that keratinocytes could also provide mechanisms involved in inflammation control and tissue repair (68).

Neutrophils

During dermatophytosis, neutrophils are the first leukocytes recruited to the site of infection (51, 69) and are thought to be responsible for fungal elimination from the skin (21, 70, 71) (**Figures 1** and **2**). In human infection, as well as in experimental dermatophytosis models, neutrophils form epidermal microabscesses surrounding the hyphae in the *stratum corneum* (50, 51, 72, 73) (**Figure 1**). According to this, $CD11b^+$ $Ly6G^+$ neutrophils can be detected by flow cytometry in epidermal cell suspensions as early as 2 days after *M. canis* epicutaneous infection in mice (51). Early studies performed by Calderon and Hay (70) demonstrated that human peripheral blood neutrophils exhibited potent cytotoxic activity against *T. quinckeanum* and *T. rubrum* hyphae. Moreover, dermatophyte-stimulated human neutrophils were able to phagocyte conidia, produce CXCL8, IL-1β, IL-6, IL-8, and TNF, and stimulate extracellular traps (NETs) formation (21, 74).

Despite all the experimental evidence suggesting a main role of neutrophils as the first 'defenders' against dermatophytes, neutropenic patients are not frequently susceptible to extracutaneous invasive infection as they are to other fungi (including normally non-pathogenic species) (75). Instead, neutropenic patients frequently present widespread superficial infections and dermal granulomas resistant to antifungal treatment (Majocchi's granulomas) (76, 77). In agreement with this, De Sousa et al. (74) studied a cohort of patients with chronic widespread dermatophytosis without noticeable predisposing conditions or signs of immunodeficiency and found that their blood-derived neutrophils and macrophages presented impaired *in vitro* killing of *T. rubrum*. Additionally, neutrophils from patients displayed defects in hydrogen peroxide, nitric oxide and cytokine production compared to neutrophils from patients with typical dermatophytosis (*tinea pedis*) or healthy donors. However, this study did not further demonstrate the cause of antifungal defects showed by the phagocytic cells.

Furthermore, impairment in neutrophil mobilization to the site of infection or fungal killing mechanisms could be associated with inherited CARD9 deficiency and dermatophytic disease in humans (78, 79). Nevertheless, to which extent neutrophils control cutaneous defenses against dermatophytes and restrain extracutaneous fungal invasion remains not fully understood.

Antimicrobial Peptides

Antimicrobial peptides and proteins (AMP) are innate immune effector molecules that not only have microbicidal activity but also function as chemoattractants and proteinase inhibitors, have proangiogenic activity, promote wound repair, and can modulate adaptive immunity. The importance of AMP as antimicrobial effector molecules relies on fast killing mechanisms like forming pores in the microbial cell wall or nutrient depletion by extracellular Zn^{2+} and Mn^{2+} chelation (80, 81).

In the skin, there are more than 20 AMP including human β-defensins (hBDs), cathelicidins (LL-37), S100 proteins, RNase 7 and lactoferrin, among others (82). Keratinocytes constitutively express hBD1 whereas hBD2, hBD3, and hBD4 require TLR signaling or induction through TNF, IL-1β, or other cytokines (83). Additionally, other signaling pathways also regulate AMP production by keratinocytes, such as insulin-like growth factor 1 (IGF-1), vitamin D signaling and epidermal growth factor receptor (EGFR) ligands (83). In this regard, EGFR regulates transcription of downstream AMP genes (hBD-2 and -3, RNase 7, S100A7, elafin) and several cytokines and chemokines (CXCL8, IL-6, IL-20, IL-24, CXCL1) (80, 82). Keratinocyte stimulation of G-coupled receptors and certain cytokine receptors (such as IL-17RA/IL-17RC) results in matrix metalloproteinase (MMP)-mediated shedding of EGFR ligands (amphiregulin and heparin-binding epidermal growth factor-like growth factor, HB-EGF, and transforming growth factor-alpha, TGF-α) leading to transactivation of EGFR and further AMP expression in the skin (**Figure 2**). Strikingly, EGFR blocking in keratinocytes significantly decreased AMP expression in response to *T. rubrum* which could explain the increased dermatophyte infection rate observed in patients receiving therapy with anti-EGFR (81).

Lopez-Garcia et al. (84) firstly reported that cathelicidins may play a role in the skin defense against dermatophytes. They detected increased cathelicidin protein expression in the skin from patients with *tinea pedis* and *in vitro* inhibition of *Trichophyton* sp. growth by cathelicidin-derived synthetic peptides LL-37 and CRAMP. Similar data were later reported by Brasch et al. (44), demonstrating that AMP psoriasin (S100A7), hBD-2 and RNase 7 also inhibit dermatophyte growth *in vitro* (85). In agreement, Firat et al. (81) published that human foreskin-derived keratinocytes exposed to *T. rubrum* strongly boosted RNase 7 and hBD-3 expression and this phenomenon was synergistically increased in the presence of

IFN-γ and IL-17A. Moreover, Sawada et al. (67) observed that expression of epidermal hBD-2 and LL-37 was significantly lower in Adult T-cell leukemia/lymphoma (ATLL) patients with dermatophytosis than in infected non-ATLL patients, and this correlated with a significantly decreased frequency of peripheral T helper 17 (Th17) lymphocytes and lower IL-17 levels in serum. The ATLL immune condition revealed that Th17 cells are deeply involved in keratinocyte production of antimicrobial peptides against dermatophytes.

TYPE 17 (IL-17-MEDIATED) IMMUNITY IN DERMATOPHYTOSIS

Type 17 immunity have a critical role in innate and adaptive immunity at barrier tissues such as oral, intestinal and lung mucosa as well as the skin. IL-17 cytokines play a major role in maintaining local homeostasis with microbiota, protecting against infections and mediating severe inflammatory diseases such as inflammatory bowel disease or psoriasis (86–88). IL-17 family members comprise six related proteins: IL-17A, IL-17B, IL-17C, IL-17D, IL-17E (IL-25), IL-17F, and the heterodimer IL-17AF. Among them, IL-17A has been the most studied cytokine and, therefore, associated with human health and disease (86). IL-17A is produced by hematopoietic cells from both innate and adaptive immune system, including $CD4^+$ T helper (Th17), $CD8^+$ cytotoxic T (Tc17), γδT, natural killer (NK), group 3 innate lymphoid (ILC3), and 'natural' Th17 cells. Members of the IL-17 family act like "local cytokines" mainly on non-classical immune cells such as epithelial, endothelial, and fibroblastic cells. IL-17 signals through heterodimeric receptors composed of the subunit IL-17RA associated with either IL-17RC, IL-17RE, or IL-17RB, which are specifically stimulated by IL-17A and F, IL-17C, and IL-17E (IL-25), respectively (89). Upon signaling on keratinocytes, IL-17 stimulates the production of various cytokines (such as GM-CSF, TNF, IL-6), chemokines (CXCL1, CXCL8), and vascular endothelial growth factor (VEGF). IL-17 can also enhance the expression of AMP such as hBD-2 and LL-37 and promote keratinocyte proliferation (80). All these mechanisms may play a major role in clearing cutaneous fungal infection (90, 91) (**Figure 2**).

In the skin, fungal recognition by PRR on myeloid cells (DC, macrophages, neutrophils) and, probably, keratinocytes and fibroblasts trigger the production of cytokines like IL-23, IL-6, IL-1β, and IL-21 (51, 53, 90). Cytokine binding to its receptor on lymphocytes selectively triggers intracellular Signal Transducer and Activator of Transcription 3 (STAT3) phosphorylation, Retinoic-acid-receptor-related orphan nuclear receptor gamma (RORγt) transcription factor activation and, eventually, leads to the induction of Th17 lineage or the synthesis of type 17-cytokines (IL-17, GM-CSF, IL-22) (92). Noteworthily, IL-17A can also activate STAT3 in keratinocytes and amplify IL-6 production (80) (**Figure 2**). In line with this, patients with STAT3 mutations (Autosomal dominant hyperimmunoglobulin E syndrome, AD-HIES) have increased susceptibility to candidiasis and dermatophytosis due to a diminished Th17 response (62).

It is well known that mucocutaneous candidiasis (CMC), a chronic and recalcitrant clinical syndrome, is associated with several genetic diseases related to dysregulation or inhibition of the IL-23/IL-17 pathway (33, 93). In this sense, IL-17-producing memory $CD4^+$ T cells in peripheral blood expand specifically upon *Candida albicans* stimuli (94) and skin resident Th17 lymphocytes mediate protective immunity to this yeast (95). However, much less is known about the skin T cell response during dermatophytosis. Deficiencies in type 17 immunity associated with susceptibility to widespread chronic dermatophytosis have been reported in patients with ATLL (67), autoimmune polyendocrinopathy-candidiasis-ectodermal dystrophy (APECED) (72), Dectin-1 mutations (39), loss-of-function mutations in STAT3 (62), autosomal gain-of-function mutations in STAT1 (96, 97), and anti-IL-17 antibody treatment (secukinumab) (73, 98). Furthermore, IL-17 impairment was also associated with inherited CARD9 deficiency and deep dermatophytosis (40, 99).

EXPERIMENTAL DERMATOPHYTOSIS AS MODELS OF HUMAN DISEASE

In contrast to research on *Candida* sp. infection, the lack of murine experimental models for dermatophytosis that mimic natural human infection long-hindered the possibility of in-depth studies on immunological mechanisms involved in the susceptibility to these mycoses. In the 1980s, Hay et al. (100, 101) made important contributions to the understanding of the anti-dermatophytic immunity by developing a highly inflammatory dermatophytosis model, similar to favus in humans, after epicutaneous infection of BALB/c mice with the murine pathogen *T. quinckeanum*. They showed that mice self-controlled the infection with a peak of skin lesions at 7–10 days, characterized by epidermal proliferation (acanthosis), neutrophil recruitment (epidermal microabscesses) and increased antigen-specific lymphocyte proliferation (69). Furthermore, they found that the adoptive transfer of T lymphocytes conferred resistance to sub-lethally irradiated mice (101) and that immunological memory was evidenced in re-infected mice (secondary infection) as they quickly cleared fungi and showed an augmented lymphoproliferative response to fungal antigens (100).

After almost 30 years of the studies published by Hay and colleagues, in 2014, Cambier et al. (50) developed a similar model in C57BL/6 mice with the zoophilic species *Arthroderma benhamiae* and *A. vanbreuseghemii* (both from the *Trichophyton mentagrophytes* complex) that cause highly inflammatory dermatophytosis in humans (102, 103). In this regard, experimental models of human diseases developed in a C57BL/6 mice background are remarkably important for the study of immunological mechanisms due to the wide variety of genetically modified strains available (104). Mice epicutaneously infected with *Arthroderma* self-healed at approximately 30 days with a clinical course and features similar to the inflammatory dermatophytosis in humans (50). Interestingly, *Arthroderma*-infected skin showed mRNA overexpression of proinflammatory

cytokines like transforming growth factor-beta (TGF-β), IL-1β, IL-6, and IL-22 at days 7 and 21 post-infection, suggesting a role of type 17-immunity in host defense. In this line, we later demonstrated that IL-17-mediated immunity is key for host protection in an experimental epicutaneous infection of C57BL/6 mice with *Microsporum canis* (51), a zoophilic dermatophyte that causes highly prevalent *tinea capitis* and *tinea corporis* in children (105–107) (**Figure 1**). Similarly to the *Arthroderma* model, *M. canis*-infected mice showed skin lesions only limited to the epidermis and hair follicles, with a maximal clinical score at 8 days post-infection and fungal clearance around day 28. However, in contrast to that observed in *Arthroderma*-infected mice, *M. canis* infection was characterized by mild cutaneous lesions resembling non-inflammatory human disease (**Figure 1**). Re-stimulation of skin draining lymph node cells with heat-killed *M. canis* showed that Th17 adaptive immunity predominates during infection (51). As demonstrated for *Candida* and *Malassezia* (108, 109), *M. canis* selectively triggers a type 17 immune response mainly by $CD4^+$T and, to a lesser extent, by $CD8^+$T lymphocytes in lymph nodes around 8 days post-infection. Furthermore, IL-17-deficient mice (IL-17RA KO or IL-17A/F KO) were extensively colonized with *M. canis* hyphae as demonstrated by a forty-fold increase in skin fungal burden compared to WT infected mice (**Figure 1**). IL-17-deficient mice showed less epidermal thickening (acanthosis) nevertheless, pro-inflammatory cytokine production was up-regulated after infection. Moreover, in the absence of a functional IL-17 pathway, *M. canis* did not invade dermis or deep tissues in mice (51) in coincidence with clinical evidence showing that humans with deficiencies in type 17 immunity or treated with anti-IL-17 antibody (secukinumab) are susceptible to widespread superficial infections rather than deep dermatophytosis (67, 73).

Strikingly, in our model, neutrophil function and mobilization to the site of infection were uncoupled from IL-17 signaling since IL-17-deficient mice had a significantly higher frequency of neutrophils in the skin (51) (**Figure 1**). Supporting these findings, neutrophilic microabscesses were observed next to hyphae in the epidermis of a patient with dermatophytosis after 4 weeks of treatment with anti- IL-17 antibody (73). Further research is needed to establish the *in vivo* role of neutrophils in dermatophytosis and the molecular pathways driving its mobilization to the skin. Considering that dermatophytes induce a robust production of chemokines and cytokines (CXCL8, CXCL1, IL-6) by keratinocytes (53, 60, 65, 110), these chemotactic factors are probably the main mediators of neutrophil recruitment, independently of IL-17 signaling.

Altogether, these experimental and clinical results reveal that type 17 immunity is important to boost keratinocyte proliferation and probably early production of AMP after dermatophyte skin invasion. Eventually, IL-17 deficient hosts are able to overcome infection but at the expense of an exacerbated inflammation and tissue damage (51, 111).

On the other hand, anthropophilic dermatophytes (e.g. *T. rubrum, T. interdigitale, T. tonsurans*) are evolutionarily adapted to human keratin and consequently, murine experimental models might have limitations in recapitulating the features of inflammation and specific immune response occurring in a natural setting. Nevertheless, Baltazar et al. (112) have reported some interesting data by developing a model of *T. rubrum* infection in C57BL/6 mice after epicutaneous and intradermal inoculation of conidia. Likewise to the *M. canis* model, *T. rubrum* infected mice showed a peak of fungal burden after 7 days of infection (112) that significantly decreased by day 14. Along with *T. rubrum* infection, myeloperoxidase (MPO) and N-acetylglucosamine (NAG) activity was detected in the skin, suggesting recruitment of neutrophils and macrophages to the site of infection. Interestingly, MPO activity decreased in parallel with fungal load (14 days post-infection), but NAG activity remained elevated, even after fungal clearance (112). The authors hypothesized that skin macrophages might be involved not only in fungal killing, but also in the resolution of inflammation. In this sense, phagocytosis of apoptotic neutrophils by macrophages is a key mechanism to down-modulate inflammation and return to tissue homeostasis during infectious diseases (113) (**Figure 2**).

TYPE 1 (IFN-Γ-MEDIATED) IMMUNITY

The role of IFN-γ-mediated (type 1 or Th1) response in protective skin immunity against dermatophytes remains less clear than IL-17-driven immunity. In the *M. canis* model, dermatophyte infection in WT mice did not trigger the expansion of antigen-specific IFN-γ-producing T cells in skin draining lymph nodes (51). In contrast, IL-17-deficient mice experienced a shift to a type 1 response suggesting the establishment of IFN-γ-mediated compensatory mechanisms to restraint *M. canis* infection. Nonetheless, *in vivo* IFN-γ neutralization in IL-17RA KO mice (at days 3 and 6 post-infection) increased skin production of Th17-lineage cytokines (IL-22, IL-17, IL-1β, IL-6) and significantly inhibited fungal growth (51). These surprising data open the possibility that IFN-γ deregulation, in the absence of IL-17 signaling, might contribute to superficial *M. canis* overgrowth by inhibiting type 17-related responses. However, the mechanisms by which Th1 cytokines may interfere with cutaneous immunity against dermatophytes and counter-regulate the IL-17 pathway remain unknown. Therefore, in this model, type 17 immunity has a dual role during infection by inhibiting dermatophyte growth and controlling Th1-mediated inflammation (51, 111).

In line with the experimental data observed in the *M. canis* mouse model, patients with mutations that lead to the gain of function in the transcription factor STAT1 (STAT1 GOF), that promote type I and type II IFN genes transcription, have reduced type 17 immunity and are susceptible to chronic mucocutaneous candidiasis (CMC) and dermatophytosis (96, 97, 114–117). Consistent with this, increased STAT1 responses to Th1 cytokines (IFN-γ and IL-27) were shown to repress the differentiation of IL-17-producing T cells through mechanisms that are not yet completely understood (114, 118). In fact, increased STAT1 phosphorylation induced by IFN-γ can be

reversed upon treatment with the JAK kinase inhibitor, ruxolitinib (113) and, interestingly, patients with STAT1 GOF condition treated with ruxolitinib have shown remission of mucocutaneous candidiasis (119). Altogether, the clinical data supports the experimental results from *M. canis* model (51), showing that dermatophyte susceptibility is mainly due to deficiencies in IL-17-driven immunity and that type 17 and type 1 immunity would eventually counter-regulate each other.

Nevertheless, Heinen et al. (120) observed that, after *Trichophyton benhamiae* epicutaneous infection in C57BL/6 mice, Th17 along with Th1 responses function in a complementary manner and, only when both IL-17 and IFN-γ pathways are deficient, mice suffer from superficial persistent infection. In contrast, Baltazar et al. (112) reported that IL-12p40 KO mice (lacking common β-subunit of IL-12 and IL-23 and thus, with impaired IL-17 and IFN-γ signaling) or IFN-γ KO mice were able to control *T. rubrum* infection after 14 days, but showed an increased fungal burden in the first week compared to infected WT mice. Eventually, as described for the *M. canis* model (51), deep dermatophytosis was not observed in the absence of IL-17 and IFN-γ in neither infection models (112, 120), suggesting that several immune pathways must be compromised to establish invasive dermatophytosis. The effector mechanisms of IFN-γ remains unclear but Verma and Gaffen (121) hypothesized that, as observed in *Candida* skin infection, IFN-γ may contribute to *T. benhamiae* destruction and expulsion by activating the fibrinolytic system in the epidermal abscess (122) or promoting M1 macrophages at a later infection stage (**Figure 2**). In line with this, peritoneal macrophages from IFN-γ KO mice showed decreased ROS production and were unable to efficiently phagocyte and kill *T. rubrum* conidia *in vitro* (112) indicating that macrophages might play a role in clearing infection.

The most noticeable difference between the *M. canis* (51) and the *T. benhamiae* (120) model is that mice infected with *T. benhamiae* had a more aggressive infection with significantly augmented fungal burden and skin inflammation, compared to *M. canis*-infected mice. Therefore, undefined specific virulence factors produced by these two pathogens may selectively activate different immune pathways in the skin. In addition, the route of infection in the *T. rubrum* model (intradermal conidia inoculation) might activate specific subsets of dermal dendritic cells that could eventually promote IFN-γ-mediated response (112) (**Figure 2**). This was observed in *Candida albicans* skin infection, where epicutaneous infection induces Th17 response through Langerhans cells (LC), while invasive *Candida* hyphae in dermis triggers Th1 immunity mediated by $CD103^+$ dermal dendritic cells (108).

In conclusion, the experimental data confirm clinical evidence showing that type 17 immunity is crucial for preventing uncontrolled superficial dermatophyte growth and for restricting an exacerbated cutaneous inflammation. The function of type 1 immunity is less clear since it inhibits type 17-mediated protective mechanisms (in the absence of an optimal IL-17 signaling) as observed in the mild inflammatory *M. canis* model or, in contrast, it might contribute to clear the infection as observed in the *T. benhamiae* inflammatory model.

SKIN ANTIGEN-PRESENTING CELLS AND INNATE VERSUS ADAPTIVE RESPONSE

In the steady-state skin, there is a coexistence of several antigen-presenting cells (APC) with the capacity to initiate and shape the immune response against pathogens. Langerhans cells are the most abundant population of skin APC and are constitutively localized in the epidermis. Other major populations of migratory skin DC are present within the dermis: $CD103^+$ DC subset, $CD11b^+$ DC ($CD1c^+$ DC in humans) and double negative DC. The current consensus is that these defined DC subsets contribute differently to antimicrobial immunity depending on the pathogen, the site or the stage of infection (123). The paradigm of adaptive immunology poses that after pathogen invasion, skin DC capture antigens and migrate to lymph nodes to present them to T lymphocytes in an MHC-TCR (Major Histocompatibility Complex–T cell receptor) context, thereby expanding antigen-specific T helper or T regulatory clones which return to the skin to fight the infection and modulate inflammation, respectively. In *Candida albicans* or *Malassezia* epicutaneous infections, IL-6- or IL-23-producing LC migrate and induce an antigen-specific Th17 response by 7–10 days post-infection (90, 109). At the same time, cutaneous DC are also able to rapidly and locally activate resident skin cells to arm the innate immune response. Notably, *C. albicans* directly stimulates sensory neurons to produce a neuropeptide that, in turn, induces IL-23 production by dermal DC and promotes a rapid protective response by IL-17-producing γδT cells (124). Moreover, as early as 2 days during *Malassezia* infection, not only LC but also neutrophils produced IL-23 to stimulate IL-17A-production by γδT, ILC and αβT cells in the skin (109). Nonetheless, the precise mechanisms involved in the induction of protective immunity in dermatophytosis are far less clear. Type 17 immunity-instructing factors IL-1β, IL-6, TGF-β and IL-23 were produced by epidermal cells after *M. canis* and *T. benhamiae* dermatophytosis in mice (51, 120). In the *M. canis* model, langerin expressing-dendritic cells (LC and a minor population of dermal DC) contributed critically to the regulation of the *M. canis*-specific Th17 response in draining lymph nodes (51), which is reminiscent of Th17 induction in response to epicutaneous infection with *C. albicans* (125) and *Malassezia* (109). However, *M. canis* fungal burden was not affected by fungal-specific Th17 cell reduction after depletion of langerin-expressing DC (51), pointing towards alternative innate sources of IL-17 for controlling dermatophytosis (**Figure 2**). In this sense, Heinen et al. (120) observed that IL-17 mRNA expression was early induced (3 days post-infection) in the skin of *T. benhamiae*-infected mice and showed a remarkably strong contribution of innate immunity in clearing dermatophytes from the skin. They demonstrated that *Rag2*$^{-/-}$ mice (lacking T and B cells) presented a long-lasting infection but were ultimately able to clear *T. benhamiae* from the skin.

INHERITED CARD9 DEFICIENCY AND DEEP DERMATOPHYTOSIS

The clearest evidence of innate immunity involvement in restricting dermatophyte extracutaneous invasion was the

discovery of loss-of-function mutations in the adapter protein CARD9 as the primary immunodeficiency underlying deep dermatophytosis (126). Deep dermatophytosis is a severe, recalcitrant and, sometimes, a life-threatening infection characterized by extensive invasion of the dermis (106) (**Figure 1**), hypodermis, and deeper tissues, by dermatophytes (6). As described above, CARD9 is a caspase recruitment domain-containing signaling protein crucial for CLR downstream signaling and gene activation by fungal glycans but it is also involved in cross-signaling with other innate receptors, such as TLR and NLR (107). Thus, CARD9 protein plays a critical role in innate immunity probably controlling various innate immune pathways (**Figure 2**).

In 2013, Lanternier et al. (40) first demonstrated that 17 non-consanguineous patients with deep dermatophytosis by *T. rubrum* or *T. violaceum*, had autosomal recessive CARD9 deficiency without other associated infectious conditions, except oral candidiasis in six of them. These authors described two CARD9 mutations: a homozygous premature stop codon mutation (Q289), identified in 15 patients from seven unrelated Algerian and Tunisian families, and a homozygous missense mutation (R101C) in two Moroccan siblings. The functional consequence of CARD9 mutations was a markedly low level of IL-6 production after stimulation of whole-blood leukocytes with heat-killed *C. albicans* or *S. cerevisiae*, but not with TLR agonists. Furthermore, peripheral Th17 cells from CARD9-deficient patients were significantly less frequent than healthy controls. CARD9 Q289 mutation was later described in Egyptian patients with widespread superficial *T. rubrum* infection of the skin and nails without significant visceral involvement (127). Recently, this mutation was also reported in an Algerian woman who suffered from cutaneous chronic dermatophytosis by *T. rubrum* from her childhood and developed an invasive brain infection in her adulthood (128).

The phenotypic variability of dermatophytic infection observed in patients with CARD9 deficiency ranges from extensive skin and nail lesions to potentially lethal lymph node and central nervous system infection. In 2015, Grumach et al. (129). reported a Brazilian patient with deep dermatophytosis by *T. mentagrophytes* harboring a novel CARD9 mutation, R101L. The patient displayed impaired fungal killing by neutrophils and low numbers of $CD16^{+}/CD56^{+}$ NK cells in peripheral blood. Similarly, Alves de Medeiros et al. (130) described a homozygous R70W CARD9 mutation in a Turkish family with resistant chronic cutaneous and deep dermatophytosis along with mucocutaneous and invasive candidiasis. In these patients, circulating IL-17 and IL-22 producing T cells were decreased as well as IL-6 and GM-CSF secretion by peripheral mononuclear cells upon stimulation with *Candida albicans*. Furthermore, high levels of serum IgE and eosinophilia were also a feature in all patients with CARD9 deficiency and invasive fungal invasion, but the link of these responses with the absence of CARD9 remains unexplained so far (40, 127, 130).

The cellular and molecular pathways related to CARD9 signaling in the skin have been scarcely investigated (131, 132) and it is currently unknown how CARD9 precisely drives cutaneous antifungal immunity (**Figure 2**). The accumulating evidence in humans has shown, so far, that susceptibility to fungal diseases in CARD9-deficient patients is related to the poor production of inflammatory cytokines by myeloid cells in response to fungal antigens along with an impairment in type 17-mediated immunity (126). Furthermore, CARD9 signaling was required in tissue-resident cells for an appropriate induction of CXC chemokines for neutrophil recruitment to the site of fungal infection (79). Noteworthily, Queiroz-Telles et al. (78) have recently reported a successful allogeneic hematopoietic stem cell transplantation (HSCT) in two patients with inherited CARD9 deficiency and deep dermatophytosis. More than 3 years after HSCT, both patients have achieved complete clinical remission and stopped antifungal therapy. This evidence points toward deep dermatophytosis pathogenesis in CARD9-deficiency settings might be largely due to the disruption of myeloid cell antifungal response.

CONCLUSIONS AND FUTURE DIRECTIONS

Over the last years, remarkable progress has been made for immunity to fungal pathogens while the physiopathogenesis of dermatophytosis remains poorly explored. So far, clinical and experimental evidence shows that type 17 immunity controls superficial infection, probably by promoting antimicrobial peptide production and keratinocyte proliferation, and independently of early recruited neutrophils with fungicidal function at the site of infection. Additionally, in the setting of mild inflammatory infections, IL-17-mediated response would be crucial to control cutaneous homeostasis preventing detrimental Th1 inflammation. The susceptibility to extracutaneous deep dermatophytosis would be related to deficiencies in various immunity pathways converging in CARD9 activation and probably restricted to the myeloid cell compartment.

In addition to causing symptomatic infections with different severity degrees (**Figure 1**), dermatophytes also colonize 30%–70% of the human population without causing clinical disease (1, 2, 133), thus these keratin parasites could be considered as a component of the human microbiota. Strikingly, the presence of dermatophyte in the skin, either in commensal or pathogenic relationship with susceptible hosts, has been related to asthma, allergy or eczematous skin (5, 13, 134). Therefore, the colonization of the skin by dermatophytes is an interesting concept to explore for its potential ability to induce migratory or tissue-resident immune cells that could participate in inflammatory pathological settings.

The increasing dermatophytosis incidence in certain geographic areas, the growing evidence of susceptible hosts with severe clinical presentations and the emerging antifungal resistance (7, 33, 135) highlight the need for a deeper understanding of the dermatophyte-host interaction. The next challenges are thoroughly defining which are the virulence factors responsible for dermatophyte pathogenesis and the mechanisms involved in limiting the infection, or, otherwise, those favoring chronicity or asymptomatic colonization.

AUTHOR CONTRIBUTIONS

The review results from the discussion and the consensus of all authors listed. The review was written by VLB and LSC. **Figure 2** was graphed by IB. All authors contributed to the article and approved the submitted version.

FUNDING

The authors acknowledge financial support from SECyT-UNC, ANPCYT-PICT 2018-1349, and CONICET-PIP (GI11220150100260), Argentina. VLB is a postdoctoral fellow of CONICET, and LSC is a member of the scientific career of CONICET.

REFERENCES

1. White TC, Findley K, Dawson TL, Scheynius A, Boekhout T, Cuomo CA, et al. Fungi on the skin: dermatophytes and Malassezia. *Cold Spring Harb Perspect Med* (2014) 4:a019802. doi: 10.1101/cshperspect.a019802
2. Hay RJ, Johns NE, Williams HC, Bolliger IW, Dellavalle RP, Margolis DJ, et al. The global burden of skin disease in 2010: an analysis of the prevalence and impact of skin conditions. *J Invest Dermatol* (2014) 134:1527–34. doi: 10.1038/jid.2013.446
3. Rouzaud C, Chosidow O, Brocard A, Fraitag S, Scemla A, Anglicheau D, et al. Severe dermatophytosis in solid organ transplant recipients: A French retrospective series and literature review. *Transpl Infect Dis* (2018) 20: e12799. doi: 10.1111/tid.12799
4. de Hoog GS, Dukik K, Monod M, Packeu A, Stubbe D, Hendrickx M, et al. Toward a Novel Multilocus Phylogenetic Taxonomy for the Dermatophytes. *Mycopathologia* (2017) 182:5–31. doi: 10.1007/s11046-016-0073-9
5. de Hoog S, Monod M, Dawson T, Boekhout T, Mayser P, Graser Y. Skin Fungi from Colonization to Infection. *Microbiol Spectr* (2017) 5(4). doi: 10.1128/microbiolspec.FUNK-0049-2016
6. Rouzaud C, Hay R, Chosidow O, Dupin N, Puel A, Lortholary O, et al. Severe Dermatophytosis and Acquired or Innate Immunodeficiency: A Review. *J Fungi Basel* (2015) 2:4. doi: 10.3390/jof2010004
7. Verma SB. Emergence of recalcitrant dermatophytosis in India. *Lancet Infect Dis* (2018) 18:718–9. doi: 10.1016/S1473-3099(18)30338-4
8. Bishnoi A, Vinay K, Dogra S. Emergence of recalcitrant dermatophytosis in India. *Lancet Infect Dis* (2018) 18:250–1. doi: 10.1016/S1473-3099(18) 30079-3
9. Mercer DK, Stewart CS. Keratin hydrolysis by dermatophytes. *Med Mycol* (2019) 57:13–22. doi: 10.1093/mmy/myx160
10. Cafarchia C, Iatta R, Latrofa MS, Graser Y, Otranto D. Molecular epidemiology, phylogeny and evolution of dermatophytes. *Infect Genet Evol* (2013) 20:336–51. doi: 10.1016/j.meegid.2013.09.005
11. Elavarashi E, Kindo AJ, Rangarajan S. Enzymatic and Non-Enzymatic Virulence Activities of Dermatophytes on Solid Media. *J Clin Diagn Res* (2017) 11:DC23–5. doi: 10.7860/JCDR/2017/23147.9410
12. Graser Y, Monod M, Bouchara JP, Dukik K, Nenoff P, Kargl A, et al. New insights in dermatophyte research. *Med Mycol* (2018) 56:2–9. doi: 10.1093/mmy/myx141
13. Woodfolk JA, Wheatley LM, Piyasena RV, Benjamin DC, Platts-Mills TA. Trichophyton antigens associated with IgE antibodies and delayed type hypersensitivity. Sequence homology to two families of serine proteinases. *J Biol Chem* (1998) 273:29489–96. doi: 10.1074/jbc.273.45.29489
14. Gao J, Takashima A. Cloning and characterization of Trichophyton rubrum genes encoding actin, Tri r2, and Tri r4. *J Clin Microbiol* (2004) 42:3298–9. doi: 10.1128/JCM.42.7.3298-3299.2004
15. Burmester A, Shelest E, Glockner G, Heddergott C, Schindler S, Staib P, et al. Comparative and functional genomics provide insights into the pathogenicity of dermatophytic fungi. *Genome Biol* (2011) 12:R7. doi: 10.1186/gb-2011-12-1-r7
16. Eymann C, Wachlin G, Albrecht D, Tiede S, Krummrei U, Junger M, et al. Exoproteome Analysis of Human Pathogenic Dermatophyte Species and Identification of Immunoreactive Proteins. *Proteomics Clin Appl* (2018) 12: e1800007. doi: 10.1002/prca.201800007
17. Karami Robati A, Khalili M, Hashemi Hazaveh SJ, Bayat M. Assessment of the subtilisin genes in Trichophyton rubrum and Microsporum canis from dermatophytosis. *Comp Clin Pathol* (2018) 27:1343–7. doi: 10.1007/s00580-018-2745-y
18. Mehul B, de Coi N, Grundt P, Genette A, Voegel JJ, Monod M. Detection of Trichophyton rubrum and Trichophyton interdigitale in onychomycosis using monoclonal antibodies against Sub6 (Tri r 2). *Mycoses* (2019) 62:32–40. doi: 10.1111/myc.12843
19. Martinez DA, Oliver BG, Gräser Y, Goldberg JM, Li W, Martinez-Rossi NM, et al. Comparative Genome Analysis of Trichophyton rubrum and Related Dermatophytes Reveals Candidate Genes Involved in Infection. *mBio* (2012) 3:e00259–12. doi: 10.1128/mBio.00259-12
20. Grumbt M, Monod M, Yamada T, Hertweck C, Kunert J, Staib P. Keratin degradation by dermatophytes relies on cysteine dioxygenase and a sulfite efflux pump. *J Invest Dermatol* (2013) 133:1550–5. doi: 10.1038/jid.2013.41
21. Heddergott C, Bruns S, Nietzsche S, Leonhardt I, Kurzai O, Kniemeyer O, et al. The Arthroderma benhamiae hydrophobin HypA mediates hydrophobicity and influences recognition by human immune effector cells. *Eukaryot Cell* (2012) 11:673–82. doi: 10.1128/EC.00037-12
22. Bitencourt TA, Rezende CP, Quaresemin NR, Moreno P, Hatanaka O, Rossi A, et al. Extracellular Vesicles From the Dermatophyte Trichophyton interdigitale Modulate Macrophage and Keratinocyte Functions. *Front Immunol* (2018) 9:2343. doi: 10.3389/fimmu.2018.02343
23. Kar B, Patel P, Free SJ. Trichophyton rubrum LysM proteins bind to fungal cell wall chitin and to the N-linked oligosaccharides present on human skin glycoproteins. *PloS One* (2019) 14:e0215034. doi: 10.1371/journal.pone.0215034
24. Martinez-Rossi NM, Jacob TR, Sanches PR, Peres NTA, Lang EAS, Martins MP, et al. Heat Shock Proteins in Dermatophytes: Current Advances and Perspectives. *Curr Genomics* (2016) 17:99–111. doi: 10.2174/1389202917666151116212437
25. Martins MP, Silva LG, Rossi A, Sanches PR, Souza LDR, Martinez-Rossi NM. Global Analysis of Cell Wall Genes Revealed Putative Virulence Factors in the Dermatophyte Trichophyton rubrum. *Front Microbiol* (2019) 10:2168. doi: 10.3389/fmicb.2019.02168
26. Martinez-Rossi NM, Peres NT, Rossi A. Pathogenesis of Dermatophytosis: Sensing the Host Tissue. *Mycopathologia* (2017) 182:215–27. doi: 10.1007/s11046-016-0057-9
27. Shende R, Wong SSW, Rapole S, Beau R, Ibrahim-Granet O, Monod M, et al. *Aspergillus fumigatus* conidial metalloprotease Mep1p cleaves host complement proteins. *J Biol Chem* (2018) 293:15538–55. doi: 10.1074/jbc.RA117.001476
28. Ho J, Wickramasinghe DN, Nikou SA, Hube B, Richardson JP, Naglik JR. Candidalysin Is a Potent Trigger of Alarmin and Antimicrobial Peptide Release in Epithelial Cells. *Cells* (2020) 9:699. doi: 10.3390/cells9030699
29. Aimanianda V, Bayry J, Bozza S, Kniemeyer O, Perruccio K, Elluru SR, et al. Surface hydrophobin prevents immune recognition of airborne fungal spores. *Nature* (2009) 460:1117–21. doi: 10.1038/nature08264
30. Salazar F, Brown GD. Antifungal Innate Immunity: A Perspective from the Last 10 Years. *J Innate Immun* (2018) 10:373–97. doi: 10.1159/000488539
31. Kasper L, Konig A, Koenig PA, Gresnigt MS, Westman J, Drummond RA, et al. The fungal peptide toxin Candidalysin activates the NLRP3 inflammasome and causes cytolysis in mononuclear phagocytes. *Nat Commun* (2018) 9:4260. doi: 10.1038/s41467-018-06607-1
32. Goyal S, Castrillon-Betancur JC, Klaile E, Slevogt H. The Interaction of Human Pathogenic Fungi With C-Type Lectin Receptors. *Front Immunol* (2018) 9:1261. doi: 10.3389/fimmu.2018.01261
33. Lionakis MS, Levitz SM. Host Control of Fungal Infections: Lessons from Basic Studies and Human Cohorts. *Annu Rev Immunol* (2018) 36:157–91. doi: 10.1146/annurev-immunol-042617-053318
34. Saijo S, Iwakura Y. Dectin-1 and Dectin-2 in innate immunity against fungi. *Int Immunol* (2011) 23:467–72. doi: 10.1093/intimm/dxr046
35. Sato K, Yang XL, Yudate T, Chung JS, Wu J, Luby-Phelps K, et al. Dectin-2 is a pattern recognition receptor for fungi that couples with the Fc receptor gamma chain to induce innate immune responses. *J Biol Chem* (2006) 281:38854–66. doi: 10.1074/jbc.M606542200

36. Yoshikawa FS, Yabe R, Iwakura Y, de Almeida SR, Saijo S. Dectin-1 and Dectin-2 promote control of the fungal pathogen Trichophyton rubrum independently of IL-17 and adaptive immunity in experimental deep dermatophytosis. *Innate Immun* (2016) 22:316–24. doi: 10.1177/1753425916645392
37. Yoshikawa FS, Ferreira LG, de Almeida SR. IL-1 signaling inhibits Trichophyton rubrum conidia development and modulates the IL-17 response in vivo. *Virulence* (2015) 6:449–57. doi: 10.1080/21505594.2015.1020274
38. Santiago K, Bomfim GF, Criado PR, Almeida SR. Monocyte-derived dendritic cells from patients with dermatophytosis restrict the growth of Trichophyton rubrum and induce CD4-T cell activation. *PloS One* (2014) 9: e110879. doi: 10.1371/journal.pone.0110879
39. Ferwerda B, Ferwerda G, Plantinga TS, Willment JA, van Spriel AB, Venselaar H, et al. Human dectin-1 deficiency and mucocutaneous fungal infections. *N Engl J Med* (2009) 361:1760–7. doi: 10.1056/NEJMoa0901053
40. Lanternier F, Pathan S, Vincent QB, Liu L, Cypowyj S, Prando C, et al. Deep dermatophytosis and inherited CARD9 deficiency. *N Engl J Med* (2013) 369:1704–14. doi: 10.1056/NEJMoa1208487
41. Heyl KA, Klassert TE, Heinrich A, Muller MM, Klaile E, Dienemann H, et al. Dectin-1 is expressed in human lung and mediates the proinflammatory immune response to nontypeable Haemophilus influenzae. *mBio* (2014) 5: e01492–14. doi: 10.1128/mBio.01492-14
42. van den Berg LM, Zijlstra-Willems EM, Richters CD, Ulrich MM, Geijtenbeek TB. Dectin-1 activation induces proliferation and migration of human keratinocytes enhancing wound re-epithelialization. *Cell Immunol* (2014) 289:49–54. doi: 10.1016/j.cellimm.2014.03.007
43. Huang XZ, Liang PP, Ma H, Yi JL, Yin SC, Chen ZR, et al. Effect of Culture Supernatant Derived from Trichophyton Rubrum Grown in the Nail Medium on the Innate Immunity-related Molecules of HaCaT. *Chin Med J Engl* (2015) 128:3094–100. doi: 10.4103/0366-6999.169106
44. Brasch J, Morig A, Neumann B, Proksch E. Expression of antimicrobial peptides and toll-like receptors is increased in tinea and pityriasis versicolor. *Mycoses* (2014) 57:147–52. doi: 10.1111/myc.12118
45. Celias DP, Motrán CC, Cervi L. Helminths Turning on the NLRP3 Inflammasome: Pros and Cons. *Trends Parasitol* (2020) 36:87–90. doi: 10.1016/j.pt.2019.10.012
46. Tavares AH, Burgel PH, Bocca AL. Turning Up the Heat: Inflammasome Activation by Fungal Pathogens. *PloS Pathog* (2015) 11:e1004948. doi: 10.1371/journal.ppat.1004948
47. Mao L, Zhang L, Li H, Chen W, Wang H, Wu S, et al. Pathogenic fungus Microsporum canis activates the NLRP3 inflammasome. *Infect Immun* (2014) 82:882–92. doi: 10.1128/IAI.01097-13
48. Li H, Wu S, Mao L, Lei G, Zhang L, Lu A, et al. Human pathogenic fungus Trichophyton schoenleinii activates the NLRP3 inflammasome. *Protein Cell* (2013) 4:529–38. doi: 10.1007/s13238-013-2127-9
49. Pietrella D, Pandey N, Gabrielli E, Pericolini E, Perito S, Kasper L, et al. Secreted aspartic proteases of Candida albicans activate the NLRP3 inflammasome. *Eur J Immunol* (2013) 43:679–92. doi: 10.1002/eji.201242691
50. Cambier L, Weatherspoon A, Defaweux V, Bagut ET, Heinen MP, Antoine N, et al. Assessment of the cutaneous immune response during Arthroderma benhamiae and A. vanbreuseghemii infection using an experimental mouse model. *Br J Dermatol* (2014) 170:625–33. doi: 10.1111/bjd.12673
51. Burstein VL, Guasconi L, Beccacece I, Theumer MG, Mena C, Prinz I, et al. IL-17-Mediated Immunity Controls Skin Infection and T Helper 1 Response during Experimental Microsporum canis Dermatophytosis. *J Invest Dermatol* (2018) 138:1744–53. doi: 10.1016/j.jid.2018.02.042
52. Willcocks S, Offord V, Seyfert HM, Coffey TJ, Werling D. Species-specific PAMP recognition by TLR2 and evidence for species-restricted interaction with Dectin-1. *J Leukoc Biol* (2013) 94:449–58. doi: 10.1189/jlb.0812390
53. Hesse-Macabata J, Morgner B, Elsner P, Hipler UC, Wiegand C. Tryptanthrin promotes keratinocyte and fibroblast responses in vitro after infection with Trichophyton benhamiae DSM6916. *Sci Rep* (2020) 10:1863. doi: 10.1038/s41598-020-58773-2
54. Cambier LC, Heinen MP, Bagut ET, Antoine NA, Mignon BR. Overexpression of TLR-2 and TLR-4 mRNA in feline polymorphonuclear neutrophils exposed to Microsporum canis. *Vet Dermatol* (2016) 27:78–81e22. doi: 10.1111/vde.12295
55. Celestrino GA, Reis APC, Criado PR, Benard G, Sousa MGT. Trichophyton rubrum Elicits Phagocytic and Pro-inflammatory Responses in Human Monocytes Through Toll-Like Receptor 2. *Front Microbiol* (2019) 10:2589. doi: 10.3389/fmicb.2019.02589
56. Almeida D de F, Fraga-Silva TF de C, Santos AR, Finato AC, Marchetti CM, Golim M de A, et al. TLR2-/- Mice Display Increased Clearance of Dermatophyte Trichophyton mentagrophytes in the Setting of Hyperglycemia. *Front Cell Infect Microbiol* (2017) 7:8. doi: 10.3389/fcimb.2017.00008
57. Netea MG, Sutmuller R, Hermann C, Van der Graaf CAA, Van der Meer JWM, van Krieken JH, et al. Toll-like receptor 2 suppresses immunity against Candida albicans through induction of IL-10 and regulatory T cells. *J Immunol Baltim Md 1950* (2004) 172:3712–8. doi: 10.4049/jimmunol.172.6.3712
58. Dillon S, Agrawal S, Banerjee K, Letterio J, Denning TL, Oswald-Richter K, et al. Yeast zymosan, a stimulus for TLR2 and dectin-1, induces regulatory antigen-presenting cells and immunological tolerance. *J Clin Invest* (2006) 116:916–28. doi: 10.1172/JCI27203
59. Moore BB, Kunkel SL. Attracting Attention: Discovery of IL-8/CXCL8 and the Birth of the Chemokine Field. *J Immunol Baltim Md 1950* (2019) 202:3–4. doi: 10.4049/jimmunol.1801485
60. Tani K, Adachi M, Nakamura Y, Kano R, Makimura K, Hasegawa A, et al. The effect of dermatophytes on cytokine production by human keratinocytes. *Arch Dermatol Res* (2007) 299:381–7. doi: 10.1007/s00403-007-0780-7
61. Ho AW, Kupper TS. T cells and the skin: from protective immunity to inflammatory skin disorders. *Nat Rev Immunol* (2019) 19:490–502. doi: 10.1038/s41577-019-0162-3
62. Simpson JK, Frobel P, Seneviratne SL, Brown M, Lowe DM, Grimbacher B, et al. Invasive dermatophyte infection with Trichophyton interdigitale is associated with prurigo-induced pseudoperforation and a signal transducer and activator of transcription 3 mutation. *Br J Dermatol* (2018) 179:750–4. doi: 10.1111/bjd.15781
63. Li J, Vinh DC, Casanova JL, Puel A. Inborn errors of immunity underlying fungal diseases in otherwise healthy individuals. *Curr Opin Microbiol* (2017) 40:46–57. doi: 10.1016/j.mib.2017.10.016
64. Drummond RA, Lionakis MS. Organ-specific mechanisms linking innate and adaptive antifungal immunity. *Semin Cell Dev Biol* (2018) 89:78–90. doi: 10.1016/j.semcdb.2018.01.008
65. Nakamura Y, Kano R, Hasegawa A, Watanabe S. Interleukin-8 and tumor necrosis factor alpha production in human epidermal keratinocytes induced by Trichophyton mentagrophytes. *Clin Diagn Lab Immunol* (2002) 9:935–7. doi: 10.1128/CDLI.9.4.935-937.2002
66. Faway E, Cambier L, De Vuyst E, Evrard C, Thiry M, Lambert de Rouvroit C, et al. Responses of Reconstructed Human Epidermis to Trichophyton rubrum Infection and Impairment of Infection by the Inhibitor PD169316. *J Invest Dermatol* (2019) 139:2080–9.e6. doi: 10.1016/j.jid.2019.03.1147
67. Sawada Y, Nakamura M, Kabashima-Kubo R, Shimauchi T, Kobayashi M, Tokura Y. Defective epidermal innate immunity and resultant superficial dermatophytosis in adult T-cell leukemia/lymphoma. *Clin Cancer Res* (2012) 18:3772–9. doi: 10.1158/1078-0432.CCR-12-0292
68. Day AJ, Milner CM. TSG-6: A multifunctional protein with anti-inflammatory and tissue-protective properties. *Matrix Biol* (2019) 78–79:60–83. doi: 10.1016/j.matbio.2018.01.011
69. Hay RJ, Calderon RA, Mackenzie CD. Experimental dermatophytosis in mice: correlation between light and electron microscopic changes in primary, secondary and chronic infections. *Br J Exp Pathol* (1988) 69:703–16.
70. Calderon RA, Hay RJ. Fungicidal activity of human neutrophils and monocytes on dermatophyte fungi, Trichophyton quinckeanum and Trichophyton rubrum. *Immunology* (1987) 61:289–95.
71. Cambier L, Mathy A, Baldo A, Bagut ET, Tabart J, Antoine N, et al. Feline polymorphonuclear neutrophils produce pro-inflammatory cytokines following exposure to Microsporum canis. *Vet Microbiol* (2013) 162:800–5. doi: 10.1016/j.vetmic.2012.10.016
72. Hay RJ. Immune Responses to Dermatophytoses. *New Insights Med Mycology* (2007) 227–39. doi: 10.1007/978-1-4020-6397-8_10
73. Neema S, Singh S, Pathak N, Khan MA. Widespread Superficial Dermatophytosis in Patient on Secukinumab for Treatment of Chronic

Plaque Psoriasis. *Indian Dermatol Online J* (2019) 10:76–8. doi: 10.4103/idoj.IDOJ_170_18
74. de Sousa Mda G, Santana GB, Criado PR, Benard G. Chronic widespread dermatophytosis due to Trichophyton rubrum: a syndrome associated with a Trichophyton-specific functional defect of phagocytes. *Front Microbiol* (2015) 6:801. doi: 10.3389/fmicb.2015.00801
75. Ogawa H, Summerbell RC, Clemons KV, Koga T, Ran YP, Rashid A, et al. Dermatophytes and host defence in cutaneous mycoses. *Med Mycol* (1998) 36 Suppl 1:166–73.
76. Lourdes LS, Mitchell CL, Glavin FL, Schain DC, Kaye FJ. Recurrent dermatophytosis (Majocchi granuloma) associated with chemotherapy-induced neutropenia. *J Clin Oncol* (2014) 32:e92–4. doi: 10.1200/JCO.2012.47.3330
77. Mays SR, Bogle MA, Bodey GP. Cutaneous fungal infections in the oncology patient: recognition and management. *Am J Clin Dermatol* (2006) 7:31–43. doi: 10.2165/00128071-200607010-00004
78. Queiroz-Telles F, Mercier T, Maertens J, Sola CBS, Bonfim C, Lortholary O, et al. Successful Allogenic Stem Cell Transplantation in Patients with Inherited CARD9 Deficiency. *J Clin Immunol* (2019) 39:462–9. doi: 10.1007/s10875-019-00662-z
79. Drummond RA, Swamydas M, Oikonomou V, Zhai B, Dambuza IM, Schaefer BC, et al. CARD9(+) microglia promote antifungal immunity via IL-1beta- and CXCL1-mediated neutrophil recruitment. *Nat Immunol* (2019) 20:559–70. doi: 10.1038/s41590-019-0377-2
80. Furue M, Furue K, Tsuji G, Nakahara T. Interleukin-17A and Keratinocytes in Psoriasis. *Int J Mol Sci* (2020) 21:1275. doi: 10.3390/ijms21041275
81. Firat YH, Simanski M, Rademacher F, Schroder L, Brasch J, Harder J. Infection of keratinocytes with Trichophytum rubrum induces epidermal growth factor-dependent RNase 7 and human beta-defensin-3 expression. *PloS One* (2014) 9:e93941. doi: 10.1371/journal.pone.0093941
82. Buchau AS. EGFR (trans)activation mediates IL-8 and distinct human antimicrobial peptide and protein production following skin injury. *J Invest Dermatol* (2010) 130:929–32. doi: 10.1038/jid.2009.371
83. Buchau AS, Gallo RL. Innate immunity and antimicrobial defense systems in psoriasis. *Clin Dermatol* (2007) 25:616–24. doi: 10.1016/j.clindermatol.2007.08.016
84. Lopez-Garcia B, Lee PH, Gallo RL. Expression and potential function of cathelicidin antimicrobial peptides in dermatophytosis and tinea versicolor. *J Antimicrob Chemother* (2006) 57:877–82. doi: 10.1093/jac/dkl078
85. Fritz P, Beck-Jendroschek V, Brasch J. Inhibition of dermatophytes by the antimicrobial peptides human beta-defensin-2, ribonuclease 7 and psoriasin. *Med Mycol* (2012) 50:579–84. doi: 10.3109/13693786.2012.660203
86. Prinz I, Sandrock I, Mrowietz U. Interleukin-17 cytokines: Effectors and targets in psoriasis-A breakthrough in understanding and treatment. *J Exp Med* (2020) 217(1):e20191397. doi: 10.1084/jem.20191397
87. Ridaura VK, Bouladoux N, Claesen J, Chen YE, Byrd AL, Constantinides MG, et al. Contextual control of skin immunity and inflammation by Corynebacterium. *J Exp Med* (2018) 215:785–99. doi: 10.1084/jem.20171079
88. Dutzan N, Kajikawa T, Abusleme L, Greenwell-Wild T, Zuazo CE, Ikeuchi T, et al. A dysbiotic microbiome triggers TH17 cells to mediate oral mucosal immunopathology in mice and humans. *Sci Transl Med* (2018) 10(463): eaat0797. doi: 10.1126/scitranslmed.aat0797
89. Monin L, Gaffen SL. Interleukin 17 Family Cytokines: Signaling Mechanisms, Biological Activities, and Therapeutic Implications. *Cold Spring Harb Perspect Biol* (2018) 10:a028522. doi: 10.1101/cshperspect.a028522
90. Kashem SW, Kaplan DH. Skin Immunity to Candida albicans. *Trends Immunol* (2016) 37:440–50. doi: 10.1016/j.it.2016.04.007
91. Dainichi T, Kitoh A, Otsuka A, Nakajima S, Nomura T, Kaplan DH, et al. The epithelial immune microenvironment (EIME) in atopic dermatitis and psoriasis. *Nat Immunol* (2018) 19:1286–98. doi: 10.1038/s41590-018-0256-2
92. Chong WP, Mattapallil MJ, Raychaudhuri K, Bing SJ, Wu S, Zhong Y, et al. The Cytokine IL-17A Limits Th17 Pathogenicity via a Negative Feedback Loop Driven by Autocrine Induction of IL-24. *Immunity* (2020) 53:384–97.e5. doi: 10.1016/j.immuni.2020.06.022
93. Puel A, Döffinger R, Natividad A, Chrabieh M, Barcenas-Morales G, Picard C, et al. Autoantibodies against IL-17A, IL-17F, and IL-22 in patients with chronic mucocutaneous candidiasis and autoimmune polyendocrine syndrome type I. *J Exp Med* (2010) 207:291–7. doi: 10.1084/jem.20091983
94. Acosta-Rodriguez EV, Rivino L, Geginat J, Jarrossay D, Gattorno M, Lanzavecchia A, et al. Surface phenotype and antigenic specificity of human interleukin 17-producing T helper memory cells. *Nat Immunol* (2007) 8:639–46. doi: 10.1038/ni1467
95. Park CO, Fu X, Jiang X, Pan Y, Teague JE, Collins N, et al. Staged development of long-lived T-cell receptor αβ T H 17 resident memory T-cell population to Candida albicans after skin infection. *J Allergy Clin Immunol* (2018) 142:647–62. doi: 10.1016/j.jaci.2017.09.042
96. Okada S, Asano T, Moriya K, Boisson-Dupuis S, Kobayashi M, Casanova JL, et al. Human STAT1 Gain-of-Function Heterozygous Mutations: Chronic Mucocutaneous Candidiasis and Type I Interferonopathy. *J Clin Immunol* (2020) 40:1065–81. doi: 10.1007/s10875-020-00847-x
97. Toubiana J, Okada S, Hiller J, Oleastro M, Lagos Gomez M, Aldave Becerra JC, et al. Heterozygous STAT1 gain-of-function mutations underlie an unexpectedly broad clinical phenotype. *Blood* (2016) 127:3154–64. doi: 10.1182/blood-2015-11-679902
98. Quach OL, Hsu S. Perianal Dermatophytosis During Secukinumab Therapy for Plaque Psoriasis. *JAMA Dermatol* (2016) 152:486–7. doi: 10.1001/jamadermatol.2015.4992
99. Corvilain E, Casanova J-L, Puel A. Inherited CARD9 Deficiency: Invasive Disease Caused by Ascomycete Fungi in Previously Healthy Children and Adults. *J Clin Immunol* (2018) 38:656–93. doi: 10.1007/s10875-018-0539-2
100. Hay RJ, Calderon RA, Collins MJ. Experimental dermatophytosis: the clinical and histopathologic features of a mouse model using Trichophyton quinckeanum (mouse favus). *J Invest Dermatol* (1983) 81:270–4. doi: 10.1111/1523-1747.ep12518292
101. Calderon RA, Hay RJ. Cell-mediated immunity in experimental murine dermatophytosis. II. Adoptive transfer of immunity to dermatophyte infection by lymphoid cells from donors with acute or chronic infections. *Immunology* (1984) 53:465–72.
102. de Freitas RS, de Freitas THP, Siqueira LPM, Gimenes VMF, Benard G. First report of tinea corporis caused by Arthroderma benhamiae in Brazil. *Braz J Microbiol Publ Braz Soc Microbiol* (2019) 50:985–7. doi: 10.1007/s42770-019-00141-y
103. Gupta AK, MacLeod MA, Foley KA, Gupta G, Friedlander SF. Fungal Skin Infections. *Pediatr Rev* (2017) 38:8–22. doi: 10.1542/pir.2015-0140
104. Monod M. Development of a mouse infection model to bridge the gap between molecular biology and immunology in dermatophyte research. *Br J Dermatol* (2014) 170:491–2. doi: 10.1111/bjd.12866
105. Hay RJ. Tinea Capitis: Current Status. *Mycopathologia* (2017) 182:87–93. doi: 10.1007/s11046-016-0058-8
106. Chiapello LS, Dib MD, Nuncira CT, Nardelli L, Vullo C, Collino C, et al. Mycetoma of the scalp due to Microsporum canis: hystopathologic, mycologic, and immunogenetic features in a 6-year-old girl. *Diagn Microbiol Infect Dis* (2011) 70:145–9. doi: 10.1016/j.diagmicrobio.2011.02.003
107. Spesso MF, Nuncira CT, Burstein VL, Masih DT, Dib MD, Chiapello LS. Microsatellite-primed PCR and random primer amplification polymorphic DNA for the identification and epidemiology of dermatophytes. *Eur J Clin Microbiol Infect Dis* (2013) 32:1009–15. doi: 10.1007/s10096-013-1839-3
108. Kashem SW, Igyarto BZ, Gerami-Nejad M, Kumamoto Y, Mohammed J, Jarrett E, et al. Candida albicans morphology and dendritic cell subsets determine T helper cell differentiation. *Immunity* (2015) 42:356–66. doi: 10.1016/j.immuni.2015.01.008
109. Sparber F, De Gregorio C, Steckholzer S, Ferreira FM, Dolowschiak T, Ruchti F, et al. The Skin Commensal Yeast Malassezia Triggers a Type 17 Response that Coordinates Anti-fungal Immunity and Exacerbates Skin Inflammation. *Cell Host Microbe* (2019) 25:389–403.e6. doi: 10.1016/j.chom.2019.02.002
110. Shiraki Y, Ishibashi Y, Hiruma M, Nishikawa A, Ikeda S. Cytokine secretion profiles of human keratinocytes during Trichophyton tonsurans and Arthroderma benhamiae infections. *J Med Microbiol* (2006) 55:1175–85. doi: 10.1099/jmm.0.46632-0
111. Sparber F, LeibundGut-Landmann S. IL-17 Takes Center Stage in Dermatophytosis. *J Invest Dermatol* (2018) 138:1691–3. doi: 10.1016/j.jid.2018.03.1518
112. Baltazar L de M, Santos PC, de Paula TP, Rachid MA, Cisalpino PS, Souza DG, et al. IFN-γ impairs Trichophyton rubrum proliferation in a murine model of dermatophytosis through the production of IL-1β and reactive oxygen species. *Med Mycol* (2014) 52:293–302. doi: 10.1093/mmy/myt011

113. Stark MA, Huo Y, Burcin TL, Morris MA, Olson TS, Ley K. Phagocytosis of apoptotic neutrophils regulates granulopoiesis via IL-23 and IL-17. *Immunity* (2005) 22:285–94. doi: 10.1016/j.immuni.2005.01.011
114. Liu L, Okada S, Kong XF, Kreins AY, Cypowyj S, Abhyankar A, et al. Gain-of-function human STAT1 mutations impair IL-17 immunity and underlie chronic mucocutaneous candidiasis. *J Exp Med* (2011) 208:1635–48. doi: 10.1084/jem.20110958
115. Martinez-Martinez L, Martinez-Saavedra MT, Fuentes-Prior P, Barnadas M, Rubiales MV, Noda J, et al. A novel gain-of-function STAT1 mutation resulting in basal phosphorylation of STAT1 and increased distal IFN-gamma-mediated responses in chronic mucocutaneous candidiasis. *Mol Immunol* (2015) 68:597–605. doi: 10.1016/j.molimm.2015.09.014
116. Baris S, Alroqi F, Kiykim A, Karakoc-Aydiner E, Ogulur I, Ozen A, et al. Severe Early-Onset Combined Immunodeficiency due to Heterozygous Gain-of-Function Mutations in STAT1. *J Clin Immunol* (2016) 36:641–8. doi: 10.1007/s10875-016-0312-3
117. Zheng J, van de Veerdonk FL, Crossland KL, Smeekens SP, Chan CM, Al Shehri T, et al. Gain-of-function STAT1 mutations impair STAT3 activity in patients with chronic mucocutaneous candidiasis (CMC). *Eur J Immunol* (2015) 45:2834–46. doi: 10.1002/eji.201445344
118. Depner M, Fuchs S, Raabe J, Frede N, Glocker C, Doffinger R, et al. The Extended Clinical Phenotype of 26 Patients with Chronic Mucocutaneous Candidiasis due to Gain-of-Function Mutations in STAT1. *J Clin Immunol* (2016) 36:73–84. doi: 10.1007/s10875-015-0214-9
119. Higgins E, Al Shehri T, McAleer MA, Conlon N, Feighery C, Lilic D, et al. Use of ruxolitinib to successfully treat chronic mucocutaneous candidiasis caused by gain-of-function signal transducer and activator of transcription 1 (STAT1) mutation. *J Allergy Clin Immunol* (2015) 135:551–3. doi: 10.1016/j.jaci.2014.12.1867
120. Heinen MP, Cambier L, Antoine N, Gabriel A, Gillet L, Bureau F, et al. Th1 and Th17 Immune Responses Act Complementarily to Optimally Control Superficial Dermatophytosis. *J Invest Dermatol* (2019) 139:626–37. doi: 10.1016/j.jid.2018.07.040
121. Verma AH, Gaffen SL. Dermatophyte Immune Memory Is Only Skin-Deep. *J Invest Dermatol* (2019) 139:517–9. doi: 10.1016/j.jid.2018.10.022
122. Santus W, Barresi S, Mingozzi F, Broggi A, Orlandi I, Stamerra G, et al. Skin infections are eliminated by cooperation of the fibrinolytic and innate immune systems. *Sci Immunol* (2017) 2:eaan2725. doi: 10.1126/sciimmunol.aan2725
123. Belkaid Y, Tamoutounour S. The influence of skin microorganisms on cutaneous immunity. *Nat Rev Immunol* (2016) 16:353–66. doi: 10.1038/nri.2016.48
124. Kashem SW, Riedl MS, Yao C, Honda CN, Vulchanova L, Kaplan DH. Nociceptive Sensory Fibers Drive Interleukin-23 Production from CD301b+ Dermal Dendritic Cells and Drive Protective Cutaneous Immunity. *Immunity* (2015) 43:515–26. doi: 10.1016/j.immuni.2015.08.016
125. Igyarto BZ, Haley K, Ortner D, Bobr A, Gerami-Nejad M, Edelson BT, et al. Skin-resident murine dendritic cell subsets promote distinct and opposing antigen-specific T helper cell responses. *Immunity* (2011) 35:260–72. doi: 10.1016/j.immuni.2011.06.005
126. Drummond RA, Franco LM, Lionakis MS. Human CARD9: A Critical Molecule of Fungal Immune Surveillance. *Front Immunol* (2018) 9:1836. doi: 10.3389/fimmu.2018.01836
127. Jachiet M, Lanternier F, Rybojad M, Bagot M, Ibrahim L, Casanova JL, et al. Posaconazole treatment of extensive skin and nail dermatophytosis due to autosomal recessive deficiency of CARD9. *JAMA Dermatol* (2015) 151:192–4. doi: 10.1001/jamadermatol.2014.2154
128. Boudghene Stambouli O, Amrani N, Boudghene Stambouli K, Bouali F. Dermatophytic disease with deficit in CARD9: A new case with a brain impairment. *J Mycol Med* (2017) 27:250–3. doi: 10.1016/j.mycmed.2017.01.001
129. Grumach AS, de Queiroz-Telles F, Migaud M, Lanternier F, Filho NR, Palma SM, et al. A homozygous CARD9 mutation in a Brazilian patient with deep dermatophytosis. *J Clin Immunol* (2015) 35:486–90. doi: 10.1007/s10875-015-0170-4
130. Alves de Medeiros AK, Lodewick E, Bogaert DJA, Haerynck F, Van daele S, Lambrecht B, et al. Chronic and Invasive Fungal Infections in a Family with CARD9 Deficiency. *J Clin Immunol* (2016) 36:204–9. doi: 10.1007/s10875-016-0255-8
131. Kanno E, Kawakami K, Tanno H, Suzuki A, Sato N, Masaki A, et al. Contribution of CARD9-mediated signalling to wound healing in skin. *Exp Dermatol* (2017) 26:1097–104. doi: 10.1111/exd.13389
132. Yasukawa S, Miyazaki Y, Yoshii C, Nakaya M, Ozaki N, Toda S, et al. An ITAM-Syk-CARD9 signalling axis triggers contact hypersensitivity by stimulating IL-1 production in dendritic cells. *Nat Commun* (2014) 5:3755. doi: 10.1038/ncomms4755
133. Bongomin F, Gago S, Oladele RO, Denning DW. Global and Multi-National Prevalence of Fungal Diseases-Estimate Precision. *J Fungi* (2017) 3:57. doi: 10.3390/jof3040057
134. Woodfolk JA. Allergy and dermatophytes. *Clin Microbiol Rev* (2005) 18:30–43. doi: 10.1128/CMR.18.1.30-43.2005
135. Ebert A, Monod M, Salamin K, Burmester A, Uhrlass S, Wiegand C, et al. Alarming India-wide phenomenon of antifungal resistance in dermatophytes: A multicentre study. *Mycoses* (2020) 63:717–28. doi: 10.1111/myc.13091

Conflict of Interest: The authors declare that the research was conducted in the absence of any commercial or financial relationships that could be construed as a potential conflict of interest.

frontiers in Immunology

REVIEW
published: 03 February 2021
doi: 10.3389/fimmu.2020.615402

Interactions of the Skin Pathogen *Haemophilus ducreyi* With the Human Host

Julie A. Brothwell[1]*, *Brad Griesenauer*[1], *Li Chen*[2] and *Stanley M. Spinola*[1,2,3]

[1] Department of Microbiology and Immunology, Indiana University School of Medicine, Indianapolis, IN, United States, [2] Department of Medicine, Indiana University School of Medicine, Indianapolis, IN, United States, [3] Department of Pathology and Laboratory Medicine, Indiana University School of Medicine, Indianapolis, IN, United States

The obligate human pathogen *Haemophilus ducreyi* causes both cutaneous ulcers in children and sexually transmitted genital ulcers (chancroid) in adults. Pathogenesis is dependent on avoiding phagocytosis and exploiting the suppurative granuloma-like niche, which contains a myriad of innate immune cells and memory T cells. Despite this immune infiltrate, long-lived immune protection does not develop against repeated *H. ducreyi* infections—even with the same strain. Most of what we know about infectious skin diseases comes from naturally occurring infections and/or animal models; however, for *H. ducreyi*, this information comes from an experimental model of infection in human volunteers that was developed nearly three decades ago. The model mirrors the progression of natural disease and serves as a valuable tool to determine the composition of the immune cell infiltrate early in disease and to identify host and bacterial factors that are required for the establishment of infection and disease progression. Most recently, holistic investigation of the experimentally infected skin microenvironment using multiple "omics" techniques has revealed that non-canonical bacterial virulence factors, such as genes involved in central metabolism, may be relevant to disease progression. Thus, the immune system not only defends the host against *H. ducreyi*, but also dictates the nutrient availability for the invading bacteria, which must adapt their gene expression to exploit the inflammatory metabolic niche. These findings have broadened our view of the host-pathogen interaction network from considering only classical, effector-based virulence paradigms to include adaptations to the metabolic environment. How both host and bacterial factors interact to determine infection outcome is a current focus in the field. Here, we review what we have learned from experimental *H. ducreyi* infection about host-pathogen interactions, make comparisons to what is known for other skin pathogens, and discuss how novel technologies will deepen our understanding of this infection.

Keywords: *Haemophilus ducreyi*, interactome, metabolome, skin, immune response

OPEN ACCESS

Edited by:
Roberta Olmo Pinheiro, Oswaldo Cruz Foundation, Brazil

Reviewed by:
Michael Marks, University of London, United Kingdom
Yu-Ching Su, Lund University, Sweden
Kristian Riesbeck, Lund University, Sweden

***Correspondence:**
Julie A. Brothwell
jbrothwe@iu.edu

Specialty section:
This article was submitted to Microbial Immunology, a section of the journal Frontiers in Immunology

Received: *09 October 2020*
Accepted: *21 December 2020*
Published: *03 February 2021*

Citation:
Brothwell JA, Griesenauer B, Chen L and Spinola SM (2021) Interactions of the Skin Pathogen Haemophilus ducreyi With the Human Host. Front. Immunol. 11:615402. doi: 10.3389/fimmu.2020.615402

INTRODUCTION

As a primary barrier to infection, the skin possesses multiple defense mechanisms including antimicrobial peptides, immune cells, and the commensal microbiome. These factors, among others, contribute to inter-person variability in response to infection. Studies investigating natural infection outcomes have been very useful for determining pathology later in infection (1), but are limited in their ability to inform what happens early in infection, since patients generally do not seek care at these times. Differences in host factors as well as different strains of a given pathogen, which may have varying degrees of virulence, further confound understanding how the immune system responds to infection.

The skin immune response differs among pathogens despite the general conservation of cell types that either reside in and patrol the skin or that are recruited to combat the infectious agent. Much of what we know about skin immunology has been inferred from murine infection models or by comparing datasets from convenience human skin samples obtained from plastic surgery (2) and from biopsy of diseased skin (3, 4). Both strategies have elucidated important players in the skin immune response, but have notable caveats. While animal models allow for better controlled studies, the skin of mice differs from human skin in terms of thickness, time to healing, microbiome, and immune response, which can all be attributed to differences in both genetics and environments. Thus, interpretations of animal studies are limited to pathogenesis and immune mechanisms shared by both the animal model and humans. Extrapolation of differential gene expression between diseased and either healthy or reference datasets from different anatomical locales, such as convenience human tissue samples, can have similar limitations.

To circumvent these limitations and further our understanding of how human skin responds to infection in a controlled fashion, we have used experimental skin infection of human volunteers with the extracellular, Gram-negative bacterium *Haemophilus ducreyi* for nearly thirty years (5, 6). *H. ducreyi* is the causative agent of two diseases: the sexually transmitted genital ulcer (GU) disease chancroid and cutaneous ulcers (CU) in children (7). Chancroid is a sexually transmitted genital ulcer disease and facilitates the transmission of HIV-1 (8). Due to syndromic management, defined as the provision of treatment without diagnostic testing, the epidemiology of chancroid is not well understood, but chancroid remains endemic in developing countries *via* reservoirs of infected commercial sex workers (7). Recently, in tropical or equatorial regions with high prevalence of CU caused by *Treponema pallidum* subsp. *pertenue* (yaws), *H. ducreyi* was found to be the etiological agent in ~40-60% of lesions (9–11). For both yaws and *H. ducreyi*, the ulcers are primarily found on the lower leg and affect approximately 4-10% of children in endemic regions. While the prevalence of *H. ducreyi*-associated CU initially decreased following mass drug administration of azithromycin, the disease was not eliminated due to environmental reservoirs (12, 13). Thus, there is a continuing need to understand *H. ducreyi* pathogenesis and the host response to this infection.

There are two classes of *H. ducreyi* isolates; class I and II strains can be differentiated based on several variable extracellular or secreted proteins (DsrA, NcaA, DltA, LspA1, LspA2, and others), and lipooligosaccharide (LOS) structure (14), but are otherwise highly conserved, clinically indistinguishable, and found in significant proportions of both CU and GU (12, 15–17). Although the majority of CU are typically caused by a single genotype, coinfections with both classes are common in CU (12); such studies have not been done in GU. Most *in vitro* work and experimental human infection utilizes *H. ducreyi* 35000HP, a human-passaged class I GU strain. By whole genome sequencing, ~70% of CU strains are nearly identical to 35000HP, indicating that our model is highly relevant to both GU and CU (15, 16).

Although both class I and II strains cause CU and GU, whether individual isolates can cause both diseases within a population is unknown due to a lack of surveillance of GU in CU endemic areas and *vice versa*. In addition, the number of HD isolates that have been sequenced is quite limited, and syndromic management of GU precludes our understanding of how prevalent each class is in the population. Whether there are differences in infectivity or the ability each class to cause disease in different anatomical locales in natural infection is unknown. To date, 35000HP is the only strain used in experimental human infection. Since 35000HP is a GU isolate and able to infect nongenital skin following the same disease kinetics and pathology seen in GU, it appears that its pathogenic potential is similar in genital and nongenital skin.

Here, we highlight and discuss the recent advances made in understanding *H. ducreyi* pathogenesis *via* mutant versus parent comparison trials, the immune response to *H. ducreyi* infection, and how *H. ducreyi* may be exploiting the immune system to promote its pathogenesis.

OVERVIEW OF THE HUMAN CHALLENGE MODEL

The *H. ducreyi* experimental infection model is arguably one of the best studied human infection model systems. It is also a powerful model for investigating bacterial pathogenesis due to FDA approval for not only experimental infection of wild type and mutant bacterial strains but also the ability to perform punch biopsies of infected sites. In this model, as few as one bacterium introduced into wounded skin on the upper arm is sufficient to cause infection (18). This suggests that experimental human infection mimics natural infection—especially considering that infection of animal models requires 3–6 log-fold higher inocula. Although most individuals experimentally infected with wild type *H. ducreyi* form papules within 24 hours of infection, only ~70% of individuals progress to the pustular stage; the other ~30% spontaneously resolve the infection within 2 to 5 days (5) (**Figure 1**). The clinical endpoints are resolution of infection or development of a painful pustule; volunteers with pustules (N=231) are infected for 8.1 ± 2.4 (mean ± SD) days. As subject safety considerations preclude progression of

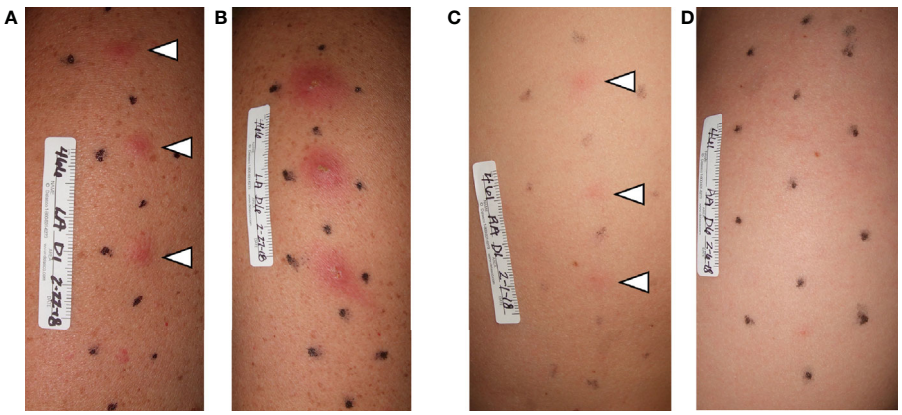

FIGURE 1 | Photographs of clinical outcomes in the *H. ducreyi* human challenge model. Volunteers were infected in three sites and mock infected in the fourth, bottom-most site. On day 1 (24 hpi), both volunteers had papules at all three infected sites (**A**, **C**; white arrowheads). On day 6 of infection, the volunteer in **(A)** had developed pustules at all infected sites **(B)**. In contrast, by day 6, the volunteer in **(C)** had resolved infection at all three infected sites **(D)**.

experimental infection to the ulcerative stage, experimental infection mirrors natural disease only until the pustular stage. Pustule formation is dependent on host effects and gender, as men are twice as likely to form pustules as women (5). Re-infection of individuals from past *H. ducreyi* challenge studies demonstrated that individuals who initially formed pustules tend to form pustules and individuals who resolved infection the first time tend to resolve infection a second time at different statistically significant rates (19). This was not attributable to serum bactericidal or opsonizing antibodies. Similarly, in patients with natural chancroid, there is no apparent protection to re-infection. Although the underlying molecular mechanisms leading to pustule formation or resolution are unknown, varying degrees of immune tolerance—particularly with regard to dendritic cells (DCs)—are hypothesized to play a role.

To date, 34 mutants have been tested in the human model to define which virulence factors are required for infection (**Table 1**). The methods for these double-blinded, multi-stage, dose ranging studies have been reviewed previously (5). Mutants are categorized as virulent (form pustules at doses similar to the parent), partially attenuated (form pustules at doses 2- or 3-fold that of the parent, but not at doses equivalent to the parent) or as attenuated (unable to form pustules even at doses 10-fold that of the parent). Of the 34 mutants, 10 were attenuated, 9 were partially attenuated, and 15 were virulent. The trials have shown the importance of evasion of phagocytosis, resistance to complement mediated killing and antimicrobial peptides, the ability to form aggregates, quorum sensing, adherence to collagen and fibrin, nutrient uptake, and adaptation to starvation as pathogenic mechanisms for disease progression. The interaction of some of these virulence determinants with the host immune response will be discussed in detail below.

To our knowledge, the only other active human challenge model using a skin pathogen is the Bacille Calmette-Guérin (BCG) model, which was developed about twelve years ago to assess BCG vaccine efficiency against BCG infection (52). Later the BCG vaccine challenge model was used to evaluate if specific *Mycobacterium tuberculosis* (53) and *M. leprae* (54) proteins were cross-reactive. This model injects BCG into the forearm skin and has also been instrumental in defining the immune infiltrate and cytokines released into the microenvironment (52).

THE ROLE OF THE HOST DURING *H. DUCREYI* INFECTION

Histopathology of the Cutaneous Ulcer

Our understanding of the role of the host during disease has been aided by histological examination of both experimental and natural infections (1, 55). A schematic of the progression of disease from the papular to pustular stage is found in **Figure 2**. Infection is dependent on entry through wounds in the skin; intact skin is resistant to infection. *H. ducreyi* first encounters keratinocytes, fibroblasts, tissue resident and memory T cells, and tissue resident DCs in healthy skin but remains extracellular throughout infection (1, 18, 55). Collagen and fibrin are deposited in the wounds, and innate immune cells are recruited to the site of infection (55, 57). Neutrophils initially surround and attempt to phagocytose the bacteria, forming a microabscess in the epidermis and dermis (55, 57). Macrophages concurrently migrate into the tissue and form a "collar" around the base of the abscess (1, 57). Immature DCs, natural killer (NK) cells, T cells, and a few B cells are simultaneously recruited and localize primarily below the macrophage collar (58–61). If the phagocytic response fails to clear the organism, the papule evolves into a pustule that resembles a suppurative granuloma and eventually erodes into a painful ulcer (1).

Immunocytochemistry of papules and pustules revealed that the bacteria are mainly confined to the upper levels of the pustule, where they are surrounded by neutrophils (1, 55, 57). In experimental infection, *H. ducreyi* is localized to the epidermis and upper dermis, which contrasts to the localization of other

TABLE 1 | *H. ducreyi* mutants tested in the human challenge model.

Gene	Definition	Function	Results	Source of Mutant (Reference)
hhdB	secretion/activation of hemolysin	lyses fibroblasts	Virulent	Munson (20)
losB	D-glycero-D-manno-heptosyltransferase	extends LOS beyond KDO-triheptose-glucose	Virulent	Munson (21)
lst	lipooligosaccharide sialytransferase	adds sialic acid to major glycoform of LOS	Virulent	Munson (21)
ftpA	fine tangled pilus major subunit	unknown	Virulent	Spinola (22)
hgbA	hemoglobin binding outer membrane protein	heme/iron acquisition and transport from hemoglobin	Attenuated	Elkins (23)
momp	major outer membrane protein	OmpA homologue; minor role in fibronectin binding	Virulent	Spinola & Hansen (24)
pal	peptidoglycan associated lipoprotein	lipoprotein; OM stability	Attenuated	Spinola (25)
dsrA	ducreyi serum resistance A	OMP; major role in serum resistance	Attenuated	Elkins (26)
cdtC	cytolethal distending toxin	toxic for T cells, epithelial cells, fibroblasts	Virulent	Hansen (27)
cdtC/hhdB	double mutant, cytolethal distending toxin, hemolysin	toxic for T cells, epithelial cells, fibroblasts; lyses fibroblasts	Virulent	Hansen & Munson (27)
glu	glucosyltransferase gene	adds glucose to KDO-triheptose LOS core	Virulent	Campagnari & Munson (28)
sodC	superoxide dismutase C	detoxifies ROS for bacteria in phagolysosomes	Virulent	Kawula (29)
tadA	tight adherence protein A	type 1V secretion; secretion of Flp proteins	Attenuated	Hansen (30)
lspA1/lspA2	double mutant, large supernatant proteins	secreted proteins; prevent Fc-γRmediated phagocytosis	Attenuated	Hansen (31)
ompP2A/ompP2B	double mutant, porin proteins	encode known classical trimeric porins	Virulent	Campagnari (32)
dltA	ducreyi lectin A	OMP; partial serum resistance	Partially Attenuated	Elkins (33)
ncaA	necessary for collagen adherence	OMP; confers collagen binding	Attenuated	Kawula (34)
wecA	first enzyme in the ECA biosynthetic pathway	initiates synthesis of putative ECA glycoconjugate	Partially Attenuated	Munson (35)
tdX/tdhA	double mutant; ton B dependent receptors	heme uptake	Virulent	Elkins (36)
fgbA	putative fibrinogen binding adhesion	OMP that confers binding to fibrinogen	Partially Attenuated	Bauer & Janowicz (37)
luxS	homolog of *V. harveyi luxS*	Autoinducer; quorum sensing	Partially Attenuated	Hansen (38)
sapA	Susceptibility to antimicrobial peptides	Confers partial resistance to LL-37	Partially Attenuated	Bauer (39)
cpxA	Sensor kinase of CpxRA 2-component system	Uncontrolled activation of CpxR	Attenuated	Munson & Spinola (40)
flp-1,-2,-3	Fimbria-like proteins 1,2,3	Microcolony formation	Attenuated	Munson (41)
cpxR	Response Regulator of CpxRA system	Senses Extracytoplasmic Stress	Virulent	Hansen (42)
sapBC	Susceptibility to antimicrobial peptides	Confers resistance to LL-37	Attenuated	Bauer (43)
neuA	CMP sialic acid synthetase	Makes required substrate for all sialyltransferases	Virulent	Munson (44)
csrA	Carbon storage regulator	Post transcriptional regulator; affects mRNA stability and translation	Partially Attenuated	Spinola (45)
ompP4	OMP with homology to *H. influenzae ompP4*	putative lipoprotein expressed *in vivo*	Virulent	Janowicz (46)

(Continued)

TABLE 1 | Continued

Gene	Definition	Function	Results	Source of Mutant (Reference)
hfq	Facilitates binding of sRNAs with mRNAs	Post transcriptional regulator	Attenuated	Spinola (47)
relA spoT double mutant	Encode enzymes for synthesis/ hydrolysis of (p)ppGpp	Transcriptional regulator; mediates the stringent response to starvation	Partially Attenuated	Spinola (48)
35000HPΔPEA (*HD0371*, *HD0852*, *HD1598* triple mutant)	Encode 3 putative PEA transferases	Alters LOS charge; confers resistance to α and β defensins	Virulent	Bauer (49)
dksA mutant	RNA polymerase (RNAP)-binding transcription factor	Co-regulator of RNAP with (p)ppGpp; has independent transcriptional effects	Partially Attenuated	Spinola (50)
35000HP*hgbA*$_{II}$	class I *hgbA* allele replaced by a class II allele in 35000HP	Heme/iron acquisition; possible surrogate for class II strains for vaccine studies	Partially Attenuated	Leduc (51)

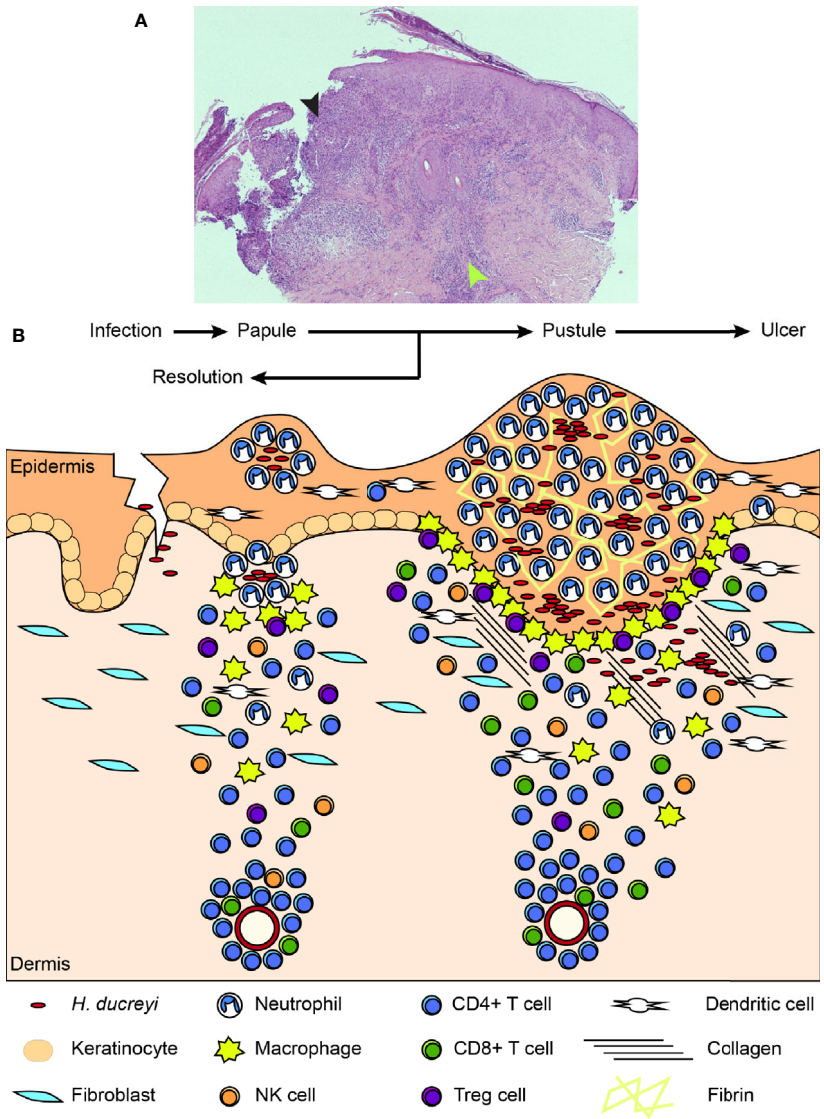

FIGURE 2 | Histology of an experimental lesion and the evolution of disease progression. **(A)** H & E staining of an endpoint pustule. The black arrowhead indicates the site of the pustule, which has eroded through the epidermis. The green arrowhead indicates the mononuclear cell infiltrate in the dermis. **(B)** Schematic of disease progression from time of infection to papule and pustule formation. Details of this process appear in the text. Adapted from Atlas of Sexually Transmitted Diseases and AIDS, 4th edition (56).

skin pathogens that form granulomas in the deep dermis. For instance, *Mycobacterium leprae* is an intracellular skin pathogen that lives in macrophages. Similar to *H. ducreyi*, the immune response appears to involve walling off the infection, so the infected macrophages are surrounded by T cells whose subtype determines whether a pro- or anti-inflammatory environment is created (62, 63). Another mycobacterium, *M. ulcerans* remains extracellular due to secretion of mycolactone and, ideally, is prevented from spreading further into the tissue by macrophages like *H. ducreyi*, but ulcers can progress to the deep dermis if the infection cannot be controlled (64).

When considering other genital skin infections, chancroidal ulcers can be macroscopically similar to syphilitic chancres caused by *T. pallidum*. However, in syphilis, bacterial replication is typically in the deep dermis and involves the vasculature (65). Like chancroid, neutrophils are first recruited, but macrophages and the T cells required for infection control are not recruited until late in the second week of infection with *T. pallidum* (65).

How immune cells are recruited to the site of infection and how *H. ducreyi* responds to the immune system is discussed below and summarized in **Figure 3**.

Antigen Presentation and Cytokine Secretion by Dendritic Cells

Myeloid DCs are among the most important antigen presenting cells recruited to sites of *H. ducreyi* infection (58). DCs have both surface and intracellular pattern recognition receptors (PRRs) that recognize foreign molecules or molecules from damaged cells. Ligand binding to PRRs activates DCs, leading to phagocytosis and the transcription of pro- and anti-inflammatory immune response genes that influence the subsequent T cell response. While large supernatant protein (Lsp) A1 and LspA2 have been shown to inhibit phagocytosis of *H. ducreyi* by neutrophils and macrophages (66), their expression does not impact DC uptake of *H. ducreyi* (58). Whether this is because DCs are not as sensitive to phagocytic inhibition by LspA1 and LspA2 or whether DCs use a different mechanism to phagocytose *H. ducreyi* compared to neutrophils and macrophages remains to be determined. DCs can also be activated by *H. ducreyi* LOS in a non-contact-dependent manner (67), indicating that phagocytosis of *H. ducreyi* by DCs is sufficient but not necessary to promote DC activitation. *H. ducreyi* is able to partially inhibit DC activation and maturation through an unknown mechanism; however, DCs are still able to secrete high levels of IL-6 and TNF-α in response to live *H. ducreyi* (58). Secretion of high levels of IL-6 along with partially activated or immature DCs are hypothesized to be mechanisms by which *H. ducreyi* avoids a full adaptive immune response and survives immune onslaught.

DCs present antigen to activate T cells and subsequently secrete cytokines that polarize T cells; however, *H. ducreyi* also partially inhibits DC activation and maturation (58). Despite this, *H. ducreyi*-specific T cell lines have been isolated from pustules of volunteers who have not been previously exposed to *H. ducreyi*, which suggests

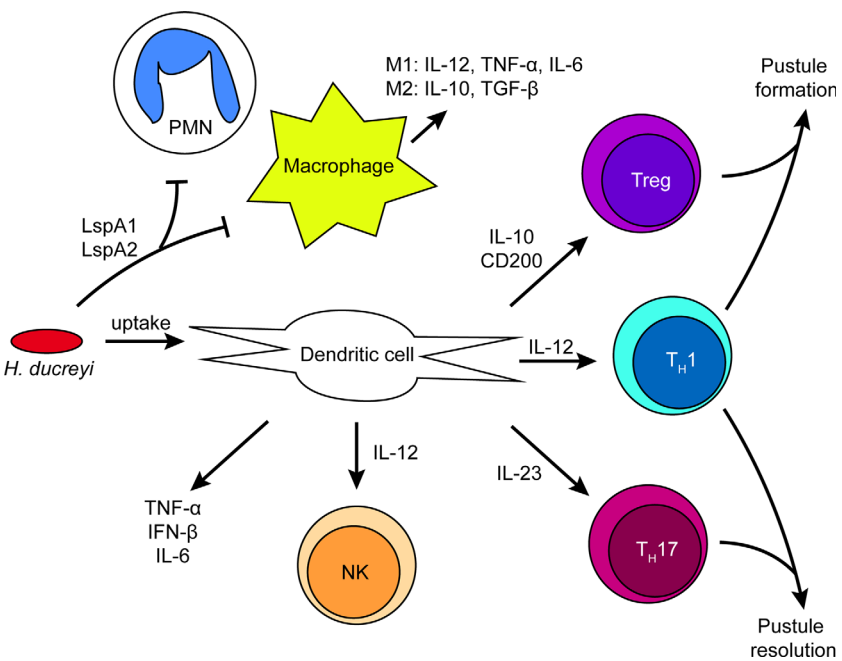

FIGURE 3 | Summary of immune cell activation by *H. ducreyi* in a pustule. Schematic of immune cell interactions and the cytokine environment in experimental infection based on transcriptomics and *in vitro* data. *H. ducreyi* secretes Large supernatant protein (Lsp)A1 and LspA2 to inhibit phagocytosis by neutrophils and macrophages. However, *H. ducreyi* is directly taken up by dendritic cells; ingested bacteria and/or soluble antigens from lysed bacteria such as lipooligosaccharide (LOS) result in dendritic cell activation. Dendritic cells subsequently secrete the indicated cytokines that lead to activation of NK cells and T cell subsets. The ratio of different T cell subsets in the lesion may be correlated with disease outcome. Further details appear in the text.

that DCs are able to present antigen to naïve T cells that differentiate into memory cells (68). Differences in pathogen detection and cytokine production that could influence T cell responses have been examined in experimental *H. ducreyi* infection. Single-nucleotide polymorphisms in Toll-like receptor 9 and interleukin-10 alleles have been identified and are predictive of pustule formation or resolution in experimental infection (69). Microarray analysis of infected and mock infected skin obtained from pustule formers and resolvers who were re-infected for 48 hours suggested that the two groups had both core and distinct tissue transcriptional responses to infection (19). Compared to resolvers, pustule formers had a hyperinflammatory, dysregulated response in the tissue. Monocyte-derived myeloid DCs obtained from resolvers and pustule formers who were re-infected with *H. ducreyi* also shared a core transcriptional response that should promote Th1 responses. However, resolver DC transcriptomes also suggested the promotion of a Th17 response and the upregulation of IL-23, whereas pustule former DCs promoted a Treg response and the upregulation of IL-10 and CD200. LOS binding to TLR4 on DCs leads to production of TNF-α and IFN-β, which induces indolamine 2,3-dioxygenase (IDO) expression, and IDO induction in DCs may explain the increased number of Tregs found in pustules (67). IDO expression in DCs can promote conversion of naïve T cells to Tregs, prevent Treg conversion to effector T cells, inhibit T cell activation/proliferation, and promote T cell death through tryptophan depletion and production of pro-apoptotic metabolites (70–72), which would result in a decrease in the number of effector T cells and an increase in Tregs. These data suggest that *H. ducreyi* infection simultaneously increases both pro-inflammatory and anti-inflammatory cytokines and that the balance between the pro-inflammatory and anti-inflammatory signals in different hosts may dictate whether a pustule forms or resolves.

Along with T cells, DCs also activate NK cells (60). *H. ducreyi*-infected DCs activate NK cells *in vitro* through production of IL-12 and subsequently lead to NK cell secretion of IFN-γ. IFN-γ secretion, primarily originating from NK cells early in infection, could increase immune-mediated phagocytosis of *H. ducreyi*.

T Cell Response in Infection

In experimental lesions, CD4+ T cells are primarily recruited and localize beneath the macrophage collar; the average CD4:CD8 ratio is 3:1 (61). T cells comprise 50% of leukocytes in papules at two days post infection. Approximately 70% of T cells collected from papules are $CD45RO^+$ memory T cells, which are likely a mix of skin-resident memory T cells and circulating central memory T cells that responded to chemokines released at the infected site. Whether the T cells in the papule can respond to *H. ducreyi* has not been tested. We previously observed that DCs in pustule formers and resolvers upregulate different transcripts; these transcripts suggest that the DCs in resolvers promote a type 1 and type 17 response while the DCs in pustule formers promote a type 1 and regulatory response (19). Therefore, we hypothesize that the T cells in the skin of resolvers and pustule formers may similarly differ. In the skin, CD49a (integrin α_1) expression has been used to differentiate IFN-γ- versus IL-17-expressing $CD8^+$ cells, which are $CD49a^+$ and $CD49a^-$, respectively (73). Although the differences between $CD49a^+$ and $CD49a^-$ CD4 T cells have yet to be determined, CD4 T cells in diseased skin can also express $CD49a^+$ (74). If the T cells identified in papules do respond to *H. ducreyi* either directly or through an unknown cross-reactive memory T cell response, then pustule formers may have more $CD49a^+$ T cells and resolvers may have more $CD49a^-$ T cells. Alternatively, if the T cells are not responding to *H. ducreyi*, then the T cells that were observed in papules are likely representative of the basal level of T cells in the skin and of non-specific memory T cells that may be following chemotactic gradients.

A hallmark of the adaptive immune system is the recall response. T cell lines have been derived from pustules that were biopsied 6-14 days after experimental infection (68). Treatment of the T cell lines with *H. ducreyi* antigen in the presence of autologous peripheral blood mononuclear cells (PBMCs), but not irradiated allogeneic PBMCs, led to proliferation and cytokine production from T cells, indicating that the response is MHC restricted. The T cell lines produced minimal responses to related members of the *Pasteurellaceae* family, demonstrating that the T cell lines are *H. ducreyi* antigen-specific. Interestingly, this antigen-specific response does not seem to confer protection against re-challenge, as 88% of pustule formers form pustules when re-challenged (75, 76). The reason for the lack of immunity is unclear, but it may in part be due to the lack of antibody responses during experimental infection. Antibody responses are made late in the ulcerative stage of natural infection, but these antibodies are not bactericidal (77).

Avoiding Phagocytosis by Macrophages and Neutrophils

H. ducreyi remains extracellular and prevents its uptake by both neutrophils and macrophages primarily by the secretion of two proteins: LspA1 and LspA2 (66). LspA1 and LspA2 are the largest proteins encoded by the *H. ducreyi* 35000HP genome, have proportionately higher numbers of SNPs compared to most *H. ducreyi* genes (16), and are secreted by the LspB transporter. Secreted LspA1 and LspA2 are taken up by neutrophils and macrophages by an unknown mechanism, bind to and are phosphorylated by the human C-terminal tyrosine kinase Csk, and increase Csk activity *via* a positive feedback loop (78). This increased Csk activity prevents human Src kinases from inducing the actin rearrangements required for FcγR-dependent phagocytosis. Phagocytes with inhibited FcγR-dependent phagocytosis are unable to engulf opsonized bacteria. Ducreyi serum resistance protein A (DsrA) is an outer membrane protein that inhibits IgM from binding to the bacterial surface thereby preventing complement deposition and serum killing (79, 80); theoretically, DsrA could also inhibit complement-mediated phagocytosis. Both DsrA and fibrinogen binding protein A (FgbA) are adhesins that bind fibrinogen, similar to the M proteins of *Streptococcus pyogenes* (37, 81). Although the role of FgbA and DsrA in resistance to phagocytosis has not been established, binding to fibrinogen in other bacteria is thought to help prevent phagocytosis through adhesion to host cells, steric hindrance, and shielding pathogen associated molecular patterns (PAMPs) that would be recognized by phagocytes (82, 83). Deletion mutants of *lspA1* and *lspA2*, *dsrA*, or *fgbA* are

attenuated for pustule formation in humans (26, 31, 37). Thus, despite appearing somewhat redundant, they are all required to establish productive infection and, given their posited *in vitro* functions, to avoid phagocytosis.

With so many mechanisms to prevent phagocytosis, how does the immune response manage to help kill the bacteria and resolve infection? Characterization of macrophages from biopsies of *H. ducreyi* infected pustules and from *in vitro H. ducreyi* -infected monocyte-derived macrophages has shown that infection produces a mixed M1/M2 macrophage population (84). The M1 phenotype is characterized by being microbicidal, producing high levels of IL-12, TNF-α, IL-6, and reactive nitrogen and oxygen intermediates; the M2 phenotype is associated with tissue repair and reducing inflammation, producing IL-10 and TGF-β (85). M2 macrophages are also better at phagocytosis than M1 macrophages, especially M2c macrophages, which are polarized by IL-10 and are efficient at phagocytosing *H. ducreyi via* class A scavenger receptors (84). The proportion of M1 versus M2 macrophages may play an important role in resolving *H. ducreyi* infection, but is yet to be studied in the context of pustule formation and resolution. Given that resolvers who are re-infected upregulate IL-10 transcripts in tissue compared to pustule formers (19), we hypothesize that resolvers may have more M2c macrophages than pustule formers and are therefore better able to phagocytose and clear *H. ducreyi* infection *via* class A scavenger receptor uptake.

The ratio of type 1 and type 2 immune cells has been instrumental in predicting disease progression for bacterial pathogens. *M. leprae* infection is dynamic. Type 1 and type 17 cells dominate in tuberculoid lesions and type 2 and regulatory cells dominate in lepromatous lesions; oscillation between these two states during natural disease correlates with changes of immune cell phenotypes (62). Similarly, prevention of *Staphylococcus aureus* and *Streptococcus pyogenes* skin infections requires a predominantly type 1 immune response rather than a type 2 immune response (86–89). Interestingly, the immune cell typing that controls infection of *M. leprae* (90), *S. aureus* (86), or *S. pyogenes* (89) favors skewing towards a predominately type 1 response, whereas the immune cell typing that controls infection of *H. ducreyi* may favor a mixed type 1 and type 17 response (19). Important distinctions between these pathogens may account for this difference. For instance, M2 macrophages express an *M. leprae* entry receptor, CD163 (91), which would explain why leprosy lesions worsen with increased numbers of M2 macrophages. The skewing of macrophage typing towards an M2 response leads to their release of cytokines that can also push the T cells toward a type 2 response.

Defensin and Cathelicidin Resistance

In addition to avoiding phagocytosis, *H. ducreyi* also resists antimicrobial peptides that are secreted by phagocytes and keratinocytes. *H. ducreyi* encodes two transporters that confer resistance to some human defensins and the cathelicidin LL-37. A proton motive force-dependent transmembrane efflux pump, Mtr, confers resistance to LL-37 and β-defensins—especially HBD-3. A *mtrC* deletion mutant had decreased expression of *lspB* and *dsrA*, indicating that multiple virulence factors are impacted by the absence of MtrC (92). Another transporter system, Sap, also ameliorates LL-37 activity (93). SapB and SapC form a heterodimeric transporter that transports cargo bound by the periplasmic chaperone SapA. A *sapA* deletion mutant is 25-50% more sensitive to killing by LL-37 *in vitro* and has an approximately 50% reduction in pustule formation in the human infection model (39). However, deletion of *sapBC* results in a mutant that is fully attenuated for pustule formation in the human infection model, suggesting that SapBC may be secreting additional SapA-like protein(s) that serve redundant functions (43).

The positive charge of the *H. ducreyi* outer membrane was also hypothesized to repulse antimicrobial peptide binding (49). The outer membrane of most Gram-negative bacteria contains lipopolysaccharide (LPS); however, *H. ducreyi* has a similar, less decorated version—LOS (94). Class I strains have a sialylated nonasaccharide (95), while Class II stains have a non-sialylated pentasaccharide (96). Deletion of either the sialyltransferase *lst* or the N-acylneuraminate cytidylyltransferase *neuA* eliminates LOS sialylation in the Class I strain *H. ducreyi* 35000HP (44). Both mutants are fully virulent and form pustules in human volunteers. This contrasts to the pathogenic *Neisseria* spp. in which sialylation of LOS is a major virulence determinant (97). *H. ducreyi* LOS and core oligosaccharide each contain a positively charged phosphoethanolamine (PEA) group (96, 98), which helps to neutralize the otherwise negatively charged LOS and was hypothesized to repel positively charged LL-37. However, deletion of *lptA*, which attaches PEA to the LOS, did not affect pustule formation (49). Overall, cathelicidin resistance is primarily mediated by the Sap and Mtr transporters rather than membrane charge or sialylation (43, 92).

Interaction of the Host With *H. ducreyi*

While cytokines and redox species certainly shape the lesion environment, what the microenvironment contains on a molecular level is a current focus of investigation. The molecular composition of the lesion bridges bacterial growth and the recruitment of immune cells. Transcriptomic data were used to first investigate how *H. ducreyi* alters its gene expression from *in vitro* growth to the environment of a pustule (99). Comparison of biopsy samples to historic mid-log, transition, and stationary phase *in vitro* data sets showed that the *in vivo* transcriptome of *H. ducreyi* was unique (99). The genes that consistently differed between all growth stages and the biopsies are involved in essential growth pathways and suggest a shift towards anaerobiosis and the use of alternative carbon sources, such as ascorbic acid and citrate, as well as increased amino acid and metal transport, protein folding chaperones, growth arrest, and DNA replication and repair. Given that the *in vitro* and skin environments are metabolically distinct, a differential growth signature is unsurprising.

A limitation of differential gene expression studies is that only differences at the transcript level are detected and, depending on the gene, may or may not accurately reflect the other biology at the site such as post-transcriptional regulatory mechanisms or the metabolome. Since many terminally differentiated cells, such as neutrophils, generally do not contain high levels of mRNA, genes that are not well-expressed or that are post-transcriptionally regulated may not be detected in RNA-seq datasets, but their metabolic products may be detected by metabolomics. Expanding

on the previous study, the *H. ducreyi* mid-log phase inoculum used to infect volunteers and biopsies of pustules along with their matched wounded skin controls were subjected to unbiased bulk RNA-seq and metabolic profiling (100). The most differentially regulated host genes in the lesion indicated a robust immune response. This metabolomics data showed that there are elevated levels of ascorbic acid as well as the presence of prostaglandins, glutamate, linoleate, and glycosphingolipids in pustules versus sham inoculated skin (100).

The matched metabolomes and transcriptomes support a richer understanding of the lesion. The elevated levels of ascorbic acid in the pustule coupled with the upregulation of *H. ducreyi* genes that metabolize ascorbic acid suggests that *H. ducreyi* is using ascorbic acid as an alternative carbon source (99, 100). Although the definitive cellular source of ascorbic acid (and other) metabolites are unknown, neutrophils take up and sequester ascorbic acid and likely release it into the abscess as they become necrotic (101). Thus, this data set helps to generate hypotheses about how different carbon sources are used by *H. ducreyi* and what host cells may be responsible for producing these carbon sources.

Since spatial information is lost during sample processing, a limitation of tissue metabolomics is that whether the metabolite is sequestered in host cells or freely available extracellularly cannot be determined. Therefore, the outstanding questions involve both sides of the host-pathogen interaction. In addition, because of the extreme difference in the amount of host material compared to the bacteria, the metabolome overwhelmingly reflects host components. For *H. ducreyi*, we hypothesize that, given the upregulation of genes to metabolize a given compound, such as ascorbic acid, coupled with the inability to synthesize the input metabolite of the pathway, *H. ducreyi* is using these metabolites as energy sources (99, 100). Generation of gene deletion mutant strains and subsequent experimental infection with these strains will confirm whether these are important carbon sources for *H. ducreyi*.

Because both the host and bacterial transcripts present in the pustule were captured from the infected samples, it was possible to use bioinformatics to generate an interaction network of host-bacterial gene clusters in an unbiased manner that were either positively or negatively correlated. Notably, genes involved in anaerobiosis were correlated with several pro-inflammatory host genes that are upregulated during infection (100). A similar strategy was used to determine an interaction network for naturally occurring lepromatous *M. leprae* biopsies; an interactome for tuberculoid *M. leprae* infection could not be established, since there were too few bacterial reads in the biopsies (4). The *M. leprae* interaction network confirmed that the type I interferon response is upregulated and that lepromatous lesions have increased bacterial metabolism (4). This was correlated to class switching in B cells (4). Application of these techniques to biopsies of lesions caused by other organisms will also elucidate whether immune system metabolism is altered along a common pathway(s) or whether infections differentially influence host metabolism. Thus, dual RNA-seq provides a tool to examine interaction networks that may identify therapeutic targets.

TOWARD UNCOVERING METABOLIC SHIFTS IN SPECIFIC CELL TYPES

Understanding how the host contributes to these differences is more complicated; central carbon metabolites—namely citrate, α-ketogluterate, and succinate—have been shown to have alternative uses outside of central metabolism during inflammation (102). These metabolites can be transported out of the mitochondria to form antimicrobial metabolites, protect against oxidation, and alter protein functions through post-translational modification (102). Furthermore, whether the differences observed in *H. ducreyi* pustules are representative of changes in local cellular metabolism (e.g., from keratinocytes and fibroblasts), the infiltration of specific cell types that are high in a given metabolite, or both is not known. As such, determining whether these compounds become available to *H. ducreyi* through diffusion or secretion from live host cells or become available after host cell death and lysis is an outstanding question. Utilization of emerging spatial metabolomics approaches in the future will further advance our understanding of the lesion on the molecular level (103).

Emerging technologies are providing new insights into specific host cell contributions to disease. Instead of restricting lesional cell characterization by using pre-selected phenotypic markers for flow cytometry, next generation sequencing provides the possibility of identifying the source of transcripts at the single cell level as well as their physical location within a lesion using spatial transcriptomics. This will allow us to better correlate the proportion of different cell types observed in previous studies (57–61); determine the cellular source(s) of differentially expressed genes observed in bulk RNA-seq studies (99, 100); and better estimate the effectiveness of the immune response in individual volunteers. In preliminary experiments, we have generated single cell suspensions and performed droplet single cell RNA sequencing on biopsies of pustules. Using Seurat (104) to cluster cells, macrophages, monocytes, DCs, T cells, NK cells, as well as endothelial cells, fibroblasts, and keratinocytes were identified in the biopsies (**Figure 4**). Interestingly, neutrophils were not detected perhaps because they are terminally differentiated and do not have high levels of mRNA. Nevertheless, the results of single cell RNA-seq studies can then be compared to our bulk transcriptomics data sets and to other publicly available single cell data sets that are available from normal and diseased human skin (2).

In previous studies, we showed that papules of pustule formers and resolvers who were re-infected for 48 hours had distinct transcription profiles that correlated with disease progression versus resolution (19). Due to the limitations of technology available at that time, we were not able to identify the cells responsible for differential transcript expression. Although we have shown that women are less susceptible to pustule formation than men, we have not been able to identify the cause(s) of the gender difference. A similar gender difference has been observed for progression from tuberculoid to lepromatous lesions for *M. leprae*, where more men progress to lepromatous lesions (90). Interestingly, some immunometabolites that are known to be regulated by sex hormones, such as prostaglandins, are upregulated in pustules (19, 100) and prostaglandin E2 has

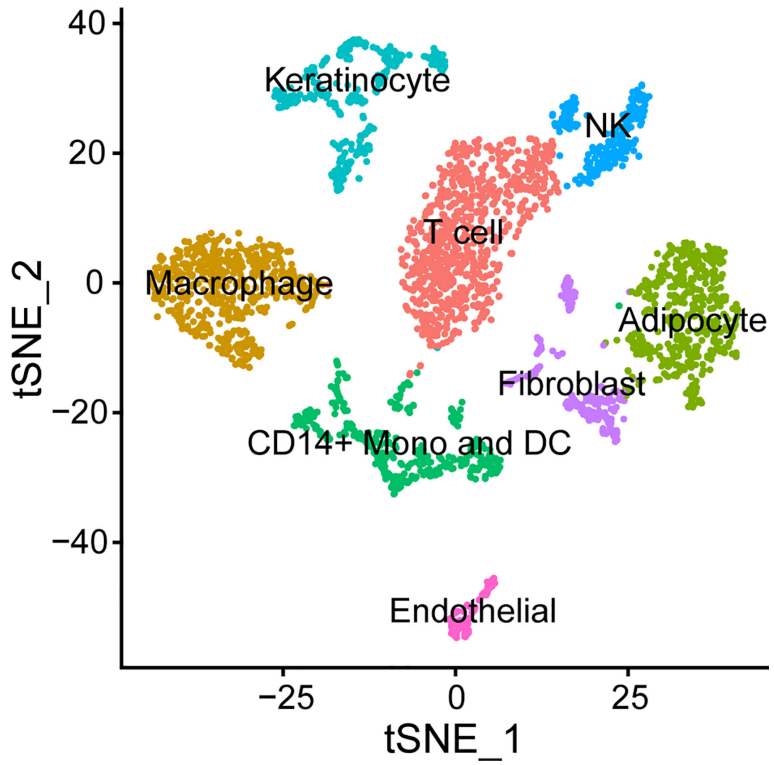

FIGURE 4 | Cell types found in the *H. ducreyi* pustule by single cell RNA-seq. Cells from a pustule were dissociated and single cell sequencing was performed. Cells were clustered in Seurat (104) and identified based off the unique, abundant transcripts in each cluster.

been shown to increase cytokine secretion in a monocyte-derived DC model (67). During infection, these cytokines are predicted to promote inflammatory responses in leukocytes and tissue repair in keratinocytes and fibroblasts. Single cell RNA-seq and metabolomics have the potential to unravel the differences in the tissues of pustule formers and resolvers who are re-infected and of men and women.

THE FUTURE OF UNDERSTANDING HOST-PATHOGEN INTERACTION IN THE SKIN

A full understanding of how an immune response is mounted in infectious human skin diseases will require determining the metabolic environment during infection and the cell-cell signaling involved as the lesion is first formed. Because of the difficulty of obtaining sufficient numbers of cells responding to invading pathogens early in infection, the first cells to initiate the immune response is largely unknown. Thus, we do not know the *in vivo* signal(s) received by the immune system that begins the recruitment of additional leukocytes. We anticipate that new "omics" technologies will help close this knowledge gap and help the field to generate a more holistic model of skin infection.

In addition to the interaction between the pathogen and host, other environmental factors, such as the skin microbiome, may play a role in determining infection outcome. In a prospective study, the pre-infection microbiomes of sites of people who resolved experimental infection clustered together while those of pustule formers were more diverse (105). In the course of experimental infection, the microbiomes of resolvers did not change, while the microbiomes of pustule formers were driven to a similar composition; in the latter, *H. ducreyi* dominates the lesion, and the proportions of the other genera decrease substantially during disease progression (105). The pre-infection microbiomes of resolvers tend to have higher levels of *Actinobacteria*, *Firmicutes*, and *Bacteroidetes* and lower levels of *Proteobacteria* compared to pustule formers, which had higher levels of micrococci and *Staphylococcus*. Whether these microbiome differences are because the former genera actively outcompete *H. ducreyi* (e.g., secrete toxins or metabolites that *H. ducreyi* is sensitive to), are a product of environmental factors (e.g., different hygiene practices and/or products), or underlying immune responsiveness is not known. However, the data suggest that the environment of a pustule drives the microbiome to a more uniform composition.

Future of Treatment Options for Skin Pathogens

H. ducreyi is currently only reliably susceptible to macrolides, quinolones, and third generation cephalosporins. For chancroid,

the preferred Center for Diseases Control and Prevention regimens include a single dose of oral azithromycin, a single dose of intramuscular ceftriaxone or a 3 day course of oral ciprofloxacin (8). For CU, a single oral dose of azithromycin has been the only regimen that has been studied and is highly effective (106). Further emergence of antibiotic resistance in endemic regions may require alternative treatment strategies. The higher differential expression of genes involved in carbon source switching and hypoxia/anaerobiosis *in vivo* indicates that interfering with bacterial nutrition may be a viable treatment tactic (99, 100).

If *H. ducreyi* is found to be dependent on "unique" metabolite (s), it may be possible to develop inhibitors to enzymes used in its metabolism in *H. ducreyi*. This strategy would require that host enzymes—and potentially those of other members of the healthy skin microbiome—are not impacted by the inhibitor. If the metabolite is only used by *H. ducreyi*, then it may also be possible to prevent its uptake and essentially starve the bacteria of a carbon source. Given the emergence of (multiple) drug resistant skin pathogens such as *S. aureus* or sexually transmitted bacteria such as *N. gonorrhoeae*, limiting broad spectrum antibiotics may help to decrease the prevalence of drug resistant strains in the population. Because *H. ducreyi* infects the upper layers of the skin, topical treatments could also be developed.

Finally, experimental human infection with deletion of candidate gene targets has been used to define essential virulence genes. Identification of vaccine antigens that produce high titers of opsonizing antibody have been complicated by the low tendency of *H. ducreyi* antigens to elicit long lasting immune responses. Evaluating vaccine efficacy in animal models is challenging because animal models lead to pathogen clearance and/or require very high dosages for infection. Nevertheless, two vaccine candidates have been studied in the porcine ear model. They are Class I specific and are most likely ineffective against Class II strains because the evaluated genes are among the genes with the most sequence diversity between Class I and Class II strains (107, 108). Therefore, these results are not wholly unanticipated, but suggest that targeting essential specific outer membrane proteins may not be as fruitful of a strategy as originally thought.

CONCLUSIONS

The ability to infect humans with *H. ducreyi* has been instrumental in exploring host-pathogen interaction at the tissue level. Nearly thirty years of human challenge experiments are helping to confirm previous studies as well as guide us toward new biological insights for future study on the cellular and molecular levels. This model is beneficial for both the skin immunology community, since it is one of the few human experimental infection models that captures the cells and metabolites of the lesion microenvironment. Thus, a rich understanding of cell types in the lesion, immune activation, and lesion architecture is achieved.

Advancements in "omics" technologies afford researchers a more holistic view of host-pathogen adaptions during infection. Bacterial virulence has expanded from primarily being thought of as the result of extracellular and secreted bacterial effectors to including how metabolism—both in the host and the bacteria—influence infection outcomes. Increased awareness of differences in microbiomes (105) and nutrient availability *in vivo* (99, 100) has highlighted that bacteria differentially regulate genes in the context of the host response and alterations in nutrient availability.

As we investigate skin inflammatory responses, we must also acknowledge that responses can differ not only by pathogen but also potentially by skin site. For other inflammatory conditions such as psoriasis, single cell RNA-seq revealed that while most dysregulated genes in psoriasis are independent of location on the body, some differentially expressed genes are unique to where psoriatic lesions are located (2). Most notably, different T cell subsets are activated based on location, which may influence therapeutic intervention strategies and outcomes (2). Similarly, location of disease may be of particular interest in *H. ducreyi* infection, since it infects both cutaneous lower leg and arm skin as well as genital skin. How or if the immune response significantly differs in these two locations has not been studied; however, the relationships between *H. ducreyi* and host cells are similar in experimental and natural infection (1). The use of clinical samples in infectious disease will be instrumental in elucidating the mechanisms behind various skin pathologies and in appreciating both inter-person and intra-person response diversity. As more data become available for different diseases, we anticipate that common immune response pathways will emerge, giving us a better understanding of how skin infections and the immune system interact.

AUTHOR CONTRIBUTIONS

JB, BG, and SS conceptualized the manuscript. JB and BG wrote the original draft. LC analyzed transcriptomic data. JB, BG, LC, and SS revised the final draft of the manuscript. All authors contributed to the article and approved the submitted version.

FUNDING

JB and BG were supported by T32AI007637. This work was supported by grant UL RR052761 from the Indiana Clinical and Translational Sciences Institute and the Indiana Clinical Research Center and by R01AI134727 and R01AI137116 from the National Institute of Allergy and Infectious Diseases to SS.

ACKNOWLEDGMENTS

We would like to thank Drs. Byron Batteiger and Margaret Bauer for critiquing this manuscript. We are also grateful to all the volunteers that have participated in the human challenge model.

REFERENCES

1. Bauer ME, Townsend CA, Ronald AR, Spinola SM. Localization of Haemophilus ducreyi in naturally acquired chancroidal ulcers. *Microbes Infect* (2006) 8(9-10):2465–8. doi: 10.1016/j.micinf.2006.06.001
2. Cheng JB, Sedgewick AJ, Finnegan AII, Harirchian P, Lee J, Kwon S, et al. Transcriptional Programming of Normal and Inflamed Human Epidermis at Single-Cell Resolution. *Cell Rep* (2018) 25(4):871–83. doi: 10.1016/j.celrep.2018.09.006
3. Zhu J, Koelle DM, Cao J, Vazquez J, Huang ML, Hladik F, et al. Virus-specific CD8+ T cells accumulate near sensory nerve endings in genital skin during subclinical HSV-2 reactivation. *J Exp Med* (2007) 204(3):595–603. doi: 10.1084/jem.20061792
4. Montoya DJ, Andrade P, Silva BJA, Teles RMB, Ma F, Bryson B, et al. Dual RNA-Seq of Human Leprosy Lesions Identifies Bacterial Determinants Linked to Host Immune Response. *Cell Rep* (2019) 26(13):3574–85.e3. doi: 10.1016/j.celrep.2019.02.109
5. Janowicz DM, Ofner S, Katz BP, Spinola SM. Experimental infection of human volunteers with *Haemophilus ducreyi*: fifteen years of clinical data and experience. *J Infect Dis* (2009) 199(11):1671–9. doi: 10.1086/598966
6. Spinola SM, Wild LM, Apicella MA, Gaspari AA, Campagnari AA. Experimental human infection with Haemophilus ducreyi. *J Infect Dis* (1994) 169(5):1146–50. doi: 10.1093/infdis/169.5.1146
7. Gonzalez-Beiras C, Marks M, Chen CY, Roberts S, Mitja O. Epidemiology of Haemophilus ducreyi Infections. *Emerg Infect Dis* (2016) 22(1):1–8. doi: 10.3201/eid2201.150425
8. Spinola SM. Chancroid and Haemophilus ducreyi. In: PF Sparling, KK Holmes, WE Stamm, P Piot, JN Wasserheit, L Corey, MS Cohen, DH Watts, editors. *Sexually Transmitted Diseases*. New York: McGraw-Hill (2008).
9. Mitja O, Godornes C, Houinei W, Kapa A, Paru R, Abel H, et al. Re-emergence of yaws after single mass azithromycin treatment followed by targeted treatment: a longitudinal study. *Lancet* (2018) 391(10130):1599–607. doi: 10.1016/S0140-6736(18)30204-6
10. Ghinai R, El-Duah P, Chi KH, Pillay A, Solomon AW, Bailey RL, et al. A cross-sectional study of 'yaws' in districts of Ghana which have previously undertaken azithromycin mass drug administration for trachoma control. *PLoS Negl Trop Dis* (2015) 9(1):e0003496. doi: 10.1371/journal.pntd.0003496
11. Marks M, Chi KH, Vahi V, Pillay A, Sokana O, Pavluck A, et al. Haemophilus ducreyi associated with skin ulcers among children, Solomon Islands. *Emerg Infect Dis* (2014) 20(10):1705–7. doi: 10.3201/eid2010.140573
12. Grant JC, Gonzalez-Beiras C, Amick KM, Fortney KR, Gangaiah D, Humphreys TL, et al. and Class II Haemophilus ducreyi Strains Cause Cutaneous Ulcers in Children on an Endemic Island. *Clin Infect Dis* (2018) 67(11):1768–74. doi: 10.1093/cid/ciy343
13. Houinei W, Godornes C, Kapa A, Knauf S, Mooring EQ, Gonzalez-Beiras C, et al. *Haemophilus ducreyi* DNA is detectable on the skin of asymptomatic children, flies and fomites in villages of Papua New Guinea. *PLoS Negl Trop Dis* (2017) 11(5):e0004958. doi: 10.1371/journal.pntd.0004958
14. White CD, Leduc I, Olsen B, Jeter C, Harris C, Elkins C. Haemophilus ducreyi Outer membrane determinants, including DsrA, define two clonal populations. *Infect Immun* (2005) 73(4):2387–99. doi: 10.1128/IAI.73.4.2387-2399.2005
15. Gangaiah D, Spinola SM. *Haemophilus ducreyi* Cutaneous Ulcer Strains Diverged from Both Class I and Class II Genital Ulcer Strains: Implications for Epidemiological Studies. *PLoS Negl Trop Dis* (2016) 10(12):e0005259. doi: 10.1371/journal.pntd.0005259
16. Gangaiah D, Webb KM, Humphreys TL, Fortney KR, Toh E, Tai A, et al. *Haemophilus ducreyi* Cutaneous Ulcer Strains Are Nearly Identical to Class I Genital Ulcer Strains. *PLoS Negl Trop Dis* (2015) 9(7):e0003918. doi: 10.1371/journal.pntd.0003918
17. Marks M, Fookes M, Wagner J, Ghinai R, Sokana O, Sarkodie YA, et al. Direct Whole-Genome Sequencing of Cutaneous Strains of Haemophilus ducreyi. *Emerg Infect Dis* (2018) 24(4):786–9. doi: 10.3201/eid2404.171726
18. Spinola SM, Bauer ME, Munson RS Jr. Immunopathogenesis of Haemophilus ducreyi infection (chancroid). *Infect Immun* (2002) 70 (4):1667–76. doi: 10.1128/iai.70.4.1667-1676.2002
19. Humphreys TL, Li L, Li X, Janowicz DM, Fortney KR, Zhao Q, et al. Dysregulated immune profiles for skin and dendritic cells are associated with increased host susceptibility to Haemophilus ducreyi infection in human volunteers. *Infect Immun* (2007) 75(12):5686–97. doi: 10.1128/IAI.00777-07
20. Palmer KL, Thornton AC, Fortney KR, Hood AF, Munson RS Jr, Spinola SM. Evaluation of an isogenic hemolysin-deficient mutant in the human model of Haemophilus ducreyi infection. *J Infect Dis* (1998) 178(1):191–9. doi: 10.1086/515617
21. Young RS, Fortney K, Haley JC, Hood AF, Campagnari AA, Wang J, et al. Expression of sialylated or paragloboside-like lipooligosaccharides are not required for pustule formation by Haemophilus ducreyi in human volunteers. *Infect Immun* (1999) 67(12):6335–40. doi: 10.1128/IAI.67.12.6335-6340.1999
22. Al-Tawfiq JA, Bauer ME, Fortney KR, Katz BP, Hood AF, Ketterer M, et al. A pilus-deficient mutant of Haemophilus ducreyi is virulent in the human model of experimental infection. *J Infect Dis* (2000) 181(3):1176–9. doi: 10.1086/315310
23. Al-Tawfiq JA, Fortney KR, Katz BP, Hood AF, Elkins C, Spinola SM. An isogenic hemoglobin receptor-deficient mutant of Haemophilus ducreyi is attenuated in the human model of experimental infection. *J Infect Dis* (2000) 181(3):1049–54. doi: 10.1086/315309
24. Throm RE, Al-Tawfiq JA, Fortney KR, Katz BP, Hood AF, Slaughter CA, et al. Evaluation of an isogenic major outer membrane protein-deficient mutant in the human model of Haemophilus ducreyi infection. *Infect Immun* (2000) 68(5):2602–7. doi: 10.1128/iai.68.5.2602-2607.2000
25. Fortney KR, Young RS, Bauer ME, Katz BP, Hood AF, Munson RS Jr, et al. Expression of peptidoglycan-associated lipoprotein is required for virulence in the human model of Haemophilus ducreyi infection. *Infect Immun* (2000) 68(11):6441–8. doi: 10.1128/iai.68.11.6441-6448.2000
26. Bong CT, Throm RE, Fortney KR, Katz BP, Hood AF, Elkins C, et al. DsrA-deficient mutant of Haemophilus ducreyi is impaired in its ability to infect human volunteers. *Infect Immun* (2001) 69(3):1488–91. doi: 10.1128/IAI.69.3.1488-1491.2001
27. Young RS, Fortney KR, Gelfanova V, Phillips CL, Katz BP, Hood AF, et al. Expression of cytolethal distending toxin and hemolysin is not required for pustule formation by Haemophilus ducreyi in human volunteers. *Infect Immun* (2001) 69(3):1938–42. doi: 10.1128/IAI.69.3.1938-1942.2001
28. Young RS, Filiatrault MJ, Fortney KR, Hood AF, Katz BP, Munson RS Jr, et al. Haemophilus ducreyi lipooligosaccharide mutant defective in expression of beta-1,4-glucosyltransferase is virulent in humans. *Infect Immun* (2001) 69(6):4180–4. doi: 10.1128/IAI.69.6.4180-4184.2001
29. Bong CT, Fortney KR, Katz BP, Hood AF, San Mateo LR, Kawula TH, et al. A superoxide dismutase C mutant of Haemophilus ducreyi is virulent in human volunteers. *Infect Immun* (2002) 70(3):1367–71. doi: 10.1128/iai.70.3.1367-1371.2002
30. Spinola SM, Fortney KR, Katz BP, Latimer JL, Mock JR, Vakevainen M, et al. Haemophilus ducreyi requires an intact flp gene cluster for virulence in humans. *Infect Immun* (2003) 71(12):7178–82. doi: 10.1128/iai.71.12.7178-7182.2003
31. Janowicz DM, Fortney KR, Katz BP, Latimer JL, Deng K, Hansen EJ, et al. Expression of the LspA1 and LspA2 proteins by Haemophilus ducreyi is required for virulence in human volunteers. *Infect Immun* (2004) 72 (8):4528–33. doi: 10.1128/IAI.72.8.4528-4533.2004
32. Janowicz D, Luke NR, Fortney KR, Katz BP, Campagnari AA, Spinola SM. Expression of OmpP2A and OmpP2B is not required for pustule formation by Haemophilus ducreyi in human volunteers. *Microb Pathog* (2006) 40 (3):110–5. doi: 10.1016/j.micpath.2005.11.005
33. Janowicz D, Leduc I, Fortney KR, Katz BP, Elkins C, Spinola SM. A DltA mutant of Haemophilus ducreyi Is partially attenuated in its ability to cause pustules in human volunteers. *Infect Immun* (2006) 74(2):1394–7. doi: 10.1128/IAI.74.2.1394-1397.2006
34. Fulcher RA, Cole LE, Janowicz DM, Toffer KL, Fortney KR, Katz BP, et al. Expression of Haemophilus ducreyi collagen binding outer membrane protein NcaA is required for virulence in swine and human challenge models of chancroid. *Infect Immun* (2006) 74(5):2651–8. doi: 10.1128/IAI.74.5.2651-2658.2006
35. Banks KE, Fortney KR, Baker B, Billings SD, Katz BP, Munson RS Jr, et al. The enterobacterial common antigen-like gene cluster of Haemophilus

ducreyi contributes to virulence in humans. *J Infect Dis* (2008) 197 (11):1531–6. doi: 10.1086/588001
36. Leduc I, Banks KE, Fortney KR, Patterson KB, Billings SD, Katz BP, et al. Evaluation of the repertoire of the TonB-dependent receptors of Haemophilus ducreyi for their role in virulence in humans. *J Infect Dis* (2008) 197(8):1103–9. doi: 10.1086/586901
37. Bauer ME, Townsend CA, Doster RS, Fortney KR, Zwickl BW, Katz BP, et al. A fibrinogen-binding lipoprotein contributes to the virulence of Haemophilus ducreyi in humans. *J Infect Dis* (2009) 199(5):684–92. doi: 10.1086/596656
38. Labandeira-Rey M, Janowicz DM, Blick RJ, Fortney KR, Zwickl B, Katz BP, et al. Inactivation of the Haemophilus ducreyi luxS gene affects the virulence of this pathogen in human subjects. *J Infect Dis* (2009) 200(3):409–16. doi: 10.1086/600142
39. Mount KL, Townsend CA, Rinker SD, Gu X, Fortney KR, Zwickl BW, et al. Haemophilus ducreyi SapA contributes to cathelicidin resistance and virulence in humans. *Infect Immun* (2010) 78(3):1176–84. doi: 10.1128/IAI.01014-09
40. Spinola SM, Fortney KR, Baker B, Janowicz DM, Zwickl B, Katz BP, et al. Activation of the CpxRA system by deletion of cpxA impairs the ability of Haemophilus ducreyi to infect humans. *Infect Immun* (2010) 78(9):3898–904. doi: 10.1128/IAI.00432-10
41. Janowicz DM, Cooney SA, Walsh J, Baker B, Katz BP, Fortney KR, et al. Expression of the Flp proteins by Haemophilus ducreyi is necessary for virulence in human volunteers. *BMC Microbiol* (2011) 11:208. doi: 10.1186/1471-2180-11-208
42. Labandeira-Rey M, Dodd D, Fortney KR, Zwickl B, Katz BP, Janowicz DM, et al. A Haemophilus ducreyi CpxR deletion mutant is virulent in human volunteers. *J Infect Dis* (2011) 203(12):1859–65. doi: 10.1093/infdis/jir190
43. Rinker SD, Gu X, Fortney KR, Zwickl BW, Katz BP, Janowicz DM, et al. Permeases of the sap transporter are required for cathelicidin resistance and virulence of Haemophilus ducreyi in humans. *J Infect Dis* (2012) 206 (9):1407–14. doi: 10.1093/infdis/jis525
44. Spinola SM, Li W, Fortney KR, Janowicz DM, Zwickl B, Katz BP, et al. Sialylation of lipooligosaccharides is dispensable for the virulence of Haemophilus ducreyi in humans. *Infect Immun* (2012) 80(2):679–87. doi: 10.1128/IAI.05826-11
45. Gangaiah D, Li W, Fortney KR, Janowicz DM, Ellinger S, Zwickl B, et al. Carbon storage regulator A contributes to the virulence of Haemophilus ducreyi in humans by multiple mechanisms. *Infect Immun* (2013) 81 (2):608–17. doi: 10.1128/IAI.01239-12
46. Janowicz DM, Zwickl BW, Fortney KR, Katz BP, Bauer ME. Outer membrane protein P4 is not required for virulence in the human challenge model of Haemophilus ducreyi infection. *BMC Microbiol* (2014) 14:166. doi: 10.1186/1471-2180-14-166
47. Gangaiah D, Labandeira-Rey M, Zhang X, Fortney KR, Ellinger S, Zwickl B, et al. Haemophilus ducreyi Hfq contributes to virulence gene regulation as cells enter stationary phase. *mBio* (2014) 5(1):e01081–13. doi: 10.1128/mBio.01081-13
48. Holley C, Gangaiah D, Li W, Fortney KR, Janowicz DM, Ellinger S, et al. A (p)ppGpp-null mutant of Haemophilus ducreyi is partially attenuated in humans due to multiple conflicting phenotypes. *Infect Immun* (2014) 82 (8):3492–502. doi: 10.1128/IAI.01994-14
49. Trombley MP, Post DM, Rinker SD, Reinders LM, Fortney KR, Zwickl BW, et al. Phosphoethanolamine Transferase LptA in *Haemophilus ducreyi* Modifies Lipid A and Contributes to Human Defensin Resistance In Vitro. *PLoS One* (2015) 10(4):e0124373. doi: 10.1371/journal.pone.0124373
50. Holley CL, Zhang X, Fortney KR, Ellinger S, Johnson P, Baker B, et al. DksA and (p)ppGpp have unique and overlapping contributions to Haemophilus ducreyi pathogenesis in humans. *Infect Immun* (2015) 83(8):3281–92. doi: 10.1128/IAI.00692-15
51. Leduc I, Fortney KR, Janowicz DM, Zwickl B, Ellinger S, Katz BP, et al. A Class I Haemophilus ducreyi Strain Containing a Class II hgbA Allele Is Partially Attenuated in Humans: Implications for HgbA Vaccine Efficacy Trials. *Infect Immun* (2019) 87(7):e00112-19. doi: 10.1128/IAI.00112-19
52. Minassian AM, Satti I, Poulton ID, Meyer J, Hill AV, McShane H. A human challenge model for Mycobacterium tuberculosis using Mycobacterium bovis bacille Calmette-Guerin. *J Infect Dis* (2012) 205(7):1035–42. doi: 10.1093/infdis/jis012
53. Tameris MD, Hatherill M, Landry BS, Scriba TJ, Snowden MA, Lockhart S, et al. Safety and efficacy of MVA85A, a new tuberculosis vaccine, in infants previously vaccinated with BCG: a randomised, placebo-controlled phase 2b trial. *Lancet* (2013) 381(9871):1021–8. doi: 10.1016/S0140-6736(13)60177-4
54. Duthie MS, Saunderson P, Reed SG. The potential for vaccination in leprosy elimination: new tools for targeted interventions. *Mem Inst Oswaldo Cruz* (2012) 107 Suppl 1:190–6. doi: 10.1590/s0074-02762012000900027
55. Bauer ME, Spinola SM. Localization of Haemophilus ducreyi at the pustular stage of disease in the human model of infection. *Infect Immun* (2000) 68 (4):2309–14. doi: 10.1128/iai.68.4.2309-2314.2000
56. Spinola SM, Ballard R. Chancroid. In: SA Morse, RC Ballard, KK Holmes, AA Moreland, editors. *Atlas of Sexually Transmitted Diseases and AIDS*, *4th ed*. London, UK: Elsevier Ltd (2010).
57. Bauer ME, Goheen MP, Townsend CA, Spinola SM. Haemophilus ducreyi associates with phagocytes, collagen, and fibrin and remains extracellular throughout infection of human volunteers. *Infect Immun* (2001) 69(4):2549–57. doi: 10.1128/IAI.69.4.2549-2557.2001
58. Banks KE, Humphreys TL, Li W, Katz BP, Wilkes DS, Spinola SM. Haemophilus ducreyi partially activates human myeloid dendritic cells. *Infect Immun* (2007) 75(12):5678–85. doi: 10.1128/IAI.00702-07
59. Humphreys TL, Baldridge LA, Billings SD, Campbell JJ, Spinola SM. Trafficking pathways and characterization of CD4 and CD8 cells recruited to the skin of humans experimentally infected with Haemophilus ducreyi. *Infect Immun* (2005) 73(7):3896–902. doi: 10.1128/IAI.73.7.3896-3902.2005
60. Li W, Janowicz DM, Fortney KR, Katz BP, Spinola SM. Mechanism of human natural killer cell activation by Haemophilus ducreyi. *J Infect Dis* (2009) 200(4):590–8. doi: 10.1086/600123
61. Palmer KL, Schnizlein-Bick CT, Orazi A, John K, Chen CY, Hood AF, et al. The immune response to Haemophilus ducreyi resembles a delayed-type hypersensitivity reaction throughout experimental infection of human subjects. *J Infect Dis* (1998) 178(6):1688–97. doi: 10.1086/314489
62. de Sousa JR, Sotto MN, Simões Quaresma JA. Leprosy As a Complex Infection: Breakdown of the Th1 and Th2 Immune Paradigm in the Immunopathogenesis of the Disease. *Front Immunol* (2017) 8:1635. doi: 10.3389/fimmu.2017.01635
63. Pinheiro RO, Schmitz V, Silva BJA, Dias AA, de Souza BJ, de Mattos Barbosa MG, et al. Innate Immune Responses in Leprosy. *Front Immunol* (2018) 9:518. doi: 10.3389/fimmu.2018.00518
64. Roltgen K, Pluschke G. Buruli ulcer: The Efficacy of Innate Immune Defense May Be a Key Determinant for the Outcome of Infection With Mycobacterium ulcerans. *Front Microbiol* (2020) 11:1018. doi: 10.3389/fmicb.2020.01018
65. Carlson JA, Dabiri G, Cribier B, Sell S. The immunopathobiology of syphilis: the manifestations and course of syphilis are determined by the level of delayed-type hypersensitivity. *Am J Dermatopathol* (2011) 33(5):433–60. doi: 10.1097/DAD.0b013e3181e8b587
66. Vakevainen M, Greenberg S, Hansen EJ. Inhibition of phagocytosis by *Haemophilus ducreyi* requires expression of the LspA1 and LspA2 proteins. *Infect Immun* (2003) 71:5994–6003. doi: 10.1128/iai.71.10.5994-6003.2003
67. Li W, Katz BP, Spinola SM. Haemophilus ducreyi lipooligosaccharides induce expression of the immunosuppressive enzyme indoleamine 2,3-dioxygenase *via* type I interferons and tumor necrosis factor alpha in human dendritic cells. *Infect Immun* (2011) 79(8):3338–47. doi: 10.1128/IAI.05021-11
68. Gelfanova V, Humphreys TL, Spinola SM. Characterization of *Haemophilus ducreyi*-specific T cell lines from lesions of experimentally infected human subjects. *Infect Immun* (2001) 69:4224–31. doi: 10.1128/IAI.69.7.4224-4231.2001
69. Singer M, Li W, Morre SA, Ouburg S, Spinola SM. Host Polymorphisms in TLR9 and IL10 Are Associated With the Outcomes of Experimental *Haemophilus ducreyi* Infection in Human Volunteers. *J Infect Dis* (2016) 214(3):489–95. doi: 10.1093/infdis/jiw164
70. Baban B, Chandler PR, Sharma MD, Pihkala J, Koni PA, Munn DH, et al. IDO activates regulatory T cells and blocks their conversion into

Th17-like T cells. *J Immunol* (2009) 183(4):2475–83. doi: 10.4049/jimmunol.0900986
71. Mellor AL, Baban B, Chandler P, Jhaver K, Hansen A, Koni PA, et al. Cutting edge: induced indoleamine 2,3 dioxygenase expression in dendritic cell subsets suppresses T cell clonal expansion. *J Immunol* (2003) 171:1652–5. doi: 10.4049/jimmunol.171.4.1652
72. Fallarino F, Grohmann U, Vacca C, Bianchi R, Orabona C, Spreca A, et al. T cell apoptosis by tryptophan catabolism. *Cell Death Differ* (2002) 9 (10):1069–77. doi: 10.1038/sj.cdd.4401073
73. Cheuk S, Schlums H, Gallais Sérézal I, Martini E, Chiang SC, Marquardt N, et al. CD49a Expression Defines Tissue-Resident CD8(+) T Cells Poised for Cytotoxic Function in Human Skin. *Immunity* (2017) 46(2):287–300. doi: 10.1016/j.immuni.2017.01.009
74. Conrad C, Boyman O, Tonel G, Tun-Kyi A, Laggner U, de Fougerolles A, et al. Alpha1beta1 integrin is crucial for accumulation of epidermal T cells and the development of psoriasis. *Nat Med* (2007) 13(7):836–42. doi: 10.1038/nm1605
75. Al-Tawfiq JA, Palmer KL, Chen C-Y, Haley JC, Katz BP, Hood AF, et al. Experimental infection of human volunteers with *Haemophilus ducreyi* does not confer protection against subsequent challenge. *J Infect Dis* (1999) 179:1283–7. doi: 10.1086/314732
76. Spinola SM, Bong CTH, Faber AL, Fortney KR, Bennett SL, Townsend CA, et al. Differences in host susceptibility to disease progression in the human challenge model of *Haemophilus ducreyi* infection. *Infect Immun* (2003) 71:6658–63. doi: 10.1128/iai.71.11.6658-6663.2003
77. Chen CY, Mertz KJ, Spinola SM, Morse SA. Comparison of enzyme immunoassays for antibodies to *Haemophilus ducreyi* in a community outbreak of chancroid in the United States. *J Infect Dis* (1997) 175:1390–5. doi: 10.1086/516471
78. Dodd DA, Worth RG, Rosen MK, Grinstein S, van Oers NS, Hansen EJ. The *Haemophilus ducreyi* LspA1 Protein Inhibits Phagocytosis By Using a New Mechanism Involving Activation of C-Terminal Src Kinase. *MBio* (2014) 5 (3):1–11. doi: 10.1128/mBio.01178-14
79. Elkins C, Morrow KJ, Olsen B. Serum resistance in *Haemophilus ducreyi* requires outer membrane protein *DsrA*. *Infect Immun* (2000) 68:1608–19. doi: 10.1128/iai.68.3.1608-1619.2000
80. Abdullah M, Nepluev I, Afonina G, Ram S, Rice P, Cade W, et al. Killing of *dsrA* mutants of *Haemophilus ducreyi* by normal human serum occurs *via the* classical complement pathway and is initiated by immunoglobulin M binding. *Infect Immun* (2005) 73:3431–9. doi: 10.1128/IAI.73.6.3431-3439.2005
81. Herwald H, Cramer H, Mörgelin M, Russell W, Sollenberg U, Norrby-Teglund A, et al. M protein, a classical bacterial virulence determinant, forms complexes with fibrinogen that induce vascular leakage. *Cell* (2004) 116 (3):367–79. doi: 10.1016/s0092-8674(04)00057-1
82. Berends ET, Kuipers A, Ravesloot MM, Urbanus RT, Rooijakkers SH. Bacteria under stress by complement and coagulation. *FEMS Microbiol Rev* (2014) 38(6):1146–71. doi: 10.1111/1574-6976.12080
83. Vaca DJ, Thibau A, Schutz M, Kraiczy P, Happonen L, Malmstrom J, et al. Interaction with the host: the role of fibronectin and extracellular matrix proteins in the adhesion of Gram-negative bacteria. *Med Microbiol Immunol* (2020) 209(3):277–99. doi: 10.1007/s00430-019-00644-3
84. Li W, Katz BP, Spinola SM. *Haemophilus ducreyi*-induced IL-10 promotes a mixed M1 and M2 activation program in human macrophages. *Infect Immun* (2012) 80(12):4426–34. doi: 10.1128/IAI.00912-12
85. Atri C, Guerfali FZ, Laouini D. Role of Human Macrophage Polarization in Inflammation during Infectious Diseases. *Int J Mol Sci* (2018) 19(6):1–15. doi: 10.3390/ijms19061801
86. Brown AF, Murphy AG, Lalor SJ, Leech JM, O'Keeffe KM, Mac Aogáin M, et al. Memory Th1 Cells Are Protective in Invasive Staphylococcus aureus Infection. *PLoS Pathog* (2015) 11(11):e1005226. doi: 10.1371/journal.ppat.1005226
87. Travers JB. Toxic interaction between Th2 cytokines and Staphylococcus aureus in atopic dermatitis. *J Invest Dermatol* (2014) 134(8):2069–71. doi: 10.1038/jid.2014.122
88. Veckman V, Miettinen M, Pirhonen J, Sirén J, Matikainen S, Julkunen I. Streptococcus pyogenes and Lactobacillus rhamnosus differentially induce maturation and production of Th1-type cytokines and chemokines in human monocyte-derived dendritic cells. *J Leukoc Biol* (2004) 75(5):764–71. doi: 10.1189/jlb.1003461
89. Mortensen R, Nissen TN, Blauenfeldt T, Christensen JP, Andersen P, Dietrich J. Adaptive Immunity against Streptococcus pyogenes in Adults Involves Increased IFN-γ and IgG3 Responses Compared with Children. *J Immunol* (2015) 195(4):1657–64. doi: 10.4049/jimmunol.1500804
90. Bezerra-Santos M, do Vale-Simon M, Barreto AS, Cazzaniga RA, de Oliveira DT, Barrios MR, et al. Mycobacterium leprae Recombinant Antigen Induces High Expression of Multifunction T Lymphocytes and Is Promising as a Specific Vaccine for Leprosy. *Front Immunol* (2018) 9:2920. doi: 10.3389/fimmu.2018.02920
91. Moura DF, de Mattos KA, Amadeu TP, Andrade PR, Sales JS, Schmitz V, et al. CD163 favors Mycobacterium leprae survival and persistence by promoting anti-inflammatory pathways in lepromatous macrophages. *Eur J Immunol* (2012) 42(11):2925–36. doi: 10.1002/eji.201142198
92. Rinker SD, Trombley MP, Gu X, Fortney KR, Bauer ME. Deletion of *mtrC* in *Haemophilus ducreyi* increases sensitivity to human antimicrobial peptides and activates the CpxRA regulon. *Infect Immun* (2011) 79:2324–34. doi: 10.1128/IAI.01316-10
93. Groisman EA, Parra-Lopez C, Salcedo M, Lipps CJ, Heffron F. Resistance to host antimicrobial peptides is necessary for *Salmonella* virulence. *Proc Natl Acad Sci U S A* (1992) 89:11939–43. doi: 10.1073/pnas.89.24.11939
94. Campagnari AA, Spinola SM, Lesse AJ, Abu Kwaik Y, Mandrell RE, Apicella MA. Lipooligosaccharide epitopes shared among gram-negative non-enteric mucosal pathogens. *Microb Pathog* (1990) 8:353–62. doi: 10.1016/0882-4010(90)90094-7
95. Melaugh W, Campagnari AA, Gibson BW. The lipooligosaccharides of *Haemophilus ducreyi* are highly sialylated. *J Bacteriol* (1996) 178:564–70. doi: 10.1128/jb.178.2.564-570.1996
96. Post DMB, Munson RSJr, Baker B, Zhong H, Bozue JA, Gibson BW. Identification of genes involved in the expression of atypical lipooligosaccharide structures from a second class of *Haemophilus ducreyi*. *Infect Immun* (2007) 75:113–21. doi: 10.1128/IAI.01016-06
97. Vogel U, Frosch M. Mechanisms of neisserial serum resistance. *Mol Microbiol* (1999) 32:1133–9. doi: 10.1046/j.1365-2958.1999.01469.x
98. Melaugh W, Phillips NJ, Campagnari AA, Tullius MV, Gibson BW. Structure of the major oligosaccharide from the lipooligosaccharide of *Haemophilus ducreyi* strain 35000 and evidence for additional glycoforms. *Biochemistry* (1994) 33:13070–8. doi: 10.1021/bi00248a016
99. Gangaiah D, Zhang X, Baker B, Fortney KR, Gao H, Holley CL, et al. Haemophilus ducreyi Seeks Alternative Carbon Sources and Adapts to Nutrient Stress and Anaerobiosis during Experimental Infection of Human Volunteers. *Infect Immun* (2016) 84(5):1514–25. doi: 10.1128/IAI.00048-16
100. Griesenauer B, Tran TM, Fortney KR, Janowicz DM, Johnson P, Gao H, et al. Determination of an Interaction Network between an Extracellular Bacterial Pathogen and the Human Host. *MBio* (2019) 10(3):1–15. doi: 10.1128/mBio.01193-19
101. Wang Y, Russo TA, Kwon O, Chanock S, Rumsey SC, Levine M. Ascorbate recycling in human neutrophils: induction by bacteria. *Proc Natl Acad Sci U S A* (1997) 94(25):13816–9. doi: 10.1073/pnas.94.25.13816
102. Diskin C, Palsson-McDermott EM. Metabolic Modulation in Macrophage Effector Function. *Front Immunol* (2018) 9:270. doi: 10.3389/fimmu.2018.00270
103. Geier B, Sogin EM, Michellod D, Janda M, Kompauer M, Spengler B, et al. Spatial metabolomics of *in situ* host-microbe interactions at the micrometre scale. *Nat Microbiol* (2020) 5(3):498–510. doi: 10.1038/s41564-019-0664-6
104. Stuart T, Butler A, Hoffman P, Hafemeister C, Papalexi E, Mauck WM3rd, et al. Comprehensive Integration of Single-Cell Data. *Cell* (2019) 177 (7):1888–902.e21. doi: 10.1016/j.cell.2019.05.031
105. van Rensburg JJ, Lin H, Gao X, Toh E, Fortney KR, Ellinger S, et al. The Human Skin Microbiome Associates with the Outcome of and Is Influenced by Bacterial Infection. *mBio* (2015) 6(5):e01315–15. doi: 10.1128/mBio.01315-15
106. Gonzalez-Beiras C, Kapa A, Vall-Mayans M, Paru R, Gavilan S, Houinei W, et al. Single-Dose Azithromycin for the Treatment of Haemophilus ducreyi Skin Ulcers in Papua New Guinea. *Clin Infect Dis* (2017) 65(12):2085–90. doi: 10.1093/cid/cix723

107. Fusco WG, Afonina G, Nepluev I, Cholon DM, Choudhary N, Routh PA, et al. Immunization with the Haemophilus ducreyi hemoglobin receptor HgbA with adjuvant monophosphoryl lipid A protects swine from a homologous but not a heterologous challenge. *Infect Immun* (2010) 78 (9):3763–72. doi: 10.1128/IAI.00217-10
108. Fusco WG, Choudhary NR, Routh PA, Ventevogel MS, Smith VA, Koch GG, et al. The Haemophilus ducreyi trimeric autotransporter adhesin DsrA protects against an experimental infection in the swine model of chancroid. *Vaccine* (2014) 32(30):3752–8. doi: 10.1016/j.vaccine.2014.05.031

Conflict of Interest: The authors declare that the research was conducted in the absence of any commercial or financial relationships that could be construed as a potential conflict of interest.

frontiers in Immunology

REVIEW
published: 01 March 2021
doi: 10.3389/fimmu.2021.649348

The Impact of Neutrophil Recruitment to the Skin on the Pathology Induced by *Leishmania* Infection

*Katiuska Passelli, Oaklyne Billion and Fabienne Tacchini-Cottier**

Department of Biochemistry, WHO Collaborative Centre for Research and Training in Immunology, University of Lausanne, Lausanne, Switzerland

Leishmania (*L.*) are obligate intracellular protozoan parasites that cause the leishmaniases, a spectrum of neglected infectious vector-borne diseases with a broad range of clinical manifestations ranging from local cutaneous, to visceral forms of the diseases. The parasites are deposited in the mammalian skin during the blood meal of an infected female phlebotomine sand fly. The skin is a complex organ acting as the first line of physical and immune defense against pathogens. Insults to skin integrity, such as that occurring during insect feeding, induces the local secretion of pro-inflammatory molecules generating the rapid recruitment of neutrophils. At the site of infection, skin keratinocytes play a first role in host defense contributing to the recruitment of inflammatory cells to the infected dermis, of which neutrophils are the first recruited cells. Although neutrophils efficiently kill various pathogens including *Leishmania*, several *Leishmania* species have developed mechanisms to survive in these cells. In addition, through their rapid release of cytokines, neutrophils modulate the skin microenvironment at the site of infection, a process shaping the subsequent development of the adaptive immune response. Neutrophils may also be recruited later on in unhealing forms of cutaneous leishmaniasis and to the spleen and liver in visceral forms of the disease. Here, we will review the mechanisms involved in neutrophil recruitment to the skin following *Leishmania* infection focusing on the role of keratinocytes in this process. We will also discuss the distinct involvement of neutrophils in the outcome of leishmaniasis.

Keywords: skin, keratinocytes, wound healing, neutrophils, *Leishmania*, cutaneous leishmaniasis, visceral leishmaniasis, leishmaniasis

OPEN ACCESS

Edited by:
Abhay Satoskar, The Ohio State University, United States

Reviewed by:
Tamás Laskay, University of Lübeck, Germany
James Alexander, University of Strathclyde, United Kingdom
Ranadhir Dey, United States Food and Drug Administration, United States

****Correspondence:***
Fabienne Tacchini-Cottier
Fabienne.Tacchini-Cottier@unil.ch

Specialty section:
This article was submitted to Microbial Immunology, a section of the journal Frontiers in Immunology

Received: *04 January 2021*
Accepted: *04 February 2021*
Published: *01 March 2021*

Citation:
Passelli K, Billion O and Tacchini-Cottier F (2021) The Impact of Neutrophil Recruitment to the Skin on the Pathology Induced by Leishmania Infection. Front. Immunol. 12:649348. doi: 10.3389/fimmu.2021.649348

THE LEISHMANIASES

The Leishmaniases are a group of neglected vector-borne diseases caused by protozoan parasites belonging to the *Leishmania (L.)* genus. Parasites are deposited into the mammalian host skin during the blood meal of infected female phlebotomine sand flies. At least twenty different *Leishmania* species can infect humans causing three main clinical manifestations including cutaneous, mucocutaneous and visceral forms (1, 2). The outcome of the disease depends on the infecting species along with host factors. Cutaneous leishmaniasis (CL) is the most common form characterized by the appearance of a skin ulcer at the sand fly bite site, usually on exposed body parts. Although skin lesions are most of the time self-healing and localized, they can leave

seriously disfiguring and disabling life-long scars (3). The frequency of self-healing lesions depends, amongst other factors, on the *Leishmania* species. For instance, more than 75% of lesions caused by *L. mexicana* and the 60–70% caused by *L. major* heal within 3 months. In contrast, lesions caused by other New World *Leishmania* spp. such as *L. panamensis* and *L. braziliensis* take longer to heal, with an average frequency of only 35 and 10% that, respectively, self-heal after 3 months (4). Disseminated forms of CL have also been observed, where CL can manifest as multiple non-ulcerative nodules disseminating to the entire body (5). Mucocutaneous leishmaniasis (MCL) is a major CL complication that can manifest days to years following the cutaneous lesion. There are between 0.4 and 20% of CL cases in Brazil and Bolivia, respectively (6). The most endemic area for MCL is Latin America, where it results from infection with *L. braziliensis, L. panamensis, L. guyanensis,* and *L. amazonensis* (1, 7). MCL develops when the parasites migrate from the localized skin lesion to mucosal tissues of the nose, mouth and throat cavities, through lymphatics and blood vessels. This can lead to massive destruction of the oral or nasal mucosa and potentially become life-threatening (8). Visceral leishmaniasis (VL) is the deadliest form of the disease resulting from parasite dissemination from the skin to visceral organs, such as the spleen and the liver. This leads to organ dysfunction, fever, weight loss, and is usually fatal if left untreated (9). Between 700,000 and 1 million new leishmaniasis cases are reported each year across 100 countries (2, 10). The disease predominantly affects poor populations living in precarious hygiene and housing conditions (2). Several efforts have been made in order to develop a vaccine, but no effective and safe vaccine to prevent human leishmaniasis is currently available (11). Several drugs are available to treat leishmaniasis but many of them present toxicity with severe side effects and low efficacy, correlating with frequent treatment interruptions promoting the development of drug resistance (12). Currently, resistance has been reported for most of the drugs in use. It is, therefore, crucial to gain a better understanding of the local immune response to *Leishmania* infection with the long-term goal to develop anti-leishmanial drugs, which are efficient, less toxic, easy to administrate and affordable for emerging countries (13).

THE SKIN AND PARASITE ENTRY

The skin acts as the first line of physical and immune defense against *Leishmania* parasites. The two main layers composing the skin are the epidermis and the dermis. The outer surface is the epidermis, characterized by overlapping layers of keratinocytes infiltrated by melanocytes. The dermis is composed of intermingled fibroblasts and extracellular matrix and is drained by blood and lymphatic vessels. The skin also includes a vast population of immune cells including Langerhans cells (skin resident dendritic cells), T lymphocytes and recruited inflammatory cells such as natural killers, macrophages, mast cells, dendritic and neutrophils, all of which participate to the immune defense against *Leishmania* infection (14).

Keratinocytes sense pathogens and initiate the inflammatory immune response. To do this, these epidermal cells possess several innate immune receptors able to sense invading microbes. These receptors include mostly Toll-like receptors (TLR), NOD-like receptors (NLR), RIG-I-like receptors (RLR), and C-type lectin receptors (CLR). Notably, keratinocytes express TLR1, TLR2, TLR4, TLR5, TLR6, and TLR10 on their cell surface, and TLR3, and TLR9 on the endosomal surface (15–22). The activation of the TLR-signaling pathways in keratinocytes mediates the secretion of pro-inflammatory cytokines and chemokines, which are mainly involved in the activation of the Th1 immune response and the recruitment of myeloid cells, including neutrophils (23). In response to pathogens, the activation of these receptors in keratinocytes enables the secretion of innate immune mediators participating in the skin immune response. Notably, in humans, keratinocytes generate antimicrobial peptides, including β-defensins (24, 25) and cathelicidins (26, 27). In addition to the direct killing of bacteria, fungi and viruses, these antimicrobial peptides can activate leukocytes. Furthermore, keratinocytes are a source of chemotactic mediators and cytokines, that enable the recruitment and activation of immune cells in the skin. For example, epidermal cells contribute to the recruitment of neutrophils in response to CXCL1 and CXCL8 release (28, 29). Keratinocytes produce cytokines such as tumor necrosis factor (TNF)-α, IL-1α, IL-1β, IL-6, IL-18, and IL-10 (29). Keratinocytes can also recruit effector T cells, following the secretion of CXCL9, CXCL10, CXCL11, and CCL20 (29).

LEISHMANIA DEPOSITION IN THE SKIN

Phlebotomine sand flies probe the exposed skin several times to find vessels and create a blood pool from which they feed. During this process, *Leishmania* parasites are deposited and they get in contact with keratinocytes. Although *Leishmania* are not internalized by keratinocytes (30–33), the parasites have been observed to interact with these cells (33). Several studies demonstrated that, during *Leishmania* infection, keratinocytes secrete factors that modulate the immune response. Indeed, *L. major* phosphoglycans, some of the major surface glycans of the parasite, trigger TLR2 in non-hematopoietic cells including keratinocytes, promoting the release of chemokines essential for early neutrophil recruitment (33). Scorza et al. showed that, in response to *L. infantum* but not *L. major*, human keratinocytes upregulate the expression of pro-inflammatory cytokines such as IL-6, CXCL8, TNFα, and IL-1β. Conversely, IL-4 expression was increased in keratinocytes exposed to *L. major* (32). The same study further showed that keratinocytes exposed to *L. infantum* released factors promoting parasite control in monocytes (32). In the same line, Ehrchen et al. showed an increased expression of cytokines and chemokines in mouse keratinocytes isolated from *L. major*-resistant but not susceptible mice (34). In visceral leishmaniasis patients, the expression of IL-10 in keratinocytes correlated with increased pathogenesis (35). Finally, the apoptosis of keratinocytes in CL correlated with skin ulceration, a process which relies on the Fas/TRAIL apoptotic pathway (36–38).

Notably, the study of Ehrchen et al. suggested that IL-4 produced by keratinocytes promoted the development of a protective Th1 immune response in C57BL/6 mice infected with *L. major* (34). In order to assess whether the IL-4 secreted by keratinocytes acted in an autocrine manner, mice with specific deletion of the IL-4Rα in keratinocytes were generated on the C57BL/6 and BALB/c genetic background, that are, respectively, resistant, or susceptible to *L. major* infection. C57BL/6 mice deficient for IL-4Rα in keratinocytes were able to develop a Th1 immune response and to heal their lesions following *L. major* infection. These data indicated that, in C57BL/6 mice, IL-4 signaling in keratinocytes is not required for the development of a protective Th1 immune response (39). In a similar manner, infection of BALB/c mice deficient for IL-4Rα in keratinocytes developed non-healing lesions characterized by a Th2 immune response, which was similar to those developed in WT BALB/c mice (40). These results showed that autocrine stimulation of keratinocytes by IL-4 is not involved in disease evolution following *L. major* infection.

The contribution of keratinocytes in the activation of antigen-specific T cells has also been reported. In this regard, studies documented that keratinocytes express MHCII, but are lacking the expression of CD80 and CD86 co-stimulatory molecules, that are essential for the priming of naïve T cells (41). Indeed, despite the ability of keratinocytes to support T cell proliferation, they fail to activate naïve T cells and they induce T cell anergy (42, 43). The expression of the costimulatory molecule B7.2 was shown to be downregulated in keratinocytes from resistant but not susceptible mice infected with *L. major* (31). More recent data have shown that keratinocytes can process antigens and present them to antigen-specific CD4 and CD8 T cells, leading to cytokine production (44). However, the role of these interactions during *Leishmania* infection remains to be investigated.

In the skin, a heterogeneous population of resident immune cells, maintains the homeostasis and is critical for host defense. In addition to the epidermal layer described above, insults to epidermis and dermis integrity lead to the recruitment of circulating immune cells including dendritic cells, T cells, natural killer cells, monocytes and neutrophils. Amongst these, neutrophils are the first cells massively recruited to the damaged skin. We shall focus on the importance of neutrophils in the response to infection.

NEUTROPHILS AND *LEISHMANIA*

Neutrophil General Functions

Neutrophils are the most abundant leukocytes in the human blood circulation. They can be rapidly recruited to sites of injury or infection and are major players in innate immune defense against various pathogens (45). At the site of infection, neutrophils phagocytose microorganisms and kill them using a variety of mechanisms. The cytoplasm of neutrophils is rich in pre-stored granules that contain microbicidal proteins that can be rapidly released in the phagosomes or into the local microenvironment in order to eliminate pathogens. Neutrophil activation also triggers a respiratory burst leading to the production of reactive oxygen species (ROS) that is toxic for microorganisms (46, 47). Moreover, neutrophils can extrude neutrophil extracellular traps (NETs), which are extracellular web-like fibers consisting of chromatin associated with antimicrobial granule proteins. NETs trap microorganisms, a process that reduces parasite spreading. They can also kill pathogens through their association with a high concentration of microbicidal components (48).

In addition to their primary killing functions, neutrophils are increasingly reported to play significant immunoregulatory roles. Indeed, they can secrete a vast repertoire of cytokines or chemokines that may impact on the recruitment and function of various cell types. Through interactions with other immune cells, neutrophils can also contribute to the orchestration of the adaptive immune response (49, 50).

Neutrophils are the first cells to be recruited when the skin barrier is injured. Their importance in limiting microbial dissemination is highlighted by the predisposition of patients with neutropenia, or defective neutrophils, to harbor severe bacterial, parasitic or invasive fungal infections (51, 52). In contrast to these protective functions, neutrophils can also induce important tissue damage and inflammation that need to be tightly controlled (53). Deregulated neutrophil function is a feature of a heterogeneous group of skin pathologies named neutrophilic dermatosis (ND). These are conditions characterized by a wide spectrum of cutaneous lesions due to accumulation of neutrophils in the skin. ND are mainly caused by genetic mutations leading to excessive activity or production of inflammatory meditators involved in neutrophil recruitment and activation (54, 55).

Neutrophils are also major players engaged upon tissue injury and they also actively contribute to wound healing. However, neutrophils can also exert a negative impact on wound healing in some contexts. They can for instance contribute to the development of non-healing diabetic wounds. It was demonstrated that diabetes primes neutrophils to produce NETs, which impair healthy tissue healing (56, 57). Neutrophils were also recently shown to contribute to the pathogenesis of leprosy, a process contributing to the formation of skin lesions and lesions of peripheral nerves observed in this disease (58).

THE MECHANISMS INVOLVED IN EARLY NEUTROPHIL RECRUITMENT TO THE SKIN FOLLOWING *LEISHMANIA* INFECTION

Neutrophils are rapidly recruited to the site of *Leishmania* inoculation during infection. The infiltration of these cells is regulated by intertwined mechanisms related to the initial skin tissue damage caused by sand flies probing for blood (59). Several studies using experimental mouse models have shown that neutrophils are recruited following natural infection with sand flies (60–62) and that several factors contribute to this process. These include salivary gland components and the promastigote secretory gel that is synthesized by *Leishmania* in the sand fly (63–65). Furthermore, recent data showed that sand fly gut bacteria induce IL-1β secretion, a cytokine that also contributes

to the recruitment of neutrophils (62). Of note, neutrophil recruitment to the site of infection following natural infection is more sustained compared to intradermal inoculation of parasites by needle injection (60, 61).

Neutrophils were similarly observed to be rapidly recruited when *Leishmania* are needle inoculated in mice (33, 60, 66–75). Phosphate buffer saline (PBS) or parasite injection promoted similar neutrophil recruitment during the first hour of injection, however, already 2 h after *L. major* or *L. mexicana* infection, the neutrophil infiltration became parasite-dependent (60, 71, 74). In experimental models of CL, a relatively high dose of *Leishmania* has been commonly injected either subcutaneously (s.c) in the footpad (66–68), or in more recent studies intradermally (i.d.) in the ear (33, 60, 69–75). Since the sand fly deposits the parasite in the host dermis, i.d. inoculation into the skin is closer to the natural infection and injection of a low dose of parasites (10^3 or 10^4) would be more related to the parasite load transmitted in natural infection (76). Interestingly, differences in neutrophil recruitment were observed depending on the site of infection. Intradermal injection led to a higher infiltration of neutrophils compared to s.c injection, while monocytes were more rapidly recruited following s.c. infection, indicating a site-dependent recruitment of myeloid cells in the skin (75, 77). Although most of the sand flies transmit a low dose of *Leishmania* parasites, needle injection of at least 10^5 *Leishmania* is required to promote rapid parasite-dependent recruitment of neutrophils (70, 74, 76), further revealing the importance of sand fly derived components in the recruitment of these cells. Recently, it has been reported that depending on the distance of parasite deposition to the bite site, the predominant cells to contain parasites can be either neutrophils or dermal macrophages (78).

The group of Laskay first proposed that *Leishmania* parasites are silently transmitted to macrophages following phagocytosis of apoptotic and infected neutrophils in a model called the "Trojan Horse." This way of entry promotes the persistence of the parasites and their subsequent propagation in the host (79, 80). This model was recently validated *in vivo* and few dermal macrophages were visualized acquiring parasites through phagocytosis of apoptotic and parasitized neutrophils. In the same context, depletion of neutrophils before the infection reduced the number of infected dermal macrophages (78).

In mice, the recruitment of neutrophils to the site of infection following sand fly bite, or needle injection of a high dose of parasites, was shown to be bimodal, with a first rapid wave peaking during the first day post-infection (p.i), returning to basal levels by the second or third day p.i. (33, 61, 67, 69–71, 73, 74). A second wave of neutrophils occurring approximately 1 week post *L. major* infection was also observed, at a time that correlates with the appearance of the lesion (71). Following *L. panamensis* infection, the second peak of neutrophils was observed several weeks p.i and was shown to be significantly stronger than the first one (81). A second wave of neutrophils was also shown to infiltrate the skin tissue 7 weeks post *L. major* infection (82), 5 weeks post-*L. major* co-infection with lymphocytic choriomeningitis virus (LCMV) (83), and neutrophils were observed in the skin of unhealing chronic *L. mexicana* lesions (84). The timing of the second wave of neutrophils is thus well documented and its timing likely varies depending on the virulence of the parasites, the parasite dose injected as well as the *Leishmania* spp.

In line with these studies, amastigotes were shown to infect both human and mouse neutrophils (84–86). Furthermore, following *L. mexicana* infection, not only are lesional neutrophils heavily infected, but a subset of neutrophils was shown to be permissive for parasite replication, suggesting that neutrophils may also serve as a replicating niche and/or safe temporary host target in chronic infection (84). Of interest, *L. major* amastigotes were not observed to replicate in C57BL/6 neutrophils (75), a difference likely linked to the distinct formation of a parasitophorous vacuole and/or to differences in the composition of the parasite surface in the two *Leishmania* spp.

Several skin chemotactic factors are responsible for the recruitment of neutrophils following *Leishmania* infection. For instance, the chemokines CXCL1 (KC) and CXCL2 (MIP-2) in mice and CXCL8 (IL-8) in humans, granulocyte chemotactic protein 2 (GCP-2/CXCL6) in mice and the cleaved complement C3 were all shown to promote neutrophil recruitment (59, 87–89). Additionally, during the second wave of neutrophils, IL-17 also contributes to their recruitment (90).

EFFECTOR FUNCTION OF NEUTROPHILS DURING LEISHMANIASIS

Although neutrophils possess an arsenal of mechanisms to kill infecting pathogens, some species of *Leishmania* can survive inside these cells and use them as a safe shelter while some others are killed by neutrophils (74, 84, 86, 91–96). The mechanisms involved in parasite escape in neutrophils will not be discussed as they have been recently reviewed (97), but we will discuss the impact of neutrophil presence on the *Leishmania*-induced pathology.

The impact of neutrophils on the development of leishmaniasis has been observed to be either protective or detrimental depending on the infecting *Leishmania* species and the host genetics and immune system (**Figure 1**). Most of the current knowledge acquired related to the impact of neutrophils in experimental *Leishmania* infection has been obtained either following mAb-induced neutrophil depletion at the onset of infection or using genetically neutropenic mice (60, 67, 70, 72, 74, 82, 98–100). In order to transiently deplete neutrophils in mice, three monoclonal antibodies have been used, each of them with some limitations. Several studies have used the RB6-8RC5 monoclonal antibody that recognizes the Gr1 epitope which is common between cells expressing Ly6G and Ly6C (101). The RB6-8RC5 antibody efficiently depletes neutrophils and inflammatory monocytes (77). The NIMP-R14 mAb depletes neutrophils and also a subset of inflammatory monocytes (77, 102). Finally, the 1A8 monoclonal antibody targets specifically Ly6G that is expressed exclusively in neutrophils (103) but depletion is transient, and if used for more than a week, an increased release of neutrophils from the BM is observed. Differences in mAb isotypes also results in

different depletion efficacy. Novel mAb administration strategies may circumvent this problem (104). One thus has to be critical in evaluating studies using only mAb depletion strategies. Complementary approaches abolishing or reducing the presence of neutrophils are needed to better understand the implications of these cells in the outcome of infection. Nevertheless, compiling results obtained with these different approaches completed by *in vitro* studies in human neutrophils allowed us to shed a new light on the importance of these cells in *Leishmania* pathogenicity, with either protective or pathogenic roles (**Table 1**).

PROTECTIVE ROLE FOR NEUTROPHILS IN LEISHMANIASIS

The first evidence suggesting a positive role of neutrophils during *Leishmania* infection was suggested in mice infected with the Bokkara strain of *L. major*. C57BL/6 mice depleted of neutrophils and monocytes (RB6-8RC5 antibody) at −3, 0 and 3 days post infection, and infected s.c. with 10^7 *L. major,* showed increased lesion size and a higher parasite burden (98). Similarly, depletion of neutrophils using the NIMP-R14 antibody in C57BL/6 mice promoted the development of a more prominent lesion during the first weeks following *L. major* LV39 infection, but the lesion eventually healed (67). BALB/c mice infected with *L. major* Bokkara and depletion of neutrophils using the RB6-8RC5 antibody, showed increased lesion progression during the first 6 weeks post infection, without affecting the chronic progression of the disease (98). These latter results contrasted with other data (see below), and these differences might be explained by the distinct species or strains of parasite inoculated, different dose of parasite injected and the specificity of the antibodies used to deplete neutrophils.

Neutrophils were further reported to secrete CCL3, a chemokine that contributes to the recruitment of dendritic cells (DC) to the site of *L. major* infection in C57BL/6 mice, a process shown to contribute to the development of a protective immune response (69). In contrast, apoptotic neutrophils containing live *Leishmania* were shown to be uptaken by dermal dendritic cells, a process inhibiting the development of an adaptive immune response (71). These data further demonstrated a complex role for neutrophils in self-healing experimental CL. In addition, the sensing of *L. major* by neutrophil endosomal TLR7, was shown to be critical for the early regulation of parasite burden and subsequent disease control in *L. major* LV39 infected C57BL/6 mice (75).

The presence of neutrophils was also shown to be protective during the first week post-infection in BALB/c mice infected with *L. amazonensis* in a study using the RB6-8RC5 antibody to deplete neutrophils (72). *L. amazonensis* promastigotes were efficiently killed by neutrophils *in vitro*, whereas the amastigote form of the parasite resisted neutrophil killing (86), suggesting that neutrophils may have a distinct role early post-infection than during the chronic phase of the disease. In addition, following infection of mice with *L. amazonensis,* neutrophil programmed cell death was altered due to genetic defective ROS production, and pathology was shown to be associated with the presence of necrotic neutrophils, suggesting that appropriated neutrophil programmed cell death is essential for the control of *L. amazonensis*-induced dermal lesions (105). Similarly, the presence of neutrophils co-cultured *in vitro* with macrophages reduced *L. amazonensis* burden in macrophages (106). The depletion of neutrophils using the RB6-8RC5 antibody in BALB/c mice infected with *L. braziliensis*, also promoted the development of a more prominent lesion with increased parasite burden during the first 2 weeks post-infection (100). Moreover, Carlsen et al. showed that the internalization of *L. braziliensis* amastigotes by neutrophils induced a strong activation of these cells, leading to efficient killing of the parasite (107). Collectively, these data show that neutrophils are efficient in controlling the parasites following infection with these *Leishmania* spp.

Neutrophils were also shown to play a protective role following needle injection of *L. donovani* and *L. infantum*, two *Leishmania* spp. causing visceral leishmaniasis (VL). The infection of neutrophil-depleted C57BL/6 mice with *L. donovani* resulted in a hepatosplenomegaly and a higher parasite burden in the spleen and liver compared to neutrophil-sufficient mice. In this study, the RB6-8RC5 antibody was used for depletion purposes (108). In the same vein, neutrophils contributed to the development of a protective immune response during *L. donovani* infection of BALB/c mice. In this latter study, neutropenic mice had a splenomegaly with a higher parasite load in the spleen and bone marrow. This phenotype was associated with increased IL-4 and IL-10 secretion and reduced IFN-γ levels in the spleen whereby the NIMP-R14 antibody was used to deplete neutrophils (109). Additionally, using the RB6-8C5 depleting antibody, neutrophils were also shown to contribute to the early control of infection in BALB/c mice infected with *L. infantum* (70, 110). During *L. infantum* infection, TLR2 and TLR9 were shown to be critical for the recruitment of neutrophils to the inflammatory site, contributing to the control of infection (111, 112). Collectively, these studies show that, although the mAb used for neutrophil depletion was not always specific for neutrophils, neutrophils can play their well-known protective role in CL and VL.

A DETRIMENTAL ROLE FOR NEUTROPHILS DURING LEISHMANIASIS

The contribution of neutrophils in the development of a non-protective immunity was first reported using the classical *L. major* s.c. infection in BALB/c mice, that develop Th2 immune response correlating with the development of unhealing skin lesions. The transient depletion of neutrophils at the onset of infection in BALB/c mice, using the NIMP-R14 antibody, allowed better resolution of skin lesions and parasite burden, than mice injected with a control mAb, a process correlating with a decreased Th2 immune response (67). In addition, using the RB6-8RC5 antibody, Ribeiro-Gomes et al., also showed that neutrophil depletion reduced the parasite burden in *L. major*-infected BALB/c mice (99). Th17 cells secrete IL-17, a cytokine which recruits neutrophils. Following *L. major* infection, this

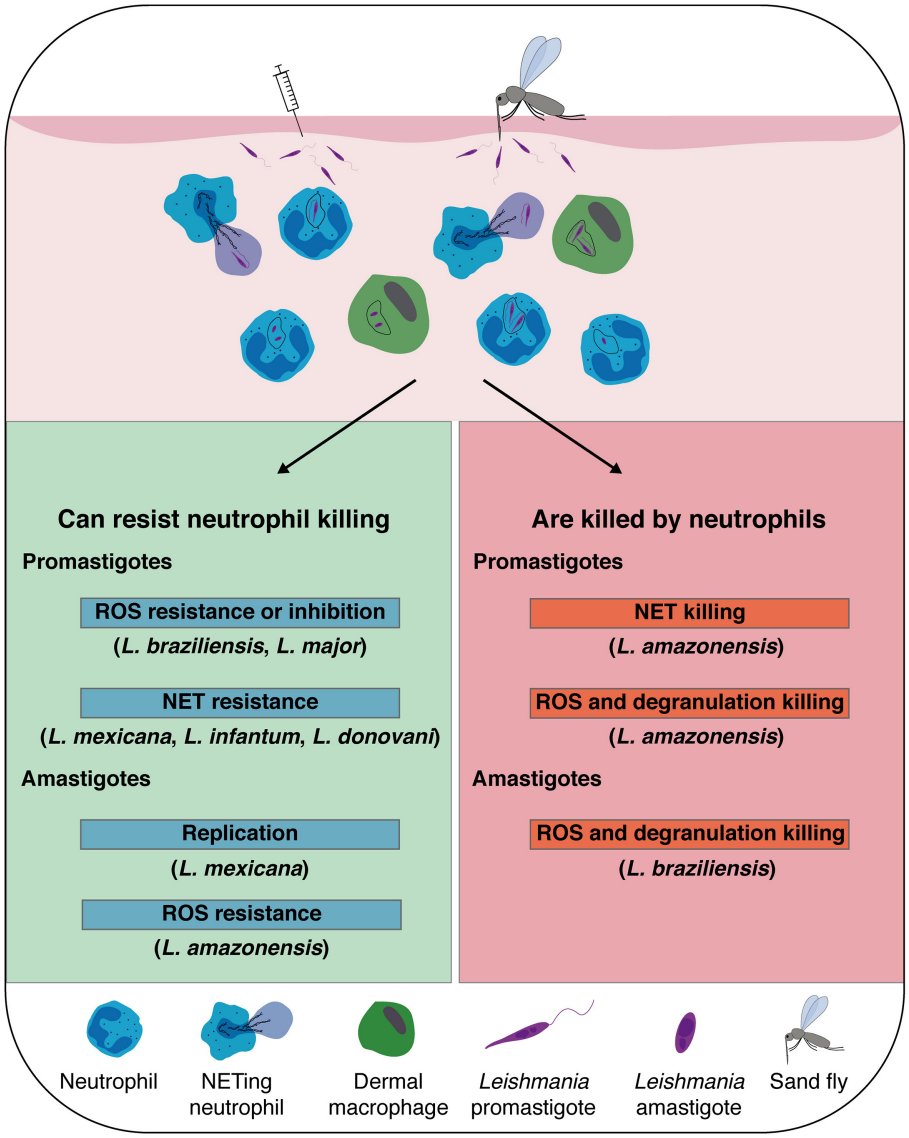

FIGURE 1 | *Leishmania* spp. that are susceptible, or that escape neutrophil killing: *Leishmania* inoculation in the host dermis by natural sand fly bite, or experimental needle injection, promotes a rapid recruitment of neutrophils, which sequestrate the parasite by phagocytosis or release of neutrophil extracellular traps (NETs). In addition to neutrophils, dermal macrophages are also heavily infected early post-infection contributing to the establishment of the infection. Although neutrophil killing mechanisms efficiently eliminate some spp. of *Leishmania* promastigotes and amastigotes, some *Leishmania* developed mechanisms to resist or inhibit reactive oxygen species (ROS) formation and survive inside neutrophils and NETs. Notably, *L. mexicana* amastigotes were shown to replicate inside neutrophils.

IL-17-induced neutrophil recruitment was shown to promote CL pathogenicity in infected BALB/c mice (90).

Neutrophil recruitment to the skin also contributed to the severe pathology associated with infection with a low dose of *L. major* Seidman, a parasite that causes severe disease in C57BL/6 mice despite the development of a strong Th1 immune response (82, 113). Neutropenic *Genista* mice infected with *L. major* Seidman developed a healing lesion associated with a decreased parasite burden and an increased protective Th1 immune response, further emphasizing the role of neutrophils in influencing the adaptive immune response (82). Of note, the negative role of neutrophils was associated with the activation of the NLRP3 inflammasome and the subsequent secretion of IL-1β (82). Using a different approach, we recently showed that the recruitment of neutrophils induced by *L. major*-triggered TLR2 activation in non-hematopoietic cells, delayed the control of the disease in C57BL/6 mice infected with *L. major* LV39 (33).

Neutrophils contribute to the chronicity of *L. mexicana* disease in C57BL/6 mice and also play a negative role in the disease. This was demonstrated using mice either genetically neutropenic or depleted of neutrophils during the first days of infection after injection of the Ly6G mAb (74). Following

TABLE 1 | Protective and detrimental role of neutrophils during *Leishmania* infection: Neutrophils play protective (resolution of the disease), or detrimental (enhanced disease) roles in cutaneous and visceral leishmaniasis depending on the infecting *Leishmania* spp., the genetic background of the host, the mode of infection and the host immune response.

Role of neutrophils in infection	*Leishmania*		Source of neutrophils	Route of infection	References
	species	strain			
Protective	*L. major*	Bokkara	C57BL/6, BALB/c	s.c.[a]	(98)
		LV39	C57BL/6	s.c.	(67, 99)
		LV39	C57BL/6	i.d.[b]	(69, 75)
	L. amazonensis		BALB/c, C57BL/6	i.d.	(72, 105)
	L. amazonensis		BALB/c (Promastigote and amastigote parasites) C57BL/6, C3H/HePas, C3H/HeJ (promastigote parasites)	*in vitro*	(86, 106)
	L. amazonensis		Human	*in vitro*	(93, 115, 116)
	L. braziliensis		BALB/c	i.d.	(100)
	L. braziliensis		C57BL/6	*in vitro*	(73, 107)
	L. donovani		C57BL/6, BALB/c	i.v.[c]	(108, 109)
	L. infantum		C57BL/6, BALB/c	i.v. or i.d.	(70, 110–112)
Detrimental	*L. major*	LV39	BALB/c	s.c.	(67, 99)
		LV39	C57BL/6	i.d.	(33)
		IL81	Human	*in vitro*	(79)
		5ASKH	BALB/c	s.c.	(88)
		Friedlin	C57BL/6 (LCMV coinfection)	i.d.	(83)
		Friedlin	C57BL/6	i.d. (sand fly)	(60, 61)
		Friedlin	BALB/c	i.d	(90)
		Seidman	C57BL/6	i.d.	(82)
		Ryan	C57BL/6	i.d. (sand fly and needle)	(78)
	L. mexicana		C57BL/6, BALB/c	i.d.	(74, 114)
	L. mexicana		C57BL/6	i.d and *in vitro*	(84)
	L. amazonensis		C57BL/6 (amastigote parasites)	*in vitro*	(86)
	L. panamensis		Human	*ex vivo*	(118)
	L. donovani		BALB/c	i.d. (sand fly)	(62)

[a] *s.c.: subcutaneous in the footpad.*
[b] *i.d.: intradermal in the ear.*
[c] *i.v.: intravenous.*
Light gray: CL; dark gray: VL. Parasites are needle injected. When parasites are deposited following natural infection, "sand fly" is indicated.

i.d. infection with *L. mexicana,* neutropenic mice developed a small lesion that ultimately healed, in contrast to neutrophil sufficient mice that showed a persistent unhealing lesion. In addition, healing was shown to correlate with the development of a protective Th1 response and a decreased parasite burden (74). Furthermore, crosstalk between Th17 cells and neutrophils was shown to contribute to the enhanced susceptibility toward a chronic disease following *L. mexicana* infection in BALB/c mice (114). These studies further strengthen the role of neutrophils on the developing adaptive immune response. An important number of neutrophils has also been reported following co-infection of mice with *L. major* and LCMV and the development of chronic lesions highly infiltrated with neutrophils, correlated with the development of a more prominent lesion (83).

Finally, natural infection with *L. major* infected sand flies also showed that neutrophils contribute to the cutaneous pathology (60). Recently, the microbiota of sand flies was shown to be associated with neutrophil recruitment to the site of *L. donovani* infection. Treating the sand flies with antibiotics decreased neutrophil recruitment and impaired parasite visceralization, suggesting a pathological role for neutrophils in this model of infection (62). Of note these data contrast with the protective role for neutrophils in VL observed following needle injection of a high dose of parasites.

Collectively these studies suggest that, to firmly assign a role for neutrophils in *Leishmania* infection, several parameters need to be taken into account including the dose of infection, the site of parasite injection, the mode of parasite delivery, the genetic background and immune status of the host as well as the neutropenic model used.

NEUTROPHILS IN HUMAN LEISHMANIASIS

To understand the role of neutrophils upon *Leishmania* infection, mouse models have predominantly been used but an increasing number of studies has been performed using peripheral blood neutrophils *in vitro* or *ex vivo* and using transcriptomics studies of infected skin biopsies. Results from these studies also suggest a dual role for neutrophils in human leishmaniasis, that can also be beneficial or detrimental depending on the infecting *Leishmania* species.

PROTECTIVE ROLE OF HUMAN NEUTROPHILS DURING *LEISHMANIA* INFECTION

Human neutrophils infected *in vitro* with *L. amazonensis* were reported to be activated and to produce ROS. Moreover, infected human neutrophils were shown to produce leukotriene B4 (LTB4), which promotes neutrophil degranulation and the killing of the parasite (115). Neutrophil degranulation in response to *L. amazonensis* was further shown to promote the killing of the parasite in infected macrophages (116).

DELETERIOUS ROLE OF HUMAN NEUTROPHILS DURING *LEISHMANIA* INFECTION

The transcriptional profile of primary human macrophages infected *in vitro* with *L. (Vianna) panamensis,* causing tegumentary leishmaniasis, differed significantly in response to infection depending on whether infection was undertaken with parasites isolated from self-healing patients or those showing chronic disease. Interestingly, expression levels of neutrophil-recruiting chemokines were predominantly observed in the transcriptomics analysis of macrophages infected with parasites isolated from chronic lesions, suggesting that the presence of neutrophils likely contributes to the sustained inflammation observed in chronic dermal leishmaniasis (117). In addition, performing transcriptomics of infected skin biopsies of patients that cured or failed to heal after meglumine antimoniate treatment, further showed that downregulation of the neutrophil activation genes was linked to cure of the disease, further supporting a deleterious role for neutrophils in chronic forms of the disease (118).

Neutrophils have been detected in patients with active cutaneous lesions of American tegumentary leishmaniasis from *L. braziliensis* patients (119–121). Neutrophils isolated from disseminated leishmaniasis patients infected with *L. brazililensis* were shown to be less activated and may thus contribute to parasite survival and dissemination (122).

In patients with active VL the number of circulating blood neutrophils was reduced and a considerable proportion of these blood peripheral cells was immature (123). Furthermore, neutrophils from VL patients were shown to be activated but to display impaired effector functions, suggesting that during active disease, neutrophils may contribute to the immunosuppression observed in VL patients (123, 124). Saliva components from the sand fly vector were shown to induce IL-17-induced neutrophil recruitment, a process favoring *L. infantum* infection (125) revealing, as was previously shown in murine models, an important role for this cytokine in neutrophil recruitment.

CONCLUSION AND PERSPECTIVES

Neutrophils are rapidly recruited to the skin following *Leishmania* infection and they play a critical role in phagocytosing the parasites and in shaping the immune response. In addition, neutrophils are also present in established lesions and were shown to contribute to parasite persistence. The impact of neutrophils on the development of leishmaniasis can be either protective, or detrimental, depending on a range of intricate factors including the infecting *Leishmania* spp., the host genetic background and immune response, as well as the local microenvironment induced by the parasite inoculation into the skin. In the last decade, keratinocytes have been identified as important cells for the modulation of the immune response following *Leishmania* infection, including neutrophil recruitment, further highlighting the importance of skin resident cells in the response against infection.

Many questions on the mechanism of action of neutrophils in leishmaniasis remain open. These include the understanding of the interactions between neutrophils and mast cells at the site of infection, the mechanisms involved in neutrophil recruitment to the draining lymphoid organs following infection and the interactions taking place between neutrophils and other recruited and resident cells in these organs. Further studies will help to identify potential targets for the treatment of leishmaniasis, in which neutrophils are contributing to the severity of the disease.

AUTHOR CONTRIBUTIONS

KP and FT-C wrote the review. OB, KP, and FT-C contributed to the figure and the table. All authors gave input on the review.

ACKNOWLEDGMENTS

We thank Drs. Miriam Diaz Varela and Borja Prat Luri and for critical reading of the manuscript and we acknowledge the financial support of the Swiss National Foundation for Scientific Research (310030_184751/1 to FT-C).

REFERENCES

1. Pace D. Leishmaniasis. *J Infect.* (2014) 69:S10–8. doi: 10.1016/j.jinf.2014.07.016
2. WHO (2020). Available online at: who.int/leishmaniasis/en/
3. Ameen M. Cutaneous leishmaniasis: advances in disease pathogenesis, diagnostics and therapeutics. *Clin Exp Dermatol.* (2010) 35:699–705. doi: 10.1111/j.1365-2230.2010.03851.x
4. Murray HW, Berman JD, Davies CR, Saravia NG. Advances in leishmaniasis. *Lancet.* (2005) 366:1561–77. doi: 10.1016/S0140-6736(05)67629-5
5. Burza S, Croft SL, Boelaert M. Leishmaniasis. *Lancet.* (2018) 392:951–70. doi: 10.1016/S0140-6736(18)31204-2
6. Goto H, Lindoso JA. Current diagnosis and treatment of cutaneous and mucocutaneous leishmaniasis. *Expert Rev Anti Infect Ther.* (2010) 8:419–33. doi: 10.1586/eri.10.19
7. Sakthianandeswaren A, Foote SJ, Handman E. The role of host genetics in leishmaniasis. *Trends Parasitol.* (2009) 25:383–91. doi: 10.1016/j.pt.2009.05.004
8. Reithinger R, Dujardin J-C, Louzir H, Pirmez C, Alexander B, Brooker S. Cutaneous leishmaniasis. *Lancet Infect Dis.* (2007) 7:581–96. doi: 10.1016/S1473-3099(07)70209-8
9. Chappuis F, Sundar S, Hailu A, Ghalib H, Rijal S, Peeling RW, et al. Visceral leishmaniasis: what are the needs for diagnosis, treatment and control? *Nat Rev Microbiol.* (2007) 5:873–82. doi: 10.1038/nrmicro1748
10. Alvar J, Vélez ID, Bern C, Herrero M, Desjeux P, Cano J, et al. Leishmaniasis worldwide and global estimates of its incidence. *PLoS ONE.* (2012) 7:e35671. doi: 10.1371/journal.pone.0035671
11. Singh B, Sundar S. Leishmaniasis: vaccine candidates and perspectives. *Vaccine.* (2012) 30:3834–42. doi: 10.1016/j.vaccine.2012.03.068
12. Bekhit AA, El-Agroudy E, Helmy A, Ibrahim TM, Shavandi A, Bekhit AEA. *Leishmania* treatment and prevention: natural and synthesized drugs. *Eur J Med Chem.* (2018) 160:229–44. doi: 10.1016/j.ejmech.2018.10.022
13. Croft SL, Sundar S, Fairlamb AH. Drug resistance in leishmaniasis. *Clin Microbiol Rev.* (2006) 19:111–26. doi: 10.1128/CMR.19.1.111-126.2006
14. Scott P, Novais FO. Cutaneous leishmaniasis: immune responses in protection and pathogenesis. *Nat Rev Immunol.* (2016) 16:581–92. doi: 10.1038/nri.2016.72
15. Kawai K, Shimura H, Minagawa M, Ito A, Tomiyama K, Ito M. Expression of functional Toll-like receptor 2 on human epidermal keratinocytes. *J Dermatol Sci.* (2002) 30:185–94. doi: 10.1016/S0923-1811(02)00105-6
16. Song PI, Park YM, Abraham T, Harten B, Zivony A, Neparidze N, et al. Human keratinocytes express functional CD14 and Toll-like receptor 4. *J Invest Dermatol.* (2002) 119:424–32. doi: 10.1046/j.1523-1747.2002.01847.x
17. Baker BS, Ovigne JM, Powles AV, Corcoran S, Fry L. Normal keratinocytes express Toll-like receptors (TLRs) 1, 2 and 5: modulation of TLR expression in chronic plaque psoriasis. *Br J Dermatol.* (2003) 148:670–9. doi: 10.1046/j.1365-2133.2003.05287.x
18. Mempel M, Voelcker V, Köllisch G, Plank C, Rad R, Gerhard M, et al. Toll-like receptor expression in human keratinocytes: nuclear factor kappaB controlled gene activation by *Staphylococcus aureus* is Toll-like receptor 2 but not Toll-like receptor 4 or platelet activating factor receptor dependent. *J Invest Dermatol.* (2003) 121:1389–96. doi: 10.1111/j.1523-1747.2003.12630.x
19. Pivarcsi A, Bodai L, Réthi B, Kenderessy-Szabó A, Koreck A, Széll M, et al. Expression and function of Toll-like receptors 2 and 4 in human keratinocytes. *Int Immunol.* (2003) 15:721–30. doi: 10.1093/intimm/dxg068
20. Miller LS, Sørensen OE, Liu PT, Jalian HR, Eshtiaghpour D, Behmanesh BE, et al. TGF-alpha regulates TLR expression and function on epidermal keratinocytes. *J Immunol.* (2005) 174:6137–43. doi: 10.4049/jimmunol.174.10.6137
21. Köllisch G, Kalali BN, Voelcker V, Wallich R, Behrendt H, Ring J, et al. Various members of the Toll-like receptor family contribute to the innate immune response of human epidermal keratinocytes. *Immunology.* (2005) 114:531–41. doi: 10.1111/j.1365-2567.2005.02122.x
22. Lebre MC, van der Aar AM, van Baarsen L, van Capel TM, Schuitemaker JH, Kapsenberg ML, et al. Human keratinocytes express functional Toll-like receptor 3, 4, 5, and 9. *J Invest Dermatol.* (2007) 127:331–41. doi: 10.1038/sj.jid.5700530
23. Miller LS, Modlin RL. Human keratinocyte Toll-like receptors promote distinct immune responses. *J Invest Dermatol.* (2007) 127:262–3. doi: 10.1038/sj.jid.5700559
24. Harder J, Bartels J, Christophers E, Schroder JM. Isolation and characterization of human beta -defensin-3, a novel human inducible peptide antibiotic. *J Biol Chem.* (2001) 276:5707–13. doi: 10.1074/jbc.M008557200
25. Liu L, Roberts AA, Ganz T. By IL-1 signaling, monocyte-derived cells dramatically enhance the epidermal antimicrobial response to lipopolysaccharide. *J Immunol.* (2003) 170:575–80. doi: 10.4049/jimmunol.170.1.575
26. Frohm M, Agerberth B, Ahangari G, Ståhle-Bäckdahl M, Lidén S, Wigzell H, et al. The expression of the gene coding for the antibacterial peptide LL-37 is induced in human keratinocytes during inflammatory disorders. *J Biol Chem.* (1997) 272:15258–63. doi: 10.1074/jbc.272.24.15258
27. Dorschner RA, Pestonjamasp VK, Tamakuwala S, Ohtake T, Rudisill J, Nizet V, et al. Cutaneous injury induces the release of cathelicidin anti-microbial peptides active against group A Streptococcus. *J Invest Dermatol.* (2001) 117:91–7. doi: 10.1046/j.1523-1747.2001.01340.x
28. O'Toole EA, Mak LL, Guitart J, Woodley DT, Hashimoto T, Amagai M, et al. Induction of keratinocyte IL-8 expression and secretion by IgG autoantibodies as a novel mechanism of epidermal neutrophil recruitment in a pemphigus variant. *Clin Exp Immunol.* (2000) 119:217–24. doi: 10.1046/j.1365-2249.2000.01104.x
29. Albanesi C, Scarponi C, Giustizieri ML, Girolomoni G. Keratinocytes in inflammatory skin diseases. *Curr Drug Targets Inflamm Allergy.* (2005) 4:329–34. doi: 10.2174/1568010054022033
30. Vasconcellos C, Sotto MN. Experimental cutaneous leishmaniasis: transmission electron microscopy of the inoculation site. *Int J Exp Pathol.* (1997) 78:81–9. doi: 10.1046/j.1365-2613.1997.d01-243.x
31. Mbow ML, DeKrey GK, Titus RG. *Leishmania major* induces differential expression of costimulatory molecules on mouse epidermal cells. *Eur J Immunol.* (2001) 31:1400–9. doi: 10.1002/1521-4141(200105)31:5<1400::AID-IMMU1400>3.0.CO;2-J
32. Scorza BM, Wacker MA, Messingham K, Kim P, Klingelhutz A, Fairley J, et al. Differential activation of human keratinocytes by *Leishmania* species causing localized or disseminated disease. *J Invest Dermatol.* (2017) 137:2149–56. doi: 10.1016/j.jid.2017.05.028
33. Ronet C, Passelli K, Charmoy M, Scarpellino L, Myburgh E, Hauyon La Torre Y, et al. TLR2 signaling in skin nonhematopoietic cells induces early neutrophil recruitment in response to *Leishmania major* infection. *J Invest Dermatol.* (2019) 139:1318–28. doi: 10.1016/j.jid.2018.12.012
34. Ehrchen JM, Roebrock K, Foell D, Nippe N, von Stebut E, Weiss JM, et al. Keratinocytes determine Th1 immunity during early experimental leishmaniasis. *PLoS Pathog.* (2010) 6:e1000871. doi: 10.1371/journal.ppat.1000871
35. Gasim S, Elhassan AM, Khalil EA, Ismail A, Kadaru AM, Kharazmi A, et al. High levels of plasma IL-10 and expression of IL-10 by keratinocytes during visceral leishmaniasis predict subsequent development of post-kala-azar dermal leishmaniasis. *Clin Exp Immunol.* (1998) 111:64–9. doi: 10.1046/j.1365-2249.1998.00468.x
36. Eidsmo L, Nylen S, Khamesipour A, Hedblad MA, Chiodi F, Akuffo H. The contribution of the Fas/FasL apoptotic pathway in ulcer formation during *Leishmania major*-induced cutaneous leishmaniasis. *Am J Pathol.* (2005) 166:1099–108. doi: 10.1016/S0002-9440(10)62330-9
37. Eidsmo L, Fluur C, Rethi B, Eriksson Ygberg S, Ruffin N, De Milito A, et al. FasL and TRAIL induce epidermal apoptosis and skin ulceration upon exposure to *Leishmania major*. *Am J Pathol.* (2007) 170:227–39. doi: 10.2353/ajpath.2007.060068
38. Tasew G, Nylén S, Lieke T, Lemu B, Meless H, Ruffin N, et al. Systemic FasL and TRAIL neutralisation reduce *Leishmaniasis* induced skin ulceration. *PLoS Negl Trop Dis.* (2010) 4:e844. doi: 10.1371/journal.pntd.0000844
39. Descatoire M, Hurrell BP, Govender M, Passelli K, Martinez-Salazar B, Hurdayal R, et al. IL-4Rα signaling in keratinocytes and early IL-4 production are dispensable for generating a curative T Helper 1 response in *Leishmania major*-Infected C57BL/6 mice. *Front Immunol.* (2017) 8:1265. doi: 10.3389/fimmu.2017.01265

40. Govender M, Hurdayal R, Martinez-Salazar B, Gqada K, Pillay S, Gcanga L, et al. Deletion of interleukin-4 receptor alpha-responsive keratinocytes in BALB/c mice does not alter susceptibility to cutaneous leishmaniasis. *Infect Immun.* (2018) 86:e00710–18. doi: 10.1128/IAI.00710-18
41. Nickoloff BJ, Turka LA. Immunological functions of non-professional antigen-presenting cells: new insights from studies of T-cell interactions with keratinocytes. *Immunol Today.* (1994) 15:464–9. doi: 10.1016/0167-5699(94)90190-2
42. Gaspari AA, Katz SI. Induction of *in vivo* hyporesponsiveness to contact allergens by hapten-modified Ia+ keratinocytes. *J Immunol.* (1991) 147:4155–61.
43. Nickoloff BJ, Mitra RS, Green J, Zheng XG, Shimizu Y, Thompson C, et al. Accessory cell function of keratinocytes for superantigens. Dependence on lymphocyte function-associated antigen-1/intercellular adhesion molecule-1 interaction. *J Immunol.* (1993) 150:2148–59.
44. Black AP, Ardern-Jones MR, Kasprowicz V, Bowness P, Jones L, Bailey AS, et al. Human keratinocyte induction of rapid effector function in antigen-specific memory CD4+ and CD8+ T cells. *Eur J Immunol.* (2007) 37:1485–93. doi: 10.1002/eji.200636915
45. Hidalgo A, Chilvers ER, Summers C, Koenderman L. The neutrophil life cycle. *Trends Immunol.* (2019) 40:584–97. doi: 10.1016/j.it.2019.04.013
46. Mócsai A. Diverse novel functions of neutrophils in immunity, inflammation, and beyond. *J Exp Med.* (2013) 210:1283–99. doi: 10.1084/jem.20122220
47. Borregaard N. Neutrophils, from marrow to microbes. *Immunity.* (2010) 33:657–70. doi: 10.1016/j.immuni.2010.11.011
48. Brinkmann V, Reichard U, Goosmann C, Fauler B, Uhlemann Y, Weiss DS, et al. Neutrophil extracellular traps kill bacteria. *Science.* (2004) 303:1532–5. doi: 10.1126/science.1092385
49. Mantovani A, Cassatella MA, Costantini C, Jaillon S. Neutrophils in the activation and regulation of innate and adaptive immunity. *Nat Rev Immunol.* (2011) 11:519–31. doi: 10.1038/nri3024
50. Schuster S, Hurrell B, Tacchini-Cottier F. Crosstalk between neutrophils and dendritic cells: a context-dependent process. *J Leukoc Biol.* (2013) 94:671–5. doi: 10.1189/jlb.1012540
51. Kolaczkowska E, Kubes P. Neutrophil recruitment and function in health and inflammation. *Nat Rev Immunol.* (2013) 13:159–75. doi: 10.1038/nri3399
52. Burke VE, Lopez FA. Approach to skin and soft tissue infections in non-HIV immunocompromised hosts. *Curr Opin Infect Dis.* (2017) 30:354–63. doi: 10.1097/QCO.0000000000000378
53. Mortaz E, Alipoor SD, Adcock IM, Mumby S, Koenderman L. Update on neutrophil function in severe inflammation. *Front Immunol.* (2018) 9:2171. doi: 10.3389/fimmu.2018.02171
54. Marzano AV, Borghi A, Wallach D, Cugno M. A comprehensive review of neutrophilic diseases. *Clin Rev Allergy Immunol.* (2018) 54:114–30. doi: 10.1007/s12016-017-8621-8
55. Marzano AV, Ortega-Loayza AG, Heath M, Morse D, Genovese G, Cugno M. Mechanisms of inflammation in neutrophil-mediated skin diseases. *Front Immunol.* (2019) 10:1059. doi: 10.3389/fimmu.2019.01059
56. Phillipson M, Kubes P. The healing power of neutrophils. *Trends Immunol.* (2019) 40:635–47. doi: 10.1016/j.it.2019.05.001
57. Wong SL, Demers M, Martinod K, Gallant M, Wang Y, Goldfine AB, et al. Diabetes primes neutrophils to undergo NETosis, which impairs wound healing. *Nat Med.* (2015) 21:815–9. doi: 10.1038/nm.3887
58. Schmitz V, Tavares IF, Pignataro P, Machado AdM, Pacheco FdS, dos Santos JB, et al. Neutrophils in leprosy. *Front Immunol.* (2019) 10:495. doi: 10.3389/fimmu.2019.00495
59. van Zandbergen G, Hermann N, Laufs H, Solbach W, Laskay T. *Leishmania* promastigotes release a granulocyte chemotactic factor and induce interleukin-8 release but inhibit gamma interferon-inducible protein 10 production by neutrophil granulocytes. *Infect Immun.* (2002) 70:4177–84. doi: 10.1128/IAI.70.8.4177-4184.2002
60. Peters NC, Egen JG, Secundino N, Debrabant A, Kimblin N, Kamhawi S, et al. *In vivo* imaging reveals an essential role for neutrophils in leishmaniasis transmitted by sand flies. *Science.* (2008) 321:970–4. doi: 10.1126/science.1159194
61. Peters NC, Kimblin N, Secundino N, Kamhawi S, Lawyer P, Sacks DL. Vector transmission of *Leishmania* abrogates vaccine-induced protective immunity. *PLoS Pathog.* (2009) 5:e1000484. doi: 10.1371/journal.ppat.1000484
62. Dey R, Joshi AB, Oliveira F, Pereira L, Guimarães-Costa AB, Serafim TD, et al. Gut microbes egested during bites of infected sand flies augment severity of leishmaniasis via inflammasome-derived IL-1β. *Cell Host Microbe.* (2018) 23:134–43.e6. doi: 10.1016/j.chom.2017.12.002
63. Teixeira CR, Teixeira MJ, Gomes RBB, Santos CS, Andrade BB, Raffaele-Netto I, et al. Saliva from *Lutzomyia longipalpis* induces CC chemokine ligand 2/monocyte chemoattractant protein-1 expression and macrophage recruitment. *J Immunol.* (2005) 175:8346–53. doi: 10.4049/jimmunol.175.12.8346
64. de Moura TR, Oliveira F, Rodrigues GC, Carneiro MW, Fukutani KF, Novais FO, et al. Immunity to *Lutzomyia intermedia* saliva modulates the inflammatory environment induced by *Leishmania braziliensis*. *PLoS Negl Trop Dis.* (2010) 4:e712. doi: 10.1371/journal.pntd.0000712
65. Rogers M, Kropf P, Choi B-S, Dillon R, Podinovskaia M, Bates P, et al. Proteophosophoglycans regurgitated by *Leishmania*-infected sand flies target the L-Arginine metabolism of host macrophages to promote parasite survival. *PLoS Pathog.* (2009) 5:e1000555. doi: 10.1371/journal.ppat.1000555
66. Beil WJ, Meinardus-Hager G, Neugebauer D-C, Sorg C. Differences in the onset of the inflammatory response to cutaneous leishmaniasis in resistant and susceptible mice. *J Leukoc Biol.* (1992) 52:135–42. doi: 10.1002/jlb.52.2.135
67. Tacchini-Cottier F, Zweifel C, Belkaid Y, Mukankundiye C, Vasei M, Launois P, et al. An immunomodulatory function for neutrophils during the induction of a CD4+ Th2 response in BALB/c mice infected with *Leishmania major*. *J Immunol.* (2000) 165:2628–36. doi: 10.4049/jimmunol.165.5.2628
68. Xin L, Vargas-Inchaustegui DA, Raimer SS, Kelly BC, Hu J, Zhu L, et al. Type I IFN receptor regulates neutrophil functions and innate immunity to *Leishmania* parasites. *J Immunol.* (2010) 184:7047–56. doi: 10.4049/jimmunol.0903273
69. Charmoy M, Brunner-Agten S, Aebischer D, Auderset F, Launois P, Milon G, et al. Neutrophil-derived CCL3 is essential for the rapid recruitment of dendritic cells to the site of *Leishmania major* inoculation in resistant mice. *PLoS Pathog.* (2010) 6:e1000755. doi: 10.1371/journal.ppat.1000755
70. Thalhofer CJ, Chen Y, Sudan B, Love-Homan L, Wilson ME. Leukocytes infiltrate the skin and draining lymph nodes in response to the protozoan *Leishmania infantum chagasi*. *Infect Immun.* (2011) 79:108–17. doi: 10.1128/IAI.00338-10
71. Ribeiro-Gomes FL, Peters NC, Debrabant A, Sacks DL. Efficient capture of infected neutrophils by dendritic cells in the skin inhibits the early anti-*Leishmania* response. *PLoS Pathog.* (2012) 8:e1002536. doi: 10.1371/journal.ppat.1002536
72. Sousa LMA, Carneiro MBH, Resende ME, Martins LS, dos Santos LM, Vaz LG, et al. Neutrophils have a protective role during early stages of *Leishmania amazonensis* infection in BALB/c mice. *Parasite Immunol.* (2014) 36:13–31. doi: 10.1111/pim.12078
73. Falcão SAC, Weinkopff T, Hurrell BP, Celes FS, Curvelo RP, Prates DB, et al. Exposure to *Leishmania braziliensis* triggers neutrophil activation and apoptosis. *PLoS Negl Trop Dis.* (2015) 9:e0003601. doi: 10.1371/journal.pntd.0003601
74. Hurrell BP, Schuster S, Grün E, Coutaz M, Williams RA, Held W, et al. Rapid sequestration of *Leishmania mexicana* by neutrophils contributes to the development of chronic lesion. *PLoS Pathog.* (2015) 11:e1004929. doi: 10.1371/journal.ppat.1004929
75. Regli IB, Passelli K, Martínez-Salazar B, Amore J, Hurrell BP, Müller AJ, et al. TLR7 sensing by neutrophils is critical for the control of cutaneous leishmaniasis. *Cell Rep.* (2020) 31:107746. doi: 10.1016/j.celrep.2020.107746
76. Kimblin N, Peters N, Debrabant A, Secundino N, Egen J, Lawyer P, et al. Quantification of the infectious dose of *Leishmania major* transmitted to the skin by single sand flies. *Proc Natl Acad Sci USA.* (2008) 105:10125–30. doi: 10.1073/pnas.0802331105
77. Ribeiro-Gomes FL, Roma EH, Carneiro MBH, Doria NA, Sacks DL, Peters NC. Site-dependent recruitment of inflammatory cells determines the effective dose of *Leishmania major*. *Infect Immun.* (2014) 82:2713–27. doi: 10.1128/IAI.01600-13

78. Chaves MM, Lee SH, Kamenyeva O, Ghosh K, Peters NC, Sacks D. The role of dermis resident macrophages and their interaction with neutrophils in the early establishment of *Leishmania major i*nfection transmitted by sand fly bite. *PLoS Pathog.* (2020) 16:e1008674. doi: 10.1371/journal.ppat.1008674
79. van Zandbergen G, Klinger M, Mueller A, Dannenberg S, Gebert A, Solbach W, et al. Cutting edge: neutrophil granulocyte serves as a vector for *Leishmania* entry into macrophages. *J Immunol.* (2004) 173:6521–5. doi: 10.4049/jimmunol.173.11.6521
80. Ritter U, Frischknecht F, van Zandbergen G. Are neutrophils important host cells for *Leishmania* parasites? *Trends Parasitol.* (2009) 25:505–10. doi: 10.1016/j.pt.2009.08.003
81. Peniche AG, Bonilla DL, Palma GI, Melby PC, Travi BL, Osorio EY. A secondary wave of neutrophil infiltration causes necrosis and ulceration in lesions of experimental American cutaneous leishmaniasis. *PLoS ONE.* (2017) 12:e0179084. doi: 10.1371/journal.pone.0179084
82. Charmoy M, Hurrell BP, Romano A, Lee SH, Ribeiro-Gomes F, Riteau N, et al. The Nlrp3 inflammasome, IL-1β, and neutrophil recruitment are required for susceptibility to a nonhealing strain of *Leishmania major* in C57BL/6 mice. *Eur J Immunol.* (2016) 46:897–911. doi: 10.1002/eji.201546015
83. Crosby EJ, Clark M, Novais FO, Wherry EJ, Scott P. Lymphocytic choriomeningitis virus expands a population of NKG2D+CD8+ T cells that exacerbates disease in mice coinfected with *Leishmania major*. *J Immunol.* (2015) 195:3301–10. doi: 10.4049/jimmunol.1500855
84. Hurrell BP, Beaumann M, Heyde S, Regli IB, Müller AJ, Tacchini-Cottier F. Frontline science: *Leishmania mexicana* amastigotes can replicate within neutrophils. *J Leukoc Biol.* (2017) 102:1187–98. doi: 10.1189/jlb.4HI0417-158R
85. Dabiri S, Hayes MM, Meymandi SS, Basiri M, Soleimani F, Mousavi MR. Cytologic features of "dry-type" cutaneous leishmaniasis. *Diagn Cytopathol.* (1998) 19:182–5. doi: 10.1002/(SICI)1097-0339(199809)19:3<182::AID-DC5>3.0.CO;2-F
86. Carlsen ED, Hay C, Henard CA, Popov V, Garg NJ, Soong L. *Leishmania amazonensis* amastigotes trigger neutrophil activation but resist neutrophil microbicidal mechanisms. *Infect Immun.* (2013) 81:3966–74. doi: 10.1128/IAI.00770-13
87. Müller K, van Zandbergen G, Hansen B, Laufs H, Jahnke N, Solbach W, et al. Chemokines, natural killer cells and granulocytes in the early course of *Leishmania major* infection in mice. *Med Microbiol Immunol.* (2001) 190:73–6. doi: 10.1007/s004300100084
88. Jacobs T, Andrä J, Gaworski I, Graefe S, Mellenthin K, Krömer M, et al. Complement C3 is required for the progression of cutaneous lesions and neutrophil attraction in *Leishmania major* infection. *Med Microbiol Immunol.* (2005) 194:143–9. doi: 10.1007/s00430-004-0229-y
89. Uyttenhove C, Marillier RG, Tacchini-Cottier F, Charmoy M, Caspi RR, Damsker JM, et al. Amine-reactive OVA multimers for auto-vaccination against cytokines and other mediators: perspectives illustrated for GCP-2 in *L.* major infection. *J Leukoc Biol.* (2011) 89:1001–7. doi: 10.1189/jlb.1210699
90. Lopez Kostka S, Dinges S, Griewank K, Iwakura Y, Udey MC, von Stebut E. IL-17 promotes progression of cutaneous leishmaniasis in susceptible mice. *J Immunol.* (2009) 182:3039–46. doi: 10.4049/jimmunol.0713598
91. Laufs H, Müller K, Fleischer J, Reiling N, Jahnke N, Jensenius JC, et al. Intracellular survival of *Leishmania major* in neutrophil granulocytes after uptake in the absence of Heat-Labile Serum Factors. *Infect Immun.* (2002) 70:826–35. doi: 10.1128/IAI.70.2.826-835.2002
92. Gueirard P, Laplante A, Rondeau C, Milon G, Desjardins M. Trafficking of *Leishmania donovani* promastigotes in non-lytic compartments in neutrophils enables the subsequent transfer of parasites to macrophages. *Cell Microbiol.* (2008) 10:100–11. doi: 10.1111/j.1462-5822.2007.01018.x
93. Guimarães-Costa AB, Nascimento MT, Froment GS, Soares RP, Morgado FN, Conceição-Silva F, et al. *Leishmania amazonensis* promastigotes induce and are killed by neutrophil extracellular traps. *Proc Natl Acad Sci USA.* (2009) 106:6748–53. doi: 10.1073/pnas.0900226106
94. Mollinedo F, Janssen H, de la Iglesia-Vicente J, Villa-Pulgarin JA, Calafat J. Selective fusion of azurophilic granules with *Leishmania*-containing phagosomes in human neutrophils. *J Biol Chem.* (2010) 285:34528–36. doi: 10.1074/jbc.M110.125302
95. Gabriel C, McMaster WR, Girard D, Descoteaux A. *Leishmania donovani* promastigotes evade the antimicrobial activity of neutrophil extracellular traps. *J Immunol.* (2010) 185:4319–27. doi: 10.4049/jimmunol.1000893
96. Guimarães-Costa AB, DeSouza-Vieira TS, Paletta-Silva R, Freitas-Mesquita AL, Meyer-Fernandes JR, Saraiva EM. 3'-nucleotidase/nuclease activity allows *Leishmania* parasites to escape killing by neutrophil extracellular traps. *Infect Immun.* (2014) 82:1732–40. doi: 10.1128/IAI.01232-13
97. Regli IB, Passelli K, Hurrell BP, Tacchini-Cottier F. Survival mechanisms used by some *Leishmania* species to escape neutrophil killing. *Front Immunol.* (2017) 8:1558. doi: 10.3389/fimmu.2017.01558
98. Lima GM, Vallochi AL, Silva UR, Bevilacqua EM, Kiffer MM, Abrahamsohn IA. The role of polymorphonuclear leukocytes in the resistance to cutaneous leishmaniasis. *Immunol Lett.* (1998) 64:145–51. doi: 10.1016/S0165-2478(98)00099-6
99. Ribeiro-Gomes FL, Otero AC, Gomes NA, Moniz-De-Souza MC, Cysne-Finkelstein L, Arnholdt AC, et al. Macrophage interactions with neutrophils regulate *Leishmania major* infection. *J Immunol.* (2004) 172:4454–62. doi: 10.4049/jimmunol.172.7.4454
100. Novais FO, Santiago RC, Báfica A, Khouri R, Afonso L, Borges VM, et al. Neutrophils and macrophages cooperate in host resistance against *Leishmania braziliensis* infection. *J Immunol.* (2009) 183:8088–98. doi: 10.4049/jimmunol.0803720
101. Fleming TJ, Fleming ML, Malek TR. Selective expression of Ly-6G on myeloid lineage cells in mouse bone marrow. RB6-8C5 mAb to granulocyte-differentiation antigen (Gr-1) detects members of the Ly-6 family. *J Immunol.* (1993) 151:2399–408.
102. Lopez AF, Strath M, Sanderson CJ. Differentiation antigens on mouse eosinophils and neutrophils identified by monoclonal antibodies. *Br J Haematol.* (1984) 57:489–94. doi: 10.1111/j.1365-2141.1984.tb02923.x
103. Daley JM, Thomay AA, Connolly MD, Reichner JS, Albina JE. Use of Ly6G-specific monoclonal antibody to deplete neutrophils in mice. *J Leukoc Biol.* (2008) 83:64–70. doi: 10.1189/jlb.0407247
104. Boivin G, Faget J, Ancey PB, Gkasti A, Mussard J, Engblom C, et al. Durable and controlled depletion of neutrophils in mice. *Nat Commun.* (2020) 11:2762. doi: 10.1038/s41467-020-16596-9
105. Carneiro MBH, Roma EH, Ranson AJ, Doria NA, Debrabant A, Sacks DL, et al. NOX2-Derived reactive oxygen species control inflammation during *Leishmania amazonensis* infection by mediating infection-induced neutrophil apoptosis. *J Immunol.* (2018) 200:196–208. doi: 10.4049/jimmunol.1700899
106. Carmo ÉVdS, Katz S, Barbiéri CL. Neutrophils reduce the parasite burden in *Leishmania* (*Leishmania*) *amazonensis*-infected macrophages. *PLoS ONE.* (2010) 5:e13815. doi: 10.1371/journal.pone.0013815
107. Carlsen ED, Jie Z, Liang Y, Henard CA, Hay C, Sun J, et al. Interactions between neutrophils and *Leishmania braziliensis* amastigotes facilitate cell activation and parasite clearance. *J Innate Immun.* (2015) 7:354–63. doi: 10.1159/000373923
108. Smelt SC, Cotterell SE, Engwerda CR, Kaye PM. B cell-deficient mice are highly resistant to *Leishmania donovani* infection, but develop neutrophil-mediated tissue pathology. *J Immunol.* (2000) 164:3681–8. doi: 10.4049/jimmunol.164.7.3681
109. McFarlane E, Perez C, Charmoy M, Allenbach C, Carter KC, Alexander J, et al. Neutrophils contribute to development of a protective immune response during onset of infection with *Leishmania donovani*. *Infect Immun.* (2008) 76:532–41. doi: 10.1128/IAI.01388-07
110. Rousseau D, Demartino S, Ferrua B, François Michiels J, Anjuère F, Fragaki K, et al. *In vivo* involvement of polymorphonuclear neutrophils in *Leishmania infantum* infection. *BMC Microbiol.* (2001) 1:17. doi: 10.1186/1471-2180-1-17
111. Sacramento L, Trevelin SC, Nascimento MS, Lima-Jùnior DS, Costa DL, Almeida RP, et al. Toll-like receptor 9 signaling in dendritic cells regulates neutrophil recruitment to inflammatory foci following *Leishmania infantum* infection. *Infect Immun.* (2015) 83:4604–16. doi: 10.1128/IAI.00975-15
112. Sacramento LA, da Costa JL, de Lima MHF, Sampaio PA, Almeida RP, Cunha FQ, et al. Toll-Like receptor 2 is required for inflammatory process development during *Leishmania infantum* infection. *Front Microbiol.* (2017) 8:262. doi: 10.3389/fmicb.2017.00262

113. Anderson CF, Mendez S, Sacks DL. Nonhealing infection despite Th1 polarization produced by a strain of *Leishmania major* in C57BL/6 mice. *J Immunol.* (2005) 174:2934–41. doi: 10.4049/jimmunol.174.5.2934
114. Pedraza-Zamora CP, Delgado-Domínguez J, Zamora-Chimal J, Becker I. Th17 cells and neutrophils: close collaborators in chronic *Leishmania mexicana* infections leading to disease severity. *Parasite Immunol.* (2017) 39. doi: 10.1111/pim.12420
115. Tavares NM, Araújo-Santos T, Afonso L, Nogueira PM, Lopes UG, Soares RP, et al. Understanding the mechanisms controlling *Leishmania amazonensis* infection *in vitro*: the role of LTB4 derived from human neutrophils. *J Infect Dis.* (2014) 210:656–66. doi: 10.1093/infdis/jiu158
116. Tavares N, Afonso L, Suarez M, Ampuero M, Prates DB, Araújo-Santos T, et al. Degranulating neutrophils promote leukotriene B4 production by infected macrophages to kill *Leishmania amazonensis* parasites. *J Immunol.* (2016) 196:1865–73. doi: 10.4049/jimmunol.1502224
117. Navas A, Vargas DA, Freudzon M, McMahon-Pratt D, Saravia NG, Gómez MA. Chronicity of dermal leishmaniasis caused by *Leishmania panamensis* is associated with parasite-mediated induction of chemokine gene expression. *Infect Immun.* (2014) 82:2872–80. doi: 10.1128/IAI.01133-13
118. Navas A, Fernández O, Gallego-Marín C, Castro MdM, Rosales-Chilama M, Murillo J, et al. Profiles of local and systemic inflammation in the outcome of treatment of human cutaneous leishmaniasis caused by *Leishmania Viannia*. *Infect Immun.* (2020) 88:e00764–19. doi: 10.1128/IAI.00764-19
119. Boaventura VS, Santos CS, Cardoso CR, de Andrade J, Dos Santos WL, Clarêncio J, et al. Human mucosal leishmaniasis: neutrophils infiltrate areas of tissue damage that express high levels of Th17-related cytokines. *Eur J Immunol.* (2010) 40:2830–6. doi: 10.1002/eji.200940115
120. Morgado FN, Nascimento MTC, Saraiva EM, Oliveira-Ribeiro Cd, Madeira MdF, Costa-Santos Md, et al. Are neutrophil extracellular traps playing a role in the parasite control in active american tegumentary leishmaniasis lesions? *PLoS ONE.* (2015) 10:e0133063. doi: 10.1371/journal.pone.0133063
121. Conceição J, Davis R, Carneiro PP, Giudice A, Muniz AC, Wilson ME, et al. Characterization of neutrophil function in human cutaneous leishmaniasis caused by *Leishmania braziliensis*. *PLoS Negl Trop Dis.* (2016) 10:e0004715. doi: 10.1371/journal.pntd.0004715
122. Cardoso T, Bezerra C, Medina LS, Ramasawmy R, Scheriefer A, Bacellar O, et al. *Leishmania braziliensis* isolated from disseminated leishmaniasis patients downmodulate neutrophil function. *Parasite Immunol.* (2019) 41:e12620. doi: 10.1111/pim.12620
123. Yizengaw E, Getahun M, Tajebe F, Cruz Cervera E, Adem E, Mesfin G, et al. Visceral leishmaniasis patients display altered composition and maturity of neutrophils as well as impaired neutrophil effector functions. *Front Immunol.* (2016) 7:517. doi: 10.3389/fimmu.2016.00517
124. Sharma S, Srivastva S, Davis RE, Singh SS, Kumar R, Nylén S, et al. The phenotype of circulating neutrophils during visceral leishmaniasis. *Am J Trop Med Hyg.* (2017) 97:767–70. doi: 10.4269/ajtmh.16-0722
125. Teixeira CR, Santos CDS, Prates DB, Dos Santos RT, Araújo-Santos T, de Souza-Neto SM, et al. *Lutzomyia longipalpis* saliva drives Interleukin-17-induced neutrophil recruitment favoring *Leishmania infantum* infection. *Front Microbiol.* (2018) 9:881. doi: 10.3389/fmicb.2018.00881

Conflict of Interest: The authors declare that the research was conducted in the absence of any commercial or financial relationships that could be construed as a potential conflict of interest.

frontiers in Immunology

ORIGINAL RESEARCH
published: 09 March 2021
doi: 10.3389/fimmu.2021.632667

PD-1 Blockade Modulates Functional Activities of Exhausted-Like T Cell in Patients With Cutaneous Leishmaniasis

Renan Garcia de Moura[1†], Luciana Polaco Covre[1,2†], Carlos Henrique Fantecelle[1], Vitor Alejandro Torres Gajardo[1], Carla Baroni Cunha[1], Lorenzzo Lyrio Stringari[1], Ashton Trey Belew[3,4], Camila Batista Daniel[5], Sandra Ventorin Von Zeidler[5], Carlos Eduardo Tadokoro[6], Herbert Leonel de Matos Guedes[7,8], Raphael Lubiana Zanotti[9], David Mosser[3], Aloisio Falqueto[10], Arne N. Akbar[2] and Daniel Claudio Oliveira Gomes[1,5]*

[1] Núcleo de Doenças Infecciosas, Universidade Federal do Espírito Santo, Vitoria, Brazil, [2] Division of Medicine, University College London, London, United Kingdom, [3] Department of Cell Biology and Molecular Genetics, University of Maryland, College Park, MD, United States, [4] Center for Bioinformatics and Computational Biology, University of Maryland, College Park, MD, United States, [5] Núcleo de Biotecnologia, Universidade Federal do Espírito Santo, Vitoria, Brazil, [6] Universidade Vila Velha, Vila Velha, Brazil, [7] Instituto de Biofísica Carlos Chagas Filho, Universidade Federal do Rio de Janeiro, Rio de Janeiro, Brazil, [8] Instituto Oswaldo Cruz, Fundação Oswaldo Cruz, Rio de Janeiro, Brazil, [9] Secretaria Estadual de Saúde do Espírito Santo-SESA, Vitoria, Brazil, [10] Departamento de Medicina Social, Universidade Federal do Espírito Santo, Vitoria, Brazil

Patients infected by *Leishmania braziliensis* develop debilitating skin lesions. The role of inhibitory checkpoint receptors (ICRs) that induce T cell exhaustion during this disease is not known. Transcriptional profiling identified increased expression of ICRs including PD-1, PDL-1, PDL-2, TIM-3, and CTLA-4 in skin lesions of patients that was confirmed by immunohistology where there was increased expression of PD-1, TIM-3, and CTLA-4 in both $CD4^+$ and $CD8^+$ T cell subsets. Moreover, PDL-1/PDL-2 ligands were increased on skin macrophages compared to healthy controls. The proportions $PD1^+$, but not TIM-3 or CTLA-4 expressing T cells in the circulation were positively correlated with those in the lesions of the same patients, suggesting that PD-1 may regulate T cell function equally in both compartments. Blocking PD-1 signaling in circulating T cells enhanced their proliferative capacity and IFN-γ production, but not TNF-α secretion in response to *L. braziliensis* recall antigen challenge *in vitro*. While we previously showed a significant correlation between the accumulation of senescent $CD8^+CD45RA^+CD27^-$ T cells in the circulation and skin lesion size in the patients, there was no such correlation between the extent of PD-1 expression by circulating on T cells and the magnitude of skin lesions suggesting that exhausted-like T cells may not contribute to the cutaneous immunopathology. Nevertheless, we identified exhausted-like T cells in both skin lesions and in the blood. Targeting this population by PD-1 blockade may improve T cell function and thus accelerate parasite clearance that would reduce the cutaneous pathology in cutaneous leishmaniasis.

Keywords: cutaneous leishmaniasis, *Leishmania braziliensis*, T cell exhaustion, PD-1, inhibitory checkpoint receptors, senescent T cells, immunosenescence

OPEN ACCESS

Edited by:
Roberta Olmo Pinheiro, Oswaldo Cruz Foundation, Brazil

Reviewed by:
Sara Passos, Federal University of Bahia, Brazil
Braulio Mark Valencia Arroyo, Kirby Institute, Australia

***Correspondence:**
Daniel Claudio Oliveira Gomes
dgomes@ndi.ufes.br

†These authors have contributed equally to this work

Specialty section:
This article was submitted to Microbial Immunology, a section of the journal Frontiers in Immunology

Received: *23 November 2020*
Accepted: *20 January 2021*
Published: *09 March 2021*

Citation:
Garcia de Moura R, Covre LP, Fantecelle CH, Gajardo VAT, Cunha CB, Stringari LL, Belew AT, Daniel CB, Zeidler SVV, Tadokoro CE, de Matos Guedes HL, Zanotti RL, Mosser D, Falqueto A, Akbar AN and Gomes DCO (2021) PD-1 Blockade Modulates Functional Activities of Exhausted-Like T Cell in Patients With Cutaneous Leishmaniasis. Front. Immunol. 12:632667. doi: 10.3389/fimmu.2021.632667

INTRODUCTION

Leishmaniasis is caused by intracellular parasites belonging to *Leishmania* genus and has a global estimated prevalence of 12 million infected people, with 2 million new cases reported annually worldwide (1). *Leishmania braziliensis* is the most prevalent of the cutaneous species in Brazil, causing chronic infections and skin tissue damage associated with a wide spectrum of clinical manifestations (2, 3).

The activity of antigen-specific T cells plays a central role in the clinical outcome of the disease, where nature, characteristics and profile of cytokines produced may influence the healing process or disease progression (4, 5). It is well recognized that interferon gamma (IFN-γ)-producing T cells are essential for mediating the leishmanicidal mechanisms and disease resolution. In contrast, increased production of TNF-α and non-specific cytotoxic mechanisms are linked to skin inflammation and lesion pathology (6, 7). Moreover, the absence of inhibitory mechanisms also has been correlated with tissue damage and severity of CL (8). Therefore, both insufficient and hyperactive non-specific immune responses may lead to pathology and provide avenues for therapeutic intervention.

T cells are subdued to avoid tissue damage during prolonged antigen exposure or chronic inflammation, progressively losing individual effector capabilities. This is regulated by the expression of inhibitory checkpoint receptors (iCRs) such as programmed death 1 (PD-1), T cell immunoglobulin-3 (TIM-3); Cytotoxic T-lymphocyte-associated protein 4 (CTLA-4); Lymphocyte activation gene-3 (LAG-3); and T cell immunoglobulin and ITIM domain (TIGIT) (9–11).

Evidence has highlighted a potentially deleterious role of IRCs during leishmania parasite infection (12–17). In this scenario, both CTLA-4 and PD-1 are highly expressed by $CD8^+$ T cells from patients with visceral (13, 18) and diffuse cutaneous leishmaniasis (19). Similar, exhausted T cells expressing PD-1, TIM-3, 2B4, and CTLA-4 receptors are found on post-Kala-azar dermal (PKDL) and cutaneous leishmaniasis caused by *L. panamensis*, linked with the severity of the diseases (16, 20). In complement to these studies, the ICR blockade, particularly PD-1, has shown promise for augmenting specific T cell immunity in chronic inflammatory state, infectious diseases and cancer (9, 21–24). Although this may inadvertently exacerbate deleterious pro-inflammatory responses, it may also improve specific IFN-γ-dependent immunity (25). It has been noted that blocking ICR may limit exaggerated pro-inflammatory responses (26) which may be very relevant in the context of cutaneous leishmaniasis. This is supported by data from mice and dogs showing that PD-1 blockade and its ligands reduce the parasite burden, restores T cell proliferation and IFN-γ production (14, 17, 18, 27, 28). Furthermore, the expression of inhibitory checkpoint receptors decreases in VL cured patients (13). This suggests a potentially deleterious role of ICRs during infection that is poorly understood in the context of cutaneous leishmaniasis.

In this study, we identified the lesional transcriptomic signature and expression pattern of ICRs on circulating and skin lesional T cells during infection by *L. braziliensis*. We hypothesized that that PD-1 blockade could re-establish the functional activity of Ag-specific exhausted T cells to promote anti-*Leishmania* immunity. We found that exhausted T cells are widely distributed in both blood and lesional skin compartments during CL and that their function is inhibited by the PD-1 receptor. Moreover, the number of circulating PD-1 expressing T cells does not correlate with skin lesion size, suggesting that they are not involved in the disease pathology.

Overall the data present here suggests that exhausted cells co-exist with senescent T cells in the circulation and skin of patients with cutaneous leishmaniasis. While senescent T cells but not exhausted populations may contribute to the skin lesions, the exhausted population contributes to decreased immunity to the pathogen. The inhibition of PD-1 signaling may improve the immune response to the parasite in these patients.

MATERIALS AND METHODS

Study Subjects

Peripheral blood from 15 untreated patients with cutaneous leishmaniasis (CL) attended at the University Hospital (HUCAM) of Universidade Federal do Espírito Santo, Brazil, were investigated in this study. They consisted of eight males and seven females with illness duration ranging from 30 to 120 days, lesion sizes ranging from 200–550 mm^2 and age of 37 ± 13.6 years. The diagnosis of CL was based on clinical and laboratory criteria and all patients in this study tested positive for the PCR/restriction fragment length polymorphism of *L. braziliensis* and reported no prior infections or treatments. The control group (HC) consisted of 15 healthy age (41.4 ± 11.9) and gender-matched individuals with no history of leishmaniasis. All participants (patients and healthy volunteers) had seronegative testing for HIV, HBV and HCV infections, and had no history of chemotherapy, radiotherapy or treatment with immunosuppressive medications within the last 6 months. The patient and control samples were obtained before the COVID-19 outbreak. Patients provided written informed consent, and study procedures were performed in accordance with the principles of the Declaration of Helsinki. This study was registered at HUCAM ethical committee reference number 735.274.

PBMC Isolation, Cell Sorting, and Culture

PBMC from HC and CL patients were isolated by centrifuging whole blood through a Ficoll-Hypaque (GE Healthcare) gradient followed by hemocytometry to determine the absolute number of viable then cryopreserved. Cells from both controls and patients were thawed in RPMI complete medium supplemented with 10% of fetal calf serum. Viability and recovery were measured using trypan blue dye exclusion.

Flow Cytometric Analysis

For phenotypic and functional analysis, at least 10^6 cells were stained washed and subsequently stained at 4°C for 20 min with the combination of surface antibodies. For intracellular analysis of cytokine secretion, cells were cultured at 37°C in the presence of monensin (used according to the manufacturer's indication, BioLegend) and brefeldin A (5 mg/ml) (Sigma-Aldrich), added for the last 6 and 4 h of stimulation, respectively. Then, cells were

fixed and permeabilized using the Cytofix/Cytoperm kit (BD Pharmingen), stained with NIR viability stain (Invitrogen) followed by cytokine intracellular antibodies on ice for 30 min. Data from 50.000 events obtained within $CD3^+$ cells were acquired in a Fortessa X-20 cytometer (BD Biosciences) and analysed using FlowJo software (Treestar). ICRs gates were based on pooled fluorescence minus one control samples and applied identically across all samples. Gate strategy and used antibodies are described in the **Supplementary Figure 1** and **Table 1**, respectively.

PD-1 Blockade

PBMCs were thawed, resuspended in complete media and incubated overnight at 37°C. The following day, cells were incubated with 10 μg/ml each of anti-PD-L1 (29E.2A3.C6) and anti-PD-L2 (24F.10C12.G12, both from Biolegend) antibodies as described previously (24) prior cell activation with anti-CD3 (OKT3, 0.5 μg/ml, Biolegend) or *L. braziliensis* promastigote antigens (LbAg, 10 μg/ml). After activation, cells were culture for 72 h. 10 μg/ml each of IgG2a (Mg2a-53) and IgG2b (MPC-11) isotype controls (Abcam) were used as control.

Cytokine Determination

Cell culture were stimulated with 10 μg/ml of *L. braziliensis* promastigote antigens (LbAg) or 0.5 μg/ml plate-coated anti-CD3 (OKT3) and 5 ng/ml rhIL-2, with or without anti-PDL1/2 or isotype control antibodies. Culture supernatants were collected at 72h for the measurement of IFN-γ, TNF-α, and IL-10 by Cytokine Bead Array (CBA) (BD Biosciences) according to the manufacturer's protocol.

Proliferation Assay

Stimulated PBMC were cultured in the presence of PD-1 blocking or isotype control antibodies and rhIL-2 for 72 h as previously described (24). The proliferation was accessed by intracellular staining for the cell cycle related nuclear antigen Ki67 Alexa Fluor 647 (BD Bioscience) that was performed with Foxp3 Staining Buffer Set (Miltenyi Biotec) and analyzed by flow cytometric analysis.

RNA-Seq Analysis

The RNA-Seq data was obtained from a previous study (29), which is available at the Sequence Read Archive (www.ncbi.nlm.nih.gov). Data as accessed through project accession reference #PRJNA307599, where paired-end reads (100 bp) were obtained through Illumina HiSeq 1500 platform. Samples analysed consisted of skin biopsies from uninfected controls (from endemic areas) (n= 10) and skin biopsies collected from patients infected with *Leishmania braziliensis* (n= 25). Initially, samples were trimmed using Trimmomatic (v. 0.39) to remove sequence adapters and filter low-quality (threshold of 25) bases at the start or end of reads. Samples were then aligned to the human reference genome (hg38/GRCh38 release 99) obtained from ENSEMBL (https://www.ensembl.org/) using Salmon (v 0.12.0) using the selective alignment option (–validateMappings) and correction for GC content bias (–gcBias). Transcript abundance at the gene-level was then calculated using tximport to obtain the counts table. Non-expressed, weakly expressed and non-protein code genes were removed prior to subsequent analyses, resulting in a count table of 17.668 genes. DESeq2, a package from Bioconductor, was used to define differentially expressed genes (30), considering genes with Benjamini-Hochberg p-adjusted value less than 0.05 as significant. The Variance Stabilizing Transformation (vst), available in the DESeq2 package, was used for visualization and clustering purposes. The function plotPCA, also available on the DESeq2 package, was used for the Principal Component Analysis. The ComplexHeatmap package (31) ggplot2 package (32) were used to generate the heatmap and plots, respectively. The heatmap was constructed to show the relative gene expression, where the vst normalized values were mean-centered across samples.

tSNE Analysis

t-SNE is a non-linear dimensionality reduction method that optimally places cells with similar expression levels near to each other and cells with dissimilar expression levels further apart. Unbiased representations of multi-parameter flow cytometry data were generated using the t-distributed stochastic neighbour embedding (tSNE) algorithm. The R package "Rtsne" available on CRAN (github.com/jkrijthe/Rtsne) was used to perform the Barnes Hut implementation of tSNE on flow cytometry data. FlowJo software was used to export events of interest (in fcs format) for each sample. After using the Bioconductor "flowCore" R package to import.fcs file data and the Logicle transform to scale the data similarly to that displayed in FlowJo. 10,000 events from each sample analyzed in parallel were merged and the relevant fluorescent parameters were used.

Skin Biopsies

Punch biopsies (8 mm in diameter) from the border of lesional skin were obtained from cutaneous leishmaniasis patients. Control skin punch biopsy specimens from healthy volunteers were also obtained. Biopsy specimens were frozen in OCT compound (Sakura, Alphen aan den Riji, The Netherlands). Six-micrometer sections were longitudinally sectioned to expose all skin layers and placed in poly-L-lysine coated slides (Star Frost®). Tissues were then fixed in acetone and ethanol and stored in -80°C until use.

Immunohistochemistry

Frozen sections from HC skin and CL lesions were blocked with 1% bovine serum albumin (BSA) solution and incubated with primary antibodies (described in **Supplementary Table 1**). Staining was detected using Novolink™ Polymer Detection System Kit (Leica, RE7150-K) according to the manufacturer instructions. Slides were then dehydrated with xylol and ethanol and mounted with Entellan® (MERK, 107960).

Immunofluorescence

Immunofluorescence staining was performed using optimal dilutions of primary antibodies for 18 h at 4°C, followed by an appropriate fluorochrome-conjugated secondary antibody (described in **Supplementary Table 1**) incubation and mounting with Flouroshield Mounting Medium with DAPI (ABCAM, ab104139). Three images of the papillary and

reticular dermis were captured at 200x magnification using fluorescence microscopy (Leica DMi8, Wetzlar, Germany). The number of positively stained cells was manually counted using computer-assisted image analysis (National Institutes of Health Image Software ImageJ 1.52j; https://imagej.nih.gov/ij/) and expressed as a percentage.

Statistics

GraphPad Prism (version 7) was used to perform statistical analysis. Data distribution was verified using the Shapiro-Wilk test. Statistical significance was evaluated using the paired Student t-test. Mann-Whitney with Welch correction or Kruskal-Wallis test was performed for all continuous and nonparametric variables. Differences were considered significant when p was <0.05.

RESULTS

Transcriptional Profiling Indicates that Inhibitory Checkpoint Receptors and Ligands Are Enriched in *Leishmania braziliensis* Lesions

First, we analysed RNA-Seq data from a previous study where skin biopsies from uninfected controls were compared to biopsies collected from the border of lesions from patients infected with *Leishmania braziliensis* (29). We investigated transcriptional signatures for inhibitory receptors and their ligands in the skin during the active disease. Transcriptional profiles of skin from lesions were very different from healthy skin from control subjects, as demonstrated by principal component analysis (PCA) (**Figure 1A**). We found 9,955 genes identified as differentially expressed between the two groups that included inhibitory checkpoint receptors and their ligands that were uniquely associated with patient skin lesions (**Figures 1B, C**). Many genes associated with cellular exhaustion were increased in lesional skin and this included PD-1 (28.8 fold), TIM-3 (16.4 fold), CTLA-4 (40.9 fold), PDL-1 (32.0 fold), and PDL-2 (13.8 fold) (**Figures 1C, D**).

Extensive Inflammatory Infiltrate with Increased Expression of Exhaustion-Related Receptors and Ligands in CL Lesions

The expression of ICRs and senescence-associated receptors have been associated with several cell populations in inflammatory and non-inflammatory contexts. We next evaluated the expression of PD-1 and their ligands as well as TIM-3, CTLA-4, CD57, and KLRG1 (Killer cell lectin-like receptor G1) expression on lesional site. Histopathological analysis by H&E staining showed epidermal hyperplasia with a dense and diffuse inflammatory cell infiltrate involving the junction of the epidermis and dermis up to hypodermis, consisting mainly of lymphocytes, macrophages and plasma cells (**Figures 2A, B**). Immunohistochemical analysis revealed that this intense cell infiltration had increased expression of PD-1, TIM-3, and CTLA-4 compared to control skin (**Figures 2C–H**), supporting the RNAseq data. We also found that both $CD4^+$ and $CD8^+$ T cells were increased in the lesional inflammatory infiltrates compared to control skin (**Supplementary Figure 2A**). Furthermore, significantly greater proportions of these cells in the skin lesions of CL patients expressed PD-1, TIM-3, CTLA-4, CD57 and KLRG1 compared to the skin of healthy controls (**Figures 2I–R** and **Supplementary Figure 2B**). Moreover, there was increased expression of both PD-1 ligands (PDL-1 and PDL-2) (**Figures 2S–V**) that was found on lesional macrophages ($CD68^+$) (**Figures 2W–Y** and **Supplementary Figure 2C**) and also neutrophils and fibroblasts (data not shown).

Circulating T Cells of CL Patients Express Elevated Levels of Immune Checkpoint Receptors

Circulating T cells are recruited to the skin during CL (33, 34). We next investigated the heterogeneity of ICRs on circulating T cell compartments. Both $CD4^+$ and $CD8^+$ T cells from CL patients exhibited elevated frequencies of cells that expressed PD-1, TIM-3, and CTLA-4 individually or combined (**Figures 3A, B**). We confirmed this by the tSNE algorithm that arbitrarily identified two different clusters of healthy control (Green) and cutaneous leishmaniasis patients (Red) groups (**Figure 3C**). In addition, the expression intensities and distribution of markers in each cluster were remarkably associated with both $CD4^+$ and $CD8^+$ T cells in CL patients.

Taken together these data suggest that T cells of CL patients have increased expression of ICRs that is not observed in healthy individuals. Thus, we next investigated whether there was an association between the level of individual ICRS on T cells in the circulation and in the skin lesions in individuals. We found a strong correlation between PD-1 expression in both compartments that was not observed with either TIM-3 or CTLA-4 (**Figures 3D, E**). This suggested that PD-1 may regulate T cell activity in both tissue compartments of CL patients to the same extent.

Blocking PD-1 Enhances Leishmania-Specific Functions of T Cells from CL Patients

PD-1- expressing T cells from CL patients are less responsive to both polyclonal and Ag-specific stimulation. We next investigated whether blockade of PD-1 signaling of circulating $CD4^+$ and $CD8^+$ T cells from CL patients, using antibodies to its ligands PDL-1 and PDL-2 blockade could enhance specific T cell functions linked to a leishmanicidal response after stimulation with *L. braziliensis* antigen (LbAg). The addition of anti- PDL1/2 significantly enhanced the proliferative capacity of $CD4^+$ and $CD8^+$ T cells, compared to cells that were activated in the absences of the blocking antibodies (**Figures 4A, B**). We also performed the same blocking experiment by stimulating T cells from both groups (HC and CL) with anti-CD3 and confirmed that blocking PD-1 signaling enhanced the proliferative capacity of T circulating cells from CL patients (**Supplementary Figure 3**).

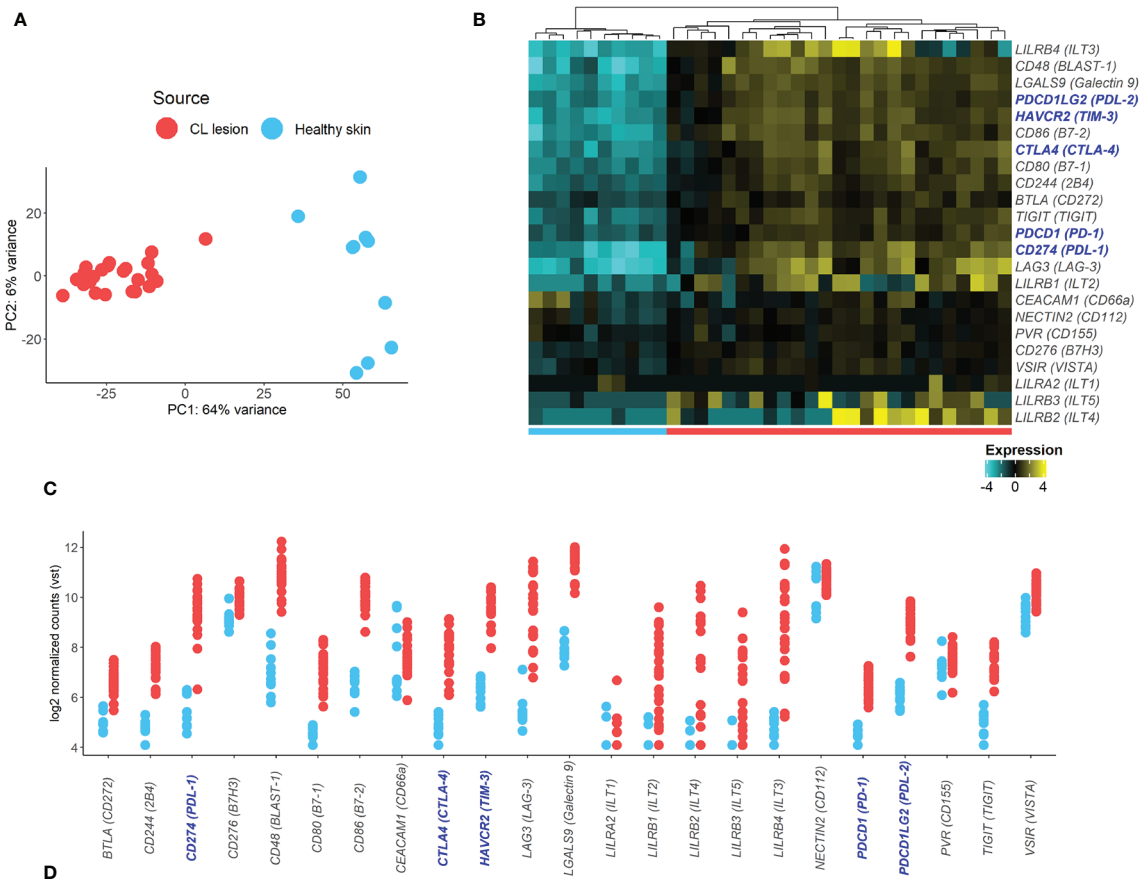

D

Gene Symbol	Gene Name	log2 fold change*	p value	Adjusted p value*
BTLA	CD272	3,26	4,13E-25	8,90E-24
CD244	2B4	4,36	7,28E-42	3,88E-40
CD274	PDL-1	5,00	5,69E-42	3,05E-40
CD276	B7H3	0,87	5,23E-10	3,13E-09
CD48	BLAST-1	4,12	6,52E-47	4,48E-45
CD80	B7-1	6,40	7,03E-37	2,91E-35
CD86	B7-2	4,02	7,43E-84	5,05E-81
CEACAM1	CD66a	-0,55	1,69E-01	2,38E-01
CTLA4	CTLA-4	5,36	7,37E-43	4,20E-41
HAVCR2	TIM-3	4,04	4,42E-67	8,30E-65
LAG3	LAG-3	5,61	4,42E-33	1,51E-31
LGALS9	Galectin 9	3,68	4,48E-103	7,91E-100
LILRA2	ILT1	-1,93	3,41E-01	4,29E-01
LILRB1	ILT2	6,46	2,96E-14	2,71E-13
LILRB2	ILT4	7,98	1,52E-09	8,61E-09
LILRB3	ILT5	6,57	4,76E-07	1,96E-06
LILRB4	ILT3	6,89	1,59E-28	4,22E-27
NECTIN2	CD112	0,45	2,77E-02	4,93E-02
PDCD1	PD-1	4,85	6,76E-32	2,16E-30
PDCD1LG2	PDL-2	3,79	1,05E-74	3,56E-72
PVR	CD155	0,38	7,21E-02	1,14E-01
TIGIT	TIGIT	4,03	6,85E-39	3,17E-37
VSIR	VISTA	0,95	1,39E-08	7,01E-08

* log2 fold changes of CL patients in comparison with controls
** Adjusted p-value (Benjamini-Hochberg method).

FIGURE 1 | Identification of inhibitory checkpoint receptors gene expression signatures in CL lesions. **(A)** Principal components analysis showing principal component 1 (PC1) with variance of 64% and PC2 with variance of 6% of human transcriptome from 10 healthy volunteers (blue circle) and 25 CL patients (red circle). **(B)** Heatmap of exhaustion receptors and ligands genes expression. Columns represent individual healthy controls and CL patients and rows represent individual genes, colored to indicate relative expression levels (genes were mean centered across samples). **(C)** Plots showing expression of receptors [*PDCD1* (PD-1), *HAVCR2* (TIM-3), *CTLA4* (CTLA-4), *LAG3* (LAG-3), *TIGIT*, *CD244* (2B4), *NECTIN2* (CD112), *CD48* (BLAST-1), *PVR* (CD155), *TNFRSF14* (HVEM), *CD276* (B7H3), *CEACAM1* (CD66a), *LILRA2* (ILT1), *LILRB1* (ILT2), *LILRB4* (ILT3), *LILRB2* (ILT4), *LILRB3* (ILT5), *VSIR* (VISTA)] and ligands [*CD274* (PDL-1), *PDCD1LG2* (PDL-2), *CD80* (B7-1), *CD86* (B7-2), *LGALS9* (Galectin 9), *BTLA* (CD272), *VSIR* (VISTA)] in healthy skin (blue) and CL lesions (*red*). **(D)** Table with fold change and *p*-values of the analysed inhibitory checkpoint receptors lesional gene expression.

We next investigated whether blocking PD-1 signaling affected cytokine production of CL patients after LbAg stimulation. We found that after blockade, the frequency of both IFN-γ TNF-α producing cells were significantly increased in $CD4^+$ and $CD8^+$ T cell compartments (**Figures 4C, D**). Interestingly, analysis of these cytokines in supernatants of cultures after LbAg stimulation in the presence or absence of PD-1 blockade demonstrated that only levels of IFN-γ

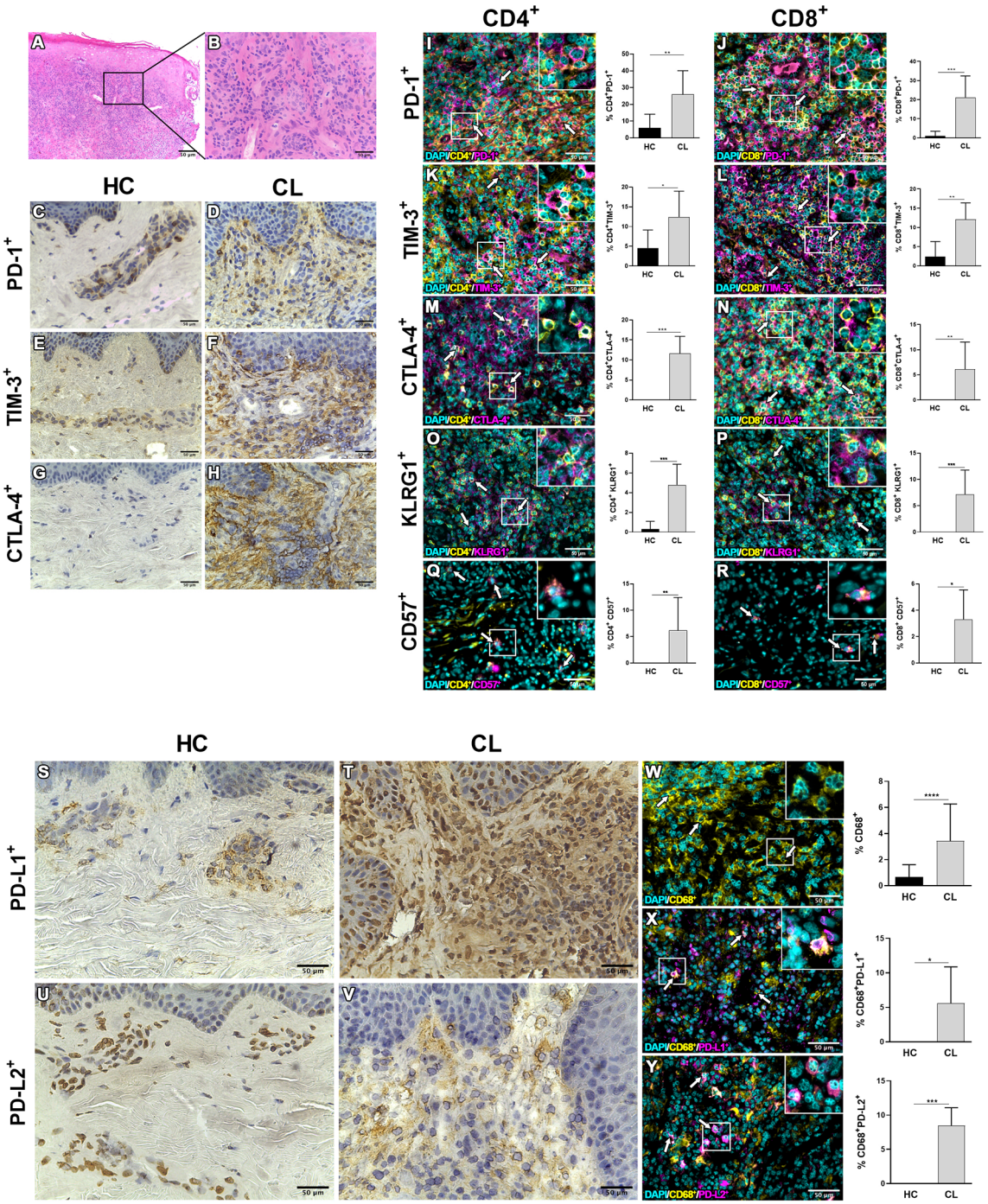

FIGURE 2 | Inhibitory molecules and senescent-associated receptors are enriched in lesional skin during cutaneous leishmaniasis. **(A)** Representative hematoxylin and eosin staining of cutaneous leishmaniasis lesion with **(B)** dense inflammatory infiltrate. Immunohistochemistry staining (in brown) in healthy skin and CL lesions for PD-1 **(C, D)**, TIM-3 **(E, F)**, CTLA-4 **(G, H)**, PD-L1 **(S, T)**, and PD-L2 **(U, V)**. Immunofluorescence staining and cumulative data of the inhibitory checkpoint receptors PD-1, TIM-3, CTLA-4, and the senescence markers KLRG1 and CD57 expressed on $CD4^+$ **(I, K, M, O, Q)** and $CD8^+$ **(J, L, N, P, R)** cells from healthy controls (n = 8) and CL patients (n = 10). **(W–Y)** Representative staining and cumulative data of the expression of the inhibitory ligands PDL-1 or PDL-2 on dermal macrophages ($CD68^+$) in healthy (n = 7) and lesional skin (n = 8). The white arrows indicate double-stained cells. The graphs show the mean ± SD. The p-values were calculated using Student's t test with Welch's correction or Mann-Whitney U-test. $^*p < 0.05$, $^{**}p < 0.01$, $^{***}p < 0.001$, $^{****}p < 0.0001$.

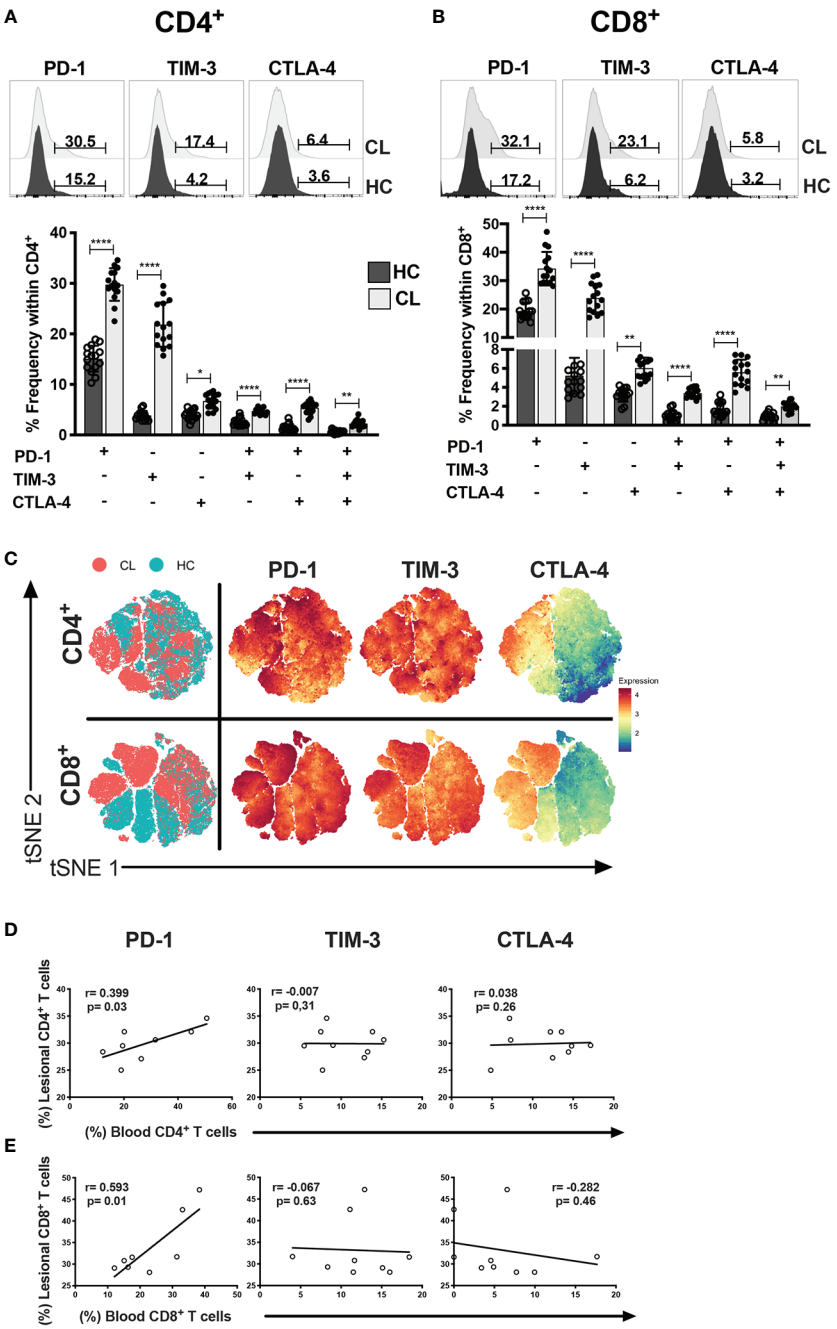

FIGURE 3 | CL patients have multiple and single exhaustion receptor expression on circulating T cells. Representative histograms and cumulative data of percentage of PD-1, TIM-3 and CTLA-4 in CD4+ **(A)** and CD8+ **(B)** T cells isolated from healthy control- HC (n = 15) or patients with active cutaneous leishmaniasis-CL (n = 15). **(C)** tSNE performed gating on CD4+ and CD8+ cells from HC (blue dots) and CL (red dots) groups. The level of expression of PD-1, TIM-3, and CTLA-4 were evaluated separately on live cells generating the expression levels of the hierarchical clusters, represented in red for high expression, whereas blue represents low expression (cold-to-hot heat map). Scatterplot showing the Spearman's correlation test relationship between frequencies of lesional and circulating **(D)** CD4+ and **(E)** CD8+ T cells expressing PD-1, TIM-3, or CTLA-4 (n = 10). The graphs show the mean with 95% of confidence. The p-values were calculated using Mann-Whitney test. *$p < 0.05$, **$p < 0.01$, ****$p < 0.0001$.

production was significantly enhanced (**Figure 4E**). We also did not observe any effect of PD-1 blockade on the production of IL-10 in the same experiments (**Figure 4E**). The dominant cytokine response after PD-1 blockade was the enhancement of IFN-γ production and the ratio of IFN-γ to TNF-α and IFN-γ to IL-10 were both increased significantly (**Figure 4F**). As IFN-γ production has a role in protective immune responses while TNF-α secretion has an immunopathogenic consequences in

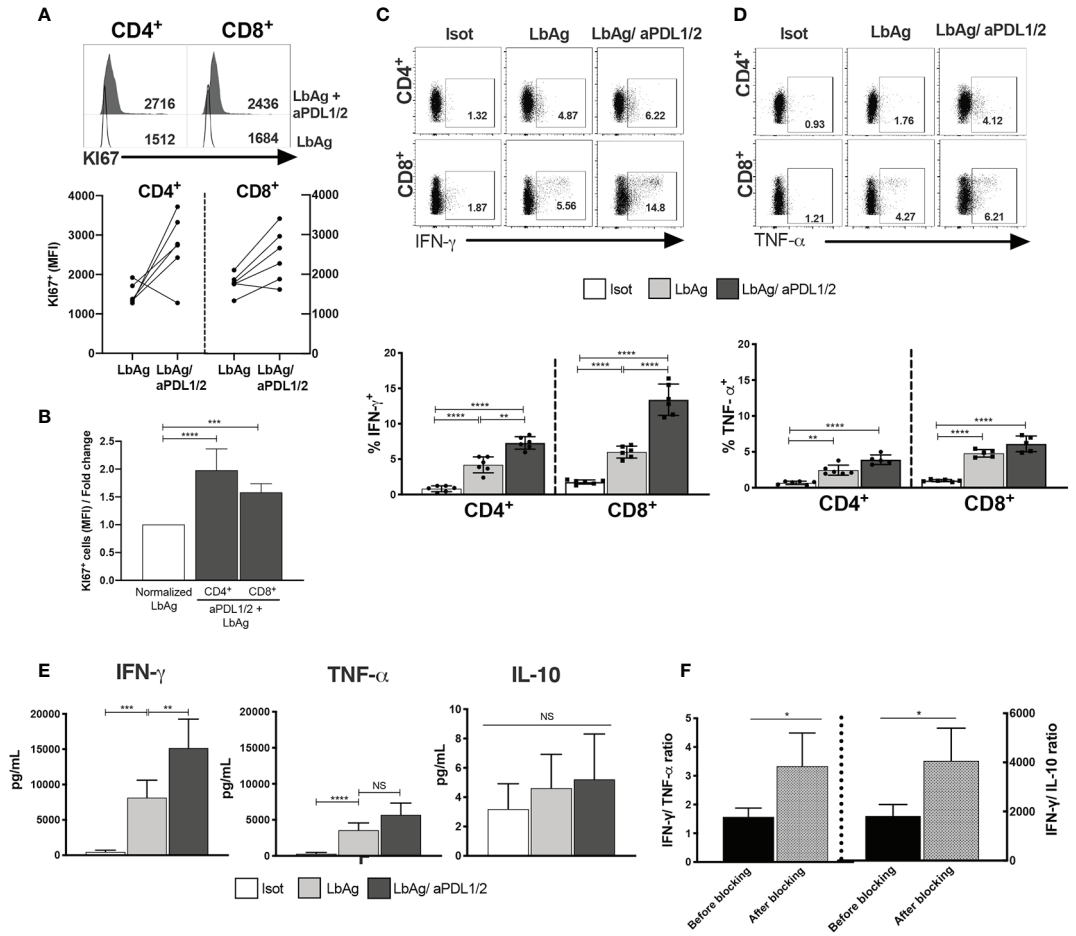

FIGURE 4 | Proliferative and pro-inflammatory cytokines are increased by blocking PD-1 pathway in CL CD4$^+$ and CD8$^+$ T cells. **(A)** Representative histograms and pooled data showing Ki67 staining on CD4$^+$ and CD8$^+$ T cells from PBMC measured by flow cytometry after 72 h stimulation with 10 μg/ml of *L. braziliensis* promastigote antigens (LbAg). The cell cultures ware performed in the presence of 10 μg/ml anti-PDL1/2 antibodies. In control cultures, 10 μg/mL IgG2a, IgG2b were added (n= 6). **(B)** fold change of quantitative fluorescence intensity levels normalized with CD4$^+$/CD8$^+$ T cells stimulated with LbAg. **(C, D)** Representative dotplots and pooled data of frequencies of IFN-γ and TNF-α within CD4$^+$ and CD8$^+$ T cells after activation in the presence of PD-1 blocker. **(E)** Production of IFN-γ, TNF-α and IL-10 determined in the culture supernatants by CBA after activation with LbAg in the presence of PD-1 blockade. **(F)** Ratio between Ag-specific cytokines production before and after PD1 blockade. The graphs show the mean ± SEM. The p-values were calculated using Mann-Whitney test. *$p < 0.05$, **$p < 0.01$, ***$p < 0.001$, ****$p < 0.0001$, NS, not statistically significant.

this disease (5), the inhibition of PD-1 signaling would shift cytokine production towards immune protection in CL.

PD-1 Expressing Cells Do Not Correlate with Lesion Size of CL Patients

We showed previously that the size of skin lesions in CL correlated with the proportion of senescent CD8$^+$CD45RA$^+$CD27$^-$ T cells in the circulation (34). We therefore investigated whether PD-1 expressing CD8$^+$ T cells in peripheral blood were also associated with the cutaneous pathology in the patients. The relative expression of CD45RA and CD27 defined 4 different subsets of CD8$^+$ T cells in both healthy controls and CL patients (**Figure 5A**). We investigated PD-1 expression within each of the 4 subsets and showed that PD-1 was significantly increased in all these population compared to healthy controls (**Figure 5B**). However, in both patients and controls, the senescent (CD45RA$^+$CD27$^-$) population expressed significantly less PD-1 compared to central memory (CM) or effector memory (EM) CD8$^+$ T cells (**Figure 5B** bottom panel). In addition, we found increased frequencies of CM and EM subsets, but not senescent cells expressing PD-1 and CLA (**Figure 5C**). This suggest that a proportion of PD-1$^+$ cells in the skin (**Figure 2**) may be derived from circulating populations. The proportions of total circulating CD4$^+$PD1$^+$ (data not shown) and CD8$^+$PD1$^+$ T cells and their subsets do not correlate with lesion size (**Figure 5D**). This suggests that despite the accumulation of PD1-expressing T cells in the circulation and in the skin, these cells may not be associated with the skin pathology that occurs in patients.

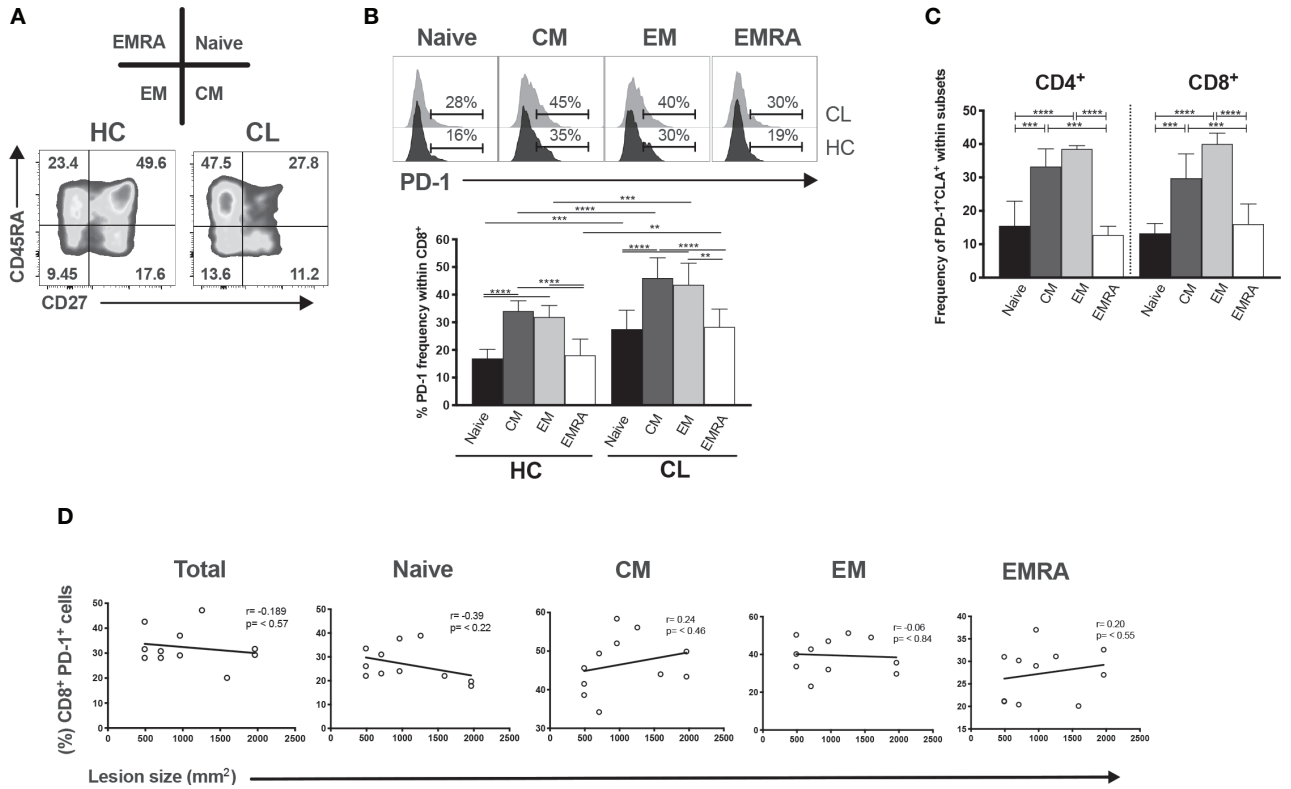

FIGURE 5 | PD-1 expression is increased in differentiated CD8+ T cells but not correlated with lesion size of CL patients. **(A)** Representative plots of CD8+ T cells subsets isolated from HC and characterized by expressing CD45RA and CD27 markers (naïve-CD45RA+ CD27+; CM-central memory, CD45RA- CD27+; EM-effector memory, CD45RA-CD27-; and EMRA-effector memory T cells that re-express CD45RA, CD45RA+ CD27-). **(B)** Representative histogram and cumulative data of the ex vivo PD-1 frequencies within CD8+ subsets. **(C)** Pearson's correlation test between frequencies of CD8+PD1+ T subsets (Naïve, CM, EM, and EMRA) and lesions size (mm^2) of CL patients. **(D)** Cumulative data of the ex vivo PD1+ CLA+ within CD4+ and CD8+ subsets. The graphs show the mean ± SEM. The p-values were calculated using Mann-Whitney test. *$p < 0.05$, **$p < 0.01$, ***$p < 0.001$, ****$p < 0.0001$.

DISCUSSION

Immune checkpoint receptors regulate the magnitude of immune responses to protect against collateral tissue damage during immune responses to infection and to maintain peripheral self-tolerance. However their expression in chronic infection is associated with T cell exhaustion and pathogens persistence.

Here we identified a unique transcriptomic signature and expression pattern of these receptors on circulating and lesional T cells in patients with CL during infection by *L. braziliensis*. Previous studies have shown increased frequencies of ICRs on T cells during cutaneous leishmaniasis caused by *L. mexicana* (19) and *L. guyanensis* (16). Similarly, the increased expression of PD-1, PDL1 in patients with diffuse cutaneous leishmaniasis (DCL) or post-Kala-azar dermal leishmaniasis have been linked with a pronounced non-responsiveness of CTLs, diseases progression and parasite evasion (19, 20, 35). Conversely, it is well-recognized that CL late lesions contain few parasites, so the expression of ICRs as a mechanism that reduces immune activity and maintain parasite survival does not apply to *L. braziliensis* infection. Alternatively, it is possible that the chronic inflammatory state in the skin lesions promotes the expression of ICRs. This hypothesis is supported by accumulation of ICR expressing T cells during chronic inflammatory diseases such as Crohn's, ulcerative colitis and rheumatoid arthritis, mainly maintained by TNF-α, IFN-γ, and IL-6, that are also seen in CL lesions (7, 8). In support of this, ICR- expressing cells have great ability to release a variety of inflammatory cytokines and mediate cytotoxicity, contributing to the progression of deleterious clinical outcomes (36–39). Therefore, the progression of tissue damage in leishmania infection would happen regardless of the ICRs expression.

CTLA-4 and PD-1 inhibit T cell function during *Leishmania* parasite infection (13, 16, 18, 20). Interestingly, the inhibition of PD-1 or CTLA-4 signaling on T cells is accompanied by an increase in proliferation and IFN-γ secretion that is correlated to better clinical status (14, 17, 18). Therefore, blocking ICRs could contribute to enhancing immunity against *L. braziliensis*. In our experiments the treatment with PD-1 blockade restored the proliferative capacity of T cells and preferentially augmented IFN-γ relative to TNF-α secretion in both $CD4^+$ T and $CD8^+$ T cell populations. While IFN-γ has been shown to have a protective role in CL, TNF-α secretion may promote pathology

in the skin (33, 40, 41). Previous studies have shown that the control of inflammatory potential by blocking TNF-α *in vitro* or during antimonial therapy for CL *in vivo* are able to promote faster healing of lesions and higher cure rates than patients with anti-*Leishmania* treatment alone (42, 43). From our results we predict that this skewing of cytokine production may induce protective and non-pathogenic immunity since PD-1 blockade of $CD8^+$ T cells does not exacerbate TNF-α secretion but instead induces protective IFN-γ based immune responses. Nevertheless, it will be important to ensure that checkpoint inhibitor inhibition does not inadvertently activate other inflammatory immune cells leading the exacerbation of CL

Our data also suggests for the first time the co-existence of senescent T cells and ICR-expressing (exhausted) T cells in the patients with CL. While the presence of senescent $CD45RA^+CD27^-$ (TEMRA) $CD8^+$T cells in the circulation express CLA and are closely associated with skin lesion size (33), PD-1 expressing $CD8^+$ T cells can also home to the skin but are not associated with lesion size. Senescent $CD8^+$ T cells do not express high levels of PD-1 reinforcing the possibility that senescent and exhausted CD8+ T cells are distinct populations, as suggested previously (24).

Overall, the present study extends the understanding of local and systemic inhibitory checkpoint receptors expression patterns that occur in the context of *L. braziliensis* infection. Moreover, our data provide information about the compartmentalization of exhausted and senescent T cells in the blood and skin lesions of CL patients and provide a new rationale for therapeutic intervention against *Leishmania* infection.

DATA AVAILABILITY STATEMENT

The RNA-Seq datasets used in this study can be found in the online repository Sequence Read Archive (www.ncbi.nlm.nih.gov) through the project accession number PRJNA307599.

ETHICS STATEMENT

The studies involving human participants were reviewed and approved by the Research and Ethics Committee of the Federal University of Espírito Santo, under reference number 735.274. The patients/participants provided their written informed consent to participate in this study.

AUTHOR CONTRIBUTIONS

LC, RG, CD, HM, SZ, VG, CC, and LS performed experiments. LC, DG, RG, CT, AB, and CF analyzed data. AF and RZ selected the patients. DG, AA, DM, and AF designed the project and discussed data. DG, AA, RG, LC, CF, and DM wrote the manuscript with the support from all other co-authors. All authors contributed to the article and approved the submitted version.

FUNDING

This work was financially supported by the Fundação de Amparo a Pesquisa do Espírito Santo- FAPES/Newton Fund and Medical Research Council (Grant 72939273/16); the Fundação de Amparo a Pesquisa do Espírito Santo- FAPES (Grant 90/2017); the Fundação de Amparo a Pesquisa do Espírito Santo-FAPES/Ministério da Saúde (Grant 83152997/2018); and the Coordination for the Improvement of Higher Education Personnel - CAPES- Brazil and Medical Research Council (UK) (Grant MR/T015853/1).

ACKNOWLEDGMENTS

Authors would like to thank the Laboratório de Histologia Molecular e Imuno-histoquímica- UFES for technical support and facilities use; and MSc. Hugh Trahair and Dr. Sian Henson for technical support.

SUPPLEMENTARY MATERIAL

The Supplementary Material for this article can be found online at: https://www.frontiersin.org/articles/10.3389/fimmu.2021.632667/full#supplementary-material

Supplementary Figure 1 | Representative gate strategy from healthy control donors and patients with cutaneous leishmaniasis.

Supplementary Figure 2 | (A) Representative immunofluorescence staining and frequency of $CD4^+$ and $CD8^+$ cells (yellow) in healthy ($n = 7$) and lesional skin ($n = 8$). **(B)** Representative healthy skin sections stained for PD-1, TIM-3, CTLA-4, KLRG1 and CD57 (magenta) expression on $CD4^+$ and $CD8^+$ cells, and **(C)** PD-L1 and PD-L2 (magenta) on dermal macrophages ($CD68^+$) (yellow). Nuclei (cyan) were stained with DAPI (ABCAM, ab104139). The graphs show the mean ± SD. The *p*-values were calculated using Kruskal-Wallis test. $^{****}p < 0.0001$.

Supplementary Figure 3 | Combined data showing Ki67 staining on $CD4^+$ and $CD8^+$ T cells from PBMC of heathy control donors (HC) and cutaneous leishmanisis patients (CL) measured by flow cytometry after 72 h stimulation with 0.5 μg/ml of anti-CD3. The cell culture was performed in the presence of 10 μg/mL anti-PDL1/2 antibodies. In control cultures, 10 μg/mL IgG2a, IgG2b were added. The *p*-values were calculated using Student's *t* test with Welch's correction or Mann-Whitney U-test. $^{**}p < 0.01$, $^{***}p < 0.001$, $^{****}p < 0.0001$.

Supplementary Table 1 | List of antibodies used for immunofluorescence, Immunohistochemistry and flow cytometry.

REFERENCES

1. World Health Organization. OMS | Leishmaniasis. In: *WHO*, vol. 375. (2015). Available at: http://whqlibdoc.who.int/trs/WHO_TRS_949_eng.pdf.
2. Ribeiro-Romao RP, Moreira OC, Osorio EY, Cysne-Finkelstein L, Gomes-Silva A, Valverde JG, et al. Comparative Evaluation of Lesion Development, Tissue Damage, and Cytokine Expression in Golden Hamsters (Mesocricetus auratus) Infected by Inocula with Different Leishmania (Viannia) braziliensis Concentrations. *Infect Immun* (2014) 82:5203–13. doi: 10.1128/IAI.02083-14
3. Costa JML, Saldanha ACR, Nasciento D, Sampaio G, Carneiro F, Lisboa E, et al. Clinical modalities, diagnosis and therapeutic approach of tegumentary leishmaniasis in Brazil. *Gaz Med Da Bahia* (2009) 143:70–83.

4. Carvalho LP, Passos S, Schriefer A, Carvalho EM. Protective and pathologic immune responses in human tegumentary leishmaniasis. *Front Immunol* (2012) 3:301. doi: 10.3389/fimmu.2012.00301
5. Scott P, Novais FO. Cutaneous leishmaniasis: immune responses in protection and pathogenesis. *Nat Rev Immunol* (2016) 16:581–92. doi: 10.1038/nri.2016.72
6. Faria DR, Souza PEA, Durães FV, Carvalho EM, Gollob KJ, Machado PR, et al. Recruitment of CD8(+) T cells expressing granzyme A is associated with lesion progression in human cutaneous leishmaniasis. *Parasite Immunol* (2009) 31:432–9. doi: 10.1111/j.1365-3024.2009.01125.x
7. Bacellar O, Lessa H, Schriefer A, Machado P, De Jesus AR, Dutra WO, et al. Up-regulation of Th1-type responses in mucosal leishmaniasis patients. *Infect Immun* (2002) 70:6734–40. doi: 10.1128/IAI.70.12.6734-6740.2002
8. Faria DR, Gollob KJ, Barbosa J, Schriefer A, Machado PRL, Lessa H, et al. Decreased in situ expression of interleukin-10 receptor is correlated with the exacerbated inflammatory and cytotoxic responses observed in mucosal leishmaniasis. *Infect Immun* (2005) 73:7853–9. doi: 10.1128/IAI.73.12.7853-7859.2005
9. Fuertes Marraco SA, Neubert NJ, Verdeil G, Speiser DE. Inhibitory receptors beyond T cell exhaustion. *Front Immunol* (2015) 6:310. doi: 10.3389/fimmu.2015.00310
10. Wherry EJ. T cell exhaustion. *Nat Immunol* (2011) 12:492–9. doi: 10.1038/ni.2035
11. Yi JS. Cox M a, Zajac AJ. T-cell exhaustion: characteristics, causes and conversion. *Immunology* (2010) 129:474–81. doi: 10.1111/j.1365-2567.2010.03255.x
12. Chiku VM, Silva KLO, de Almeida BFM, Venturin GL, Leal AAC, de Martini CC, et al. PD-1 function in apoptosis of T lymphocytes in canine visceral leishmaniasis. *Immunobiology* (2016) 221:879–88. doi: 10.1016/j.imbio.2016.03.007
13. Gautam S, Kumar R, Singh N, Singh AK, Rai M, Sacks D, et al. CD8 T cell exhaustion in human visceral leishmaniasis. *J Infect Dis* (2014) 209:290–9. doi: 10.1093/infdis/jit401
14. Oliveira Silva KL, Marin Chiku V, Luvizotto Venturin G, Correa Leal AA, de Almeida BF, De Rezende Eugenio F, et al. PD-1 and PD-L1 regulate cellular immunity in canine visceral leishmaniasis. *Comp Immunol Microbiol Infect Dis* (2019) 62:76–87. doi: 10.1016/j.cimid.2018.12.002
15. Habib S, El Andaloussi A, Elmasry K, Handoussa A, Azab M, Elsawey A, et al. PDL-1 blockade prevents T cell exhaustion, inhibits autophagy, and promotes clearance of Leishmania donovani. *Infect Immun* (2018) 86(6):e00019. doi: 10.1128/IAI.00019-18
16. Egui A, Ledesma D, Pérez-Antón E, Montoya A, Gómez I, Robledo SM, et al. Phenotypic and Functional Profiles of Antigen-Specific CD4+ and CD8+ T Cells Associated With Infection Control in Patients With Cutaneous Leishmaniasis. *Front Cell Infect Microbiol* (2018) 8:393. doi: 10.3389/fcimb.2018.00393
17. da Fonseca-Martins AM, Ramos TD, Pratti JES, Firmino-Cruz L, Gomes DCO, Soong L, et al. Immunotherapy using anti-PD-1 and anti-PD-L1 in Leishmania amazonensis-infected BALB/c mice reduce parasite load. *Sci Rep* (2019) 9:1–13. doi: 10.1038/s41598-019-56336-8
18. Esch KJ, Juelsgaard R, Martinez PA, Jones DE, Petersen CA. Programmed Death 1-Mediated T Cell Exhaustion during Visceral Leishmaniasis Impairs Phagocyte Function. *J Immunol* (2013) 191:5542–50. doi: 10.4049/jimmunol.1301810
19. Hernández-Ruiz J, Salaiza-Suazo N, Carrada G, Escoto S, Ruiz-Remigio A, Rosenstein Y, et al. CD8 cells of patients with diffuse cutaneous leishmaniasis display functional exhaustion: The latter is reversed, in vitro, by TLR2 agonists. *PloS Negl Trop Dis* (2010) 4(11):e871. doi: 10.1371/journal.pntd.0000871
20. Mukherjee S, Sengupta R, Mukhopadhyay D, Braun C, Mitra S, Roy S, et al. Impaired activation of lesional CD8+ T-cells is associated with enhanced expression of Programmed Death-1 in Indian Post Kala-azar Dermal Leishmaniasis. *Sci Rep* (2019) 9:1–12. doi: 10.1038/s41598-018-37144-y
21. Pardoll DM. The blockade of immune checkpoints in cancer immunotherapy. *Nat Rev Cancer* (2012) 12:252–64. doi: 10.1038/nrc3239
22. Fromentin R, DaFonseca S, Costiniuk CT, El-Far M, Procopio FA, Hecht FM, et al. PD-1 blockade potentiates HIV latency reversal ex vivo in CD4 + T cells from ART-suppressed individuals. *Nat Commun* (2019) 814(2019):1–7. doi: 10.1038/s41467-019-08798-7
23. Henson SM, MaCaulay R, Franzese O, Akbar AN. Reversal of functional defects in highly differentiated young and old CD8 T cells by PDL blockade. *Immunology* (2012) 135:355–63. doi: 10.1111/j.1365-2567.2011.03550.x
24. Henson SM, Macaulay R, Riddell NE, Nunn CJ, Akbar AN. Blockade of PD-1 or p38 MAP kinase signaling enhances senescent human $CD8^+$ T-cell proliferation by distinct pathways. *Eur J Immunol* (2015) 45:1441–51. doi: 10.1002/eji.201445312
25. Teigler JE, Zelinskyy G, Eller MA, Bolton DL, Marovich M, Gordon AD, et al. Differential Inhibitory Receptor Expression on T Cells Delineates Functional Capacities in Chronic Viral Infection. *J Virol* (2017) 91:1–15. doi: 10.1128/JVI.01263-17
26. Rao M, Valentini D, Dodoo E, Zumla A, Maeurer M. Anti-PD-1/PD-L1 therapy for infectious diseases: learning from the cancer paradigm. *Int J Infect Dis* (2017) 56:221–8. doi: 10.1016/j.ijid.2017.01.028
27. Mou Z, Muleme HM, Liu D, Jia P, Okwor IB, Kuriakose SM, et al. Parasite-derived arginase influences secondary anti-Leishmania immunity by regulating PD-1-mediated CD4+ T cell exhaustion. *J Immunol* (2013) 190:3380–9. doi: 10.4049/jimmunol.1202537.Parasite-derived
28. Joshi T, Rodriguez S, Perovic V, Cockburn IA, Stäger S. B7-H1 blockade increases survival of dysfunctional CD8+ T cells and confers protection against Leishmania donovaniinfections. *PloS Pathog* (2009) 5(5):e1000431. doi: 10.1371/journal.ppat.1000431
29. Christensen SM, Dillon LAL, Carvalho LP, Passos S, Novais FO, Hughitt VK, et al. Meta-transcriptome Profiling of the Human-Leishmania braziliensis Cutaneous Lesion. *PloS Negl Trop Dis* (2016) 10:1–17. doi: 10.1371/journal.pntd.0004992
30. Love MI, Huber W, Anders S. Moderated estimation of fold change and dispersion for RNA-seq data with DESeq2. *Genome Biol* (2014) 15:1–21. doi: 10.1186/s13059-014-0550-8
31. Gu Z, Eils R, Schlesner M. Complex heatmaps reveal patterns and correlations in multidimensional genomic data. *Bioinformatics* (2016) 32:2847–9. doi: 10.1093/bioinformatics/btw313
32. Wickham H. *ggplot2: Elegant Graphics for Data Analysis*. New York, NY: Springer-Verlag New York (2016).
33. Covre LP, Devine OP, Garcia de Moura R, Vukmanovic-Stejic M, Dietze R, Ribeiro-Rodrigues R, et al. Compartmentalized cytotoxic immune response leads to distinct pathogenic roles of natural killer and senescent CD8+ T cells in human cutaneous leishmaniasis. *Immunology* (2020) 159:429–40. doi: 10.1111/imm.13173
34. Covre LP, Martins RF, Devine OP, Chambers ES, Vukmanovic-Stejic M, Silva JA, et al. Circulating senescent T cells are linked to systemic inflammation and lesion size during human cutaneous leishmaniasis. *Front Immunol* (2019) 10:3001. doi: 10.3389/fimmu.2018.03001
35. Barroso DH, Falcão SDAC, da Motta J de OC, dos Santos LS, Takano GHS, Gomes CM, et al. PD-L1 May Mediate T-Cell Exhaustion in a Case of Early Diffuse Leishmaniasis Caused by Leishmania (L.) amazonensis. *Front Immunol* (2018) 9:1021. doi: 10.3389/fimmu.2018.01021
36. Legat A, Speiser DE, Pircher H, Zehn D, Fuertes Marraco SA. Inhibitory receptor expression depends more dominantly on differentiation and activation than "exhaustion" of human CD8 T cells. *Front Immunol* (2013) 4:455. doi: 10.3389/fimmu.2013.00455
37. Wherry EJ, Ha S-J, Kaech SM, Haining WN, Sarkar S, Kalia V, et al. Molecular Signature of CD8+ T Cell Exhaustion during Chronic Viral Infection. *Immunity* (2007) 27:670–84. doi: 10.1016/j.immuni.2007.09.006
38. Youngblood B, Wherry EJ, Ahmed R. Acquired transcriptional programming in functional and exhausted virus-specific CD8 T cells. *Curr Opin HIV AIDS* (2012) 7(1):50–7. doi: 10.1097/COH.0b013e32834ddcf2
39. Sakhdari A, Mujib S, Vali B, Yue FY, MacParland S, Clayton K, et al. Tim-3 negatively regulates cytotoxicity in exhausted CD8+ T cells in HIV infection. *PloS One* (2012) 7(7):e40146. doi: 10.1371/journal.pone.0040146
40. Santos C da S, Boaventura V, Ribeiro Cardoso C, Tavares N, Lordelo MJ, Noronha A, et al. CD8+ Granzyme B+–Mediated Tissue Injury vs. CD4+IFNγ+–Mediated Parasite Killing in Human Cutaneous Leishmaniasis. *J Invest Dermatol* (2013) 133:1533–40. doi: 10.1038/jid.2013.4
41. Cardoso TM, Machado Á, Costa DL, Carvalho LP, Queiroz A, Machado P, et al. Protective and pathological functions of CD8+ T cells in Leishmania braziliensis infection. *Infect Immun* (2015) 83:898–906. doi: 10.1128/IAI.02404-14
42. Carvalho AM, Novais FO, Paixão CS, de Oliveira CI, Machado PRL, Carvalho LP, et al. Glyburide, a NLRP3 Inhibitor, Decreases Inflammatory Response

and Is a Candidate to Reduce Pathology in Leishmania braziliensis Infection. *J Invest Dermatol* (2019) 140:1–3.e2. doi: 10.1016/j.jid.2019.05.025

43. Macedo SRA, De Figueiredo Nicolete LD, Ferreira ADS, De Barros NB, Nicolete R. The pentavalent antimonial therapy against experimental Leishmania amazonensis infection is more effective under the inhibition of the NF-κB pathway. *Int Immunopharmacol* (2015) 28:554–9. doi: 10.1016/j.intimp.2015.07.020

Conflict of Interest: The authors declare that the research was conducted in the absence of any commercial or financial relationships that could be construed as a potential conflict of interest.

The handling editor declared a shared affiliation, though no other collaboration, with one of the authors HM.

frontiers in Immunology

ORIGINAL RESEARCH
published: 11 March 2021
doi: 10.3389/fimmu.2021.647385

Presence of Senescent and Memory CD8+ Leukocytes as Immunocenescence Markers in Skin Lesions of Elderly Leprosy Patients

Pedro Henrique Lopes da Silva[1†], Katherine Kelda Gomes de Castro[1†], Mayara Abud Mendes[1†], Thyago Leal-Calvo[1†], Júlia Monteiro Pereira Leal[1†], José Augusto da Costa Nery[1†], Euzenir Nunes Sarno[1†], Roberto Alves Lourenço[2†], Milton Ozório Moraes[1†], Flávio Alves Lara[3†] and Danuza Esquenazi[1,4*†]*

[1] Laboratório de Hanseníase, Instituto Oswaldo Cruz, Fundação Oswaldo Cruz, Rio de Janeiro, Brazil, [2] Laboratorio de Envelhecimento Humano, GeronLab, Policlínica Piquet Carneiro, Universidade do Estado do Rio de Janeiro, Rio de Janeiro, Brazil, [3] Laboratório de Microbiologia Celular, Instituto Oswaldo Cruz, Fundação Oswaldo Cruz, Rio de Janeiro, Brazil, [4] Disciplina de Patologia Geral, Faculdade de Ciências Médicas, Universidade do Estado do Rio de Janeiro, Rio de Janeiro, Brazil

Leprosy is an infectious disease that remains endemic in approximately 100 developing countries, where about 200,000 new cases are diagnosed each year. Moreover, multibacillary leprosy, the most contagious form of the disease, has been detected at continuously higher rates among Brazilian elderly people. Due to the so-called immunosenescence, characterized by several alterations in the quality of the immune response during aging, this group is more susceptible to infectious diseases. In view of such data, the purpose of our work was to investigate if age-related alterations in the immune response could influence the pathogenesis of leprosy. As such, we studied 87 individuals, 62 newly diagnosed and untreated leprosy patients distributed according to the age range and to the clinical forms of the disease and 25 healthy volunteers, who were studied as controls. The frequency of senescent and memory $CD8^+$ leukocytes was assessed by immunofluorescence of biopsies from cutaneous lesions, while the serum levels of IgG anti-CMV antibodies were analyzed by chemiluminescence and the gene expression of T cell receptors' inhibitors by RT-qPCR. We noted an accumulation of memory $CD8^+$ T lymphocytes, as well as reduced $CD8^+CD28^+$ cell expression in skin lesions from elderly patients, when compared to younger people. Alterations in *LAG3* and *PDCD1* gene expression in cutaneous lesions of young MB patients were also observed, when compared to elderly patients. Such data suggest that the age-related alterations of T lymphocyte subsets can facilitate the onset of leprosy in elderly patients, not to mention other chronic inflammatory diseases.

Keywords: leprosy, elderly, immunosenescence, skin lesions, memory T cell, cytomegalovirus

OPEN ACCESS

Edited by:
Fabienne Tacchini-Cottier, University of Lausanne, Switzerland

Reviewed by:
Mirian Nacagami Sotto, University of São Paulo, Brazil
Guillaume Sarrabayrouse, Vall d'Hebron Research Institute (VHIR), Spain

****Correspondence:***
Danuza Esquenazi
danuza@ioc.fiocruz.br
Pedro Henrique Lopes da Silva
peddro.henrique10@gmail.com

†ORCID:
Pedro Henrique Lopes da Silva
orcid.org/0000-0001-7683-398X
Katherine Kelda Gomes de Castro
orcid.org/0000-0003-4324-0744
Mayara Abud Mendes
orcid.org/0000-0002-9689-6440
Thyago Leal-Calvo
orcid.org/0000-0001-9520-4791
Júlia Monteiro Pereira Leal
orcid.org/0000-0002-1048-2088
José Augusto da Costa Nery
orcid.org/0000-0003-0550-9327
Euzenir Nunes Sarno
orcid.org/0000-0003-0129-2159
Roberto Alves Lourenço
orcid.org/0000-0003-0838-1285
Milton Ozório Moraes
orcid.org/0000-0003-2653-0037
Flávio Alves Lara
orcid.org/0000-0002-2717-6597
Danuza Esquenazi
orcid.org/0000-0002-1312-7161

Specialty section:
This article was submitted to Microbial Immunology, a section of the journal Frontiers in Immunology

Received: *29 December 2020*
Accepted: *15 February 2021*
Published: *11 March 2021*

INTRODUCTION

Leprosy is a neglected chronic infectious disease caused by *Mycobacterium leprae*, which remains a public health problem in low-income countries (1, 2). *M. leprae* affects mainly the skin and peripheral nervous system, where the bacilli are responsible for neurological damage, bone resorption, and irreversible physical disabilities (3–5). Genetic and environmental factors contribute to disease progression (3). Fortunately, around 95% of people are genetically resistant to *M. leprae* infection (3, 6).

Leprosy presents a wide spectrum of clinical forms, which is essentially determined by the presence (or absence) of cell-mediated immunity (CMI) against the pathogen. According to the Ridley and Jopling classification (7), tuberculoid forms (T-Lep) are characterized by a strong immune response to localized disease with a single (or few) skin lesion(s) without bacilli detection. On the other side, lepromatous forms (L-Lep) are characterized by several disseminated skin lesions with many bacilli, and the absence of CMI against *M. leprae*. Between these polar forms (TT and LL) there are borderline forms (BT, BB, and BL), which comprise most of the patients. In addition, there is also a WHO classification, a more practical and operational classification, which classifies leprosy patients into two groups: paucibacillary leprosy (PB leprosy) that presents five or less skin lesions and no apparent bacilli in slit-skin smears; and multibacillary leprosy (MB leprosy) with more than five skin lesions (8).

During the aging process, significant changes in the composition of peripheral T lymphocytes occur (9). These changes are mostly caused by decline in the output of naïve T cells due to thymic involution and exposure to pathogens over the lifetime, especially latent viruses, such as cytomegalovirus (CMV), which are related to the accumulation of highly differentiated $CD8^+$ memory T cells (9, 10). Although a mechanism of compensation by homeostatic proliferation partly maintains the numbers of naïve T cells in the periphery, the adaptive immune system in elderly people is characterized by higher proportions of memory T cells and lower proportions of naïve T cells (11). $CD8^+$ T cells play a central role in the recognition and clearance of intracellular pathogens, such as *M. leprae*. $CD8^+$ T cell frequency is similar between the leprosy clinical forms, although functional features such as higher IL-10 levels in MB compared to PB patients in this T cell subset has been observed (12). Moreover, TNF-producing $CD8^+$ T cells are essential in the pathogenesis of the type 2 leprosy reaction in MB patients, these reactions are episodes of acute hypersensitivity presenting as aggravation of the previous symptoms and skin lesions (13).

During the aging process, the T cell costimulatory molecule, CD28 (needed for activation and survival), is lost, interfering in cellular signaling and functional aspects of these cells (14, 15). The binding of CD28, expressed on the T cell surface, to CD80 or CD86 stimulates IL-2 production leading to T cell activation and proliferation, while signals through the TCR/CD3 complex in the absence of a costimulatory signal induces anergy (16). Recent works have shown that the loss of CD28 expression is a hallmark of senescent $CD8^+$ T cells, and proportion changes in $CD8^+CD28^-$ cells have been reported in aging-related diseases such as cancer, cardiovascular disease, and other chronic inflammatory diseases (17–19). Accumulating evidence indicates that $CD8^+CD28^-$ T cells play a relevant role in immune response suppression, such as impairing T cell activation and proliferation, and inducing apoptosis in these cells *in vitro* (20, 21). The immunosuppressive mechanisms performed by these cells are diverse, including secretion of anti-inflammatory cytokines, increased expression of programmed cell death protein 1 (PD-1) and its ligands, and FasL (22, 23). Several studies showed that the CD28 constitutive expression level is similar between PB patients and healthy individuals, while MB patients presented lower CD28 expression (24–26). This suggests that upregulation of the CD28 molecule plays a critical role in the cell-mediated immunity response against *M. leprae,* restricting the proliferation of the pathogen.

The present study aimed at investigating potential age-related alterations that are associated with $CD8^+$ cells in elderly leprosy patients. For this purpose, blood and skin lesion samples from young and elderly patients were evaluated for the frequency of memory and senescent $CD8^+$ T cells, anti-CMV IgG titers, and gene expression of inhibitory T cell receptors. We observed the accumulation of memory $CD8^+$ cells in the skin lesions of all elderly patients, followed by a lower frequency of $CD8^+CD28^+$ in elderly PB patients compared to young ones. We also observed changes in gene expression of the *LAG3* and *PDCD1* receptors in cutaneous lesions of young MB patients and not in elderly leprosy patients.

METHODS

Participants and Study Design

All enrolled leprosy patients were classified according to the Ridley and Jopling scale (1966), then the diagnosis was confirmed by clinical examination and histopathological analysis of skin lesions. Blood and skin lesion samples were collected before treatment (**Figure 1**). Patients were classified according to clinical forms and also stratified into two groups: young (20–40 years old) and elderly (over 60 years old). All patients and healthy volunteers resided in the metropolitan region of Rio de Janeiro state, Brazil, a leprosy endemic area. Exclusion criteria for leprosy patients and healthy elderly volunteers were: relapse cases, pregnancy or breast-feeding women, co-infections such as tuberculosis, hepatitis B and C, and HIV. Hypertensive and diabetic elderly individuals under drug control were included. As previously mentioned, our work used clinical samples of young and elderly patients diagnosed according to the R&J criteria. Nevertheless, in order to avoid repetitions, BL and LL individuals shall be hereinafter grouped as MB patients, and BT and TT as PB patients.

Ethical Considerations

The study was approved by the Institutional Ethics Committee of Oswaldo Cruz Foundation/FIOCRUZ (permit protocol number 27052919.0.0000.5248). Leprosy patients and healthy volunteers signed a written consent form to participate in the study. The biological samples from leprosy patients were obtained

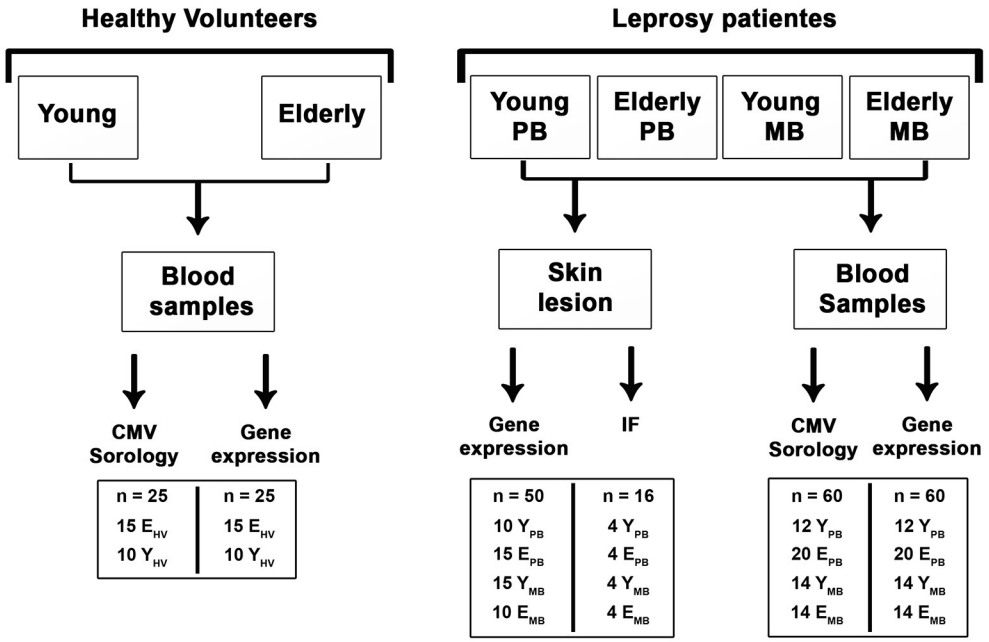

FIGURE 1 | Study design. Groups of individuals evaluated and tests performed. A total of 62 leprosy patients and 25 healthy volunteers were clinically and/or laboratory assessed. At each analysis performed, the numbers of individuals tested by group are shown (inside the boxes).

at the Leprosy outpatient clinic (FIOCRUZ/Rio de Janeiro). Elderly healthy individuals were recruited at the Human Aging Laboratory – GeronLab, Policlínica Piquet Carneiro (UERJ/Rio de Janeiro).

Immunofluorescence Assay

Frozen skin lesion section assays were performed in a Leica LM3000 cryostat, fixed in paraformaldehyde. Unspecific binding sites were blocked with 10% Fetal Calf Serum (FCS, GIBCO, Life Technologies) in 0.01 M of PBS for 1 h at room temperature. Permeabilization was performed by incubating the sections with 0.05% Triton X-100 for 15 min. Rat IgG2b anti-human CD8 (1:50; Abcam, ab60076), mouse IgG2a anti-human CD45RO (1:25; Abcam, ab86080), and rabbit IgG anti-human CD28 (1:50; Abcam, ab243228) or their respective isotypes were diluted in 1% Bovine Serum Albumin (BSA, Sigma-Aldrich) in 0.01 M of PBS and incubated at 4°C overnight. Tissue sections were washed three times and incubated with Alexa Fluor 594 goat anti-Rat IgG (1:1,000, Abcam, ab150164), Alexa Fluor 633 goat anti-mouse IgG1 (1:1,000, ThermoFisher Scientific, A-21126), and Alexa Fluor 488 goat anti-rabbit IgG (1:1,000, Abcam, ab150077) secondary antibodies for 1.5 h at room temperature. The nuclei were stained with 4′-6-diamidino-2-phenylindole (DAPI; 1:10,000, Molecular Probes, D1306), and slides were mounted with VECTASHIELD Mounting Medium (Vector Laboratories, H-1000). Tissues were imaged using an Axio Observer.Z1 (Carl Zeiss, Oberkochen, Germany) using an EC Plan-Neofluar 20×/0.50 objective and Plan-Apochromat 63×/1.3 oil objective. Images were acquired with an AxioCam HRm digital camera, in the format of structured confocal images by Apotome (Carl Zeiss), mathematically deconvoluted by the AxioVision Rel. 4.6 software (Carl Zeiss). For quantitative analysis of $CD8^+$, $CD45RO^+$, and $CD28^+$ cells, 10 microscopic fields were imaged and the number of positive cells was counted in each field. The results were summarized as the average of fields' counts, as determined by three independent observers.

CMV Serology

IgG antibodies against CMV were determined in sera samples with a commercially available chemiluminescent microparticle immunoassay according to the manufacturer's instructions (Architect CMV IgG, Abbott Laboratories, Diagnostic Division, Sligo, Ireland). Absorbance was measured and an optical density (OD) ratio was calculated. The default result unit for the assay was AU/mL. Specimens with concentration values $\geq$15.0 AU/mL were considered reactive for IgG antibodies to CMV and indicated past or acute infection.

Total RNA Isolation and cDNA Synthesis

The total RNA from whole blood obtained by venous puncture was isolated using the PAXgene™ Blood RNA kit (Qiagen, Hilden, Germany) in accordance with the manufacturer's instructions. For biopsy specimens, RNA from skin lesion samples (6 mm^3 punch) was obtained using the Polytron Homogenizer Model PT3100 apparatus (Kinematica AG, Lucerne, Switzerland) in 2 mL of TRIzol™ Reagent (ThermoFisher Scientific, Massachusetts, USA), following the manufacturer's instructions. Total RNA was treated with TURBO™ DNase (ThermoFisher Scientific) according to the manufacturer's standard protocol, quantified, and their integrity was evaluated by agarose gel electrophoresis. RNA

reverse transcription into cDNA was performed as previously described (27).

Gene Expression Analysis by RT-qPCR

Quantitative RT-PCR was carried out with a final volume of 10 μL containing 200 nM of each primers (**Supplementary Table 1**), 1X Fast SYBR™ Green Master Mix (ThermoFisher Scientific), and 10 ng of cDNA. All reactions were conducted with three technical replicates for each biological sample. No reverse transcriptase negative controls and no template controls were included in each run. The assays were performed on a StepOnePlus™ Real-Time PCR Systems thermocycler (ThermoFisher Scientific) as detailed elsewhere (27). The relative expression levels of the genes of interest were normalized by ribosomal protein L13. qPCR data analysis was performed with the N_0 method implemented in LinRegPCR v. 2020.0, which considers qPCR mean efficiencies estimated by the window-of-linearity method as proposed by Ramakers et al. (28) and Ruijter et al. (29). Briefly, N0 values were calculated in LinRegPCR using default parameters. Then, N0 values from the gene of interest (GOI) were normalized by taking its ratio to the N0 of the reference gene (REF) *RPL13a* ($N0_{GOI}/N0_{REF}$).

Biomark Fluidigm Gene Expression

Gene expression from whole blood was measured using Biomark's microfluidic-based qPCR technology. cDNA was obtained from RNA as described above. Then, 1.25 μL of cDNA (from stock concentration of 5 ng/μL) was pre-amplified with a pool of 96 primer pairs (final concentration of 50 nM) with the TaqMan PreAmp Master Mix 2X (Applied Biosystems, USA, # 4391128) in a GeneAmp PCR System 9700 thermocycler for 14 cycles. All subsequent steps are detailed in research by Guerreiro et al. (27). For data analysis, initial quality control was performed based on melting curve analysis (MCA) using the Fluidigm Real-Time PCR Analysis Software v. 4.5.2, where targets with multiple dissociation curve peaks were removed from further analysis. Later, raw data were exported and processed with custom R scripts as described elsewhere by Guerreiro et al. (27). In brief, foreground data (EvaGreen) were adjusted by the subtraction of background (Rox) intensity to generate Rn (background-adjusted accumulated fluorescence). Then, qPCR reaction efficiency was estimated by fitting a four-parameter sigmoid model according to Rutledge and Stewart (30), with functions from the R package qpcR v.1.41-1 (31). Cycle thresholds (Ct) were determined from the maximum of the second derivative from the fitted sigmoid curve. Cts and efficiencies were used to estimate relative expression based on the method proposed by Pfaffl (32). The normalization factor used in the denominator for relative expression consisted of the geometric mean from *RPS16*, *RPL13,* and *RPL35* genes, selected as the most stable by the R implementation of the geNorm algorithm (33, 34).

Statistical Analysis

Results were analyzed using Statistical Package for the Social Sciences (SPSS) V. 10.1 (SPSS, Inc., Chicago, IL, USA) and Graph Prism V. 8 (San Diego, CA, USA) software. After testing for normality (Shapiro-Wilk normality test), non-normally distributed data were analyzed through non-parametric tests. The Mann/Whitney U-test was used to test the differences between two groups, and comparisons between more than two groups were examined through the Kruskal-Wallis test followed by *post-hoc* Dunn's correction. Normally distributed data were compared using one-way ANOVA followed by Tukey's multiple comparisons test. A P-value < 0.05 was considered statistically significant.

RESULTS

Subject Demographics and Clinical Data

The present study enrolled 87 individuals, 62 of whom were patients diagnosed with leprosy and 25 were healthy volunteers (HV). Both patients and HV were divided into two groups according to age: young (20–40 years age) and elderly (60 years age or older). The mean age of the young groups was 30 years of age (29.3 for young HV, 29.3 for young PB, 31.7 for young MB). In the elderly groups, the mean ages were 79.1, 69.1, and 67.7 years for elderly HV, elderly PB, and elderly MB patients, respectively. Participants' clinical and demographic data are shown in **Table 1**.

According to the Ridley and Jopling classification of patient clinical spectrums, those in the MB group were classified as BL (40%) or LL (60%), while PB patients were either TT (12.5%) or BT (87.5%). Among elderly MB patients, there was a high frequency of male individuals when compared to the other groups. This unequal gender distribution was expected due to the influence of sex hormones on the immune response to infectious diseases. Lower education level (average of 5 years) of elderly patients was not related to a delay in diagnosing the disease. Although young patients had higher education levels when compared to elderly patients ($p = 0.0035$), especially in the PB group (10 years), the time from symptoms onset to disease diagnosis was, on average, 1 year for both young and elderly participants.

Bacterial load, as measured by the bacterial index (BI) in slit skin smears samples, was greater in young MB patients than in the elderly patients, although this difference was not significant ($p = 0.2932$). On the other hand, bacterial lesion index (BLI) was significantly greater in young MB patients than in elderly patients ($p = 0.0112$). This information is particularly interesting considering that the frequency of MB patients in young and elderly groups was similar.

Memory Cutaneous $CD8^+$ Cell Populations are More Frequent in Elderly Leprosy Patients

Memory $CD8^+$ cells ($CD8^+CD45RO^+$) presence was detected in patients' skin lesions by labeling with anti-CD8 and anti-CD45RO antibodies, as described in the methods section. **Figure 2A** represents results from the four studied groups. $CD8^+$ leukocytes were significantly higher in elderly skin lesions when compared to those of young patients, regardless of clinical form (**Figure 2B**). Memory $CD8^+$ cells ($CD8^+CD45RO^+$) were also greater in elderly than in young patients (**Figure 2C**),

TABLE 1 | Characteristics of study population.

Groups	*N*	Age, years (Mean ± SD)	Sex (%male)	BI (Mean ± SD)	LBI (Mean ± SD)	DG (%)			Education level (Mean ± SD)	Time to diagnosis (median)
						0	I	II		
Y HV	10	29.3 ± 7.1	40	–	–	–	–	–	16.1 ± 5.7	–
E HV	15	79.1 ± 6.3	46.7	–	–	–	–	–	10.4 ± 4.1	–
Y PB	12	29.3 ± 6.2	66.7	0	0	83.3	16.7	0	10.1 ± 4.3	12
E PB	20	69.1 ± 7.5	30	0	0	90	5	5	5.9 ± 4.4	10
Y MB	15	31.7 ± 3.2	60	4.5 ± 1.2	4.9 ± 1.1	53.3	33.3	13.4	7.9 ± 4.3	11.5
E MB	15	67.7 ± 6.7	73.3	4.1 ± 1.1	3.7 ± 1.4	33.3	46.7	20	3.5 ± 2.8	11.5

Y, Young; E, Elderly; HV, Healthy Volunteers; PB, Paucibacillary leprosy; MB, Multibacillary leprosy; BI, Bacillary Index; LBI, Lesion Bacillary Index; DG, Disability Degree.

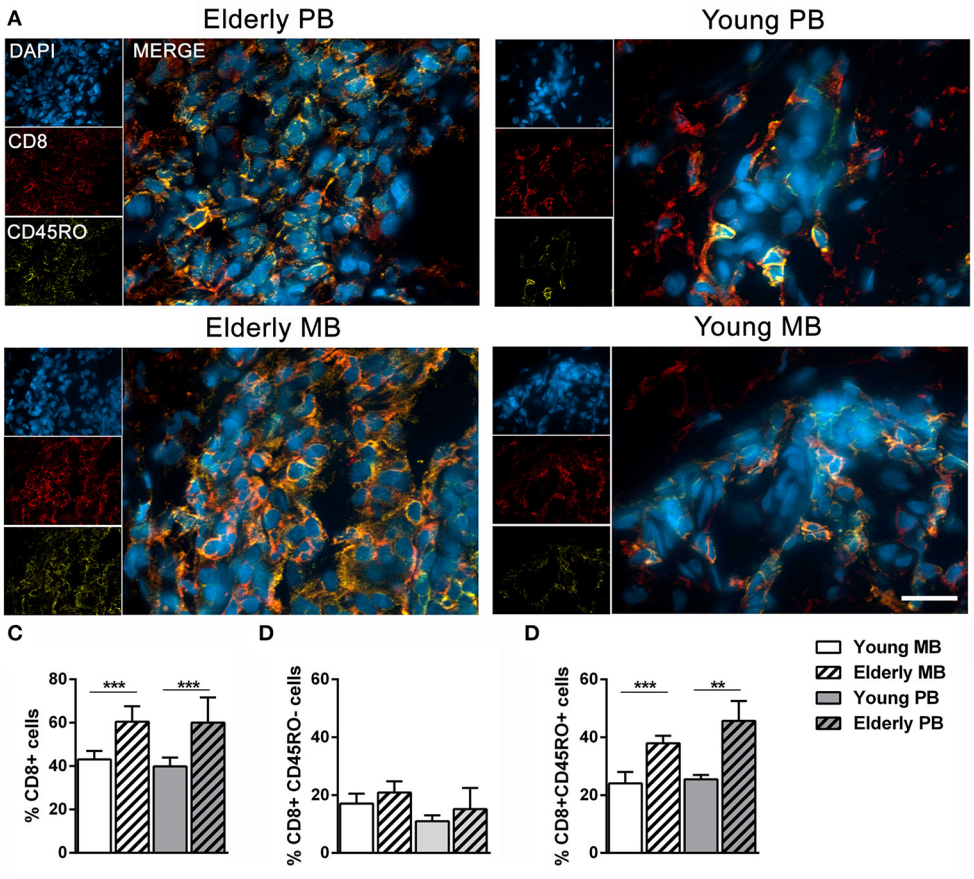

FIGURE 2 | Frequency of memory $CD8^+$ T cells in skin lesions samples. Immunofluorescence assays were performed to determine the number of memory $CD8^+$ T cells ($CD8^+CD45RO^+$) in skin lesions of leprosy patients. The images are representative of a patient from each group of four individuals, where CD8 (red, Alexa Fluor 594), CD45RO (yellow, Alexa Fluor 633), and the nuclei (blue) were stained with DAPI **(A)**. The images were visualized and obtained by a Zeiss Colibri fluorescent microscope, and the scale bar was 20 μm. The graphs show the frequency of **(B)** $CD8^+$ T cells, **(C)** $CD8^+CD45RO^-$ T cells, and **(D)** $CD8^+CD45RO^+$ T cells. Analysis was performed by one-way ANOVA followed by Tukey's multiple comparison test. Data are representative of four individuals in each group and the results are shown as means ± SD, where $^{**}P < 0.01$, and $^{***}P < 0.001$.

irrespective of clinical form. On the other hand, naïve cells ($CD8^+CD45RO^-$) were not significantly different in skin lesions from young and elderly patients (**Figure 2D**). As expected, these results demonstrate an accumulation of memory $CD8^+$ cells in elderly patient skin lesions, which is a process linked to immunosenescence.

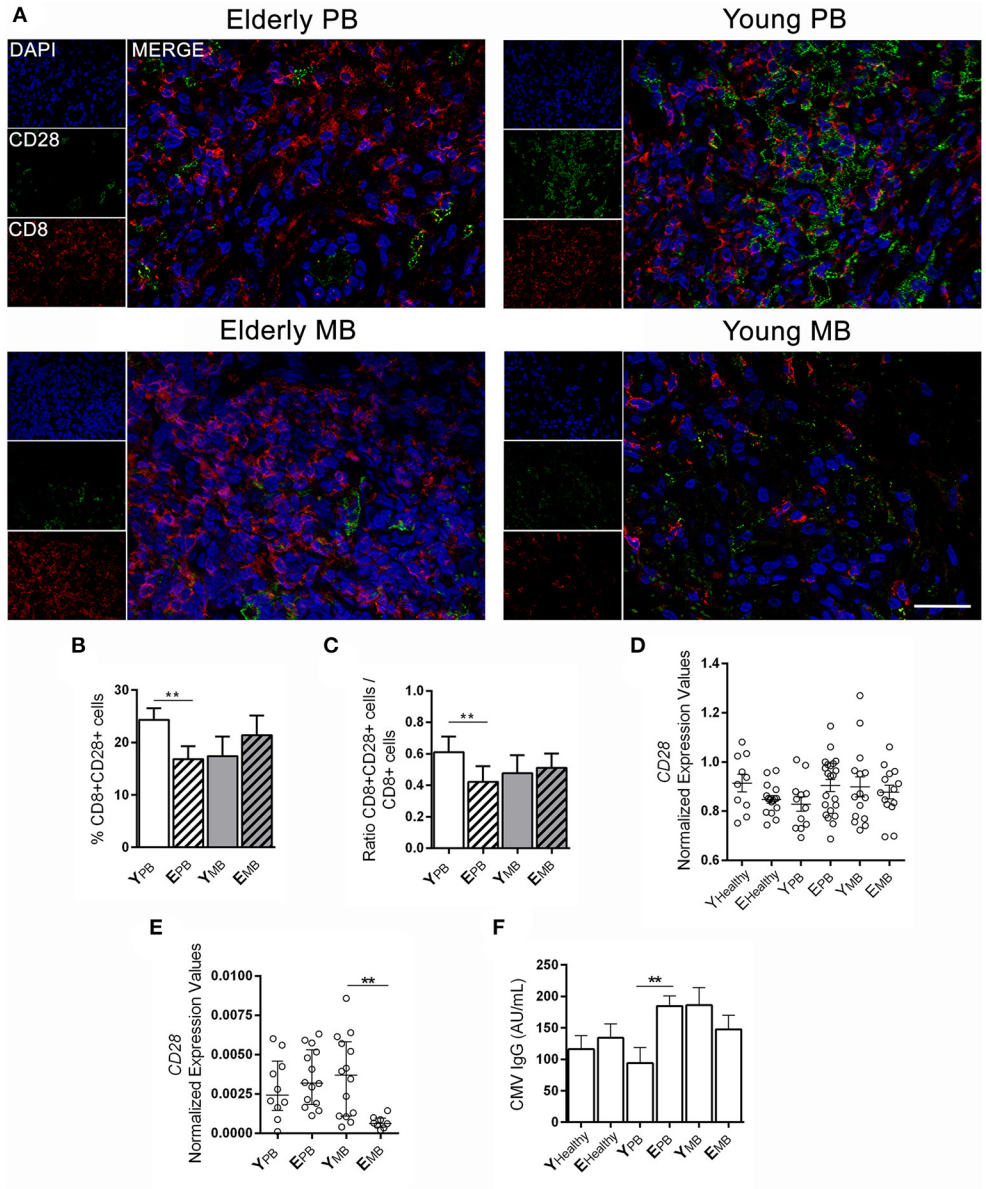

FIGURE 3 | CD28 expression in blood and skin lesion samples. Fluorescence immunostaining of CD28 (green) and CD8 (red) in skin lesions. **(A)** The images are representative of a patient from each group of four individuals. Images were visualized and obtained by a Zeiss Colibri fluorescent microscope and the scale bar was 20 μm. The graphs show the frequency of **(B)** $CD8^+CD28^+$ T cells, **(C)** ratio between $CD8^+CD28^+$ cells and $CD8^+$ T cells, and the data are demonstrated by means ± SD. The results of CD28 gene expression in **(D)** blood samples and **(E)** skin lesion samples are shown in normalized expression values. Whole blood samples were measured using Biomark's microfluidic-based qPCR technology and experiments with skin lesions were performed with RT-qPCR. Each circle represents an individual, horizontal bars indicate the mean. **(F)** IgG anti-CMV antibodies in sera samples in the studied groups were performed by a chemiluminescence method. Bars represent mean ± SD. Analysis was performed by one-way ANOVA followed by Tukey's multiple comparison test, and $^{**}P < 0.01$.

Low Frequency of $CD8^+CD28^+$ Cells in Skin Lesion Samples of Elderly Leprosy Patients

Although $CD8^+$ T lymphocytes play an important part in controlling *M. leprae* proliferation, the presence of these senescent lymphocytes ($CD8^+CD28^-$) may hinder the control of infection due to their regulatory T cell activities. **Figure 3A** presents CD8 and CD28 expression in skin lesions of the groups of patients in this study. $CD8^+CD28^+$ cells were significantly more frequent in young PB than elderly PB patients in skin lesions ($p = 0.0015$; **Figure 3B**). However, the same was not observed among patients in MB groups, in which both young and elderly exhibited similar levels of $CD8^+CD28^+$ cells (**Figure 3B**). Ratios were calculated between $CD8^+CD28^+$ and total $CD8^+$ cells in order to confirm the higher frequency of $CD8^+CD28^+$

cells in young PB patients when compared to total $CD8^+$ cells (**Figure 3C**).

Gene expression of co-stimulating *CD28* in whole blood samples showed no difference in *CD28* mRNA expression in blood across the studied groups (**Figure 3D**). However, when it comes to *CD28* mRNA expression in skin lesions by RT-qPCR, elderly MB patients showed a significant reduction when compared to other groups in the study, including young patients with the same clinical form (**Figure 3E**; $p = 0.0024$).

Latent subclinical infection caused by CMV may lead to immunological alterations linked to aging, such as the accumulation of memory $CD8^+$ cells that do not express CD28. We carried out detection of anti-CMV IgG in the serum of studied participants. All elderly patients were positive for anti-CMV IgG, while 85% of young patients were positive. The lowest frequency of anti-CMV IgG positive individuals occurred in the young and healthy group (72%). However, antibody titers were not correlated to $CD8^+CD28^+$ cells in any of the studied groups. Furthermore, in elderly PB patients, only those with significantly lower $CD8^+CD28^+$ cells presented higher anti-CMV IgG levels, as opposed to young PB patients (**Figure 3F**; $p = 0.0054$).

Regardless of Age, MB Patients Presented Higher Gene Expression of T Cell Inhibitory Receptors Than PB Patients

Regulatory T lymphocytes use diverse strategies to suppress the immune response mediated by other subpopulations of T lymphocytes. Therefore, we hypothesized that PD-1 and LAG3 T lymphocyte inhibition receptors (also known as CD279 and CD223, respectively) could be part of the suppression strategy, linked to greater susceptibility to infectious diseases such as leprosy. Furthermore, CMV infection may induce these inhibition receptors.

We carried out gene expression analysis of programmed cell death 1 (*PDCD1*) receptor and its ligands *PDCD1lg1* and *PDCD1lg2*, as well as lymphocyte activation protein (*LAG3*) in blood and skin lesion samples. Blood samples from patients and healthy controls showed similar expression levels of *LAG3* and *PDCD1* (**Figures 4A**,**B**). In skin lesions, differences were observed between groups regardless of age. MB patients presented increased expression of *LAG3* and *PDCD1* in skin lesions in comparison to PB patients ($p < 0.0001$, $p = 0.0031$, respectively; **Figures 4C**,**D**). Furthermore, young MB patients presented significantly higher expression in skin lesions than PB patients ($p = 0.0219$).

It seems that *LAG3* and *PDCD1* could be associated with mechanisms leading to weaker T lymphocyte response to *M. leprae* in MB patients. However, the expression of these receptors does not seem to be related to aging, at least not under these studied conditions. Then, we analyzed putative age-related changes in programmed cell death receptor (*PDCD1*, i.e., *PDCD1lg1* and *PDCD1lg2*) gene expression in blood and skin lesions (**Supplementary Figure 1**) and no differences were observed among all groups tested. *PDCD1lg1* and *PDCD1lg2* also demonstrated no difference in gene expression between PB and MB patients, as opposed to *PDCD1*.

DISCUSSION

The aging process leads to a myriad of innate and adaptive immune system adaptations, which result in increased susceptibility to infections, reduction in vaccine response, and even greater incidence of cancer (35). Although these alterations are related to T cell mediated immune response, the mechanisms by which they increase susceptibility to infectious diseases remain unknown (36). Cunha and collaborators addressed these factors among elderly people affected by SARS-CoV-2 infection (37). Considering that *M. leprae* is capable of infecting a large amount of people, and only a minority will progress toward the disease (1), factors behind delayed disease onset that could be associated with changes in T lymphocyte subpopulations remain unclear. Studies in this area are even more relevant considering epidemiological tendencies of increased disease detection in the population over 60 years of age and stabilization in those between 15 and 60 years (38, 39), which could be increased in a transition from high-endemic to middle-endemicity.

The social impact of leprosy is high due to the physical sequelae that it may render, which are even more serious in the elderly population. Our work identified the increased frequency of physical incapacity in elderly, especially in MB patients, which is in agreement with other findings in the Brazilian population (38–40). Similarly, the greater frequency of males among MB patients has also been documented previously due to the progressive increase in MB leprosy with age (38, 39). It is known from experimental models of intracellular pathogens such as *Leishmania* (41), *Mycobacterium tuberculosis* (42), and *Paracoccidioides brasiliensis* (43) that testosterone is capable of increasing the levels of Th2 anti-inflammatory cytokines, such as IL-10 and IL-4, while estrogen induces a Th1 response, such as IL-2 and IFN-γ. These findings may explain the higher susceptibility of men for developing the multibacillary form of leprosy.

Herein, the observation of increased memory $CD8^+$ cells in skin lesions of elderly patients corroborates preceding evidence that demonstrated increased subpopulations of these cells during aging (9, 44). Although T lymphocytes are essential for the elimination of *M. leprae*, many subpopulations have reduced activation and proliferation due to the absence of the CD28 costimulatory molecule. $CD8^+CD28^-$ T cells exhibit a senescence profile along with severe reduction in telomere function due to a long replication history (45). Although other cells may express CD8 molecules, such as NK (CD8+CD3–CD56+) cells (46), it is highly likely that these CD8+ cells found in the skin of our patients studied herein are T lymphocytes. NK cells are also present in granulomatous diseases, such as tuberculosis and tuberculoid leprosy (47). Nevertheless, few studies disclosed the frequency of these cells in skin lesions of patients affected by such diseases.

While reduced expression of CD28 in peripheral blood T lymphocytes of MB patients has been previously described (24, 25), the current work provides new information correlating these data with age. We observed lower expression of CD28 molecules in $CD8^+$ of elderly PB patients in comparison with young patients with the same clinical form. These findings could compromise the activation and proliferation of these cells,

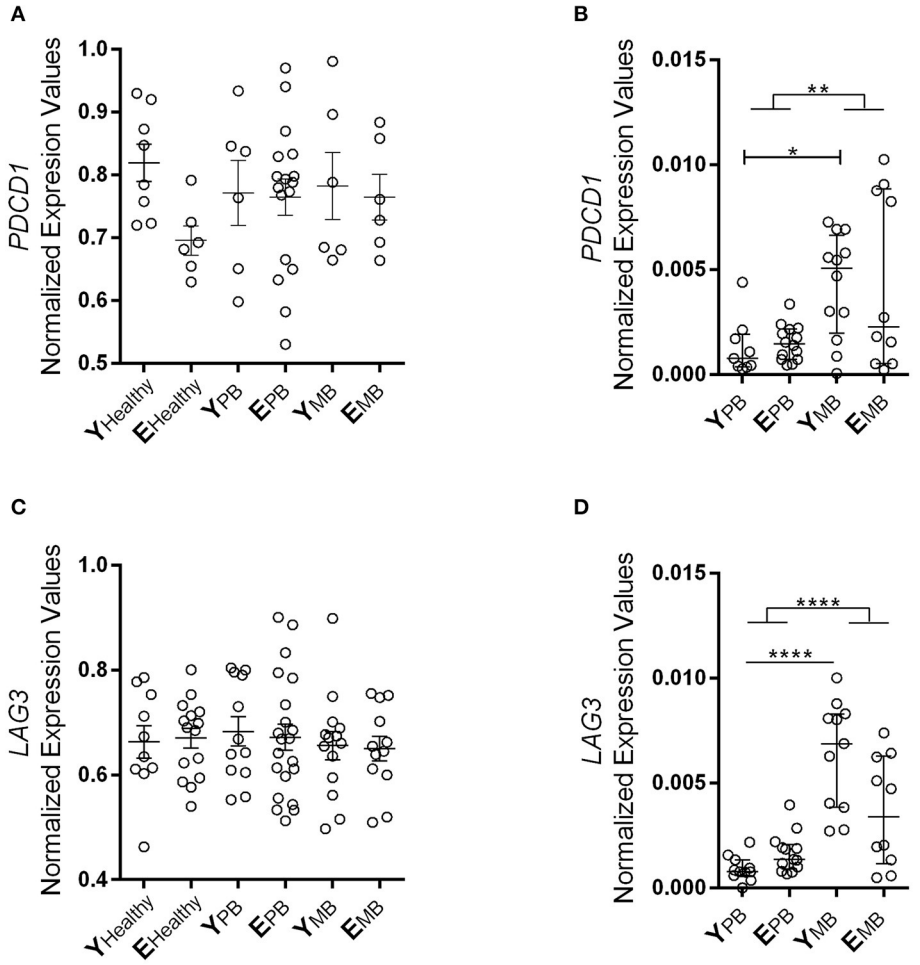

FIGURE 4 | PD-1 and LAG3 gene expression in whole blood and skin lesion samples. Expression of *PDCD1* gene on **(A)** blood and **(B)** skin samples. Expression of *LAG3* gene on **(C)** blood and **(D)** skin lesion samples. The results of these two inhibitory receptors are represented in normalized expression values. Whole blood samples were measured using Biomark's microfluidic-based qPCR technology and fragments of lesions were performed by RT-qPCR. Each circle represents an individual, and the horizontal bars indicate the mean. Kruskal-Wallis test with Dunn's multiple comparison test correction was used to compare the groups. $^{*}P < 0.05$, $^{**}P < 0.01$, and $^{****}P < 0.0001$.

favoring bacilli proliferation in elderly patients. Furthermore, $CD8^+CD28^-$ cells disclosed its ability to suppress immune activity, which could hamper the activation and proliferation of Th lymphocytes through different mechanisms, such as TGF-β and IL-10 secretion and expression of PDL-1 and FasL ligands (20, 21). Nonetheless, $CD8^+CD28^-$ T lymphocytes may also reduce the capacity of dendritic cells and monocytes to present *M. leprae*-derived antigens, through increased expression of *Ig-like transcript 3* (ILT3) and *4* (ILT4) (48). In summary, increased expression of senescent leukocytes in elderly patients could constitute a permissive environment that favors *M. leprae* replication and spread.

Our data are even more striking in the elderly PB patient group since they not only present lower $CD8^+CD28^+$ cells in skin lesions but showed increased detection of anti-CMV IgG antibodies in serum. Longitudinal studies have demonstrated that elderly people have a reduced capacity to resist new infections due to an excess of memory leukocytes, especially $CD8^+CD28^-$. Another contributing factor is the scarcity of naïve T lymphocytes that present a T lymphocyte receptor (TCR) repertoire (49–51). Studies suggest that T cell subsets frequencies may be caused, in part, by latent CMV control (52, 53). In fact, CMV seropositivity seems to be a determinant factor of life expectancy, CMV^+ individuals who present other risk factors, such as increase in $CD8^+CD28^-$ cells tend to have a shorter life span (54, 55).

As age advances, a decline of distinct intensity in adaptive immune functions is observed. It is speculated that this decline may be explained by regulatory T lymphocytes (Treg), however, these data are still inconsistent. Some studies describe a reduction in Treg ($CD4^+CD25^+$) suppressive activity during aging (54), while others show that blood Treg frequency is higher in the elderly and that their depletion improves conventional $CD4^+$ T lymphocyte activity in these individuals (55). Here, expression of two receptors (PD-1 and LAG3) related to the suppression mechanisms of Treg cells does not appear to be associated to age

in leprosy patients. Our results show that, regardless of age, MB patients present higher expression levels of these two receptors in skin samples than PB patients. These results are in accordance with the fact that MB patients present a permissive environment for the proliferation of *M. leprae*, considering their high bacilli counts in cutaneous lesions.

LAG3 receptor function seems to be influenced by different cytokines as well as by persistent antigen exposure (56). We found evidence that corroborates other studies showing that high bacillary load in MB patients may provide an environment that increases immunosuppressive action of Treg through LAG3. This could hinder the containment of bacilli, since LAG3 tends to increase Treg activity in an environment with high antigen exposure (57, 58). Similarly, increased PD-1 expression hampers effector T lymphocyte actions in containing *M. leprae* proliferation, resulting in high bacillary load, a characteristic of MB leprosy (59). For example, in a chronic infection model, blocking of PD-1 interaction with its ligands with nivolumab was able to revert the exhaustion of T lymphocytes (60).

Taken together, our data suggest that changes in cell subpopulations associated with aging may facilitate the appearance of signs and symptoms of leprosy in elderly people exposed to *M. leprae*. Thus, the accumulation of memory $CD8^+$ and reduced frequency of $CD8^+CD28^+$ cells in elderly patients constitute important immunosenescence changes that compromise the activation of resistance mechanisms against *M. leprae*. Future studies are necessary to evaluate the senescent cells response to bacterial challenge, confirm their hyporesponsiveness when compared to non-senescent cells and still, verify the functional profile of these subsets. On this basis, the data shown in this study provide information and perspectives on the implications of immunosenescence in leprosy progression, which can be extended to other models of chronic infectious diseases.

DATA AVAILABILITY STATEMENT

The original contributions presented in the study are included in the article/**Supplementary Material**, further inquiries can be directed to the corresponding author/s.

ETHICS STATEMENT

The studies involving human participants were reviewed and approved by Institutional Ethics Committee of Oswaldo Cruz Foundation/FIOCRUZ (permit protocol number 27052919.0.0000.5248). The patients/participants provided their written informed consent to participate in this study.

AUTHOR CONTRIBUTIONS

DE: conceptualization. ES, MMo, RL, and DE: funding acquisition. PS, KC, TL-C, MMe, and JL: performed the experiments. JN, RL, and ES: clinical follow-up. PS, TL-C, MMe, FL, MMo, and DE: analyzed the data and writing. PS, MMo, and DE: review and editing. All authors contributed to the article and approved the submitted version.

FUNDING

PS was a postgraduate student sponsored by FIOCRUZ/CAPES (in Portuguese: Coordenação de Aperfeiçoamento de Pessoal de Nível Superior, number16.11.38.106). KC and TL-C were postgraduate students sponsored by FIOCRUZ/CNPq (in Portuguese: Conselho Nacional de Pesquisa e Desenvolvimento Tecnológico, numbers 18.08.38.140 and 18.08.18.013 respectively). MMe and JL were postgraduate student sponsored by FIOCRUZ/CNPq, numbers 15.06.38.062 and 18.03.37.105, respectively. MMo (process 313657/2018-1), ES (process 305105/2019-1), FL (process 31633/2017-7), and RL (process 309853/2019-2) are fellows sponsored by CNPq. This investigation received financial support from PAEF (in Portuguese: Projeto de Ações Estratégicas para Desenvolvimento e Fortalecimento dos Laboratórios Credenciados e das Áreas de Apoio à Pesquisa do IOC, process number IOC-023-FIO-18-2-41, MMo) and PAPES VI/CNPq/Fiocruz (process number 422.103/2017-9, DE). The funders had no role in the study design, data collection and analysis, decision to publish, or preparation of the manuscript.

ACKNOWLEDGMENTS

We are grateful to all the leprosy patients and non-leprosy volunteers for agreeing to participate in the study, as well as to Cristiane Domingues and José Augusto da Silva for their administrative assistance. Our recognition goes to Anna Beatriz Robottom Ferreira, a native speaker for editing the text.

SUPPLEMENTARY MATERIAL

The Supplementary Material for this article can be found online at: https://www.frontiersin.org/articles/10.3389/fimmu.2021.647385/full#supplementary-material

Supplementary Figure 1 | PD-1 ligands gene expression in blood and skin lesion samples. Expression of *PDCD1LG1* gene on **(A)** whole blood samples and **(B)** skin samples, and *PDCD1LG2* gene on **(C)** whole blood samples and **(D)** skin specimens. The results of gene expression of these PD-1 ligands are represented in normalized expression values. In the whole blood, the analysis was performed by Bio mark's microfluidic-based qPCR technology and in the cutaneous fragments, analysis was performed by RT-qPCR. Each circle represents an individual, and horizontal bars indicate the mean. Kruskal-Wallis test with Dunn's multiple comparison test correction was used to compare the groups.

Supplementary Table 1 | Oligonucleotides used in the study.

REFERENCES

1. Scollard DM, Adams LB, Gillis TP, Krahenbuhl JL, Truman RW, Williams DL. The continuing challenges of leprosy. *Clin Microbiol Rev.* (2006) 19:338–81. doi: 10.1128/CMR.19.2.338-381.2006
2. Foss NT, Motta AC. Leprosy, a neglected disease that causes a wide variety of clinical conditions in tropical countries. *Mem Inst Oswaldo Cruz.* (2012) 107(Suppl.1):28–33. doi: 10.1590/S0074-02762012000900006
3. Scollard DM, Truman RW, Ebenezer GJ. Mechanisms of nerve injury in leprosy. *Clin Dermatol.* (2015) 33:46–54. doi: 10.1016/j.clindermatol.2014.07.008
4. Lockwood DN, Saunderson PR. Nerve damage in leprosy: a continuing challenge to scientists, clinicians and service providers. *Int Health.* (2012) 4:77–85. doi: 10.1016/j.inhe.2011.09.006
5. Silva SR, Illarramendi X, Tempone AJ, Silva PH, Nery JA, Monteiro AM, et al. Downregulation of PHEX in multibacillary leprosy patients: observational cross-sectional study. *J Transl Med.* (2015) 13:296. doi: 10.1186/s12967-015-0651-5
6. Britton WJ, Lockwood DN. Leprosy. *Lancet.* (2004) 363:1209–19. doi: 10.1016/S0140-6736(04)15952-7
7. Ridley DS, Jopling WH. Classification of leprosy according to immunity. A five-group system. *Int J Lepr Other Mycobact Dis.* (1966) 34:255–73.
8. World Health Organization (WHO). *Guide to Eliminate Leprosy as a Public Health Problem*. 1st ed. Geneva: World Health Organization (1995).
9. Boyd SD, Liu Y, Wang C, Martin V, Dunn-Walters DK. Human lymphocyte repertoires in ageing. *Curr Opin Immunol.* (2013) 25:511–5. doi: 10.1016/j.coi.2013.07.007
10. Fülöp T, Larbi A, Pawelec G. Human T cell aging and the impact of persistent viral infections. *Front Immunol.* (2013) 4:271. doi: 10.3389/fimmu.2013.00271
11. Goronzy JJ, Fang F, Cavanagh MM, Qi Q, Weyand CM. Naïve T cell maintenance and function in human aging. *J Immunol.* (2015) 194:4073–80. doi: 10.4049/jimmunol.1500046
12. Carvalho JC, Araújo MG, Coelho-Dos-Reis JGA, Peruhype-Magalhães V, Alvares CC, Moreira ML, et al. Phenotypic and functional features of innate and adaptive immunity as putative biomarkers for clinical status and leprosy reactions. *Microb Pathog.* (2018) 125:230–9. doi: 10.1016/j.micpath.2018.09.011
13. Silva PHL, Santos LN, Mendes MA, Nery JAC, Sarno EN, Esquenazi D. Involvement of TNF-Producing CD8+ effector memory T cells with immunopathogenesis of erythema nodosum leprosum in leprosy patients. *Am J Trop Med Hyg.* (2019) 100:377–85. doi: 10.4269/ajtmh.18-0517
14. Vallejo AN, Brandes JC, Weyand CM, Goronzy JJ. Modulation of CD28 expression: distinct regulatory pathways during activation and replicative senescence. *J Immunol.* (1999) 162:6572–9.
15. Esensten JH, Helou YA, Chopra G, Weiss A, Bluestone JA. CD28 costimulation: from mechanism to therapy. *Immunity.* (2016) 44:973–88. doi: 10.1016/j.immuni.2016.04.020
16. Bour-Jordan H, Esensten JH, Martinez-Llordella M, Penaranda C, Stumpf M, Bluestone JA. Intrinsic and extrinsic control of peripheral T-cell tolerance by costimulatory molecules of the CD28/ B7 family. *Immunol Rev.* (2011) 241:180–205. doi: 10.1111/j.1600-065X.2011.01011.x
17. Huff WX, Kwon JH, Henriquez M, Fetcko K, Dey M. The evolving role of CD8+CD28- immunosenescent T cells in cancer immunology. *Int J Mol Sci.* (2019) 20:2810. doi: 10.3390/ijms20112810
18. Pera A, Caserta S, Albanese F, Blowers P, Morrow G, Terrazzini N, et al. CD28null pro-atherogenic CD4 T-cells explain the link between CMV infection and an increased risk of cardiovascular death. *Theranostics.* (2018) 8:4509–4519. doi: 10.7150/thno.27428
19. Teteloshvili N, Dekkema G, Boots AM, Heeringa P, Jellema P, de Jong D, et al. Involvement of MicroRNAs in the aging-related decline of CD28 expression by human T cells. *Front Immunol.* (2018) 9:1400. doi: 10.3389/fimmu.2018.01400
20. Liu Z, Tugulea S, Cortesini R, Suciu-Foca N. Specific suppression of T helper alloreactivity by allo-MHC class I-restricted CD8+CD28- T cells. *Int Immunol.* (1998) 10:775–83. doi: 10.1093/intimm/10.6.775
21. Chen X, Liu Q, Xiang AP. CD8+CD28- T cells: not only age-related cells but a subset of regulatory T cells. *Cell Mol Immunol.* (2018) 15:734–6. doi: 10.1038/cmi.2017.153
22. Liu Q, Zheng H, Chen X, Peng Y, Huang W, Li X, et al. Human mesenchymal stromal cells enhance the immunomodulatory function of CD8(+)CD28(-) regulatory T cells. *Cell Mol Immunol.* (2015) 12:708–18. doi: 10.1038/cmi.2014.118
23. Reiser J, Banerjee A. Effector, memory, and dysfunctional CD8(+) T cell fates in the antitumor immune response. *J Immunol Res.* (2016) 2016:8941260. doi: 10.1155/2016/8941260
24. Sridevi K, Neena K, Chitralekha KT, Arif AK, Tomar D, Rao DN. Expression of costimulatory molecules (CD80, CD86, CD28, CD152), accessory molecules (TCR alphabeta, TCR gammadelta) and T cell lineage molecules (CD4+, CD8+) in PBMC of leprosy patients using *Mycobacterium leprae* antigen (MLCWA) with murabutide and T cell peptide of T rat protein. *Int Immunopharmacol.* (2004) 4:1–4. doi: 10.1016/j.intimp.2003.09.001
25. Palermo Mde L, Trindade MÂ, Duarte AJ, Cacere CR, Benard G. Differential expression of the costimulatory molecules CD86, CD28, CD152 and PD-1 correlates with the host-parasite outcome in leprosy. *Mem Inst Oswaldo Cruz.* (2012) 107(Suppl.1):167–73. doi: 10.1590/S0074-02762012000900024
26. Dagur PK, Sharma B, Kumar G, Khan NA, Katoch VM, Sengupta U, et al. Mycobacterial antigen(s) induce anergy by altering TCR- and TCR/CD28-induced signalling events: insights into T-cell unresponsiveness in leprosy. *Mol Immunol.* (2010) 47:943–52. doi: 10.1016/j.molimm.2009.11.009
27. Guerreiro LTA, Robottom-Ferreira AB, Ribeiro-Alves M, Toledo-Pinto TG, Rosa Brito T, Rosa PS, et al. Gene expression profiling specifies chemokine, mitochondrial and lipid metabolism signatures in leprosy. *PLoS ONE.* (2013) 8:e64748. doi: 10.1371/journal.pone.0064748
28. Ramakers C, Ruijter JM, Lekanne Deprez RH, Moorman AFM. Assumption-free analysis of quantitative real-time PCR data. *Neurosci Lett.* (2003) 339:62–6. doi: 10.1016/S0304-3940(02)01423-4
29. Ruijter JM, Ramakers C, Hoogaars W, Bakker O, van den Hoff MJB, Karlen Y, et al. Amplification efficiency: linking baseline and bias in the analysis of quantitative PCR data. *Nucleic Acids Res.* (2009) 37:e45. doi: 10.1093/nar/gkp045
30. Rutledge R, Stewart D. A kinetic-based sigmoidal model for the polymerase chain reaction and its application to high-capacity absolute quantitative real-time PCR. *BMC Biotechnology.* (2008) 8:47. doi: 10.1186/1472-6750-8-47
31. R Core Team. *R: A Language and Environment for Statistical Computing.* (2020). Available online at: http://cran.r-project.org/ (accessed July 2, 2020).
32. Pfaffl, MW. A new mathematical model for relative quantification in real-time RT-PCR. *Nucleic Acids Res.* (2001) 29:e45. doi: 10.1093/nar/29.9.e45
33. Vandesompele J, De Preter K, Pattyn F, Poppe B, Van Roy N, De Paepe A, et al. Accurate normalization of real-time quantitative RT-PCR data by geometric averaging of multiple internal control genes. *Genome Biol.* (2002) 3:34. doi: 10.1186/gb-2002-3-7-research0034
34. Perkins JR, Dawes JM, Orengo C, McMahon SB, Bennett DL, Kohl M. ReadqPCR and NormqPCR: R packages for the reading, quality checking and normalisation of RT-qPCR quantification cycle (Cq) data. *BMC Genomics.* (2012) 13:296. doi: 10.1186/1471-2164-13-296
35. McElhaney JE, Effros RB. Immunosenescence: what does it mean to health outcomes in older adults? *Curr Opin Immunol.* (2009) 4:418–24. doi: 10.1016/j.coi.2009.05.023
36. Hakim FT, Gress RE. Immunosenescence: deficits in adaptive immunity in the elderly. *Tissue Antigens.* (2007) 70:179–89. doi: 10.1111/j.1399-0039.2007.00891.x
37. Cunha LL, Perazzio SF, Azzi J, Cravedi P, Riella LV. Remodeling of the immune response with aging: immunosenescence and its potential impact on COVID-19 immune response. *Front Immunol.* (2020) 11:1748. doi: 10.3389/fimmu.2020.01748
38. Oliveira JSS, Reis ALMD, Margalho LP, Lopes GL, Silva ARD, Moraes NS, et al. Leprosy in elderly people and the profile of a retrospective cohort in an endemic region of the Brazilian Amazon. *PLoS Negl Trop Dis.* (2019) 13:e0007709. doi: 10.1371/journal.pntd.0007709
39. Nobre ML, Illarramendi X, Dupnik KM, Hacker MA, Nery JA, Jerônimo SM, et al. Multibacillary leprosy by population groups in Brazil: Lessons from an observational study. *PLoS Negl Trop Dis.* (2017) 11:e0005364. doi: 10.1371/journal.pntd.0005364

40. Matos TS, Carmo RFD, Santos FGB, Souza CDF. Leprosy in the elderly population and the occurrence of physical disabilities: is there cause for concern? *Ann Bras Dermatol.* (2019) 94:243–5. doi: 10.1590/abd1806-4841.20198067
41. Snider H, Lezama-Davila C, Alexander J, Satoskar AR. Sex hormones and modulation of immunity against leishmaniasis. *Neuroimmunomodulation.* (2009) 16:106–13. doi: 10.1159/000180265
42. Bini EI, Mata Espinosa D, Marquina Castillo B, Barrios Payán J, Colucci D, Cruz AF, et al. The influence of sex steroid hormones in the immunopathology of experimental pulmonary tuberculosis. *PLoS ONE.* (2014) 9:e93831. doi: 10.1371/journal.pone.0093831
43. Pinzan CF, Ruas LP, Casabona-Fortunato AS, Carvalho FC, Roque-Barreira MC. Immunological basis for the gender differences in murine *Paracoccidioides brasiliensis* infection. *PLoS ONE.* (2010) 5:e10757. doi: 10.1371/journal.pone.0010757
44. Gupta S, Bi R, Su K, Yel L, Chiplunkar S Gollapudi S. Characterization of naive, memory and effector CD8+ T cells: effect of age. *Exp Gerontol.* (2004) 4:545–50. doi: 10.1016/j.exger.2003.08.013
45. Effros RB, Boucher N, Porter V, Zhu X, Spaulding C, Walford RL, et al. Decline in CD28+ T cells in centenarians and in long-term T cell cultures: a possible cause for both in vivo and *in vitro* immunosenescence. *Exp Gerontol.* (1994) 29:601–9. doi: 10.1016/0531-5565(94)90073-6
46. McKinney EF, Cuthbertson I, Harris KM, Smilek DE, Connor C, Manferrari G, et al. A CD8+ NK cell transcriptomic signature associated with clinical outcome in relapsing remitting multiple sclerosis. *Nat Commun.* (2021) 12:635. doi: 10.1038/s41467-020-20594-2
47. Sadhu S, Mitra DK. Emerging concepts of adaptive immunity in leprosy. *Front Immunol.* (2018) 9:604. doi: 10.3389/fimmu.2018.00604
48. Vlad G, Cortesini R, Suciu-Foca N. License to heal: bidirectional interaction of antigen-specific regulatory T cells and tolerogenic APC. *J Immunol.* (2005) 174:5907–14. doi: 10.4049/jimmunol.174.10.5907
49. Reker-Hadrup S, Strindhall J, Kollgaard T, Seremet T, Johansson B, Pawelec G, et al. Longitudinal studies of clonally expanded CD8 T cells reveal a repertoire shrinkage predicting mortality and increased number of dysfunctional cytomegalovirus-specific T cells in the elderly. *J Immunol.* (2006) 176:2645–53. doi: 10.4049/jimmunol.176.4.2645
50. Wikby A, Månsson IA, Johansson B, Strindhall J, Nilsson SE. The immune risk profile is associated with age and gender: findings from three Swedish population studies of individuals 20-100 years of age. *Biogerontology.* (2008) 9:299–308. doi: 10.1007/s10522-008-9138-6
51. Derhovanessian E, Larbi A, Pawelec G. Biomarkers of human immunosenescence: impact of Cytomegalovirus infection. *Curr Opin Immunol.* (2009) 21:440–5. doi: 10.1016/j.coi.2009.05.012
52. Schwanninger A, Weinberger B, Weiskopf D, Herndler-Brandstetter D, Reitinger S, Gassner C, et al. Age-related appearance of a CMV-specific high-avidity CD8+ T cell clonotype which does not occur in young adults. *Immun Ageing.* (2008) 5:14. doi: 10.1186/1742-4933-5-14
53. Nikolich-Zugich J. Ageing and life-long maintenance of T-cell subsets in the face of latent persistent infections. *Nat Rev Immunol.* (2008) 8:512–22. doi: 10.1038/nri2318
54. Tsaknaridis L, Spencer L, Culbertson N, Hicks K, LaTocha D, Chou YK, et al. Functional assay for human CD4+CD25+ Treg cells reveals an age-dependent loss of suppressive activity. *J Neurosci Res.* (2003) 74:296–308. doi: 10.1002/jnr.10766
55. Lages CS, Suffia I, Velilla PA, Huang B, Warshaw G, Hildeman DA, et al. Functional regulatory T cells accumulate in aged hosts and promote chronic infectious disease reactivation. *J Immunol.* (2008) 181:1835–48. doi: 10.4049/jimmunol.181.3.1835
56. Graydon CG, Balasko AL, Fowke KR. Roles, function and relevance of LAG3 in HIV infection. *PLoS Pathog.* (2019) 15:e1007429. doi: 10.1371/journal.ppat.1007429
57. Do JS, Visperas A, Sanogo YO, Bechtel JJ, Dvorina N, Kim S, et al. An IL-27/Lag3 axis enhances Foxp3+ regulatory T cell-suppressive function and therapeutic efficacy. *Mucosal Immunol.* (2016) 9:137–45. doi: 10.1038/mi.2015.45
58. Huang CT, Workman CJ, Flies D, Pan X, Marson AL, Zhou G, et al. Role of LAG-3 in regulatory T cells. *Immunity.* (2004) 21:503–13. doi: 10.1016/j.immuni.2004.08.010
59. Chaves AT, Ribeiro-Junior AF, Lyon S, Medeiros NI, Cassirer-Costa F, Paula KS, et al. Regulatory T cells: Friends or foe in human *Mycobacterium leprae* infection? *Immunobiology.* (2018) 223:397–404. doi: 10.1016/j.imbio.2017.11.002
60. Nguyen LT, Ohashi PS. Clinical blockade of PD1 and LAG3-potential mechanisms of action. *Nat Rev Immunol.* (2015) 15:45–56. doi: 10.1038/nri3790

Conflict of Interest: The authors declare that the research was conducted in the absence of any commercial or financial relationships that could be construed as a potential conflict of interest.

Citation: da Silva PHL, de Castro KKG, Mendes MA, Leal-Calvo T, Leal JMP, Nery JAdC, Sarno EN, Lourenço RA, Moraes MO, Lara FA and Esquenazi D (2021) Presence of Senescent and Memory CD8+ Leukocytes as Immunocenescence Markers in Skin Lesions of Elderly Leprosy Patients. Front. Immunol. 12:647385. doi: 10.3389/fimmu.2021.647385

frontiers in Immunology

ORIGINAL RESEARCH
published: 16 March 2021
doi: 10.3389/fimmu.2021.642711

Staphylococcus aureus-Specific Tissue-Resident Memory CD4$^+$ T Cells Are Abundant in Healthy Human Skin

Astrid Hendriks[1,2†], *Malgorzata Ewa Mnich*[1,2†], *Bruna Clemente*[1], *Ana Rita Cruz*[1,2], *Simona Tavarini*[1], *Fabio Bagnoli*[1] *and Elisabetta Soldaini*[1*]

[1] GSK, Siena, Italy, [2] Medical Microbiology, University Medical Center Utrecht, Utrecht University, Utrecht, Netherlands

The skin is an immunocompetent tissue that harbors several kinds of immune cells and a plethora of commensal microbes constituting the skin microbiome. *Staphylococcus aureus* is a prominent skin pathogen that colonizes a large proportion of the human population. We currently have an incomplete understanding of the correlates of protection against *S. aureus* infection, however genetic and experimental evidence has shown that CD4$^+$ T cells play a key role in orchestrating a protective anti-*S. aureus* immune response. A high *S. aureus*-specific memory CD4$^+$ T cell response has been reported in the blood of healthy subjects. Since T cells are more abundant in the skin than in blood, we hypothesized that *S. aureus*-specific CD4$^+$ T cells could be present in the skin of healthy individuals. Indeed, we observed proliferation of tissue-resident memory CD4$^+$ T cells and production of IL-17A, IL-22, IFN-γ and TNF-β by cells isolated from abdominal skin explants in response to heat-killed *S. aureus*. Remarkably, these cytokines were produced also during an *ex vivo* epicutaneous *S. aureus* infection of human skin explants. These findings highlight the importance of tissue-resident memory CD4$^+$ T cells present at barrier sites such as the skin, a primary entry site for *S. aureus*. Further phenotypical and functional characterization of these cells will ultimately aid in the development of novel vaccine strategies against this elusive pathogen.

Keywords: *Staphylococcus aureus*, infection, immunity, human skin, tissue-resident memory T cells, CD4$^+$ T cells

OPEN ACCESS

Edited by:
Fabienne Tacchini-Cottier, University of Lausanne, Switzerland

Reviewed by:
Mirian Nacagami Sotto, University of São Paulo, Brazil
Oliver Harrison, Benaroya Research Institute, United States

***Correspondence:**
Elisabetta Soldaini
elisabetta.x.soldaini@gsk.com

†These authors have contributed equally to this work and share first authorship

Specialty section:
This article was submitted to Microbial Immunology, a section of the journal Frontiers in Immunology

Received: *16 December 2020*
Accepted: *18 February 2021*
Published: *16 March 2021*

Citation:
Hendriks A, Mnich ME, Clemente B, Cruz AR, Tavarini S, Bagnoli F and Soldaini E (2021) Staphylococcus aureus-Specific Tissue-Resident Memory CD4$^+$ T Cells Are Abundant in Healthy Human Skin. Front. Immunol. 12:642711. doi: 10.3389/fimmu.2021.642711

INTRODUCTION

The skin provides a physical and immunological barrier for invading pathogens, while also maintaining symbiotic interactions with skin commensals. There are numerous specialized immune cells present in the skin that maintain skin homeostasis and act as the first line of defense against pathogens. It has been estimated that human skin contains roughly twice as many memory T cells than blood (1). Different memory T cell subsets can be phenotypically identified in human skin based on the presence of surface markers and the capacity to emigrate and enter the circulation. Tissue resident memory T (Trm) cells are a subset of memory T cells phenotypically and functionally distinct from their circulating counterparts (1, 2). In particular, human skin-resident memory T (Tsrm) cells can be identified through the surface expression of the skin-homing marker cutaneous lymphocyte-associated antigen (CLA), the memory T cell marker CD45RO and the tissue-retention marker CD69. CLA binds selectively and avidly to the vascular lectin

E-selectin while CD69 prevents sphingosine-1-phosphate receptor 1 mediated egress from tissues into the circulation (3). Skin-resident T cell memory has been observed in response to *Candida albicans*, *Leishmania major*, Herpes simplex virus as well as commensal bacteria. Most importantly, Tsrm cells contribute to localized protection against re-infection with cutaneous pathogens (4–9). In addition, Trm cell development has been tracked in mice following vaccination and was positively correlated with vaccination efficacy (10–13), making Trm cells a promising target for vaccination (14–19).

The Gram-positive bacterium *Staphylococcus aureus* is the leading cause of skin and soft tissue infections globally (20). In addition, the rapid emergence of antibiotic resistance has highlighted the need for alternative treatments such as vaccination to combat *S. aureus* infections. However, to design an efficacious vaccine, it is important to have a complete understanding of the correlates of protection against this pathogen, which is currently lacking (21, 22).

Based on data from mouse and human studies, there is a general consensus that $CD4^+$ T cells, and in particular Th17 and Th1 subsets, contribute to protective immunity against *S. aureus* infection (23–26). Furthermore, healthy individuals have a considerable number of circulating memory $CD4^+$ T cells specific for *S. aureus*, likely due to repeated encounters over time with this skin pathobiont (27, 28). However, to our knowledge, the existence of *S. aureus*-specific tissue resident memory $CD4^+$ T cells in healthy human skin has not yet been addressed.

Using human skin explants, which represent a valuable model to study skin-resident immune responses of human skin to microbes (29), we here show that *S. aureus*-specific $CD4^+$ Tsrm cells are commonly found in the skin of healthy individuals. This finding uncovers $CD4^+$ Tsrm cells as previously neglected cellular players in the cutaneous human immune response to *S. aureus* and thus may aid in the development of novel vaccine strategies against *S. aureus* SSTIs.

MATERIALS AND METHODS

Preparation of Single Cell Suspensions From Human Skin Explants

Fresh human skin explants (16 cm^2) derived from abdominoplasty surgical waste of healthy women (age 40 ± 11, body mass index 25 ± 3) were purchased from Biopredic (France). Explants were shipped at 4°C and received within 48 h following the surgery. Upon arrival, samples were immediately processed as shown in **Figure 1A**. In short, adipose tissue was removed with dissection scissors followed by additional scraping with a disposable scalpel (Swann-Morton, Sheffield). Skin was cut in 1 cm^2 pieces, washed repeatedly with PBS and incubated for 1 h at RT in RPMI 1640 (Invitrogen) containing 1 mg/ml collagenase type 1 (Life technologies). Next, skin pieces were extensively minced with disposable scalpels and incubated overnight at 37°C at 5% CO_2 in a 6-well plate with 1 mg/ml collagenase type 1 (Life technologies) and 20 μg/ml DNAse (Sigma) in 5 ml c-RPMI [RPMI 1640 containing penicillin-streptomycin-glutamine, sodium pyruvate, minimum essential medium non-essential amino acids (all from Gibco), and 10% heat-inactivated FBS (Hyclone)]. The next day, the skin cell suspension was pipetted vigorously, pooled and filtered sequentially through a 100 μm and a 40 μm cell strainers (Corning). Skin debris was further removed by Ficoll-Paque Premium (GE Healthcare) gradient separation. The viability (83% ± 6.5) and the cell yield (0.63 ± 0.33 × 10^6 cells/cm^2 skin) of the obtained single cell suspensions were assessed with a Vi-CELL XR cell counter (Beckman Coulter).

Heat-Killed (HK) Microbes

Methicillin resistant *S. aureus* USA300 LAC strain and the coagulase negative staphylococci *S. epidermidis* 1457 strain and *S. lugdunensis* SL13 strain were grown to mid-exponential phase (OD_{600} 0.6) (30, 31). Next, bacteria were washed with PBS to remove secreted proteins, resuspended in sterile PBS, plated on Tryptic Soy Agar (TSA) for CFU counts and inactivated in a dry block heater at 90°C for 45 min. After inactivation bacteria were washed three times with PBS and protein content was measured using the Pierce™ BCA Protein Assay kit (Thermo Scientific). Samples concentrations were adjusted to 25 μg/ml, which corresponds to ∼1 × 10^8 CFU/ml (25). Bacterial killing was verified by plating the HK bacteria for 5 days on TSA. Heat-killed (HK) bacteria were aliquoted and stored at −20°C. HK *S. epidermidis* (FDA strain PCI 1200), HK *C. albicans* (ATCC 10231), and HK *E. coli* (O111:B4) were purchased from Invivogen.

$CD4^+$ T Cell Proliferation and Cytokine Production in Response to HK Microbes by Click-iT EdU/V-PLEX Assay

Single cell suspensions obtained from the skin explants were seeded at 500,000 live cells/well for all conditions but CD3/CD28 (for which half the number of cells were plated) in a final volume of 200 μl c-RPMI in round-bottom 96 wells plates (Corning). Cells were rested for at least 24 h at 37°C with 5% CO_2 to restore surface marker expression and reduce cellular stress due to the isolation procedure. Cell culture medium was replaced with: (1) fresh medium alone (no stimulation, negative control) or containing: (2) 10^6 CFU HK microbes corresponding to a multiplicity of infection of 2; (3) Tetanus toxoid (5 μg/ml, Novartis); (4) anti-CD28 (2 μg/ml, clone CD28.2, BD Bioscience, cat # 555725) added to anti-CD3 (1 μg/ml, clone OKT3, BD Bioscience, cat # 566685) coated wells (CD3/CD28, polyclonal stimulation, positive control). After 3 days of culture the thymidine analog EdU (10 μM) was added to the cultures for the last 16 h. At day four, cell culture supernatants were collected and stored at −20°C for cytokine analysis while $CD4^+$ T cell proliferation was assessed by Click-iT EdU assay (Click-iT Plus EdU Alexa Fluor 488 Flow cytometry assay kit, Invitrogen), as recently described (Clemente et al., manuscript in preparation). Cytokines were measured using the 27-V-PLEX human kit (MesoScale Discovery) following manufacturer's instructions. Plates were analyzed by a MESO Quickplex SQ 120 reader and cytokine concentrations were determined using MSD discovery

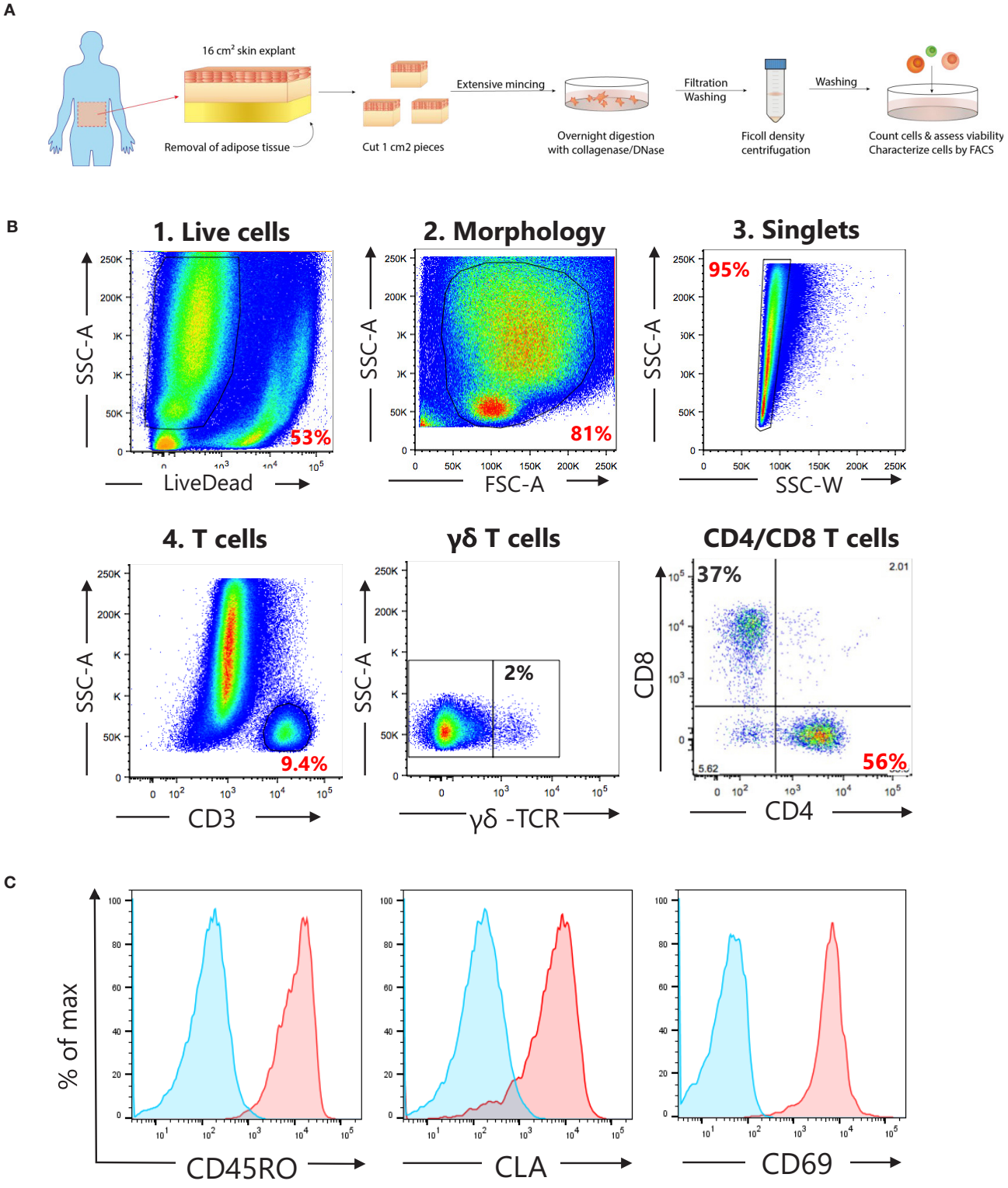

FIGURE 1 | Characterization of T cell subsets in cell suspensions obtained from human skin explants. **(A)** Schematic overview of the protocol used to obtain single cell suspensions from human skin explants. **(B)** Gating strategy to analyze T cell subsets, γδ-, $CD4^+$, and $CD8^+$ T cells, in single cell suspensions. **(C)** Representative histograms (in red) showing the surface expression for skin resident memory T cells markers, CD45RO (memory), CLA (skin homing), and CD69 (tissue retention) on live $CD4^+$ cells. Blue histograms represent unstained cells.

workbench 4.0. Values below or above the detection limits were given the value of ½ LLOD (Lower Limit Of Detection) or 2x ULOD (Upper Limit Of Detection), respectively. Cytokines that were consistently above or below the detection limits, or showed no differences across all stimuli were excluded from further analysis.

Flow Cytometry

For the phenotypic characterization of T cell subsets in the single skin cell suspensions, cells were stained with Live/Dead Near-IR Dead cell stain kit (Invitrogen) for 20 min at room temperature (RT), washed and blocked with 2% rabbit serum in PBS on ice for 20 min. Next, cells were stained for CD4, CD8, γδ-TCR, CD45RO, CLA, and CD69 for 20 min at 4°C, washed with PBS, and fixed with Cytofix (BD Bioscience). Gating strategy is shown in **Figure 1B**.

For T cell proliferation experiments, after surface staining with CD4, CD8, CD45RO and CLA and fixation, cells were permeabilized with PBS 1% BSA, 0.5% saponin for 30 min at 4°C, washed with PBS 1% BSA, 0.5% saponin followed by the Click-iT reaction (Click-iT Plus EdU Alexa Fluor 488 Flow cytometry assay kit, Invitrogen). After 30 min at RT, cells were washed with PBS 1% BSA, 0.5% saponin and stained for CD3 for 15 min at RT. After two washes, the cells were analyzed on a BD LSR II flow cytometer, and data was analyzed using FlowJo 10 (TreeStars). All antibodies used in this study are shown in **Supplementary Table 1**.

Cytokine Production in Response to *ex vivo* Epicutaneous *S. aureus* Infection of Human Skin Explants

Infection of human skin explants was performed according to a previously described protocol (32). In short, after removal of adipose tissue, the skin sheet was pinned in a dissection board and stripped 30 times with a hypoallergenic tape (Transpore, 3M). Eight mm punch biopsies were collected using disposable biopsy punches (Kai Medical). The punches were washed with culture medium (Advanced DMEM; Gibco) once, followed by two washes with PBS to remove antibiotics. Next, the punches were placed in 12-well transwell plates with 0.4 μm pore size (Corning), containing 1 ml of culture medium. Finally, the punches were infected in duplicate with USA300 LAC strain (5×10^6 CFU in 1 μl PBS) and cultured at air-liquid interface for 2, 24, or 72 h at 37°C, 5% CO_2. At each indicated time point, culture supernatants were collected, filtered and stored at −20°C for cytokine analysis that was performed using the 27-V-PLEX human kit (MesoScale Discovery).

Statistical Analysis

GraphPad Prism 8.0.1 was used to perform statistical analysis. Data were analyzed using one-way ANOVA with Dunnett's test, paired Wilcoxon test or paired *t*-test, as indicated. Significant differences ($p < 0.05$) are shown.

RESULTS

Tissue-Resident Memory CD4$^+$ T Cells Present in the Skin of Healthy Subjects Proliferate in Response to *S. aureus*

To investigate if healthy human skin contains CD4$^+$ Tsrm cells specific for *S. aureus,* we stimulated single cell suspensions prepared from skin explants from eight healthy donors with heat-killed (HK) *S. aureus*. The vast majority (>90%) of the isolated CD4$^+$ T cells had a Tsrm phenotype based on the surface expression of the memory marker CD45RO, the skin-tropic marker CLA and the tissue-retention marker CD69 (**Figure 1C**). After 4 day stimulation with HK microbes, we identified CD4$^+$ T cells that have neo-synthesized DNA by the flow cytometry-based Click-iT EdU proliferation assay (CD4$^+$EdU$^+$ cells, **Figures 2A,B**). These cells were CD4$^+$ Tsrm based on their expression of CD45RO and CLA (**Supplementary Figure 1**). As shown in **Figure 2C**, the analysis of 8 healthy subjects showed a statistically significant CD4$^+$ Tsrm cell proliferation in response to HK *S. aureus* but not to HK *S. epidermidi*s, which is a major component of the human skin microbiome (33). In agreement with previous studies, we observed specific CD4$^+$ Tsrm cell proliferation in response to *C. albicans* (**Figure 2C**) (6), while no proliferation was observed in response to *E. coli*, which is not part of the skin microbiome (**Figure 2C**). Interestingly, a strong proliferation of CD4$^+$ Tsrm cells was also induced by the recall antigen Tetanus toxoid (**Figure 2C**) that commonly induces a strong T cell response in human blood (27, 34). Polyclonal T cell stimulation with anti-CD3/CD28 antibodies, which was used as positive control, induced the strongest CD4$^+$ Tsrm cell proliferation in all donors as expected (**Figure 2C**).

Heat-inactivated intact bacteria have been described to be devoid of superantigens, which stimulate T cells in a non-specific manner (25, 35). To further prove that the observed CD4$^+$ Tsrm cell proliferation was antigen-specific, we added MHC class-II blocking antibodies or the isotype control to the skin cell cultures. Indeed, in the presence of MHC-II blocking antibodies, CD4$^+$ T cell proliferation in response to HK *S. aureus* was abolished while the isotype control had no effect (**Figure 2D**). In addition, no CD4$^+$ T cell proliferation was detected by Click-iT EdU assay upon stimulation of peripheral blood mononuclear cells (PBMCs) of some healthy subjects with HK *S. aureus*, while a strong proliferation was observed in response to the staphylococcal T cell superantigen SEB, as expected (**Supplementary Figure 2A**).

To further assess the staphylococcal species-specificity on CD4$^+$ Tsrm cell proliferation, we analyzed the proliferative response to the coagulase-negative *S. lugdunensis*, which is also a skin commensal (33). Analysis of cells obtained from explants from five healthy subjects showed no proliferation in response to either *S. lugdunensis* SL13 strain or *S. epidermidis* 1457 strain while proliferation to *S. aureus* USA300 LAC strain was confirmed (**Supplementary Figure 2B**). Taken together, these findings support the presence of *S. aureus*-specific CD4$^+$ tissue-resident memory T cells in healthy human skin.

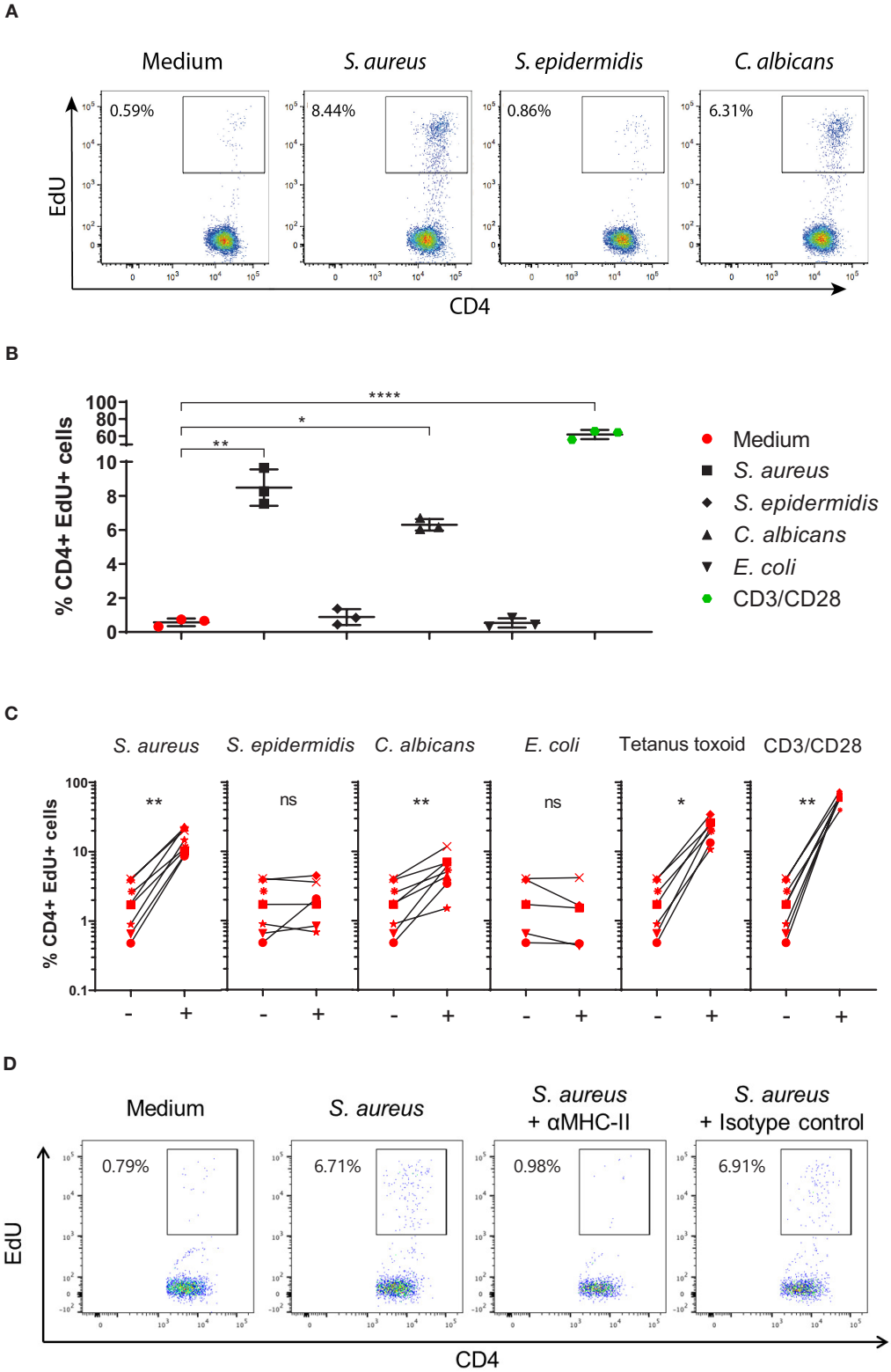

FIGURE 2 | Tissue-resident memory CD4$^+$ T cells present in the skin of healthy subjects proliferate in response to *S. aureus*. **(A)** Representative dot-plots showing CD4$^+$EdU$^+$ cells in cell cultures, obtained from a skin explant of an healthy subject, stimulated for 4 days with heat-killed (HK): *S. aureus* USA300 LAC strain,

(Continued)

FIGURE 2 | *S. epidermidis* PCI 1200 strain, *C. albicans*, or left unstimulated (medium). **(B)** Reproducibility of the Click-iT EdU assay. Representative results showing the percentages of $CD4^+EdU^+$ T cells obtained from triplicate skin cell cultures from the healthy subject shown in **(A)** in response to different stimuli. $^*p < 0.05$, $^{**}p < 0.01$, $^{****}p < 0.0001$ as assessed by one-way ANOVA. **(C)** Proliferation of $CD4^+$ Tsrm cells from skin explants of 8 healthy subjects in response to different HK microbes, Tetanus toxoid, anti-CD3/anti-CD28 antibodies or medium alone. Average percentages of $CD4^+EdU^+$ cells of each of the 8 subjects analyzed, in triplicate, are shown by an identifying symbol. Per donor, each stimulated group, indicated by a +, was compared to the non-stimulated group (medium), indicated by a –, by paired Wilcoxon test, $^*p < 0.05$, $^{**}p < 0.01$. **(D)** Representative dot plots showing proliferating $CD4^+$ Tsrm cells ($CD4^+EdU^+$) after 4-day culture in medium alone (negative control) or with HK *S. aureus* alone or in combination with MHC class-II blocking antibodies or isotype control antibodies.

Cells Isolated From the Skin of Healthy Subjects Produce Pro-inflammatory Cytokines in Response to *S. aureus*

To further investigate the response of healthy human skin to *S. aureus*, we analyzed the cytokine profile in the supernatants of *S. aureus*-specific $CD4^+$ Tsrm cells analyzed by Click-iT EdU assay (**Figure 2C**), collected after 4 days of stimulation, by 27-V-PLEX. As shown in **Figure 3**, significant increases in production of IL-17A (141.20 vs. 12.34 pg/ml), IL-22 (131.67 vs. 4.22 pg/ml), IFN-γ (176.61 vs. 78.82 pg/ml), GM-CSF (138.73 vs. 13.34 pg/ml), and TNF-β (18.48 vs. 1.84 pg/ml) were observed in response to HK *S. aureus* stimulation while HK *S. epidermidis* induced a significant increase in IL-17A production only (48.29 vs. 12.34 pg/ml). Interestingly, *C. albicans,* as well as Tetanus toxoid and the polyclonal stimulation with anti-CD3/CD28 antibodies induced the same pattern of cytokines as *S. aureus* while in response to *E. coli* none of the analyzed cytokines was induced. Remarkably, the production of IL-17A, IL-22, IFN-γ, GM-CSF, and TNF-β in response to HK *S. aureus* stimulation were substantially decreased by MHC class II blocking antibodies, indicating that $CD4^+$ Tsrm cells were a major source of these cytokines (data not shown). In addition we obtained direct evidence of IL-17A and IL-22 production by $CD4^+EdU^+$ Tsrm cells by intracellular cytokine staining (data not shown).

Ex vivo Epicutaneous *S. aureus* Infection of Healthy Human Skin Induces Pro-inflammatory Cytokines

To understand the local immune response to *S. aureus* within healthy human skin, we used an *ex vivo* epicutaneous infection model (32). Skin explants were tape-stripped to remove the *stratum corneum,* followed by topical application of 5×10^6 CFU *S. aureus* USA300 LAC strain. Cytokines were quantified in the skin explants culture media by 27-V-PLEX at different time-points post infection (p.i.). At 24 h p.i. only IL-10, IL-1α, and IL-2 were produced at significantly higher levels compared to the non-infected control while at 72 h p.i. also IL-17A, IL-22, IFN-γ, IL-1α, IL-1β, GM-CSF, IL-12p40, TNF-α, and TNF-β levels were increased (**Figure 4**). These data show that, while at an initial stage of *S. aureus* infection the cytokine response of the skin is limited, it becomes strongly proinflammatory at later stages of infection. Furthermore, the cytokines induced by stimulation of cells extracted from the skin with HK *S. aureus*, namely IL-17A, IL-22, GM-CSF, IFN-γ, and TNF-β, were induced also by epicutaneous infection of human skin with live *S. aureus*, strengthening the value of this *in vitro* model.

DISCUSSION

Here, we show that *S. aureus*-specific $CD4^+$ tissue-resident memory T cells are abundant in the skin of healthy subjects. In particular, by the use of a novel assay, Click-iT EdU/V-PLEX, which allows simultaneous detection of $CD4^+$ T cell proliferation and cytokine quantification in cell culture supernatants, we revealed that stimulation of cells isolated from abdominal skin explants with HK *S. aureus* USA300 LAC strain induced: (1) The proliferation of $CD4^+$ T cells that were identified as skin-resident memory T (Tsrm) cells based on the expression of the CLA skin-homing, CD45RO memory, and CD69 tissue-retention markers. (2) The secretion of proinflammatory cytokines, namely IL-17A, IL-22, GM-CSF, IFN-γ, and TNF-β. Remarkably, neither proliferation of $CD4^+$ Tsrm cells nor secretion of proinflammatory cytokines except for IL-17A was observed in response to the common skin commensal *S. epidermidis*.

Mechanisms enabling the host to mount protective immune responses against pathogens while establishing a privileged relationship with commensal bacteria have been intensively studied but still remain largely unknown. One important feature of commensal-specific immunity is its uncoupling from inflammation and the maintenance of tissue homeostasis (8). Cytokines play a key role not only in the promotion of skin inflammation but also in skin homeostasis. Cytokine analysis of culture medium of both isolated skin cells stimulated with HK *S. aureus* and human skin explants infected *ex vivo* with *S. aureus* showed the production of cytokines involved in skin inflammation and tissue repair. Genetic evidence has highlighted a key role for IL-17-mediated immunity in protection against *S. aureus* skin infection, but not invasive staphylococcal disease, similarly to what has been observed for *C. albicans* infections (36, 37). IL-17 enhances the recruitment of neutrophils, which can kill *S. aureus*, to the site of infection, and stimulates the production of antimicrobial peptides (AMPs) that can be directly bactericidal (38–40). IL-22 promotion of skin inflammation is well-established (41), however a role of IL-22 in skin homeostasis has also emerged. In particular, IL-22 has been shown to induce the proliferation of keratinocytes and AMPs production (42, 43). In addition, IL-22 induces MHC class II expression on keratinocytes thereby promoting the selective accumulation of commensal-induced IFN-γ producing $CD4^+$ T cells within murine skin (44). TNF-β induces angiogenesis, thereby contributing to wound repair (45, 46). Interestingly, cytokine analysis of human skin explants infected epicutaneously with *S. aureus* revealed also a significant production of IL-1α and IL-1β (**Figure 4**). These results are in agreement with previous studies showing that these cytokines were produced by

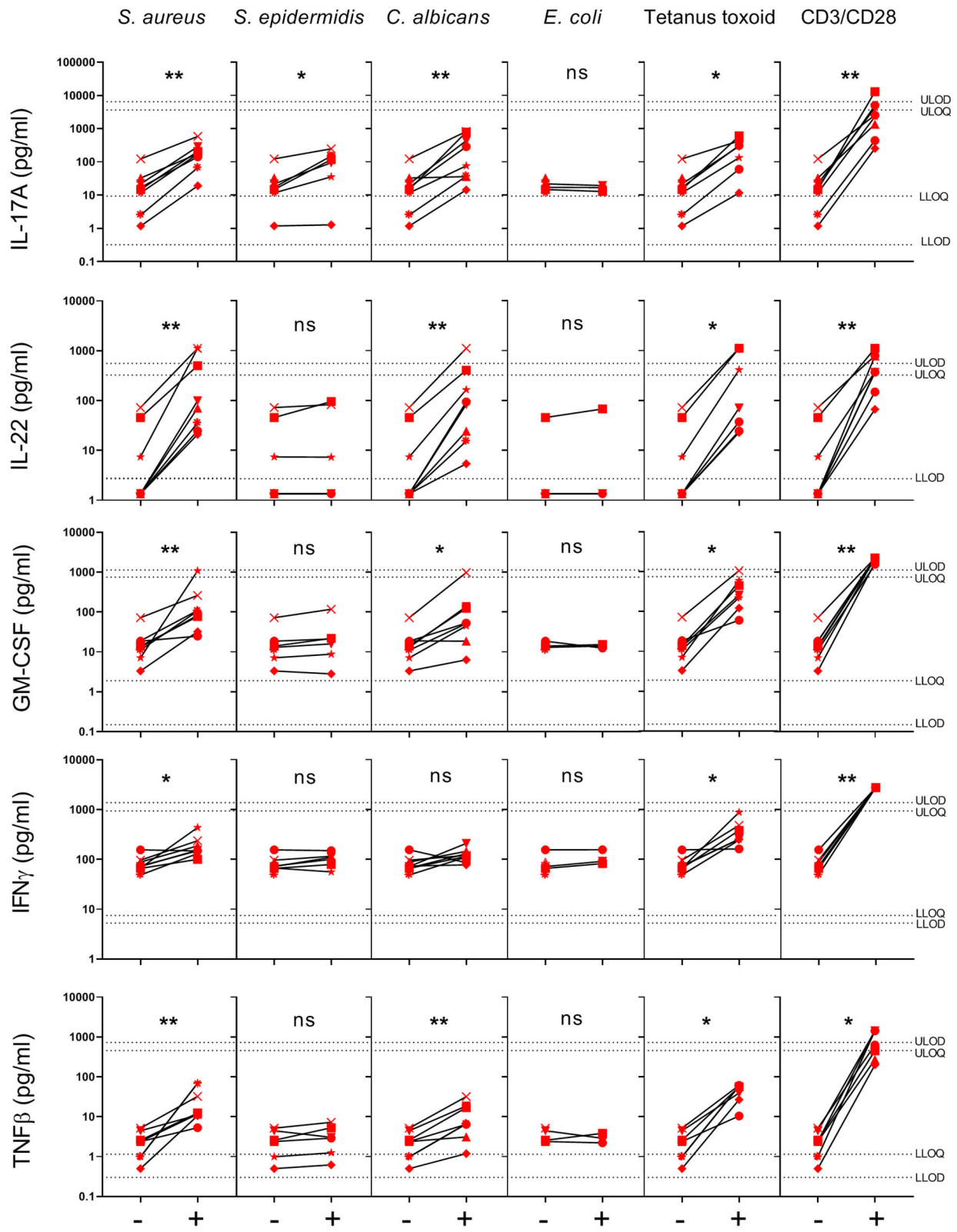

FIGURE 3 | Cytokines secreted in the supernatants of skin cell cultures stimulated with different HK microbes. Supernatants were collected from samples used to determine $CD4^+$ Tsrm cell proliferation by the Click-iT EdU assay. Cytokines were quantified by V-PLEX assays. Cytokine production in response to the different stimuli is shown for 8 donors (indicated by individual symbols), except for Tetanus toxoid (7), *S. epidermidis* (6) and *E. coli* (3). Per donor, each stimulated group, indicated by a +, was compared to the non-stimulated group (medium), indicated by a –, by paired Wilcoxon test, $^*p < 0.05$, $^{**}p < 0.01$. LLOD, Lower limit of detection; ULOD, upper limit of detection; LLOQ, lower limit of quantification; ULOQ, upper limit of quantification.

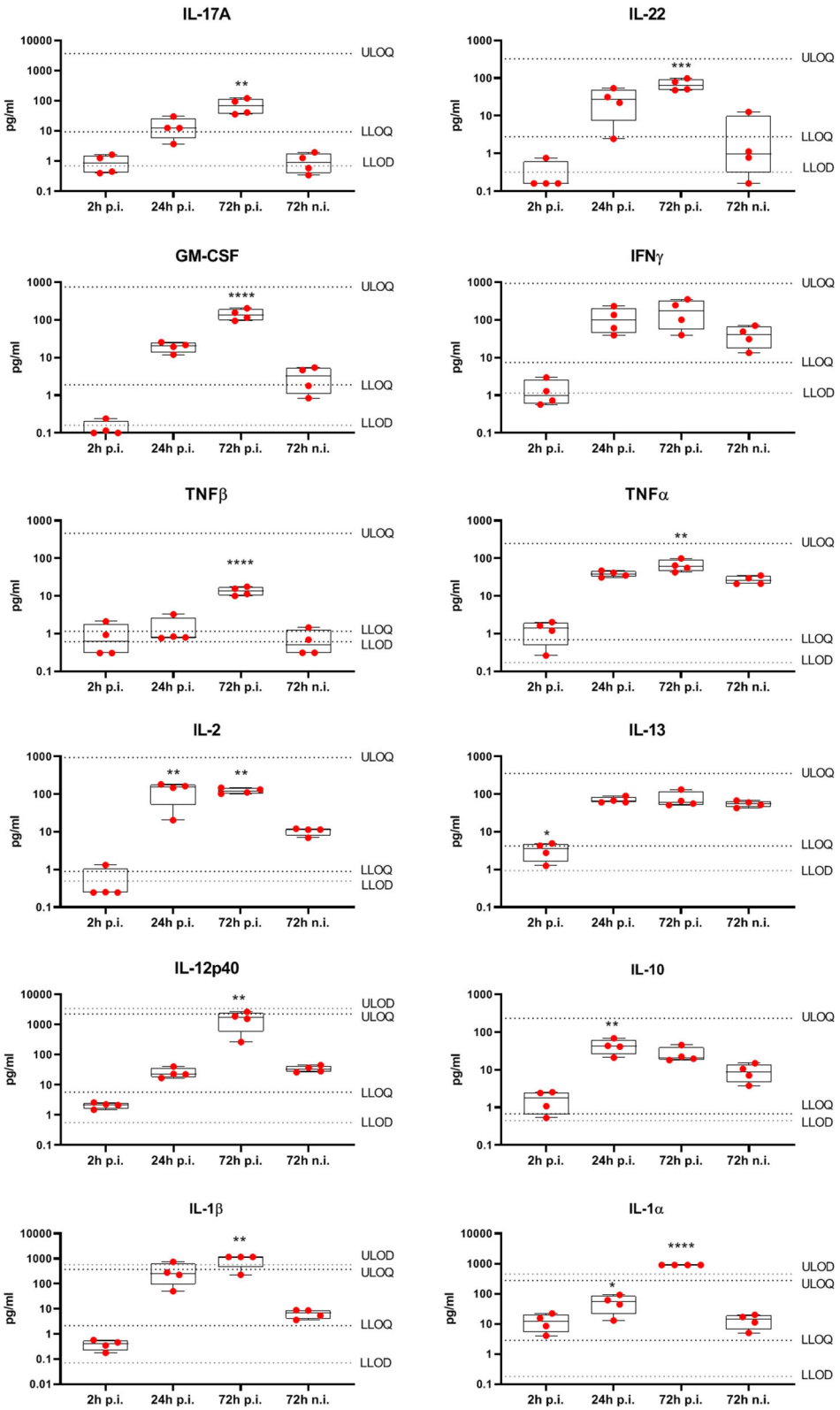

FIGURE 4 | Cytokines produced by human skin from healthy subjects in response to *ex vivo* epicutaneous *S. aureus* USA300 LAC infection. Eight mm biopsy punches, prepared from tape stripped human skin explants from four donors, were put in transwells at air-liquid interface and infected epicutaneously with 5×10^6 CFU

(Continued)

FIGURE 4 | *S. aureus* USA300 LAC strain in duplicate, or were left non-infected (n.i.) for 2, 24, or 72 h when culture medium was collected. Cytokine concentrations were assessed by V-PLEX assay. Box-and-whiskers extend from the 25th to 75th percentiles and the line inside the box represents the median. LLOD, Lower limit of detection; ULOD, upper limit of detection; LLOQ, lower limit of quantification; ULOQ, upper limit of quantification. Differences between cytokine concentrations measured at 2, 24, 72 hpi were compared with non-infected control at 72 h using an one-way ANOVA, $^{*}p < 0.05$, $^{**}p < 0.01$, $^{***}p < 0.001$, $^{****}p < 0.0001$.

murine keratinocytes after an epicutaneous *S. aureus* challenge (47, 48). The lack of IL-1 production by isolated human skin cells stimulated with HK *S. aureus* could be due to the lack of secreted bacterial proteins, including alpha-toxin that has a prominent role in the induction of IL-1 production by keratinocytes (49).

The Click-iT EdU/V-PLEX assay does not allow the identification of the cellular source of the detected cytokines. However, since we observed that the polyclonal T cell stimulation with anti-CD3/CD28 antibodies induced the same cytokine profile as HK *S. aureus* stimulation, and MHC class II blocking antibodies substantially decreased the production of these cytokines in response to HK *S. aureus* stimulation (data not shown) it seems likely that $CD4^+$ Tsrm cells are a major source of the observed cytokines (50), although cytokine production by non-classical T cells cannot be ruled out (51–53). In addition we obtained direct evidence of IL-17A and IL-22 production by $CD4^+EdU^+$ Tsrm cells by intracellular cytokine staining (data not shown). It should be noted that studies, performed both in human and murine skin, suggest that Trm cells accumulate in the skin as a function of the number of infectious and inflammatory events over time. Indeed, laboratory mice, like newborn, but not adult, humans lack effector-differentiated and peripherally distributed memory T cells, including Tsrm cells (54, 55). In mice, γδ T cells have been identified as key IL-17 producers upon *S. aureus* infection (52). However, it has been shown that following infection of laboratory mice with *C. albicans*, while the initial IL-17-producing cells were γδ T cells, at later times the majority of *C. albicans*-reactive IL-17-producing T cells were $CD4^+$ Tsrm cells. Importantly, IL-17-producing $CD4^+$ Trm cells that responded to *C. albicans* were identified in normal human skin (4). Similarly, since humans, unlike laboratory mice, naturally encounter *S. aureus* repeatedly over time, we hypothesize that $CD4^+$ Tsrm cells are the primary source of IL-17 produced in response to this bacterium in human skin. Indeed, comparable levels of IL-17A were produced in response to HK *S. aureus* or *C. albicans* in our experiments. On the other hand, *S. epidermidis* colonization of mouse skin has been shown to induce IL-17A-producing $CD8^+$ T cells restricted to non-classical MHC class I molecules and characterized by immunoregulatory and tissue-repair signatures, which home to the epidermis (9). These cells could be the source of IL-17A produced in response to HK *S. epidermidis* in our experiments, although further research is needed to address this point.

A major difference between *S. aureus* and *S. epidermidis* is the secretion of numerous virulence factors including proteases and toxins such as alpha-toxin, that can damage the skin epithelial integrity (32, 56). Our results suggest that in order to halt *S. aureus* invasion, the cutaneous immunity deploys $CD4^+$ Tsrm cells that secrete several cytokines with proven anti-*S. aureus* and tissue-repair activities. Induction of such a mild anti-bacterial immune response might be a strategy to limit local infection and prevent systemic spread, promoting a long-lasting equilibrium between this pathobiont and the host. Interestingly, this could be achieved through alpha-toxin that has been shown to modulate mouse $CD4^+$ T cell differentiation limiting Th1 while promoting Th17 responses (57). However, once the skin is breached, the local immunity is dampened or the bacterial load is exceedingly high, this local response is no longer sufficient to control *S. aureus* (37). Indeed, the importance of antibodies and Th1 cells in controlling systemic *S. aureus* infections has been highlighted (25, 58).

Interestingly, a recent paper showed that neonatal mouse skin colonization with *S. epidermidis* facilitated immune tolerance to this bacterium via the induction of regulatory T (Treg) cells (49). This was not the case for *S. aureus* that, through alpha-toxin mediated IL-1β production by myeloid cells, limited the development of *S. aureus*-specific Treg cells thus enhancing skin inflammation upon later-life exposure to *S. aureus* (49). Similarly, we cannot rule out the presence of *S. epidermidis*-specific Treg cells, which are known to proliferate under homeostatic conditions, in our experiments (6).

The immune response of the skin to *S. aureus* has been intensively investigated in a number of elegant mouse studies (19). However, the anatomical and immunological differences between murine and human skin together with the different composition and exposure to skin microbiome limit the translational value of the results obtained in mice (29, 59). As a more biologically relevant model, we used human skin explants generated as surgical waste from cosmetic surgery performed on the abdomen. Of note, although *Staphylococcus aureus* colonization is most consistently identified in humans in the anterior nares, colonization has also been reported at other body sites including axilla, inguinal and rectal areas (60). In addition, *S. aureus* was cultured from 30% of abdominal skin swabs from healthy subjects (61). Since variability was reported among different skin sites, as a consequence differences in the relative abundance in $CD4^+$ Trm cells specific for *S. aureus* at different locations can be envisaged. Nevertheless, studies have shown that following skin infection, Tsrm cells can migrate out of the skin and populate distant skin sites thus forming global skin immunity (16, 62). Interestingly, *S. aureus*-specific $CD4^+$ Trm cells have been identified in gut tissue of healthy individuals. These cells showed increased IL-17A and reduced IFN-γ production as compared to cells with similar reactivity present in the circulation (63), similarly to what we report here for *S. aureus*-specific $CD4^+$ Tsrm cells. Indeed, this seems to be a common characteristic of barrier-protective Trm cells. In addition, since some inborn errors of IL-17 immunity predispose not only to skin but also to lung *S. aureus* infection (37), the presence of *S. aureus*-specific $CD4^+$ Tsrm cells in the lungs and their phenotype should be assessed.

While numerous efforts have been made toward designing a vaccine against *S. aureus*, unfortunately to this date none have been successful (64). Perhaps the most fundamental reason explaining the past failures of *S. aureus* vaccines is the lack of a complete understanding of protective immunity. Our results enforce the conclusion that since the contribution of local immune memory within tissues is becoming evident, it should be evaluated in vaccination efficacy studies (50). Since a sizable percentage of people experiencing *S. aureus* SSTI has recurrent infections (22, 65), it will be very informative to analyze the $CD4^+$ Tsrm response to *S. aureus* in this population. In addition, it would be interesting to investigate the *S. aureus*-specific $CD4^+$ Tsrm response in patients with atopic dermatitis, a chronic and relapsing inflammatory skin disorder associated with skin barrier impairment and the predominant *S. aureus* colonization (66).

In summary, we describe a skin-resident memory $CD4^+$ T cell population within healthy human skin that is specific for the human skin pathogen *S. aureus*. While further research is needed to better characterize the phenotype, the antigen-specificity and the protective potential of these cells, this finding highlights that skin-resident memory $CD4^+$ T cells could be a powerful and exploitable arm of adaptive immunity against this elusive pathobiont.

DATA AVAILABILITY STATEMENT

The raw data supporting the conclusions of this article will be made available by the authors, without undue reservation.

ETHICS STATEMENT

The studies involving human participants were reviewed and approved by French Ministry of Higher Education, Research and Innovation. The patients/participants provided their written informed consent to participate in this study.

AUTHOR CONTRIBUTIONS

AH, MEM, and ES were involved in designing the study and wrote the paper. AH, MEM, BC, and ARC performed experiments. ST and BC set up the Click-iT EdU assay. ST provided valuable technical support with flow cytometry. AH, MEM, BC, and ES analyzed the data. FB and ES supervised the project. All authors critically revised the manuscript and approved it before submission.

FUNDING

This work was supported by the European Union's Horizon 2020 research and innovation program under the Marie Skłodowska-Curie grant agreement no. 675106 coordinated by FB (GSK, Siena, Italy).

ACKNOWLEDGMENTS

We would like to thank Rachael Clark and Thomas Kupper for sharing their expertise and technical details on the skin digestion protocol, Nina van Sorge and Jonah Clegg for providing critical feedback on the manuscript, Federica Baffetta for statistical support, Michela Brazzoli and Oretta Finco for support and scientific advice.

SUPPLEMENTARY MATERIAL

The Supplementary Material for this article can be found online at: https://www.frontiersin.org/articles/10.3389/fimmu.2021.642711/full#supplementary-material

REFERENCES

1. Clark RA, Chong B, Mirchandani N, Brinster NK, Yamanaka K, Dowgiert RK, et al. The vast majority of CLA^+ T cells are resident in normal skin. *J Immunol.* (2006) 176:4431–9. doi: 10.4049/jimmunol.176.7.4431
2. Watanabe R, Gehad A, Yang C, Scott LL, Teague JE, Schlapbach C, et al. Human skin is protected by four functionally and phenotypically discrete populations of resident and recirculating memory T cells. *Sci Transl Med.* (2015) 7:279RA39. doi: 10.1126/scitranslmed.3010302
3. Kumar BV, Ma W, Miron M, Granot T, Guyer RS, Carpenter DJ, et al. Human tissue-resident memory T cells are defined by core transcriptional and functional signatures in lymphoid and mucosal sites. *Cell Rep.* (2017) 20:2921–34. doi: 10.1016/j.celrep.2017.08.078
4. Park CO, Fu X, Jiang X, Pan Y, Teague JE, Collins N, et al. Staged development of long-lived T-cell receptor αβ T_H17 resident memory T-cell population to *Candida albicans* after skin infection. *J Allergy Clin Immunol.* (2018) 142:647–62. doi: 10.1016/j.jaci.2017.09.042
5. Glennie ND, Yeramilli VA, Beiting DP, Volk SW, Weaver CT, Scott P. Skin-resident memory $CD4^+$ T cells enhance protection against *Leishmania major* infection. *J Exp Med.* (2015) 212:1405–14. doi: 10.1084/jem.20142101
6. Seneschal J, Clark RA, Gehad A, Baecher-Allan CM, Kupper TS. Human epidermal langerhans cells maintain immune homeostasis in skin by activating skin resident regulatory T cells. *Immunity.* (2012) 36:873–84. doi: 10.1016/j.immuni.2012.03.018
7. Sparber F, De Gregorio C, Steckholzer S, Ferreira FM, Dolowschiak T, Ruchti F, et al. The skin commensal yeast malassezia triggers a type 17 response that coordinates anti-fungal immunity and exacerbates skin inflammation. *Cell Host Microbe.* (2019) 25:389–403.e6. doi: 10.1016/j.chom.2019.02.002
8. Naik S, Bouladoux N, Linehan JL, Han SJ, Harrison OJ, Wilhelm C, et al. Commensal-dendritic-cell interaction specifies a unique protective skin immune signature. *Nature.* (2015) 520:104–8. doi: 10.1038/nature14052
9. Linehan JL, Harrison OJ, Han SJ, Byrd AL, Vujkovic-Cvijin I, Villarino AV. et al. Non-classical immunity controls microbiota impact on skin immunity and tissue repair. *Cell.* (2018) 172:784–96. doi: 10.1016/j.cell.2017.12.033
10. Wakim LM, Smith J, Caminschi I, Lahoud MH, Villadangos JA. Antibody-targeted vaccination to lung dendritic cells generates tissue-resident memory CD8 T cells that are highly protective against influenza virus infection. *Mucosal Immunol.* (2015) 8:1060–71. doi: 10.1038/mi.2014.133
11. Wilk MM, Mills KHG. CD4 T_{RM} cells following infection and immunization: Implications for more effective vaccine design. *Front Immunol.* (2018) 9:1860. doi: 10.3389/fimmu.2018.01860
12. Kadoki M, Patil A, Thaiss CC, Brooks DJ, Pandey S, Deep D, et al. Organism-level analysis of vaccination reveals networks of protection across tissues. *Cell.* (2017) 171:398–413. doi: 10.1016/j.cell.2017.08.024
13. Louis L, Clark M, Wise MC, Glennie N, Wong A, Broderick K, et al. Intradermal synthetic DNA vaccination generates leishmania-specific T cells in the skin and protection against leishmania major. *Infect Immun.* (2019) 87:e00227–19. doi: 10.1128/IAI.00227-19

14. Seidel JA, Vukmanovic-Stejic M, Muller-Durovic B, Patel N, Fuentes-Duculan J, Henson SM, et al. Skin resident memory $CD8^+$ T cells are phenotypically and functionally distinct from circulating populations and lack immediate cytotoxic function. *Clin Exp Immunol.* (2018) 194:79–92. doi: 10.1111/cei.13189
15. Pan Y, Tian T, Park CO, Lofftus SY, Mei S, Liu X, et al. Survival of tissue-resident memory T cells requires exogenous lipid uptake and metabolism. *Nature.* (2017) 543:252–6. doi: 10.1038/nature21379
16. Jiang X, Clark RA, Liu L, Wagers AJ, Fuhlbrigge RC, Kupper TS. Skin infection generates non-migratory memory $CD8^+$ T_{RM} cells providing global skin immunity. *Nature.* (2012) 483:227–31. doi: 10.1038/nature10851
17. Beura LK, Mitchell JS, Thompson EA, Schenkel JM, Mohammed J, Wijeyesinghe S, et al. Intravital mucosal imaging of $CD8^+$ resident memory T cells shows tissue-autonomous recall responses that amplify secondary memory article. *Nat Immunol.* (2018) 19:173–82. doi: 10.1038/s41590-017-0029-3
18. Ariotti S, Hogenbirk MA, Dijkgraaf FE, Visser LL, Hoekstra ME, Song JY, et al. Skin-resident memory $CD8^+$ T cells trigger a state of tissue-wide pathogen alert. *Science.* (2014) 346:101–5. doi: 10.1126/science.1254803
19. Clegg J, Soldaini E, Bagnoli F, McLoughlin RM. Targeting skin-resident memory T cells via vaccination to combat *Staphylococcus aureus* infections. *Trends Immunol.* (2020) 42:6–17. doi: 10.1016/j.it.2020.11.005
20. Ray GT, Suaya JA, Baxter R. Microbiology of skin and soft tissue infections in the age of community-acquired methicillin-resistant *Staphylococcus aureus*. *Diagn Microbiol Infect Dis.* (2013) 76:24–30. doi: 10.1016/j.diagmicrobio.2013.02.020
21. Montgomery CP, Daniels M, Zhao F, Alegre ML, Chong AS, Daum RS. Protective immunity against recurrent *Staphylococcus aureus* skin infection requires antibody and interleukin-17A. *Infect Immun.* (2014) 82:2125–34. doi: 10.1128/IAI.01491-14
22. Montgomery CP, David MZ, Daum RS. Host factors that contribute to recurrent staphylococcal skin infection. *Curr Opin Infect Dis.* (2015) 28:253–8. doi: 10.1097/QCO.0000000000000156
23. Minegishi Y, Saito M, Nagasawa M, Takada H, Hara T, Tsuchiya S, et al. Molecular explanation for the contradiction between systemic Th17 defect and localized bacterial infection in hyper-IgE syndrome. *J Exp Med.* (2009) 206:1291–301. doi: 10.1084/jem.20082767
24. Utay NS, Roque A, Timmer JK, Morcock DR, DeLeage C, Somasunderam A, et al. MRSA infections in HIV-infected people are associated with decreased MRSA-specific Th1 immunity. *PLoS Pathog.* (2016) 12:e1005580. doi: 10.1371/journal.ppat.1005580
25. Brown AF, Murphy AG, Lalor SJ, Leech JM, O'Keeffe KM, Mac Aogáin M, et al. Memory Th1 Cells Are Protective In Invasive *Staphylococcus aureus* infection. *PLoS Pathog.* (2015) 11:1–32. doi: 10.1371/journal.ppat.1005226
26. Lin L, Ibrahim AS, Xu X, Farber JM, Avanesian V, Baquir B, et al. Th1-Th17 cells mediate protective adaptive immunity against *Staphylococcus aureus* and Candida albicans infection in mice. *PLoS Pathog.* (2009) 5:e1000703. doi: 10.1371/journal.ppat.1000703
27. Kolata JB, Kühbandner I, Link C, Normann N, Vu CH, Steil L, et al. The fall of a Dogma? Unexpected high T-cell memory response to *Staphylococcus aureus* in humans. *J Infect Dis.* (2015) 212:830–8. doi: 10.1093/infdis/jiv128
28. Zielinski CE, Mele F, Aschenbrenner D, Jarrossay D, Ronchi F, Gattorno M, et al. Pathogen-induced human T_H17 cells produce IFN-γ or IL-10 and are regulated by IL-1β. *Nature.* (2012) 484:514–8. doi: 10.1038/nature10957
29. Boero E, Mnich ME, Manetti AGO, Soldaini E, Grimaldi L, Bagnoli F. Human three-dimensional models for studying skin pathogens. In: *Current Topics in Microbiology and Immunology*. Berlin: Springer (2020).
30. Chassain B, Lemée L, Didi J, Thiberge JM, Brisse S, Pons JL, et al. Multilocus sequence typing analysis of *Staphylococcus lugdunensis* implies a clonal population structure. *J Clin Microbiol.* (2012) 50:3003–9. doi: 10.1128/JCM.00988-12
31. Mack D, Siemssen N, Laufs R. Parallel induction by glucose of adherence and a polysaccharide antigen specific for plastic-adherent *Staphylococcus epidermidis*: Evidence for functional relation to intercellular adhesion. *Infect Immun.* (1992) 60:2048–57. doi: 10.1128/IAI.60.5.2048-2057.1992
32. Olaniyi RO, Pancotto L, Grimaldi L, Bagnoli F. Deciphering the pathological role of staphylococcal α-Toxin and panton-valentine leukocidin using a novel ex vivo human skin model. *Front Immunol.* (2018) 9:951. doi: 10.3389/fimmu.2018.00951
33. Byrd AL, Belkaid Y, Segre JA. The human skin microbiome. *Nat Rev Microbiol.* (2018) 16:143–55. doi: 10.1038/nrmicro.2017.157
34. Da Silva Antunes R, Paul S, Sidney J, Weiskopf D, Dan JM, Phillips E, et al. Definition of human epitopes recognized in tetanus toxoid and development of an assay strategy to detect Ex vivo tetanus $CD4^+$ T cell responses. *PLoS ONE.* (2017) 12:e0169086. doi: 10.1371/journal.pone.0169086
35. Choi Y, Kotzin B, Herron L, Callahan J, Marrack P, Kappler J. Interaction of *Staphylococcus aureus* toxin "superantigens" with human T cells. *Proc Natl Acad Sci USA.* (1989) 86:8951–45. doi: 10.1073/pnas.86.22.8941
36. Puel A, Cypowyj S, Maródi L, Abel L, Picard C, Casanova JL. Inborn errors of human IL-17 immunity underlie chronic mucocutaneous candidiasis. *Curr Opin Allergy Clin Immunol.* (2012) 12:616–22. doi: 10.1097/ACI.0b013e328358cc0b
37. Puel A. Human inborn errors of immunity underlying superficial or invasive candidiasis. *Hum Genet.* (2020) 139:1011–22. doi: 10.1007/s00439-020-02141-7
38. Peric M, Koglin S, Kim S-M, Morizane S, Besch R, Prinz JC, et al. IL-17A enhances vitamin D3 -induced expression of cathelicidin antimicrobial peptide in human keratinocytes. *J Immunol.* (2008) 181:8504–12. doi: 10.4049/jimmunol.181.12.8504
39. Archer NK, Adappa ND, Palmer JN, Cohen NA, Harro JM, Lee SK, et al. Interleukin-17A (IL-17A) and IL-17F are critical for antimicrobial peptide production and clearance of *Staphylococcus aureus* nasal colonization. *Infect Immun.* (2016) 84:3575–83. doi: 10.1128/IAI.00596-16
40. Ishigame H, Kakuta S, Nagai T, Kadoki M, Nambu A, Komiyama Y, et al. Differential roles of interleukin-17A and−17F in host defense against mucoepithelial bacterial infection and allergic responses. *Immunity.* (2009) 30:108–19. doi: 10.1016/j.immuni.2008.11.009
41. Dudakov JA, Hanash AM, Van Den Brink MRM. Interleukin-22: immunobiology and pathology. *Annu Rev Immunol.* (2015) 33:747–85. doi: 10.1146/annurev-immunol-032414-112123
42. Avitabile S, Odorisio T, Madonna S, Eyerich S, Guerra L, Eyerich K, et al. Interleukin-22 promotes wound repair in diabetes by improving keratinocyte pro-healing functions. *J Invest Dermatol.* (2015) 135:2862–70. doi: 10.1038/jid.2015.278
43. Mulcahy ME, Leech JM, Renauld JC, Mills KHG, McLoughlin RM. Interleukin-22 regulates antimicrobial peptide expression and keratinocyte differentiation to control *Staphylococcus aureus* colonization of the nasal mucosa. *Mucosal Immunol.* (2016) 9:1429–41. doi: 10.1038/mi.2016.24
44. Tamoutounour S, Han SJ, Deckers J, Constantinides MG, Hurabielle C, Harrison OJ, et al. Keratinocyte-intrinsic MHCII expression controls microbiota-induced Th1 cell responses. *Proc Natl Acad Sci USA.* (2019) 116:23643–52. doi: 10.1073/pnas.1912432116
45. Upadhyay V, Fu YX. Lymphotoxin signalling in immune homeostasis and the control of microorganisms. *Nat Rev Immunol.* (2013) 13:270–9. doi: 10.1038/nri3406
46. Mounzer RH, Svendsen OS, Baluk P, Bergman CM, Padera TP, Wiig H, et al. Lymphotoxin-alpha contributes to lymphangiogenesis. *Blood.* (2010) 116:2173–82. doi: 10.1182/blood-2009-12-256065
47. Nakagawa S, Matsumoto M, Katayama Y, Oguma R, Wakabayashi S, Nygaard T, et al. *Staphylococcus aureus* virulent PSMα peptides induce keratinocyte alarmin release to orchestrate IL-17-dependent skin inflammation. *Cell Host Microbe.* (2017) 22:667–77. doi: 10.1016/j.chom.2017.10.008
48. Liu H, Archer NK, Dillen CA, Wang Y, Ashbaugh AG, Ortines RV. et al. *Staphylococcus aureus* epicutaneous exposure drives skin inflammation via IL-36-mediated T cell responses. *Cell Host Microbe.* (2017) 22:653–66. doi: 10.1016/j.chom.2017.10.006
49. Leech JM, Dhariwala MO, Lowe MM, Chu K, Merana GR, Cornuot C, et al. Toxin-triggered interleukin-1 receptor signaling enables early-life discrimination of pathogenic versus commensal skin bacteria. *Cell Host Microbe.* (2019) 26:795–809.e5. doi: 10.1016/j.chom.2019.10.007
50. Amezcua Vesely MC, Pallis P, Bielecki P, Low JS, Zhao J, Harman CCD, et al. Effector T_H17 cells give rise to long-lived T_{RM} cells that are essential for an immediate response against bacterial infection. *Cell.* (2019) 178:1176–88.e15. doi: 10.1016/j.cell.2019.07.032

51. Constantinides MG, Link VM, Tamoutounour S, Wong AC, Perez-Chaparro PJ, Han SJ, et al. MAIT cells are imprinted by the microbiota in early life and promote tissue repair. *Science.* (2019) 366:eaax6624. doi: 10.1126/science.aax6624
52. Marchitto MC, Dillen CA, Liu H, Miller RJ, Archer NK, Ortines RV, et al. Clonal $V\gamma6^+V\delta4^+$ T cells promote IL-17–mediated immunity against *Staphylococcus aureus* skin infection. *Proc Natl Acad Sci USA.* (2019) 116:10917–26. doi: 10.1073/pnas.1818256116
53. Visvabharathy L, Id SG, Id LC, He Y, Alonzo F, Id III, et al. Group 1 CD1-restricted T cells contribute to control of systemic *Staphylococcus aureus* infection. *PLoS Pathog.* (2020) 16:e1008443. doi: 10.1371/journal.ppat.1008443
54. Beura LK, Hamilton SE, Bi K, Schenkel JM, Odumade OA, Casey KA, et al. Normalizing the environment recapitulates adult human immune traits in laboratory mice. *Nature.* (2016) 532:512–6. doi: 10.1038/nature17655
55. Reese TA, Bi K, Kambal A, Filali-Mouhim A, Beura LK, Bürger MC, et al. Sequential infection with common pathogens promotes human-like immune gene expression and altered vaccine response. *Cell Host Microbe.* (2016) 19:713–9. doi: 10.1016/j.chom.2016.04.003
56. Williams MR, Cau L, Wang Y, Kaul D, Sanford JA, Zaramela LS, et al. Interplay of staphylococcal and host proteases promotes skin barrier disruption in netherton syndrome. *Cell Rep.* (2020) 30:2923–33.e7. doi: 10.1016/j.celrep.2020.02.021
57. Bonifacius A, Goldmann O, Floess S, Holtfreter S, Robert PA, Nordengrün M, et al. *Staphylococcus aureus* alpha-toxin limits type 1 while fostering type 3 immune responses. *Front Immunol.* (2020) 11:1579. doi: 10.3389/fimmu.2020.01579
58. Zhang F, Ledue O, Jun M, Goulart C, Malley R, Lu YJ. Protection against *Staphylococcus aureus* colonization and infection by B-and T-cell-mediated mechanisms. *MBio.* (2018) 9:1–13. doi: 10.1128/mBio.01949-18
59. Pasparakis M, Haase I, Nestle FO. Mechanisms regulating skin immunity and inflammation. *Nat Rev Immunol.* (2014) 14:289–301. doi: 10.1038/nri3646
60. Yang ES, Tan J, Eells S, Rieg G, Tagudar G, Miller LG. Body site colonization in patients with community-associated methicillin-resistant *Staphylococcus aureus* and other types of *S. aureus* skin infections. *Clin Microbiol Infect.* (2010) 16:425–31. doi: 10.1111/j.1469-0691.2009.02836.x
61. Williams RE. Healthy carriage of *Staphylococcus aureus*: its prevalence and importance. *Bacteriol Rev.* (1963) 27:56–71. doi: 10.1128/BR.27.1.56-71.1963
62. Klicznik MM, Morawski PA, Höllbacher B, Varkhande SR, Motley SJ, Kuri-Cervantes L, et al. Human $CD4^+CD103^+$ cutaneous resident memory T cells are found in the circulation of healthy individuals. *Sci Immunol.* (2019) 4:eaav8995. doi: 10.1126/sciimmunol.aav8995
63. Hegazy AN, West NR, Stubbington MJT, Wendt E, Suijker KIM, Datsi A, et al. Circulating and tissue-resident $CD4^+$ T cells with reactivity to intestinal microbiota are abundant in healthy individuals and function is altered during inflammation. *Gastroenterology.* (2017) 153:1320–37.e16. doi: 10.1053/j.gastro.2017.07.047
64. Bagnoli F, Bertholet S, Grandi G. Inferring reasons for the failure of *Staphylococcus aureus* vaccines in clinical trials. *Front Cell Infect Microbiol.* (2012) 2:16. doi: 10.3389/fcimb.2012.00016
65. Vella V, Galgani I, Polito L, Arora AK, Creech CB, David MZ, et al. *Staphylococcus aureus* skin and soft tissue infection recurrence rates in outpatients: a retrospective database study at three US medical centers. *Clin Infect Dis.* (2020). doi: 10.1093/cid/ciaa1717
66. Kong HH, Oh J, Deming C, Conlan S, Grice EA, Beatson MA, et al. Temporal shifts in the skin microbiome associated with disease flares and treatment in children with atopic dermatitis. *Genome Res.* (2012) 22:850–9. doi: 10.1101/gr.131029.111

Conflict of Interest: AH, MEM, and ARC are Ph.D. fellows and are enrolled in the Infection and Immunity Ph.D. program, part of the graduate school of Life Sciences at Utrecht University and participated in a post graduate studentship program at GSK. BC was a PhD student from the University of Siena funded by GSK. ST, FB, and ES are employees of the GSK group of companies. FB hold shares in the GSK group of companies and holds pending and issued patents (WO/2019/158537, WO/2015/144691, WO/2015/144653, WO/2015/144655, WO/2014/033190, WO/2014/033191, WO/2014/033192, WO/2014/033193, WO/2013/030378, and WO/2010/119343) on *S. aureus* vaccine formulations.

frontiers in Immunology

REVIEW
published: 26 March 2021
doi: 10.3389/fimmu.2021.660183

Host-Directed Therapies for Cutaneous Leishmaniasis

Fernanda O. Novais[1]*, *Camila Farias Amorim*[2] and *Phillip Scott*[2]*

[1] Department of Microbial Infection and Immunity, College of Medicine, The Ohio State University, Columbus, OH, United States,
[2] Department of Pathobiology, School of Veterinary Medicine, University of Pennsylvania, Philadelphia, PA, United States

Cutaneous leishmaniasis exhibits a wide spectrum of clinical presentations from self-resolving infections to severe chronic disease. Anti-parasitic drugs are often ineffective in the most severe forms of the disease, and in some cases the magnitude of the disease can result from an uncontrolled inflammatory response rather than unrestrained parasite replication. In these patients, host-directed therapies offer a novel approach to improve clinical outcome. Importantly, there are many anti-inflammatory drugs with known safety and efficacy profiles that are currently used for other inflammatory diseases and are readily available to be used for leishmaniasis. However, since leishmaniasis consists of a wide range of clinical entities, mediated by a diverse group of leishmanial species, host-directed therapies will need to be tailored for specific types of leishmaniasis. There is now substantial evidence that host-directed therapies are likely to be beneficial beyond autoimmune diseases and cancer and thus should be an important component in the armamentarium to modulate the severity of cutaneous leishmaniasis.

Keywords: cutaneous leishmaniasis, host-directed therapies, skin immunity, immunopathology, cytokines

OPEN ACCESS

Edited by:
Fabienne Tacchini-Cottier, University of Lausanne, Switzerland

Reviewed by:
Christian Engwerda, Queensland Children's Medical Research Institute, Australia
Maria Adelaida Gomez, Centro Internacional de Entrenamiento e Investigaciones Medicas, Colombia

***Correspondence:**
Fernanda O. Novais
Fernanda.Novais@osumc.edu
Phillip Scott
Pscott@upenn.edu

Specialty section:
This article was submitted to Microbial Immunology, a section of the journal Frontiers in Immunology

Received: *28 January 2021*
Accepted: *11 March 2021*
Published: *26 March 2021*

Citation:
Novais FO, Amorim CF and Scott P (2021) Host-Directed Therapies for Cutaneous Leishmaniasis. Front. Immunol. 12:660183. doi: 10.3389/fimmu.2021.660183

INTRODUCTION

Cutaneous leishmaniasis is caused by several different species of protozoa transmitted by sand flies, and has a variety of clinical forms, ranging from self-healing lesions to chronic disfiguring mucosal disease (1, 2). There is no vaccine for the disease, and drug treatment is not always effective (3, 4). Moreover, in some forms of leishmaniasis the magnitude of the disease appears to be due to the uncontrolled inflammatory response at the cutaneous site of infection. It is clear that new therapeutic approaches are needed, and host-directed therapies to either enhance protective immune responses or to ameliorate excessive cutaneous inflammation represent novel therapeutic strategies worthy of pursuit.

Host-directed therapies for infectious diseases are designed to either amplify protective immune responses, divert non-protective immune responses towards protective responses, or block pathologic immune responses (5). Fortunately, our in-depth understanding of both protective and pathologic immune responses and identification of agents that can be used clinically to influence immune responses has revolutionized treatment of a wide range of diseases. While many of these new treatments are for non-communicable diseases, repurposing such treatments for infectious diseases, such as cutaneous leishmaniasis is advantageous, as their safety and efficacy profiles have often already been established.

In order to be successful, host-directed therapies must not overstimulate the immune response, or block protective immune responses necessary to control the pathogen. These are not theoretical possibilities. For example, checkpoint blockade has revolutionized cancer treatment, but some patients develop adverse events associated with these treatments, including cytokine storms that can be lethal (6, 7). Similarly, anti-inflammatory treatments run the risk of increased susceptibility to infections. Thus, the key to using host-directed therapy with infectious diseases is to lessen the chances of adverse events by defining the mechanisms mediating protection as well as those promoting immunopathologic responses associated with the disease. In cutaneous leishmaniasis there is a good understanding of the protective mechanisms, and thus one strategy is to promote those responses. Here we will review the host-directed therapies that could be used to enhance protection in patients. Many of the studies discussed focus on murine models where potential host-directed therapies can be assessed prior to initiation of clinical trials with patients.

We will also discuss what we know about destructive inflammation seen in patients with chronic cutaneous leishmaniasis and identify potential targets for therapies to promote disease resolution.

SPECTRUM OF CLINICAL PRESENTATIONS IN CUTANEOUS LEISHMANIASIS

A challenging aspect in lessening disease in cutaneous leishmaniasis is the variety of clinical presentations associated with the infection. The type of clinical presentation is driven by the nature of the immune response invoked, which is influenced by both host genetics and the specific species or strain of the parasite causing the infection (1, 2). Following infection by a sand fly, patients develop a small nodule which progresses to an ulcerated lesion that will eventually heal in several months. However, in some cases, the lesions fail to resolve, or the parasites spread to many cutaneous sites without any evidence of control, a form of leishmaniasis known as diffuse cutaneous leishmaniasis (DCL) (8–10). These patients fail to develop a delayed-type hypersensitivity response or a strong IFN-γ response, and thus parasite burdens in the lesions are extremely high (9, 10). Histologically, these lesions appear as masses of macrophages with large numbers of intracellular parasites, and few infiltrating lymphocytes (10). It is clear that enhancing a protective immune response would be important for this disease.

At the other end of the spectrum, parasites can spread to the naso-oropharyngeal mucosa and cause extensive damage mediated by an uncontrolled immune response. This disease, termed mucosal leishmaniasis, is most often caused by *L. braziliensis* parasites and is refractory to anti-parasitic treatment. While the parasites are largely controlled by the immune response, there is a large infiltration of inflammatory cells into the lesions, suggesting that the damage is due to an overexuberant inflammatory response rather than uncontrolled parasite growth (11). While mucosal leishmaniasis is the most severe form of the disease at the inflammatory end of the spectrum, single lesions in patients infected by *L. braziliensis* can also be chronic, resistant to drug treatment, and associated with a severe inflammatory response with a low parasite burden in the lesions.

Patients who fail to develop a protective Th1 cell response develop disease, often in spite of a strong antibody response. This is most clearly observed in DCL patients (9). In contrast, patients with a strong Th1 cell response also develop severe disease, but in this case due to inflammation rather than massive parasite numbers (11). This spectrum is not unique to cutaneous leishmaniasis. For example, in another cutaneous disease, leprosy, the disease ranges from lepromatous leprosy in which there is an absence of a strong T cell response and no control of the bacteria to tuberculoid leprosy in which bacteria are scarce, and the immune response causes disease (12, 13). Unfortunately, drug treatment for cutaneous leishmaniasis patients with severe disease at either end of the spectrum can be ineffective, which provides support for considering alternative treatment strategies (8, 10, 14). However, what is clearly evident is that any host-directed therapy will need to take into consideration where a patient is on this immunologic spectrum.

Experimental models of cutaneous leishmaniasis have been critical for understanding the disease, and important in defining the mechanisms associated with T cell subset development. For example, infection of mice with *Leishmania major* helped define the factors driving CD4 Th1 and CD4 Th2 cell development and maintenance (15–17). These studies established the critical role of IFN-γ produced by CD4 T cells in protection, and the lack of a protective role for antibodies. In contrast, infection of BALB/c mice with *L. major* results in an uncontrolled infection, which is in part due to the development of a Th2 response. While these uncontrolled infections mimic some aspects of DCL (or visceral leishmaniasis), the role of IL-4 in promoting increased disease in patients is less clear than in murine models (18). Many studies have been done with *L. major*, but these do not represent the whole breadth of disease patterns that can be seen with other species of *Leishmania*. For example, while C57BL/6 mice resolve disease following infection with *L. major*, lesions induced by either *L. amazonensis* or *L. mexicana* infections do not resolve (19, 20). In these cases, susceptibility is linked with the failure to develop a strong Th1 response, rather than a Th2 response. *Leishmania* strain differences can also influence disease outcome. For example, the *L. major* Seidman strain causes a non-healing infection in C57BL/6 mice in spite of the development of a Th1 response (21, 22). Although all murine models have their limitations, many of these different host-parasite models are useful to assess host-directed therapies that can enhance immune responses. In contrast, fewer models have been available that mimic the excessive inflammatory responses associated with patients infected with *L. braziliensis* parasites (see below).

ENHANCING PROTECTION IN CUTANEOUS LEISHMANIASIS BY HOST-DIRECTED THERAPIES

Leishmania parasites replicate in myeloid cells, including macrophages, monocytes and dendritic cells. Control of the parasites is dependent upon activation of these cells by IFN-γ, leading to increased production of nitric oxide and/or reactive oxygen species, although the role of these molecules may vary depending upon the host and the parasite species (23–26). The primary source of IFN-γ that leads to protection in cutaneous leishmaniasis is the CD4 T cell, although CD8 T cells and NK cells can also contribute to protection (27–29). Once an infection has resolved, resident memory CD4 Th1 cells in the skin, central memory CD4 T cells and circulating effector CD4 Th1 cells maintained by persistent parasites provide protection against a secondary challenge (30, 31). Since resident memory Th1 cells can be maintained in the absence of persistent parasites, they are a good target for vaccine development. While we understand how the immune response can control these parasites, there are multiple mechanisms that can block or lessen the development of protective responses, which is why lesions often take so long to resolve. Defining these barriers to protection can provide targets for host-directed therapies in patients in whom limited Th1 responses develop.

A reasonable first line approach to promote healing is treatment with agents that directly increase protective immunity (**Figure 1**). One can define protective immunity in both experimental models and humans as the ability to protect against the development of disease, which may not lead to complete elimination of the parasites. While this protection may require IFN-γ, as discussed above it is also clear that IFN-γ by itself does not always lead to lack of disease.

As would be expected, treatment with IFN-γ has shown increased control in patients who are refractory to standard treatment (32, 33), and experimentally, IL-12 can promote healing even after lesions have developed when given in conjunction with an anti-parasitic drug (34, 35). In addition, clinical trials have been done with GM-CSF, in which topical treatment was found to promote increased healing (36, 37). Similarly, topical treatment with the TLR7 agonist imiquimod has shown increased healing rates (38), although there have been mixed results in clinical trials (39).

Alternatively, another potential therapeutic approach would be to block pathways that downregulate protective immunity (**Figure 1**). DCL patients fail to generate a protective IFN-γ response, and the pathology seen in these individuals is due to uncontrolled parasite growth in macrophages in the skin. While IL-4 blockade of protective responses can contribute to the uncontrolled *Leishmania* replication in experimental models, IL-4 appears to be less important in DCL patients (9) or indeed in any form of human leishmaniasis. Instead, a recent study suggests that DCL patients exhibit an overwhelming B cell response, and little evidence of either a Th1 or Th2 response (9). In contrast, IL-10 plays a critical role in promoting susceptibility to *L. major* in BALB/c mice, suggesting that blocking IL-10 might increase protective responses. Consistent with this possibility are studies in visceral leishmaniasis patients who can also develop

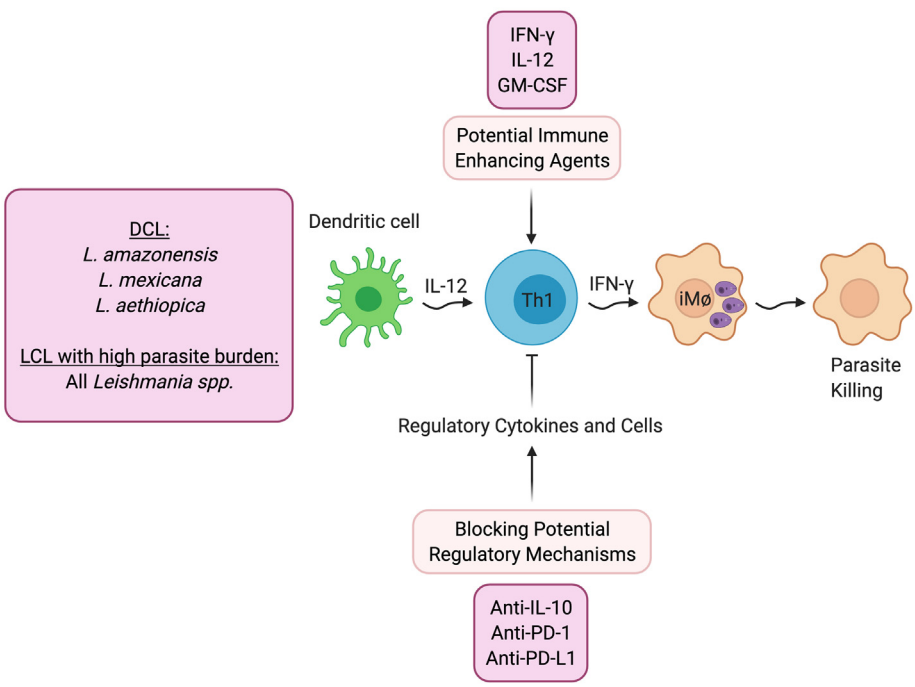

FIGURE 1 | Host directed therapies that promote better parasite control. DCL- Diffuse cutaneous leishmaniasis; LCL- Localized cutaneous leishmaniasis.

uncontrolled infections. In these patients IL-10, rather than IL-4, has been linked with susceptibility. Importantly, a study with splenic aspirates from visceral leishmaniasis (VL) patients demonstrated that blockade of IL-10 enhanced control of the parasites (40), which provides the experimental foundation for a host-directed therapy where IL-10 would be blocked in VL patients (41). Experimentally, other regulatory cytokines have been shown to block protective Th1 responses in cutaneous leishmaniasis. For example, TGF-β inhibits protection in *L. amazonensis* infected mice (42), and IL-27 promotes IL-10 responses and increased susceptibility (43). Thus, blocking these regulatory pathways might promote better protective responses.

The role of inhibitory receptors in modulating the outcome of infectious diseases is an area of active investigation, since checkpoint blockade is effective in promoting control of cancer (44). One might predict, therefore, that blocking this regulatory pathway might be protective in cutaneous leishmaniasis as well. However, to date the experimental results in leishmaniasis are unclear. A study with arginase-deficient *L. major* in mice unable to resolve their infections found that anti-PD-1 monoclonal antibody promoted healing. However, blockade of PD-1 or PD-L1 in *L. amazonensis* infected mice (45) or infection of PD-L1 knockout mice with *L. mexicana* (46), had minimal effects on parasite control. A recent study found that T cells with an exhausted phenotype were present in the blood and lesions of *L. braziliensis* patients, and blocking PD-1 signaling in circulating T cells from patients enhanced their proliferation and production of IFN-γ (47). Clearly, more studies need to be done to understand the role of PD-1/PD-L1, as well as other checkpoint molecules, in cutaneous leishmaniasis.

CONTROLLING IMMUNOPATHOLOGY IN CUTANEOUS LEISHMANIASIS BY HOST-DIRECTED THERAPIES

Enhancing Th1 responses directly or blocking pathways that lessen Th1 responses will not be effective for every type of cutaneous leishmaniasis. This is particularly true for patients at the immunopathologic end of the spectrum who develop chronic lesions in spite of their ability to generate a strong Th1 response. This clinical presentation is best exemplified by *L. braziliensis* infections, where chronic lesions are associated with a strong Th1 response and few parasites. While IFN-γ and TNF are important for macrophage activation and parasite control, in excess both cytokines can be associated with pathologic immune responses and it is possible that a poorly regulated Th1 response leading to high levels of IFN-γ and TNF contributes to this chronic inflammation. Moreover, since blocking TNF is a successful host-directed therapy for patients with rheumatoid arthritis, it is reasonable to consider its role in blocking pathology in cutaneous leishmaniasis. In support, a recent study suggests that TNF in *L. mexicana* infections promotes T cell exhaustion (48). While clinical trials have not yet been done with humanized monoclonal antibodies against TNF, the drug pentoxifylin, which blocks TNF, has been used in *L. braziliensis*, but with mixed results (49–51).

The optimal pathway to target in patients at the inflammatory end of the spectrum would be one that is not associated with protection. Notably, studies in *L. braziliensis* patients uncovered a major pathway leading to disease that was independent of protective immune responses. These studies found that cytolysis by CD8 T cells correlated with increased pathology in cutaneous leishmaniasis patients (23, 52–61). Importantly, these studies were followed up with the demonstration that patients who eventually fail drug therapy can be identified prior to treatment based upon expression level of genes associated with cytotoxicity (59).

The identification of CD8 T cells as drivers of disease was initially confusing, since CD8 T cells were protective in models of cutaneous leishmaniasis. For example, infection of CD8 deficient mice with low doses of *L. major* leads to susceptibility (28). The protective role of CD8 T cells appears to be mediated primarily by promoting Th1 responses in the draining lymph nodes (27, 28). This paradox was resolved by the finding that CD8 T cells in the lesions made little IFN-γ, but were instead cytolytic (53, 54, 56). The mechanisms involved in the differential function of CD8 T cells in the draining lymph nodes and cutaneous lesions has yet to be understood, although one factor may involve the lack of local signals in the lesions that would promote IFN-γ production by CD8 T cells (62). These results raised the question of how cytolytic CD8 T cells promote disease in cutaneous leishmaniasis. Based upon other infections, one might predict that killing of *Leishmania*-infected cells would lead to better parasite control. However, the evidence suggests that instead of killing the parasites, lysing the infected cell results in parasite dissemination, which then go on to infect other cells (54). Thus, cytolysis may be one mechanism that promotes metastasis in patients.

As the pathologic role for CD8 T cells is difficult to ascertain in standard experimental models of cutaneous leishmaniasis new models to define the mechanisms leading to CD8 T cell mediated pathology needed to be created. The most straightforward model was the adoptive transfer of CD8 T cells into RAG mice followed by infection with *Leishmania* (28, 54). Importantly, RAG mice infected with *L. braziliensis* do not develop substantial lesions over many weeks of infection, in spite of a large number of parasites present at the site of infection (54). These results, and previous studies in RAG mice (63), demonstrate the critical role T cells play in developing ulcerated lesions. RAG mice receiving CD4 and CD8 T cells developed small lesions and controlled parasite replication. In contrast, RAG mice that received CD8 T cells alone and were infected with *L. braziliensis* developed severe uncontrolled lesions (54). Surprisingly, the number of parasites in infected RAG mice and RAG mice that received CD8 T cells was the same, highlighting the critical role for CD8 T cells in immunopathology. This CD8 T cell dependent pathology required the cytotoxic molecule perforin, but not IFN-γ, since transfer of perforin deficient T cells to RAG mice failed to induce pathology, while IFN-γ -/- CD8 T cells did (54). In a complementary model, bystander cytolytic CD8 T cells were

also found to promote increased disease, as mice that had resolved an infection with lymphocytic choriomeningitis virus (LCMV) developed more severe disease than mice that had not previously been infected with LCMV in response to *Leishmania* challenge weeks after viral clearance (64, 65). In this model, LCMV specific NKG2D expressing CD8 T cells were recruited to the cutaneous lesions non-specifically and mediated killing of targets expressing NKG2D ligands that were upregulated on cells in the lesions due to inflammation. The relevance of bystander CD8 T cells to human leishmaniasis is suggested by the finding that lesions from patients who have been infected with *Toxoplasma* contained *Toxoplasma* specific CD8 T cells (66). Thus, studies in both experimental models, as well as gene transcriptional analysis of lesions from patients, identified an immunopathologic pathway dependent upon cytolysis in cutaneous leishmaniasis.

The transcriptional analysis of lesions from patients provided clues as to how cytolysis might promote increased disease (23, 67). Not only were genes associated with cytolysis upregulated in lesions, but those associated with inflammasome activation, including NLRP3, Caspase 1 and IL-1β, were similarly upregulated. The immunopathologic pathway hypothesized from gene transcriptional analysis of lesions was confirmed using the experimental models of CD8 T cell mediated disease described above. Thus, CD8 T cell mediated disease could be blocked by inhibitors of NLRP3, such as MCC950 and glyburide, or blockade of IL-1β with the IL-1 receptor antagonist anakinra or with anti- IL-1β antibody treatment (56) (**Figure 2**). The pathologic role for IL-1β is not limited to situations where there is uncontrolled CD8 T cell mediated cytolysis. Others have shown that inflammasome-dependent IL-1β mediates the severe disease seen with a virulent *L. major* strain, and IL-1β administration can exacerbate disease following *L. major* and *L. amazonensis* infection (22, 68, 69). In addition, IL-1 serum levels correlate with increased disease severity in *L. mexicana* patients (70), and more serious disease was reported in mice lacking the natural inhibitor of IL-1β signaling (IL-1RA) (71). In the *L. amazonensis* model IL-1β was found to promote resistance, although these mice fail to resolve with or without IL-1β (72). IL-1β has many roles in the immune response, but the pathologic role of IL-1β in cutaneous leishmaniasis appears to be when the cytokine is in excess. Notably, because both the inflammasome and IL-1β are associated with many chronic diseases, including autoimmune diseases, cancer and cardiovascular diseases, a number of inhibitors designed to block this pathway are in clinical use or are in clinical trials that can be tested in cutaneous leishmaniasis.

Blocking CD8 T cell cytotoxicity, an initiator of this pathway, could be another important target in lessening pathology. IL-15 is a potential target for such treatment, as it is highly expressed in lesions of human cutaneous leishmaniasis patients and promotes the expression of granzyme B dependent CD8 T cell cytotoxicity. Tofacitinib is a small molecule inhibitor of janus kinase (Jak)3 which is required for IL-15 signaling (73). It is currently being used clinically to treat certain types of arthritis under the trade name Xeljanz, and experimentally treats alopecia areata by blocking NKG2D dependent cytolysis (74). In experimental *Leishmania* models of CD8 T cell mediated pathology, systemic and topical treatment with tofacitinib blocked pathology (75). Notably, tofacitinib did not alter protective Th1 responses or parasite control. Thus, local targeting of CD8 T cell-mediated cytotoxicity can be a safe strategy to block immunopathologic responses locally while sparing protective responses.

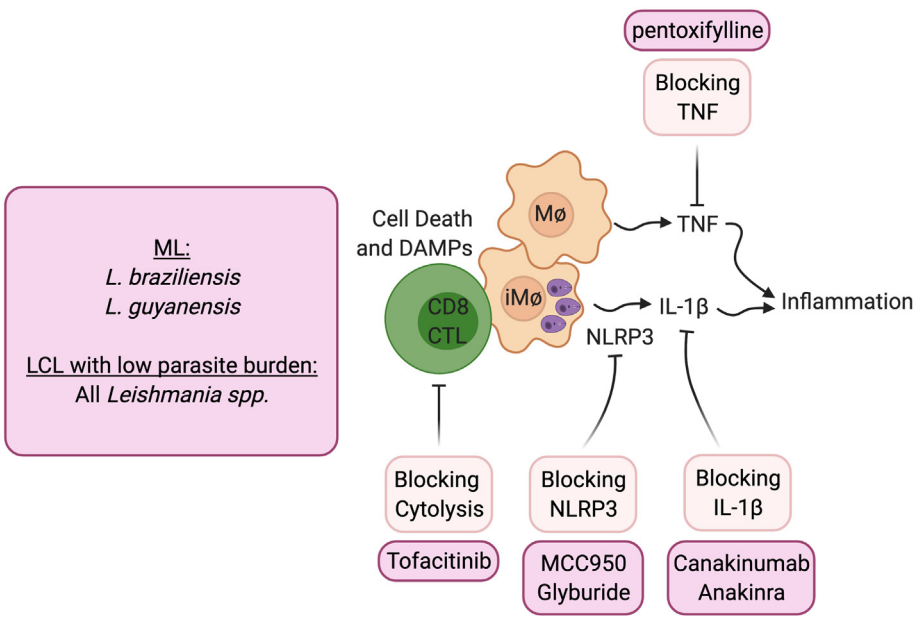

FIGURE 2 | Host directed therapies that block immunopathologic mediated cytolysis. ML, mucosal leishmaniasis; LCL, Localized cutaneous leishmaniasis.

CONCLUSIONS

Host-directed therapies hold great promise for lessening the more severe forms of cutaneous leishmaniasis. The ease of monitoring the efficacy of host-directed therapies in cutaneous diseases is a significant advantage to such treatments, and particularly important is the potential to develop topical treatments that may reduce untoward systemic responses. While in many diseases host-directed therapies are administered systemically, for those that might be used in cutaneous leishmaniasis it will be important to test whether topical application might be effective. One successful experimental example is the treatment with tofacitinib, which we found was as effective at controlling disease given topically as given systemically (75).

It is evident that care must be taken in the development of such therapies, as there remains the potential for blocking a pathway critical for control of *Leishmania*. Importantly, all of these therapies should be used in conjunction with standard anti-parasite drug treatment which lessens the risk of unchecked *Leishmania* multiplication. While increased susceptibility to other pathogens might remain, the short treatment period required would also lessen this risk. Finally, a practical consideration for developing therapies for neglected tropical diseases, such as cutaneous leishmaniasis, is the cost of treatment. Clearly the utility of any new host-directed therapy will depend on cost. However, identification of the targets for a successful host-directed therapy is the first step and can provide the rationale for a search for cheaper alternative treatments targeting the same immunologic pathways.

With the seeming endless development of new approaches to modulate the immune response with cytokines, small molecule inhibitors, humanized monoclonal antibodies, and drugs directed against immune targets, there is a growing interest in applying host-directed therapies to infectious diseases. Cutaneous diseases, such as leishmaniasis, can clearly benefit from such treatments. However, the key to success will be a continued focus on understanding the mechanisms leading to protective and pathologic responses in the skin, where many unanswered questions remain to be addressed. Most studies of cutaneous leishmaniasis have focused on systemic responses, or those occurring in local lymph nodes, and have ignored the unique aspects of the skin. Differences in cell types, metabolism, oxygen levels, and temperature can influence the outcome of cutaneous leishmaniasis, but have been little studied in this disease. Further, the skin directly interacts with the external environment and the skin microbiome can have significant effects on the outcome of infection (76, 77). It is fair to say that the success of host-directed therapies for cutaneous leishmaniasis will depend upon a better understanding of the skin, and for leishmaniasis we have just "scratched the surface" in that arena.

AUTHOR CONTRIBUTIONS

FN and PS contributed to the conception and design of the review. FN, PS, and CA contributed to aspects of the review and writing. All authors contributed to the article and approved the submitted version.

FUNDING

The authors were supported funding from NIH grants R01-AI-150606 and R01-AI-149456.

REFERENCES

1. Scott P, Novais FO. Cutaneous leishmaniasis: immune responses in protection and pathogenesis. *Nat Rev Immunol* (2016) 16:581–92. doi: 10.1038/nri.2016.72
2. Kaye P, Scott P. Leishmaniasis: complexity at the host-pathogen interface. *Nat Rev Microbiol* (2011) 9:604–15. doi: 10.1038/nrmicro2608
3. Carvalho AM, Guimarães LH, Costa R, Saldanha MG, Prates I, Carvalho LP, et al. Impaired Th1 response is associated therapeutic failure in patients with cutaneous leishmaniasis caused by Leishmania braziliensis. *J Infect Dis* (2020) 223:527–35. doi: 10.1093/infdis/jiaa374
4. Unger A, O'Neal S, Machado PRL, Guimarães LH, Morgan DJ, Schriefer A, et al. Association of treatment of American cutaneous leishmaniasis prior to ulcer development with high rate of failure in northeastern Brazil. *Am J Trop Med Hyg* (2009) 80:574–9. doi: 10.4269/ajtmh.2009.80.574
5. Kaufmann SHE, Dorhoi A, Hotchkiss RS, Bartenschlager R. Host-directed therapies for bacterial and viral infections. *Nat Rev Drug Discovery* (2018) 17:35–56. doi: 10.1038/nrd.2017.162
6. Burke KP, Grebinoski S, Sharpe AH, Vignali DAA. Understanding adverse events of immunotherapy: A mechanistic perspective. *J Exp Med* (2021) 218:1. doi: 10.1084/jem.20192179
7. Martins F, Sofiya L, Sykiotis GP, Lamine F, Maillard M, Fraga M, et al. Adverse effects of immune-checkpoint inhibitors: epidemiology, management and surveillance. *Nat Rev Clin Oncol* (2019) 16:563–80. doi: 10.1038/s41571-019-0218-0
8. Convit J, Kerdel-Vegas F. Disseminated cutaneous leishmaniasis; innoculation to laboratory animals, electron microscopy and fluorescent antibodies studies. *Arch Dermatol* (1965) 91:439–47. doi: 10.1001/archderm.1965.01600110025007
9. Christensen SM, Belew AT, El-Sayed NM, Tafuri WL, Silveira FT, Mosser DM. Host and parasite responses in human diffuse cutaneous leishmaniasis caused by L. amazonensis. *PloS Negl Trop Dis* (2019) 13:e0007152. doi: 10.1371/journal.pntd.0007152
10. Barral A, Costa JM, Bittencourt AL, Barral-Netto M, Carvalho EM. Polar and subpolar diffuse cutaneous leishmaniasis in Brazil: clinical and immunopathologic aspects. *Int J Dermatol* (1995) 34:474–9. doi: 10.1111/j.1365-4362.1995.tb00613.x
11. Saldanha MG, Pagliari C, Queiroz A, Machado PRL, Carvalho L, Scott P, et al. Tissue damage in human cutaneous leishmaniasis: correlations between inflammatory cells and molecule expression. *Front Cell Infect Microbiol* (2020) 10:355. doi: 10.3389/fcimb.2020.00355
12. Sansonetti P, Lagrange PH. The immunology of leprosy: speculations on the leprosy spectrum. *Rev Infect Dis* (1981) 3:422–69. doi: 10.1093/clinids/3.3.422
13. Ridley DS, Jopling WH. A classification of leprosy for research purposes. *Lepr Rev* (1962) 33:119–28. doi: 10.5935/0305-7518.19620014
14. García-Bustos MF, González-Prieto G, Pániz-Mondolfi AE, Parodi C, Beckar J, Monroig S, et al. Risk factors for antimony treatment failure in American Cutaneous Leishmaniasis in Northwestern-Argentina. *PloS Negl Trop Dis* (2021) 15:e0009003. doi: 10.1371/journal.pntd.0009003
15. Coffman RL, Varkila K, Scott P, Chatelain R. Role of cytokines in the differentiation of CD4+ T-cell subsets in vivo. *Immunol Rev* (1991) 123:189–207. doi: 10.1111/j.1600-065X.1991.tb00611.x

16. Locksley RM, Scott P. Helper T-cell subsets in mouse leishmaniasis: induction, expansion and effector function. *Immunol Today* (1991) 12:A58–61. doi: 10.1016/S0167-5699(05)80017-9
17. Sacks D, Noben-Trauth N. The immunology of susceptibility and resistance to Leishmania major in mice. *Nat Rev Immunol* (2002) 2:845–58. doi: 10.1038/nri933
18. Sacks D, Anderson C. Re-examination of the immunosuppressive mechanisms mediating non-cure of Leishmania infection in mice. *Immunol Rev* (2004) 201:225–38. doi: 10.1111/j.0105-2896.2004.00185.x
19. Alexander J, Kaye PM. Immunoregulatory pathways in murine leishmaniasis: different regulatory control during Leishmania mexicana mexicana and Leishmania major infections. *Clin Exp Immunol* (1985) 61:674–82.
20. Afonso LC, Scott P. Immune responses associated with susceptibility of C57BL/10 mice to Leishmania amazonensis. *Infect Immun* (1993) 61:2952–9. doi: 10.1128/IAI.61.7.2952-2959.1993
21. Anderson CF, Mendez S, Sacks DL. Nonhealing infection despite Th1 polarization produced by a strain of Leishmania major in C57BL/6 mice. *J Immunol* (2005) 174:2934–41. doi: 10.4049/jimmunol.174.5.2934
22. Charmoy M, Hurrell BP, Romano A, Lee SH, Ribeiro-Gomes F, Riteau N, et al. The Nlrp3 inflammasome, IL-1β, and neutrophil recruitment are required for susceptibility to a nonhealing strain of Leishmania major in C57BL/6 mice. *Eur J Immunol* (2016) 46:897–911. doi: 10.1002/eji.201546015
23. Novais FO, Carvalho LP, Passos S, Roos DS, Carvalho EM, Scott P, et al. Genomic profiling of human Leishmania braziliensis lesions identifies transcriptional modules associated with cutaneous immunopathology. *J Invest Dermatol* (2015) 135:94–101. doi: 10.1038/jid.2014.305
24. Glennie ND, Volk SW, Scott P. Skin-resident CD4+ T cells protect against Leishmania major by recruiting and activating inflammatory monocytes. *PloS Pathog* (2017) 13:e1006349. doi: 10.1371/journal.ppat.1006349
25. Roma EH, Macedo JP, Goes GR, Gonçalves JL, de CW, Cisalpino D, et al. Impact of reactive oxygen species (ROS) on the control of parasite loads and inflammation in Leishmania amazonensis infection. *Parasit Vectors* (2016) 9:193. doi: 10.1186/s13071-016-1472-y
26. Carneiro MBH, Roma EH, Ranson AJ, Doria NA, Debrabant A, Sacks DL, et al. NOX2-Derived Reactive Oxygen Species Control Inflammation during Leishmania amazonensis Infection by Mediating Infection-Induced Neutrophil Apoptosis. *J Immunol* (2018) 200:196–208. doi: 10.4049/jimmunol.1700899
27. Uzonna JE, Joyce KL, Scott P. Low dose Leishmania major promotes a transient T helper cell type 2 response that is down-regulated by interferon gamma-producing CD8+ T cells. *J Exp Med* (2004) 199:1559–66. doi: 10.1084/jem.20040172
28. Belkaid Y, Von Stebut E, Mendez S, Lira R, Caler E, Bertholet S, et al. CD8+ T cells are required for primary immunity in C57BL/6 mice following low-dose, intradermal challenge with Leishmania major. *J Immunol* (2002) 168:3992–4000. doi: 10.4049/jimmunol.168.8.3992
29. Scharton-Kersten T, Afonso LC, Wysocka M, Trinchieri G, Scott P. IL-12 is required for natural killer cell activation and subsequent T helper 1 cell development in experimental leishmaniasis. *J Immunol* (1995) 154:5320–30.
30. Glennie ND, Yeramilli VA, Beiting DP, Volk SW, Weaver CT, Scott P. Skin-resident memory CD4+ T cells enhance protection against Leishmania major infection. *J Exp Med* (2015) 212:1405–14. doi: 10.1084/jem.20142101
31. Peters NC, Pagán AJ, Lawyer PG, Hand TW, Henrique Roma E, Stamper LW, et al. Chronic parasitic infection maintains high frequencies of short-lived Ly6C+CD4+ effector T cells that are required for protection against re-infection. *PloS Pathog* (2014) 10:e1004538. doi: 10.1371/journal.ppat.1004538
32. Kolde G, Luger T, Sorg C, Sunderkotter C. Successful treatment of cutaneous leishmaniasis using systemic interferon-gamma. *Dermatol (Basel)* (1996) 192:56–60. doi: 10.1159/000246316
33. Falcoff E, Taranto NJ, Remondegui CE, Dedet JP, Canini LM, Ripoll CM, et al. Clinical healing of antimony-resistant cutaneous or mucocutaneous leishmaniasis following the combined administration of interferon-gamma and pentavalent antimonial compounds. *Trans R Soc Trop Med Hyg* (1994) 88:95–7. doi: 10.1016/0035-9203(94)90518-5
34. Heinzel FP, Schoenhaut DS, Rerko RM, Rosser LE, Gately MK. Recombinant interleukin 12 cures mice infected with Leishmania major. *J Exp Med* (1993) 177:1505–9. doi: 10.1084/jem.177.5.1505
35. Nabors GS, Afonso LC, Farrell JP, Scott P. Switch from a type 2 to a type 1 T helper cell response and cure of established Leishmania major infection in mice is induced by combined therapy with interleukin 12 and Pentostam. *Proc Natl Acad Sci USA* (1995) 92:3142–6. doi: 10.1073/pnas.92.8.3142
36. Santos JB, de Jesus AR, Machado PR, Magalhães A, Salgado K, Carvalho EM, et al. Antimony plus recombinant human granulocyte-macrophage colony-stimulating factor applied topically in low doses enhances healing of cutaneous Leishmaniasis ulcers: a randomized, double-blind, placebo-controlled study. *J Infect Dis* (2004) 190:1793–6. doi: 10.1086/424848
37. Almeida RP, Brito J, Machado PL, DE Jesus AR, Schriefer A, Guimarães LH, et al. Successful treatment of refractory cutaneous leishmaniasis with GM-CSF and antimonials. *Am J Trop Med Hyg* (2005) 73:79–81.
38. Miranda-Verástegui C, Llanos-Cuentas A, Arévalo I, Ward BJ, Matlashewski G. Randomized, double-blind clinical trial of topical imiquimod 5% with parenteral meglumine antimoniate in the treatment of cutaneous leishmaniasis in Peru. *Clin Infect Dis* (2005) 40:1395–403. doi: 10.1086/429238
39. Berbert TRN, de Mello TFP, Wolf Nassif P, Mota CA, Silveira AV, Duarte GC, et al. Pentavalent Antimonials Combined with Other Therapeutic Alternatives for the Treatment of Cutaneous and Mucocutaneous Leishmaniasis: A Systematic Review. *Dermatol Res Pract* (2018) 2018:9014726. doi: 10.1155/2018/9014726
40. Gautam S, Kumar R, Maurya R, Nylén S, Ansari N, Rai M, et al. IL-10 neutralization promotes parasite clearance in splenic aspirate cells from patients with visceral leishmaniasis. *J Infect Dis* (2011) 204:1134–7. doi: 10.1093/infdis/jir461
41. Faleiro RJ, Kumar R, Bunn PT, Singh N, Chauhan SB, Sheel M, et al. Combined immune therapy for the treatment of visceral leishmaniasis. *PloS Negl Trop Dis* (2016) 10:e0004415. doi: 10.1371/journal.pntd.0004415
42. Barral-Netto M, Barral A, Brownell CE, Skeiky YA, Ellingsworth LR, Twardzik DR, et al. Transforming growth factor-beta in leishmanial infection: a parasite escape mechanism. *Science* (1992) 257:545–8. doi: 10.1126/science.1636092
43. Anderson CF, Stumhofer JS, Hunter CA, Sacks D. IL-27 regulates IL-10 and IL-17 from CD4+ cells in nonhealing Leishmania major infection. *J Immunol* (2009) 183:4619–27. doi: 10.4049/jimmunol.0804024
44. Waldman AD, Fritz JM, Lenardo MJ. A guide to cancer immunotherapy: from T cell basic science to clinical practice. *Nat Rev Immunol* (2020) 20:651–68. doi: 10.1038/s41577-020-0306-5
45. da Fonseca-Martins AM, Ramos TD, Pratti JES, Firmino-Cruz L, Gomes DCO, Soong L, et al. Immunotherapy using anti-PD-1 and anti-PD-L1 in Leishmania amazonensis-infected BALB/c mice reduce parasite load. *Sci Rep* (2019) 9:20275. doi: 10.1038/s41598-019-56336-8
46. Liang SC, Greenwald RJ, Latchman YE, Rosas L, Satoskar A, Freeman GJ, et al. PD-L1 and PD-L2 have distinct roles in regulating host immunity to cutaneous leishmaniasis. *Eur J Immunol* (2006) 36:58–64. doi: 10.1002/eji.200535458
47. Garcia De Moura R, Covre LP, Fantecelle CH, Gajardo VAT, Cunha CB, Stringari LL, et al. PD-1 blockade modulates functional activities of exhausted-like T cell in patients with cutaneous leishmaniasis. *Front Immunol* (2021), 1–12. doi: 10.3389/fimmu.2021.632667
48. González-Tafoya E, Diupotex M, Zamora-Chimal J, Salaiza-Suazo N, Ruiz-Remigio A, Becker I. TNF contributes to T-cell exhaustion in chronic L. mexicana infections of mice through PD-L1 up-regulation. *Cell Immunol* (2020) 358:104196. doi: 10.1016/j.cellimm.2020.104196
49. Machado PRL, Lessa H, Lessa M, Guimarães LH, Bang H, Ho JL, et al. Oral pentoxifylline combined with pentavalent antimony: a randomized trial for mucosal leishmaniasis. *Clin Infect Dis* (2007) 44:788–93. doi: 10.1086/511643
50. Brito G, Dourado M, Guimarães LH, Meireles E, Schriefer A, de Carvalho EM, et al. Oral Pentoxifylline Associated with Pentavalent Antimony: A Randomized Trial for Cutaneous Leishmaniasis. *Am J Trop Med Hyg* (2017) 96:1155–9. doi: 10.4269/ajtmh.16-0435
51. Lessa HA, Machado P, Lima F, Cruz AA, Bacellar O, Guerreiro J, et al. Successful treatment of refractory mucosal leishmaniasis with pentoxifylline plus antimony. *Am J Trop Med Hyg* (2001) 65:87–9. doi: 10.4269/ajtmh.2001.65.87
52. Brodskyn CI, Barral A, Boaventura V, Carvalho E, Barral-Netto M. Parasite-driven in vitro human lymphocyte cytotoxicity against autologous infected macrophages from mucosal leishmaniasis. *J Immunol* (1997) 159:4467–73.

53. Faria DR, Souza PEA, Durães FV, Carvalho EM, Gollob KJ, Machado PR, et al. Recruitment of CD8(+) T cells expressing granzyme A is associated with lesion progression in human cutaneous leishmaniasis. *Parasite Immunol* (2009) 31:432–9. doi: 10.1111/j.1365-3024.2009.01125.x
54. Novais FO, Carvalho LP, Graff JW, Beiting DP, Ruthel G, Roos DS, et al. Cytotoxic T cells mediate pathology and metastasis in cutaneous leishmaniasis. *PloS Pathog* (2013) 9:e1003504. doi: 10.1371/journal.ppat.1003504
55. Novais FO, Scott P. CD8+ T cells in cutaneous leishmaniasis: the good, the bad, and the ugly. *Semin Immunopathol* (2015) 37:251–9. doi: 10.1007/s00281-015-0475-7
56. Novais FO, Carvalho AM, Clark ML, Carvalho LP, Beiting DP, Brodsky IE, et al. CD8+ T cell cytotoxicity mediates pathology in the skin by inflammasome activation and IL-1β production. *PloS Pathog* (2017) 13: e1006196. doi: 10.1371/journal.ppat.1006196
57. Santos C da S, Boaventura V, Ribeiro Cardoso C, Tavares N, Lordelo MJ, Noronha A, et al. CD8(+) granzyme B(+)-mediated tissue injury vs. CD4(+) IFNγ(+)-mediated parasite killing in human cutaneous leishmaniasis. *J Invest Dermatol* (2013) 133:1533–40. doi: 10.1038/jid.2013.4
58. Cardoso TM, Machado Á, Costa DL, Carvalho LP, Queiroz A, Machado P, et al. Protective and pathological functions of CD8+ T cells in Leishmania braziliensis infection. *Infect Immun* (2015) 83:898–906. doi: 10.1128/IAI.02404-14
59. Amorim CF, Novais FO, Nguyen BT, Misic AM, Carvalho LP, Carvalho EM, et al. Variable gene expression and parasite load predict treatment outcome in cutaneous leishmaniasis. *Sci Transl Med* (2019) 11:eaax4204. doi: 10.1126/scitranslmed.aax4204
60. Campos TM, Novais FO, Saldanha M, Costa R, Lordelo M, Celestino D, et al. Granzyme B produced by natural killer cells enhances inflammatory response and contributes to the immunopathology of cutaneous leishmaniasis. *J Infect Dis* (2020) 221:973–82. doi: 10.1093/infdis/jiz538
61. Covre LP, Devine O, Garcia de Moura R, Vukmanovic-Stejic M, Dietze R, Rodrigues RR, et al. Compartmentalized cytotoxic immune response leads to distinct pathogenic roles of natural killer and senescent CD8+ T cells in human cutaneous leishmaniasis. *Immunology* (2020) 159:429–40. doi: 10.1111/imm.13173
62. Novais FO, Wong AC, Villareal DO, Beiting DP, Scott P. CD8+ T Cells Lack Local Signals To Produce IFN-γ in the Skin during Leishmania Infection. *J Immunol* (2018) 200:1737–45. doi: 10.4049/jimmunol.1701597
63. Soong L, Chang CH, Sun J, Longley BJ, Ruddle NH, Flavell RA, et al. Role of CD4+ T cells in pathogenesis associated with Leishmania amazonensis infection. *J Immunol* (1997) 158:5374–83.
64. Crosby EJ, Goldschmidt MH, Wherry EJ, Scott P. Engagement of NKG2D on bystander memory CD8 T cells promotes increased immunopathology following Leishmania major infection. *PloS Pathog* (2014) 10:e1003970. doi: 10.1371/journal.ppat.1003970
65. Crosby EJ, Clark M, Novais FO, Wherry EJ, Scott P. Lymphocytic Choriomeningitis Virus Expands a Population of NKG2D+CD8+ T Cells That Exacerbates Disease in Mice Coinfected with Leishmania major. *J Immunol* (2015) 195:3301–10. doi: 10.4049/jimmunol.1500855
66. Da-Cruz AM, Oliveira-Neto MP, Bertho AL, Mendes-Aguiar CO, Coutinho SG. T cells specific to leishmania and other nonrelated microbial antigens can migrate to human leishmaniasis skin lesions. *J Invest Dermatol* (2010) 130:1329–36. doi: 10.1038/jid.2009.428
67. Christensen SM, Dillon LAL, Carvalho LP, Passos S, Novais FO, Hughitt VK, et al. Meta-transcriptome Profiling of the Human-Leishmania braziliensis Cutaneous Lesion. *PloS Negl Trop Dis* (2016) 10:e0004992. doi: 10.1371/journal.pntd.0004992
68. Xin L, Li Y, Soong L. Role of interleukin-1beta in activating the CD11c(high) CD45RB- dendritic cell subset and priming Leishmania amazonensis-specific CD4+ T cells in vitro and in vivo. *Infect Immun* (2007) 75:5018–26. doi: 10.1128/IAI.00499-07
69. Voronov E, Dotan S, Gayvoronsky L, White RM, Cohen I, Krelin Y, et al. IL-1-induced inflammation promotes development of leishmaniasis in susceptible BALB/c mice. *Int Immunol* (2010) 22:245–57. doi: 10.1093/intimm/dxq006
70. Fernández-Figueroa EA, Rangel-Escareño C, Espinosa-Mateos V, Carrillo-Sánchez K, Salaiza-Suazo N, Carrada-Figueroa G, et al. Disease severity in patients infected with Leishmania mexicana relates to IL-1β. *PloS Negl Trop Dis* (2012) 6:e1533. doi: 10.1371/journal.pntd.0001533
71. Kautz-Neu K, Kostka SL, Dinges S, Iwakura Y, Udey MC, von Stebut E. A role for leukocyte-derived IL-1RA in DC homeostasis revealed by increased susceptibility of IL-1RA-deficient mice to cutaneous leishmaniasis. *J Invest Dermatol* (2011) 131:1650–9. doi: 10.1038/jid.2011.99
72. Lima-Junior DS, Costa DL, Carregaro V, Cunha LD, Silva ALN, Mineo TWP, et al. Inflammasome-derived IL-1β production induces nitric oxide-mediated resistance to Leishmania. *Nat Med* (2013) 19:909–15. doi: 10.1038/nm.3221
73. Schwartz DM, Kanno Y, Villarino A, Ward M, Gadina M, O'Shea JJ. JAK inhibition as a therapeutic strategy for immune and inflammatory diseases. *Nat Rev Drug Discovery* (2017) 16:843–62. doi: 10.1038/nrd.2017.201
74. Xing L, Dai Z, Jabbari A, Cerise JE, Higgins CA, Gong W, et al. Alopecia areata is driven by cytotoxic T lymphocytes and is reversed by JAK inhibition. *Nat Med* (2014) 20:1043–9. doi: 10.1038/nm.3645
75. Novais FO, Nguyen BT, Scott P. Granzyme B inhibition by tofacitinib blocks the pathology induced by CD8 T cells in cutaneous leishmaniasis. *J Invest Dermatol* (2020) 141:575–85. doi: 10.1016/j.jid.2020.07.011
76. Naik S, Bouladoux N, Wilhelm C, Molloy MJ, Salcedo R, Kastenmuller W, et al. Compartmentalized control of skin immunity by resident commensals. *Science* (2012) 337:1115–9. doi: 10.1126/science.1225152
77. Gimblet C, Meisel JS, Loesche MA, Cole SD, Horwinski J, Novais FO, et al. Cutaneous Leishmaniasis Induces a Transmissible Dysbiotic Skin Microbiota that Promotes Skin Inflammation. *Cell Host Microbe* (2017) 22:13–24.e4. doi: 10.1016/j.chom.2017.06.006

Conflict of Interest: The authors declare that the research was conducted in the absence of any commercial or financial relationships that could be construed as a potential conflict of interest.

frontiers in Immunology

ORIGINAL RESEARCH
published: 16 April 2021
doi: 10.3389/fimmu.2021.647832

Large-Scale Gene Expression Signatures Reveal a Microbicidal Pattern of Activation in *Mycobacterium leprae*-Infected Monocyte-Derived Macrophages With Low Multiplicity of Infection

*Thyago Leal-Calvo[1], Bruna Leticia Martins[2,3], Daniele Ferreira Bertoluci[2,3], Patricia Sammarco Rosa[2], Rodrigo Mendes de Camargo[2,3], Giovanna Vale Germano[2,3], Vania Nieto Brito de Souza[2,3], Ana Carla Pereira Latini[2,3] and Milton Ozório Moraes[1]**

[1] Laboratório de Hanseníase, Instituto Oswaldo Cruz, FIOCRUZ, Rio de Janeiro, Brazil, [2] Divisão de Pesquisa e Ensino, Instituto Lauro de Souza Lima, Bauru, Brazil, [3] Departamento de Doenças Tropicais, Faculdade de Medicina de Botucatu, Universidade Estadual Paulista, Botucatu, Brazil

OPEN ACCESS

Edited by:
Fabienne Tacchini-Cottier, University of Lausanne, Switzerland

Reviewed by:
Ricardo Silvestre, University of Minho, Portugal
Gaurav Gupta, NIIT University, India

***Correspondence:**
Milton Ozório Moraes
milton.moraes@fiocruz.br

Specialty section:
This article was submitted to Microbial Immunology, a section of the journal Frontiers in Immunology

Received: *30 December 2020*
Accepted: *31 March 2021*
Published: *16 April 2021*

Citation:
Leal-Calvo T, Martins BL, Bertoluci DF, Rosa PS, Camargo RM, Germano GV, Brito de Souza VN, Pereira Latini AC and Moraes MO (2021) Large-Scale Gene Expression Signatures Reveal a Microbicidal Pattern of Activation in Mycobacterium leprae-Infected Monocyte-Derived Macrophages With Low Multiplicity of Infection. Front. Immunol. 12:647832. doi: 10.3389/fimmu.2021.647832

Leprosy is a disease with a clinical spectrum of presentations that is also manifested in diverse histological features. At one pole, lepromatous lesions (L-pole) have phagocytic foamy macrophages heavily parasitized with freely multiplying intracellular *Mycobacterium leprae*. At the other pole, the presence of epithelioid giant cells and granulomatous formation in tuberculoid lesions (T-pole) lead to the control of *M. leprae* replication and the containment of its spread. The mechanism that triggers this polarization is unknown, but macrophages are central in this process. Over the past few years, leprosy has been studied using large scale techniques to shed light on the basic pathways that, upon infection, rewire the host cellular metabolism and gene expression. *M. leprae* is particularly peculiar as it invades Schwann cells in the nerves, reprogramming their gene expression leading to a stem-like cell phenotype. This modulatory behavior exerted by *M. leprae* is also observed in skin macrophages. Here, we used live *M. leprae* to infect (10:1 multiplicity of infection) monocyte-derived macrophages (MDMs) for 48 h and analyzed the whole gene expression profile using microarrays. In this model, we observe an intense upregulation of genes consistent with a cellular immune response, with enriched pathways including peptide and protein secretion, leukocyte activation, inflammation, and cellular divalent inorganic cation homeostasis. Among the most differentially expressed genes (DEGs) are *CCL5/RANTES* and *CYP27B1*, and several members of the metallothionein and metalloproteinase families. This is consistent with a proinflammatory state that would resemble macrophage rewiring toward granulomatous formation observed at the T-pole. Furthermore, a comparison with a dataset retrieved from the Gene Expression Omnibus of *M. leprae*-infected Schwann cells (MOI 100:1) showed that the patterns among the DEGs are highly distinct, as the

Schwann cells under these conditions had a scavenging and phagocytic gene profile similar to M2-like macrophages, with enriched pathways rearrangements in the cytoskeleton, lipid and cholesterol metabolism and upregulated genes including *MVK*, *MSMO1*, and *LACC1/FAMIN*. In summary, macrophages may have a central role in defining the paradigmatic cellular (T-pole) vs. humoral (L-pole) responses and it is likely that the multiplicity of infection and genetic polymorphisms in key genes are gearing this polarization.

Keywords: macrophages, *Mycobacterium leprae*, eQTLs, SNPs, host-directed therapy, leprosy, tuberculosis

INTRODUCTION

Schwann cells in the peripheral nerves and macrophages in the skin are the major host cells for *Mycobacterium leprae* (ML) infection (1). These cells operate with high plasticity, induced by different environmental factors, and *M. leprae* has a unique ability to subvert and reprogram these host cells in order to establish a more favorable niche in which to replicate and spread. Huge transcriptomic variations may induce phenotypic modifications, as evidenced by transformations in Schwann to mesenchymal-like cells upon infection (2). Furthermore, increased glucose uptake, mitochondrial shutdown, and lipid biosynthesis resembling the Warburg effect are all phenomena induced upon *M. leprae* infection in these cells, although some of these are restricted to specific clinical forms (3).

Clinical presentation of leprosy is a spectrum encompassing a myriad of manifestations (1), where the tuberculoid pole (T-pole) is restrictive to bacillus growth leading to localized disease, while the lepromatous forms (L-pole) present a permissive and disseminated clinical form with high bacterial loads (1). *M. leprae* has suffered a reductive evolution resulting in low genetic variability, which suggests that the diversity of the disease phenotypes is attributable to the host responses (4). This landscape makes leprosy a unique model to understand the mechanisms involved in the immunopathogenesis of infectious diseases.

In the skin, macrophages are pivotal in the host-pathogen interaction, having important roles from proinflammatory and microbicidal activity to tissue remodeling and wound healing, which are features of the so-called M1 and M2 macrophages, respectively. Most of the skin macrophages are derived from monocytes that migrate and differentiate under inflammatory stimuli, referred to as monocyte-derived macrophages (MDMs) (5). Macrophages present huge functional plasticity according to the milieu in order to maintain skin homeostasis (6). Although less efficient in T cell activation than dendritic cells, they are vastly superior in their phagocytic ability (7). Additionally, monocytes engulf the bacillus through phagocytosis and produce cytokines helping to dictate the host-specific immune response at the lesion. The initial immune events involved in leprosy disease progression are probably triggered by the macrophage-*M. leprae* interaction. This hypothesis can be reinforced by the fact that key innate immune genes, pattern recognition receptors, and autophagic genes have been associated with disease outcome in the mouse model for bacilli replication (infected footpads of Balb/C lineage mice) that carries the *NRAMP1* polymorphism. Furthermore, human genome-wide association studies and other genetic analysis has identified *PRKN*, *LRRK2*, *NOD2*, *TLR1*, and *MRC1* as genes associated with disease outcome and are expressed in *M. leprae*-infected macrophages (8). In this regard, polarized macrophages are found according to the clinical form of leprosy. In tuberculoid lesions, there is a predominance of classically-activated macrophages, which are able to partially contain *M. leprae* replication by activation of cellular responses, vitamin D-dependent pathways, and granuloma formation consistent with the M1 profile (9). On the other hand, lepromatous lesions present permissive, scavenging, phagocytic, and foamy macrophages with anti-inflammatory profile harboring a large number of bacilli, associated with a poor microbicide activity, which are the phenotypes of M2 macrophages (9, 10).

Pathways such as apoptosis and autophagy, combined with lower levels of proinflammatory cytokines and antigen presentation molecules are inhibited by live, but not dead, *M. leprae* in macrophages and Schwann cells (11–13). This type of response is triggered by type I interferons (IFNs) through a STING/TBK/IRF3 pathway that inhibits IFN-gamma and other microbicidal mechanisms within infected macrophages *in vitro* (12).

In a recent re-analysis of leprosy public microarray datasets, mainly comparing skin lesions from different clinical forms, we confirmed previous genes and pathways corroborating the predominance of cellular immunity, leukocyte differentiation, vitamin D receptor (VDR)-mediated microbicidal responses, and granuloma formation at the T-pole, while the L-pole exhibited scavenger receptors and lipid metabolism genes (14). Nevertheless, we also pointed out new differentially expressed genes (DEGs) in leprosy related to skin development and keratinocyte differentiation (14).

Macrophages play a central role in orchestrating gene modulation within the nerve or skin microenvironment. Nevertheless, genome-wide expression patterns from *M. leprae*-infected macrophages have never been obtained. The gene expression signatures of these macrophages can provide target discoveries for therapies and prevention strategies to interfere with leprosy outcomes. Herein, we show the DEGs of macrophages related to immune and other responses after *M. leprae* infection. Our data indicate that *M. leprae*-infected MDMs

submitted to a low multiplicity of infection (10:1) for 48 h overly express a cellular immunity profile. This suggests an *M. leprae*-induced program that might create a granuloma formation type of response in the tissues. Moreover, a comparison between the dataset generated in this study with that of a previously published dataset involving *M. leprae*-infected primary Schwann cells *in vitro* was performed. Through this comparison it was found that the expression profile obtained after a higher multiplicity of infection (100:1) for 48 h has a distinct activation pattern, with genes associated with lipid biosynthesis and consistent with a scavenging and phagocytic profile. Understanding the interaction between macrophage and *M. leprae* is highly relevant in deciphering key features that could further aid in the definition of the clinical forms.

MATERIALS AND METHODS

Study Subjects

Volunteers were recruited from the staff of the Lauro de Souza Lima Institute (Secretary of Health of São Paulo State, Brazil) including health care, cleaning, and security workers, as well as students. Firstly, 29 healthy individuals (14 men and 15 women, from 20 to 30 years), free from cancer and infectious and autoimmune diseases, were enrolled for the collection of peripheral blood. A signed, written informed consent was obtained from all participants. The study was approved by the Local Ethics Committee (Protocol: 56169616.5.0000.5475).

Monocyte-Derived Macrophage (MDM) Differentiation

Fifty milliliters of peripheral blood were collected by venipuncture in tubes with anticoagulant (heparin). Peripheral blood mononuclear cells (PBMCs) were purified by density gradient (Histopaque 1077, Sigma Co., St. Louis, MO, USA) and monocytes were isolated by positive selection employing anti-CD14-coated magnetic microbeads (Miltenyi Biotec, Auburn, CA, USA) according to the manufacturer's instructions. Purity greater than 95% was confirmed by flow cytometry using an anti-CD14 antibody (BD Biosciences, Franklin Lakes, NJ, USA).

Macrophages were differentiated by adherence, without using recombinant cytokines, in order to obtain a non-polarized macrophage with M0 phenotype, according described by Vogel and collaborators (15) with modifications. Briefly, monocytes were cultured in 24-well plates (5×10^5 cells/well) in Iscove's modified Dulbecco's medium (IMDM, Gibco, Grand Island, NY, USA) supplemented with 10% of pooled human sera from the participants and 100 units/mL of penicillin and 100 µg/mL of streptomycin (Gibco; Thermo Fisher Scientific, Inc.) for 6 days at 37°C in 5% CO_2 humidified atmosphere for the differentiation into macrophages. Cultures were fed by replacing half part of the complete medium on the third day. The percentage of differentiated macrophages was evaluated during the standardization of the protocols considering the expression of CD68 and was greater than 95%.

M. leprae Purification and Macrophages Infection

M. leprae (Thai-53 strain, kindly provided by Dr. Yuji Yamamoto, NIH, Japan) was obtained from footpads of athymic nude mice, according to a previously described protocol (16). Briefly, each footpad was inoculated with 3×10^6 acid-fast bacilli in 30 µL of saline solution. After 6-7 months, mice were euthanized and the footpads were collected (CEUA 06/2006). The protocol for bacilli recovery included footpad dissection, tissue isolation, and enzymatic digestion with 0.05% trypsin, followed by purification, quantification, and evaluation of ML viability using the Live/Dead BacLight Bacterial Viability Kit (Molecular Probes, Inc., Eugene, OR, USA). The *M. leprae* count was done after Ziehl-Neelsen staining (16, 17).

Previously differentiated MDMs were infected with *M. leprae* in the multiplicity of infection of 10 bacilli/cell (MOI = 10:1) and kept at 37°C in 5% CO_2 humidified atmosphere. After 48 h of infection, macrophages were collected in TRIzol Reagent (Thermo Fisher Scientific, Carlsbad, CA, USA). Uninfected MDMs incubated under the same conditions were used as controls.

RNA Isolation and Microarray

Total RNA was extracted by an in-house method using phenol: chloroform and isopropyl alcohol (18). Glycogen (Thermo Fisher Scientific) was added to improve RNA recovery. After centrifugation at 12,000 RPM for 5 minutes, the RNA pellet was washed with 70% ethanol, air dried, and resuspended in DEPC-treated water. RNA quality was evaluated on a Bioanalyzer 2100 Instrument (Agilent Technologies Inc., Palo Alto, CA, USA), by using the RNA 6000 Nano Kit (Agilent Technologies). For all samples, the RNA integrity number (RIN) was higher than 8.

For the transcriptome, RNA samples were then purified with the RNeasy MinElute Cleanup Kit (QIAGEN, Hilden, Germany). The reverse transcription synthesis and biotin labeling were performed with Epicentre TargetAmp Kit (Illumina, CA, USA), and transcriptomes were obtained by chip hybridization using the HumanHT-12 v4 BeadChip followed by scanning in iScan equipment (Illumina) according to manufacturer's instructions.

Microarray Data Analysis

Raw.idat files were imported into the R v. 3.6.1 (BiocVersion 3.9.0) environment using limma v. 3.40.0. Quality control was carried out by investigating raw and normalized expression intensities across arrays with Tukey box plots. Background correction and between-array quantile normalization were performed using negative/positive control probes (19) from the manufacturer with limma::neqc function (**Figure S1C**) (20–22). Next, an ExpressionSet (Biobase v. 2.44.0) object was assembled to hold assay, gene, and phenotype data (23). Principal Component Analysis (PCA) was used to inspect dataset structure and biological and technical effects. PCA was conducted with FactoMineR v. 1.41 (24) and visualized with factoextra v. 1.0.5 and cowplot v. 1.0.0 (**Figures S2A–F**). Outlier samples were removed before attempting statistical inference based on the first three principal components (**Figure S2**).

Differential expression analysis was performed by fitting gene-wise linear models with moderated standard errors by the empirical Bayes method (22, 25). The final model included the independent variables: chip (categorical with seven levels), sex (categorical, two levels), treatment (categorical, two levels), and individuals as a random effect. Genes were mapped to Entrezid and HGNC official symbols using the illuminaHumanv4.db v. 1.26.0 annotation. Duplicated Entrezid were removed by keeping the one with the largest average across all arrays. Finally, nominal P-values were inspected with histograms and adjusted for multiple testing with the Benjamini-Hochberg method to control the false-discovery rate (FDR) (26). Genes were considered differentially expressed (DE) if FDR ≤ 10% and absolute fold-change ≥ 1.5 ($|\log_2 FC| \approx 0.58$) with alternative thresholds indicated wherever used. A volcano plot was drawn to illustrate the DE results with ggplot2 v. 3.3.0 (27). Exploratory hierarchical clustering was constructed with the top 92 DEGs using pheatmap v. 1.0.12 (28), with Euclidean distance (samples) plus average agglomeration and Pearson correlation (genes). Raw and normalized data are available in the Gene Expression Omnibus (GEO) accession GSE162416. Also, data and computer source code are readily available in Zenodo (https://dx.doi.org/10.5281/zenodo.4401968).

Over-Representation Analysis (ORA) and Gene Set Enrichment Analysis (GSEA)

Gene ontology (GO) biological processes (BP) were evaluated separately for up- and downregulated DE lists using clusterProfiler v. 3.12.0 (29), fgsea v. 1.10.0 (30) and org.Hs.eg.db v.3.8.2 annotations. The universe set contained all Entrezid genes (n = 21207) used in DE analyses. The minimum gene set size was 5 and the FDR cutoff was set at 10%. Enriched BP were visualized with dot plots or heat plots. For GSEA (**Figure S3**), the gene list was constructed using limma's estimated $\log_2 FC$. GO BP and Reactome GSEA were estimated with 5000 permutations and with gene sets containing at least five genes (29, 31, 32).

Comparison to Infected Schwann Cell Dataset

Microarray dataset GSE35423 was processed as described elsewhere (12, 14). DEGs from Schwann cells infected with *M. leprae* for 48 hours were filtered by FDR ≤ 10% and $|\log_2 FC| \geq 0.26$ (20% difference). Genes differentially expressed common to both datasets were visually compared with a dot plot along with $\log_2 FC$ and confidence intervals from original results (ggplot2 v. 3.3.0). Since the number of common DEG was large, only the top 50 DEG (sorted by decreasing $\log_2 FC$) with same and opposite modulation signs were drawn. **Table S6** contains the full results. UpSetR v.1.4.0 was used to visualize the intersection between DEG according to the dataset and modulation sign.

Gene Set Variation Analysis (GSVA)

Pathway activity was estimated using GSVA with custom gene sets (33). GSVA is an unsupervised non-parametric alternative to ORA and GSEA as it does not depend on prior selection or ranking of the genes from group comparisons. The score produced by GSVA can be interpreted as the coordinated activation of genes from the gene set, summarizing the expression profile within individual samples. The gene sets used herein were compiled from literature and functional annotation databases. The 'granulomatosis' gene set was assembled with genes sourced from the Human Phenotype Ontology (HP:0002955), Gene Ontology (GO:0002432), and DisGeneNet (granulomatous diseases with score ≥ 0.1) totaling 30 genes (**Table S7**). The macrophage polarization signatures are mainly from (34), where 'M1' (n genes = 25), 'M2' (n=20), 'M2a' (n=12), 'M2b' (n=9) and 'M2c' (n=12). 'Pro-M1' and 'Pro-M2' gene sets were built from literature (35, 36). Autophagy genes were retrieved from Reactome v.75 accessions: 'Macroautophagy' (R-HSA-1632852.8, n=137), 'Chaperone Mediated Autophagy' (R-HSA-9613829.3, n=22), and 'Late endosomal microautophagy' (R-HSA-9615710.3, n=34). Wilcoxon signed-rank test was used to test the differences between mean ranks between infected and mock macrophages signatures. Spearman's rank correlation coefficient was calculated alongside 95% confidence intervals using DescTools R package v.0.99.40 (37). Principal component analysis (PCA) was applied to further explore the macroautophagy genes in the dataset. Mean-centered and variance standardized expression matrix with the 137 genes from macroautophagy gene set was subjected to PCA computed with FactoMineR v.2.4 (24). PCA scatter plot and contribution bar plots were graphed with factoextra v.1.0.6.

RESULTS

Differentially Expressed Genes in MDMs Infected With *M. leprae*

Here, we included 29 healthy volunteers (15 females and 14 males) with an age range of 20-30 years. PBMCs were collected and used to obtain monocytes for differentiation to MDMs, which were subsequently infected with *M. leprae* at 10:1 MOI for 48 h. Microarray quality control was used to discard aberrant arrays, and outlier samples were removed (**Figure S2**).

We designed our study to evaluate early changes in the macrophage-*M. leprae* interaction. Thus, human MDMs were analyzed after 48 h of infection with *M. leprae*, which resulted in 325 unique upregulated (FDR ≤ 10% and $\log_2 FC \geq 0.58$) and 117 downregulated (FDR ≤ 10% and $\log_2 FC \leq -0.58$) genes. Genes with the largest effect size ($|\log_2 FC| > 1.5$) are annotated in the volcano plot of **Figure 1A**, of which some members of the metallothionein family can be observed, like *MT1G*, *MT1E* and *MT1P*. **Figure 1B** shows a heatmap with hierarchical clustering of all samples and the top 92 genes with an FDR ≤ 10% and $|\log_2 FC| \geq 1$. The heatmap demonstrates a cluster pattern that clearly distinguishes infected from non-infected samples (**Figure 1B**), at the same time highlighting the high heterogeneity among individuals for some genes, such as *ORM1*, *MT1G*, *MT1H*, *MMP12*, *CXCL5*, *COL22A1*, and *GAL*. Some of the gene families identified such as metallothioneins, chemokines, and interleukins are involved in inflammation and autophagy, and

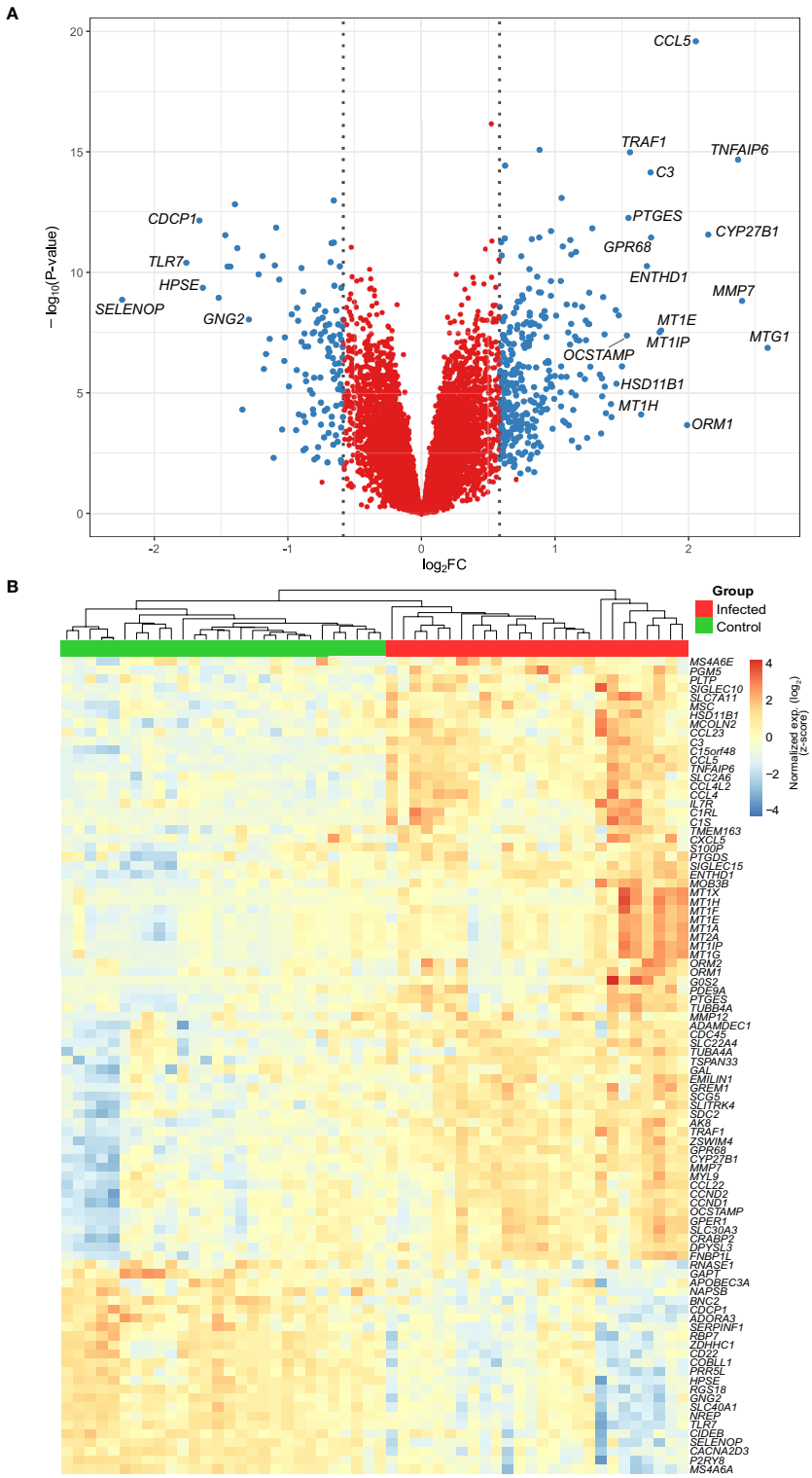

FIGURE 1 | **(A)** Volcano plot showing the DEGs from monocyte-derived macrophages infected with live *M. leprae* (MOI 10:1) for 48 h. Blue dots represent genes with an FDR ≤ 10% and $|\log_2 FC| \geq 0.58$. Gene symbols are given for those with an FDR ≤ 10% and $|\log_2 FC| \geq 1.5$. **(B)** Heatmap and unsupervised hierarchical clustering of genes with an FDR ≤ 10% and $|\log_2 FC| \geq 1$ (n = 92). Samples were clustered based on Euclidean distance and genes with Pearson correlation coefficient, both with average agglomeration. Color key displays expression values in standard deviation units away from the mean (i.e., scaled and centered row-wise). FDR, false discovery rate; FC, fold change.

among the induced genes, we found that *MT1G*, *MMP7*, *TNFAIP6*, *CYP27B1*, and *CCL5/RANTES* had the largest fold-changes (**Figure 1A** and **Table S1**). Conversely, among the most repressed were *SELENOP*, *TLR7*, *CDCP1*, *HPSE*, and *GNG2* (**Figure 1A** and **Table S1**).

To further understand which biological processes the DEGs were involved in, we performed an over-representation analysis (ORA) with Gene Ontology Biological Process annotation. ORA revealed several biological processes modulated by *M. leprae* infection, whereby the expression patterns of the MDM genes were consistent with resistant responses and a reprogramming profile that would induce *M. leprae* killing and infection control. Strikingly, the upregulated pathways had a greater number of DEGs and more robust FDR. Among these predominantly induced pathways, there were redundancies, which are expected since several of these genes participate in multiple pathways. Nevertheless, there is a clear activation of 'regulation of inflammatory response', 'regulation of leukocyte activation', 'cytokine secretion', 'regulation of T cell activation', 'response to IFN-gamma', as well as some others (**Figure 2A** and **Table S2**). On the contrary, downregulated genes pertain to biological processes such as membrane lipid metabolic process, sphingolipid metabolic process, and locomotory behavior (**Figure 2B** and **Table S3**).

Commonly Modulated Genes in Macrophages and Schwann Cells Upon Infection With Live-*M. leprae*

As a comparison, we decided to use a public dataset from *M. leprae* infected (100:1) Schwann cells where approximately 30-100 intracellular bacilli per cell were observed (2). In this case, a shift toward a de-differentiation phenotype was noticed. By comparing the lists of DEGs from this study and the results from Schwann cells infected with live *M. leprae* (100:1) for 48 h, we identified 920 DEGs with FDR ≤ 10% and a difference in mean expression of at least 20% (i.e., $|\log_2 FC| \geq 0.26$). Of these, 229 (24.89%) were upregulated in both datasets, while 179 (19.45%) were jointly downregulated (**Figure 3A** and **Table S6**). On the other hand, 512 genes (55.65%) were regulated in opposite directions in the two experiments (**Figure 3A**). We next graphed the top 50 genes with the greatest $|\log_2 FC|$ for both concordant and discordant DEG, as this can be used to further enlighten both similarities and differences in how the pathogen interacts with each host cell as well as the effect of a higher/lower multiplicity of infection (**Table S6**). Indeed, a higher multiplicity of infection (Schwann dataset) leads to activation of the type I IFN pathways (*OAS1, TRIM7, TNFSF10*) and subversion of energetic metabolism where increased glucose uptake is redirected from glycolysis/mitochondrial respiration to lipid metabolism (*MVK, DHCR7, HMGCS1, LDLR, MSMO1*) (3, 12). In the same manner, some members of TNF signaling, inflammasome pathway, and regulators of NFκB and JNK pathways were upregulated in MDMs but repressed in Schwann cells, such as *TNF*, *CXCL5*, *FAS*, *MAPK13, TRAF1, NKFB2, AIM2*, and *PANX1* (**Figure 3C** and **Table S6**). Furthermore, in Schwann cells, we observed a consistent upregulation of genes involved with prostaglandin biosynthesis, lipogenesis, mitochondrial metabolism, and negative regulation of immune *ADORA1*, *LDLR*, *NOV*, *PPARA*, *SERPINF1*, *FFAR4,* and *ARG2)*. The patterns were quite distinct from the MDMs where Schwann cells showed a more pronounced expression of genes *SELENOP*, *GAL*, *RGS18, AIF1, DEF6*, *ANGPTL6, DHCR7*, *MVK*, and *MSMO*, some involved in cholesterol biosynthesis, along with *LACC1/FAMIN*, which is also genetically associated with leprosy (**Table S6**).

Infected MDMs Express Mainly M1 Polarization Genes That Are Correlated With Granuloma Formation

The somewhat contrasting gene expression profiles identified before suggested that the infected MDMs could be expressing M1 markers with autophagic and phagocytic profiles. To examine this, we calculated gene scores representative of multiple macrophage polarization phenotypes, autophagy, and granulomatosis, which are features often observed in paucibacillary leprosy patients. **Figure 4A** shows the scores for each signature indicating a transcriptional activity increase in genes involved with M1 macrophage polarization, as well as decreased or similar activity for M2, M2a, and Pro-M2. It seems that although genes responsible for inducing M2 phenotype are unaffected, the M2b signature shows activation upon infection, which could indicate either a mixed MDM specialization phenotype or distinctive polarization patterns between individuals, like the clinical disease presentation. As for the autophagy signatures, macroautophagy is specifically active in infected MDMs, whereas chaperone-mediated autophagy appears the opposite (**Figure 4A**). Finally, we tested the correlation between granulomatosis gene scores with M1, M2, and macroautophagy scores. There was a moderated positive correlation between M1 polarization signature with granulomatosis, and no correlation with M2 score, which together corroborated our hypothesis that a pro-inflammatory macrophage profile seems predominant in this model with low MOI (**Figures 4B, C**). The granulomatosis signature does not correlate with macroautophagy, which could indicate that these processes may not be simultaneously active at the transcriptional level (**Figure 4D**). Finally, we wanted to see which macroautophagy genes were driving the signature activity signal. Principal component analysis (PCA) with the 137 genes from the macroautophagy signature revealed that the second principal component (PC2) separated MDMs according to the infection treatment, explaining around 12% of the variability (**Figure 4E**). As expected, there is considerable between-individual variation and noise captured mainly by the first and second principal components (PCs). We then explored PC1, and only the "microarray chip" variable partially correlated with this PC (data not shown). Some uninfected MDMs had basal higher expression (placed vertically higher across PC2) as seen in blue dots over the horizontal dashed line marking zero (**Figure 4E**). Next, we extracted the top 25 genes most correlating to PC2. The gene *TOMM40* alone contributed with explaining almost 4% of the variability of that axis (**Figure 4F**), where more than 25 genes

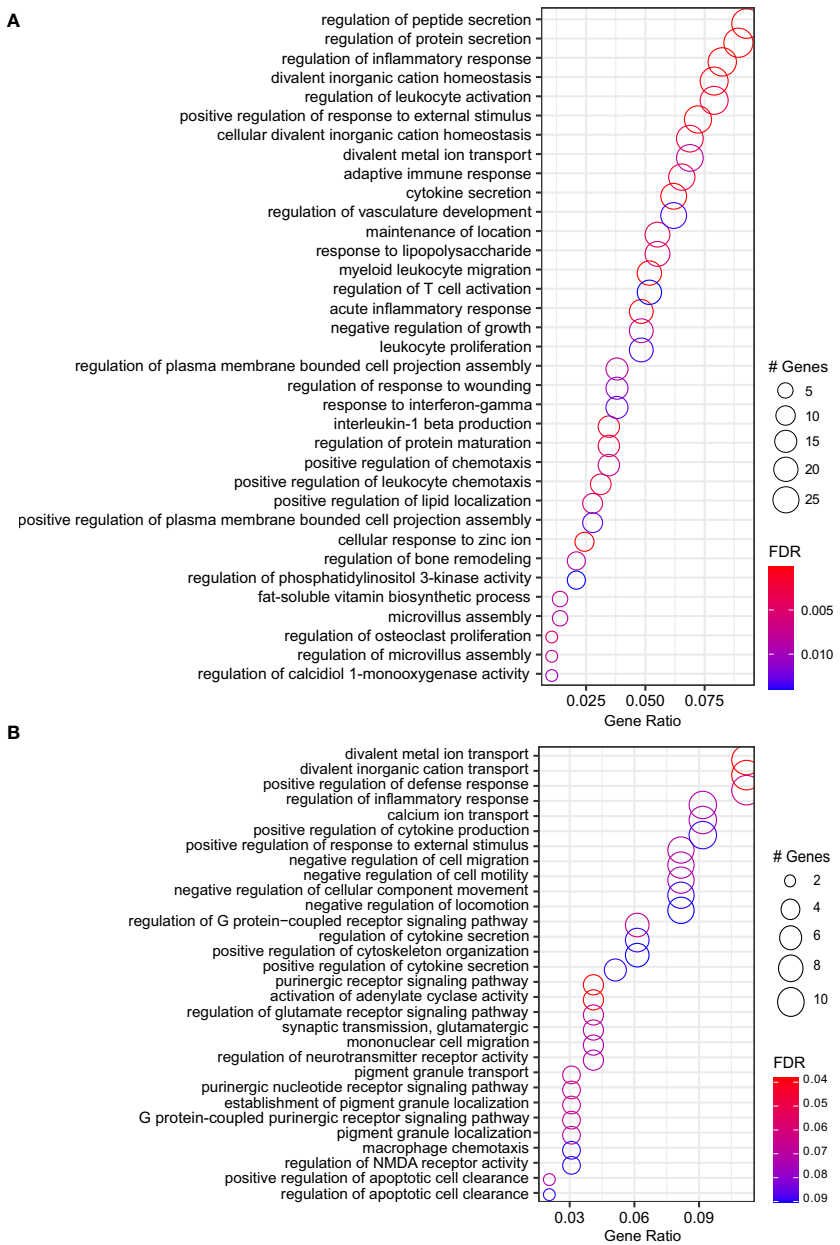

FIGURE 2 | Dot plot showing the top significant GO biological processes enriched from ORA of genes **(A)** upregulated (n = 35) or **(B)** repressed (n = 30) by *M. leprae* infection. Gene ratio is the fraction of genes belonging to an ontology over the total number of modulated genes. Circle size shows the number of modulated genes per biological process. FDR, false discovery rate.

contribute with more variability than would be expected if contributions were uniform (dashed vertical line in **Figure 4F**). Infected MDMs separated from their mock pair by great distance vertically (**Figure 4F**) are cells with the most difference in expression for the genes correlating with PC2, which varies among individuals. Most of the top genes with higher contributions to PC2 showed upregulation after infection with live *M. leprae,* with some exceptions that were significantly downregulated (**Figure 4G**).

DISCUSSION

Here, we evaluated the gene expression patterns of *M. leprae*-infected MDMs, at a 10:1 MOI for 48 h, using a large-scale technique. The data were consistent with an M1-like differentiation profile, with several enriched pathways associated with increased microbicidal activity, T cell activation, and IFN-gamma cytokine secretion. Among the most DE genes were those found in the vitamin D processing

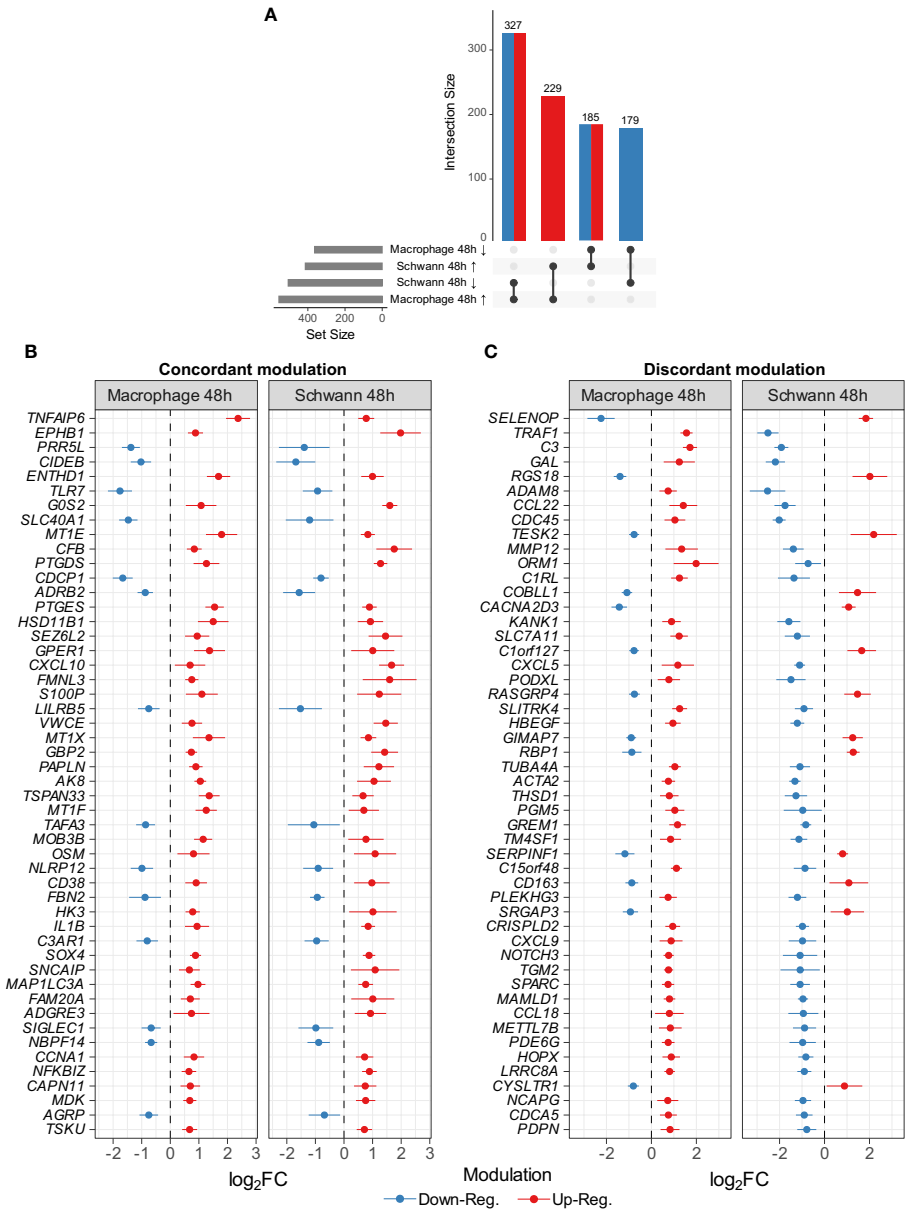

FIGURE 3 | Common DEGs between this study and Schwann cells infected with *M. leprae* (MOI 1:100 for 48 h) [GSE35423] (12). **(A)** The number of commonly DEG by dataset and modulation sign passing $|\log_2 FC| \geq 0.26$ and FDR ≤ 10% in both datasets. Arrows indicate (↑) upregulation and (↓) downregulation. Top 50 DEG common to both datasets modulated in the same manner **(B)** or oppositely **(C)**. Points represent $\log_2 FC$ (unstandardized) from each dataset original differential expression analysis alongside error lines indicating nominal 95% confidence intervals. All genes shown have an FDR ≤ 10% and a difference in mean expression of at least 56% (≈ 0.65 $\log_2 FC$).

pathway (*CYP27B1*, *VDR*, *IL1B*), CC-chemokine ligands (*CCL5, CCL4, CCL3, CCL4L2, CCL2*), receptors involved in cellular migration (*GREM1*, *MCOLN2*, *MDK*, *CCL3*), and inflammation (*CCL5/RANTES*). It seems that a combination of MDM differentiation with *M. leprae* infection at a low multiplicity of infection (10:1) induces a gene expression program in agreement with a protective response. One of these genes, *CCL5/RANTES*, is a key chemoattractant for monocytes in the skin suggesting a pro-inflammatory feedback loop during *M. leprae* infection toward M1-like macrophages, which is consistent with the higher expression in PB leprosy (38, 39). Curiously, the chemokine-clustered genomic region has been associated with leprosy indicating that genetic variations within this gene could contribute to clinical form polarization (40). We observed an upregulation of metallothionein gene's expression, like *MT1E* and *MT1G*. These genes produce proteins that regulate metal availability, while zinc homeostasis is crucial to activation of transcriptional factors and reactive oxygen species

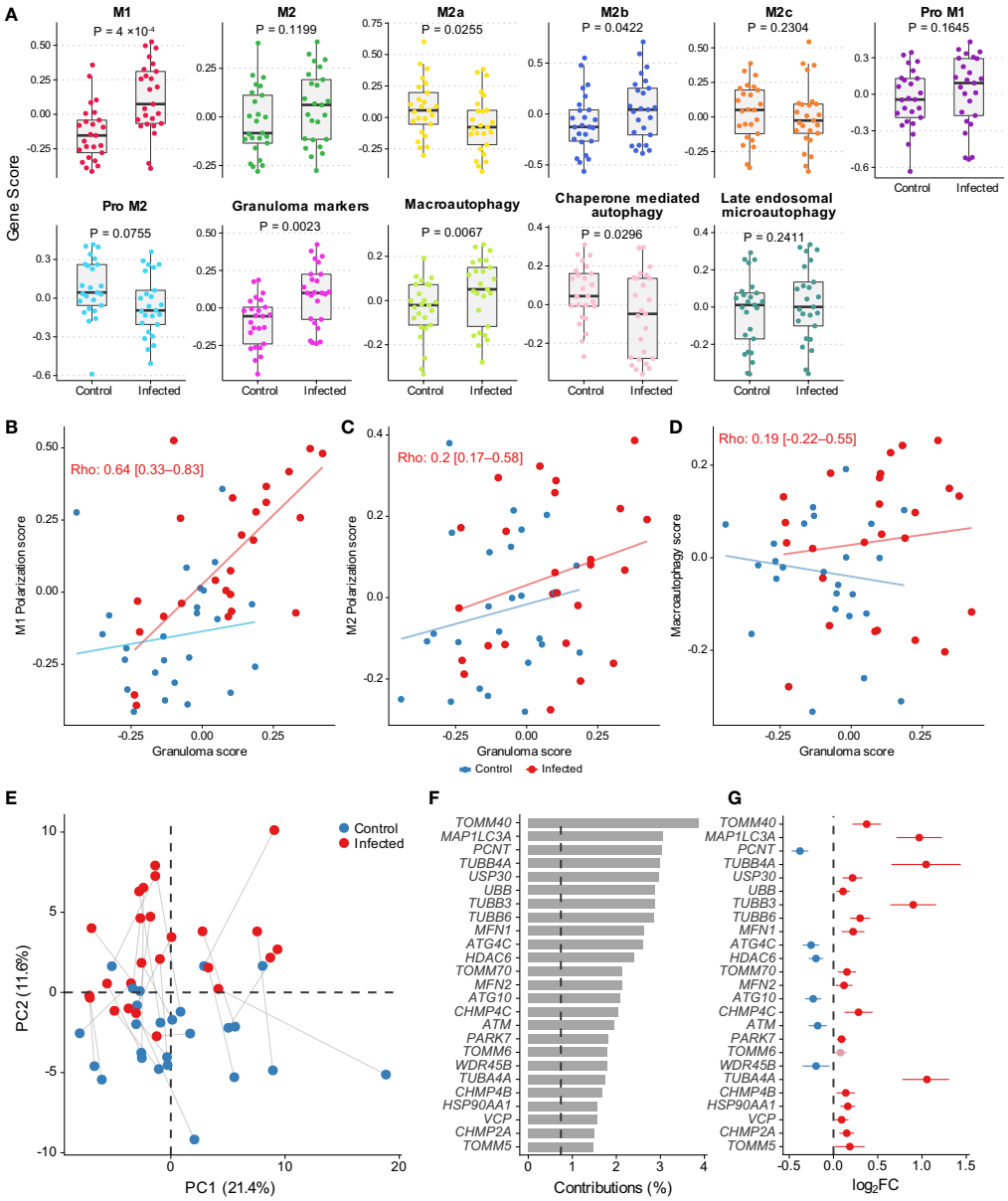

FIGURE 4 | **(A)** Gene scores for macrophage polarization profiles, granulomatosis and autophagy. Tukey box plots display first, second (median), and third quartiles with whiskers extending ± 1.5 × interquartile range (IQR). Each point illustrates a MDM culture (n=50) from one human donor in mock and infected conditions (paired within donor). Nominal P-values displayed are from Wilcoxon signed-rank test. **(B–D)** Scatter plots illustrating the correlation between granulomatosis, M1, M2, and macroautophagy gene scores. Spearman's rank correlation coefficient is shown with nominal 95% confidence intervals calculated only with the infected condition (n=25). Slope and intercept for drawing the lines were estimated using robust linear regression from the MASS v.7.3-53.1 R package. **(E)** Scatter plot with the two first principal components from PCA on the subset of 137 macroautophagy-related genes. Lines connect samples from the same donor. **(F)** Percentage contribution of the top 50 genes most correlated to PC2. **(G)** Log_2FC estimates from differential expression analysis for the top 50 macroautophagy-related genes from PCA and their nominal 95% confidence intervals. Light-shaded red indicates gene with FDR > 10%.

and have been associated with antimicrobial immune responses (41).

Some metalloproteinases, such as *MMP7*, *ADAMDEC1* and *MMP12*, were also highly differentially expressed. These are involved with tissue/matrix remodeling and host defense. It is interesting that the macrophages in this model appear to have a regulatory activation of gene expression involved in tissue remodeling. Indeed, *MMP2* and *MMP9* expression and activity were higher among T-pole patients (42). This pattern is dependable with the reshaping of cellular morphology and the adjacent tissue during M1-like macrophage differentiation observed here.

The upregulation of mitochondrial genes in *M. leprae*-infected-macrophages, as compared to Schwann cells, is also consistent

with the aforementioned alterations observed in infected MDMs toward epithelioid transformation programming. In this same direction, *NDUFAF6*, which encodes a protein that participates in the mitochondrial respiratory chain complex I (NADH: ubiquinone oxidoreductase) assembly; *TACO1*, which is involved in the translational activation of mitochondria cytochrome c; and *TOMM40*, the encoded protein of which produces a pore to channel protein precursors into mitochondria were also observed. We also detected an over-expression in MDMs of metabolite transporters across the inner mitochondrial membrane (*SLC25A12*).

Other sets of induced genes in the MDMs were involved in tubulin assembly and cytoskeleton remodeling, such as *TUBB6*. Some of these genes are involved in autophagy and the mTOR pathway (43), which is increased during macrophage differentiation in the presence of a low *M. leprae* MOI or dead mycobacteria (44). Curiously, Yang and colleagues showed that a 20:1 MOI leads to higher CD163 and an anti-inflammatory profile with higher IL-10 and lower HLA expression, although dead *M. leprae* induced proinflammatory cytokines (45). In clinical samples these patterns are observed in low bacterial index patients (T-pole) and type 1 reactional patients (RR) where vitamin D-mediated microbicidal clearance is observed. Furthermore, IFN-gamma and IL-15 have been demonstrated to gear the polarization of M1-like macrophages, exhibiting a phenotype that is probably orchestrating the milieu inducing granuloma formation and autophagy (44, 46). Thus, there is a clear antagonistic pattern that, on the one hand, we observed granuloma formation and M1-like polarization for macrophages (10:1 MOI), whereas lipid biogenesis, wound healing and a phagocytic signature were observed for Schwann cells (100:1 MOI). This M2-like profile occurred in both Schwann cells and macrophages when higher concentrations of *M. leprae* were used to infect the cells (11, 12, 47). Indeed, molecular and biochemical subversion induced by *M. leprae* infection leads to a type I IFN response reducing autophagy (12, 48) and turning on the Warburg-like effect (3). This is expected since this downregulation was detected as associated with diminished capacity to produce ATP through the respiratory chain (3) and the redirection of glycolysis to lipid biosynthesis. Furthermore, we observed a prominent upregulation toward higher MOI (100:1) when genes associated with cholesterol and fatty acid metabolism (*DHCR7*, *MVK*, and *MSMO*, and *LACC1*/*FAMIN* were analyzed, which are pathways involved in lepromatous leprosy immunopathogenesis.

Genes associated with leprosy outcome are also involved with ulcerative colitis pathogenesis and other diseases, such as Crohn's disease, Parkinson's and Alzheimer's (49). Curiously, some of the genes highlighted here, such as *TOMM40* and *TUBB6*, were associated not only with neurodegenerative diseases, like Alzheimer's, but also with ulcerative colitis (50, 51). These proteins interact with *LRRK2*, which is a gene that has been independently associated with leprosy, and Parkinson's disease (49, 52). Another important gene upregulated in *M. leprae*-Schwann cells was *LACC1*. The protein which *LACC1*/*FAMIN* encodes is involved in fatty acid oxidation and bacterial clearance. Interestingly, the gene was associated with leprosy in several studies (53, 54).

The global gene expression can also be analyzed in a genotype-phenotype correlation perspective. In leprosy, whole blood cells stimulated with *M. leprae* sonicates indicate quantitative trait loci (eQTL) associated with transcript levels when samples were compared before and after stimulation. The data revealed SNPs controlling immunoinflammatory responses such as type II IFNs and bacterial/pathogen recognition (55). Indeed, there are SNPs regulating expression of genes such as *LACC1*, which indicates that it is likely that a combination of *M. leprae*-induced activation with genetic polymorphisms may define the commitment toward the T- or L-pole. Thus, together these could contribute to identifying potential pharmacologic targets as adjuvants to personalize treatment for each specific clinical form.

DATA AVAILABILITY STATEMENT

The datasets presented in this study can be found in online repositories. The names of the repository/repositories and accession number(s) can be found below: https://www.ncbi.nlm.nih.gov/geo/, GSE162416.

ETHICS STATEMENT

The studies involving human participants were reviewed and approved by Local Ethics Committee, Lauro de Souza Lima Institute. The patients/participants provided their written informed consent to participate in this study. The animal study was reviewed and approved by Local Ethics Committee, Lauro de Souza Lima Institute.

AUTHOR CONTRIBUTIONS

AP, MM, and VB contributed to the design and implementation of the research. TL-C, AL, and MM to the writing of the manuscript. BM, DB, RC, and GG performed the experiments and processed the experimental data. TL-C performed the analysis. PR and DB contributed to *M. leprae* maintenance in athymic nude mice and purification. TL-C, MM, and AP to the analysis of the results. All authors provided critical feedback and helped shape the research, analysis and manuscript. All authors contributed to the article and approved the submitted version.

FUNDING

This study was funded in part by the Fundação de Amparo do Estado do Rio de Janeiro (FAPERJ, E_09/2019 - Cientista do Nosso Estado – 2019 and E_34/2014 - PENSA RIO – Apoio ao Estudo de Temas Relevantes e Estratégicos para o RJ - 2014) and the Conselho Nacional de Desenvolvimento Científico e

Tecnológico (CNPq) [grant #313657/2018-1 and 4000170/2017-2]. Fundação de Amparo à Pesquisa do Estado de São Paulo - FAPESP, Grant no. 2015/01744-9.

ACKNOWLEDGMENTS

TL-C was supported by a scholarship from the National Council for Scientific and Technological Development (Conselho Nacional de Desenvolvimento Científico e Tecnológico, CNPq) from 2018 to 2022.

SUPPLEMENTARY MATERIAL

The Supplementary Material for this article can be found online at: https://www.frontiersin.org/articles/10.3389/fimmu.2021.647832/full#supplementary-material

REFERENCES

1. Scollard DM, Adams LB, Gillis TP, Krahenbuhl JL, Truman W, Williams DL. The Continuing Challenges of Leprosy The Continuing Challenges of Leprosy. *Clin Microbiol Rev* (2006) 19:338–81. doi: 10.1128/CMR.19.2.338
2. Masaki T, Qu J, Cholewa-Waclaw J, Burr K, Raaum R, Rambukkana A. Reprogramming adult Schwann cells to stem cell-like cells by leprosy bacilli promotes dissemination of infection. *Cell* (2013) 152:51–67. doi: 10.1016/j.cell.2012.12.014
3. Medeiros RCA, Girardi K do C de V, Cardoso FKL, Mietto B de S, Pinto TG de T, Gomez LS, et al. Subversion of Schwann Cell Glucose Metabolism by Mycobacterium leprae. *J Biol Chem* (2016) 291:21375–87. doi: 10.1074/jbc.M116.725283
4. Cole ST, Eiglmeier K, Parkhill J, James KD, Thomson NR, Wheeler PR, et al. Massive gene decay in the leprosy bacillus. *Nature* (2001) 409:1007–11. doi: 10.1038/35059006
5. Delavary BM, van der Veer WM, van Egmond M, Niessen FB, Beelen RHJ. Macrophages in skin injury and repair. *Immunobiology* (2011) 216:753–62. doi: 10.1016/j.imbio.2011.01.001
6. Mantovani A, Biswas SK, Galdiero MR, Sica A, Locati M. Macrophage plasticity and polarization in tissue repair and remodelling. *J Pathol* (2013) 229:176–85. doi: 10.1002/path.4133
7. Kashem SW, Haniffa M, Kaplan DH. Antigen-Presenting Cells in the Skin. *Annu Rev Immunol* (2017) 35:469–99. doi: 10.1146/annurev-immunol-051116-052215
8. Cardoso CC, Pereira AC, de Sales Marques C, Moraes MO. Leprosy susceptibility: genetic variations regulate innate and adaptive immunity, and disease outcome. *Future Microbiol* (2011) 6:533–49. doi: 10.2217/fmb.11.39
9. Montoya D, Cruz D, Teles RMB, Lee DJ, Ochoa MT, Krutzik SR, et al. Divergence of Macrophage Phagocytic and Antimicrobial Programs in Leprosy. *Cell Host Microbe* (2009) 6:343–53. doi: 10.1016/j.chom.2009.09.002
10. Inkeles MS, Teles RMB, Pouldar D, Andrade PR, Madigan CA, Lopez D, et al. Cell-type deconvolution with immune pathways identifies gene networks of host defense and immunopathology in leprosy. *JCI Insight* (2016) 1:e88843. doi: 10.1172/jci.insight.88843
11. Teles RMB, Graeber TG, Krutzik SR, Montoya D, Schenk M, Lee DJ, et al. Type I Interferon Suppresses Type II Interferon-Triggered Human Anti-Mycobacterial Responses. *Science* (2013) 339:1448–53. doi: 10.1126/science.1233665
12. de Toledo-Pinto TG, Ferreira ABR, Ribeiro-Alves M, Rodrigues LS, Batista-Silva LR, Silva BJ de A, et al. STING-Dependent 2′-5′ Oligoadenylate Synthetase–Like Production Is Required for Intracellular Mycobacterium leprae Survival. *J Infect Dis* (2016) 214:311–20. doi: 10.1093/infdis/jiw144
13. Ma Y, Pei Q, Zhang L, Lu J, Shui T, Chen J, et al. Live Mycobacterium leprae inhibits autophagy and apoptosis of infected macrophages and prevents engulfment of host cell by phagocytes. *Am J Transl Res* (2018) 10:2929–39.
14. Leal-Calvo T, Moraes MO. Reanalysis and integration of public microarray datasets reveals novel host genes modulated in leprosy. *Mol Genet Genomics* (2020) 295:1355–68. doi: 10.1007/s00438-020-01705-6
15. Vogel DYS, Glim JE, Stavenuiter AWD, Breur M, Heijnen P, Amor S, et al. Human macrophage polarization in vitro: maturation and activation methods compared. *Immunobiology* (2014) 219:695–703. doi: 10.1016/j.imbio.2014.05.002
16. Trombone APF, Pedrini SCB, Diório SM, Belone A de FF, Fachin LRV, do Nascimento DC, et al. Optimized protocols for Mycobacterium leprae strain management: frozen stock preservation and maintenance in athymic nude mice. *J Vis Exp* (2014) (85):50620. doi: 10.3791/50620
17. Shepard CC. Acid-fast bacilli in nasal excretions in leprosy, and results of inoculation of mice. *Am J Hyg* (1960) 71:147–57. doi: 10.1093/oxfordjournals.aje.a120098
18. Chomczynski P. A reagent for the single-step simultaneous isolation of RNA, DNA and proteins from cell and tissue samples. *Biotechniques* (1993) 15:532–534, 536–537.
19. Shi W, Oshlack A, Smyth GK. Optimizing the noise versus bias trade-off for Illumina whole genome expression BeadChips. *Nucleic Acids Res* (2010) 38:e204–4. doi: 10.1093/nar/gkq871
20. Smyth GK, Speed T. Normalization of cDNA microarray data. *Methods* (2003) 31:265–73. doi: 10.1016/S1046-2023(03)00155-5
21. Ritchie ME, Phipson B, Wu D, Hu Y, Law CW, Shi W, et al. limma powers differential expression analyses for RNA-sequencing and microarray studies. *Nucleic Acids Res* (2015) 43:e47. doi: 10.1093/nar/gkv007
22. Phipson B, Lee S, Majewski IJ, Alexander WS, Smyth GK. Robust hyperparameter estimation protects against hypervariable genes and improves power to detect differential expression. *Ann Appl Stat* (2016) 10:946–63. doi: 10.1214/16-AOAS920
23. Huber W, Carey VJ, Gentleman R, Anders S, Carlson M, Carvalho BS, et al. Orchestrating high-throughput genomic analysis with Bioconductor. *Nat Methods* (2015) 12:115–21. doi: 10.1038/nmeth.3252
24. Lê S, Josse J, Husson F. FactoMineR : An R Package for Multivariate Analysis. *J Stat Softw* (2008) 25:1–18. doi: 10.18637/jss.v025.i01
25. Smyth GK. Linear Models and Empirical Bayes Methods for Assessing Differential Expression in Microarray Experiments Linear Models and Empirical Bayes Methods for Assessing Differential Expression in Microarray Experiments. *Stat Appl Genet Mol Biol* (2004) 3:1–26. doi: 10.2202/1544-6115.1027
26. Benjamini Y, Hochberg Y. Controlling the False Discovery Rate: A Practical and Powerful Approach to Multiple Testing. *J R Stat Soc Series B* (1995) 57 (1):289–300. doi: 10.1111/j.2517-6161.1995.tb02031.x
27. Wickham H. *ggplot2: Elegant Graphics for Data Analysis*. New York: Springer-Verlag (2016).
28. Kolde R. *pheatmap: Pretty Heatmaps*. R package version 1.0.12 (2019). Available at: https://cran.r-project.org/package=pheatmap.
29. Yu G, Wang L-G, Han Y, He Q-Y. clusterProfiler: an R Package for Comparing Biological Themes Among Gene Clusters. *OMICS: A J Integr Biol* (2012) 16:284–7. doi: 10.1089/omi.2011.0118
30. Korotkevich G, Sukhov V, Sergushichev A. Fast gene set enrichment analysis. *bioRxiv* [Preprint] (2016). Available at: https://www.biorxiv.org/content/10.1101/060012v3 (Accessed April 10, 2021).
31. Subramanian A, Tamayo P, Mootha VK, Mukherjee S, Ebert BL, Gillette MA, et al. Gene set enrichment analysis: A knowledge-based approach for interpreting genome-wide expression profiles. *Proc Natl Acad Sci U States America* (2005) 102:15545–50. doi: 10.1073/pnas.0506580102
32. Mootha VK, Lindgren CM, Eriksson K-F, Subramanian A, Sihag S, Lehar J, et al. PGC-1α-responsive genes involved in oxidative phosphorylation are coordinately downregulated in human diabetes. *Nat Genet* (2003) 34:267–73. doi: 10.1038/ng1180
33. Hänzelmann S, Castelo R, Guinney J. GSVA: gene set variation analysis for microarray and RNA-seq data. *BMC Bioinf* (2013) 14:7. doi: 10.1186/1471-2105-14-7

34. Benoit M, Desnues B, Mege J-L. Macrophage polarization in bacterial infections. *J Immunol* (2008) 181:3733–9. doi: 10.4049/jimmunol.181.6.3733
35. Murray PJ. Macrophage Polarization. *Annu Rev Physiol* (2017) 79:541–66. doi: 10.1146/annurev-physiol-022516-034339
36. Ni Y, Zhuge F, Nagashimada M, Ota T. Novel Action of Carotenoids on Non-Alcoholic Fatty Liver Disease: Macrophage Polarization and Liver Homeostasis. *Nutrients* (2016) 8:391. doi: 10.3390/nu8070391
37. Signorell A. *DescTools: Tools for Descriptive Statistics. R package version 0.99.40.* (2021). Available at: https://cran.r-project.org/package=DescTools.
38. Belone A de FF, Rosa PS, Trombone APF, Fachin LRV, Guidella CC, Ura S, et al. Genome-wide screening of mRNA expression in leprosy patients. *Front Genet* (2015) 6:334. doi: 10.3389/fgene.2015.00334
39. Zhang D-F, Wang D, Li Y-Y, Yao Y-G. Integrative analyses of leprosy susceptibility genes indicate a common autoimmune profile. *J Dermatol Sci* (2016) 82:18–27. doi: 10.1016/j.jdermsci.2016.01.001
40. Jamieson SE, Miller EN, Black GF, Peacock CS, Cordell HJ, Howson JMM, et al. Evidence for a cluster of genes on chromosome 17q11-q21 controlling susceptibility to tuberculosis and leprosy in Brazilians. *Genes Immun* (2004) 5:46–57. doi: 10.1038/sj.gene.6364029
41. Subramanian Vignesh K, Deepe. GS. Metallothioneins: Emerging Modulators in Immunity and Infection. *Int J Mol Sci* (2017) 18:2197. doi: 10.3390/ijms18102197
42. Teles RMB, Teles RB, Amadeu TP, Moura DF, Mendonca-Lima L, Ferreira H, et al. High Matrix Metalloproteinase Production Correlates with Immune Activation and Leukocyte Migration in Leprosy Reactional Lesions. *Infect Immun* (2010) 78:1012–21. doi: 10.1128/IAI.00896-09
43. Jha AK, Huang SC-C, Sergushichev A, Lampropoulou V, Ivanova Y, Loginicheva E, et al. Network Integration of Parallel Metabolic and Transcriptional Data Reveals Metabolic Modules that Regulate Macrophage Polarization. *Immunity* (2015) 42:419–30. doi: 10.1016/j.immuni.2015.02.005
44. Silva BJ de A, Barbosa MG de M, Andrade PR, Ferreira H, Nery JA da C, Côrte-Real S, et al. Autophagy Is an Innate Mechanism Associated with Leprosy Polarization. *PloS Pathog* (2017) 13:e1006103. doi: 10.1371/journal.ppat.1006103
45. Yang D, Shui T, Miranda JW, Gilson DJ, Song Z, Chen J, et al. Mycobacterium leprae-Infected Macrophages Preferentially Primed Regulatory T Cell Responses and Was Associated with Lepromatous Leprosy. *PloS Neglect Trop Dis* (2016) 10:e0004335. doi: 10.1371/journal.pntd.0004335
46. Chun Y, Kim J. Autophagy: An Essential Degradation Program for Cellular Homeostasis and Life. *Cells* (2018) 7(12):278. doi: 10.3390/cells7120278
47. Guerreiro LTA, Robottom-Ferreira AB, Ribeiro-Alves M, Toledo-Pinto TG, Rosa Brito T, Rosa PS, et al. Gene Expression Profiling Specifies Chemokine, Mitochondrial and Lipid Metabolism Signatures in Leprosy. *PloS One* (2013) 8(6):e64748. doi: 10.1371/journal.pone.0064748
48. de Toledo-Pinto TG, Batista-Silva LR, Medeiros RCA, Lara FA, Moraes MO. Type I Interferons, Autophagy and Host Metabolism in Leprosy. *Front Immunol* (2018) 9:806. doi: 10.3389/fimmu.2018.00806
49. Fava VM, Dallmann-Sauer M, Schurr E. Genetics of leprosy: today and beyond. *Hum Genet* (2020) 139:835–46. doi: 10.1007/s00439-019-02087-5
50. Law BMH, Spain VA, Leinster VHL, Chia R, Beilina A, Cho HJ, et al. A direct interaction between leucine-rich repeat kinase 2 and specific β-tubulin isoforms regulates tubulin acetylation. *J Biol Chem* (2014) 289:895–908. doi: 10.1074/jbc.M113.507913
51. Guo Y, Xu W, Li J-Q, Ou Y-N, Shen X-N, Huang Y-Y, et al. Genome-wide association study of hippocampal atrophy rate in non-demented elders. *Aging (Albany NY)* (2019) 11:10468–84. doi: 10.18632/aging.102470
52. Fava VM, Xu YZ, Lettre G, Van Thuc N, Orlova M, Thai VH, et al. Pleiotropic effects for Parkin and LRRK2 in leprosy type-1 reactions and Parkinson's disease. *Proc Natl Acad Sci* (2019) 116:15616–24. doi: 10.1073/pnas.1901805116
53. Cader MZ, Boroviak K, Zhang Q, Assadi G, Kempster SL, Sewell GW, et al. C13orf31 (FAMIN) is a central regulator of immunometabolic function. *Nat Immunol* (2016) 17:1046–56. doi: 10.1038/ni.3532
54. Wang D, Fan Y, Malhi M, Bi R, Wu Y, Xu M, et al. Missense Variants in HIF1A and LACC1 Contribute to Leprosy Risk in Han Chinese. *Am J Hum Genet* (2018) 102:794–805. doi: 10.1016/j.ajhg.2018.03.006
55. Manry J, Nédélec Y, Fava VM, Cobat A, Orlova M, Thuc NV, et al. Deciphering the genetic control of gene expression following Mycobacterium leprae antigen stimulation. *PloS Genet* (2017) 13:e1006952. doi: 10.1371/journal.pgen.1006952

Conflict of Interest: The authors declare that the research was conducted in the absence of any commercial or financial relationships that could be construed as a potential conflict of interest.

frontiers in Immunology

REVIEW
published: 25 May 2021
doi: 10.3389/fimmu.2021.674241

Autophagy as a Target for Drug Development Of Skin Infection Caused by Mycobacteria

Tamiris Lameira Bittencourt[1], *Rhana Berto da Silva Prata*[1], *Bruno Jorge de Andrade Silva*[2], *Mayara Garcia de Mattos Barbosa*[3], *Margareth Pretti Dalcolmo*[4] *and Roberta Olmo Pinheiro*[1]*

[1] Leprosy Laboratory, Oswaldo Cruz Institute, Oswaldo Cruz Foundation (Fiocruz), Rio de Janeiro, Brazil, [2] Division of Dermatology, David Geffen School of Medicine, Los Angeles, CA, United States, [3] Department of Surgery, University of Michigan, Ann Arbor, MI, United States, [4] Helio Fraga Reference Center, Sergio Arouca National School of Public Health, Fiocruz, Rio de Janeiro, Brazil

Pathogenic mycobacteria species may subvert the innate immune mechanisms and can modulate the activation of cells that cause disease in the skin. Cutaneous mycobacterial infection may present different clinical presentations and it is associated with stigma, deformity, and disability. The understanding of the immunopathogenic mechanisms related to mycobacterial infection in human skin is of pivotal importance to identify targets for new therapeutic strategies. The occurrence of reactional episodes and relapse in leprosy patients, the emergence of resistant mycobacteria strains, and the absence of effective drugs to treat mycobacterial cutaneous infection increased the interest in the development of therapies based on repurposed drugs against mycobacteria. The mechanism of action of many of these therapies evaluated is linked to the activation of autophagy. Autophagy is an evolutionary conserved lysosomal degradation pathway that has been associated with the control of the mycobacterial bacillary load. Here, we review the role of autophagy in the pathogenesis of cutaneous mycobacterial infection and discuss the perspectives of autophagy as a target for drug development and repurposing against cutaneous mycobacterial infection.

Keywords: autophagy, skin, mycobacteria, drug development, skin cells

OPEN ACCESS

Edited by:
Esther Christina De Jong, Academic Medical Center, Netherlands

Reviewed by:
Eun-Kyeong Jo, Chungnam National University, South Korea
Mirian Nacagami Sotto, University of São Paulo, Brazil

***Correspondence:**
Roberta Olmo Pinheiro
robertaolmo@gmail.com

Specialty section:
This article was submitted to Microbial Immunology, a section of the journal Frontiers in Immunology

Received: *01 March 2021*
Accepted: *28 April 2021*
Published: *25 May 2021*

Citation:
Bittencourt TL, da Silva Prata RB, de Andrade Silva BJ, de Mattos Barbosa MG, Dalcolmo MP and Pinheiro RO (2021) Autophagy as a Target for Drug Development Of Skin Infection Caused by Mycobacteria. Front. Immunol. 12:674241. doi: 10.3389/fimmu.2021.674241

INTRODUCTION

Pathogenic mycobacteria species subvert the innate immune system barriers and modulate the activation of phagocytes to cause disease not only in the respiratory tract but also in soft tissues and skin, sometimes resulting in disseminated infection (1). Cutaneous mycobacterial infections may cause different clinical manifestations, such as cutaneous manifestations of *Mycobacterium tuberculosis* (*M. tuberculosis*) infection, Buruli ulcer caused by *M. ulcerans* and other related slowly growing mycobacteria, leprosy caused by *M. leprae* and *M. lepromatosis*, and cutaneous infections caused by rapidly growing mycobacteria such as *M. abscessus* subsp. *abscessus*, *M. abscessus* subsp. *bolletti*, *M. abscessus* subsp. *massiliense*, *M. chelonae* and *M. fortuitum* (1–9). Among patients with advanced immunosuppression, *M. avium-intracellulare* complex,

the *M. haemophilum*, and *M. kansasii* may cause cutaneous or disseminated disease. Mycobacterial infections of the skin and subcutaneous tissue are associated with important stigma, deformity, and disability. The treatment for cutaneous mycobacterial infections depends on the specific pathogen, whereas for rapidly growing mycobacteria, the official treatment guidelines recommend carrying out susceptibility tests for antibacterial drugs of different classes (10, 11). Management often includes use of multiple antibiotics for several months (12). Treatment options for cutaneous tuberculosis follow the same recommendations for the treatment of other forms of TB, being limited to conventional oral therapy and surgical intervention for severe forms, such as lupus vulgaris (13, 14). The therapeutic regimen is based on the combination of isoniazid, rifampicin, pyrazinamide, ethambutol and streptomycin according to the needs of each individual. In most cases, skin manifestations result from hematogenous dissemination or are a direct extension from the focus of the infection (14, 15). In addition, treatment of leprosy is performed with multidrug therapy (MDT) and comprises 6 or 12 doses, depending on the clinical form. There is not a consensus for the treatment of cutaneous infections caused by non-tuberculous mycobacteria. Recently, much effort has been made to develop more effective therapies by modulating host responses to mycobacteria (i.e., host-directed therapy).

After recognition by skin cells, mycobacteria may use a wide range of strategies to escape the microbicidal activity of skin host cells. Some of these immune escape mechanisms are the inhibition of the maturation of phagolysosomes, inhibition of the acidification of phagolysosomes, bacterial escape to reside in the cytosol, modulation of host cell metabolism, inhibition of oxidative stress, and inhibition of apoptosis and autophagy associated with increased type 1 interferon (IFN) expression and inflammasome activation (16–23).

Autophagy is an intracellular catabolic process that may contribute to the removal of invading pathogens *via* a lysosomal degradation pathway. The activation of autophagy by diverse drugs or agents may represent a promising treatment strategy against mycobacterial diseases. In this review, we discuss the current knowledge of, advances and perspectives on new therapeutic strategies targeting autophagy against mycobacterial infections in the skin.

OVERVIEW OF AUTOPHAGY MACHINERY ON SKIN CELLS

Autophagy is a homeostatic mechanism highly conserved evolutionarily and dependent on the lysosome action (24). It is responsible for the cellular catabolism of dysfunctional organelles, components of the cytoplasm and, more recently, invading pathogens, thus determining the maintenance of homeostasis and adaptation of the cell to stress (25, 26). Autophagy has been described as having a primary role in physiological cellular processes such as development and growth, in the senescence process, and immune defense (25, 27–29). Based on the way the autophagy target is taken to the lysosome, its final destination of degradation, autophagy was didactically classified into three forms: macroautophagy, microautophagy, and chaperone-mediated autophagy. In this review, we will exclusively address the action and manipulation of the macroautophagy pathway.

Only a small amount of research has considered the impact of autophagy on the pathogenesis of skin diseases, including diseases caused by mycobacteria. Skin is the largest organ of the body and it is not only the first line of defense against numerous insults but it is also the site whereas some infectious, including mycobacterial diseases, may manifest.

Autophagy is considered an effector tool of the immune system since it is a relevant pathway of elimination and recognition of pathogens by the immune system (30). As well to cellular homeostasis, autophagy works to eliminate intracellular pathogens, including some pathogens associated with skin diseases, such as *Streptococcus pyogenes* from group A (31, 32), *Staphylococcus aureus* (33, 34), *M. leprae* (35, 36), *M. marinum* (37, 38), and *M. tuberculosis* (39–42). Through a process called xenophagy, which plays a principal role in innate immune defense, intracellular pathogens are directed to the autophagosome and then to the lysosomal degradation pathway (43, 44). Xenophagy is the process of eliminating intracellular pathogens through autophagic machinery, being a unique type of macroautophagy/selective autophagy that targets invasive pathogens, being an important defense mechanism against infectious diseases (45, 46).

Few studies have focused on deciphering autophagy machinery in skin cells, such as: keratinocytes, skin fibroblasts, melanocytes, Langerhans cells, dendritic cells, mast cells, neutrophils, NK and B cells. The current knowledge regarding skin cell autophagy during mycobacterial diseases is based mainly in studies with cell lineage and dermal macrophages.

Briefly, after pathogen recognition by host cells, the first step is the formation of the isolation membrane, which starts to grow and expand in size until sequestration and the surrounding of the target and finally closure to form the autophagosome. Subsequently, autophagosomes fuse with lysosomes to generate autolysosomes through elimination and recycling the sequestered charges *via* the lysosomal proteases (**Figure 1**) (28). A large number of proteins have been identified as highly relevant in different stages of control and action in autophagic flow. Several cell types have autophagy as an effector mechanism for homeostatic/immune functions as skin cells like keratinocytes and macrophages (**Figure 1**) (47).

A wide variety of signals regulates the activation of autophagy. The induction of autophagy can occur through the recognition of microbial factors that are ubiquitinated and recognized by autophagy cargo adaptor proteins (these include p62 (sequestosome 1), NBR1 (neighbor of BRCA1 gene 1 protein), NDP52 (calcium binding and coiled-coil domain 2), optineurin and galectin) or can occur by the production of reactive oxygen radicals and IFN-γ-mediated proteolysis, and autophagosome formation (43, 48–52). The autophagy pathway may be negatively regulated by PI3K (phosphoinositide 3-kinase)/Akt (protein kinase B)/mTOR (target of rapamycin

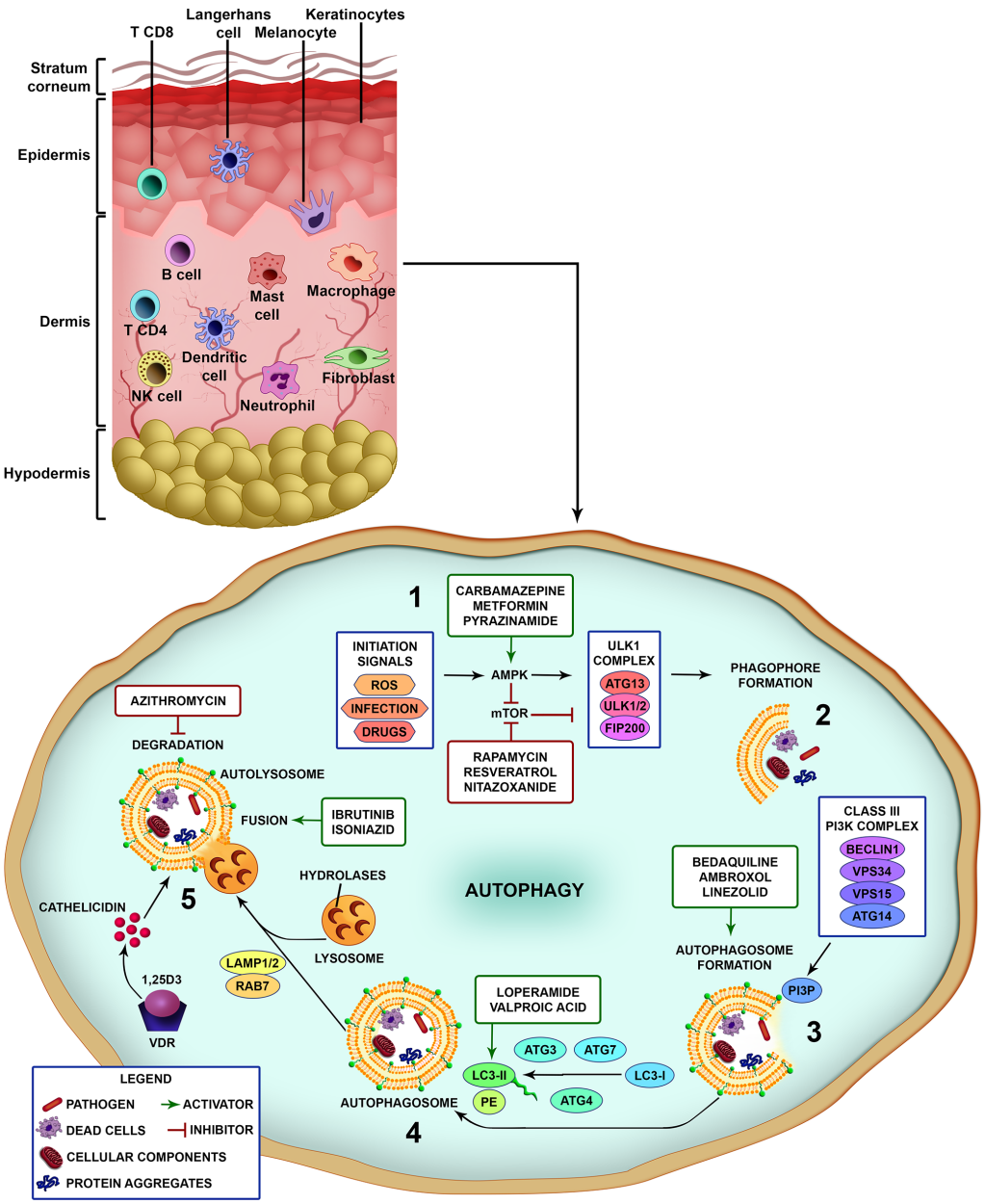

FIGURE 1 | Different steps of the autophagic pathway targeted by autophagy-modulating drugs. A schematic view of the different cell types populating the skin. Vertebrate skin is comprised of two major compartments: the epidermis and the dermis. The superficial part of the epidermis, known as the stratum corneum, is composed of dead keratinocytes and acts as a barrier. The epidermis is composed mainly of keratinocytes with few melanocytes. The major immune cells in this compartment include Langerhans cells (LCs) and CD8 T-cells. The dermis is composed of fibroblasts, NK cells, T-cells (CD4 αβ, and γδ), B cells, dermal dendritic cells, macrophages, mast cells, and neutrophils (non-exhaustive list). The knowledge of skin cell autophagy is mainly based in studies with dermal macrophages. Briefly, (1) autophagy is inhibited by mTOR and activated by AMPK. mTOR is inhibited by the autophagy-initiation signals as metabolic stress, ROS, infection and drugs, and leads to the activation of AMPK. After AMPK activation, the ULK1 complex (ATG13, ULK1/2, FIP200) initiates the phagophore formation (2), involving the targets (pathogens, dead cells, cellular components and organelles, protein aggregates), which in turn activates the Class III PI3K complex (Beclin 1, VPS34, VPS15, ATG14) (3). This complex completes the autophagosome maturation and elongation by forming PI3P in the omegasome membrane and recruiting downstream ubiquitin-like conjugation systems that convert LC3-I to LC3-II (4). Fully formed autophagosomes then fuse with lysosomes (autolysosomes), degrade the sequestered cargo *via* lysosomal hydrolases and recycle macromolecule components (5). Several drugs can interfere with the autophagic pathway by inhibiting or activating different parts of the process (see also **Table 1**). Drugs as rapamycin, resveratrol and nitazoxanide, that inhibit mTOR, or carbamazepine, metformin and pyrazinamide, that activate AMPK, induce autophagy. Bedaquiline, ambroxol and linezolid increase the formation of autophagosomes. Loperamide and valproic acid increase the colocalization of LC3-decorated autophagosomes with *M. tuberculosis*. Ibrutinib and isoniazid facilitate the fusion of phagosome and lysosome. Vitamin D3 (1,25D3) induces the expression of antimicrobial peptides as cathelicidin and upregulates the expression of Beclin 1 and ATG5, that are pivotal for the autophagosome formation. On the other hand, azithromycin was demonstrated to inhibit the acidification of the autolysosome impairing *M. abscessus* degradation.

in mammals) signalling (53). In contrast, the mitogen-activated protein kinase pathway (MAPK) can induce autophagy (54, 55).

AUTOPHAGY AS AN INNATE IMMUNE MECHANISM AGAINST MYCOBACTERIAL DISEASES

There is a strong relationship between autophagy signals and pattern recognition receptors, such as TLR (Toll-Like Receptors) that include TLR3, TLR4, TLR5, TLR6, TLR9, and the heterodimers TLR1/2, TLR7/8 that are capable of activating autophagy in macrophages, dendritic cells, and neutrophils (56–58). This activation occurs *via* signaling of the adaptor proteins MyD88 (myeloid differentiation factor 88) and TRIF (TIR-domain-containing adapter-inducing interferon-β). Xu and colleagues (59) demonstrated that after the stimulation of TLR4, positive LC3 (microtubule-associated protein 1A/1B-light chain 3) aggregates form in the macrophage cytoplasm and increase mycobacterial elimination through autophagy. Interestingly, for the LC3-aggregates induction, *via* TLR4 induction, it is necessary to activate the protein TRIF, as well as other proteins like RIP1 (receptor-interacting protein 1) and p38 for autophagic induction (56, 59). TLR4 acts as a pro-autophagic receptor in TRIF-dependent pathways. TLR4 induces the production of TNF (tumor necrosis factor) by a mechanism that is mediated both by reactive oxygen species (ROS) and nitrogen intermediates (i.e. nitric oxide), and by p38 and MAPK and the inhibition of these components may lead to total autophagy inactivity (60–62). Studies have shown that in LPS (lipopolysaccharide)-TLR4-mediated autophagy, activation of the transcription factor Nrf2 (nuclear factor erythroid 2–related factor 2) occurs, which leads to increased p62 transcription and formation of aggresome-like induced structures (ALIS) with subsequent autophagic degradation (63, 64), showing the ability of this receptor to link innate immunity with cellular oxidative response or adaptive immunity.

It is known that TLR receptors are of great importance for the activation of dendritic cells (DCs) and their subsequent maturation, some of these receptors such as TLR4 and TLR2 are already described as inducing an innate response against *M. tuberculosis* (65–67). Khan and colleagues (68) observed that the co-stimulus of CD40 and TLR4 leads to the production of pro-inflammatory cytokines such as IL-6, IL-12 and TNF, autophagy and death of mycobacteria. Interestingly, when they evaluated this co-stimulus as an adjunct to anti-TB therapy, they observed an increase *in vivo* and *in vitro* of the deadly potential of anti-TB drugs. Shin and colleagues (69) showed that stimulation of TLR2/1/CD14 by mycobacterial lipoprotein LpqH can activate antibacterial autophagy by activating vitamin D receptor signaling and inducing cathelicidin. They suggested that the TLR2/1/CD14-Ca^{2+}-AMPK (Adenosine monophosphate-activated protein kinase)-p38 MAPK pathways contribute to cathelicidin-dependent expression, which played an important role in LpqH-induced autophagy. A study comparing the induction of autophagy by different species of mycobacteria found that non-pathogenic mycobacteria, such as *M. smegmatis*, induce a more robust autophagy response than *M. tuberculosis* (strain H37Rv) (70). The group observed a decrease in LC3-II protein expression when the TLR2 receptor was blocked, as well as a reduction in the colocalization of LC3 with *M. smegmatis* ΔpmmB (lipoglycan deficient mutant), suggesting the participation of TLR2 in the activation of autophagy during infection with *M. smegmatis* (70). *M. smegmatis* can also be recognized by NOD2 (nucleotide-binding oligomerization domain-containing protein 2) and dectin-2 receptors (71).

In addition to the TLR receptors, another group of innate receptors was the nucleotide-binding oligomerization domain (NLRs). It has already been described that the presence of the NOD2 receptor is capable of synergistically amplify the production of pro-inflammatory cytokines and their bactericidal activity (72). In previous studies, Khan and colleagues (73) have demonstrated that after the induction of both receptors, an increase in the bactericidal capacity of DCs *in vitro* was observed and they required a much lower dose of the drug to kill *M. tuberculosis*, in addition, activated DCs induced a more effective T cell response *in vivo* with an increase in autophagy (73, 74). Since pathogenic mycobacteria can modulate the autophagy machinery in skin cells, we hypothesize that autophagy may be a target for new therapeutic strategies against mycobacterial infections in the skin.

AUTOPHAGY-TARGETING THERAPEUTICS UPON MYCOBACTERIAL INFECTION

Despite the efficacy of anti-TB treatment based on classic isoniazid and rifampicin, limitations in terms of drug resistance, duration of treatment, associated with the use of a complex treatment regimen (75), made the researchers use another strategy in the treatment of different bacterial disease. Besides, unlike infections caused by *M. tuberculosis* and *M. leprae* for which there is a well-established therapeutic regimen, there are no standardized and effective regimens for the treatment of non-tuberculosis mycobacteria (NTMs) (10). A promising strategy in the treatment of infectious diseases is the use of host-directed therapy. It works as an adjuvant therapy, which aims to enhance the main components of the host's antimycobacterial effector mechanisms (76–79). Several studies on immunity, host-pathogen interactions, and host-directed interventions have shown that the antimycobacterial action of anti-TB drugs (standardized scheme) is associated with the induction of autophagy (40). Thus, several drugs used in the clinical area to treat infectious diseases may have their action through the autophagic process.

We previously showed that xenophagy is a crucial mechanism in the leprosy outcome. A functional autophagy pathway driven by IFN-γ and Beclin 1 in skin lesion macrophages was associated with the self-healing paucibacillary tuberculoid form of the disease, whereas a BCL2 (apoptosis regulator Bcl-2)-mediated block of Beclin 1 autophagy axis was linked to the progressive

multibacillary lepromatous pole (35). While macrophages patrol the dermis, the human epidermis is enriched for Langerhans cells (LC). Langerhans cells restricted human immunodeficiency virus (HIV)-1 infection through the capture of viral particles by langerin and subsequent internalization into Birbeck granules and targeting of HIV-1 for destruction in the TRIM5 (tripartite motif-containing protein 5) auto lysosomal pathway (80), which in turn is induced by IFN-γ (81). In *M. leprae*-infected LC, the antimicrobial activity induced by IFN-γ treatment is achieved through autophagy, which improves the degradation of *M. leprae*-containing phagolysosomes and fine-tunes LC's power to present antigens for T cells in a CD1a-restricted manner (82). Thus, IFN-γ therapy or a drug targeting autophagy on skin cells could be favorable to the clinical management of leprosy and other skin-related mycobacteriosis such as fish-tank granuloma (83) and Buruli ulcer (1), as well as outbreak associated postsurgical and tattoo ink infections caused by rapidly growing mycobacteria (2, 4). Indeed, the acid-fast bacilli clearance in the skin of multibacillary leprosy patients is accelerated when multidrug therapy is used along with an intradermal treatment with recombinant human IFN-γ (84).

Cell-based studies in leprosy have predominantly focused on dermal cells such as macrophages, neutrophils and T cells. In the dermis, macrophages are an important cell type that promote Th1-type responses, but there is evidence about the involvement of the epidermis in the development of reactional episodes (85) which are acute inflammatory episodes that can occur before, during or after the release of multidrug therapy, being responsible for the cases of disability caused by the disease (86). The relevance of autophagy as a drug target is not only restricted to the control of *M. leprae* infection but also to its potential to regulate the exacerbated inflammation associated with leprosy reactional episodes, as autophagy tempers inflammation by hijacking active inflammasomes for destruction (87). The downregulation of autophagy observed in skin lesion macrophages of multibacillary leprosy patients also predicts the reversal reaction onset. This impairment of the autophagic pathway correlates with the activation of NLRP3 (NALP3; NACHT, LRR and PYD domains-containing protein 3) inflammasome and IL-1β production, which drive the inflammatory status found in multibacillary patients when undergoing reversal reaction (36). On the other hand, due to Th2→Th1 shift and increased IFN-γ production, autophagy levels are restored in lepromatous patients when the reversal reaction episode is established, which in turn help to reduce the bacillary load in skin cells (35). Therefore, leprosy lesion skin cells can earn a dual benefit from the use of autophagy as a platform for drug development; both inflammasome and antimicrobial optimal activities can be reached by modulating autophagy to a certain level. However, some bacterial pathogens inhibit autophagosome maturation and promote bacterial replication, such as *M. tuberculosis* (88, 89). Given the background, Silva and colleagues (35) demonstrated that live but not dead *M. leprae* can inhibit the autophagic flux in macrophages, which indicates a requirement for an active mycobacterial ESX-1 secretion system.

The ESX-1 secretion system is also involved in the targeting of *M. marinum* by LC3; however, ubiquitination does not seem to be necessary for this process (83). *Legionella pneumophila* and *Coxiella burnetii* also developed strategies to explore or subvert autophagy (88). Kim and colleagues (42) demonstrated that *M. abscessus* (UC22 – rough variant) induces autophagy and inhibits autophagic flow in murine macrophages. Also as observed, the lipid components of the clinical isolate UC22, which is highly virulent, play a critical role in the formation of the autophagosome. These data suggest that virulent *M. abscessus* can survive and grow within autophagosomes, preventing autophagosome-lysosome fusion and clearance from cells (42). A study demonstrates the role of lactoferrin, an antimicrobial peptide, in the autophagy of macrophages infected with *M. avium*. D-lactoferrin inhibits intracellular growth of *M. avium* and, at the same time, leads to structural changes in infected macrophages leading to increased lysosomal content and increased numbers of autophagic vesicles (90).

P-aminosalicylate, one of oldest drugs used against tuberculosis, inhibits the assimilation of iron (91). Depletion of iron is strongly associated with increased expression and accumulation of regulated in DNA damage and development 1 (REDD1), which inhibits mTOR activation, decrease phosphorylation of Akt and TSC2 (tuberous sclerosis complex 2) (92, 93). Iron depletion was also shown to increase the activation of HIF-1α (hypoxia-inducible factor) and AMPK and induce autophagy (92, 94).

Zinc has been shown to be a positive regulator of autophagy in several different cell types and conditions, increasing the production of ROS, the formation and turnover of autophagosomes and cellular clearance (95–101). Nevertheless, zinc depletion was found to induce non-selective autophagy in yeast to release zinc recycled from zinc-rich proteins (91, 102, 103), demonstrating the key role of autophagy on zinc homeostasis. Zinc chelation was found to arrest autophagy and impair lysosomal acidification (95, 104). Phosphorylation of ERK1/2 is necessary for the regulation of zinc-induced autophagy by either activating the Beclin 1-PI3K complex or by promoting disassembly of mTOR complex but the mechanisms in which zinc modulates autophagy are still not completely understood (95, 99, 105). Uncoupling of autophagy and zinc homeostasis in the airway epithelial cells was demonstrated to be a fundamental mechanism in the pathogenesis of chronic obstructive pulmonary disease (106). In TB, previous studies have shown that zinc levels in the peripheral blood decrease with age and during active disease but are improved after the beginning of treatment with anti-TB drugs (107–111). Oral zinc supplementation in Brazilian children exposed to adults with pulmonary TB was demonstrated to increase the positivity of tuberculin test (PPD) and induration size, decreasing false negative results (112). It is postulated that zinc supplementation could correct asymptomatic zinc deficiencies, improve the effect of autophagy-mediated therapy in TB, as well as giving a booster to immunity (109, 111, 112). There are currently several studies associating autophagy and infection by bacteria, including studies showing

the different strategies developed by bacteria to inhibit the host's autophagic responses (113–117), as well as studies that show that the activation of autophagy by starvation or by treatment with rapamycin restricts bacterial growth and is capable of improving cell resistance to infection (39, 40, 118–120). The therapeutic benefit of pharmacological agents that can modulate autophagy must be considered since a diverse variety of pathogens using autophagic machinery has been described in their favor. It is primary to understand whether the pathogen exploits this pathway as a whole (systemically) or just part of components to increase its intracellular replication and/or survival. Besides, it is necessary to consider whether the drug will act on all autophagic pathways or only on a specific component, which may, or may not, be used to replicate for the pathogen. For example, intracellular *Brucella abortus* (*B. abortus*) survives by promoting the formation of vacuoles containing *B. abortus*, which requires the activity of the autophagy initiation proteins PIK3C3 (phosphatidylinositol 3-kinase catalytic subunit type 3), ULK1 (serine/threonine-protein kinase ULK1), ATG (autophagy-related protein) 14L (Barkor; Beclin 1-associated autophagy-related key regulator), and Beclin 1, but not the autophagy activity stretching proteins ATG16L1, ATG4B, ATG5, ATG7 and LC3-II (121). In this condition, the use of inhibitors of the autophagy protein conjugation systems or inhibitors of autophagosome maturation would not have a protective effect against the survival of this bacterium. Still in this context, it is important to consider those patients who are affected by infections (for example, TB) that can be eliminated if autophagy is regulated positively, but who are co-infected with pathogens that use the autophagic pathway in their favor, such as concomitant infections with the Hepatitis B virus and HIV (122). Under other conditions, the co-infected patient is favored by autophagic activation, as is the case of patients with cystic fibrosis (CF) who are treated with cysteamine. The autophagic stimulus mediated by cysteamine in macrophages of cystic fibrosis (with the CFTRdel506 mutation) patients favors the clearance of *Pseudomonas aeruginosa*, a bacterium that frequently infects the lungs of CF patients (123). Therefore, it is primary to understand the differences between each stimulus, pathogen, and the type of cell under study so that the use of this route as a target for the development of antimycobacterial drugs can be advanced.

TREATMENTS INDUCING AUTOPHAGY DURING TUBERCULOUS MYCOBACTERIAL INFECTION

When autophagy studies were started, the only drug that was able to chronically induce this pathway was rapamycin. There is evidence of its antimycobacterial activity, where it has been observed that it significantly inhibits infection by *M. kansasii*, *M. avium*, Bacillus Calmette–Guérin (BCG), and virulent strains of *M. tuberculosis* (124, 125). However, the adverse effects of rapamycin (which were not associated with autophagy induction) made this drug unattractive for use. Several drugs are capable of inducing autophagy and treating mycobacterial diseases, some examples are summarized in **Table 1** and their activities are illustrated in **Figure 1**.

Among the various drugs described in the literature with pro-autophagic properties, ambroxol (126), metformin (127), verapamil (143), carbamazepine (128, 129), valproic acid (129, 130), and loperamide (130) are already approved for clinical use in different pathologies. The strategy of using drugs with a known safety profile for new indications related to autophagy is attractive because they do not need to undergo a complete toxicological assessment (18, 147, 148).

Regarding the pro-autophagic property of ambroxol, it has been shown to potentiate the antimicrobial activity of rifampicin in the murine model in trials for TB (126). The antidiabetic drug metformin reduced the intracellular growth of *M. tuberculosis* in a manner dependent on AMPK. Also, metformin was able to induce reactive mitochondrial oxygen species and facilitate phagosome-lysosome fusion (127). However, a more recent study failed to show the improvement in the bacterial activity of antituberculosis drugs by metformin in the murine model (149). This data makes us reflect on the importance of considering whether the anti-TB drug may or may not alter the pharmacokinetics of the repositioning drug. The use of rifampicin in this more recent study (149) may have altered the pharmacokinetics of metformin. Besides, it is also prudent to pay attention to the differences in the experimental design carried out to assess the effectiveness of the therapy, which can be combined (149) or used alone (monotherapy) (127).

Initial studies that evaluated the effect of verapamil and its analogs on macrophages infected with *M. tuberculosis* showed that the structural analog KSV21 had an additive effect on the inhibitory antimicrobial activity of Isoniazid and Rifampicin (143). In addition, the antibiotics isoniazid and pyrazinamide, two first-line cocktail drugs used to treat TB, exert their antimycobacterial activity through autophagy (40).

Recently, the impact of linezolid and bedaquiline on the intra-macrophagic behavior of *M. tuberculosis* has been reported. It was observed that the anti-Mtb effect of these new drugs occurred *via* activation of autophagy and increased formation of autolysosomes in infected macrophages (131). Bedaquiline induces metabolic stress in *M. tuberculosis*, which results in the accumulation of NADH (nicotinamide adenine dinucleotide), followed by the generation of ROS (subsequently generating ROS by the bacteria) (150). Although not directly proven, ROS can trigger autophagy activation and be responsible for antibiotic-induced death of *M. tuberculosis* (151).

Resveratrol has also been studied for its antioxidant effect and its role in inducing autophagy. Regarding the antioxidant effect, resveratrol can increase the activity of antioxidant enzymes and works by eliminating free radicals (152, 153). Resveratrol has inhibitory activity on the mTOR molecule (133, 154). Other studies have shown antibacterial properties, mainly activity against gram-positive bacteria, flavonoid, and resveratrol (132). Still, on drugs capable of stimulating the autophagic death of *M. tuberculosis*, the anticonvulsant drug carbamazepine was able

TABLE 1 | Therapeutic strategies of drug repositioning targeting autophagy of host cells against mycobacterial diseases.

Drugs	*Mycobacteria*	Model	Mechanism of Action	Reference
Rapamycin	*M. avium* subspecies *paratuberculosis* (MAP)	Inhibition of MAP growth *in vitro* (BACTEC radiometric 7H12 broth)	Inhibition of mTOR	Greenstein et al. (124)
Rapamycin	*M. smegmatis*	Murine bone marrow derived macrophages (BMDM) and RAW264.7 macrophages	Inhibition of mTOR	Zullo et al. (125)
Ambroxol	*M. tuberculosis*	BMDM and primary human macrophages	Increased autophagosomes production	Choi et al. (126)
Metformin*	*M. tuberculosis*	Monocytes differentiated to macrophage (THP-1 cell line)	Increases AMPK expression, inducing phosphorylation of ULK1	Singhal (127)
Carbamazepine*	*M. tuberculosis*	Primary human macrophages Infection of C57BL/6 mice with MDR strain	Lowers myoinositol levels, activates AMPK and induces autophagy in an mTOR independent manner	Cárdenas et al. (128); Schiebler et al. (129)
Valproic acid*	*M. tuberculosis*	Primary human macrophages	Increases colocalization of LC3 with Mtb	Schiebler et al. (129); Juárez et al. (130)
Loperamide	*M. tuberculosis*	Primary human macrophages	Decreases the production of TNF and increases the colocalization of LC3 with Mtb	Juárez et al. (130)
Bedaquiline*	*M. tuberculosis*	Human differentiated monocytes (U-937 cell line)	Increases the formation of autophagosomes	Genestet et al. (131)
Linezolid*	*M. tuberculosis*	Human differentiated monocytes (U-937 cell line)	Increases the formation of autophagosomes	Genestet et al. (131)
Resveratrol	*M. tuberculosis*	MIC values were determined against *M. tuberculosis* using the standard microbroth dilution method	Inhibits of mTOR	Sun et al. (132); Park et al. (133)
Baicalin	*M. tuberculosis*	RAW264.7 macrophages	Induces autophagy by inhibiting the PI3K/Akt/mTOR pathway	Zhang et al. (134)
Azithromycin*	*M. abscessus*	Primary human macrophages and C57BL/6 mice	Blocks lysosomal acidification	Renna et al. (135)
Rifabutin*	*M. abscessus*	MICs in dose-response assays were determined by the broth microdilution method	Undefined	Aziz et al. (136)
Nitazoxanide	*M. leprae*	C57BL/6 mice	mTOR inhibition by TSC2	Bailey et al. (137)
Isoniazid	*M. tuberculosis*	Primary BMDMs, human primary monocytes, and MDMs	Facilitates phagosome-lysosome fusion	Kim et al. (40)
Pyrazinamide	*M. tuberculosis*	Primary BMDMs, human primary monocytes, and MDMs	Activates AMPK and induces autophagy	Kim et al. (40)
Vitamin D3	*M. tuberculosis*	Human macrophages	Stimulation of VDR to induce cathelicidin expression; upregulation the expression of Atg5 and Beclin-1	Jo, (138); Palucci & Delogu, (139)
Vitamin D3	*M. leprae*	Peripheral monocytes	Stimulation of VDR to induce cathelicidin expression	Krutzik et al. (140), Montoya et al. (141)
Ibrutinib	*M. tuberculosis*	Monocytes differentiated to macrophage (THP-1 cell line) and C57BL/6 mice	Facilitates phagosome-lysosome fusion	Hu et al. (142)
Iron	–	DN TfR-1 and DMT-1 CKO model	Iron depletion increases the activation of HIF-1α (hypoxia-inducible factor) and AMPK.	Wu et al. (94); Fretham et al. (92)
Verapamil	*M. tuberculosis* *M. bovis* BCG	BMDM from ATG5(flox/flox) (control) and ATG5 (flox/flox) Lyz-Cre mice; Human monocytes	Inhibits $Ca2^+$ channel, cytosolic $Ca2^+\downarrow$	Abate et al. (143)
Zinc	–	MCF-7 cells (human breast cancer cell line)	Increasing the formation and turnover of autophagosomes	Hwang et al. (95); Cho et al. (104)
Simvastatin	*M. tuberculosis*	Peripheral blood mononuclear cells (PBMCs)	Increases the autophagic flux (autophagolysosomes)	Guerra-De-Blas et al. (144)
		PBMCs or MDMs from patients with familial hypercholesterolemia (FH) and C57BL/6 mice	Reduction of membrane cholesterol levels promotes phagosomal maturation (monocyte autophagy)	Parihar et al. (145)
Rosuvastatin	*M. tuberculosis*	PBMCs or MDMs from patients with familial hypercholesterolemia (FH) and C57BL/6 mice	Reduction of membrane cholesterol levels promotes phagosomal maturation (monocyte autophagy)	Parihar et al. (145)
Omadacycline	*Mycobacterium abscessus* *Mycobacterium chelonae* *Mycobacterium fortuitum*	Broth microtiter dilution assay	–	Shoen et al. (146)
Tigecycline	*Mycobacterium abscessus* *Mycobacterium chelonae* *Mycobacterium fortuitum*	Broth microtiter dilution assay	–	Shoen et al. (146)

**Repurposed Drugs.*

to induce autophagy in mice infected with the multidrug-resistant *M. tuberculosis* strain, resulting in a decrease in their bacterial load and improvement in pulmonary pathology (129). It was observed that carbamazepine induces antimicrobial autophagy due to decreased levels of Myoinositol (by blocking myoinositol uptake) into a pathway independent of mTOR. Furthermore, it was seen that this drug also activates AMPK (128). In that same study, the group described the induction of autophagy by the drug valproic acid, another anticonvulsant drug (129), which favored the increase in the co-localization of LC3 with *M. tuberculosis*, an effect similar to that observed after treatment with anti-diarrhea medication loperamide (130). Unlike carbamazepine, which activates AMPK, the induction of autophagy by baicalin in macrophages infected by *M. tuberculosis* occurred through inhibition of the PI3K/Akt/mTOR pathway. Additionally, baicalin showed a suppressive effect on the activation of the NLRP3 inflammasome *via* PI3K/Akt/NF-κB (nuclear factor-κB), as well as reduced the levels of the pro-inflammatory cytokine IL-1β (134). Both the induction of autophagy and the inhibition of NF-κB contribute to limit the activation of the NLRP3 inflammasome. Autophagy can limit the activation of the inflammasome indirectly or directly. Indirectly, it can reduce endogenous stimuli that favor the activation of the inflammasome (155, 156) and can directly inhibit the autophagic degradation of inflammasome components (87, 157).

Fluvastatin is a statin class drug currently used to treat hypercholesteromia and prevent cardiovascular disease, by blocking the enzyme hydroxy-methyl-glutaryl-CoA (HMG-CoA) reductase, which catalyzes a key step in cholesterol synthesis. Fluvastatin was demonstrated to be effective in targeting not only the mycobacteria but also increasing the ability of the host cells to eliminate *M. tuberculosis* infection (158). Other statins, including simvastatin and rosuvastatin were also demonstrated to control *M. tuberculosis* infection by promoting phagosomal maturation and autophagy (145).

Some studies demonstrated the protective role of autophagy in excessive inflammation during *M. tuberculosis* infection (159). Based on these studies, we conclude that autophagy plays an important role in the fight against TB, by direct killing of the pathogen, while also avoiding excessive inflammatory damage. This makes an antimycobacterial agent that has autophagy as a pharmacological target, a promising candidate to assist in therapy directed at the host.

ROLE OF AUTOPHAGY IN THERAPEUTIC APPROACHES FOR NTMS AND SKIN DISEASES

The treatment of nontuberculous mycobacteriosis is not very rewarding. Currently, the proposed therapeutic regimen for infection with NTMs is based on the use of macrolides (clarithromycin or azithromycin), ethambutol, and rifamycins (160). Azithromycin is a potent antibiotic and is often prescribed for prophylaxis and treatment regimens of mycobacterial infections (10). However, one study reported that long-term use of azithromycin by adults with CF increased the risk of infection with *M. abscessus*. That was observed because the therapeutic dosage of azithromycin impaired autophagic degradation (135). That is, these data emphasize the importance of autophagy in the host's response to infection by NTMs.

The challenge of treating lung diseases caused by *M. abscessus* is related to antibiotic resistance, including all first-line drugs for anti-TB treatment (161, 162). Even rifampicin, which has bactericidal activity against *M. tuberculosis* and *M. leprae*, has low potency against *M. abscessus*. Although rifampicin is part of the treatment regimens established for *M. kansasii* and *Mycobacterium avium* complex infections, it is not recommended against *M. abscessus* (163, 164). Recently, rifabutin (of the rifamycin group) was shown, through its bactericidal activity, to be effective against strains of clinical isolates from the three subspecies of the *M. abscessus* complex (subsp. *abscessus*, subsp. *massiliense*, and subsp. *bolletii*) (136). Recently, the *in vitro* activity of omadacycline and tigecycline against clinical isolates of *M. abscessus*, *M. chelonae* and *M. fortuitum* was evaluated (146). Omadacycline, a new tetracycline analog, approved for the treatment of acute bacterial skin and skin structure infections (ABSSSI) (165) showed activity against the three clinical isolates (146). There are reports that these microorganisms have been identified in postoperative infections caused by mycobacteria, including the three opportunistic pathogens: *M. fortuitum* (166), *M. abscessus* (167) and *M. chelonae* (168). Postoperative infections have been reported after orthopedic, laparoscopic, ophthalmic procedures and cosmetic operations (mainly liposuction, abdominoplasty, rhinoplasty) (169, 170). *M. chelona*e can cause localized skin infection after being accidentally inoculated from the environment (pedicure beds, water heaters, and tattoo parlors) (171, 172). In immunocompromised patients, the infection caused by this mycobacterium can manifest itself as a disseminated skin disease. A case report demonstrated *M. chelonae* skin and soft tissue infection in a patient with chronic lymphocytic leukemia (LLC) who was using ibrutinib, an oral drug, which acts by inhibiting Bruton tyrosine kinase (BTK) for the treatment of various malignant B-cell diseases (173, 174). After 6 months of therapy with ibrutinib, the 85-year-old man developed skin lesions on his arms and legs (175). Fiocari and colleagues (176) showed that ibrutinib promotes an M2 phenotype by modifying the function of macrophages/monocytes in the LLC. Taken together, these results showed that ibrutinib can have detrimental consequences on the microbicidal response in patients treated with ibrutinib. On the other hand, a more current study reported the impact of the drug ibrutinib on the intra-macrophagic behavior of *M. tuberculosis*. It was observed that the anti-TB effect of this medication occurred *via* activation of autophagy and facilitates phagosome-lysosome fusion in infected macrophages (142).

Nitazoxanide has also been studied for its role in inducing autophagy. The use of nitazoxanide in C57BL/6 mice infected with *M. leprae* showed a bactericidal action similar to that of

rifampicin, an antibiotic used in the therapeutic regimen against leprosy (137). Based on this study, nitazoxanide (NTZ) may be an effective option for the treatment of leprosy (137).

The epidermis is composed mainly by keratinocytes, which contributes to the defense responses against various stimuli in the environment (177). Numerous findings indicate that autophagy plays an important role in the biology and pathology of keratinocytes (177). It has already been seen that calcipotriol, a vitamin D analog, has the ability to induce autophagy in keratinocytes (178). Analogous vitamin D molecules have been used to treat different skin diseases, such as psoriasis, lamellar ichthyosis and epidermolytic hyperkeratosis (179). The autophagic pathway converges with the vitamin D3-cathelicidin pathway, which is preferably seen in the paucibacillary form of leprosy (140, 141). Vitamin D3 induces autophagy *via* cathelicidin in macrophages infected with *M. tuberculosis*, with cathelicidin being required for IFNγ-mediated antimicrobial activity (180, 181). Also, 1,25(OH)2D3-induced LL-37 (C-terminal antimicrobial peptide) enhances the colocalization of mycobacterial phagosomes and autophagosomes (182). Vitamin D3 has been used successfully in the treatment of patients with TB (183). Vitamin D3 could be one of the components for the treatment of leprosy and other chronic infectious diseases in which the cellular immune response is unregulated (184, 185). Vitamin D prevents tissue damage through the negative regulation of perforin, granzyme B and granulisine in cytotoxic T lymphocytes (186).

Many species of mycobacteria that cause skin infections are considered to have a natural ability to acquire resistance to antibiotics and to have a significant reduction in sensitivity to antibiotics, which makes treatment efficacy more difficult by increasing failure rates (187, 188). Thus, using therapies directed at the host, such as those that induce autophagy, to inhibit bacterial cell release and form biofilms or bacterial media can increase the effectiveness of currently available antibiotics, i.e. azithromycin (135) and verapamil (143, 189) already mentioned in the text, as well as, Carvacrol (190–193), Tetracycline (146, 194, 195), Thioridazine (196–199) and, Mefloquine (200, 201).

CONCLUSION

This review describes the potential of host cell autophagy as a target for the development of new strategies against mycobacterial diseases. There are few studies focusing on skin cell autophagy during mycobacterial infections but in this review we summarized autophagy mechanisms in some cells most relevant to skin mycobacterial diseases. In addition, drug repurposing presents itself as a promising perspective in the control of infections caused by mycobacteria, being used in isolation or complementary to existing treatments. Some challenges still need to be faced, such as the understanding of the mechanisms used by different species of mycobacteria to induce autophagy, the evaluation of host cell autophagy by different clinical isolates, including resistant strains, the impact of a therapy directed at the host cell in cases where there is co-infection and, finally, if the use of a drug in combination with current therapeutic regimens will have a beneficial effect on bacillary load.

AUTHOR CONTRIBUTIONS

TB, RP, BS, MG, and RP wrote the manuscript. TB, RP, and MG made the table and the figure. RP and MD provided intellectual output in the manuscript. All authors contributed to the article and approved the submitted version.

FUNDING

We thank CAPES, FAPERJ, and CNPq funding institutions for all their financial support. This study was partially supported by the Coordination for the Improvement of Higher Education Personnel (Coordenação de Aperfeiçoamento de Pessoal de Nível Superior - CAPES) - Finance Code 001. National Council for Scientific and Technological Development (CNPq) - Finance Code 303834/2017-0. Rio de Janeiro Carlos Chagas Filho Research Foundation (FAPERJ) - Finance Code E-26/010.002231/2019.

REFERENCES

1. Franco-Paredes C, Marcos LA, Henao-Martínez AF, Rodríguez-Morales AJ, Villamil-Gómez WE, Gotuzzo E, et al. Cutaneous Mycobacterial Infections. *Clin Microbiol Rev* (2018) 32(1):e00069–18. doi: 10.1128/CMR.00069-18
2. Duarte RS, Lourenço MCS, Fonseca LDS, Leão SC, Amorim EDLT, Rocha ILL, et al. Epidemic of Postsurgical Infections Caused by Mycobacterium Massiliense. *J Clin Microbiol* (2009) 47(7):2149–55. doi: 10.1128/JCM.00027-09
3. Khan FA, Khakoo R. Nontuberculous Mycobacterial Cutaneous Infections: An Updated Review. *Cutis* (2011) 88(4):194–200.
4. Kennedy BS, Bedard B, Younge M, Tuttle D, Ammerman E, Ricci J, et al. Outbreak of *Mycobacterium Chelonae* Infection Associated With Tattoo Ink. *New Engl J Med* (2012) 367(11):1020–4. doi: 10.1056/nejmoa1205114
5. Gervais P, Manuel O, Jaton K, Giulieri S. Skin Infections Due to Rapid-Growing Mycobacteria. *Rev Med Suisse* (2014) 10(427):931–4.
6. Pinheiro RO, Schmitz V, Silva BJ, de A, Dias AA, de Souza BJ, et al. Innate Immune Responses in Leprosy. *Front Immunol* (2018) 9:518. doi: 10.3389/fimmu.2018.00518
7. de Macedo CS, Lara FA, Pinheiro RO, Schmitz V, de Berrêdo-Pinho M, Pereira GM, et al. New Insights Into the Pathogenesis of Leprosy: Contribution of Subversion of Host Cell Metabolism to Bacterial Persistence, Disease Progression, and Transmission. *F1000Research* (2020) 9:F1000 Faculty Rev–70. doi: 10.12688/f1000research.21383.1
8. Johansen MD, Herrmann JL, Kremer L. Non-Tuberculous Mycobacteria and the Rise of *Mycobacterium Abscessus*. *Nat Rev Microbiol* (2020) 18 (7):392–407. doi: 10.1038/s41579-020-0331-1
9. Costa LL, Veasey JV. Diagnosis of Cutaneous Tuberculosis (Lymph Node Scrofuloderma) Using the Xpert MTB/RIF® Method. *Anais Bras Dermatol* (2021) 96(1):82–4. doi: 10.1016/j.abd.2020.01.009
10. Griffith DE, Aksamit T, Brown-Elliott BA, Catanzaro A, Daley C, Gordin F, et al. An Official ATS/IDSA Statement: Diagnosis, Treatment, and Prevention of Nontuberculous Mycobacterial Diseases. *Am J Respir Crit Care Med* (2007) 175(4):367–416. doi: 10.1164/rccm.200604-571ST
11. Forbes BY, Hall GS, Miller MB, Novak S, Rowlinson MC, Salfinger M, et al. Practice Guidelines for Clinical Microbiology Laboratories: Mycobacteria. *Clin Microbiol Rev* (2018) 31(2):e00038–17. doi: 10.1128/CMR.00038-17
12. Wang SH, Pancholi P. Mycobacterial Skin and Soft Tissue Infection. *Curr Infect Dis Rep* (2014) 16(11):438. doi: 10.1007/s11908-014-0438-5

13. Barbagallo J, Tager P, Ingleton R, Hirsch RJ, Weinberg JM. Cutaneous Tuberculosis: Diagnosis and Treatment. *Am J Clin Dermatol* (2002) 3 (5):319–28. doi: 10.2165/00128071-200203050-00004
14. Zyl LV, du Plessis J, Vilijoen J. Cutaneous Tuberculosis Overview and Current Treatment Regimens. *Tuberculosis* (2015) 95(6):629–38. doi: 10.1016/j.tube.2014.12.006
15. Bravo FG, Gotuzzo E. Cutaneous Tuberculosis. *Clinics Dermatol* (2007) 25 (2):173–80. doi: 10.1016/j.clindermatol.2006.05.005
16. Rahman SA, Singh Y, Kohli S, Ahmad J, Ehtesham NZ, Tyagi AK, et al. Comparative Analyses of Nonpathogenic, Opportunistic, and Totally Pathogenic Mycobacteria Reveal Genomic and Biochemical Variabilities and Highlight the Survival Attributes of *Mycobacterium Tuberculosis*. *mBio* (2014) 5(6):e02020. doi: 10.1128/mbio.02020-14
17. Carranza C, Chavez-Galan L. Several Routes to the Same Destination: Inhibition of Phagosome-Lysosome Fusion by *Mycobacterium Tuberculosis*. *Am J Med Sci* (2019) 357(3):184–94. doi: 10.1016/j.amjms.2018.12.003
18. Kim YS, Silwal P, Kim SY, Yoshimori T, Jo EK. Autophagy-Activating Strategies to Promote Innate Defense Against Mycobacteria. *Exp Mol Med* (2019) 51(12):1–10. doi: 10.1038/s12276-019-0290-7
19. Kim JK, Silwal P, Jo EK. Host-Pathogen Dialogues in Autophagy, Apoptosis, and Necrosis During Mycobacterial Infection. *Immune Netw* (2020) 20(5): e37. doi: 10.4110/in.2020.20.e37
20. Chai Q, Wang L, Liu CH, Ge B. New Insights Into the Evasion of Host Innate Immunity by *Mycobacterium Tuberculosis*. *Cell Mol Immunol* (2020) 17 (9):901–13. doi: 10.1038/s41423-020-0502-z
21. Ankley L, Thomas S, Olive AJ. Fighting Persistence: How Chronic Infections With *Mycobacterium Tuberculosis* Evade T Cell-Mediated Clearance and New Strategies to Defeat Them. *Infect Immun* (2020) 88(7):e00916–19. doi: 10.1128/IAI.00916-19
22. Bernard EM, Fearns A, Bussi C, Santucci P, Peddie CJ, Lai RJ, et al. *M. Tuberculosis* Infection of Human iPSC-derived Macrophages Reveals Complex Membrane Dynamics During Xenophagy Evasion. *J Cell Sci* (2020) 134(5):jcs252973. doi: 10.1242/jcs.252973
23. Naeem MA, Ahmad W, Tyagi R, Akram Q, Younus M, Liu X. Stealth Strategies of Mycobacterium Tuberculosis for Immune Evasion. *Curr Issues Mol Biol* (2021) 41:597–616. doi: 10.21775/cimb.041.597
24. Deter RL, Baudhuin P, De Duve C. Participation of Lysosomes in Cellular Autophagy Induced in Rat Liver by Glucagon. *J Cell Biol* (1967) 35(2):C11–6. doi: 10.1083/jcb.35.2.c11
25. Klionsky DJ, Emr SD. Autophagy as a Regulated Pathway of Cellular Degradation. *Science* (2000) 290(5497):1717–21. doi: 10.1126/science.290.5497.1717
26. Wileman T. Autophagy as a Defence Against Intracellular Pathogens. *Essays Biochem* (2013) 55(1):153–63. doi: 10.1042/BSE0550153
27. Tsukamoto S, Kuma A, Mizushima N. The Role of Autophagy During the Oocyte-to-Embryo Transition. *Autophagy* (2008) 4(8):1076–8. doi: 10.4161/auto.7065
28. Gottlieb RA, Carreira RS. Mitophagy as a Way of Life. *Am J Physiol Cell Physiol* (2010) 299(2):C203–210. doi: 10.1152/ajpcell.00097.2010
29. Guan JL, Simon AK, Prescott M, Menendez JA, Liu F, Wang F, et al. Autophagy in Stem Cells. *Autophagy* (2013) 9(6):830–49. doi: 10.4161/auto.24132
30. Deretic V, Levine B. Autophagy Balances Inflammation in Innate Immunity. *Autophagy* (2018) 14(2):243–51. doi: 10.1080/15548627.2017.1402992
31. Nakagawa I, Amano A, Mizushima N, Yamamoto A, Yamaguchi H, Kamimoto T, et al. Autophagy Defends Cells Against Invading Group A Streptococcus. *Science* (2004) 306(5698):1037–40. doi: 10.1126/science.1103966
32. Nakajima S, Aikawa C, Nozawa T, Minowa-Nozawa A, Toh H, Nakagawa I. Bcl-Xl Affects Group a Streptococcus-Induced Autophagy Directly, by Inhibiting Fusion Between Autophagosomes and Lysosomes, and Indirectly, by Inhibiting Bacterial Internalization Via Interaction With Beclin 1-UVRAG. *PloS One* (2017) 12(1):e0170138. doi: 10.1371/journal.pone.0170138
33. Muñoz-Sánchez S, van der Vaart M, Meijer AH. Autophagy and Lc3-Associated Phagocytosis in Zebrafish Models of Bacterial Infections. *Cells* (2020) 9(11):2372. doi: 10.3390/cells9112372
34. Prajsnar TK, Serba JJ, Dekker BM, Gibson JF, Masud S, Fleming A, et al. The Autophagic Response to *Staphylococcus Aureus* Provides an Intracellular Niche in Neutrophils. *Autophagy* (2020) 17(4):888–902. doi: 10.1080/15548627.2020.1739443
35. Silva BJ, de A, Barbosa MG deM, Andrade PR, Ferreira H, Nery JA daC, et al. Autophagy Is an Innate Mechanism Associated With Leprosy Polarization. *PloS Pathog* (2017a) 13(1):1–29. doi: 10.1371/journal.ppat.1006103
36. de Mattos Barbosa MG, de Andrade Silva BJ, Assis TQ, Prata RB, da S, Ferreira H, et al. Autophagy Impairment is Associated With Increased Inflammasome Activation and Reversal Reaction Development in Multibacillary Leprosy. *Front Immunol* (2018) 9:1223. doi: 10.3389/fimmu.2018.01223
37. Chen Z, Shao X, Wang C, Hua Mh, Wang Cn, Wang X, et al. Mycobacterium Marinum Infection in Zebrafish and Microglia Imitates the Early Stage of Tuberculous Meningitis. *J Mol Neurosci* (2018) 64(2):321–30. doi: 10.1007/s12031-018-1026-1
38. Zhang R, Varela M, Vallentgoed W, Forn-Cuni G, van der Vaart M, Meijer AH. The Selective Autophagy Receptors Optineurin and p62 are Both Required for Zebrafish Host Resistance to Mycobacterial Infection. *PloS Pathog* (2019) 15(2):e1007329. doi: 10.1371/journal.ppat.1007329
39. Gutierrez MG, Master SS, Singh SB, Taylor GA, Colombo MI, Deretic V. Autophagy is a Defense Mechanism Inhibiting BCG and *Mycobacterium Tuberculosis* Survival in Infected Macrophages. *Cell* (2004) 119(6):753–66. doi: 10.1016/j.cell.2004.11.038
40. Kim JJ, Lee HM, Shin DM, Kim W, Yuk JM, Jin HS, et al. Host Cell Autophagy Activated by Antibiotics Is Required for Their Effective Antimycobacterial Drug Action. *Cell Host Microbe* (2012) 11(5):457–68. doi: 10.1016/j.chom.2012.03.008
41. Watson RO, Bell SL, MacDuff DA, Kimmey JM, Diner EJ, Olivas J, et al. The Cytosolic Sensor Cgas Detects *Mycobacterium Tuberculosis* DNA to Induce Type I Interferons and Activate Autophagy. *Cell Host Microbe* (2015) 17 (6):811–9. doi: 10.1016/j.chom.2015.05.004
42. Kim JK, Lee HM, Park KS, Shin DM, Kim TS, Kim YS, et al. MIR144* Inhibits Antimicrobial Responses Against *Mycobacterium Tuberculosis* in Human Monocytes and Macrophages by Targeting the Autophagy Protein DRAM2. *Autophagy* (2017b) 13(2):423–41. doi: 10.1080/15548627.2016.1241922
43. Virgin HW, Levine B. Autophagy Genes in Immunity. *Nat Immunol* (2009) 10(5):461–70. doi: 10.1038/ni.1726
44. Levine B, Mizushima N, Virgin HW. Autophagy in Immunity and Inflammation. *Nature* (2011) 469(7330):323–35. doi: 10.1038/nature09782
45. Ravenhill BJ, Boyle KB, von Muhlinen N, Ellison CJ, Masson GR, Otten EG, et al. The Cargo Receptor NDP52 Initiates Selective Autophagy by Recruiting the ULK Complex to Cytosol-Invading Bacteria. *Mol Cell* (2019) 74(2):320–329.e6. doi: 10.1016/j.molcel.2019.01.041
46. Wen X, Klionsky DJ. How Bacteria can Block Xenophagy: An Insight From *Salmonella*. *Autophagy* (2020) 16(2):193–4. doi: 10.1080/15548627.2019.1666580
47. Puleston DJ, Simon AK. Autophagy in the Immune System. *Immunology* (2013) 141(1):1–8. doi: 10.1111/imm.12165
48. Wild P, Farhan H, McEwan DG, Wagner S, Rogov VV, Brady NR, et al. Phosphorylation of the Autophagy Receptor Optineurin Restricts Salmonella Growth. *Science* (2011) 333(6039):228–33. doi: 10.1126/science.1205405
49. Oh JE, Lee HK. Modulation of Pathogen Recognition by Autophagy. *Front Immunol* (2012) 3:44. doi: 10.3389/fimmu.2012.00044
50. Paik S, Jo EK. An Interplay Between Autophagy and Immunometabolism for Host Defense Against Mycobacterial Infection. *Front Immunol* (2020) 11:603951. doi: 10.3389/fimmu.2020.603951
51. Randow F, Youle RJ. Self and Nonself: How Autophagy Targets Mitochondria and Bacteria. in. *Cell Host Microbe* (2014) 15(4):403–11. doi: 10.1016/j.chom.2014.03.012
52. Da Silva Prata RB, de Mattos Barbosa MG, de Andrade Silva BJ, Oliveira JAP, Bittencourt TL, et al. Macrophages in the Pathogenesis of Leprosy. In: *Macrophage activation - Biology and Disease*. United Kingdom: Intech Open (2019), p. 1–19. doi: 10.5772/INTECHOPEN.88754 IntechOpen.
53. Heras-Sandoval D, Pérez-Rojas JM, Hernández-Damián J, Pedraza-Chaverri J. The Role of PI3K/AKT/mTOR Pathway in the Modulation of Autophagy and

the Clearance of Protein Aggregates in Neurodegeneration. *Cell Signal* (2014) 26(12):2694–701. doi: 10.1016/j.cellsig.2014.08.019
54. Krishna M, Narang H. The Complexity of Mitogen-Activated Protein Kinases (Mapks) Made Simple. *Cell Mol Life Sci* (2008) 65(22):3525–44. doi: 10.1007/s00018-008-8170-7
55. Zhou YY, Li Y, Jiang WQ, Zhou LF. MAPK/JNK Signalling: A Potential Autophagy Regulation Pathway. *Biosci Rep* (2015) 35(3):1–10. doi: 10.1042/BSR20140141
56. Delgado MA, Elmaoued RA, Davis AS, Kyei G, Deretic V. Toll-Like Receptors Control Autophagy. *EMBO J* (2008) 27(7):1110–21. doi: 10.1038/emboj.2008.31
57. Fitzgerald KA, Kagan JC. Toll-Like Receptors and the Control of Immunity. *Cell* (2020) 180(6):1044–66. doi: 10.1016/j.cell.2020.02.041
58. Pellegrini JM, Sabbione F, Morelli MP, Tateosian NL, Castello FA, Amiano NO, et al. Neutrophil Autophagy During Human Active Tuberculosis is Modulated by SLAMF1. *Autophagy* (2020) 16:1–10. doi: 10.1080/15548627.2020.1825273
59. Xu Y, Jagannath C, Liu X, Sharafkhaneh A, Kolodziejska KE, Eissa NT. Toll-Like Receptor 4 Is a Sensor for Autophagy Associated With Innate Immunity. *Immunity* (2007) 27(1):135–44. doi: 10.1016/j.immuni.2007.05.022
60. Asehnoune K, Strassheim D, Mitra S, Kim JY, Abraham E. Involvement of Reactive Oxygen Species in Toll-Like Receptor 4-Dependent Activation of NF-κb. *J Immunol* (2004) 172(4):2522–9. doi: 10.4049/jimmunol.172.4.2522
61. Zhou M, Xu W, Wang J, Yan J, Shi Y, Zhang C, et al. Boosting mTOR-dependent Autophagy Via Upstream TLR4-MyD88-MAPK Signalling and Downstream NF-κb Pathway Quenches Intestinal Inflammation and Oxidative Stress Injury. *EBioMedicine* (2018) 35:345–60. doi: 10.1016/j.ebiom.2018.08.035
62. Hasan A, Akhter N, Al-Roub A, Thomas R, Kochumon S, Wilson A, et al. Tnf-α in Combination With Palmitate Enhances IL-8 Production Via the MyD88- Independent TLR4 Signaling Pathway: Potential Relevance to Metabolic Inflammation. *Int J Mol Sci* (2019) 20(17):4112. doi: 10.3390/ijms20174112
63. Fujita KI, Srinivasula SM. TLR4-Mediated Autophagy in Macrophages is a p62-dependent Type of Selective Autophagy of Aggresome-Like Induced Structures (ALIS). *Autophagy* (2011a) 7(5):552–4. doi: 10.4161/auto.7.5.15101
64. Fujita KI, Maeda D, Xiao Q, Srinivasula SM. Nrf2-mediated Induction of p62 Controls Toll-like receptor-4-driven Aggresome-Like Induced Structure Formation and Autophagic Degradation. *Proc Natl Acad Sci USA* (2011b) 108(4):1427–32. doi: 10.1073/pnas.1014156108
65. Shinya E, Owaki A, Norose Y, Sato S, Takahashi H. Quick Method of Multimeric Protein Production for Biologically Active Substances Such as Human GM-CSF (Hgm-CSF). *Biochem Biophys Res Commun* (2009) 386 (1):40–4. doi: 10.1016/j.bbrc.2009.05.125
66. Pompei L, Jang S, Zamlynny B, Ravikumar S, McBride A, Hickman SP, et al. Disparity in IL-12 Release in Dendritic Cells and Macrophages in Response to *Mycobacterium Tuberculosis* is Due to Use of Distinct TLRs. *J Immunol* (2007) 178(8):5192–9. doi: 10.4049/jimmunol.178.8.5192
67. Drage MG, Pecora ND, Hise AG, Febbraio M, Silverstein RL, Golenbock DT, et al. TLR2 and its Co-Receptors Determine Responses of Macrophages and Dendritic Cells to Lipoproteins of Mycobacterium Tuberculosis. *Cell Immunol* (2009) 258(1):29–37. doi: 10.1016/j.cellimm.2009.03.008
68. Khan N, Pahari S, Vidyarthi A, Aqdas M, Agrewala JN. Stimulation Through CD40 and TLR-4 is an Effective Host Directed Therapy Against *Mycobacterium Tuberculosis*. *Front Immunol* (2016a) 7:386. doi: 10.3389/fimmu.2016.00386
69. Shin DM, Yuk JM, Lee HM, Lee SH, Son JW, Harding CV, et al. Mycobacterial Lipoprotein Activates Autophagy Via TLR2/1/CD14 and a Functional Vitamin D Receptor Signalling. *Cell Microbiol* (2010) 12 (11):1648–65. doi: 10.1111/j.1462-5822.2010.01497
70. Bah A, Lacarrière C, Vergne I. Autophagy-Related Proteins Target Ubiquitin-Free Mycobacterial Compartment to Promote Killing in Macrophages. *Front Cell Infect Microbiol* (2016) 6:53. doi: 10.3389/fcimb.2016.00053
71. Travassos LH, Carneiro LAM, Ramjeet M, Hussey S, Kim YG, Magalhes JG, et al. Nod1 and Nod2 Direct Autophagy by Recruiting ATG16L1 to the Plasma Membrane At the Site of Bacterial Entry. *Nat Immunol* (2010) 11 (1):55–62. doi: 10.1038/ni.1823
72. Ferwerda G, Girardin SE, Kullberg BJ, Le Bourhis L, De Jong DJ, Langenberg DML, et al. NOD2 and Toll-Like Receptors are Nonredundant Recognition Systems of Mycobacterium Tuberculosis. *PloS Pathog* (2005) 1(3):279–85. doi: 10.1371/journal.ppat.0010034
73. Khan N, Pahari S, Vidyarthi A, Aqdas M, Agrewala JN. NOD-2 and TLR-4 Signaling Reinforces the Efficacy of Dendritic Cells and Reduces the Dose of TB Drugs Against Mycobacterium Tuberculosis. *J Innate Immun* (2016b) 8 (3):228–42. doi: 10.1159/000439591
74. Khan N, Vidyarthi A, Pahari S, Negi S, Aqdas M, Nadeem S, et al. Signaling Through NOD-2 and TLR-4 Bolsters the T Cell Priming Capability of Dendritic Cells by Inducing Autophagy. *Sci Rep* (2016c) 6:19084. doi: 10.1038/srep19084
75. Zumla A, Rao M, Parida SK, Keshavjee S, Cassell G, Wallis R, et al. Inflammation and Tuberculosis: Host-directed Therapies. in. *J Internal Med* (2015) 277(4):373–87. doi: 10.1111/joim.12256
76. Hawn TR, Matheson AI, Maley SN, Vandal O. Host-Directed Therapeutics for Tuberculosis: can We Harness the Host? *Microbiol Mol Biol Rev* (2013) 77(4):608–27. doi: 10.1128/mmbr.00032-13
77. Zumla A, Rao M, Wallis RS, Kaufmann SHE, Rustomjee R, Mwaba P, et al. Host-directed Therapies for Infectious Diseases: Current Status, Recent Progress, and Future Prospects. *Lancet Infect Dis* (2016) 16(4):e47–63. doi: 10.1016/S1473-3099(16)00078-5
78. Machelart A, Song OR, Hoffmann E, Brodin P. Host-Directed Therapies Offer Novel Opportunities for the Fight Against Tuberculosis. *Drug Discovery Today* (2017) 22(8):1250–7. doi: 10.1016/j.drudis.2017.05.005
79. Yang CS. Advancing Host-Directed Therapy for Tuberculosis. *Microb Cell* (2017) 4(3):105–7. doi: 10.15698/mic2017.03.565
80. Ribeiro CMS, Sarrami-Forooshani R, Setiawan LC, Zijlstra-Willems EM, Van Hamme JL, Tigchelaar W, et al. Receptor Usage Dictates HIV-1 Restriction by Human TRIM5α in Dendritic Cell Subsets. *Nature* (2016) 540(7633):448–52. doi: 10.1038/nature20567
81. Kimura T, Jain A, Choi SW, Mandell MA, Schroder K, Johansen T, et al. TRIM-Mediated Precision Autophagy Targets Cytoplasmic Regulators of Innate Immunity. *J Cell Biol* (2015) 210(6):973–89. doi: 10.1083/jcb.201503023
82. Dang AT, Teles RMB, Liu PT, Choi A, Legaspi A, Sarno EN, et al. Autophagy Links Antimicrobial Activity With Antigen Presentation in Langerhans Cells. *JCI Insight* (2019) 4(8):e126955. doi: 10.1172/jci.insight.126955
83. Lerena MC, Colombo MI. *Mycobacterium Marinum* Induces a Marked LC3 Recruitment to its Containing Phagosome That Depends on a Functional ESX-1 Secretion System. *Cell Microbiol* (2011) 13(6):814–35. doi: 10.1111/j.1462-5822.2011.01581.x
84. Sampaio E, Malta A, Sarno E, Kaplan G. Effect of rhuIFN-gamma Treatment in Multibacillary Leprosy Patients. *Int J Lepr Other Mycobact Dis* (1996) 64 (3):268–73.
85. Cogen AL, Walker SL, Roberts CH, Hagge DA, Neupane KD, Khadge S, et al. Human Beta-Defensin 3 Is Up-Regulated in Cutaneous Leprosy Type 1 Reactions. *PloS Neglect Trop Dis* (2012) 6(11):e1869. doi: 10.1371/journal.pntd.0001869
86. Scollard DM, Adams LB, Gillis TP, Krahenbuhl JL, Truman RW, Williams DL. The Continuing Challenges of Leprosy. *Clin Microbiol Rev* (2006) 19 (2):338–81. doi: 10.1128/CMR.19.2.338-381.2006
87. Shi CS, Shenderov K, Huang NN, Kabat J, Abu-Asab M, Fitzgerald KA, et al. Activation of Autophagy by Inflammatory Signals Limits IL-1β Production by Targeting Ubiquitinated Inflammasomes for Destruction. *Nat Immunol* (2012) 13(3):255–63. doi: 10.1038/ni.2215
88. Campoy E, Colombo MI. Autophagy Subversion by Bacteria. *Curr Topics Microbiol Immunol* (2009) 335:227–50. doi: 10.1007/978-3-642-00302-8_11
89. Cemma M, Brumell JHH. Interactions of Pathogenic Bacteria With Autophagy Systems. *Curr Biol* (2012) 22(13):R540–5. doi: 10.1016/j.cub.2012.06.001
90. Silva T, Moreira AC, Nazmi K, Moniz T, Vale N, Rangel M, et al. Lactoferricin Peptides Increase Macrophages' Capacity to Kill *Mycobacterium Avium*. *mSphere* (2017b) 2(4):301–17. doi: 10.1128/mSphere
91. Periyasamy KM, Ranganathan UD, Tripathy SP, Bethunaickan R. Vitamin D – A Host Directed Autophagy Mediated Therapy for Tuberculosis. *Mol Immunol* (2020) 127:238–44. doi: 10.1016/j.molimm.2020.08.007

92. Fretham SJB, Carlson ES, Georgieff MK. Neuronal-Specific Iron Deficiency Dysregulates Mammalian Target of Rapamycin Signaling During Hippocampal Development in Nonanemic Genetic Mouse Models. *J Nutr* (2013) 143(3):260–6. doi: 10.3945/jn.112.168617
93. Watson A, Lipina C, McArdle HJ, Taylor PM, Hundal HS. Iron Depletion Suppresses mTORC1-directed Signalling in Intestinal Caco-2 Cells Via Induction of REDD1. *Cell Signal* (2016) 28(5):412–24. doi: 10.1016/j.cellsig.2016.01.014
94. Wu Y, Li X, Xie W, Jankovic J, Le W, Pan T. Neuroprotection of Deferoxamine on Rotenone-Induced Injury Via Accumulation of HIF-1 Alpha and Induction of Autophagy in SH-SY5Y Cells. *Neurochem Int* (2010) 57(3):198–205. doi: 10.1016/j.neuint.2010.05.008
95. Hwang JJ, Ha NK, Kim J, Cho D, Mi JK, Kim Y, et al. Zinc (II) Ion Mediates Tamoxifen-Induced Autophagy and Cell Death in MCF-7 Breast Cancer Cell Line. *Biometals* (2010) 23(6):997–1013. doi: 10.1007/s10534-010-9346-9
96. Lee S, Koh J. Roles of Zinc and Metallothionein-3 in Oxidative Stress-Induced Lysosomal Dysfunction, Cell Death, and Autophagy in Neurons and Astrocytes. *Mol Brain* (2010) 3(1):30. doi: 10.1186/1756-6606-3-30
97. Kim KW, Speirs CK, Jung DK, Lu B. The Zinc Ionophore PCI-5002 Radiosensitizes Non-Small Cell Lung Cancer Cells by Enhancing Autophagic Cell Death. *J Thorac Oncol* (2011) 6(9):1542–52. doi: 10.1097/JTO.0b013e3182208fac
98. Hung H, Huang W, Pan C. Dopamine-and Zinc-Induced Autophagosome Formation Facilitates PC12 Cell Survival. *Cell Biol Toxicol* (2013) 29(6):415–29. doi: 10.1007/s10565-013-9261-2
99. Liuzzi JP, Yoo C. Role of Zinc in the Regulation of Autophagy During Ethanol Exposure in Human Hepatoma Cells. *Biol Trace Element Res* (2013) 156(1-3):350–6. doi: 10.1007/s12011-013-9816-3
100. Pan R, Timmins GS, Liu W, Liu KJ. Autophagy Mediates Astrocyte Death During Zinc-Potentiated Ischemia–Reperfusion Injury. *Biol Trace Element Res* (2015) 166(1):89–95. doi: 10.1007/s12011-015-0287-6
101. Popp L, Segatori L. Zinc Oxide Particles Induce Activation of the Lysosome–Autophagy System. *ACS Omega* (2019) 4(1):573–81. doi: 10.1021/acsomega.8b01497
102. Kawamata T, Horie T, Matsunami M, Sasaki M, Ohsumi Y. Zinc Starvation Induces Autophagy in Yeast. *J Biol Chem* (2017) 292(20):8520–30. doi: 10.1074/jbc.M116.762948
103. Ding B, Zhong Q. Zinc Deficiency: An Unexpected Trigger for Autophagy. *J Biol Chem* (2017) 292(20):8531–2. doi: 10.1074/jbc.H116.762948
104. Cho YH, Lee SH, Lee SJ, Kim HN, Koh JY. A Role of Metallothionein-3 in Radiation-Induced Autophagy in Glioma Cells. *Sci Rep* (2020) 10(1):2015. doi: 10.1038/s41598-020-58237-7
105. Liuzzi JP, Guo L, Yoo C, Stewart TS. Zinc and Autophagy. *Biometals* (2014) 27(6):1087–96. doi: 10.1007/s10534-014-9773-0
106. Roscioli E, Tran HB, Jersmann H, Nguyen PT, Hopkins E, Lester S, et al. The Uncoupling of Autophagy and Zinc Homeostasis in Airway Epithelial Cells as a Fundamental Contributor to COPD. *Am J Physiol Lung Cell Mol Physiol* (2017) 313(3):L453–65. doi: 10.1152/ajplung.00083.2017
107. Taneja DP. Observations on Serum Zinc in Patients of Pulmonary Tuberculosis. *J Indian Med Assoc* (1990) 88(10):280–1.
108. Ray M, Kumar L, Prasad R. Plasma Zinc Status in Indian Childhood Tuberculosis: Impact of Antituberculosis Therapy. *Int J Tuberculosis Lung Dis* (1998) 2(9):719–25.
109. Karyadi E, Schultink W, Nelwan RH, Gross R, Amin Z, Dolmans WM, et al. Poor Micronutrient Status of Active Pulmonary Tuberculosis Patients in Indonesia. *J Nutr* (2000) 130(12):2953–8. doi: 10.1093/jn/130.12.2953
110. Koyanagi A, Kuffó D, Gresely L, Shenkin A, Cuevas LE. Relationships Between Serum Concentrations of C-reactive Protein and Micronutrients, in Patients With Tuberculosis. *Ann Trop Med Parasitol* (2004) 98(4):391–9. doi: 10.1179/000349804225003424
111. Ghulam H, Kadri SM, Manzoor A, Waseem Q, Aatif MS, Khan GQ, et al. Status of Zinc in Pulmonary Tuberculosis. *J Infect Dev Ctries* (2009) 3(5):365–8. doi: 10.3855/jidc.244
112. Cuevas LE, Almeida LM, Mazunder P, Paixão AC, Silva AM, Maciel L, et al. Effect of Zinc on the Tuberculin Response of Children Exposed to Adults With Smear-Positive Tuberculosis. *Ann Trop Paediatr* (2002) 22(4):313–9. doi: 10.1179/027249302125001967
113. Yoshikawa Y, Ogawa M, Hain T, Chakraborty T, Sasakawa C. Listeria Monocytogenes ActA is a Key Player in Evading Autophagic Recognition. *Autophagy* (2009) 5(8):1220–1. doi: 10.4161/auto.5.8.10177
114. Shahnazari S, Namolovan A, Mogridge J, Kim PK, Brumell JH. Bacterial Toxins can Inhibit Host Cell Autophagy Through cAMP Generation. *Autophagy* (2011) 7(9):957–65. doi: 10.4161/auto.7.9.16435
115. Tattoli I, Sorbara MT, Philpott DJ, Girardin SE. Bacterial Autophagy: The Trigger, the Target and the Timing. *Autophagy* (2012) 8(12):1848–50. doi: 10.4161/auto.21863
116. Dong N, et al. Structurally Distinct Bacterial TBC-like Gaps Link Arf Gtpase to Rab1 Inactivation to Counteract Host Defenses. *Cell* (2012) 150(5):1029–41. doi: 10.1016/j.cell.2012.06.050
117. O'Keeffe KM, Wilk MM, Leech JM, Murphy AG, Laabei M, Monk IR, et al. Manipulation of Autophagy in Phagocytes Facilitates Staphylococcus Aureus Bloodstream Infection. *Infect Immun* (2015) 83(9):3445–57. doi: 10.1128/IAI.00358-15
118. Lapaquette P, Bringer MA, Darfeuille-Michaud A. Defects in Autophagy Favour Adherent-Invasive Escherichia Coli Persistence Within Macrophages Leading to Increased Pro-Inflammatory Response. *Cell Microbiol* (2012) 14(6):791–807. doi: 10.1111/j.1462-5822.2012.01768.x
119. Kuo SY, Castoreno AB, Aldrich LN, Lassen KG, Goel G, Dančík V, et al. Small-molecule Enhancers of Autophagy Modulate Cellular Disease Phenotypes Suggested by Human Genetics. *Proc Natl Acad Sci USA* (2015) 112(31):E4281–7. doi: 10.1073/pnas.1512289112
120. Miao Y, Li G, Zhang X, Xu H, Abraham SN. A TRP Channel Senses Lysosome Neutralization by Pathogens to Trigger Their Expulsion. *Cell* (2015) 161(6):1306–19. doi: 10.1016/j.cell.2015.05.009
121. Starr T, Child R, Wehrly TD, Hansen B, Hwang S, López-Otin C, et al. Selective Subversion of Autophagy Complexes Facilitates Completion of the Brucella Intracellular Cycle. *Cell Host Microbe* (2012) 11(1):33–45. doi: 10.1016/j.chom.2011.12.002
122. Li J, Liu Y, Wang Z, Liu K, Wang Y, Liu J, et al. Subversion of Cellular Autophagy Machinery by Hepatitis B Virus for Viral Envelopment. *J Virol* (2011) 85(13):6319–33. doi: 10.1128/JVI.02627-10
123. Ferrari E, Monzani R, Villella VR, Esposito S, Saluzzo F, Rossin F, et al. Cysteamine Re-Establishes the Clearance of Pseudomonas Aeruginosa by Macrophages Bearing the Cystic Fibrosis-Relevant F508del-CFTR Mutation. *Cell Death Dis* (2017) 8(1):e2544. doi: 10.1038/cddis.2016.476
124. Greenstein RJ, Su L, Juste RA, Brown ST. On the Action of Cyclosporine A, Rapamycin and Tacrolimus on M. Avium Including Subspecies Paratuberculosis. *PloS One* (2008) 3(6):e2496. doi: 10.1371/journal.pone.0002496
125. Zullo AJ, Jurcic Smith KL, Lee S. Mammalian Target of Rapamycin Inhibition and Mycobacterial Survival are Uncoupled in Murine Macrophages. *BMC Biochem* (2014) 15(1):4. doi: 10.1186/1471-2091-15-4
126. Choi SW, Gu Y, Peters RS, Salgame P, Ellner JJ, Timmins GS, et al. Ambroxol Induces Autophagy and Potentiates Rifampin Antimycobacterial Activity. *Antimicrobial Agents Chemother* (2018) 62(9):e01019–18. doi: 10.1128/aac.01019-18
127. Singhal A, Jie L, Kumar P, Hong GS, Leow MKS, Paleja B, et al. Metformin as Adjunct Antituberculosis Therapy. *Sci Trans Med* (2014) 6(263):263ra159. doi: 10.1126/scitranslmed.3009885
128. Cárdenas-Rodríguez N, Coballase-Urrutia E, Rivera-Espinosa L, Romero-Toledo A, Sampieri AI, Ortega-Cuellar D, et al. Modulation of Antioxidant Enzymatic Activities by Certain Antiepileptic Drugs (Valproic Acid, Oxcarbazepine, and Topiramate): Evidence in Humans and Experimental Models. *Oxid Med Cell Longevity* (2013) 2013:598493. doi: 10.1155/2013/598493
129. Schiebler M, Brown K, Hegyi K, Newton SM, Renna M, Hepburn L, et al. Functional Drug Screening Reveals Anticonvulsants as Enhancers of mTOR-Independent Autophagic Killing of *Mycobacterium Tuberculosis* Through Inositol Depletion. *EMBO Mol Med* (2015) 7(2):127–39. doi: 10.15252/emmm.201404137
130. Juárez E, Carranza C, Sánchez G, González M, Chávez J, Sarabia C, et al. Loperamide Restricts Intracellular Growth of *Mycobacterium Tuberculosis* in Lung Macrophages. *Am J Respir Cell Mol Biol* (2016) 55(6):837–47. doi: 10.1165/rcmb.2015-0383OC
131. Genestet C, Bernard-Barret F, Hodille E, Ginevra C, Ader F, Goutelle S, et al. Antituberculous Drugs Modulate Bacterial Phagolysosome Avoidance and

Autophagy in *Mycobacterium Tuberculosis*-Infected Macrophages. *Tuberculosis* (2018) 111:67–70. doi: 10.1016/j.tube.2018.05.014
132. Sun D, Hurdle JG, Lee R, Lee R, Cushman M, Pezzuto JM. Evaluation of Flavonoid and Resveratrol Chemical Libraries Reveals Abyssinone II as a Promising Antibacterial Lead. *ChemMedChem* (2012) 7(9):1541–5. doi: 10.1002/cmdc.201200253
133. Park D, Jeong H, Lee MN, Koh A, Kwon O, Yang YR, et al. Resveratrol Induces Autophagy by Directly Inhibiting mTOR Through ATP Competition Dohyun Park1. *Sci Rep* (2016) 23:6–21772. doi: 10.1038/srep21772
134. Zhang Q, Sun J, Wang Y, He W, Wang L, Zheng Y, et al. Antimycobacterial and Anti-Inflammatory Mechanisms of Baicalin Via Induced Autophagy in Macrophages Infected With *Mycobacterium Tuberculosis*. *Front Microbiol* (2017) 8:2142. doi: 10.3389/fmicb.2017.02142
135. Renna M, Schaffner C, Brown K, Shang S, Tamayo MH, Hegyi K, et al. Azithromycin Blocks Autophagy and may Predispose Cystic Fibrosis Patients to Mycobacterial Infection. *J Clin Invest* (2011) 121(9):3554–63. doi: 10.1172/JCI46095
136. Aziz DB, Low JL, Wu ML, Gengenbacher M, Teo JWP, Dartois V, et al. Rifabutin Is Active Against *Mycobacterium Abscessus* Complex. *Antimicrobial Agents Chemother* (2017) 61(6):e00155–17. doi: 10.1128/AAC.00155-17
137. Bailey MA, Na H, Duthie MS, Gillis TP, Lahiri R, Parish T. Nitazoxanide is Active Against *Mycobacterium Leprae*. *PloS One* (2017) 12(8):e0184107. doi: 10.1371/journal.pone.0184107
138. Jo EK. Innate Immunity to Mycobacteria: Vitamin D and Autophagy. *Cell Microbiol* (2010) 12(8):1026–35. doi: 10.1111/j.1462-5822.2010.01491.x
139. Palucci I, Delogu G. Host Directed Therapies for Tuberculosis: Futures Strategies for an Ancient Disease. *Chemotherapy* (2018) 63(3):172–80. doi: 10.1159/000490478
140. Krutzik SR, Hewison M, Liu PT, Robles JA, Stenger S, Adams JS, et al. Il-15 Links Tlr2/1-Induced Macrophage Differentiation to the Vitamin D-Dependent Antimicrobial Pathway. *J Immunol* (2008) 181(10):7115–20. doi: 10.4049/jimmunol.181.10.7115
141. Montoya D, Cruz D, Teles RMB, Lee DJ, Ochoa MT, Krutzik SR, et al. Divergence of Macrophage Phagocytic and Antimicrobial Programs in Leprosy. *Cell Host Microbe* (2009) 6(4):343–53. doi: 10.1016/j.chom.2009.09.002
142. Hu Y, Wen Z, Liu S, Cai Y, Guo J, Xu Y, et al. Ibrutinib Suppresses Intracellular Mycobacterium Tuberculosis Growth by Inducing Macrophage Autophagy. *J Infect* (2020) 80(6):e19–26. doi: 10.1016/j.jinf.2020.03.003
143. Abate G, Ruminiski PG, Kumar M, Singh K, Hamzabegovic F, Hoft DF, et al. New Verapamil Analogs Inhibit Intracellular Mycobacteria Without Affecting the Functions of Mycobacterium-Specific T Cells. *Antimicrobial Agents Chemother* (2016) 60(3):1216–25. doi: 10.1128/AAC.01567-15
144. Guerra-De-Blas PDC, Bobadilla-Del-Valle M, Sada-Ovalle I, Estrada-Garcia I, Torres-Gonzalez P, Lopez-Saavedra A, et al. Simvastatin Enhances the Immune Response Against Mycobacterium Tuberculosis. *Front Microbiol* (2019) 10:2097. doi: 10.3389/fmicb.2019.02097 doi: 10:2097.
145. Parihar SP, Guler R, Khutlang R, Lang DM, Hurdayal R, Mhlanga MM, et al. Statin Therapy Reduces the Mycobacterium Tuberculosis Burden in Human Macrophages and in Mice by Enhancing Autophagy and Phagosome Maturation. *J Infect Dis* (2014) 209(5):754–63. doi: 10.1093/infdis/jit550
146. Shoen C, Benaroch D, Sklaney M, Cynamon M. In Vitro Activities of Omadacycline Against Rapidly Growing Mycobacteria. *Antimicrobial Agents Chemother* (2019) 63(5):e02522–18. doi: 10.1128/AAC.02522-18
147. Sundaramurthy V, Barsacchi R, Samusik N, Marsico G, Gilleron J, Kalaidzidis I, et al. Integration of Chemical and RNAi Multiparametric Profiles Identifies Triggers of Intracellular Mycobacterial Killing. *Cell Host Microbe* (2013) 13(2):129–42. doi: 10.1016/j.chom.2013.01.008
148. Stanley RE, Ragusa MJ, Hurley JH. The Beginning of the End: How Scaffolds Nucleate Autophagosome Biogenesis. *Trends Cell Biol* (2014) 24(1):73–81. doi: 10.1016/j.tcb.2013.07.008
149. Dutta NK, Pinn ML, Karakousis PC. Metformin Adjunctive Therapy Does Not Improve the Sterilizing Activity of the First-Line Antitubercular Regimen in Mice. *Antimicrobial Agents Chemother* (2017) 61(8):e00652–17. doi: 10.1128/AAC.00652-17
150. Bhat SA, Iqbal IK, Kumar A. Imaging the NADH: NAD+ Homeostasis for Understanding the Metabolic Response of Mycobacterium to Physiologically Relevant Stresses. *Front Cell Infect Microbiol* (2016) 6:145. doi: 10.3389/fcimb.2016.00145
151. Piccaro G, Pietraforte D, Giannoni F, Mustazzolu A, Fattorini L. Rifampin Induces Hydroxyl Radical Formation in Mycobacterium Tuberculosis. *Antimicrobial Agents Chemother* (2014) 58(12):7527–33. doi: 10.1128/AAC.03169-14
152. Alarcón De La Lastra C, Villegas I. Resveratrol as an Antioxidant and Pro-Oxidant Agent: Mechanisms and Clinical Implications. *Biochem Soc Trans* (2007) 35(5):1156–60. doi: 10.1042/BST0351156
153. Kuršvietienė L, Stanevičienė I, Mongirdienė A, Bernatonienė J. Multiplicity of Effects and Health Benefits of Resveratrol. *Med (Kaunas)* (2016) 52 (3):148–55. doi: 10.1016/j.medici.2016.03.003
154. Liu M, Wilk SA, Wang A, Zhou L, Wang RH, Ogawa W, et al. Resveratrol Inhibits mTOR Signaling by Promoting the Interaction Between mTOR and DEPTOR. *J Biol Chem* (2010) 285(47):36387–94. doi: 10.1074/jbc.M110.169284
155. Nakahira K, Haspel JA, Rathinam VAK, Lee SJ, Dolinay T, Lam HC, et al. Autophagy Proteins Regulate Innate Immune Responses by Inhibiting the Release of Mitochondrial DNA Mediated by the NALP3 Inflammasome. *Nat Immunol* (2011) 12(3):222–30. doi: 10.1038/ni.1980
156. Zhou R, Yazdi AS, Menu P, Tschopp J. A Role for Mitochondria in NLRP3 Inflammasome Activation. *Nature* (2011) 469(7329):221–6. doi: 10.1038/nature09663
157. Harris J, Lang T, Thomas JPW, Sukkar MB, Nabar NR, Kehrl JH. Autophagy and Inflammasomes. *Mol Immunol* (2017) 86:10–5. doi: 10.1016/j.molimm.2017.02.013
158. Battah B, Chemi G, Butini S, Campiani G, Brogi S, Delogu G, et al. A Repurposing Approach for Uncovering the Anti-Tubercular Activity of FDA-Approved Drugs With Potential Multi-Targeting Profiles. *Molecules* (2019) 24(23):4373. doi: 10.3390/molecules24234373
159. Castillo EF, Dekonenko A, Arko-Mensah J, Mandell MA, Dupont N, Jiang S, et al. Autophagy Protects Against Active Tuberculosis by Suppressing Bacterial Burden and Inflammation. *Proc Natl Acad Sci USA* (2012) 109 (46):3168–76. doi: 10.1073/pnas.1210500109
160. Griffith DE. Treatment of *Mycobacterium Avium* Complex (Mac). *Semin Respir Crit Care Med* (2018) 39(3):351–61. doi: 10.1055/s-0038-1660472
161. Luthra S, Rominski A, Sander P. The Role of Antibiotic-Target-Modifying and Antibiotic-Modifying Enzymes in *Mycobacterium Abscessus* Drug Resistance. *Front Microbiol* (2018) 9:2179. doi: 10.3389/fmicb.2018.02179
162. Wu ML, Aziz DB, Dartois V, Dick T. NTM Drug Discovery: Status, Gaps and the Way Forward. *Drug Discovery Today* (2018) 23(8):1502–19. doi: 10.1016/j.drudis.2018.04.001
163. Chopra S, Matsuyama K, Hutson C, Madrid P. Identification of Antimicrobial Activity Among FDA-approved Drugs for Combating *Mycobacterium Abscessus* and *Mycobacterium Chelonae*. *J Antimicrob Chemother* (2011) 66(7):1533–6. doi: 10.1093/jac/dkr154
164. Pang H, Li G, Zhao X, Liu H, Wan K, Yu P. Drug Susceptibility Testing of 31 Antimicrobial Agents on Rapidly Growing Mycobacteria Isolates From China. *BioMed Res Int* (2015) 2015:419392. doi: 10.1155/2015/419392
165. O'Riordan W, Green S, Overcash JS, Puljiz I, Metallidis S, Gardovskis J, et al. Omadacycline for Acute Bacterial Skin and Skin-Structure Infections. *New Engl J Med* (2019) 380(6):528–38. doi: 10.1056/nejmoa1800170
166. Celdrán A, Esteban J, Mañas J, Granizo JJ. Wound Infections Due to Mycobacterium Fortuitum After Polypropylene Mesh Inguinal Hernia Repair. *J Hosp Infect* (2007) 66(4):374–7. doi: 10.1016/j.jhin.2007.05.006
167. Murillo J, Torres J, Bofill L, Rios-Fabra A, Irausquin E, Istúriz R. Skin and Wound Infection by Rapidly Growing Mycobacteria: An Unexpected Complication of Liposuction and Liposculpture. The Venezuelan Collaborative Infectious and Tropical Diseases Study Group - Pubmed. *Arch Dermatol* (2000) 136(11):1347–52. doi: 10.1001/archderm.136.11.1347
168. Brickman M, Parsa AA, Parsa FD. Mycobacterium Cheloneae Infection After Breast Augmentation. *Aesthet Plast Surg* (2005) 29(2):116–8. doi: 10.1007/s00266-004-0023-7
169. Mauriello JA. Atypical Mycobacterial Infection of the Periocular Region After Periocular and Facial Surgery. *Ophthalmic Plast Reconstructive Surg* (2003) 19(3):182–8. doi: 10.1097/01.IOP.0000064994.09803.CB
170. Gravante G, Caruso R, Araco A, Cervelli V. Infections After Plastic Procedures: Incidences, Etiologies, Risk Factors, and Antibiotic

Prophylaxis. *Aesthet Plast Surg* (2008) 32(2):243–51. doi: 10.1007/s00266-007-9068-8
171. Goldman J, Caron F, De Quatrebarbes J, Pestel-Caron M, Courville P, Doré MX, et al. Infections From Tattooing: Outbreak of *Mycobacterium Chelonae* in France. *BMJ* (2010) 341:c5483. doi: 10.1136/bmj.c5483
172. Falkinham JO. Nontuberculous Mycobacteria From Household Plumbing of Patients With Nontuberculous Mycobacteria Disease. *Emerg Infect Dis* (2011) 17(3):419–24. doi: 10.3201/eid1703.101510
173. Khan M, Gibbons JL, Ferrajoli A. Spotlight on Ibrutinib and its Potential in Frontline Treatment of Chronic Lymphocytic Leukemia. *OncoTargets Ther* (2017) 10:1909–14. doi: 10.2147/OTT.S98689
174. Tran PN, O'Brien S. The Safety of Bruton's Tyrosine Kinase Inhibitors for the Treatment of Chronic Lymphocytic Leukemia. *Expert Opin Drug Saf* (2017) 16(9):1079–88. doi: 10.1080/14740338.2017.1344213
175. Dousa KM, Babiker A, Van Aartsen D, Shah N, Bonomo RA, Johnson JL, et al. Ibrutinib Therapy and *Mycobacterium Chelonae* Skin and Soft Tissue Infection. *Open Forum Infect Dis* (2018) 5(7):ofy168. doi: 10.1093/ofid/ofy168
176. Fiorcari S, Maffei R, Audrito V, Martinelli S, Hacken E, Zucchini P, et al. Ibrutinib Modifies the Function of Monocyte/Macrophage Population in Chronic Lymphocytic Leukemia. *Oncotarget* (2016) 7(40):65968–81. doi: 10.18632/oncotarget.11782
177. Li L, Chen X, Gu H. The Signaling Involving in Autophagy Machinery in Keratinocytes and Therapeutic Approaches for Skin Diseases. *Oncotarget* (2016) 7(31):50682–97. doi: 10.18632/oncotarget.9330
178. Wang RC, Levine B. Calcipotriol Induces Autophagy in Hela Cells and Keratinocytes. *J Invest Dermatol* (2011) 131(4):990–3. doi: 10.1038/jid.2010.423
179. Ito K, Koga M, Shibayama Y, Tatematsu S, Nakayama J, Imafuku S. Proactive Treatment With Calcipotriol Reduces Recurrence of Plaque Psoriasis. *J Dermatol* (2016) 43(4):402–5. doi: 10.1111/1346-8138.13158
180. Yuk JM, Shin DM, Lee HM, Yang CS, Jin HS, Kim KK, et al. Vitamin D3 Induces Autophagy in Human Monocytes/Macrophages Via Cathelicidin. *Cell Host Microbe* (2009) 6(3):231–43. doi: 10.1016/j.chom.2009.08.004
181. Fabri M, Stenger S, Shin DM, Yuk JM, Liu PT, Realegeno S, et al. Vitamin D is Required for IFN-γ-Mediated Antimicrobial Activity of Human Macrophages. *Sci Trans Med* (2011) 3(104):104ra102. doi: 10.1126/scitranslmed.3003045
182. Vickers NJ. Animal Communication: When I'm Calling You, Will You Answer Too? *Curr Biol* (2017) 27(14):R713–5. doi: 10.1016/j.cub.2017.05.064
183. Martineau AR, Honecker FU, Wilkinson RJ, Griffiths CJ. Vitamin D in the Treatment of Pulmonary Tuberculosis. *J Steroid Biochem Mol Biol* (2007) 103(3–5):793–8. doi: 10.1016/j.jsbmb.2006.12.052
184. Selvaraj P. Vitamin D, Vitamin D Receptor, and Cathelicidin in the Treatment of Tuberculosis. *Vitam Horm* (2011) 86:307–25. doi: 10.1016/B978-0-12-386960-9.00013-7
185. Liu PT, Wheelwright M, Teles R, Komisopoulou E, Edfeldt K, Ferguson B, et al. MicroRNA-21 Targets the Vitamin D-dependent Antimicrobial Pathway in Leprosy. *Nat Med* (2012) 18(2):267–73. doi: 10.1038/nm.2584
186. Afsal K, Selvaraj P, Harishankar M. 1, 25-Dihydroxyvitamin D_3 Downregulates Cytotoxic Effector Response in Pulmonary Tuberculosis. *Int Immunopharmacol* (2018) 62:251–60. doi: 10.1016/j.intimp.2018.07.018
187. Sanguinetti M, Ardito F, Fiscarelli E, La Sorda M, D'Argenio P, Ricciotti G, et al. Fatal Pulmonary Infection Due to Multidrug-Resistant Mycobacterium Abscessus in a Patient With Cystic Fibrosis. *J Clin Microb* (2001) 39(2):816–9. doi: 10.1128/JCM.39.2.816-819.2001
188. Nessar R, Cambau E, Reyrat JM, Murray A, Gicquel B. *Mycobacterium Abscessus*: A New Antibiotic Nightmare. *J Antimicrob Chemother* (2012) 67(4):810–8. doi: 10.1093/jac/dkr578
189. Williams A, Sarkar S, Cuddon P, Ttofi EK, Saiki S, Siddiqi FH, et al. Novel Targets for Huntington's Disease in an mTOR-independent Autophagy Pathway. *Nat Chem Biol* (2008) 4(5):295–305. doi: 10.1038/nchembio.79
190. Nowotarska SW, Nowotarski K, Grant IR, Elliott CT, Friedman M, Situ C. Mechanisms of Antimicrobial Action of Cinnamon and Oregano Oils, Cinnamaldehyde, Carvacrol, 2,5-Dihydroxybenzaldehyde, and 2-Hydroxy-5-Methoxybenzaldehyde Against *Mycobacterium Avium* Subsp. *Paratuberculosis* (Map). *Foods* (2017) 6(9):72. doi: 10.3390/foods6090072
191. Potoènjak I, Gobin I, Domitroviæ R. Carvacrol Induces Cytotoxicity in Human Cervical Cancer Cells But Causes Cisplatin Resistance: Involvement of MEK–ERK Activation. *Phytother Res* (2018) 32(6):1090–7. doi: 10.1002/ptr.6048
192. Spalletta S, Flati V, Toniato E, Di Gregorio J, Marino A, Pierdomenico L, et al. Carvacrol Reduces Adipogenic Differentiation by Modulating Autophagy and ChREBP Expression. *PloS One* (2018) 13(11):e0206894. doi: 10.1371/journal.pone.0206894
193. Marini E, Di Giulio M, Ginestra G, Magi G, Di Lodovico S, Marino A, et al. Efficacy of Carvacrol Against Resistant Rapidly Growing Mycobacteria in the Planktonic and Biofilm Growth Mode. *PloS One* (2019) 14(7):e0219038. doi: 10.1371/journal.pone.0219038
194. Brüning A, Brem GJ, Vogel M, Mylonas I. Tetracyclines Cause Cell Stress-Dependent ATF4 Activation and mTOR Inhibition. *Exp Cell Res* (2014) 320(2):281–9. doi: 10.1016/j.yexcr.2013.11.012
195. Kaushik A, Ammerman NC, Martins O, Parrish NM, Nuermberger EL. *In Vitro* Activity of New Tetracycline Analogs Omadacycline and Eravacycline Against Drug-Resistant Clinical Isolates of *Mycobacterium Abscessus*. *Antimicrob Agents Chemother* (2019) 63(6):e470–19. doi: 10.1128/aac.00470-19
196. Rodrigues L, Wagner D, Viveiros M, Sampaio D, Couto I, Vavra M, et al. Thioridazine and Chlorpromazine Inhibition of Ethidium Bromide Efflux in *Mycobacterium Avium* and *Mycobacterium Smegmatis*. *J Antimicrob Chemother* (2008) 61(5):1076–82. doi: 10.1093/jac/dkn070
197. Deshpande D, Srivastava S, Musuka S, Gumbo T. Thioridazine as Chemotherapy for *Mycobacterium Avium* Complex Diseases. *Antimicrob Agents Chemother* (2016) 60(8):4652–8. doi: 10.1128/aac.02985-15
198. Seervi M, Rani A, Sharma AK, Santhosh, Kumar TR. ROS Mediated ER Stress Induces Bax-Bak Dependent and Independent Apoptosis in Response to Thioridazine. *Biomed Pharmacother* (2018) 106:200–9. doi: 10.1016/j.biopha.2018.06.123
199. Chu CW, Ko HJ, Chou CH, Cheng TS, Cheng HW, Liang YH, et al. Thioridazine Enhances P62-Mediated Autophagy and Apoptosis Through Wnt/β-Catenin Signaling Pathway in Glioma Cells. *Int J Mole Sci* (2019) 20(3):473. doi: 10.3390/ijms20030473
200. Bermudez LE, Kolonoski P, Wu M, Aralar PA, Inderlied CB, Young LS. Mefloquine Is Active In Vitro and In Vivo Against Mycobacterium Avium Complex. *Antimicrob Agents Chemother* (1999) 43(8):1870–4. doi: 10.1128/aac.43.8.1870
201. Shin JH, Park SJ, Jo YK, Kim ES, Kang H, Park JH, et al. Suppression of Autophagy Exacerbates Mefloquine-mediated Cell Death. *Neurosci Lett* (2012) 515(2):162–7. doi: 10.1016/j.neulet.2012.03.040

Conflict of Interest: The authors declare that the research was conducted in the absence of any commercial or financial relationships that could be construed as a potential conflict of interest.

frontiers in Microbiology

ORIGINAL RESEARCH
published: 14 June 2021
doi: 10.3389/fmicb.2021.615383

Skin Immune Response of Immunocompetent and Immunosuppressed C57BL/6 Mice After Experimental Subcutaneous Infection Caused by *Purpureocillium lilacinum*

Danielly Corrêa-Moreira[1,2], Arethuza dos Santos[2], Rodrigo C. Menezes[3], Fernanda N. Morgado[2], Cintia M. Borba[1] and Joseli Oliveira-Ferreira[2]**

[1] Laboratory of Taxonomy, Biochemistry and Bioprospecting of Fungi, Oswaldo Cruz Institute, Oswaldo Cruz Foundation, Rio de Janeiro, Brazil, [2] Laboratory of Immunoparasitology, Oswaldo Cruz Institute, Oswaldo Cruz Foundation, Rio de Janeiro, Brazil, [3] Laboratory of Clinical Research in Dermatozoonosis in Domestic Animals, Evandro Chagas National Institute of Infectious Diseases, Oswaldo Cruz Foundation, Rio de Janeiro, Brazil

Hyalohyphomycosis is a fungal infection characterized by the presence of a hyaline mycelium in the host. It is caused by several agents, such as *Purpureocillium lilacinum*. Our study aimed to evaluate some cell subsets and inflammatory markers involved in the *in situ* immune response to subcutaneous hyalohyphomycosis by *P. lilacinum* in C57BL/6 murine models. The fungal isolate was inoculated in mice randomly distributed in immunocompetent/infected (CI) and immunosuppressed/infected (SI) groups. Mice were evaluated on days 1, 3, 5, and 7 after inoculation. Histopathological studies showed several lesions in the site of infection as well as the formation of multifocal and mixed inflammatory infiltrates, which differed between the CI and SI groups. This analysis also revealed conidia and hypha-like structures in subcutaneous tissues of mice of both groups. The immunohistochemical analysis showed lower percentages of macrophages and neutrophils in the SI group compared to those in the CI group. Moreover, the intensity of interleukin (IL)-1β and nitric oxide synthase 2 production by cells of immunosuppressed mice was discreet, compared to immunocompetent mice that ranged from moderate to intense over time. The quantitative interference of dexamethasone in the response to the fungus was also demonstrated. We concluded that our results can be useful not only to broaden the knowledge on *P. lilacinum* but also, based on this host–parasite relationship, to contribute to the understanding of the mechanisms of infection.

Keywords: *Purpureocillium lilacinum*, skin immune response, experimental model, immunosuppression, immunohistochemistry

OPEN ACCESS

Edited by:
Stéphane Ranque, Aix-Marseille Université, France

Reviewed by:
Patricia Talamás-Rohana, Instituto Politécnico Nacional de México (CINVESTAV), Mexico
Rogelio De J. Treviáo-Rangel, Autonomous University of Nuevo León, Mexico

****Correspondence:***
Danielly Corrêa-Moreira
dcorrea@ioc.fiocruz.br
Joseli Oliveira-Ferreira
lila@ioc.fiocruz.br

Specialty section:
This article was submitted to Microbial Immunology, a section of the journal Frontiers in Microbiology

Received: *09 October 2020*
Accepted: *11 May 2021*
Published: *14 June 2021*

Citation:
Corrêa-Moreira D, dos Santos A, Menezes RC, Morgado FN, Borba CM and Oliveira-Ferreira J (2021) Skin Immune Response of Immunocompetent and Immunosuppressed C57BL/6 Mice After Experimental Subcutaneous Infection Caused by Purpureocillium lilacinum. Front. Microbiol. 12:615383. doi: 10.3389/fmicb.2021.615383

INTRODUCTION

Hyalohyphomycosis is a fungal infection characterized by the presence of a hyaline mycelium in the host (Ajello, 1986). It is caused by several agents, such as *Paecilomyces* spp., *Fusarium* spp., *Scedosporium* spp., *Scopulariopsis* spp., *Penicillium* spp., and *Purpureocillium lilacinum*. Some species, including *P. lilacinum*, in addition to hyaline mycelium have the ability to produce adventitious forms in the tissue, which are structures morphologically similar to phialides and microconidias that spread through the blood, causing occlusion, infarction, and vascular necrosis (Perfect and Schell, 1996; Das et al., 2010).

Purpureocillium lilacinum (Thom) Luangsa-ard, Houbraken, Hywel-Jones and Samson, comb. nov 2011, previously called *Paecilomyces lilacinus*, is a filamentous, hyaline, anamorphic fungus (Luangsa-Ard et al., 2011) considered as an emerging pathogen for humans, especially for immunosuppressed patients, although the number of immunocompetent hosts infected by this fungus has also increased in recent years (Shivaprasad et al., 2013; Turner and Conrad, 2015; Borba and Brito, 2016; Juyal et al., 2018).

Immunocompetent individuals present clinical manifestations that may vary from cutaneous to subcutaneous nodular lesions and constitute one third of the cases of hyalohyphomycosis by *P. lilacinum* (Pastor and Guarro, 2006). In immunosuppressed patients, the majority of reported cases were disseminated infections (Pastor and Guarro, 2006; Antas et al., 2011; Ding et al., 2014).

As the population of immunosuppressed individuals increases, fungal diseases have emerged as the major cause of human diseases (Shoham and Levitz, 2005; Antas et al., 2011). Patients with immune deficiencies frequently have recurrent mycoses and, in some cases, develop severe forms, which emphasize the importance of understanding how the immune system controls infection.

Although evaluations of immunological responses against *P. lilacinum* are scarce, it is generally believed that the main fungal defense mechanism is developed by phagocytes, which destroy fungi through the production of nitric oxide (NO) and other substances secreted by these cells (Romani, 2011). Usually, inflammatory infiltrates in cutaneous fungal infections are composed of lymphocytes, neutrophils, and macrophages. Granulomatous reactions, often suppurative, are observed, depending on the immunological status of the patient (Guarner and Brandt, 2011).

Miranda et al. (2016) evaluated cats naturally infected with *Sporothrix* spp. and demonstrated that the fungus stimulates the development of granulomas with phagocytes that are unable to destroy fungal cells and that the inhibition of macrophage functions increased host susceptibility. These results corroborate the data of Antachopoulos and Roilides (2005), who mentioned the participation of granulocyte colony-stimulating factor (G-CSF), macrophage colony-stimulating factor (M-CSF), and granulocyte-macrophage colony-stimulating factor (GM-CSF), important glycoproteins in the production and activation of phagocytes that are crucial in the defense against fungi. Previously, Sa et al. (2007) also demonstrated the presence of Langerhans cells in the cutaneous tissue of patients with chromoblastomycosis, pointing out that the persistence of the fungus in the tissue is related to the activation of macrophages and the production of NO.

In patients with cutaneous forms of hyalohyphomycosis caused by *P. lilacinum*, several authors describe the presence of mixed inflammatory infiltrates in the lesions, composed of macrophages, neutrophils, and dendritic cells (DCs) (Gutierrez-Rodero et al., 1999; Lin et al., 2008; Huang et al., 2011). Since cutaneous infections constitute the majority of cases of fungal hyalohyphomycosis, it is necessary to emphasize the importance of these cells in the phagocytosis and presentation of antigens and, consequently, in the efficiency of the adaptive response (Antachopoulos and Roilides, 2005).

The impact of immunosuppression by glucocorticoids on the immune response is due to their mechanisms, which promote the inhibitory effect of the synthesis of pro-inflammatory cytokines such as interleukin (IL)-2, IL-6, and tumor necrosis factor (TNF)-α, and prostaglandins (Song et al., 2005). According to Lionakis and Kontoyiannis (2003), glucocorticoids affect the number of mononuclear leukocytes, causing reversible lymphopenia and monocytopenia. The drug primarily affects cellular immunity, both qualitatively and functionally, depleting circulating $CD4^{++}$ T lymphocytes, and to a lesser extent $CD8^{+}$ T lymphocytes, in addition to monocytes, macrophages, and polymorphonuclear cells. In the murine model of systemic infection, de Sequeira et al. (2017) demonstrated that immunosuppressive drugs such as dexamethasone interfere with lymphoproliferative responses. However, the authors did not evaluate the influence of the drug on subcutaneous infection.

Thus, this study aimed to evaluate some cell subsets and inflammatory markers involved in the skin immune response in subcutaneous hyalohyphomycosis by *P. lilacinum* due to its emerging and opportunistic potential in an immunocompetent and immunosuppressed murine model, characterizing phenotypically and functionally some cells involved in this process.

MATERIALS AND METHODS

Ethics Statement

This study was performed in strict accordance with the Brazilian College of Animal Experimentation (COBEA). All experimental procedures involving animals followed the regulations for animal experiments of the Ethics Committee for Animal Study of FIOCRUZ (license number L-031/2015-CEUA/IOC-FIOCRUZ) and were performed under anesthesia. All efforts were made to minimize the suffering of the animals.

Mice

Ninety-six male C57BL/6 mice, aged 6–8 weeks, weighing approximately 21 g were used in the experiments. The number of animals used in this study was calculated to guarantee statistically valid results obtained with as few individuals as

possible without compromising the degree of reliability and avoiding the unnecessary use of animals.

Mice were randomly allocated to each experimental group and were kept under specific pathogen-free conditions at the Laboratory of the Animal Experimentation Center (IOC FIOCRUZ) and maintained in micro-insulators made of polypropylene, autoclavable, containing pine beds. Micro-insulators were disposed in ventilated racks (ALESCO) with air exchange measures of 350 m^3/h. Breeding room was managed at room temperature; 23–25°C, humidity; 30–70%, light/dark cycle; 12 h, and water and food were given *ad libitum*. We took the utmost care to alleviate any pain and suffering on the part of the mice. Mice were submitted to euthanasia by CO_2 exposure prior to analysis.

Purpureocillium lilacinum

One human strain of *P. lilacinum* was used in this study: S2, kindly provided by Dr. Annette Fothergill (Fungus Testing Laboratory, University of Texas Health Science Center–San Antonio, San Antonio, TX, United States), isolated from skin biopsy on the left foot of a female patient. The strain was molecularly authenticated and deposited in GenBank® sequences database with access number MF590109 (de Sequeira et al., 2017).

Culture Conditions and Inoculum

The isolate was subcultured on potato dextrose agar (PDA) medium at room temperature for 12 days, and then, conidia were collected by scraping the colonies, suspended in phosphate buffered saline (PBS), followed by thermal shock protocol to separate conidia from hyphae, according to de Sequeira et al. (2017). The supernatant was collected for quantification in a Neubauer hemocytometer. Cell viability was assessed by colony-forming unit (CFU) (Goihman-Yahr et al., 1980). The resulting suspensions were adjusted to the desired inoculum.

Immunosuppression by Dexamethasone

To perform immunosuppression, mice received 1 mg/kg of dexamethasone (Hypofarma, Ribeirão das Neves, Brazil) administered *ad libitum* in the drinking water for 3 days before fungal inoculation and during all the experiments (Brito et al., 2011). We chose dexamethasone because of its ability to deplete $CD4^+$ T lymphocytes, similar to the condition provoked by HIV infection, one of the preexisting factors for fungal infections. Tetracycline (1,000 mg/L; Teuto, São Paulo, Brazil) was also added to the drinking water in parallel to prevent bacterial infections. The route of administration of the drug had already been demonstrated by our group as safe and effective in inducing immunosuppression without, however, causing stress in animals as do invasive methods like gavage (Brito et al., 2011; de Sequeira et al., 2013, 2017).

Experimental Hyalohyphomycosis

The fungal isolate was inoculated subcutaneously by a syringe at the base of the tail in 32 mice randomly distributed into two groups: immunocompetent (CI) and immunosuppressed mice (SI). Sixteen mice were distributed into immunocompetent (CC) and immunosuppressed mice (SC) control groups and similarly inoculated with PBS. In dorsal–ventral position, mice were inserted in an acrylic container, and after trichotomy and asepsis of the tail base region, the CI and SI groups were inoculated with 0.02 ml of the cell suspension containing 1×10^5 conidia of *P. lilacinum* with more than 80% viability. Control groups (CC and SC) were similarly inoculated with PBS. Mice were checked daily for 7 days to observe abnormal behaviors and pathological changes, with the aim of minimizing suffering. On each observation point (days 1, 3, 5, and 7 after inoculation), four animals from the CI and SI groups and two from the CC and SC groups were euthanized.

Histopathology

Mice were submitted to anesthesia with 10% ketamine hydrochloride associated with 2% xylazine hydrochloride (Syntec, Santana de Parnaíba, Brazil) and submitted to euthanasia by CO_2 exposure. After asepsis of the region, two skin fragments of approximately 3 mm in diameter around the point of inoculation were removed. One skin fragment was submitted to histological analysis and the other to immunohistochemistry.

The skin fragment destined for histopathology was fixed in 10% neutral buffered formalin, dehydrated, and embedded in paraffin. Sections were cut and stained with hematoxylin–eosin (H&E), periodic acid-Schiff (PAS), and Grocott (methenamine silver), and the photographs were taken with a Leica DM 1000 (Leica, Werzlar, Germany). The inflammatory infiltrate in tissues was classified into: granulomatous, predominance of macrophages, and non-granulomatous, predominance of other types of inflammatory cells (such as lymphocytes, plasma cells, and neutrophils). The intensity of the inflammatory infiltrate was classified as follows: absent or mild (cellular infiltrate absent or mild and dispersed foci) and moderate to intense (cellular infiltrate dense and diffuse).

Immunohistochemistry

Biopsy fragments frozen in OCT resin (Sakura Finetek, Alphen aan den Rijn, Netherlands) were cut into 3-μm-thick sections and mounted on microscope silanized slides (Dako Cytomation, Carpinteria, CA, United States). The slides were fixed in acetone PA (Merck, Darmstadt, Germany) and hydrated in PBS, pH 7.4. Blockage of endogenous peroxidase (peroxidase blocking reagent; Dako, Carpinteria, CA, United States) and non-specific staining (normal goat serum; Zymed Laboratories Inc., San Francisco, CA, United States) were performed before the use of specific antibodies.

The specimens were then incubated with the primary antibodies directed to surface receptors: $CD68^+$ macrophages, anti-neutrophilic elastase, nitric oxide synthase type 2 (NOS2), and IL-1β (all from BD Biosciences Pharmingen, San Diego, CA, United States), followed by incubation with the biotinylated secondary antibody (Zymed) and the streptavidin–biotin–peroxidase complex (ABC kit; Dako Cytomation). Aminoethylcarbazole (AEC kit; Zymed) was used as the

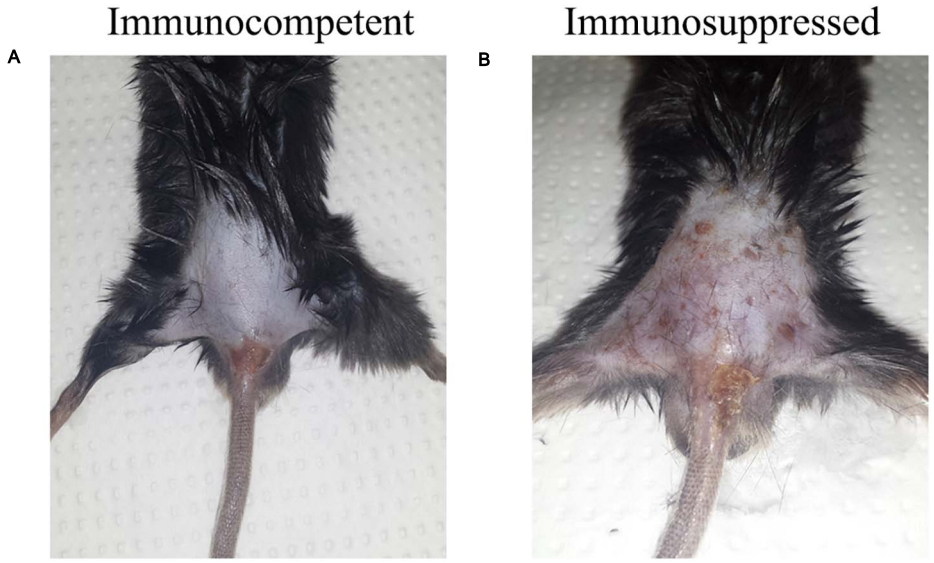

FIGURE 1 | Macroscopic aspects of the epidermis of the immunocompetent (CI) and immunosuppressed (SI) mice inoculated at the tail base with 1×10^5 conidia of *Purpureocillium lilacinum* on day 5 after infection. **(A)** Discreet, non-ulcerative, and non-suppurative lesion at the point of inoculation; **(B)** Crusted lesion at the point of inoculation, extending to the base of the tail.

substrate–chromogen system, and the slides were counterstained with Mayer's hematoxylin (Dako). The slides were examined under a light microscope (E400 model; Nikon Instruments Inc., Melville, NY, United States), and the percentage of stained cells was determined by counting 500 cells as standard. The intensity of IL-1β and NOS2 was scored in 10 microscope fields. + = discreet (at least one positive site per field); ++ = moderate (two or three positive sites per field); +++ = intense (four or five positive sites per field).

Statistical Analysis

Data were analyzed using GraphPad Prism R software, version 8 (GraphPad Software, Inc., San Diego, CA, United States). The Kolmogorov–Smirnov test was used to evaluate the distribution of variables. Mann–Whitney test was used to perform comparisons between groups. Data are expressed as mean ± standard deviation. The *p*-value cutoff for statistical significance was 0.05, and the n value for each group on each time point = 4.

All the experiments were carried out twice to ensure reproducibility.

RESULTS

Clinical Signs

Mice were observed for 7 days. No clinical alterations as apathy and weight and/or hair loss were observed in the immunocompetent (CI/CC) group. The inflammatory response at the site of the infection was discreet, non-suppurative, and non-ulcerative (**Figure 1A**). On the other hand, mice in the immunosuppressed group (SI/SC) presented apathy and hair loss and crusted lesions at the point of inoculation, extending to the base of the tail (**Figure 1B**).

Histological Studies

Figure 2 shows histological findings in the cutaneous and subcutaneous tissues of immunocompetent and immunosuppressed mice inoculated at the tail base with *P. lilacinum*.

Immunocompetent mice inoculated with *P. lilacinum* (CI group) presented dermatitis, panniculitis, and skin ulcerations with diffuse inflammatory infiltrate reaching superficial and deep dermis (**Figure 2A**–day 1), consisting mainly of neutrophils and macrophages in all days during the follow-up (1, 3, 5, and 7 days) after inoculation. From the third day after the inoculation, hyphae were detected, as well as abundant intracellular and extracellular conidia (**Figure 2C**), and on day 5, necrosis of the skeletal muscle and foci of fibrosis in the dermis and subcutaneous tissue were observed (**Figure 2B**). Conidia within macrophages and neutrophils were observed in the subcutaneous tissue and also in the superficial dermis in the middle of the inflammatory infiltrate. On day 7 after inoculation, the skin of these mice presented acanthosis, and there were conidia inside the macrophages (data not shown).

In general, immunosuppressed mice inoculated with *P. lilacinum* (Group SI) had more severe lesions and more fungal structures than the immunocompetent ones (CI Group) from the first day after inoculation. In all the sampling days, the histological analysis of the tissue collected from these animals revealed the formation of diffuse and/or multifocal inflammatory infiltrate, which intensified until the end of the experiment. Extensive areas of ulcer covered by crusts, dermatitis, and suppurative panniculitis were also observed (data not shown).

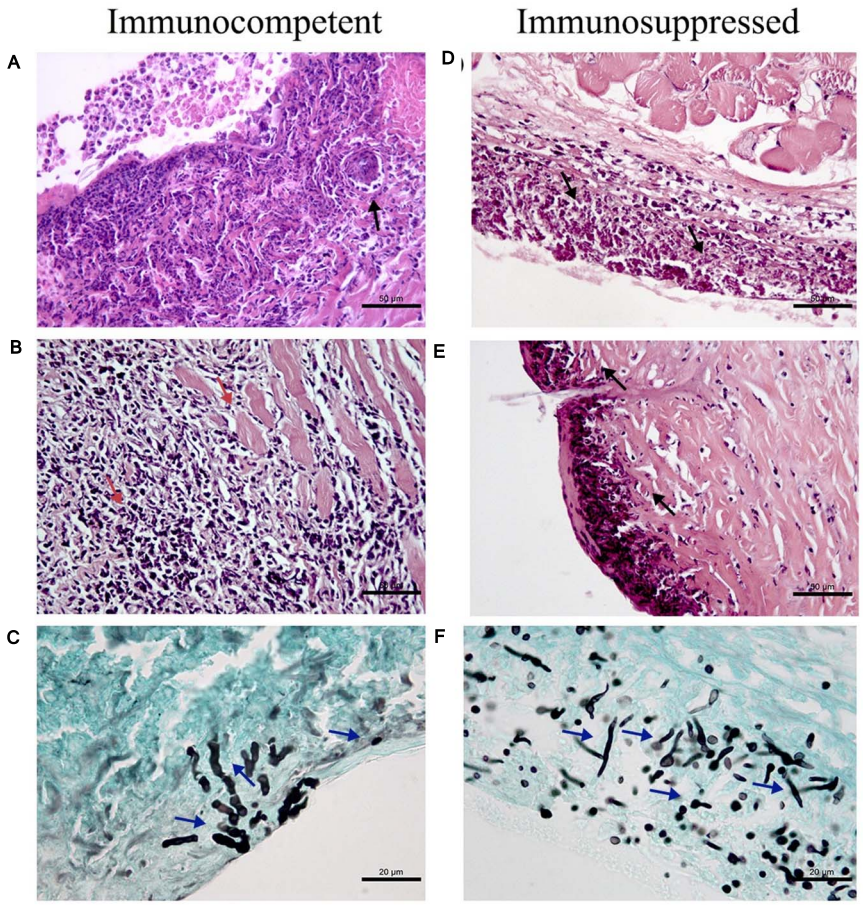

FIGURE 2 | Histological findings in the cutaneous and subcutaneous tissues of immunocompetent (CI–left column) and immunosuppressed mice (SI–right column) inoculated at the tail base with 1 × 10^5 conidia of *Purpureocillium lilacinum*. **(A)** Diffuse inflammatory infiltrate (black arrow) constituted mainly by macrophages and neutrophils reaching superficial and deep dermis on day 1 after infection, H&E. **(B)** Necrosis in the skeletal muscle and fibrosis in the dermis and subcutaneous tissue (red arrows) on day 5 after infection, H&E. **(C)** Hyphae in the dermis (blue arrows) on the third day after infection, Grocott. **(D)** Severe inflammatory infiltrate (black arrows) affecting the superficial and deep dermis and adjacent skeletal muscles on day 3 after infection, H&E. **(E)** Suppurative dermatitis and panniculitis (black arrows) with diffuse inflammatory infiltrate ranging from mild to severe consisting mainly of neutrophils, with fewer macrophages on day 7 after infection, H&E; **(F)** Abundant hyphae, pseudohyphae (blue arrows) in the subcutaneous tissue on day 1 after inoculation, Grocott.

On day 1, similarly to the immunocompetent group, numerous conidia in the interior of macrophages and hyphae in the tissue were revealed (**Figure 2F**). On the third day after inoculation, the infiltrate ranged from moderate to severe, and the extension of the infiltrate affected the superficial and deep dermis and adjacent skeletal muscles (suppurative myositis), being more intense in the subcutaneous tissue (**Figure 2D**). Five days after inoculation, in addition to the presence of conidia inside the phagocytes and in the tissue, hyphae were also observed in the crusts that covered the ulcerations in the epidermis of immunosuppressed mice (data not shown), also observed at the end of the experiment (day 7), with the formation of multifocal inflammatory infiltrates, besides abundant conidia and hyphae in the crusts, dermis, and mainly subcutaneous tissue (**Figure 2E**). In all samples (CI and SI groups–1, 3, 5, and 7 days after infection), the culture was positive to *P. lilacinum*. As expected, all control mice (Groups CC and SC) were negative.

Immunohistochemistry

Figure 3 shows the differences in macrophage and neutrophil frequencies and the intensity of inflammation markers, comparing immunocompetent and immunosuppressed groups. It was possible to observe lower percentages of macrophages and neutrophils in the SI group, compared to CI, as well as a lower intensity of production of IL-1β and NO by the cells of immunosuppressed mice than by those of immunocompetent ones.

The immunohistochemical analyses during the follow-up are summarized in **Figure 4**. In the immunocompetent group infected with *P. lilacinum* (CI group), the percentages of macrophages (**Figure 4A**) were lower than those of neutrophils (**Figure 4C**), especially on day 1 after inoculation. However, concerning the quantification of macrophages, it was possible to notice that the absolute number of these cells tended to increase in the final observation points, as well as the expression of NOS2.

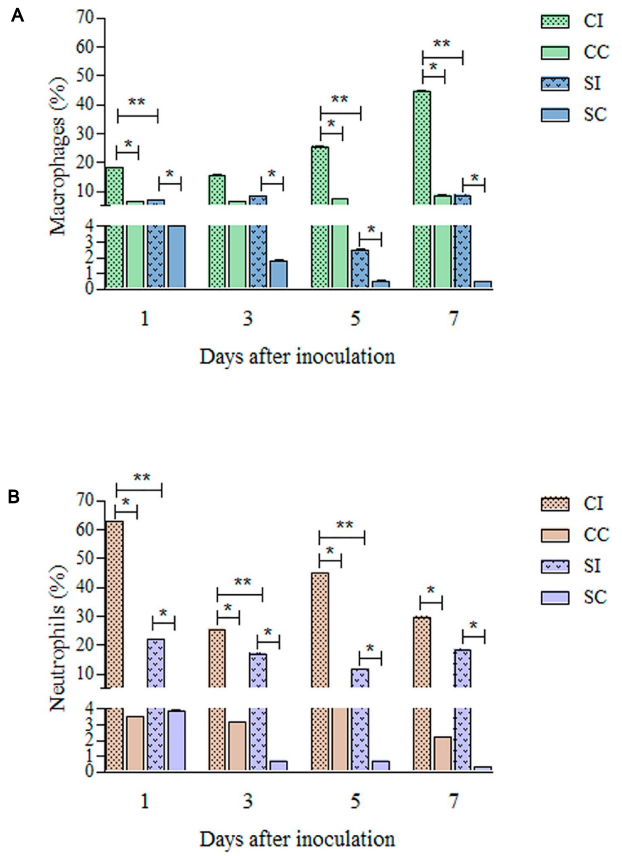

FIGURE 3 | Quantification of macrophages **(A)** and neutrophils **(B)** from skin biopsy of the tail base region of immunocompetent and immunosuppressed mice inoculated with *Purpureocillium lilacinum* and control groups inoculated with phosphate-buffered saline (PBS) by immunohistochemistry. CI, Immunocompetent mice inoculated with *P. lilacinum*; CC, Immunocompetent mice inoculated with PBS; SI, Immunosuppressed mice inoculated with *P. lilacinum*; SC, Immunosuppressed mice inoculated with PBS. *Statistical differences between infected and control groups ($p < 0.05$). **Statistical differences between immunocompetent and immunosuppressed groups ($p < 0.005$).

IL-1β (**Figure 4E**) production was high on the first day after infection, decreased on days 3 and 5, and showed an elevation at the end of the experiment. The production of NOS2 (**Figure 4G**) was moderate on days 1 and 3, increasing from day 5 until the end of the experiment. Compared to the infected group (CI), the production of IL-1β and NOS2 in the control group (CC) was discreet over time.

It was not possible to reach 500 cells in the immunosuppressed mice of both infected (SI) and control (SC) groups. Approximately 280 cells were quantified in these animals and, as observed in immunocompetent mice, there was a higher percentage of neutrophils than macrophages (**Figures 4B,D**), especially in the initial (day 1) and final (day 7) periods of the experiment. The production of NO and IL-1β remained discreet (**Figures 4F,H**), without variations over time, in the SI and SC groups.

DISCUSSION

Currently, invasive fungal infections are one of the greatest threats for immunosuppressed hosts (Antachopoulos and Roilides, 2005). Hyalohyphomycosis is caused by several agents, and *P. lilacinum* (Antas et al., 2011) is one of them.

The mechanisms of cellular and immunological response against this fungus are scarce; therefore, this work sought to investigate part of the basis of the host–parasite interaction. Previous studies of our group using peritoneal macrophages from C57BL/6 mice lineage for *in vitro* experiments demonstrated the potential of this fungus to adhere, invade, and destroy host cells (Peixoto et al., 2010). Since these results pointed out the possibility of disease establishment in this mouse strain, we chose the *in vivo* C57BL/6 murine model with the same genetic lineage of the cells previously used.

Notwithstanding *P. lilacinum* fungus has low virulence, according to some authors, and requires an immunosuppressed host to invade and produce the disease (Hubálek and Hornich, 1977; Pujol et al., 2002; Pastor and Guarro, 2006), both immunocompetent and immunosuppressed models used by our group were infected, although the immunosuppressed model seemed to be more susceptible.

The ability of the fungus to escape the immune response of the host and remain viable and circulating was demonstrated by de Sequeira et al. (2017). In this work were considered mechanisms of the adaptive immune response, as the role of $CD4^+$, $CD8^+$, regulatory T cells (Tregs), and memory T cells, of immunocompetent and immunosuppressed mice infected with *P. lilacinum* for a period of up to 45 days. It was possible to observe the impact of dexamethasone in the course of the infection, as presented here, allowing us to observe that the administration of dexamethasone can quickly (within 2 h) modify the immune response (Bain et al., 2018).

The study of de Sequeira et al. (2017) also reports that immunocompetent animals, inoculated intravenously, remained healthy during the experimental period and did not present any behavioral changes or clinical signs, such as weight loss and internal or external organ damage. However, the infection was established, since viable fungal cells were recovered from the spleen. Moreover, conidia-like structures were found in the histopathological analysis of the lung and liver of the mice of this group. In contrast, immunosuppressed mice of the same study showed weight loss, hair loss, apathy, dermatitis, internal organ damage, and keratitis, consistent with the reported cases of human infection and similar to the BALB/c model used by Brito et al. (2011).

In our study, we used the same mouse model as that of de Sequeira et al. (2017), but the route of inoculation was subcutaneous in order to evaluate the early stages of *P. lilacinum* cutaneous infection. Our results showed similar clinical signs to those of animals inoculated intravenously (Brito et al., 2011; de Sequeira et al., 2017). The immunocompetent mice did not present any clinical signs, while the immunosuppressed group presented apathy and hair loss. However, both groups presented lesions at the site of infection, dermatitis, and in some cases, keratitis.

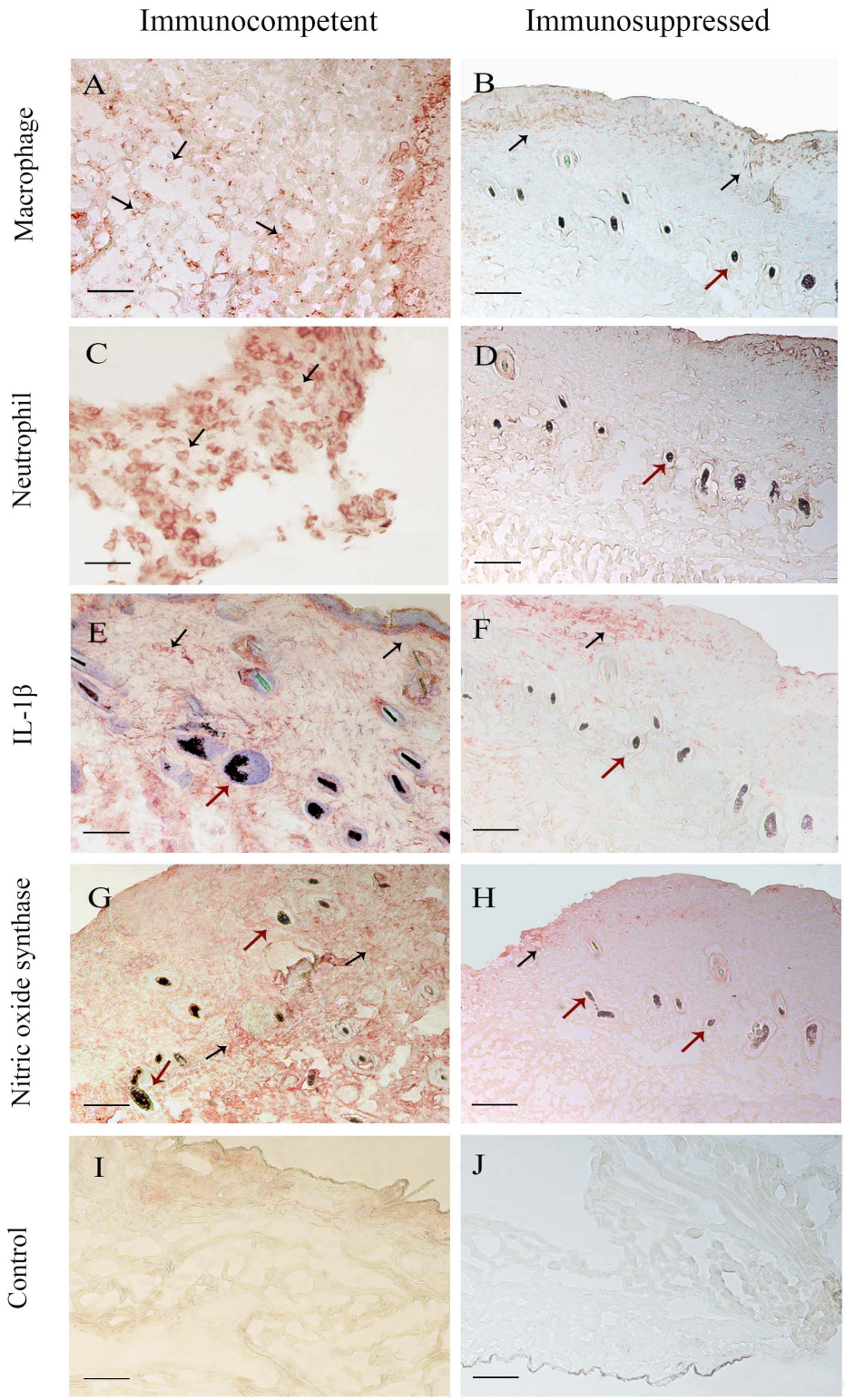

FIGURE 4 | Immunohistochemical analysis of skin biopsy of immunocompetent (left column) and immunosuppressed (right column) mice 7 days after infection. Mice were inoculated at the tail base with 1 × 10^5 conidia of *Purpureocillium lilacinum* and control groups were inoculated with phosphate-buffered saline (PBS). The black arrows show the frequencies of **(A,B)** macrophages and **(C,D)** neutrophils and the intensity of interleukin (IL)-1β **(E,F)** and nitric oxide synthase **(G,H)** production. **(I,J)** Control group. The red arrows signal the hair follicle of mice tail epidermis (— = 100 μm).

The results of this work go in line with those obtained by Permi et al. (2011); Saghrouni et al. (2013), and Bassiri-Jahromi (2014), whose histopathological analysis of the skin biopsies of immunocompetent and immunosuppressed patients infected with *P. lilacinum* revealed the formation of granulomatous reactions, in which inflammatory infiltrates are mainly composed of polymorphonuclear and macrophages. We also observed ulcerated lesions at the site of infection in mice, as well as the formation of multifocal and mixed inflammatory infiltrates, that differed between immunocompetent (CI) and immunosuppressed (SI) groups with respect to severity—more pronounced in SI. It is interesting to highlight that in the study published by Permi et al. (2011), reporting the infection caused by this fungus in an immunocompetent patient, the formation of fibrosis was observed, and the same was shown in our immunocompetent murine model. It is known that fibrosis is the formation of tissue composed of collagen fibers in an organ in response to injury or tissue damage, so we speculate that the normal host immune condition uses this mechanism to respond to the invasion and proliferation of the fungus in host tissues.

The immunohistochemical analysis of the tissue fragments collected from the immunocompetent (CI and CC) and immunosuppressed (SI and SC) mice allowed us to identify and quantify macrophages, neutrophils, and two inflammatory markers, IL-1β and NOS2, involved in the immune response *in situ*. In general, percentages of neutrophils in immunocompetent and immunosuppressed mice were higher than those of macrophages, except for the seventh day after inoculation, in the immunocompetent group. We know that *P. lilacinum* is capable of destroying macrophages that phagocytose the conidia, as well as forming germ tubes and hyphae in the first 24 h after infection *in vitro* (Peixoto et al., 2010). Thus, the marked difference in the percentages of these cells can be attributed to the fact that, although macrophages are the first line of defense against conidia, neutrophils are the cell population selected to eliminate hyphae (Schaffner et al., 1982; Cenci et al., 1997). This hypothesis is plausible to assume, since *P. lilacinum*, as well as other agents of hyalohyphomycosis, is a producer of hyphae and adventitious structures in the tissue (Perfect and Schell, 1996). These results confirm the findings of Demirezen et al. (2015), since these authors verified the predominance of neutrophils compared to macrophages in the cervicovaginal smear of patients infected with *Candida* spp., which are able to produce hypha and/or pseudohypha.

In contrast, Morgado et al. (2011) observed higher percentages of macrophages compared to neutrophils in the fixed and lymphocutaneous forms of sporotrichosis. We may suppose that these results are due to the fact that *Sporothrix* spp. in the host acquire the yeast form against which the macrophage-mediated immune response may be effective. The difference in the number of macrophages found in this study between the immunocompetent and immunosuppressed groups is also worth noting, demonstrating once again the action of dexamethasone. We know that the drug, by interfering with IL-2 synthesis, can suppress the production of inflammatory markers, such as IL-1β (Paliogianni et al., 1993; Antachopoulos and Roilides, 2005; Orlikowsky et al., 2005), leading to a deficiency in macrophage function. Our results corroborate these data, since the production of NOS2 and IL-1β by immunocompetent mice ranged from moderate to severe, especially in the final periods of observation, while in immunosuppressed mice, it remained discreet on all points.

In conclusion, our data reinforce that host conditions are crucial to the severity of opportunistic infection by *P. lilacinum*, since it is capable to infect both immunocompetent and immunosuppressed murine models but causes damage only in the immunosuppressed ones. The lower percentages of innate immune cells and their products in immunosuppressed mice demonstrate the quantitative interference of dexamethasone in the response to the fungus. Thus, we conclude that our results have not only broadened the knowledge on *P. lilacinum* but also, based on this host–parasite relationship, contributed to the understanding of the mechanisms of infection.

DATA AVAILABILITY STATEMENT

The original contributions presented in the study are included in the article/supplementary material, further inquiries can be directed to the corresponding author/s.

ETHICS STATEMENT

The animal study was reviewed and approved by Ethics Committee for Animal Study of FIOCRUZ (license number L-031/2015- CEUA/IOC-FIOCRUZ).

AUTHOR CONTRIBUTIONS

DC-M, JO-F, and CB designed the study. DC-M and AS carried out the experiments. DC-M, RM, and FM analyzed the data. DC-M wrote the manuscript. DC-M, RM, FM, CB, and JO-F revised and approved the final manuscript. All authors contributed to the article and approved the submitted version.

FUNDING

This work was supported by CAPES (DC-M fellowship–Financial code: 001). AS is a recipient of CNPq Scientific Initiation Fellowship. CB is responsible for PAPES FIOCRUZ–PAPES VI CNPq. RM and JO-F are recipients of CNPq research fellowship Code: PQ-2.

ACKNOWLEDGMENTS

We are grateful to Annette Fothergill for kindly providing the fungal isolates and to all individuals who participated in this study for their cooperation that made it possible, especially Aurea Virginia Andrade for all the support with the immunohistochemistry slides and images.

REFERENCES

Ajello, L. (1986). Hyalohyphomycosis and phaeohyphomycosis: two global disease entities of public health importance. *Eur. J. Epidemiol.* 2, 243–251.

Antachopoulos, C., and Roilides, E. (2005). Cytokines and fungal infections. *Br. J Haematol.* 129, 583–596. doi: 10.1111/j.1365-2141.2005.05498.x

Antas, P. R. Z., Brito, M. M. S., Peixoto, E., Ponte, C. G. G., and Borba, C. M. (2011). Neglected and emerging fungal infections: review of hyalohyphomycosis by *Paecilomyces lilacinus* focusing in disease burden, in vitro antifungal susceptibility and management. *Microbes Infect.* 14, 1–8.

Bain, C. R., Draxler, D. F., Taylor, R., Wallace, S., Gouldthorpe, O., Corcoran, T. B., et al. (2018). The early *in-vivo* effects of a single anti-emetic dose of dexamethasone on innate immune cell gene expression and activation in healthy volunteers. *Anaesthesia* 73, 955–966. doi: 10.1111/anae.14306

Bassiri-Jahromi, S. (2014). Cutaneous *Paecilomyces lilacinus* infections in immunocompromised and immunocompetent patients. *Indian J. Dermatol. Venereol. Leprol.* 80, 331–334. doi: 10.4103/0378-6323.136903

Borba, C. M., and Brito, M. M. S. (2016). "*Paecilomyces*: mycotoxin production and human infection," in *Molecular Biology of Food and Water Borne Mycotoxigenic and Mycotic Fungi*, eds R. M. Paterson and N. Lima (Boca Raton, FL: CRC Press), 401–423.

Brito, M. M. S., Lima, M. S., Morgado, F. N., Raibolt, P., Menezes, R. C., Conceicao-Silva, F., et al. (2011). Characteristics of *Paecilomyces lilacinus* infection comparing immunocompetent with immunosuppressed murine model. *Mycoses* 54, e513–e521. doi: 10.1111/j.1439-0507.2010.01969

Cenci, E., Perito, S., Enssle, K. H., Mosci, P., Latge, J. P., Romani, L., et al. (1997). Th1 and Th2 cytokines in mice with invasive aspergillosis. *Infect. Immun.* 65, 564–570. doi: 10.1128/iai.65.2.564-570.1997

Das, S., Saha, R., Dar, S. A., and Ramachandran, V. G. (2010). *Acremonium* species: a review of the etiological agents of emerging hyalohyphomycosis. *Mycopath* 170, 361–375. doi: 10.1007/s11046-010-9334-1

Ding, C. H., Tzar, M. N., Rahman, M. M., Muttaqillah, N. A., Redzuan, S. R., and Periyasamy, P. (2014). *Paecilomyces lilacinus* fungaemia in an AIDS patient: the importance of mycological diagnosis. *Pak. J. Med. Sci.* 30, 914–916.

de Sequeira, D. C., Peixoto, M. L., De Luca, P. M., Oliveira-Ferreira, J., Antas, P. R., and Borba, C. M. (2013). Detection of antibody to *Purpureocillium lilacinum* by immunofluorescent assay and flow cytometry in serum of infected C57BL/6 mice. *J. Immunol. Methods.* 396, 147–151. doi: 10.1016/j.jim.2013.07.002

de Sequeira, D. C. M., Menezes, R. C., Oliveira, M. M. E., Antas, P. R. Z., De Luca, P. M., Oliveira-Ferreira, J., et al. (2017). Experimental hyalohyphomycosis by *Purpureocillium lilacinum:* outcome of the infection in C57BL/6 murine models. *Front. Microbiol.* 8:1617. doi: 10.3389/fmicb.2017.01617

Demirezen, S., Donmez, H. G., Ozcan, M., and Beksac, M. S. (2015). Evaluation of the relationship between fungal infection, neutrophil leukocytes and macrophages in cervicovaginal smears: light microscopic examination. *J. Cytol.* 32, 79–84. doi: 10.4103/0970-9371.160544

Goihman-Yahr, M., Pine, L., Albornoz, M. C., Yarzabal, L., de Gomez, M. H., San Martin, B., et al. (1980). Studies on plating efficiency and estimation of viability of suspensions of *Paracoccidioides brasiliensis* yeast cells. *Mycopathologia* 71, 73–83. doi: 10.1007/BF00440612

Guarner, J., and Brandt, M. E. (2011). Histopathologic diagnosis of fungal infections in the 21st century. *Clin. Microbiol. Rev.* 24, 247–280.

Gutierrez-Rodero, F., Moragon, M., Ortiz de la Tabla, V., Mayol, M. J., and Martin, C. (1999). Cutaneous hyalohyphomycosis caused by *Paecilomyces lilacinus* in an immunocompetent host successfully treated with itraconazole: case report and review. *Eur. J. Clin. Microbiol. Infect. Dis.* 18, 814–818.

Huang, C. Y., Sun, P. L., and Tseng, H. K. (2011). Cutaneous hyalohyphomycosis caused by *Paecilomyces lilacinus* successfully treated by oral voriconazole and nystatin packing. *Mycopath* 172, 141–145. doi: 10.1007/s11046-011-9409-7

Hubálek, Z., and Hornich, M. (1977). Experimental infection of white mouse with *Chrysosporium* and *Paecilomyces*. *Mycopath* 62, 173–178.

Juyal, D., Pal, S., Sharma, M., Negi, V., Adekhandi, S., and Tyagi, M. (2018). Keratomycosis due to *Purpureocillium lilacinum*: a case report from Sub-Himalayan region of Uttarakhand. *Indian J. Pathol. Microbiol.* 61, 607–609. doi: 10.4103/IJPM.IJPM_404_17

Lin, W. L., Lin, W. C., and Chiu, C. S. (2008). *Paecilomyces lilacinus* cutaneous infection associated with peripherally inserted central catheter insertion. *J. Eur. Acad. Dermatol. Venereol.* 22, 1267–1268.

Lionakis, M. S., and Kontoyiannis, D. P. (2003). Glucocorticoids and invasive fungal infections. *Lancet* 362, 1828–1838. doi: 10.1016/s0140-6736(03)14904-5

Luangsa-Ard, J., Houbraken, J., van Doorn, T., Hong, S. B., Borman, A. M., Hywel-Jones, N. L., et al. (2011). Purpureocillium, a new genus for the medically important *Paecilomyces lilacinus*. *FEMS Microbiol. Lett.* 321, 141–149. doi: 10.1111/j.1574-6968.2011.02322

Miranda, L. H., Santiago, M. A., Schubach, T. M., Morgado, F. N., Pereira, S. A., de Oliveira, R. V., et al. (2016). Severe feline sporotrichosis associated with an increased population of $CD8^{low}$ cells and a decrease in $CD4^{(+)}$ cells. *Med. Mycol.* 54, 29–39.

Morgado, F. N., Schubach, A. O., Barros, M. B., and Conceicao-Silva, F. (2011). The *in situ* inflammatory profile of lymphocutaneous and fixed forms of human sporotrichosis. *Med. Mycol.* 49, 612–620.

Orlikowsky, T. W., Dannecker, G. E., Spring, B., Eichner, M., Hoffmann, M. K., and Poets, C. F. (2005). Effect of dexamethasone on B7 regulation and T cell activation in neonates and adults. *Pediatr. Res.* 57(Pt 1), 656–661. doi: 10.1203/01.pdr.0000156211.48307.f5

Paliogianni, F., Ahuja, S. S., Balow, J. P., Balow, J. E., and Boumpas, D. T. (1993). Novel mechanism for inhibition of human T cells by glucocorticoids. Glucocorticoids inhibit signal transduction through IL-2 receptor. *J. Immunol.* 151, 4081–4089.

Pastor, F. J., and Guarro, J. (2006). Clinical manifestations, treatment and outcome of *Paecilomyces lilacinus* infections. *Clin. Microbiol. Infect.* 12, 948–960. doi: 10.1111/j.1469-0691.2006.01481

Peixoto, E., Oliveira, J. C., Antas, P. R., and Borba, C. M. (2010). In-vitro study of the host-parasite interactions between mouse macrophages and the opportunistic fungus *Paecilomyces lilacinus*. *Ann. Trop. Med. Parasitol.* 104, 529–534. doi: 10.1179/136485910x12786389891489

Perfect, J. R., and Schell, W. A. (1996). The new fungal opportunists are coming. *Clin. Infect. Dis.* 22(Suppl. 2), S112–S118.

Permi, H. S., Sunil, K. Y., Karnaker, V. K., Kishan, P. H., Teerthanath, S., and Bhandary, S. K. (2011). A rare case of fungal maxillary sinusitis due to *Paecilomyces lilacinus* in an immunocompetent host, presenting as a subcutaneous swelling. *J. Lab. Physicians.* 3, 46–48.

Pujol, I. A., Ortoneda, C., Pastor, J., Mayayo, E., and Guarro, J. (2002). Experimental pathogenicity of three opportunist *Paecilomyces* species in a murine model. *J. Mycol. Med.* 12, 86–89.

Romani, L. (2011). Immunity to fungal infections. *Nat. Rev. Immunol.* 11, 275–288. doi: 10.1038/nri2939

Sa, V. C., Silva, T. A., Reis, C. M., Cunha, F. Q., Figueiredo, F., and Bocca, A. L. (2007). The pattern of immune cell infiltration in chromoblastomycosis: involvement of macrophage inflammatory protein-1 alpha/CCL3 and fungi persistence. *Rev. Inst. Med. Trop. Sao Paulo.* 49, 49–53. doi: 10.1590/s0036-46652007000100009

Saghrouni, F., Saidi, W., Ben Said, Z., Gheith, S., Ben Said, M., Ranque, S., et al. (2013). Cutaneous hyalohyphomycosis caused by *Purpureocillium lilacinum* in an immunocompetent patient: case report and review. *Med. Mycol.* 51, 664–668. doi: 10.3109/13693786.2012.757656

Schaffner, A., Douglas, H., and Braude, A. (1982). Selective protection against conidia by mononuclear and against mycelia by polymorphonuclear phagocytes in resistance to *Aspergillus*. Observations on these two lines of defense in vivo and in vitro with human and mouse phagocytes. *J. Clin. Invest.* 69, 617–631. doi: 10.1172/jci110489

Shivaprasad, A., Ravi, G. C., and Shivapriya, R. (2013). A rare case of nasal septal perforation due to *Purpureocillium lilacinum*: case report and review.

Indian J. Otolaryngol. Head Neck Surg. 65, 184–188. doi: 10.1007/s12070-012-0570-1

Shoham, S., and Levitz, S. M. (2005). The immune response to fungal infections. *Br. J. Haematol.* 129, 569–582. doi: 10.1111/j.1365-2141.2005.05397.x

Song, I. H., Gold, R., Straub, R. H., Burmester, G. R., and Buttgereit, F. (2005). New glucocorticoids on the Horizon: repress, Don't activate! *J. Rheumatol.* 32, 1199–1207.

Turner, L. D., and Conrad, D. (2015). Retrospective case-series of *Paecilomyces lilacinus* ocular mycoses in Queensland, Australia. *BMC Res. Notes.* 31:627.

Conflict of Interest: The authors declare that the research was conducted in the absence of any commercial or financial relationships that could be construed as a potential conflict of interest.

frontiers in Immunology

ORIGINAL RESEARCH
published: 15 June 2021
doi: 10.3389/fimmu.2021.598943

Leishmania Parasites Drive PD-L1 Expression in Mice and Human Neutrophils With Suppressor Capacity

Alessandra M. da Fonseca-Martins[1,2,3], Phillipe de Souza Lima-Gomes[2], Maísa Mota Antunes[4], Renan Garcia de Moura[5], Luciana P. Covre[5,6], Carolina Calôba[7], Vivian Grizente Rocha[7], Renata M. Pereira[7], Gustavo Batista Menezes[4], Daniel Claudio Oliveira Gomes[5], Elvira M. Saraiva[2†] and Herbert L. de Matos Guedes[1,3,8*†]*

[1] Laboratório de Imunofarmacologia, Instituto de Biofísica Carlos Chagas Filho, Universidade Federal do Rio de Janeiro, Rio de Janeiro, Brazil, [2] Departamento de Imunologia, Laboratório de Imunobiologia das Leishmanioses, Instituto de Microbiologia Paulo de Góes, Universidade Federal do Rio de Janeiro, Rio de Janeiro, Brazil, [3] Departamento de Imunologia, Laboratório de Imunobiotecnologia, Instituto de Microbiologia Paulo de Góes, Universidade Federal do Rio de Janeiro, Rio de Janeiro, Brazil, [4] Center for Gastrointestinal Biology, Departamento de Morfologia, Instituto de Ciências Biológicas, Universidade Federal de Minas Gerais, Minas Gerais, Brazil, [5] Núcleo de Doenças Infecciosas, Universidade Federal do Espírito Santo, Vitória, Brazil, [6] Division of Medicine, University College London, London, United Kingdom, [7] Departamento de Imunologia, Laboratório de Imunologia Molecular, Instituto de Microbiologia Paulo de Góes, Universidade Federal do Rio de Janeiro, Rio de Janeiro, Brazil, [8] Laboratório Interdisciplinar de Pesquisas Médicas, Instituto Oswaldo Cruz, Fundação Oswaldo Cruz, Rio de Janeiro, Brazil

Neutrophils play an important role in the outcome of leishmaniasis, contributing either to exacerbating or controlling the progression of infection, a dual effect whose underlying mechanisms are not clear. We recently reported that $CD4^+$ and $CD8^+$ T cells, and dendritic cells of *Leishmania amazonensis*-infected mice present high expression of PD-1 and PD-L1, respectively. Given that the PD-1/PD-L1 interaction may promote cellular dysfunction, and that neutrophils could interact with T cells during infection, we investigated here the levels of PD-L1 in neutrophils exposed to *Leishmania* parasites. We found that both, promastigotes and amastigotes of *L. amazonensis* induced the expression of PD-L1 in the human and murine neutrophils that internalized these parasites *in vitro*. PD-L1-expressing neutrophils were also observed in the ear lesions and the draining lymph nodes of *L. amazonensis*-infected mice, assessed through cell cytometry and intravital microscopy. Moreover, expression of PD-L1 progressively increased in neutrophils from ear lesions as the disease evolved to the chronic phase. Co-culture of infected neutrophils with *in vitro* activated $CD8^+$ T cells inhibits IFN-γ production by a mechanism dependent on PD-1 and PD-L1. Importantly, we demonstrated that *in vitro* infection of human neutrophils by *L braziliensis* induced PD-$L1^+$ expression and also PD-$L1^+$ neutrophils were detected in the lesions of patients with cutaneous leishmaniasis. Taken together, these findings suggest that the *Leishmania* parasite increases the expression of PD-L1 in neutrophils with suppressor capacity, which could favor the parasite survival through impairing the immune response.

Keywords: PD-L1, neutrophils, skin, *Leishmania*, human cutaneous leishmaniasis, murine leishmaniasis, supression

OPEN ACCESS

Edited by:
Fabienne Tacchini-Cottier, University of Lausanne, Switzerland

Reviewed by:
Jaqueline França-Costa, Federal University of Bahia, Brazil
Hira Nakhasi, Center of Biologics Evaluation and Research (FDA), United States

****Correspondence:***
Elvira M. Saraiva
esaraiva@micro.ufrj.br
Herbert L. de Matos Guedes
herbert@biof.ufrj.br;
herbert@micro.ufrj.br;
herbert@ioc.fiocruz.br

†These authors share senior authorship

Specialty section:
This article was submitted to Microbial Immunology, a section of the journal Frontiers in Immunology

Received: *26 August 2020*
Accepted: *13 April 2021*
Published: *15 June 2021*

Citation:
da Fonseca-Martins AM, de Souza Lima-Gomes P, Antunes MM, de Moura RG, Covre LP, Calôba C, Rocha VG, Pereira RM, Menezes GB, Gomes DCO, Saraiva EM and de Matos Guedes HL (2021) Leishmania Parasites Drive PD-L1 Expression in Mice and Human Neutrophils With Suppressor Capacity. Front. Immunol. 12:598943. doi: 10.3389/fimmu.2021.598943

IMPORTANCE

Neutrophils outnumber leukocytes in healthy human blood, rapidly migrate to infected or inflamed sites and have powerful mechanisms to eliminate pathogens. These cells secrete cytokines and chemokines critical for the initiation and amplification of the inflammatory response. Neutrophils also have the ability to modulate adaptive immune cells through a variety of receptors, including the programmed death ligand-1 (PD-L1), a cell surface protein that suppresses T cell activation. We report that *Leishmania amazonensis*, which can cause cutaneous leishmaniasis, severe anergic diffuse cutaneous and even visceral leishmaniasis, upon interaction with murine and human neutrophils induces the expression of PD-L1. Neutrophils expressing PD-L1 were observed in the ear lesions and draining lymph nodes of infected mice and in human cutaneous leishmaniasis biopsies. Our findings suggest that *Leishmania* could modulate PD-L1 expression in neutrophils, weakening the immune response to favor its survival, which opens up new possibilities of targeting PD-L1 for therapy.

INTRODUCTION

Neutrophils, the most abundant white blood cells in the human circulation, play a crucial role in eliminating pathogens by multiple mechanisms, and participating in the development of the inflammatory reaction. Thus, neutrophils are key components of the innate immune response and in the elimination of infectious agents. They are recognized for their broad defense repertoire that includes the production of reactive oxygen species, phagocytosis, degranulation and the release of the antimicrobial neutrophil extracellular traps (1, 2).

Within the inflammatory environment, neutrophils interact with other immune cells, and secrete cytokines and chemokines critical for the development and establishment of the necessary conditions required for the interface with the adaptive immune response (3, 4). On the other hand, these cells can also favor the progression of various diseases, such as rheumatoid arthritis, systemic lupus erythematosus, and cystic fibrosis, as well as sepsis, HIV-1 infection, and malaria (5–8).

Neutrophils may also present opposing roles in infections caused by *Leishmania* sp. In fact, it has been shown that neutrophils can both exacerbate the disease or protect the host, an outcome that is dependent on a fine balance pertaining to the *Leishmania* species and host genetic background (9).

Furthermore, neutrophils are endowed with the ability to induce T cell suppression (10). Analyses of patients with visceral leishmaniasis (VL) showed an increased frequency of CD15$^+$ neutrophils expressing high levels of arginase, an enzyme associated with immunosuppression, which, after successful treatment, returned to basal levels (11). In addition, co-culture of low-density HLA-DR$^+$-neutrophils and lymphocytes, both from VL patients, with *Leishmania* antigen increased the expression of programmed death ligand-1 (PD-L1, also called B7-H1 and CD274) in neutrophils, and of the programmed death receptor 1 (PD-1, also called CD279) in lymphocytes. These findings led to the hypothesis that low-density HLA-DR$^+$ neutrophils may be involved in promoting T-cell exhaustion (12).

PD-1 is a receptor found in Natural Killer cells, T cells, B cells and activated monocytes (13–15), while the PD-L1 ligand can be found in neutrophils, B cells, dendritic cells, macrophages, mesenchymal stem cells and in non-hematopoietic cells, such as epithelial cells, muscle cells and hepatocytes (16, 17). The function of this pathway has been widely studied revealing a dichotomous activity depending on the model in which it is applied, where often it can inhibit T cell proliferation and cytokine production or increase T cell activation (18, 19). Thus, the formation of the PD-1/PD-L1 complex can be seen as a mechanism used by pathogens to evade the immune response or as a possible regulator of tissue damage mediated by the immune system (20–22). The dysfunctional state characterized by increased expression of inhibitory receptors, like the PD-1/PD-L1 complex, and by progressive loss of function, is commonly known as cellular exhaustion (23).

The use of immunotherapy to reverse dysfunction due to T-cell exhaustion has been used successfully to treat several tumors (24, 25) and also in viral and parasitic infections (26, 27). Concerning leishmaniasis, we recently reported that mice infected with *L. amazonensis* presented high expression of PD-1 in CD4$^+$ and CD8$^+$ T cells, and PD-L1 in dendritic cells, and that treatment with anti-PD-1 or anti-PD-L1 antibodies reduced the parasite load and increased IFN-gamma production by CD4$^+$ and CD8$^+$ T cells, thus, reversing cell suppression (28).

It was demonstrated that neutrophils depletion using 1A8 increased T cells response against *Leishmania* (29). Here, we aimed to investigate whether the PD-L1 expression in murine and human neutrophils could be modulated after *in vitro* interaction with *Leishmania*, and identified PD-L1-expressing neutrophils in murine and human cutaneous lesions. We also evaluated *in vitro* the participation of PD-L1 expression by neutrophils in suppressing IFN-γ production by T cells.

MATERIALS AND METHODS

Experimental Animals

Female BALB/c mice and C57BL/6, 6-8 weeks old, from the Central Bioterium (Centro de Ciências da Saúde – Universidade Federal do Rio de Janeiro, Brazil), were housed in ventilated mini-isolators (Alesco, Brazil) and kept under controlled temperature and light conditions. All animal experiments were performed in strict accordance with the Brazilian animal protection law (Lei Arouca, Number: 11.794/08) of the National Council for the Control of Animal Experimentation (CONCEA, Brazil). The protocol was approved by the Committee for Animal Use of the Universidade Federal do Rio de Janeiro (Permit Number: 161/18).

Parasite Culture

For *in vivo* infection, *L. amazonensis* promastigotes (MHOM/BR/75/Josefa) were used. Parasites were first obtained from the macerated lesions of infected BALB/c mice and then grown at 26°C in M-199 medium (Cultilab) with 20% heat inactivated fetal

bovine serum (FBS, Cultilab). Parasites were used for the experimental infections until the fifth passage in culture.

For *in vitro* infection, *L. amazonensis* promastigotes (RAT/BA/74/LV78) and *L. braziliensis* (MHOM/BR/2005/RPL5) were cultured at 26°C in Schneider medium (Invitrogen) with 20% FBS and 50 µg/mL gentamicin (Sigma). The parasites were used in assays until the fifth passage.

Amastigotes of *L. amazonensis* (RAT/BA/74/LV78) and *L. braziliensis* (MHOM/BR/2005/RPL5) were obtained from a culture of promastigotes maintained at 32°C in Grace's medium (Invitrogen), pH 5.3 supplemented with 20% FBS and 25 µg/ml gentamicin. The amastigotes were used until the third passage in culture.

Recruitment and Isolation of Murine Peritoneal Neutrophils

Neutrophils were recruited in BALB/c or C57BL/6 mice 3 h after intraperitoneal injection of 1 ml of 9% casein solution (Sigma). Mice were euthanized and the peritoneal cavity was washed with RPMI 1640 (Sigma) without serum at room temperature. A fraction of the obtained cells was first characterized by flow cytometry using anti-Ly6G-PerCP (murine, eBioscience) revealing >95% Ly6G$^+$ cells (neutrophils). Remaining cells were centrifuged at 400 g for 5 min, resuspended in RPMI and used in the following assays.

Purification of Murine Neutrophils From Bone Marrow

Bone marrow cells were flushed from the femur and tibia of BALB/c mice with RPMI/10% FBS into a 15 ml conical tube through a 100 µm cell strainer, and then were centrifuged at 400 g for 7 min at 24°C. The cell pellet was resuspended in RPMI/10% FBS and centrifuged at 1500 g for 30 min at 24°C in a Percoll gradient (100%, 72%, 65% and 58% v/v GE Healthcare). Neutrophils collected at the interface of 65% and 72%, were washed with PBS at 400 g for 10 min at 15°C, resuspended in RPMI and used in the following assays. Cell yield was ≥80% Ly6G$^+$ cells (neutrophils) as analyzed by flow cytometry using anti-Ly6G-PerCP (murine, eBioscience).

Isolation of Dermal Cells From Mouse Ears

Mice were infected intradermally in the right ear with 2x10^6 stationary-phase promastigotes of *L. amazonensis* in 20 µl PBS. After 18 h, 15 days and 60 days post-infection, the ears were collected. Control was performed with ears from naïve mice. The dermal sheets were opened and added to the wells of a 24-well plate in DMEM (Sigma) with 1% penicillin/streptomycin and 100 µg/ml each of collagenase I and II (Sigma), followed by 90 min incubation at 37°C. The tissue was then macerated with a tissue mixer for 3 min, filtered through a 70 µm filter and washed with PBS at 400 g for 5 min at 15°C. Cells were resuspended in RPMI/10% FBS for further use.

Isolation of Cells From the Lymph Nodes Draining the Infected Lesion

Mice were infected intradermally in the right footpad with 2x10^6 *L. amazonensis* stationary-phase promastigotes in 20 µl PBS. After approximately 60 days post-infection, draining lymph nodes were removed, individually macerated and the cell suspensions were centrifuged at 400 g for 5 min at 4°C. The cell pellet was resuspended in 2 ml RPMI/10% FBS for further use.

Purification of Human Blood Neutrophils

Human neutrophils from healthy blood were obtained by centrifugation on Ficoll Histopaque density gradient (Sigma-Aldrich), followed by hypotonic lysis (155 mM NH_4Cl, 10 mM $KHCO_3$, 0.1 mM EDTA, pH 7.4) to remove red blood cells. Isolated neutrophils (≥95% of the cells) were washed in PBS and resuspended in RPMI. All the procedures dealing with human blood were performed in accordance with the guidelines of the Research Ethics Committee (Hospital Universitário Fraga Filho, UFRJ, Brazil), protocol number: 4261 015400005257.

In Vivo Infection

BALB/c mice were infected with 2x10^6 *L. amazonensis* stationary-phase promastigotes in 20 µl PBS, either intradermally in the right ear or subcutaneously in the right footpad. The lesions were followed weekly for around two months by measuring the thickness with a pachymeter.

Leishmania-Neutrophil Interaction *In Vitro*

Parasites were washed twice with PBS and incubated with 0.5 µM CFSE (carboxyfluorescein succinimidyl ester - Invitrogen) at 37°C. After 15 min, RPMI/20% FBS was added, and parasites incubated for a further 15 min on ice, followed by three washes with PBS, and resuspension in PBS. Murine neutrophils were infected with CFSE-labeled promastigotes or amastigotes of *L. amazonensis* (cell:parasite-MOI 1: 10) for 4 h at 35°C and human neutrophils were infected with CFSE-labeled promastigotes or amastigotes of *L. amazonensis* or *L. braziliensis* (MOI 1:5 or 1:10) for 4 h at 35°C.

Cell Staining for Flow Cytometry

Cells from lymph nodes (5x10^5) or ear homogenates (1x10^6) were washed with PBS at 400 g for 5 min at 4°C and blocked with Human FcX (BioLegend) for 15 min, followed by staining with the antibody cocktail for 30 min at 4°C. Cells were then washed with a cytometry buffer (PBS with 5% FBS) at 400 g for 5 min and 4°C), then fixed with 4% formaldehyde (Sigma) for 15 min at 4°C. Cells were washed and resuspended in the cytometry buffer and stored in the dark at 4°C until acquisition. The following antibodies were used: anti-PD-L1-APC, anti-CD10-APC-780 (human, eBioscience); anti-CD45-APCcy7, anti-CD11b-FITC, anti-CD11b-PE, anti-CD11b-Pecy7, anti-Ly6G-PerCP, anti-Ly6G-FITC and anti-PD-L1-APC (murine, eBioscience). Acquisition of events (lymph node, 100,000 events; ear, all cells) was performed on a BD FACSAria™. The gate strategy was performed based on the selection of cell size (FSC) and composition (SSC). After identifying the main population, a gate of FSC-A (area) and FSC-H (weight) was used, where cellular doublets were excluded. Gates for positive events were established through Fluorescence Minus One (FMO) control. The data analyzes were performed using the FlowJo software.

Imaging PD-L1 Expression by Intravital Microscopy

L. amazonensis ear-infected BALB/c mice (naïve-not infected; control with saline; 1 h, 7 days and 15 days and 60 days post-infection) were injected on the ear with 8-12 µl/animal of anti-PD-L1-APC and Ly6G-FITC antibodies. After 2 h, mice were anesthetized with ketamine and xylazine intraperitoneally. Images were obtained using a Nikon Eclipse Ti with an A1R confocal head equipped with four different lasers (excitation: 405, 488, 546 and 647 nm) and emission bandpass filters at 450/50, 515/30, 584/50 and 663/738 nm. Objective Plan Apo λ 10x. Analysis was performed using Volocity 6.3 software (PerkinElmer).

CD8$^+$ T Cells Activation And Culture *In Vitro*

Spleens were harvested from 6 to 8-week-old mice. Naïve CD8$^+$ T cells (CD44^{lo} CD62L^{hi}) T cells were purified (>95% purity) by negative selection (Dynabeads^{TM} Untouched^{TM} Mouse CD8 Cells Kit, Invitrogen) from RBC-lysed single-cell suspensions from spleen followed by cell sorting. For stimulation, purified CD8$^+$ T cells were plated at 10^6 cells/ml in 24-well plates precoated with 0,3 mg/mL goat anti-hamster and coated with anti-CD3 (clone 2C11) and anti-CD28 (clone 37.51) (1 µg/mL), as previously described (30, 31). After, 48 h, cells were removed from the TCR signal and re-cultured by diluting 1:2 in media (DMEM (11995-065, Gibco) supplemented with 10% FBS (26140079, Gibco), 1x Penicillin/Streptomycin (15140-122, Gibco), 1x L-Glutamine (25030-081, Gibco), 1x MEM Vitamins (11120-052, Gibco), 1x Sodium Pyruvate (11360-070, Gibco), 1x Essential Amino Acids (M5550, Sigma),1x Non-Essential Amino Acids (11140-050, Gibco), 10 mM HEPES (15630-080, Gibco) and 50 µM β-Mercaptoethanol (M3148, Sigma), containing 200 U/ml final concentration of recombinant murine IL-2 (Peprotech). Every 24 h, cells were diluted 1:2 with fresh media containing IL-2. On day 5, cells were stained with anti-CD25-PE, anti-CD44-FITC, anti-CD62L-APC and anti-CD127-PEcy7 antibodies (Biolegend) for phenotypic analysis and were assessed by flow cytometry.

Coculture of Murine Neutrophils and Activated CD8$^+$ T Cells

C57BL/6 neutrophils ($5x10^5$) recruited to the peritoneum with casein were infected with promastigotes of *L. amazonensis* (cell: parasite-MOI 1:5) by 4h. After that, we added 5 µg/ml anti-PD-1 (CD279, clone RMP1-14, catalog # BE0146, Bioxcell) or anti-PD-L1 (BMS-936559, Bristol-Myers Squibb) or isotype (IgG2a, SouthernBiotech) for 15 min in the culture. Following, activated CD8$^+$ T cells were added ($5x10^5$) to the culture and the media was supplemented with 200 U/ml recombinant murine IL-2 (Peprotech) for 18h. The supernatants were collected and IFN-gamma quantified by specific ELISA using a standard protocol (Peprotech), detection limits are 12 - 3000 pg/ml.

Skin Biopsies and Study Subjects

Punch biopsies (8 mm in diameter) from the border of skin lesions were obtained from 7 untreated patients with cutaneous leishmaniasis (CL) attended at the University Hospital (HUCAM) of Universidade Federal do Espírito Santo, Brazil. The diagnosis of CL was based on clinical criteria including differential diagnosis, skin lesion analysis and parasite identification by microscopy. In addition, all patients in this study tested positive for the PCR/restriction fragment length polymorphism of *L. braziliensis* and reported no prior infections or treatment. The CL group consisted of 5 males and 2 females with illness duration ranging from 30 to 120 days, lesion sizes ranging from 50–200 mm^2 and 1.42± 0.53 lesion per patient. All patients involved in this study progressed to clinical cure after Meglumine antimoniate treatment. Control skin punch biopsy specimens from 12 healthy volunteers living in a non-endemic area with no history of leishmaniasis were also obtained. Biopsy specimens were frozen in OCT compound (Sakura). Sections of 6 µM were obtained longitudinally to expose all skin layers and were placed on poly-L-lysine-coated slides (Star Frost®). Tissues were then fixed in acetone and ethanol and stored at -80°C until use. All participants (patients and healthy volunteers) were seronegative for HIV, HBV and HCV infections, and had no history of chemotherapy, radiotherapy or treatment with immunosuppressive medications within the last 6 months. They provided written informed consent, and study procedures were performed in accordance with the principles of the Declaration of Helsinki. This study was registered with the HUCAM Ethical Committee under the number 735.274.

Immunofluorescence Staining and Analysis of Human Tissues

Briefly, sections were hydrated with PBS, blocked with a 1% bovine serum albumin (BSA- Sigma) solution for 20 min and incubated with the following primary antibodies: anti-elastase (1:400; US1481001; Merk KGaA) or anti-PD-L1 (1:200; clone: ABM4E54; ab210931; Abcam) overnight at 4°C. Afterwards, slides were washed with PBS and incubated with goat anti-rabbit Alexa Fluor 488 (1:400; A11008) or goat anti-mouse Alexa Fluor 568 (1:400; A21124 or A21134) secondary antibodies (Thermo Fischer Scientific) for 1 h at room temperature. Slides were mounted with Fluoroshield Mounting Medium with DAPI (Abcam, ab104139) and analyzed by manually selecting regions of interest (ROI) using the Chromoplex Staining Detection system (Leica Biosystems). Cell and marker frequencies were defined according to the evaluated marker and cell nuclei of each ROI. Slides were imaged with a 20x objective (200× magnification) on a fluorescence microscope (Leica DMi8) with a 710 Metahead (Zeiss) by z-stack tile-scans and counted manually by using computer-assisted image analysis (National Institutes of Health Image Software ImageJ 1.52j; https://imagej.nih.gov/ij/).

DATA ANALYSIS

Results are expressed as mean ± SEM with confidence level $p \leq 0.05$. For lesion development analysis, a two-way ANOVA with Bonferroni post-test was used. For multiple comparisons, a one-way ANOVA followed by Tukey pairing was performed. Cell analyzes were performed using the paired Student's *t* test or Mann-Whitney test (indicated p value in the graph and legend). Skin biopsies were analyzed using Student's t test with Welch

correction or Mann-Whitney test. Data analysis was performed using GraphPad Prism® 8.00 software.

RESULTS

PD-L1 Expression on Neutrophils Upon Interaction With *Leishmania*

Initially, we tested whether casein-recruited peritoneal neutrophils interacted equally with CSFE-labeled promastigotes and amastigotes of *L. amazonensis*. Our results evidenced that neutrophils internalized both parasite stages at similar levels (**Figure 1A**). Next, we analyzed the expression of PD-L1 on the CSFE$^+$ neutrophils, which were the neutrophils that had internalized the parasites. We observed that uninfected neutrophils (medium) constitutively expressed PD-L1 at low levels, while both forms of the parasite induced PD-L1 expression in the infected casein-recruited peritoneal neutrophils (**Figure 1B**). It is important to note that within the neutrophil population, PD-L1 expression in cells that did not internalize the parasites (bystander CSFE$^-$ neutrophils) was not augmented, expressing similar PD-L1 levels to the control (**Figure 1C**). Similarly, we evaluated the parasite interaction with neutrophils isolated from the bone marrow. Amastigotes were internalized

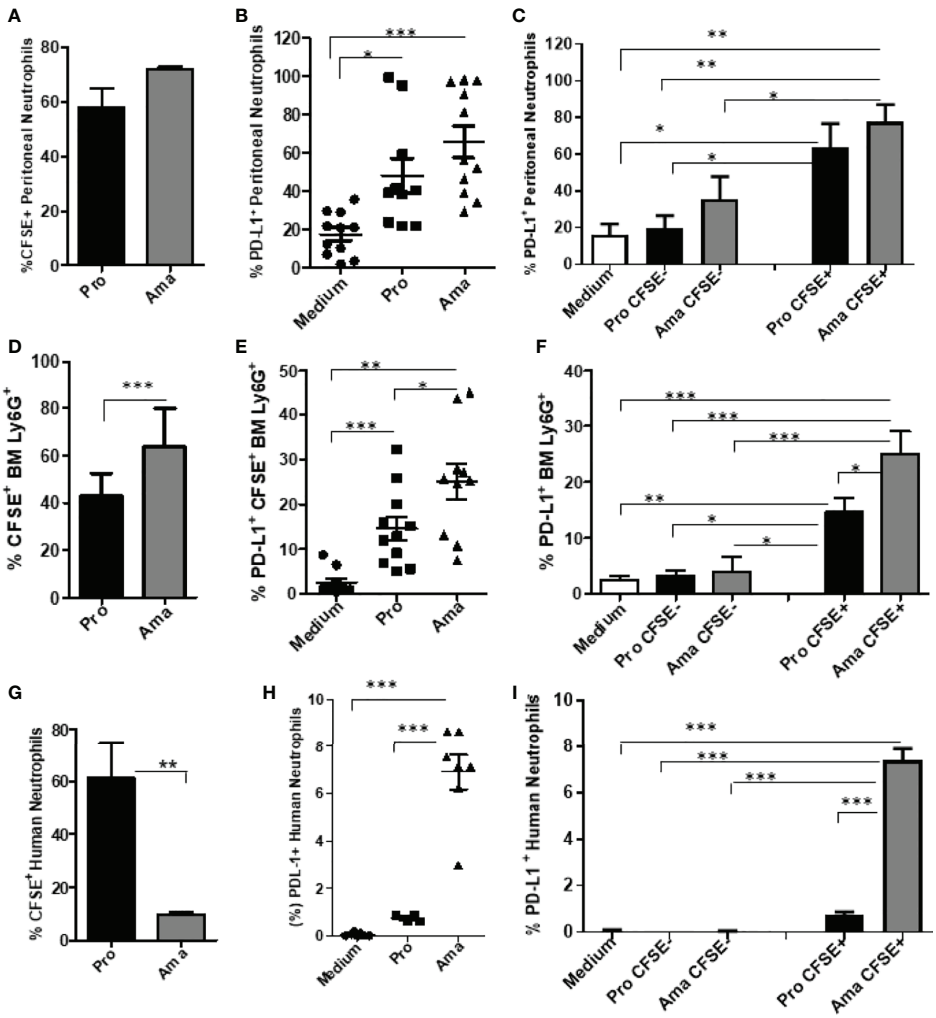

FIGURE 1 | Increased expression of PD-L1 in murine and human neutrophils exposed to challenge with *L. amazonensis*. BALB/c neutrophils (5x10^5) recruited to the peritoneum with casein, or purified from bone marrow, and human neutrophils (5x10^5) from healthy donors were incubated with CFSE-stained promastigotes (Pro) and amastigotes (Ama) of *L. amazonensis* (murine 1:10; human 1:5), for 4 h. Control was performed with neutrophils on medium. Cells were then analyzed by flow cytometry using Ly6G$^+$-Percp (neutrophils), CFSE$^+$ (*L. amazonensis*) and PD-L1$^+$-APC. **(A)** Percentage of peritoneal neutrophils infected with CFSE-labeled parasites. **(B)** Percentage of PD-L1$^+$ peritoneal neutrophils upon interaction with parasites. **(C)** Percentage of PD-L1 expression on CFSE$^-$ (bystander) and CFSE$^+$ casein-recruited neutrophils. **(D)** Percentage of bone marrow (BM) neutrophils infected with CFSE-labeled parasites. **(E)** Percentage of PD-L1$^+$ bone marrow neutrophils upon interaction with parasites. **(F)** Percentage of PD-L1 expression on CFSE$^-$ and CFSE$^+$ bone marrow neutrophils. **(G)** Percentage of human neutrophils infected with CFSE-labeled parasites. **(H)** Percentage of PD-L1$^+$ human neutrophils upon interaction with parasites. **(I)** Percentage of PD-L1 expression on CFSE$^-$ and CFSE$^+$ human neutrophils. Data are mean ± SEM (N=10-11) and human donors (N=7). Each point represents a donor. *p < 0.01, **p < 0.001, ***p < 0.001.

significantly more than promastigotes by these neutrophils (**Figure 1D**). Again, internalization of both parasite forms significantly increased PD-L1 expression in relation to the uninfected control (**Figure 1E**). Interestingly, in the bone marrow neutrophils, amastigotes induced significantly more PD-L1 expression than promastigotes (**Figure 1E**). Like the casein-recruited neutrophils, constitutive PD-L1 expression of bystander bone marrow neutrophils, was not modulated by the presence of either form of the parasite (**Figure 1F**). Comparing the levels of PD-L1 expression of the peritoneal and bone marrow neutrophils, our results demonstrated that PD-L1 expression was higher in peritoneal neutrophils, independent of the parasite infection (**Figure S1**), suggesting that the inflamed milieu or the maturation stage of the neutrophils could influence PD-L1 expression.

We next tested the interaction of human neutrophils with promastigotes and amastigotes of *L. amazonensis* (MOI 1:5). Unlike mouse neutrophils, human neutrophils internalized promastigotes more than the amastigotes (**Figure 1G**). However, PD-L1 induction occurred similarly to murine neutrophils, being significantly more expressed after interaction with amastigotes (**Figure 1H**). Interestingly, the PD-L1 constitutive expression (medium) in human neutrophils (**Figure 1I**) was lower than in mouse peritoneal (**Figure 1C**) and bone marrow (**Figure 1F**) neutrophils. Surprisingly, a reduction in PD-L1 expression was observed after human neutrophil infection with promastigotes and amastigotes at a higher MOI, although maintaining the same pattern of higher PD-L1 expression induced by amastigotes in comparison to promastigotes (**Figure S2**). Together, these results suggest that PD-L1 expression in neutrophils is modulated upon parasite interaction.

PD-L1 Expression in Cells From Ear Lesions of BALB/c Mice Infected With *L. amazonensis*

Following our observations of neutrophils *in vitro*, we assessed whether cells present at the lesion site *in vivo* would also express PD-L1 (**Figure S10**). As the peak of neutrophil infiltration has been reported to occur at 12 h after *Leishmania* infection in mice (29), we started by analyzing PD-L1 expression at this time-point. Our data shows increase in the percentage of Ly6G$^+$ cells in infected group, but, while there is an increase in the number of neutrophils, it was not statistically different from the other groups (**Figures 2A–C**). Although the number of PD-L1$^+$Ly6G$^+$ increased in the infected group (**Figure 2F**), no differences were observed in the frequency of PD-L1$^+$Ly6G$^+$ or in the MFI between the groups (**Figures 2D, E, G**). Evaluating the same parameters after 18 h post infection, although the frequency of CD11b$^+$ cells was a little higher in the infected ear, it was not significantly different from the naïve (non-infected) control; a similar observation was noted regarding the numbers of CD11b$^+$ cells in naïve and infected mouse ears (**Figures S3A, B** and **S4A**). In addition, no differences were observed between the ears of naïve and infected mice in the frequency and number of Ly6G$^+$CD11b$^+$ cells (**Figures S3C, D** and **S4B**) and the expression of PD-L1 in the Ly6G$^+$ cells (**Figures S3E–H**).

A second wave of neutrophils has been described to migrate to the infection site after 15 days (29), therefore we also evaluated PD-L1 expression at this time-point. Our results showed no statistical difference in the frequency of neutrophils between naïve and *Leishmania*-infected ear lesions (**Figure 3A**), however, a significant increase in the number of neutrophils was observed in infected mice compared with the naïve control (**Figure 3B**). Concomitantly, increased PD-L1 expression was detected in infected mice (**Figures 3C, D, F**) as well as an increased number of PD-L1-expressing neutrophils (**Figure 3E**).

The analysis of cells from infected animals in the chronic phase, after 60 days of infection, displayed an increase in the neutrophil population (**Figures 4A–C** and **S5**). The expression of PD-L1 on neutrophils from 60-day lesions followed the same pattern with increased expression of PD-L1 in the cells from the infected animals (**Figures 4D–G**). These data show that as the lesion progresses, there is an increase in the population of neutrophils that express PD-L1, and this strengthens our hypothesis that a constant *Leishmania* stimulus promotes this induction.

Intravital Images of Neutrophils Expressing PD-L1 in Infected Lesions but Not in Circulation

To validate our findings, we evaluated PD-L1 expression in neutrophils present in the lesions of *L. amazonensis*-infected mice directly *in vivo*. Initially, we analyzed the animals within 1 h of infection, since it is at this time that neutrophils begin the process of migrating to the infected site (32), in addition to the chronic lesion (60 days post-infection). Some migrating neutrophils in the tissue were expressing PD-L1, but interestingly, no expression was observed in the circulating neutrophils (**Figure S11**, **Movies S1**, **S2**). The absence of PD-L1 expression was observed in naïve and in saline-injected control mice (**Figures S11A, B**). After 1h post-infection, some migrating neutrophils in the tissue were expressing PD-L1, but interestingly, no expression was observed in the circulating neutrophils (**Figure S11C**; **Movies S1** and **S2**). Importantly, chronic lesions showed a high presence of neutrophils expressing PD-L1 (**Figure S11D**). In fact, the presence of PD-L1-expressing neutrophils, at times, formed a mass (**Movie S3**) that we could image only after cutting the lesion tissue. After this step, we could see the circulation contralateral to the injury (**Movie S4**). Interestingly, this contralateral circulation did not have circulating neutrophils expressing PD-L1. This observation is important because it demonstrates that the infection environment is conducive to the induction of the suppressive neutrophil without affecting the circulating neutrophils.

PD-L1-Expressing Neutrophils in the Draining Lymph Nodes of Mice

To better map PD-L1-expressing neutrophils we investigated these cells in the lymph nodes that drain the footpad lesions caused by *L. amazonensis*. Our results show that the neutrophil population was increased in the lymph nodes of the infected mice at 60 days (**Figures 5A–C**). The frequency and numbers of PD-L1-expressing neutrophils was also significantly increased (**Figures 5D–F**), however, the median intensity of fluorescence (MFI) was similar to the naïve control (**Figure 5G**). This data reveals that the neutrophils not only express PD-L1 at the

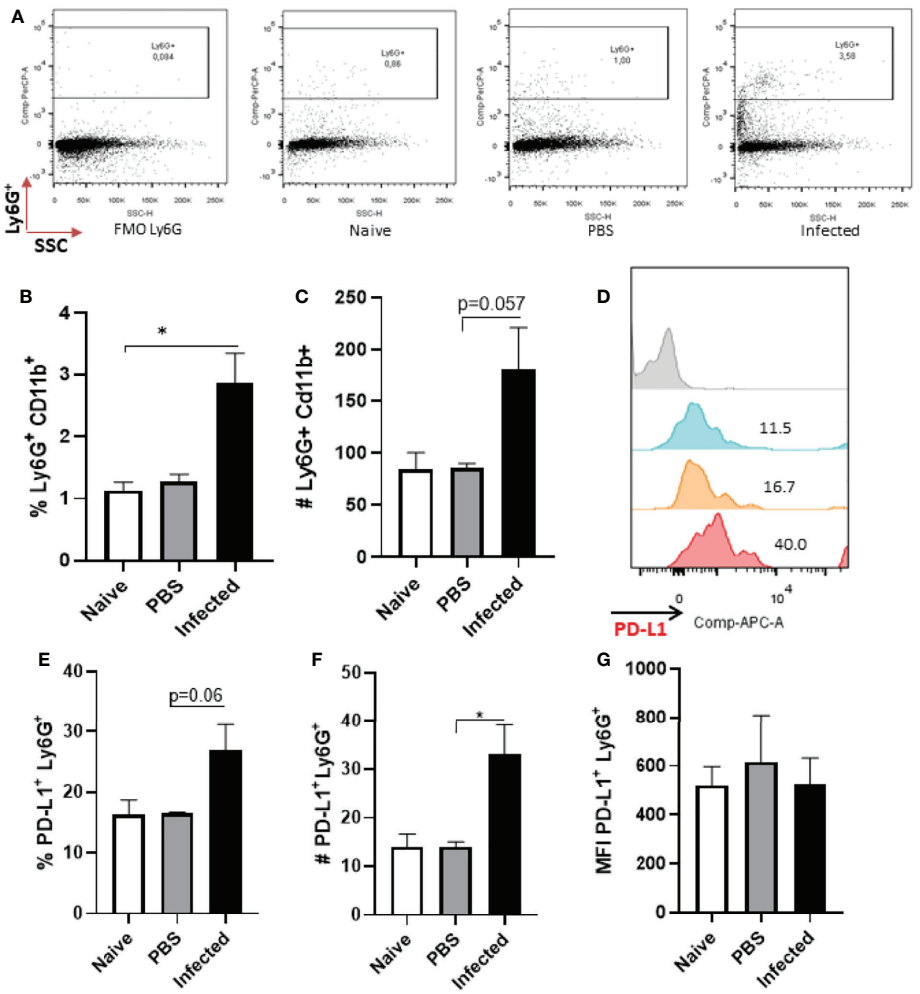

FIGURE 2 | Analysis of murine ear neutrophils after 12h of infection. Cells were collected from *L. amazonensis*-infected ears after 12h then submitted to flow cytometry. Controls were performed with uninfected (naïve) and PBS injected mice. **(A)** Dot plot showing Ly6G$^+$ cells (Ly6G-PerCP, SSC). **(B)** Percentage of Ly6G$^+$ CD11b$^+$ cells. **(C)** Number of Ly6G$^+$ CD11b$^+$ cells, p=0.057 (Mann-Whitney). **(D)** Histogram of PD-L1 expression. Grey = Fluorescence minus one control (FMO) PD-L1, Blue = Naïve, Orange = PBS and Red = Infected. **(E)** Percentage of PD-L1$^+$ Ly6G$^+$ cells, p=0,06 (Mann-Whitney). **(F)** Number of PD-L1$^+$ Ly6G$^+$ cells, p=0.06. **(G)** MFI of PD-L1$^+$ Ly6G$^+$. Data are mean ± SEM from cells of individual mice (N = 4-7 mice/group). *p < value 0,0323.

infection site, but these cells, expressing the ligand, also have the ability to be drained to the lymph nodes.

Neutrophils Expressing PD-L1 Suppress IFN-γ Production by T Cell

First, the expression of PD-L1 was evaluated in infected C57BL6 peritoneal neutrophils with *L. amazonensis* promastigotes (MOI 1:1; 1:5; 1:10). We observed 50% of infected neutrophils in 1:1 and 90% in 1:5 and 1:10 MOIs (**Figure 6A**). The expression of PD-L1 was not modulated by the infection rate, and similarly to the BALB/c neutrophils, bystander CSFE$^-$ neutrophils expressed significantly less PD-L1 (**Figures 6B, C**). Following, the capacity of PD-L1$^+$-neutrophils to inhibit the production of IFN-γ by CD8$^+$ T was evaluated by co-culturing infected neutrophils with activated CD8$^+$ T cells (**Figure 6D**). Characterization of isolated CD8$^+$ T cells is shown in **Figure S9**. We observed a significant reduction in the IFN-γ production by CD8$^+$ T cells co-cultured with infected neutrophil (1:5) compared to the non-infected neutrophils (Neu). Importantly, addition of anti-PD-L1 or anti-PD-1 to the co-culture restored the production of IFN-γ. Moreover, the isotype control was unable to reverse IFN-γ inhibition mediated by infected neutrophils. This result demonstrated that inhibition of IFN-γ production is dependent of PD-L1/PD-1 (**Figure 6D**).

PD-L1-Expressing of Human Neutrophil *In Vitro* and in the Lesions Caused by *Leishmania braziliensis*

Finally, we evaluated the expression of PD-L1 in human neutrophils after *Leishmania braziliensis* infection. Differently from *L. amazonensis*, our results evidenced that independently of

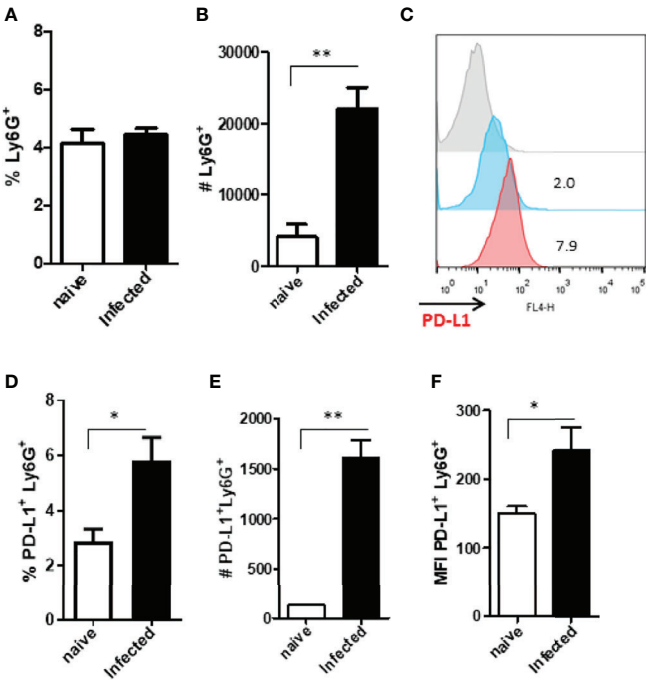

FIGURE 3 | Analysis of murine ear neutrophils after 15 days of infection. Cells were collected from *L. amazonensis*-infected ears after 15 days then submitted to flow cytometry. Controls were performed with uninfected mice (naïve). **(A)** Percentage of Ly6G$^+$ cells. **(B)** Number of Ly6G$^+$ cells. **(C)** Histogram of PD-L1 expression. Grey = Fluorescence minus one control (FMO) PD-L1$^+$, Blue = Naïve and Red = Infected. **(D)** Percentage of PD-L1$^+$ Ly6G$^+$ cells. **(E)** Number of PD-L1$^+$ Ly6G$^+$ cells. **(F)** MFI of PD-L1$^+$ Ly6G$^+$. Data are mean ± SEM from cells of individual mice (N = 4-5/group). *p < 0.03, **p < 0.005.

the MOI, neutrophils internalized both parasite stages of *L. braziliensis* at similar levels (**Figure 7A**). However, PD-L1 expression was higher in promastigotes infected-neutrophils and likewise *L. amazonensis*, PD-L1 was not expressed in the bystander neutrophils (**Figures 7B, C**).

We also investigated the PD-L1 expression on neutrophils from human cutaneous leishmaniasis biopsies obtained from untreated patients. It is already been demonstrated that cutaneous leishmaniasis lesions present hyperplasia with a dense inflammatory cellular infiltrate involving the dermal-epidermal junction, consisting mainly of lymphocytes, macrophages, neutrophils and plasma cells (33–38). Thus, we evaluated whether neutrophils in the lesions expressed PD-L1, which could directly impact on the skin immune balance during infection. Interestingly, lesional analysis revealed the expression of PD-L1 on neutrophils, that were respectively 7.44 and 3.77-fold higher than healthy controls (**Figures 8A–C** and **S6**), suggesting that neutrophils may have a role in human injuries caused by *L. braziliensis*, which still needs to be assessed.

DISCUSSION

In the present work we investigated the expression of PD-L1 in human and murine neutrophils, showing that upon interaction with promastigotes or amastigotes of *L. amazonensis*, these host cells express PD-L1, a molecule involved in T cell exhaustion. Interestingly, a higher number of murine bone marrow and human peripheral neutrophils expressing PD-L1 was evidenced after interaction with amastigotes than with promastigotes. Although, human neutrophils were less infected by *L. amazonensis* amastigotes than the murine neutrophils, this parasite stage induced higher numbers cells expressing PD-L1. However, these effects were not observed in casein-recruited murine neutrophils, where similar numbers of PD-L1$^+$ neutrophils were stimulated by both parasite developmental stages, and which did not display any differences in neutrophil infection between the two parasite forms studied. A higher number of casein-recruited neutrophils expressed PD-L1 than bone marrow neutrophils upon interaction with both parasite stages. This result could be due to the inflammation induced by casein, since it has been shown that inflammation could contribute to a higher PD-L1 expression (16). The same lack of inflammatory stimuli could explain the low frequency of human PD-L1$^+$ neutrophils in comparison with the murine neutrophils, but it should be noted that the frequency of PD-L1-expressing-neutrophils increased 8 times in relation to control (medium) after only 4h of interaction with the amastigotes. This high expression of PD-L1 in amastigote-infected neutrophils may be the consequence of its increased survival, consistent with the study highlighting the resistance of *L. amazonensis* amastigotes against microbicidal mechanisms of neutrophils, such as the oxidative burst (39).

Regardless of the source of neutrophils, the expression of PD-L1 was not affected in bystander cells irrespective of the presence

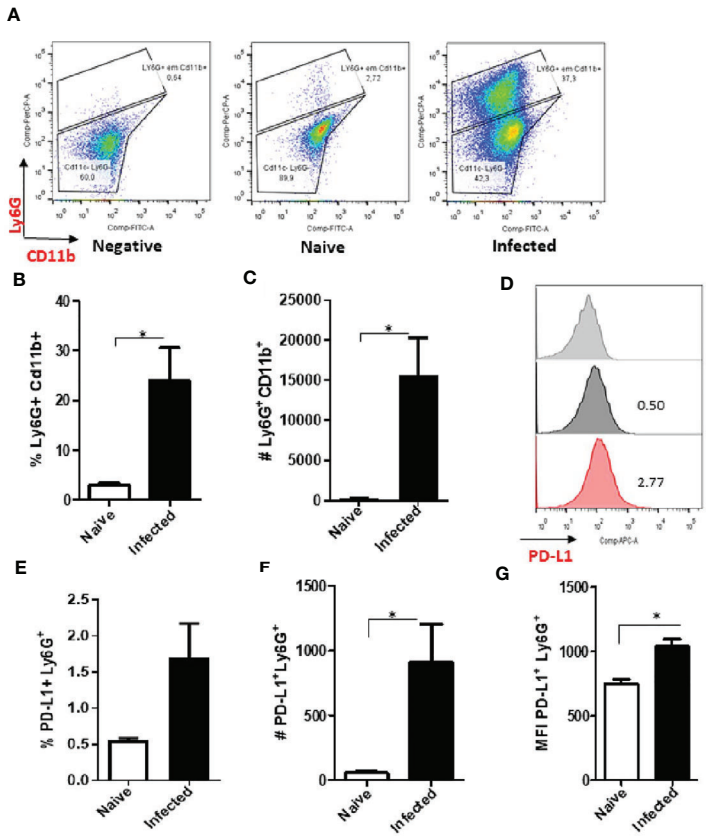

FIGURE 4 | Increase of PD-L1^{+} Ly6G^{+} cells in *L. amazonensis*-infected ear lesions. Cells were collected from *L. amazonensis*-infected mouse ears after around 50 days. Controls were performed with uninfected mice (naïve). **(A)** Dot plot showing Ly6G^{+} CD11b^{+} cells (Ly6G-PerCP, CD11b-FITC). **(B)** Percentage of Ly6G^{+} CD11b^{+} cells. **(C)** Number of Ly6G^{+} CD11b^{+} cells. **(D)** Histogram of PD-L1 expression. Grey = Fluorescence minus one control (FMO) for PD-L1, Dark grey = Naïve and Red = Infected ear cells. **(E)** Percentage of PD-L1^{+} Ly6G^{+} cells, p=0.057. **(F)** Number of PD-L1^{+} Ly6G^{+} cells. **(G)** MFI of PD-L1^{+} Ly6G^{+}. Data are mean ± SEM from two independent experiments (7-8 mice/group). *p < 0.02.

of parasite forms in the co-culture. Taken together, this suggests that upon infection of neutrophils, the parasite induces this suppression marker in the host cell. Expression of PD-L1 has been described in monocytes from a patient presenting diffuse cutaneous leishmaniasis (40), and only in low-density neutrophils (normal-density neutrophils did not expressed PD-L1) from human visceral leishmaniasis patients (12), but, to the best of the authors' knowledge, this is the first description of PD-L1 expression upon *in vitro* interaction with *Leishmania*. Interestingly, similar to our results, it was shown that incubation of neutrophils *ex vivo* with LPS for 6 h also induced PD-L1 expression (41).

A swarm of neutrophils are recruited to the *Leishmania* infection site and the presence of these cells has been reported in chronic lesions as well (32, 42–45). Thus, we investigated PD-L1 expression in neutrophils from a *L. amazonensis* cutaneous lesion in mouse ears at both these early and late time-points. Remarkably, although PD-L1^{+} neutrophils could already be observed after 12h or 18 h post-infection, and a significant number of PD-L1^{+} neutrophils was detected after 15 days post-infection, the number and frequency of which decreased a little in 2-month chronic lesions. However, the mean fluorescence intensity greatly enhanced (around 4 times) in the chronic lesion, compared to the lesion at 15 days. It was recently demonstrated that in the beginning of the infection (1h-24h) (46), resident macrophages are the predominant infected cells. In the absence of infection, neutrophils are not stimulated to express PD-L1 as observed in the frequency in 12 or 18 hours post *in vivo* infection. In the chronic phase the combination of infected neutrophils and the inflammatory cytokines can prime the express of PD-L1 as observed in 15, 30 and 60 days post infection.

Next, we sought to image the environment of an *L. amazonensis* infection *in vivo*, and our results showed that as the infection progressed, there was an accumulation of neutrophils at the site of infection, and some of them expressing PD-L1. The presence of neutrophils is in agreement with reports describing these cells in chronic lesions (60 days post infection) of animals naturally or experimentally infected with *Leishmania* (42–44). Importantly, PD-L1 expression was not seen in neutrophils circulating in vessels close to the infected site, as observed by intravital microscopy. Instead, in human

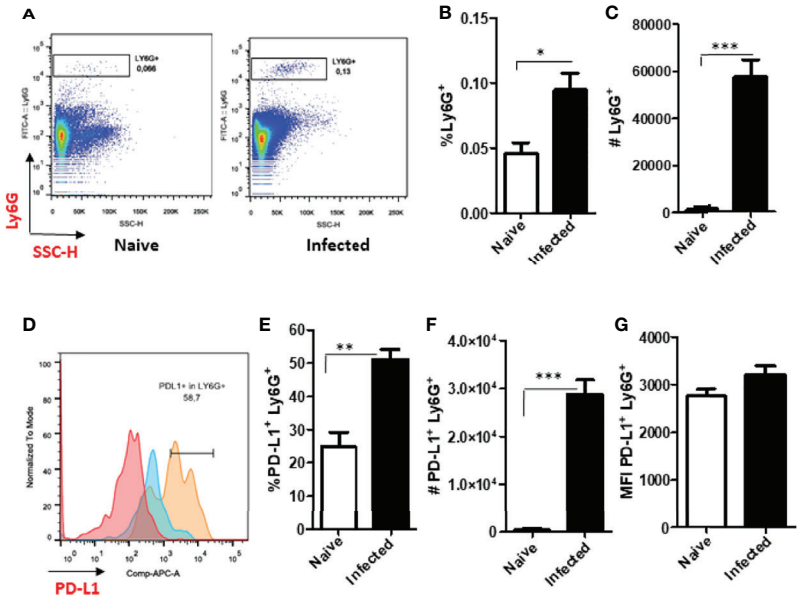

FIGURE 5 | Increased expression of Ly6G$^+$ and PD-L1$^+$ in the draining lymph nodes of infected BALB/c mice. Mice were infected in the footpad with *L. amazonensis* promastigotes (2×10^6). After approximately 60 days, the draining lymph nodes were collected, macerated and the cells analyzed by flow cytometry. Controls were performed with uninfected mice (naïve). **(A)** Dot plot showing Ly6G$^+$ cells (Ly6G-FITC x SSC-H). **(B)** Percentage of Ly6G$^+$ cells. **(C)** Number of Ly6G$^+$ cells. **(D)** Histogram of PD-L1 (PD-L1-APC) expression. Red = Fluorescence minus one control (FMO) PD-L1; Blue = Naïve lymph nodes; Orange = Infected lymph nodes. **(E)** Percentage of PD-L1$^+$ Ly6G$^+$ cells. **(F)** Number of PD-L1$^+$ Ly6G$^+$ cells. **(G)** MFI of PD-L1$^+$Ly6G$^+$. Data are mean ± SEM of individual mice (5 mice/group) shown as a representative experiment of three producing the same result profile. *p < 0.01, **p < 0.001, ***p < 0.0001.

diffuse cutaneous leishmaniasis and in visceral leishmaniasis PD-L1-expressing cells have been detected in the blood circulation (12, 40). Similarly, higher levels of blood PD-L1$^+$ neutrophils have been reported in tuberculosis and HIV-1-infected patients (7, 47), in patients with cancer (48), severe sepsis (49), while in rheumatoid disease, patients have neutrophils expressing PD-L1 in the synovial fluid, which can be related to the severity of the disease (50).

Another aspect identified in our study was the presence of PD-L1-expressing neutrophils in the draining lymph nodes of *L. amazonensis* infected mice. Upon analyzing the lymph nodes draining the chronic lesion we evidenced an increased number of neutrophils in this organ, and half of this population was expressing PD-L1. It has been reported that neutrophils have the ability to migrate to the lymph nodes, transporting and presenting antigens to T cells and inducing the activation and expansion of CD4$^+$ T cells (51–54). We recently described in the draining lymph nodes of a non-healing *L. amazonensis* infection in BALB/c mice that both, CD4$^+$ and CD8$^+$ T cells expressed PD-1, and dendritic cells PD-L1 (28). Importantly, treatment of the *L. amazonensis*-infected mice with anti-PD-1 and anti-PD-L1 antibodies significantly increased IFN-γ production by T cells and decreased the parasite load (28). Our results in *Leishmania*-infected mice confirmed the presence of neutrophils in the lesion site in the first and second waves of neutrophil infiltration as well as in the chronic phase, and we perceived a relationship between PD-L1 expression and the cutaneous disease progression in the mouse.

It has been shown that neutrophil depletion with 1A8 monoclonal antibody enhanced T cell production of IFN-γ, suggesting a suppressor function of neutrophis (29). Here, we show the direct effect of *Leishmania* in the induction of PD-L1 on neutrophils, which interacting with CD8$^+$ T cells, reduce IFN-γ production. Here, we demonstrated PD-L1 expression was detected in the skin of dogs severely infected with *L. infantum* (54), and in the spleen and in B cells of dogs infected with *L. infantum* (55–57). Several reports have identified the presence of neutrophils in chronic inflammatory infiltrate of patients with localized cutaneous (58, 59), diffuse cutaneous (60) and mucocutaneous leishmaniasis (61, 62).

Likewise to *L. amazonensis* induction of PD-L1 in human neutrophils, *L. braziliensis* infection in these cells shares the same capacity. Both promastigotes and amastigotes induced PD-L1 expression in neutrophils indicating an ability of this parasite to this phenotype. Finally, we analyzed lesions from patients with cutaneous leishmaniasis caused by *L. braziliensis*, evidencing an enhanced frequency of neutrophils expressing PD-L1 than in healthy controls. Similar increased PD-L1 transcripts have been reported in the lesions of patients infected with *L. braziliensis* (62). Our study demonstrated that neutrophils contributed to PD-L1 expression in the *Leishmania* lesion site.

Recently, it has been demonstrated by RNA-seq and immunohistochemistry that PD-1 and PD-L1 were highly up regulated in *L. braziliensis* skin lesion (63). Moreover, indicating an exhaustion process, anti-PD-L1/PD-L2 added to cultures of CD4$^+$ and CD8$^+$ T cells from cutaneous leishmaniasis patients

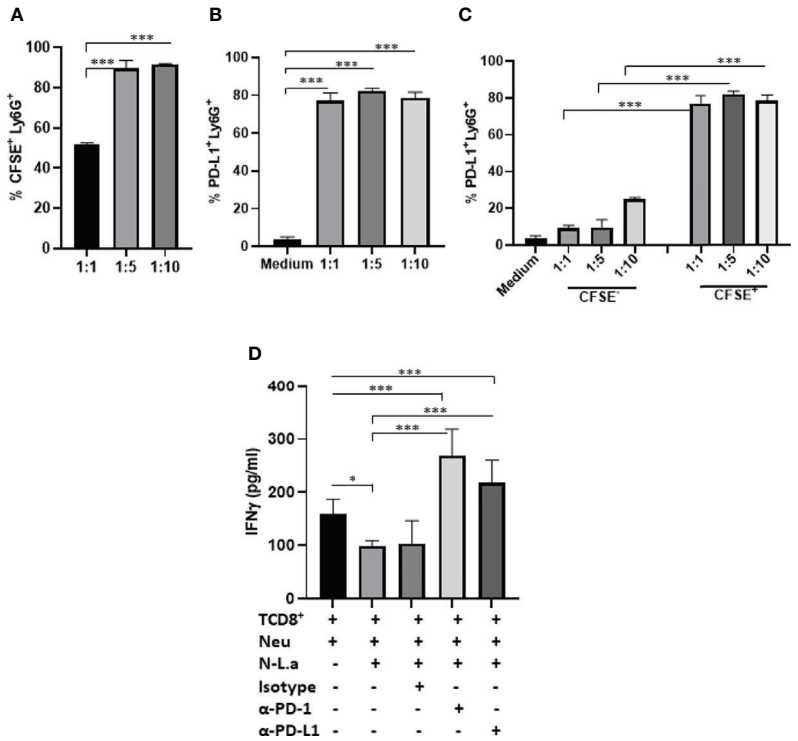

FIGURE 6 | Coculture of murine neutrophils exposed to *L. amazonensis* with CD8$^+$ T activated cells. C57BL/6 neutrophils (5x10^5) recruited to the peritoneum with casein were incubated with CFSE-stained promastigotes (Pro) of *L. amazonensis* (1:1, 1:5, 1:10), for 4 h. Control performed with neutrophils on medium. Cells were then analyzed by flow cytometry using Ly6G$^+$-Percp (neutrophils), CFSE$^+$ (*L. amazonensis*) and PD-L1$^+$-APC. **(A)** Percentage of CFSE$^+$ Ly6G$^+$ cells. **(B)** Percentage of PD-L1$^+$ Ly6G+ cells. **(C)** Percentage of PD-L1 expression on CFSE$^-$ (bystander) and CFSE$^+$ cells. **(D)** Coculture of murine neutrophils (Neu) infected or not with promastigotes of *L. amazonensis* (Leish) with CD8$^+$ T effectors cells. The coculture was treated or not with anti-PD-1 or anti-PD-L1 or isotype control for 18h. IFN-γ was analyzed in the culture supernatant by ELISA. Data are mean ± SEM. **(A–C)** N=3-4 and **(D)** N=7. *p=0.049, ***p < 0.001.

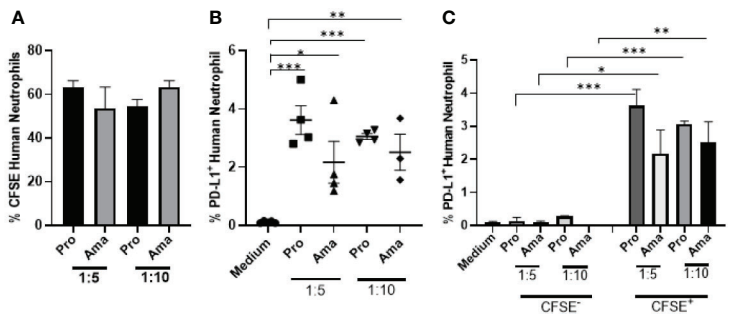

FIGURE 7 | Increased expression of PD-L1 in human neutrophils exposed to *L. braziliensis*. Human neutrophils (5x10^5) from healthy donors were incubated with CFSE-stained promastigotes (Pro) and amastigotes (Ama) of *L. braziliensis* (1:5 and 1:10), for 4 h. Control performed with neutrophils on medium. Cells were then analyzed by flow cytometry. **(A)** Percentage of neutrophils infected with CFSE-labeled parasites. **(B)** Percentage of PD-L1$^+$ neutrophils upon interaction with parasites. **(C)** Percentage of PD-L1 expression on CFSE$^-$ (bystander) and CFSE$^+$ neutrophils. Data are mean ± SEM (N=4-5). *p < 0.0303, **p < 0.0047 ***p < 0.0001.

increased the response to *L. braziliensis* antigen, and restored their IFN-γ response (63).

In summary, we show for the first time that *L. amazonensis* infection induces the expression of PD-L1 in neutrophils and that this expression increases with disease progression associated to chronic development of the disease. The induction of PD-L1 in neutrophils could favor the suppressive milieu that is important for the persistence of the parasite in human and experimental infections. Our finding is relevant because it opens new possibilities for therapeutic targets, and for understanding the local environment of the infection that may favor *Leishmania* growth.

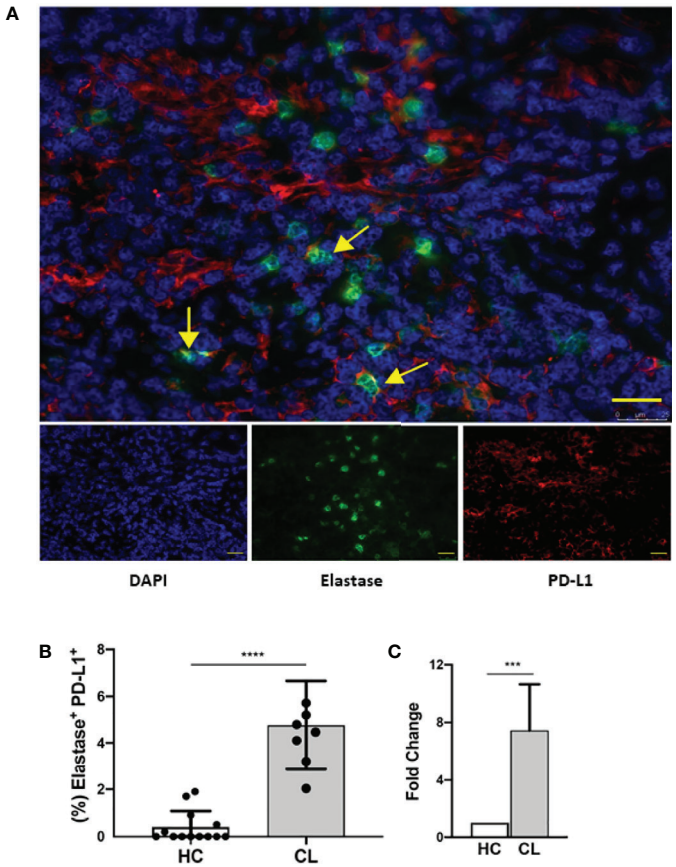

FIGURE 8 | Human lesion neutrophils present a conspicuous expression of PD-L1. Healthy human skin and human cutaneous leishmaniasis skin lesions were stained with anti-elastase (green), anti-PD-L1 (red) and counter-stained with DAPI (blue). **(A)** Representative immunofluorescence staining of a cutaneous leishmaniasis lesion. Yellow arrows indicate anti-PD-L1 and anti-elastase double-stained cells. Bars = 50 μm. **(B)** Frequency of elastase-positive PD-L1^{+} cells of cumulative data of PD-L1 in neutrophils in healthy control skin (HC, N = 12) and in cutaneous leishmaniasis skin lesions (CL, N = 7). **(C)** Frequencies of double-stained neutrophils were normalized and data are expressed as fold over the control. Data shown as median with 95% confidence. The p values were calculated using Mann-Whitney test. ***$p < 0.001$.

CONCLUSION

The present study demonstrated that both amastigotes and promastigotes of *L. amazonensis* and *L. braziliensis* are capable of inducing the expression of PD-L1 in murine and human neutrophils. It was also observed that, in a murine model, the expression is not present in the first wave of neutrophil infiltration, however, the expression increases in the lesion and in the draining lymph nodes as the disease progress. Importantly, we demonstrated the capacity of *Leishmania*-infected neutrophils to inhibit IFN-γ production by effector TCD8^{+} cells, which was reversed by anti-PD-L1. Overall, our findings strongly suggest that PD-L1 expressing neutrophils could participate in the modulation of the immune response, favoring *Leishmania* survival and persistence.

DATA AVAILABILITY STATEMENT

The raw data supporting the conclusions of this article will be made available by the authors, without undue reservation.

ETHICS STATEMENT

The studies involving human participants were reviewed and approved by the HUCAM Ethical Committee and this study was registered under the number 735.274. The patients/participants provided their written informed consent to participate in this study. The animal study was reviewed and approved by Committee for Animal Use of the Universidade Federal do Rio de Janeiro (Permit Number: 161/18).

AUTHOR CONTRIBUTIONS

AF-M: Conceived and designed the analysis, data collection, data analysis and interpretation, scientific discussion, wrote and revised the manuscript. PL-G: Data collection. MA: Data collection, data analysis and interpretation. RG Data collection, data analysis, interpretation and critical revision of the article. LC: Data collection, data analysis, interpretation and critical

revision of the article. GM: Scientific discussion. DG: Scientific discussion and critical revision of the article and funding. ES: Conceived and designed the analysis, scientific discussion, wrote and critical revised the manuscript and funding. HM: Conceived and designed the analysis, scientific discussion, wrote and critically revised the manuscript and funding. All authors contributed to the article and approved the submitted version.

ACKNOWLEDGMENTS

We would like to thank the kind donations by Dr. Milton A.P. Oliveira (Universidade Federal de Goiás, GO, Brazil), Dr. André M. Vale (Universidade Federal do Rio de Janeiro, RJ, Brazil) and Bristol-Myers Squibb (Nova York, NY, EUA), respectively of *L. braziliensis* (MHOM/BR/2005/RPL5) strain, anti-IgG2A and anti-PD-L1. The work was supported by the following Brazilian agencies: Fundação de Amparo à Pesquisa do Estado do Rio de Janeiro (FAPERJ); Programa Jovem Cientista do Nosso Estado (FAPERJ); Productivity Fellowships from Conselho Nacional de Desenvolvimento Científico e Tecnológico (CNPq) and Coordenação de Aperfeiçoamento de Pessoal de Nível Superior (CAPES) Finance code 001. The funders had no role in the study design, data collection, analysis, decision to publish or preparation of the manuscript.

SUPPLEMENTARY MATERIAL

The Supplementary Material for this article can be found online at: https://www.frontiersin.org/articles/10.3389/fimmu.2021.598943/full#supplementary-material

Supplementary Figure 1 | Comparison of PD-L1 expression in murine neutrophils from bone marrow and peritonium. Neutrophils recruited to the peritoneum with casein (Per) for 3 h or isolated from the bone marrow (BM) of mice. Cells were infected (1:10) with promastigotes (Pro) or amastigotes (Ama) of *L. amazonensis* for 4 h. Controls were performed with the same cells without infection (control). Data shown percentage of PD-L1+ cells are mean + SEM (N = 9-11). **p < 0.03, ***p < 0.0001.

Supplementary Figure 2 | PD-L1 expression in human neutrophils infected with *L. amazonensis*. Human neutrophils (5x105) from healthy donors were incubated with CFSE-stained promastigotes (Pro) and amastigotes (Ama) of *L. amazonensis* (1:5 and 1:10), for 4 h. Control performed with neutrophils on medium. Cells were then analyzed by flow cytometry. Data shown as percentage of PD-L1 expression on human neutrophils, mean ± SEM (N= 5-6). ***p < 0.0001.

Supplementary Figure 3 | Analysis of murine ear neutrophils after 18 h of infection. Cells were collected from *L. amazonensis*-infected ears after 18 h then submitted to flow cytometry. Controls were performed with uninfected mice (naïve). **(A)** Percentage of CD11b$^+$ cells. **(B)** Number of CD11b$^+$ cells. **(C)** Percentage of Ly6G$^+$ CD11b$^+$ cells. **(D)** Number of Ly6G$^+$ CD11b$^+$ cells. **(E)** Histogram of PD-L1 expression. Grey = Fluorescence minus one control (FMO) PD-L1, Blue = Naïve and Red = Infected. **(F)** Percentage of PD-L1$^+$ Ly6G$^+$ cells. **(G)** Number of PD-L1$^+$ Ly6G$^+$ cells, p=0.055. **(H)** MFI of PD-L1$^+$ Ly6G$^+$. Data are mean ± SEM from cells of individual mice (N = 4 mice/group).

Supplementary Figure 4 | Dot plots of murine cells from lesions infected with *L. amazonensis*. Cells were collected from *L. amazonensis*-infected ears after 18 h. Controls were performed with uninfected mice (naïve) and FMO for **(A)** CD11b and **(B)** Ly6G (negative). **(A)** Dot plot of CD11b$^+$ cells. **(B)** Dot plot of Ly6G$^+$ CD11b$^+$ cells. Data of individual mice (4 mice/group).

Supplementary Figure 5 | Expression of PD-L1+ Ly6G+ cells in *L. amazonensis*-infected lesions. Cells were collected from *L. amazonensis*-infected ears after approximately 60 days. Controls were performed with uninfected mice (naïve). **(A)** Dot plot showing CD11b$^+$ cells (PE-CD11b x SSC) on FMO for CD11b (negative), naïve and infected mice. **(B)** Percentage of CD11b$^+$ cells. **(C)** Number of CD11b$^+$ cells. **(D)** Dot plot showing PD-L1$^+$ Ly6G$^+$ and PD-L1$^+$ Ly6G$^-$ gates (PD-L1-APC x Ly6G-PerCP) on FMO Ly6G and PD-L1, naïve and infected mice. **p<0.008 Data are mean ± SEM of individual mice (4-5 mice/group) and are representative of three experiments producing the same result profile.

Supplementary Figure 6 | Analyses of lesion neutrophils present a conspicuous expression of PD-L1. PD-L1 expression in neutrophils from healthy skin (HC, N = 8) and cutaneous leishmaniasis lesions (CL, N = 9). **(A)** Neutrophils are a percentage of nucleated cells. **(B)** Percentage PD-L1$^+$ neutrophils. The P values were calculated using Student's *t* test with Mann-Whitney test. ***p < 0.001.

Supplementary Figure 7 | Gating strategy of CFSE+ neutrophils expressing PD-L1. **(A)** Neutrophils FSC x SSC. **(B)** Single cells - FSC-A x FSC-H. **(C)** CFSE$^+$ and CFSE$^-$ (CFSE x SSC). **(D)** Histogram of PD-L1 expression, Green = FMO (negative), Red= isotype, Orange = control not infected, Blue = infected.

Supplementary Figure 8 | Gating strategy of neutrophils expressing PD-L1 on the mice ear and on draining lymph nodes. Ear cells after processing were analyzed as follows: **(A)** Cells FSC x SSC. **(B)** Single cells - FSC-A x FSC-H. **(C)** CD45$^+$ (APC-cy7 x FSC-H). **(D)** CD11b$^+$ and Ly6G$^+$ (FITC x Percp). **(E)** Histogram of PD-L1 expression, Grey = FMO (negative), Black= naïve control (not infected), Red = infected. Draining lymph node cells were analyzed as follows: **(F)** Cells FSC x SSC. **(G)** Single cells - FSC-A x FSC-H. **(H)** CD11b$^+$ (Pe-cy7 x SSC-A). **(I)** Ly6G$^+$ CD11b$^+$ (FITC x SSC-H). **(J)** Histogram of PD-L1 expression, Red = FMO (negative), Blue= naïve control (not infected), Orange = infected.

Supplementary Figure 9 | Phenotype of CD8$^+$ T cells differentiated in vitro. Spleen cells of C57BL/6 mice were processed, and CD8$^+$ T cells purified by negative selection and sorted. **(A)** Pre-sort and Pos-sort SSC x CD8$^+$, CD62L$^+$ x CD44$^+$. **(B)** On day 5, cells were stained with CD25$^+$ x CD44$^+$, CD127$^+$ x CD44$^+$ and CD62L$^+$ x CD44$^+$.

Supplementary Figure 10 | Lesion development in *L. amazonensis*-infected mice. Mice were infected in the ear with *L. amazonensis* stationary-phase promastigotes ($2x10^6$). Ear thickness was measured weekly using a thickness gauge.

Supplementary Figure 11 | PD-L1-expressing neutrophils in infected ear lesions. BALB/c mice infected in the ear with *L. amazonensis* were injected with anti-PD-L1-APC and anti-Ly6G-FITC antibodies and imaged by intravital microscopy. Controls were performed with mice injected with PBS and non-infected (naïve) mice. Arrows show neutrophils expressing PD-L1. **(A)** Naïve mouse. **(B)** Control mouse injected with PBS. **(C)** Mouse infected for 1 h. **(D)** Mouse with chronic infection (60 days). Autofluorescence of the skin fur can be observed (Arrow head). Images were obtained using Nikon Eclipse Ti with an A1R confocal head equipped with four different lasers (excitation at: 405, 488, 546 and 647 nm) and emission bandpass filters at 450/50, 515/30, 584/50 and 663/738 nm. Objective Plan Apo λ 10x. Bars: 130 µm.

Movie S1 | Neutrophils in the blood vessels in the infected ear did not express PD-L1. Mice infected in the ears with *L. amazonensis* for 1 h were injected with anti-PD-L1-APC and anti-Ly6G-FITC antibodies. White arrows indicate circulating neutrophils with no expression of PD-L1. Images were obtained using a Nikon Eclipse Ti with an A1R confocal head equipped with four different lasers (excitation at: 405, 488, 546 and 647 nm) and emission bandpass filters at 450/50, 515/30, 584/50 and 663/738 nm. Objective Plan Apo λ 10x. Presence of skin hair autofluorescence. Bar = 130 µm.

Movie S2 | Migration of neutrophils without expression of PD-L1 to the infected ear. Mice infected in the ear with *L. amazonensis* for 1 h were injected with anti-PD-L1-APC and anti-Ly6G-FITC antibodies. Presence of skin hair autofluorescence (Arrow head). Images were obtained using a Nikon Eclipse Ti with an A1R confocal head equipped with four different lasers (excitation at four wavelengths: 405, 488, 546 and 647 nm) and emission bandpass filters at 450/50, 515/30, 584/50 and 663/738 nm. Objective Plan Apo λ 10x and 2x zoom. Bar = 62 µm.

Movie S3 | Neutrophils expressing PD-L1 in a chronic *L. amazonensis* ear infection. Mice infected in the ear with *L. amazonensis* in the chronic infection (60 days) were injected with anti-PD-L1-APC and anti-Ly6G-FITC antibodies.

Images were obtained using a Nikon Eclipse Ti with an A1R confocal head equipped with four different lasers (excitation at four wavelengths: 405, 488, 546 and 647 nm) and emission bandpass filters at 450/50, 515/30, 584/50 and 663/738 nm. Objective Plan Apo λ 10x. Bar =38,57 µm and 127,77 µm.

Movie S4 | Circulating neutrophils not expressing PD-L1 in a chronic *L. amazonensis*. Mice infected in the ear with *L. amazonensis* in the chronic infection (60 days) were injected with anti-PD-L1-APC and anti-Ly6G-FITC antibodies. Presence of skin hair autofluorescence (Arrow head). White arrows indicate circulating neutrophils with no expression of PD-L1. Images were obtained using a Nikon Eclipse Ti with an A1R confocal head equipped with four different lasers (excitation at four wavelengths: 405, 488, 546 and 647 nm) and emission bandpass filters at 450/50, 515/30, 584/50 and 663/738 nm. Objective Plan Apo λ 10x. Bar = 130 µm.

REFERENCES

1. Nordenfelt P and Tapper H. Phagosome Dynamics During Phagocytosis by Neutrophils. *J Leukoc Biol* (2011) 90:271–84. doi: 10.1189/jlb.0810457
2. Brinkmann V, Reichard U, Goosmann C, Fauler B, Uhlemann Y, Weiss DS, et al. Neutrophil Extracellular Traps Kill Bacteria. *Science* (2004) 303:(5663):1532–5. doi: 10.1126/science.1092385
3. Amulic B, Cazalet C, Hayes GL, Metzler KD, Zychlinsky A. Neutrophil Function: From Mechanisms to Disease. *Annu Rev Immunol* (2012) 30:459–89. doi: 10.1146/annurev-immunol-020711-074942
4. Yang F, Feng C, Zhang X, Lu J, Zhao Y. The Diverse Biological Functions of Neutrophils, Beyond the Defense Against Infections. *Inflammation* (2017) 40 (1):311–23. doi: 10.1007/s10753-016-0458-4
5. Castanheira FVS, Kubes P. Neutrophils and NETs in Modulating Acute and Chronic Inflammation. *Blood* (2019) 133:2178–85. doi: 10.1182/blood-2018-11-844530
6. Colón DF, Wanderley CW, Franchin M, Silva CM, Hiroki CH, Castanheira FVS, et al. Neutrophil Extracellular Traps (Nets) Exacerbate Severity of Infant Sepsis. *Crit Care* (2019) 23(1):113. doi: 10.1186/s13054-019-2407-8
7. Bowers NL, Helton ES, Huijbregts RP, Goepfert PA, Heath SL, Hel Z. Immune Suppression by Neutrophils in HIV-1 Infection: Role of PD-L1/PD-1 Pathway. *PloS Pathog* (2014) 10(3):e1003993. doi: 10.1371/journal.ppat.1003993
8. Kho S, Minigo G, Andries B, Leonardo L, Prayoga P, Poespoprodjo JR, et al. Circulating Neutrophil Extracellular Traps and Neutrophil Activation Are Increased in Proportion to Disease Severity in Human Malaria. *J Infect Dis* (2019) 219(12):1994–2004. doi: 10.1093/infdis/jiy661
9. Hurrell BP, Regli IB, Tacchini-Cottier F. Different *Leishmania* Species Drive Distinct Neutrophil Functions. *Trends Parasitol* (2016) 32:392–401. doi: 10.1016/j.pt.2016.02.003
10. Zemans RL. Neutrophil-Mediated T-Cell Suppression in Influenza: Novel Finding Raising Additional Questions. *Am J Respir Cell Mol Biol* (2018) 58 (4):423–5. doi: 10.1165/rcmb.2017-0425ED
11. Abebe T, Takele Y, Weldegebreal T, Cloke T, Closs E, Corset C, et al. Arginase Activity - A Marker of Disease Status in Patients With Visceral Leishmaniasis in Ethiopia. *PloS Neglected Trop Dis* (2013) 7(3):e2134. doi: 10.1371/journal.pntd.0002134
12. Sharma S, Davis RE, Srivastva S, Nylén S, Sundar S, Wilson ME. A Subset of Neutrophils Expressing Markers of Antigen-Presenting Cells in Human Visceral Leishmaniasis. *J Infect Dis* (2016) 214(10):1531–8. doi: 10.1093/infdis/jiw394
13. Greenwald RJ, Freeman GJ, Sharpe AH. The B7 Family Revisited. *Annu Rev Immunol* (2005) 23:515–48. doi: 10.1146/annurev.immunol.23.021704.115611
14. Okazaki T, Honjo T. The PD-1-PD-L Pathway in Immunological Tolerance. *Trends Immunol* (2006) 27(4):195–201. doi: 10.1016/j.it.2006.02.001
15. Chen L. Co-Inhibitory Molecules of the B7-CD28 Family in the Control of T-cell Immunity. *Nat Rev Immunol* (2004) 4(5):336–47. doi: 10.1038/nri1349
16. Bankey PE, Banerjee S, Zucchiatti A, De M, Sleem RW, Lin CFL, et al. Cytokine Induced Expression of Programmed Death Ligands in Human Neutrophils. *Immunol Lett* (2010) 129:100–7. doi: 10.1016/j.imlet.2010.01.006
17. Kythreotou A, Siddique A, Mauri FA, Bower M, Pinato DJ. Pd-L1. *J Clin Pathol* (2018) 71:189–94. doi: 10.1136/jclinpath-2017-204853
18. Freeman GJ, Long AJ, Iwai Y, Bourque K, Chernova T, Nishimura H, et al. Engagement of the PD-1 Immunoinhibitory Receptor by A Novel B7 Family Member Leads to Negative Regulation of Lymphocyte Activation. *J Exp Med* (2000) 192(7):1027–34. doi: 10.1084/jem.192.7.1027
19. Dong H, Zhu G, Tamada K, Chen L. B7-H1, a Third Member of the B7 Family, Co-Stimulates T-Cell Proliferation and Interleukin-10 Secretion. *Nat Med* (1999) 5(12):1365–9. doi: 10.1038/70932
20. Jones D, Como CN, Jing L, Blackmon A, Neff CP, Krueger O, et al. Varicella Zoster Virus Productively Infects Human Peripheral Blood Mononuclear Cells to Modulate Expression of Immunoinhibitory Proteins and Blocking PD-L1 Enhances Virus-Specific CD8+ T Cell Effector Function. *PloS Pathog* (2019) 15(3):e1007650. doi: 10.1371/journal.ppat.1007650
21. de Mel S, Tan JZ-C, Jeyasekharan AD, Chng W-J, Ng S-B. Transcriptomic Abnormalities in Epstein Barr Virus Associated T/NK Lymphoproliferative Disorders. *Front Pediatr* (2019) 6:405. doi: 10.3389/fped.2018.00405
22. Sanjo N, Nose Y, Shishido-Hara Y, Mizutani S, Sekijima Y, Aizawa H, et al. A Controlled Inflammation and a Regulatory Immune System are Associated With More Favorable Prognosis of Progressive Multifocal Leukoencephalopathy. *J Neurol* (2019) 266(2):369–77. doi: 10.1007/s00415-018-9140-0
23. Bardhan K, Anagnostou T, Boussiotis VA. The PD1:PD-L1/2 Pathway From Discovery to Clinical Implementation. *Front Immunol* (2016) 7:550. doi: 10.3389/fimmu.2016.00550
24. Patel R, Bock M, Polotti CF, Elsamra S. Pharmacokinetic Drug Evaluation of Atezolizumab for the Treatment of Locally Advanced or Metastatic Urothelial Carcinoma. *Expert Opin Drug Metab Toxicol* (2017) 13(2):225–32. doi: 10.1080/17425255.2017.1277204
25. Wang C, Yu X, Wang W. A Meta-Analysis of Efficacy and Safety of Antibodies Targeting PD-1/PD-L1 in Treatment of Advanced Nonsmall Cell Lung Cancer. *Med (Baltimore)* (2016) 95(52):e5539. doi: 10.1097/MD.0000000000005539
26. Chamoto K, Al-Habsi M, Honjo T. Role of PD-1 in Immunity and Diseases. *Curr Top Microbiol Immunol* (2017) 410:75–97. doi: 10.1007/82_2017_67
27. Wang J, Jebbawi F, Bellanger AP, Beldi G, Millon L, Gottstein B. Immunotherapy of Alveolar Echinococcosis *Via* PD-1/PD-L1 Immune Checkpoint Blockade in Mice. *Parasite Immunol* (2018) 40(12):e12596. doi: 10.1111/pim.12596
28. da Fonseca-Martins AM, Ramos TD, Pratti JES, Firmino-Cruz L, Gomes DCO, Soong L, et al. Immunotherapy Using Anti-PD-1 and Anti-PD-L1 in *L. amazonensis*-Infected BALB/c Mice Reduce Parasite Load. *Sci Rep* (2019) 9 (1):20275. doi: 10.1038/s41598-019-56336-8
29. Ribeiro-Gomes FL, Peters NC, Debrabant A, Sacks DL. Efficient Capture of Infected Neutrophils by Dendritic Cells in the Skin Inhibits the Early Anti-Leishmania Response. *PloS Pathog* (2012) 8(2):e1002536. doi: 10.1371/journal.ppat.1002536
30. Scott-Browne JP, López-Moyado IF, Trifari S, Wong V, Chavez L, Rao A, et al. Dynamic Changes in Chromatin Accessibility Occur in CD8^{+} T Cells Responding to Viral Infection. *Immunity* (2016) 45(6):1327–40. doi: 10.1016/j.immuni.2016.10.028
31. Pipkin ME, Sacks JA, Cruz-Guilloty F, Lichtenheld MG, Bevan MJ, Rao A. Interleukin-2 and Inflammation Induce Distinct Transcriptional Programs That Promote the Differentiation of Effector Cytolytic T Cells. *Immunity* (2010) 32(1):79–90. doi: 10.1016/j.immuni.2009.11.012
32. Peters NC, Egen JG, Secundino N, Debrabant A, Kimblin N, Kamhawi S, et al. In Vivo Imaging Reveals an Essential Role for Neutrophils in Leishmaniasis Transmitted by Sand Flies. *Science* (2008) 321(5891):970–4. doi: 10.1126/science.1159194
33. Schubach A, Cuzzi-Maya T, Oliveira AV, Sartori A, de Oliveira-Neto MP, Mattos MS, et al. Leishmanial Antigens in the Diagnosis of Active Lesions and Ancient Scars of American Tegumentary Leishmaniasis Patients. *Mem Inst Oswaldo Cruz* (2001) 96(7):987–96. doi: 10.1590/s0074-02762001000700018
34. Viana AG, Mayrink W, Fraga CA, Silva LM, Domingos PL, Bonan PR, et al. Histopathological and Immunohistochemical Aspects of American Cutaneous Leishmaniasis Before and After Different Treatments. *Bras Dermatol* (2013) 88(1):32–40. doi: 10.1590/s0365-05962013000100003
35. Mendes DS, Dantas ML, Gomes JM, Santos WL, Silva AQ, Guimarães LH, et al. Inflammation in Disseminated Lesions: An Analysis of CD4+, Cd20+,

CD68+, CD31+ and vW+ Cells in non-Ulcerated Lesions of Disseminated Leishmaniasis. *Mem Inst Oswaldo Cruz* (2013) 108(1):18–22. doi: 10.1590/s0074-02762013000100003
36. Eid AA, Badr El Dine FM, Nabil IM. Histopathologic and Ultrastructural Changes in Seminiferous Tubules of Adult Male Albino Rats Following Daily Administration of Different Doses of Tadalafil. *Urology* (2016) 90:89–96. doi: 10.1016/j.urology.2015.12.038
37. Gomes AHS, Martines RB, Kanamura CT, Barbo MLP, Iglezias SD, Lauletta Lindoso JA, et al. American Cutaneous Leishmaniasis: *In Situ* Immune Response of Patients With Recent and Late Lesions. *Parasite Immunol* (2017) 39(4):1–10. doi: 10.1111/pim.12423
38. Covre LP, Devine OP, Garcia de Moura R, Vukmanovic-Stejic M, Dietze R, Ribeiro-Rodrigues R, et al. Compartmentalized Cytotoxic Immune Response Leads to Distinct Pathogenic Roles of Natural Killer and Senescent CD8$^+$ T Cells in Human Cutaneous Leishmaniasis. *Immunology* (2020) 159 (4):429–40. doi: 10.1111/imm.13173
39. Carlsen ED, Hay C, Henard CA, Popov V, Garg NJ, Soong L. *L. amazonensis* Amastigotes Trigger Neutrophil Activation But Resist Neutrophil Microbicidal Mechanisms. *Infect Immun* (2013) 81(11):3966–74. doi: 10.1128/IAI.00770-13
40. Barroso DH, Falcão SAC, da Motta JOC, Sevilha Dos Santos L, Takano GHS, Gomes CM, et al. Pd-L1 May Mediate T-Cell Exhaustion in A Case of Early Diffuse Leishmaniasis Caused By *L. amazonensis*. *Front Immunol* (2018) 9:1021. doi: 10.3389/fimmu.2018.01021
41. de Kleijn S, Langereis JD, Leentjens J, Kox M, Netea MG, Koenderman L, et al. Ifn-γ-Stimulated Neutrophils Suppress Lymphocyte Proliferation Through Expression of PD-L1. *PloS One* (2013) 8(8):e72249. doi: 10.1371/journal.pone.0072249
42. Souza-Lemos C, de-Campos SN, Teva A, Côrte-Real S, Fonseca EC, Porrozzi R, et al. Dynamics of Immune Granuloma Formation in a Leishmania Braziliensis-Induced Self-Limiting Cutaneous Infection in the Primate Macaca Mulatta. *J Pathol* (2008) 216(3):375–86. doi: 10.1002/path.2403
43. Lopez Kostka S, Dinges S, Griewank K, Iwakura Y, Udey MC, von Stebut E. Il-17 Promotes Progression of Cutaneous Leishmaniasis in Susceptible Mice. *J Immunol* (2009) 182(5):3039–46. doi: 10.4049/jimmunol.0713598
44. Verçosa BL, Melo MN, Puerto HL, Mendonça IL, Vasconcelos AC. Apoptosis, Inflammatory Response and Parasite Load in Skin of Leishmania (Leishmania) Chagasi Naturally Infected Dogs: A Histomorphometric Analysis. *Veterinary Parasitology* (2012) 189(2-4):162–70. doi: 10.1016/j.vetpar.2012.04.035
45. Morgado FN, Nascimento MT, Saraiva EM, de Oliveira-Ribeiro C, Madeira Mde F, da Costa-Santos M, et al. Are Neutrophil Extracellular Traps Playing a Role in the Parasite Control in Active American Tegumentary Leishmaniasis Lesions? *PloS One* (2015) 10(7):e0133063. doi: 10.1371/journal.pone.0133063
46. Chaves MM, Lee SH, Kamenyeva O, Ghosh K, Peters NC, Sacks D. The Role of Dermis Resident Macrophages and Their Interaction With Neutrophils in the Early Establishment of Leishmania Major Infection Transmitted by Sand Fly Bite. *PloS Pathog* (2020) 16(11):e1008674. doi: 10.1371/journal.ppat.1008674
47. McNab FW, Berry MP, Graham CM, Bloch SA, Oni T, Wilkinson KA, et al. Programmed Death Ligand 1 is Over-Expressed by Neutrophils in the Blood of Patients With Active Tuberculosis. *Eur J Immunol* (2011) 41(7):1941–7. doi: 10.1002/eji.201141421
48. He G, Zhang H, Zhou J, Wang B, Chen Y, Kong Y, et al. Peritumoural Neutrophils Negatively Regulate Adaptive Immunity *Via* the PD-L1/PD-1 Signalling Pathway in Hepatocellular Carcinoma. *J Exp Clin Cancer Res* (2015) 34:141. doi: 10.1186/s13046-015-0256-0
49. Fallon EA, Biron-Girard BM, Chung CS, Lomas-Neira J, Heffernan DS, Monaghan SF, et al. A Novel Role for Coinhibitory Receptors/Checkpoint Proteins in the Immunopathology of Sepsis. *J Leukoc Biol* (2018) 103:1151–64. doi: 10.1002/JLB.2MIR0917-377R
50. Luo Q, Huang Z, Ye J, Deng Y, Fang L, Li X, et al. Pd-L1-Expressing Neutrophils as A Novel Indicator to Assess Disease Activity of Rheumatoid Arthritis. *Int J Clin Exp Med* (2017) 10:7716–24. doi: 10.1186/s13075-016-0942-0
51. Abadie V, Badell E, Douillard P, Ensergueix D, Leenen PJ, Tanguy M, et al. Neutrophils Rapidly Migrate Via Lymphatics After Mycobacterium Bovis BCG Intradermal Vaccination and Shuttle Live Bacilli to the Draining Lymph Nodes. *Blood* (2005) 106(5):1843–50. doi: 10.1182/blood-2005-03-1281
52. Castell SD, Harman MF, Morón G, Maletto BA, Pistoresi-Palencia MC. Neutrophils Which Migrate to Lymph Nodes Modulate Cd4$^+$ T Cell Response by a PD-L1 Dependent Mechanism. *Front Immunol* (2019) 10:105. doi: 10.3389/fimmu.2019.00105
53. Bogoslowski A, Wijeyesinghe S, Lee WY, Chen CS, Alanani S, Janne C, et al. Neutrophils Recirculate Through Lymph Nodes to Survey Tissues for Pathogens. *J Immunol* (2020) 204:2552–61. doi: 10.4049/jimmunol.2000022
54. Ordeix L, Montserrat-Sangrà S, Martínez-Orellana P, Baxarias M, Solano-Gallego L. Toll-Like Receptors 2, 4 and 7, Interferon-Gamma and Interleukin 10, and Programmed Death Ligand 1 Transcripts in Skin From Dogs of Different Clinical Stages of Leishmaniosis. *Parasit Vectors* (2019) 12(1):575. doi: 10.1186/s13071-019-3827-7
55. de Souza TL, da Silva AVA, Pereira LOR, Figueiredo FB, Mendes AAVJr, Menezes RC, et al. Pro-Cellular Exhaustion Markers are Associated With Splenic Microarchitecture Disorganization and Parasite Load in Dogs With Visceral Leishmaniasis. *Sci Rep* (2019) 9:12962. doi: 10.1038/s41598-019-49344-1
56. Chiku VM, Silva KL, de Almeida BF, Venturin GL, Leal AA, de Martini CC, et al. PD-1 Function in Apoptosis of T Lymphocytes in Canine Visceral Leishmaniasis. *Immunobiology* (2016) 221(8):879–88. doi: 10.1016/j.imbio.2016.03.007
57. Schaut RG, Lamb IM, Toepp AJ, Scott B, Mendes-Aguiar CO, Coutinho JF, et al. Regulatory Igdhi B Cells Suppress T Cell Function Via IL-10 and PD-L1 During Progressive Visceral Leishmaniasis. *J Immunol* (2016) 196(10):4100–9. doi: 10.4049/jimmunol.1502678
58. Dabiri S, Hayes MM, Meymandi SS, Basiri M, Soleimani F, Mousavi MR. Cytologic Features of "Dry-Type" Cutaneous Leishmaniasis. *Diagn Cytopathol* (1998) 19(3):182–5. doi: 10.1002/(sici)1097-0339(199809)19:3<182::aid-dc5>3.0.co;2-f
59. Morgado FN, Schubach A, Rosalino CM, Quintella LP, Santos G, Salgueiro M, et al. Is the *In Situ* Inflammatory Reaction An Important Tool to Understand the Cellular Immune Response in American Tegumentary Leishmaniasis? *Br J Dermatol* (2008) 158(1):50–8. doi: 10.1111/j.1365-2133.2007.08255.x
60. Dantas ML, Oliveira JM, Carvalho L, Passos ST, Queiroz A, Guimarães LH, et al. Comparative Analysis of the Tissue Inflammatory Response in Human Cutaneous and Disseminated Leishmaniasis. *Mem Inst Oswaldo Cruz* (2014) 109(2):202–9. doi: 10.1590/0074-0276130312
61. Boaventura VS, Santos CS, Cardoso CR, de Andrade J, Dos Santos WL, Clarêncio J, et al. Human Mucosal Leishmaniasis: Neutrophils Infiltrate Areas of Tissue Damage That Express High Levels of Th17-related Cytokines. *Eur J Immunol* (2010) 40(10):2830–6. doi: 10.1002/eji.200940115
62. Christensen SM, Dillon LA, Carvalho LP, Passos S, Novais FO, Hughitt VK, et al. Meta-Transcriptome Profiling of the Human-Leishmania Braziliensis Cutaneous Lesion. *PloS Negl Trop Dis* (2016) 10(9):e0004992. doi: 10.1371/journal.pntd.0004992
63. Garcia de Moura R, Covre LP, Fantecelle CH, Gajardo VAT, Cunha CB, Stringari LL, et al. Pd-1 Blockade Modulates Functional Activities of Exhausted-Like T Cell in Patients With Cutaneous Leishmaniasis. *Front Immunol* (2021) 12:632667. doi: 10.3389/fimmu.2021.632667

Conflict of Interest: The authors declare that the research was conducted in the absence of any commercial or financial relationships that could be construed as a potential conflict of interest.

frontiers in Immunology

ORIGINAL RESEARCH
published: 20 July 2021
doi: 10.3389/fimmu.2021.662307

Potential Role of CXCL10 in Monitoring Response to Treatment in Leprosy Patients

Helen Ferreira[1], *Mayara Abud Mendes*[1], *Mayara Garcia de Mattos Barbosa*[2], *Eliane Barbosa de Oliveira*[1], *Anna Maria Sales*[1], *Milton Ozório Moraes*[1], *Euzenir Nunes Sarno*[1] *and Roberta Olmo Pinheiro*[1]*

[1] Leprosy Laboratory, Oswaldo Cruz Institute, Oswaldo Cruz Foundation, Rio de Janeiro, Brazil, [2] Cascalho-Platt Laboratory, Department of Surgery, University of Michigan, Ann Arbor, MI, United States

The treatment of multibacillary cases of leprosy with multidrug therapy (MDT) comprises 12 doses of a combination of rifampicin, dapsone and clofazimine. Previous studies have described the immunological phenotypic pattern in skin lesions in multibacillary patients. Here, we evaluated the effect of MDT on skin cell phenotype and on the *Mycobacterium leprae*-specific immune response. An analysis of skin cell phenotype demonstrated a significant decrease in MRS1 (SR-A), CXCL10 (IP-10) and IFNG (IFN-γ) gene and protein expression after MDT release. Patients were randomized according to whether they experienced a reduction in bacillary load after MDT. A reduction in CXCL10 (IP-10) in sera was associated with the absence of a reduction in the bacillary load at release. Although IFN-γ production in response to *M. leprae* was not affected by MDT, CXCL10 (IP-10) levels in response to *M. leprae* increased in cells from patients who experienced a reduction in bacillary load after treatment. Together, our results suggest that CXCL10 (IP-10) may be a good marker for monitoring treatment efficacy in multibacillary patients.

Keywords: leprosy, skin cells, IFN-γ, CXCL-10, multidrug therapy

OPEN ACCESS

Edited by:
Nathalie Winter, Institut National de recherche pour l'agriculture, l'alimentation et l'environnement (INRAE), France

Reviewed by:
Utpal Sengupta, The Leprosy Mission Trust India, India
Patrick Brennan, Colorado State University, United States

***Correspondence:**
Roberta Olmo Pinheiro
robertaolmo@gmail.com

Specialty section:
This article was submitted to Microbial Immunology, a section of the journal Frontiers in Immunology

Received: *01 February 2021*
Accepted: *05 July 2021*
Published: *20 July 2021*

Citation:
Ferreira H, Mendes MA, de Mattos Barbosa MG, de Oliveira EB, Sales AM, Moraes MO, Sarno EN and Pinheiro RO (2021) Potential Role of CXCL10 in Monitoring Response to Treatment in Leprosy Patients. Front. Immunol. 12:662307. doi: 10.3389/fimmu.2021.662307

INTRODUCTION

Multibacillary leprosy (MB) patients are responsible for the active transmission of the disease in the community (1). Previous studies have demonstrated that macrophages present in skin lesions of MB patients have the characteristics of anti-inflammatory macrophages, with higher phagocytic properties and increased bacterial survival. These are furthermore mediated by an increased expression of proteins involved in host iron metabolism and they contribute to a higher bacillary load in these patients (2–4).

MB patients do not mount an effective cellular-mediated response to *Mycobacterium leprae* and may present numerous and symmetrically distributed lesions, with an increased ratio of CD8:CD4 T cells and increased production of Th2 cytokines such as IL-4, IL-5 and IL-10 (5). These Th2 cytokines are associated with the production of antibodies that do not confer protection against the disease. IL-10 is associated with increased phagocytic activity in skin macrophages from MB patients, as well as with a reduction in the antimicrobial properties of host cells, which are responsible for the maintenance of *M. leprae*-susceptible macrophages (6–8).

Until now, a specific drug for the treatment of leprosy was not available (9). Leprosy is a bacterial disease caused by *M. leprae*, an intracellular pathogen that infects keratinocytes, macrophages and histiocytes in the skin and Schwann cells in the peripheral nerves (10–12). MB treatment consists of a combination of rifampicin, clofazimine and dapsone in 12 doses (13). Although patients are considered "cured" after the completion of MDT, leprosy reactions, permanent disability and occasional relapse/reinfection have been observed in many patients (14). Moreover, not all patients present a reduction in bacillary load after the 12 doses of MDT.

Several studies evaluated the impact of MDT on immune response. MDT changes the profile of serum cytokines in *M. leprae*-infected patients (15, 16), and a reduction in antibody response in MB patients was considered a parameter for monitoring MDT effectiveness (17). The immunosuppressive and anti-inflammatory properties of MDT are associated with the inhibition of some cell types, and they do not seem to interfere directly in the production of mediators and cytokines (18–21). In addition, during MB clinical courses, there are disturbances in skin lipid metabolism that are modulated by MDT (22).

Here, we investigated the expression of cell markers associated with an anti-inflammatory phenotype in macrophages in skin lesion cells from MB patients that presented or showed no reduction in bacillary load after MDT. Furthermore, we evaluated whether MDT was able to restore the cellular immune response against *M. leprae* in these patients.

MATERIALS AND METHODS

Study Population

In this study, we utilized biological samples from a total of 55 adult patients. The patients were men and women between 18 and 81 years old who had been diagnosed with MB leprosy and who were categorized according to Ridley and Jopling's classification (23) as being lepromatous-lepromatous (LL), meaning they had no reaction at the onset or at the completion of treatment (release) (**Table 1**). Patients under the age of 18 with comorbidities such diabetes, hepatitis, syphilis and diseases caused by other mycobacteria, as well as patients co-infected with the human immunodeficiency virus and relapse cases were excluded. All patients enrolled were treated at the Souza Araújo Outpatient Unit at FIOCRUZ, Rio de Janeiro, Brazil. Among the recruited patients, 48 received the standard regimen of multidrug therapy (WHO-MDT): rifampicin, dapsone and clofazimine, and 7 received an alternative scheme: rifampicin, clofazimine and ofloxacin. Both groups took these regimens for twelve months. Whole blood and skin lesion samples were obtained at diagnosis, or prior to treatment (onset), and at the conclusion of treatment (release) from patients who did not exhibit any signs of leprosy at both points. Blood samples were used in the study of gene expression and for cytokine measurements, both in whole blood and in serum. Skin lesion samples were obtained with a 6 mm punch and cleaved into two fragments. One fragment was used for histopathological processing and staining by the Hematoxylin-Eosin and Wade methods in order to diagnose cases, while the second fragment was immediately frozen by immersion in liquid nitrogen and used for immunohistochemistry or real-time PCR. Blood without anticoagulants was also collected to obtain serum samples.

Ethics Statement

This study was carried out in accordance with institutional research ethics committee approval and in Resolution 466/12 of the National Health Council (CAAE 76328517.2.0000.5248, approval number 2.450.910). All volunteers agreed to participate and signed a free and informed consent form prior to their inclusion in the study and any sample collection. All the patients received clinical treatment, follow-up appointments and all information, regardless of their participation or exclusion from the study.

Immunohistochemistry

Frozen sections of skin lesion samples were examined with a Leica LM1850UV cryostat (Leica, Wetzlar, Germany). The 5 μm thick sections were fixed in cold acetone and hydrated in 0.01M phosphate buffer saline (PBS). Endogenous peroxidase was blocked in 0.3% hydrogen peroxide solution diluted in 0.01M PBS and then washed in 0.01M PBS. Unspecific binding sites were blocked with 0.01M PBS solution containing 10% normal goat serum (NGS) and 0.1% bovine serum albumin (BSA). The following primary antibodies were diluted in 0.01M PBS solution containing 1% NGS and incubated overnight at 4°C in humid chamber: anti-CD68 (1:100 Dako M0814), anti-CD163 (1:25 R&D Systems MAB1607), anti-arginase 1 (BD Transduction labs 610708), anti-IDO (1:100 Millipore MAB1009), anti-MRS-1 (SR-A, Santa Cruz, SC-166184), anti-IFN-γ (1:50 BD Biosciences N554548) and anti-CXCL10/IP-10 (1:50 Santa Cruz SC-101500). Next, sections were washed with 0.01M PBS

TABLE 1 | Demographic and clinical data of patients included in the study (n = 55).

Gender (n,%)	
Female	11 (20.0%)
Male	44 (80.0%)
Age (range, min–max)	48 (18 – 81)
BI onset (range, min–max)	4.61 (3.0 – 6.0)
BI release (range, min–max)	3.78 (1.0 – 6.0)
LBI onset (range, min–max)	5.01 (2,3 – 6.0)
LBI release (range, min–max)	2.78 (0,0 – 5,85)
Reaction during treatment (n,%)	
Yes	12 (21.82%)
No	43 (78.18%)
Treatment (n,%)	
Multidrug therapy (MDT)	48 (87.28%)
Alternative scheme	07 (12.72%)
BI Reduction (n,%)	
Yes (WR)	22 (40.0%)
No (NR)	33 (20.0%)

BI, bacillary index; LBI, logarithmic bacillary index of skin lesions; WR, with reduction; NR, no reduction.

and incubated in a HiDef signal amplifier solution for 20 min, and then washed in 0.01M PBS and incubated in a HiDef HRP polymer detector solution (kit HiDef detection HRP polymer system, Cell Marque, 954-D) for 20 minutes. Sections were washed twice with 0.01M PBS. Immunostainings were developed in 3-amino-9-ethylcarbazole solution (AEC substrate Kit, Vector Labs SK-4200). The cell nuclei were stained with Harris' Hematoxylin. Sections were mounted with coverslips using an aqueous mounting medium (Abcam 128982) and the results were analyzed under Nikon Eclipse E400 optical microscope with a plan-apochromatic 20X/0,40 objective (Nikon Instruments Inc., New York, USA).

Whole Blood Assay

Venous blood samples collected in tubes containing heparin were diluted in serum-free AIM-V medium (GIBCO 12055) in a 1:10 ratio and distributed onto plates in three series of 300 µL in triplicate. A fraction was incubated with sonicated *M. leprae* cell antigens at a 10 µg/mL concentration (BEI Resources, NR19329) and the second aliquot was stimulated with phytohemagglutinin (PHA Sigma 1668) solution at 25 µg/mL as a positive control. Negative controls were non-stimulated cells. Samples were cultured at 37°C in an environment containing 5% CO_2 for five days. Subsequently, the supernatant was collected and IFN-γ and CXCL10/IP-10 were measured by ELISA (eBiosciences, San Diego, CA, USA).

ELISA

Serum samples obtained from blood without anticoagulants or supernatants from whole blood cultures were used to determine the concentration of IFN-γ, IL-6, IL-10, IL-17A, TNF, IL-1β, TGF-β and CXCL10/IP-10 cytokines by ELISA, following the manufacturer's protocol (eBiosciences, San Diego, CA, USA).

RT-PCR

RNA was extracted from skin lesion fragments by the TRIzol method (Life Technologies15596-018), following the manufacturer's instructions. To avoid genomic DNA contamination, the RNA was treated with DNAse (RTS DNase Kit, MO BIO Laboratories); integrity was analyzed *via* 1.2% agarose gel electrophoresis. A SuperScript III First-Strand Synthesis System (Life Technologies, 18080-051) was used to perform the reverse transcription. mRNA expression of *CD163, ARGINASE1, MRS1, IDO1, NOS2A, IL15, IFNG* and *CXCL10* was evaluated using TaqMan Fast Universal PCR Master Mix (2X) (Applied Biosystems 4352042) in a StepOnePlus real-time PCR system (Applied Biosystems, MA, USA). All primers were acquired from ThermoFisher Scientific (4331182). The $2^{-\Delta CT}$ method was used to analyze gene expression data using glyceraldehyde-3-phosphate dehydrogenase (*GAPDH*; Hs02758991_g1, Thermo-Fisher Scientific) as a reference gene.

Statistical Analysis

Statistical significance was calculated by Mann–Whitney or Kruskal–Wallis tests with Dunn's multiple comparison post-test *via* GraphPad Prism 8.0 software (GraphPad, La Jolla, CA, USA). A $p \leq 0.05$ was deemed statistically significant.

RESULTS

MDT Contributes to Reducing the Anti-Inflammatory Profile of Skin Macrophages in LL Patients

Routine histopathological analyses of skin lesion fragments were performed to select representative specimens of the LL polar form of the disease, both before treatment and after the release of MDT. As previously described (24, 25), the histopathology of lepromatous leprosy is characterized by collections and sheets of macrophages diffusely distributed in the dermis, with few lymphocytes and plasma cells (**Figure 1**). Macrophages present a foamy appearance and are filled with bacilli (**Figure 1**). After 12 doses of MDT, histopathology was variable between the recruited cases, but a reduction in the infiltrate was a common finding in patients who did not develop reactional episodes during treatment (**Figure 1**). A diffuse lymphocytic infiltrate was also observed, and only few foamy cells were observed (**Figure 1**). Immunohistochemistry was performed to identify whether MDT decreases the anti-inflammatory (M2) profile in cells from treated LL patients.

To characterize the macrophage phenotype, LL skin lesions were immunostained for CD68, CD163, Arg1 (arginase), MSR1 (SR-A) and IDO-1, which are surface markers predominant in non-treated macrophages (2, 7, 8, 24). We selected representative cases to demonstrate that the inflammatory infiltrates decreases in the release and that anti-inflammatory profile disappears after MDT, with a reduction in CD68+, CD163+, SR-A+, Arg1 and IDO+ cells (**Figure 1**). Gene expression analysis revealed a significant decrease in *MRS1* (that encodes SR-A-) and an increase in *ARG1* expressions (**Figure 2**).

IFN-γ and CXCL10 (IP-10) Were Reduced in LL Skin Lesion Cells After MDT

We evaluated whether 12 doses of MDT increased the presence of pro-inflammatory macrophages in the skin cells of MB patients. We did not observe significant changes in *NOS2A* and *IL15* expression (data not shown). However, IFN-γ and CXCL10 (IP-10) production in skin lesion cells was significantly reduced after MDT, as was observed by gene expression (**Figure 3A**) and histopathology (**Figure 3B**).

CXCL10 Is Associated With a Reduction in Bacillary Load

We evaluated levels of CXCL10 (IP-10), IFN-γ, IL-6, IL-10, TNF, IL-12p70, TGF-β and IL-17A in LL patient sera. We did not observe significant differences between the levels of IFN-γ (**Figure 4A**), IL-6, IL-10, TNF, IL-12p70, TGF-β and IL-17A (**Supplementary Figure 1**) when comparing between the onset and the release of MDT. CXCL-10 serum levels decreased after MDT (**Figure 4B**).

It is well known that, after MDT, lesions can histologically clear in 2 to 5 years or more (25–27). Moreover, for unexplained reasons, some patients do not reduce their bacillary index, even after 12 doses of MDT. In this context, we divided the recruited volunteers into two groups. The first group was composed of

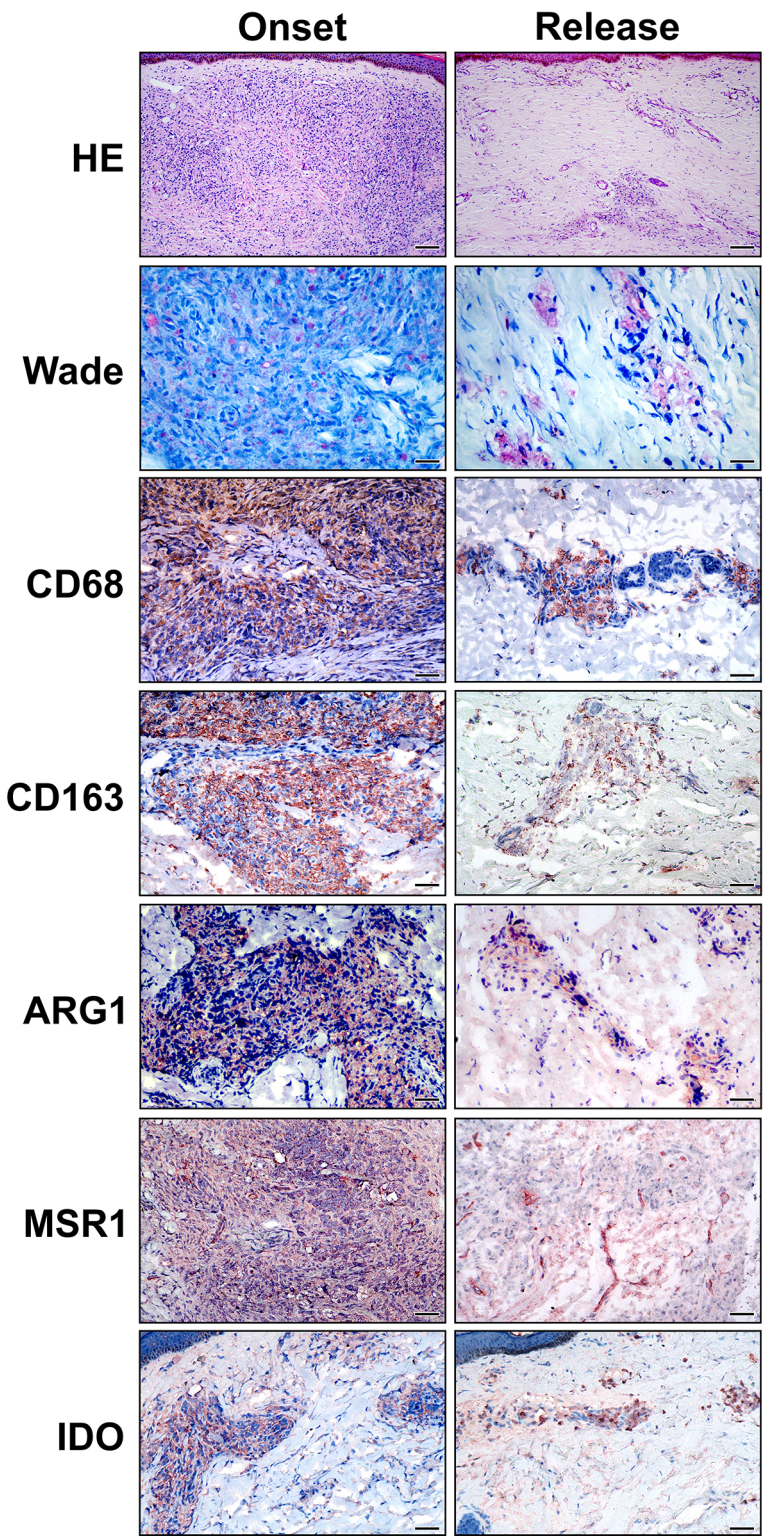

FIGURE 1 | Anti-inflammatory macrophage phenotype in LL skin lesions is reduced at 12-dose MDT release. Skin lesions fragments were collected at LL diagnosis (onset) and at release of 12-dose MDT. Routine Hematoxylin-Eosin (HE) and Wade staining were performed to characterize the inflammatory infiltrate and to verify the presence of alcohol-acid-resistant bacilli in the skin lesions. Additionally, CD68, CD163, Arginase 1 (ARG1), MSR1 (SR-A) and IDO immunostainings were performed to characterize the phenotype of the cells infiltrating the skin lesions. Representative images are shown. Bars: 100 μm (HE), 25 μm (Wade) and 50 μm (immunostaining).

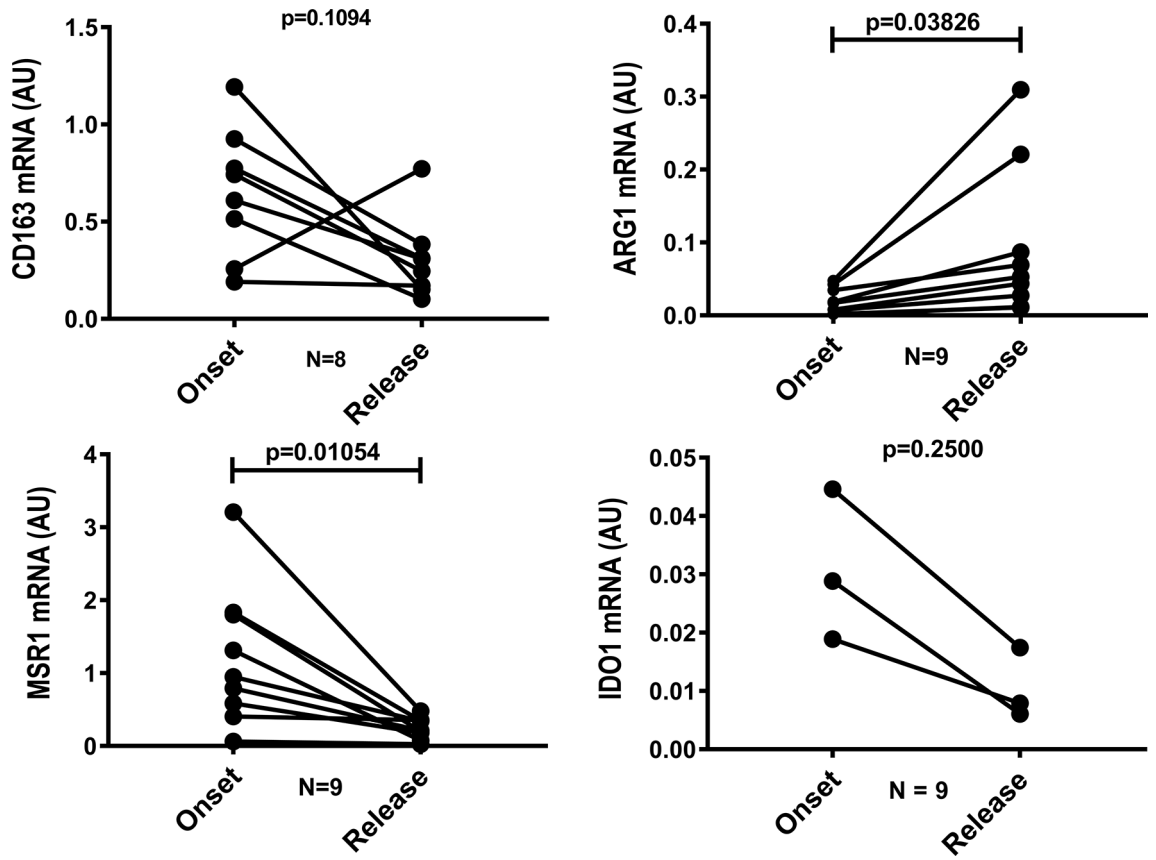

FIGURE 2 | Gene expression of *MSR1* is reduced and *ARG1* increases after 12 doses of MDT. Skin lesions fragments were collected at LL diagnosis (onset) and at release of 12-dose MDT. RNA was extracted, cDNA was synthesized and the expression of *CD163*, *ARG1*, *MSR1* and *IDO1* genes was evaluated by real-time PCR. Graph shows the gene expression of each patient at disease onset and 12-dose MDT release.

patients who presented a reduction in bacilloscopic index (WR—with reduction) and the other group was composed of patients who did not show a reduction in bacilloscopic index (NR—no reduction) after the release of 12 doses of MDT.

As observed in **Figures 4C, D**, in patients who did not present a reduction in bacilloscopic index, there was a significant decrease in CXCL10 (IP-10) levels in the sera; this was not the case in IFN-γ.

Reduction in Bacillary Load Is Associated With Increased Production of CXCL10 (IP-10) in Response to *M. leprae*

In LL, the immune system maneuvers the immune response towards antigen-specific anergy. As observed in **Figure 5A**, levels of IFN-γ were significantly increased after MDT,. CXCL10 (IP-10) levels were not affected by MDT (**Figure 5B**). However, when we separated the NR and WR groups, we observed an increase in CXCL10 (IP-10), but not IFN-γ, in *M. leprae*-stimulated cells compared to non-stimulated cells. This was true for the group that showed a reduced bacilloscopic index after 12 months of MDT (WR) (**Figures 5C, D**).

DISCUSSION

Antigen-specific T cell responses (Th1 and Th17) have been observed in paucibacillary (PB) patients and are associated with control over *M. leprae* replication (28–32). In contrast, Th2 and T regulatory cells are associated with MB presentations. Although several studies have demonstrated an association between IFN-γ-specific immune responses and protection, the assessment of T cell responses by only measuring IFN-γ may not reflect the protective potential of the response, meaning that other mediators might be involved in the control of the disease. The World Health Organization (WHO) introduced the MDT standardized regimen in 1982, but a high percentage of patients who completed a fixed duration of MDT left with residual skin lesions. In addition, upon MDT completion, patients are considered cured; however, even after MDT, some patients develop leprosy reactions (33).

Despite advances in understanding the pathogenesis of leprosy and perspectives in terms of developing new therapeutic strategies (34), the identification of biomarkers is pivotal for characterizing the immune response in different clinical forms of leprosy, as well as for determining MDT efficacy. There is strong evidence that the immunological

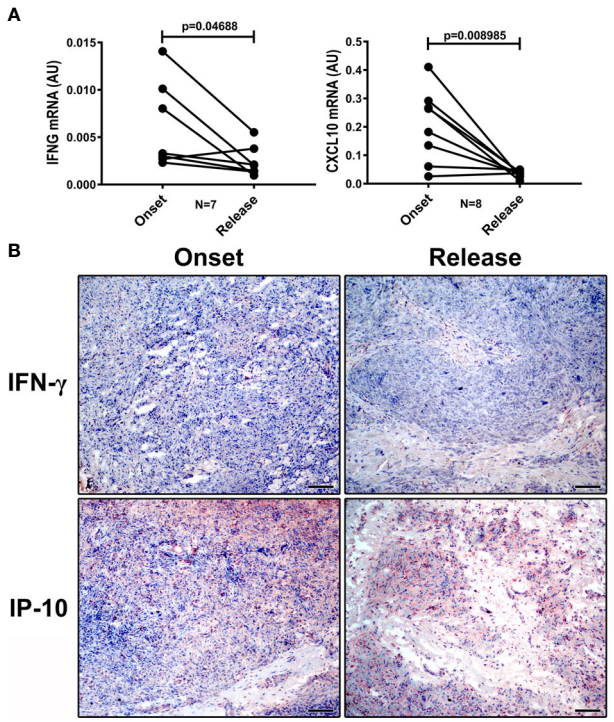

FIGURE 3 | IFN-γ and CXCL10 (IP-10) are reduced in LL skin lesions at 12-dose MDT release. Skin lesions fragments were collected at LL diagnosis (onset) and at release of 12-dose MDT: **(A)** RNA was extracted, cDNA was synthesized and the expression of *IFNG* and *CXCL10* genes was evaluated by real-time PCR. Graphs show the gene expression of each patient at disease onset and 12-dose MDT release. **(B)** Expression of IFN-γ and CXCL10 (IP-10) in the skin lesions was detected by immunohistochemistry. Representative images are shown. Bars: 50 μm.

response of infected individuals influences not only their susceptibility to *M. leprae* but also the outcome of leprosy. However, little is known regarding the capacity of MDT to modulate a host's immune response and control the disease, especially in MB patients who present reduced antigen-specific T cell responses. Antigen-specific antibody responses were readily detected in MB patients at the time of diagnosis but were reduced after MDT (35). In this scenario, we can speculate whether the mechanisms associated with control of the disease in MB patients involve increased frequencies of pro-inflammatory macrophages in skin lesions instead of specific T cell responses.

The pathogenesis of MB leprosy involves higher frequency and highly susceptible anti-inflammatory macrophages in skin lesions. Previous studies have demonstrated that MB macrophages have a high phagocytic activity mediated by IL-10 (6, 7, 36). A qPCR performed to evaluate pro- and anti-inflammatory related gene expression in skin lesions of leprosy patients revealed that pro-inflammatory genes *STAT1*, *TNF*, *IFNG*, *IL15* and *CSF2* are increased in PB cells, whereas anti-inflammatory *MSR1* and *PPARG* genes are increased in MB cells (2). Increased expressions of IDO-1, CD163, Arginase 1 and SRA-1 (MSR1) were observed in MB compared to PB cells (7, 8, 24). Although there was a predominance of an alternatively activated phenotype in MB skin lesions at the onset of the disease, the effect of MDT on the macrophage skin phenotype remains uncertain. Here, we investigated the expression of IDO-1, CD163, Arginase 1 and SRA-1 in skin cells of polar lepromatous patients (LL - MB) at onset and after the release of MDT. As expected, treatment with 12 doses of MDT decreased the inflammatory infiltrate in about 90% of the analyzed cases, which was accompanied by a reduction in the expression of scavenger receptors such as SR-A1 (*MSR1*) and CD163, as well as a decrease in IFN-γ and CXCL10 (IP-10) in skin cells associated with an increase in *ARG1*expression.

It is clear that clinically curing the disease is associated not only with bacilli clearance but with the activation of wound healing or tissue repair functions. It is well known that tissue repair comprises a spectrum of overlapping functions that include phagocytosis, secretion of cytokines and growth factors, as well as matrix remodeling (37). In this context, the reduction in proinflammatory mediators in skin cells, such as IFN-γ and CXCL10 (IP-10), could be associated with tissue repair. This hypothesis may be reinforced by an increase in arginase expression. Previous studies have demonstrated that arginase is important for tissue repair (38, 39). Arginase 1 can be produced by cells other than macrophages (40, 41) and, as human macrophages do not produce arginase, human arginase appears to be derived entirely from non-macrophage cell types (40, 42, 43).

Arginase 1 is expressed across a range of cell types involved in wound healing, including keratinocytes (44), fibroblasts (45) and inflammatory cells (46). Arginase 1-mediated metabolism of arginine is an important source of local ornithine, a proline precursor important for collagen synthesis. Previous reports from Singer and Clark (1999) (47) have demonstrated that the main sources of wound collagen are fibroblasts. Although we did not describe the phenotype of Arginase 1-producing cells in MDT-treated LL patients, our data suggest that 12 doses of MDT may modulate *ARG1* expression in LL skin cells. In humans, iNOS activity appears to be indetectable or lower (48). Since Arginase 1 and iNOS compete for the same substrate, the amino acid L-arginine, we evaluated *NOS2* expression in LL skin cells at onset and at release of MDT. No differences were observed between *NOS2* expressions when comparing treated *versus* untreated skin cells.

Cytokines might be identified as good biomarkers of the impact of MDT on the immune system and the effectiveness of treatment. IFN-γ has been studied as a diagnostic host biomarker for leprosy; it is helpful in the differential diagnosis of leprosy from other confounding dermatoses (17), and IFN-γ production in response to *M. leprae* antigens has been used as a marker of the presence of cellular immune responses against bacilli (49–53). Cassirer-Costa and colleagues (2017) (16) have demonstrated increased IFN-γ, IL-6 and IL-10 serum levels in MDT-treated MB patients, but we did not observe significant differences in the sera from LL patients at onset or MDT release. After treatment, increased IFN-γ levels were observed in supernatants from both non-stimulated and *M. leprae*-stimulated cells. The increased production of IFN-γ might be due to Clofazimine, since previous studies have demonstrated that it induces IFN-γ in the cells of treated patients (54, 55). In addition, we cannot exclude the possibility

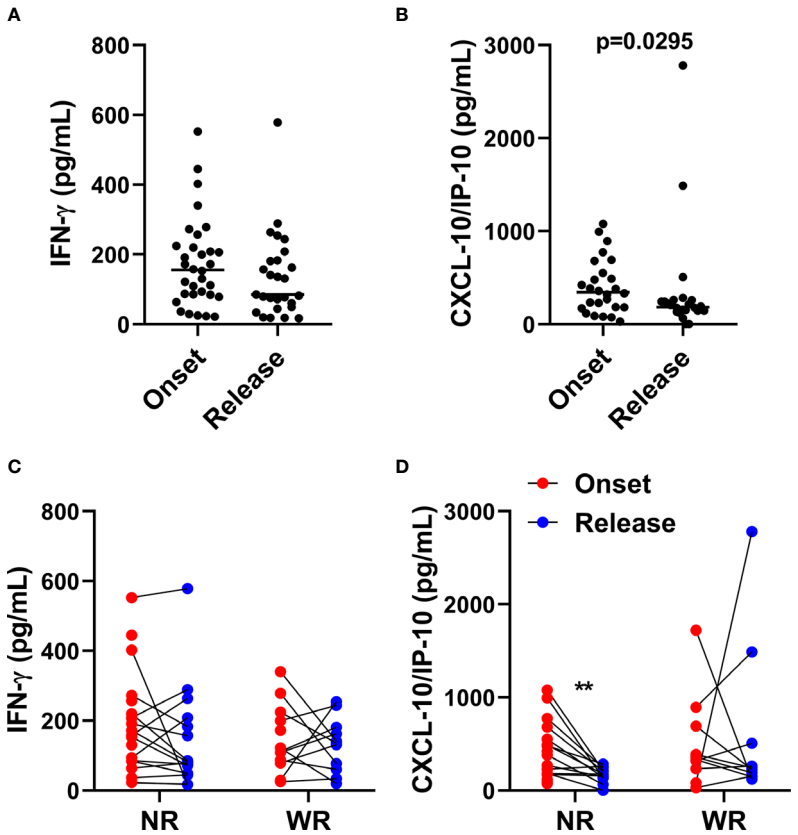

FIGURE 4 | CXCL10 (IP-10) production is associated with reduction of bacilloscopic index at 12-dose MDT release. Anticoagulant-free venous blood samples were collected at LL diagnosis (onset) and at completion of 12 doses of MDT (release), and the sera was aliquoted. Levels of IFN-γ and CXCL10 (IP-10) in the sera were evaluated by ELISA. **(A, B)** Graphs show: IFN-γ **(A)** and CXCL10 (IP-10) **(B)** levels in sera at disease onset and MDT release. **(C, D)** Graphs show: the levels of IFN-γ **(C)** and CXCL10 (IP-10) **(D)** of each patient at disease onset and 12-dose MDT release classified in two groups, one with the patients who presented a reduction in the bacilloscopic index at release (WR, with reduction) and one for the patients who did not reduce the bacilloscopic index after 12-dose MDT (NR, no reduction). **p ≤ 0.01.

that the destruction of bacilli by MDT may result in enhanced antigen presentation due to higher exposure to antigens, including new antigens such as epitopes contained within LID-1, which could lead to the stimulation of effector T cells and IFN-γ production, even in MB patients (17).

CXCL10 (IP-10) is secreted under pro-inflammatory conditions in response to IFN-γ by various cell types, including leukocytes, monocytes, activated neutrophils, epithelial cells, endothelial cells, stromal cells and keratinocytes (56, 57). In PB skin lesion cells, keratinocytes are the major producer of CXCL10 (IP-10), but this is not the case in MB cells; this is probably due to the absence of high levels of IFN-γ (58). CXCL10 (IP-10) induction may also be mediated by TNF (59). CXCL10 exerts its biological functions *via* CXCR3, which is expressed by activated T cells (60) through the induction of paracrine and/or autocrine signaling; it has been identified as an important prognostic indicator for various diseases (61–64). Here, we observed that patients who did not reduce the bacilloscopic index after MDT showed a decrease in CXCL10 (IP-10) sera levels at release, which was not observed in the sera of patients who presented a reduction in bacillary load after 12 doses of MDT; this suggests that higher levels of CXCL-10 are important for the control of bacillary load. In addition, an analysis of cellular immune responses against *M. leprae* antigens revealed that cells from patients who presented a reduction in the bacilloscopic index after the release of MDT increased the production of CXCL10 (IP-10) in response to *M. leprae*.

We acknowledge that the relatively small sample size due the loss of follow-up of some patients represent a limitation of this study. One limitation of our study is that we could not identify the cells associated with the production of CXCL10 at MDT release. Another limitation is that we only recruited volunteers who did not develop a reaction during treatment. Therefore, our future studies will evaluate the impact of immunological reactions on cell phenotype and function after MDT release.

Hungria and colleagues (2018) (35) claim that the applicability of serology in monitoring treatment efficacy seems limited for MB patients with a high bacillary load at diagnosis, especially for those who are evaluated in a short-term follow-up after the conclusion of their treatment. Therefore, the results presented in this study suggest that CXCL10 (IP-10) may be used to evaluate the efficacy of MDT in MB patients.

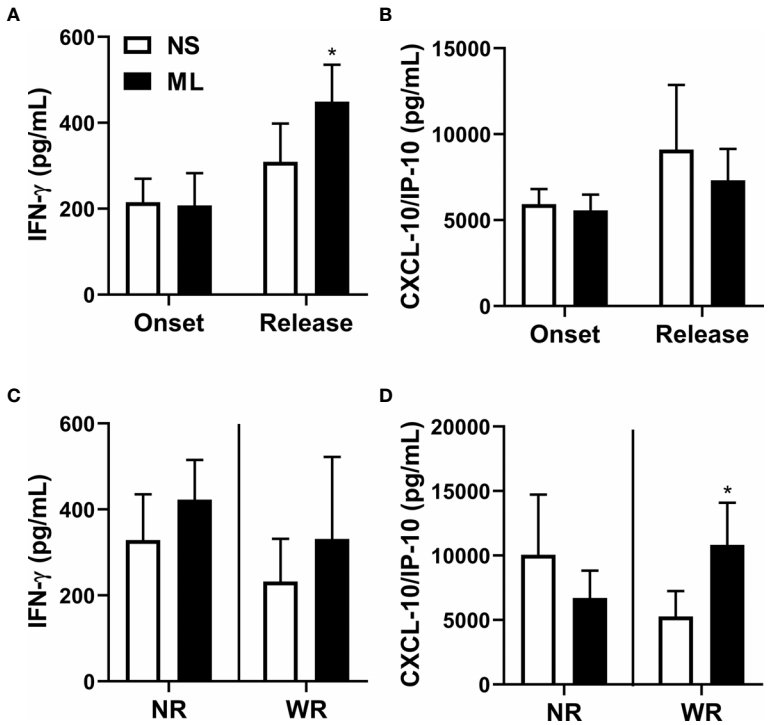

FIGURE 5 | Reduction in bacilloscopic index after 12-dose MDT is associated with increased production of CXCL10 (IP-10). Heparinized venous blood samples were collected at LL diagnosis (onset) and at completion of 12 doses of MDT (release). Whole blood was diluted in AIM-V media and stimulated (ML—stimulated with *M. leprae*) or not (NS—non-stimulated) with 10 μg/mL sonicated *M. leprae* cell antigens for 5 days at 37°C 5% CO_2. Levels of IFN-γ and CXCL10 (IP-10) in the cell culture supernatants were evaluated by ELISA. **(A, B)** Graphs show: Average ± SEM of IFN-γ **(A)** and CXCL10 (IP-10) **(B)** levels in culture supernatant at disease onset and MDT release. **(C, D)** Graphs show: Average ± SEM of the levels of IFN-γ **(C)** and CXCL10 (IP-10) **(D)** at disease onset and at 12-dose MDT release, classified into two groups. The first group contains patients who presented a reduction in the bacilloscopic index at release (WR, with reduction) and the second group comprises patients who did not reduce the bacilloscopic index after 12-dose MDT (NR, no reduction). *$p \leq 0.05$.

DATA AVAILABILITY STATEMENT

The original contributions presented in the study are included in the article/**Supplementary Material**. Further inquiries can be directed to the corresponding author.

ETHICS STATEMENT

The studies involving human participants were reviewed and approved by Oswaldo Cruz Foundation Ethical Committee. The patients/participants provided their written informed consent to participate in this study.

AUTHOR CONTRIBUTIONS

ES, MM, and RP contributed to the design and implementation of the research. HF, MB, and RP contributed to the writing of the manuscript. HF, MM, EO, and MB processed the experimental data and performed the analysis. HF, MM, and RP contributed to the analysis of the results. AS helped with patient care. All authors contributed to the article and approved the submitted version.

FUNDING

We thank CAPES, FAPERJ, and CNPq funding institutions for all their financial support. National Council for Scientific and Technological Development (CNPq) - Finance Code 303834/2017-0. Rio de Janeiro Carlos Chagas Filho Research Foundation (FAPERJ) - Finance Code E-26/010.002231/2019.

ACKNOWLEDGMENTS

We would like to thank all the patients who agreed to participate in this study. We are also grateful to the Souza Araujo Out-Patient Unit team for their support with the patients. Sonicated *M. leprae* was kindly gifted by the NIH Biodefense and Emerging Infections Research Resources Repository, NIAID, NIH.

SUPPLEMENTARY MATERIAL

The Supplementary Material for this article can be found online at: https://www.frontiersin.org/articles/10.3389/fimmu.2021.662307/full#supplementary-material

REFERENCES

1. Nobre M, Illarramendi X, Dupnik KM, Hacker MA, Nery JAC, Jerônimo SMB, et al. Multibacillary Leprosy by Population Groups in Brazil: Lessons From an Observational Study. *PloS Negl Trop Dis* (2017) 11:e0005364. doi: 10.1371/journal.pntd.0005364
2. De Mattos Barbosa MG, da Silva Prata RB, Andrade PR, Ferreira H, de Andrade Silva BJ, da Paixão Oliveira JA, et al. Indoleamine 2,3-Dioxygenase and Iron are Required For*mycobacterium Leprae* Survival. *Microbes Infect* (2017) 19:505–14. doi: 10.1016/j.micinf.2017.06.006
3. Pinheiro RO, Schmitz V, Andrade Silva BJ, Dias AA, de Souza BJ, de Mattos Barbosa MG, et al. Innate Immune Responses in Leprosy. *Front Immunol* (2018) 9:518. doi: 10.3389/fimmu.2018.00518
4. Da Silva Prata RB, De Mattos Barbosa MG, Andrade Silva BJ, Da Paixão Oliveira JA, Bittencourt TL, Pinheiro RO. Macrophages in the Pathogenesis of Leprosy. In: . *Macropahages Activation – Biology and Disease*. United Kingdom: Intech open (2019). p. 1–19. doi: 10.5772/INTECHOPEN.88754IntechOpen
5. Modlin RL. Th1-Th2 Paradigm: Insights From Leprosy. *J Invest Dermatol* (1994) 102(6):828–32. doi: 10.1111/1523-1747.ep12381958
6. Montoya D, Cruz D, Teles RM, Lee DJ, Ochoa MT, Krutzik SR, et al. Divergence of Macrophage Phagocytic and Antimicrobial Programs in Leprosy. *Cell Host Microbe* (2009) 6:343–53. doi: 10.1016/j.chom.2009.09.002
7. Fulco TO, Andrade PR, de Mattos Barbosa MG, Pinto TG, Ferreira PF, Ferreira H, et al. Effect of Apoptotic Cell Recognition on Macrophage Polarization and Mycobacterial Persistence. *Infect Immun* (2014) 82:3968–78. doi: 10.1128/IAI.02194-14
8. de Moura DF, de Mattos KA, Amadeu TP, Andrade PR, Sales JS, Schmitz V, et al. CD 163 Favors *Mycobacterium Leprae* Survival and Persistence by Promoting Anti-Inflammatory Pathways in Lepromatous Macrophages. *Eur J Immunol* (2012) 42:2925–36. doi: 10.1002/eji.201142198
9. Aamir M, Sadaf A, Khan S, Perveen S, Khan A. Recent Advancement in the Diagnosis and Treatment of Leprosy. *Curr Top Med Chem* (2018) 18:1550–58. doi: 10.2174/1568026618666181025100434
10. Polycarpou A, Walker SL, Lockwood DN. New Findings in the Pathogenesis of Leprosy and Implications for the Management of Leprosy. *Cur Op Infect Dis* (2013) 26:413–19. doi: 10.1097/QCO.Ob013e3283638b04
11. Cogen AL, Walker SL, Roberts CH, Hagge DA, Neupane KD, Khadge S, et al. Human Beta-Defensin 3 Is Up-Regulated in Cutaneous Leprosy Type 1 Reactions. *PloS Negl Trop Dis* (2012) 6(11):e1869. doi: 10.1371/journal.pntd.0001869
12. Graham A, Furlong S, Margoles LM, Owusu K, Franco-Paredes C. Clinical Management of Leprosy Reactions. *Infect Dis Clin Pract* (2010) 18:235–8. doi: 10.1097/IPC.0b013e3181deba2a
13. WHO. Global Leprosy Update, 2013; Reducing Disease Burden. *Wkly Epidemiol Rec* (2014) 89(36):389–400.
14. White C, Franco-Paredes C. Leprosy in the 21st Century. *Clin Microbiol Rev* (2015) 28:80–94. doi: 10.1128/CMR.00079-13
15. Moubasher AEA, Kamel NA, Zedan H, Raheem DEA. Cytokines in Leprosy, I. Serum Cytokine Profile in Leprosy. *Int J Dermatol* (1998) 37(10):733–40. doi: 10.1046/j.1365-4362.1998.00381.x
16. Cassirer-Costa F, Medeiros NI, Chaves AT, Lyon S, Coelho-dos-Reis JGA, Ribeiro- Junior AF, et al. Cytokines as Biomarkers to Monitoring the Impact of Multidrug Therapy in Immune Response of Leprosy Patients. *Cytokine* (2017) 97:42–8. doi: 10.1016/j.cyto.2017.05.020
17. Freitas AA, Oliveira RM, Hungria EM, Cardoso LPV, Sousa ALOM, Costa MB, et al. Alterations to Antigen-Specific Immune Responses Before and After Multidrug Therapy of Leprosy. *Diag Microbiol Infect Dis* (2015) 83:154–61. doi: 10.1016/j.diagmicrobio.2015.06.021
18. Ren YR, Pan F, Parvez S, Fleig A, Chong CR, Xu J, et al. Clofazimine Inhibits Human Kv1.3 Potassium Channel by Perturbing Calcium Oscillation in T Lymphocytes. *PloS One* (2008) 3:e4009. doi: 10.1371/journal.pone.0004009
19. Mu X, Ubagai T, Kikuchi-Ueda T, Tansho-Nagakawa S, Nakano R, Kikuchi H, et al. Effects of Erythromycin and Rifampicin on Immunomodulatory Gene Expression and Cellular Function in Human Polymorphonuclear Leukocytes. *Chemotherapy* (2013) 59(6):395–401. doi: 10.1159/000358818
20. Debol SM, Herron MJ, Nelson RD. Anti-Inflammatory Action of Dapsone: Inhibition of Neutrophil Adherence is Associated With Inhibition of Chemoattractant-Induced Signal Transduction. *J Leukoc Biol* (1997) 62(6):827–36. doi: 10.1002/jlb.62.6.827
21. Suda T, Suzuki Y, Matsui T, Inoue T, Niide O, Yoshimaru T, et al. Dapsone Suppresses Human Neutrophil Superoxide Production and Elastase Release in a Calcium-Dependent Manner. *Brit J Dermatol* (2005) 152:887–95. doi: 10.1111/j.1365-2133.2005.06559.x
22. Macedo CS, Anderson DM, Pascarelli BM, Spraggins JM, Sarno EM, Schey KL, et al. Maldi Imaging Reveals Lipid Changes in the Skin of Leprosy Patients Before and After Multidrug Therapy (MDT). *J Mass Spectrom* (2015) 50:1374–85. doi: 10.1002/jms.3708
23. Ridley DS, Jopling WH. Classification of Leprosy According to Immunity. A Five Groups System. *Int J Lepr Other Mycobact Dis* (1966) 34(3):255–73.
24. De Souza Sales J, Lara FA, Amadeu TP, de Oliveira Fulco T, da Costa Nery JA, Sampaio EP, et al. The Role of Indoleamine 2,3-Dioxygenase in Lepromatous Leprosy Immunosuppression. *Clin Exp Immunol* (2011) 165:251–63. doi: 10.1111/j.1365-2249.2011.04412.x
25. Massone C, Belachew WA, Schettini A. Histopathology of Lepromatous Skin Biopsy. *Clin Dermatol* (2015) 33(1):38–45. doi: 10.1016/j.clindermatol.2014.10.003
26. Ridley DS. Histological Classification and the Immunological Spectrum of Leprosy. *Bull World Health Organ* (1974) 51:451–65.
27. Job CK. Pathology of Leprosy. In: RC Hastings, editor. *Leprosy*, *2nd*. Edinburgh: Churchill Livingstone (1994). p. 93–224.
28. Massone C. Histopathology of the Skin. In: E Nunzi, C Massone, editors. *Leprosy, a Practical Guide*. Berlin: Springer (2012). p. 115–36.
29. Attia EAS, Abdallah M, El-Khateeb E, Saad AA, Lotfi RA, Abdallah M, et al. Serum Th17 Cytokines in Leprosy: Correlation With Circulating $CD4^+$ $CD25^{High}$ $FoxP3^+$ T-Reg Cells, as Well as Down Regulatory Cytokines. *Arch Dermatol Res* (2014) 306:793–801. doi: 10.1007/s00403-014-1486-2
30. De Sousa JR, Sotto MN, Quaresma JAS. Leprosy As a Complex Infection: Breakdown of the Th1 and Th2 Immune Paradigm in the Immunopathogenesis of the Disease. *Front Immunol* (2017) 8:1635. doi: 10.3389/fimmu.2017.01635
31. Santos DF, Mendonça MR, Antunes DE, Sabino EFP, Pereira RC, Goulart LR, et al. Revisiting Primary Neural Leprosy: Clinical, Serological, Molecular and Neurophysiological Aspects. *PloS Negl Trop Dis* (2017) 11(11):e0006086. doi: 10.1371/journal.pntd.0006086
32. Froes LAR Jr., Trindade MAB, Sotto MN. Immunology of Leprosy. *Int Rev Immunol* (2020) 39:1–21. doi: 10.1080/08830185.2020.1851370
33. WHO, World Health Organization. *MDT: Duration of Treatment FAQ* (2020). Available at: https://www.who.int/lep/mdt/duration/en/ (Accessed December 15, 2020).
34. Bittencourt TL, Da Silva Prata RB, De Andrade Silva BJ, De Mattos Barbosa MG, Dalcomo MP, Pinheiro RO. Autophagy as a Target for Drug Development of Skin Infection Caused By Mycobacteria. *Front Immunol* (2021) 12:674241. doi: 10.3389/fimmu.2021.674241
35. Hungria EM, Bührer-Sékula S, Oliveira RM, Aderaldo LC, Pontes MAA, Cruz R, et al. *Mycobacterium Leprae*-Specific Antibodies in Multibacillary Leprosy Patients Decrease During and After Treatment With Either the Regular 12 Doses Multidrug Therapy (MDT) or the Uniform 6 Doses MDT. *Front Immunol* (2018) 9:915. doi: 10.3389/fimmu.2018.00915
36. Montoya D, Modlin RL. Learning From Leprosy: Insight Into the Human Innate Immune Response. *Adv Immunol* (2010) 105:1–24. doi: 10.1016/S0065-2776(10)05001-7
37. Novak ML, Koh TJ. Macrophage Phenotypes During Tissue Repair. *J Leukoc Biol* (2013) 93(6):875–81. doi: 10.1189/jlb.1012512
38. Mosser DM, Edwards JP. Exploring the Full Spectrum of Macrophage Activation. *Nat Rev Immunol* (2008) 8:958–69. doi: 10.1038/nri2448
39. Shearer JD, Richards JR, Mills CD, Caldwell MD. Differential Regulation of Macrophage Arginine Metabolism: A Proposed Role in Wound Healing. *Am J Physiol* (1997) 272:E181–90. doi: 10.1152/ajpendo.1997.272.2.E181
40. Brancato SK, Albina JE. Wound Macrophages As Key Regulators of Repair: Origin, Phenotype and Function. *Am J Pathol* (2011) 178:19–25. doi: 10.1016/j.ajpath.2010.08.003
41. Jansen A, Lewis S, Cattel V, Cook T. Arginase is a Major Pathway of L-Arginine Metabolism in Nephritic Glomeruli. *Kidney Int* (1992) 42(5):1107–12. doi: 10.1038/ki.1992.394

42. Munder M, Molinedo F, Calafat J, Canchado J, Gil-Lamaignere C, Fuentes JM, et al. Arginase I is Constitutively Expressed in Human Granulocytes and Participates in Fungicidal Activity. *Blood* (2005) 105:2549–56. doi: 10.1182/blood-2004-07-2521
43. Raes G, Van den Berg R, De Baetselier P, Ghassabeh GH. Arginase-1 and Ym1 Are Markers for Murine, But Not Human, Alternatively Activated Myeloid Cells. *J Immunol* (2005) 174:6561. doi: 10.4049/jimmunol.174.11.6561
44. Kämpfer H, Pfeilschifter J, Frank S. Expression and Activity of Arginase Isoenzymes During Normal and Diabetes-Impaired Skin Repair. *J Invest Dermatol* (2003) 12:1544–51. doi: 10.1046/j.1523-1747.2003.12610.x
45. Witte MB, Barbul A, Schick MA, Vogt N, Becker HD. Upregulation of Arginase Expression in Wound-Derived Fibroblasts. *J Surg Res* (2002) 105:35–42. doi: 10.1006/jsre.2002.6443
46. Miao M, Niu Y, Xie T, Yuan B, Qing C, Lu S. Diabetes-Impaired Wound Healing and Altered Macrophage Activation: A Possible Pathophysiologic Correlation. *Wound Rep Reg* (2012) 20:203–13. doi: 10.1111/j.1524-475X.2012.00772.x
47. Singer AJ, Clark RA. Cutaneous Wound Healing. *N Eng J Med* (1999) 341:738–46. doi: 10.1056/NEJM199909023411006
48. Albina JE. On the Expression of Nitric Oxide Synthase By Human Macrophages. Why No No? *J Leukoc Biol* (1995) 58:643–9. doi: 10.1002/jlb.58.6.643
49. Shinde SR, Chiplunkar SV, Butlin R, Samson PD, Deo MG, Gangal SG. Lymphocyte Proliferation, IFN-Gamma Production and Limiting Dilution Analysis of T-Cell Responses to ICRC and *Mycobacterium Leprae* Antigens in Leprosy Patients. *Int J Lepr Other Mycobac Dis* (1993) 61:51–8.
50. Lima MC, Pereira GM, Rumjanek FD, Gomes HM, Duppre N, Sampaio EP, et al. Immunological Cytokine Correlates of Protective Immunity and Pathogenesis in Leprosy. *Scand J Immunol* (2000) 5:419–28. doi: 10.1046/j.1365-3083.2000.00703.x
51. Kamble RR, Shinde VS, Madhale SP, Jadhav RS. Study of Cytokine Response Against Panel of Purified Mycobacterium Leprae Antigens By Using Whole Blood Assay in Subjects Residing in a Resettlement Village of Cured Leprosy Patients. *Indian J Lepr* (2010) 82:23–31.
52. Geluk A, Bobosha K, van der Ploe-van Schipp JJ, Spencer JS, Banu S, Martins MV, et al. Newbiomarkers With Relevance to Leprosy Diagnosis Applicable in Areas Hyperendemic for Leprosy. *J Immunol* (2012) 188:4782–91. doi: 10.4049/jimmunol.1103452
53. Geluk A, van Meijgaarden KE, Wilson L, Bobosha K, van der Ploeg-van Schipp JJ, Van denEeden SJ, et al. Longitudinal Immune Responses and Gene Expression Profiles in Type 1 Leprosy Reactions. *J Clin Immunol* (2014) 34:245–55. doi: 10.1007/s10875-013-9979-x
54. Degang Y, Akama T, Hara T, Tanigawa K, Ishido Y, Gidoh M, et al. Clofazimine Modulates the Expression of Lipid Metabolism Proteins in*Mycobacterium Leprae*-Infected Macrophages. *PloS Negl Trop Dis* (2012) 6(12):e1936. doi: 10.1371/journal.pntd.0001936
55. Parak RB, Wadee A. The Synergistic Effects of Gamma Interferon and Clofazimine on Pahgocyte Function: Restoration of Inhibition Due to a 25 Kilodalton Fraction From Mycobacterium Tuberculosis. *Biotherapy* (1991) 3 (3):265–72. doi: 10.1007/BF02171691
56. Luster AD, Ravetech JV. Biochemical Characterization of a Gamma-Interferon-Inducible Cytokine (IP-10). *J Exp Med* (1987) 166:1084–97. doi: 10.1084/jem.166.4.1084
57. Dyer KD, Percopo CM, Fisher ER, Gabryszewski SJ, Rosenberg HF. Pneumoviruses Infect Eosinophils and Elicit MyD88-Dependent Release of Chemoattractant Cytokines and Interleukin-6. *Blood* (2009) 114:2649–56. doi: 10.1182/blood-2009-01-199497
58. Kaplan G, Luster AD, Hancock G, Cohn ZA. The Expression of a Gamma-Interferon-Induced Protein (IP-10) in Delayed Immune Responses in Human Skin. *J Exp Med* (1987) 166:1098–108. doi: 10.1084/jem.166.4.1098
59. Tamaru M, Tominaga Y, Yatsunami K, Narumi S. Cloning of the Murine Interferon-Inducible Protein(IP-10) and its Specific Expression in Lymphoid Organs. *Biochem Biophys Res Commun* (1998) 251:41–8. doi: 10.1006/bbrc.1998.9404
60. Loetscher M, Gerber B, Loetscher P, Jones SA, Piali L, Clark-Lewis I, et al. Chemokine Receptor Specific for IP-10 and Mig: Structure, Function and Expression in Activated T-Lymphocytes. *J ExpMed* (1996) 184:963–9. doi: 10.1084/jem.184.3.963
61. Lo BKK, Yu M, Zlot D, Cowan B, Shapiro J, McElwee KJ. CXCR-3/Ligands are Significantly Involved in the Tumorigenesis of Basal Cell Carcinomas. *Am J Pathol* (2010) 176:2435–46. doi: 10.2353/ajpath.2010.081059
62. Liu M, Guo S, Hibbert JM, Jain V, Singh N, Wilson NO, et al. CXCL10/IP-10 in Infectious Diseases Pathogenesis and Potential Therapeutic Implications. *Cytokine Growth Factor Rev* (2011) 22(3):121–30. doi: 10.1016/j.cytogfr.2011.06.001
63. Kelsen SG, Aksoy MO, Yang Y, Shahabuddin JL, Safadi F, Rogers TJ. The Chemokine Receptor CXCR3 and its Splice Variant Are Expressed in Human Airway Epithelial Cells. *Am J Physiol Lung Cell Mol Physiol* (2004) 287:L584–91. doi: 10.1152/ajplung.00453.2003
64. Ferrari SM, Fallahi P, Ruffilli I, Elia G, Ragusa F, Paparo SR, et al. Immunomodulation of CXCL10 Secretion by Hepatitis C Vírus: Could CXCL10 Be a Prognostic Marker of Chronic Hepatitis C? *J Immunol Res* (2019) 2019:5878960. doi: 10.1155/2019/5878960

Conflict of Interest: The authors declare that the research was conducted in the absence of any commercial or financial relationships that could be construed as a potential conflict of interest.

frontiers in Immunology

ORIGINAL RESEARCH
published: 26 August 2021
doi: 10.3389/fimmu.2021.695373

Identification of Genes Encoding Antimicrobial Proteins in Langerhans Cells

*Aislyn Oulee[1], Feiyang Ma[1,2,3], Rosane M. B. Teles[1], Bruno J. de Andrade Silva[1], Matteo Pellegrini[3], Eynav Klechevsky[4], Andrew N. Harman[5,6], Jake W. Rhodes[5,6] and Robert L. Modlin[1,2]**

[1] Division of Dermatology, Department of Medicine, University of California, Los Angeles, Los Angeles, CA, United States, [2] Department of Microbiology, Immunology and Molecular Genetics, University of California, Los Angeles, Los Angeles, CA, United States, [3] Department of Molecular, Cell and Developmental Biology, University of California, Los Angeles, Los Angeles, CA, United States, [4] Department of Pathology and Immunology, Washington University School of Medicine, St. Louis, MO, United States, [5] Centre for Virus Research, The Westmead Institute for Medical Research, Westmead, NSW, Australia, [6] School of Medical Sciences, Faculty of Medicine and Health Sydney, The University of Sydney, Westmead, NSW, Australia

OPEN ACCESS

Edited by:
Fatima Conceição-Silva, Oswaldo Cruz Foundation, Brazil

Reviewed by:
Patrick M. Brunner, Medical University of Vienna, Austria
Yingping Xu, Southern Medical University, China
Marta Ewa Polak, University of Southampton, United Kingdom

***Correspondence:**
Robert L. Modlin
rmodlin@mednet.ucla.edu

Specialty section:
This article was submitted to Microbial Immunology, a section of the journal Frontiers in Immunology

Received: *14 April 2021*
Accepted: *06 August 2021*
Published: *26 August 2021*

Citation:
Oulee A, Ma F, Teles RMB, de Andrade Silva BJ, Pellegrini M, Klechevsky E, Harman AN, Rhodes JW and Modlin RL (2021) Identification of Genes Encoding Antimicrobial Proteins in Langerhans Cells. Front. Immunol. 12:695373. doi: 10.3389/fimmu.2021.695373

Langerhans cells (LCs) reside in the epidermis where they are poised to mount an antimicrobial response against microbial pathogens invading from the outside environment. To elucidate potential pathways by which LCs contribute to host defense, we mined published LC transcriptomes deposited in GEO and the scientific literature for genes that participate in antimicrobial responses. Overall, we identified 31 genes in LCs that encode proteins that contribute to antimicrobial activity, ten of which were cross-validated in at least two separate experiments. Seven of these ten antimicrobial genes encode chemokines, *CCL1, CCL17, CCL19, CCL2, CCL22, CXCL14* and *CXCL2*, which mediate both antimicrobial and inflammatory responses. Of these, *CCL22* was detected in seven of nine transcriptomes and by PCR in cultured LCs. Overall, the antimicrobial genes identified in LCs encode proteins with broad antibacterial activity, including against *Staphylococcus aureus*, which is the leading cause of skin infections. Thus, this study illustrates that LCs, consistent with their anatomical location, are programmed to mount an antimicrobial response against invading pathogens in skin.

Keywords: Langerhans cells, dendritic cells, antimicrobial peptides, immunity, skin, transcriptome, bioinformatics

INTRODUCTION

Dendritic cells (DCs) are the key antigen presenting cells (APCs) that control both immunity and tolerance (1). DCs are localized in most tissues and surface barriers, where they function as sentinels for pathogen recognition. Stimulation of innate signaling receptors induce DCs to migrate from the periphery to secondary lymphoid organs, where they present antigens that drive adaptive immunity. DCs are divided into distinct subsets characterized by their unique expression of surface receptors and transcription factors, pathogen sensors and cytokines secretion profiles that contribute to their specialized capacities in activating different modules of immunity (2–6).

Human skin harbors multiple types of dendritic-appearing cells including Langerhans cells (LCs) that exclusively reside in the epidermis as well as conventional DCs (cDCs) in the underlying dermis. In addition to their localization to the epidermis, LCs are distinguished by their high expression of CD1a, the C-type lectin langerin (CD207) which induces the formation of a LC-specific organelle, the Birbeck granule, and lower expression of CD11c than dermal DCs (7). Through their dendrites, they form an extensive cellular network patrol the interface between the skin and the outside environment for pathogens (8–10), bind microbial ligands *via* toll-like receptors (TLRs) and CD207 and taking up pathogens *via* endocytosis (11–13).

LCs, although derived in mice from similar precursors as macrophages, have antigen presentation capacities similar to DCs (14, 15). Upon antigen capture, LCs undergo phenotypic changes during maturation and migrate to regional lymph nodes where they activate adaptive responses (12, 16–18). During infection, LC emigration from the epidermis is significantly enhanced by inflammatory cytokines such as IL-1 and TNF (19, 20). Migrating LCs express the DC-specific transcription factor ZBTB46 (21, 22), IL-15 (23) and IRF4, which is important for their ability to prime and cross-present antigens to $CD8^+$ T cells at that site (24, 25). Additionally, LCs enhances cellular immunity by inducing Th1 and Th2 differentiation of $CD4^+$ T cells (3, 4), they are the main skin DC subset responsible for directing IL-17 and IL-22-mediated responses (12, 26, 27), indicative of skin inflammatory and antimicrobial diseases. A subset of migratory LCs express CD5 with an even greater capacity to amplify these T cell responses (6). Moreover, a unique aspect of human LC is their ability to present antigen *via* CD1a both autoreactive (28, 29) and *Mycobacterium leprae*- and *M. tuberculosis*-reactive CD1a-restricted T cell responses have been reported (30).

Although it has been previously shown that LCs contribute to cutaneous host defense against pathogens including viruses (13, 31, 32), bacteria and fungi (33), only a few genes have been identified that directly mediate the antimicrobial response. In order to more broadly define the mechanisms by which LCs potentially contribute to an antimicrobial response, we mined public LC transcriptomes and surveyed the literature to identify "antimicrobial genes", defined as genes encoding proteins with direct antimicrobial activity.

MATERIALS AND METHODS

Gene Expression Omnibus (GEO) Analysis

We surveyed Gene Expression Omnibus (GEO) (34) for transcriptomes of human skin-derived LCs and Langerhans-like dendritic cells (LCDCs), which are derived from $CD34^+$ stem cells, using the key terms "(Langerhans AND skin) AND Homo sapiens[Organism]". Our search was for the period before August 2020 and include those studies in which the LCs were activated with pro-inflammatory stimuli and/or as compared to other myeloid populations. This search yielded 24 series, nine of which met the criteria that $n \geq 3$ samples for the LC and comparison group and did not contain only Langerhans cell histiocytosis samples. We then used GEO2R, an R-based web application, to obtain a list of genes that were differentially expressed in LCs. After obtaining the list of genes, we then filtered the comparisons by logFC>1 and adj. p-value<0.05. Of the nine series which the described criteria, one (GSE32648) did not yield any recognizable gene names on GEO2R and therefore we contacted the authors who provided us with their new RNA-seq data instead of the microarray data currently deposited in GEO2R and for a second dataset (GSE120386), GEO2R was not available. We used DESeq2 to run differential expression analysis of both of the bulk RNA-seq data with the default parameters. Genes with an adj. p value <0.05 were considered significantly differentially expressed.

LC Antimicrobial Genes

We curated our direct antimicrobial list based on the 105 antimicrobial peptides listed in the Antimicrobial Peptide Database (APD) (35). The criteria for data registration into APD are the following: the peptides must be from natural sources, their antimicrobial activities must have been demonstrated (MIC <100 ug/ml), and their amino acid sequences elucidated. We also supplemented this list with literature findings of eight genes encoding peptides with direct antimicrobial activity not yet registered into the database including *CCL2* (36), *CCL14*, *CCL15* (37), *CXCL7* (38), *CXCL17* (39), *MPEG1* (40), *S1008A* (41), and *S1009A* (42) yielding a total of 113 genes. To identify which genes encoded peptides with direct antimicrobial activity, we overlapped the results with our curated direct antimicrobial list using Venny 2.1 (43).

We also reviewed the literature for direct antimicrobial genes using the key terms "(Langerhans [Title/Abstract]) AND (antimicrobial [Title/Abstract])" which yielded 40 results of which five studies contained evidence for eight genes encoding peptides with direct antimicrobial activity in LCs. Our search "(Langerhans [Title/Abstract]) AND (antibacterial [Title/Abstract])" yielded 21 results, none of which included genes encoding peptides with direct antimicrobial in LCs.

Ingenuity Pathway Analysis (IPA) Upstream Regulator Prediction

IPA Upstream Regulator Analysis was used to identify upstream regulators and predict whether they are activated or inhibited, given the observed gene expression changes in our experimental dataset. The analysis examines the known targets of each upstream regulator in a dataset, compares the targets' actual direction of change to expectations derived from the literature, then generates a prediction for each upstream regulator. Briefly, IPA uses an 'enrichment' score [Fisher's exact test (FET) P-value] that measures the overlap of observed and predicted regulated gene sets.

RESULTS

Identification and Characteristics of Langerhans Cells Transcriptomes

To identify potential mechanisms by which LCs mount an antimicrobial response, we queried GEO and identified seven

microarray series that permitted the mining of the LC transcriptome data using GEO2R. In addition, there was one bulk RNA-seq series for which GEO2R was not available (GSE120386) and another bulk-RNA seq data series not yet deposited in GEO2R and therefore we used DESeq2 on RStudio to compute the differential gene expression for both data series (**Supplementary Table S1**).

In three of nine series, LCs were directly isolated from skin specimens by enzymatic digestion, and the transcriptomes measured immediately. In one study, $CD11c^+$ DDCs were directly isolated from skin and monocyte derived DCs and $CD1c^+$ DCs from blood (44). In another study, plasmacytoid DCs (pDCs) and myeloid DCs (mDCs) were isolated from peripheral blood (45), and in the third study, pDCs were isolated from spleen and dermal macrophages from skin (46). Five of the nine transcriptomes were derived from LCs isolated by migration, in order to represent those LCs that are in the process of migration to lymph nodes, albeit this leads to an altered phenotype. In one study each, $CD14^+$ DCs and $CD14^+$ macrophages (47), or $CD141^+$ dermal DCs, $CD14^+$ dermal DCs, and $CD141^-CD14^-$ dermal DCs (21), or dermal $langerin^-$ type 2 conventional dendritic cell (cDC2), dermal $langerin^+$ cDC2, dermal $CD14^+CD1c^-$ monocyte-derived macrophages, and dermal $CD14^+CD1c^+$ monocyte-derived dendritic cells (48) were isolated from skin by enzymatic digestion. In two of the migratory LC studies, the LC transcriptomes were measured at time zero and various timepoints following stimulation by TNF at (24, 49). In the same transcriptome, $CD11c^+$ dermal DCs were also isolated by migration (49). In the last series, Langerhans-like dendritic cells (LCDCs) were generated *in vitro* and infected with the live mosquito-derived third-stage larvae (L3) of the parasitic nematode *Brugia malayi* (50).

Identification of Antimicrobial Genes in LCs

We mined the LC transcriptomes by comparing either LCs to another myeloid cell type or a specific time point following stimulation. We filtered the comparisons by logFC>1 and adjusted p-value <0.05, then overlapped the results with the direct antimicrobial gene list consisting of 113 genes using Venny 2.1 (43). Using this approach, we identified 23 genes encoding proteins with direct antimicrobial activity in the LC transcriptomes (**Table 1**). Of these 23 genes, 11 were uniquely identified in LCs isolated by migration (then either unstimulated or cytokine activated), nine were uniquely identified in LCs derived from digested skin samples and three were presented in LCs isolated by migration as well as from digested skin samples. Although there were more genes identified in LCs obtained by migration from skin samples as compared to digested skin samples, as LCs isolated by enzymatic digestion are immature compared to those isolated by migration which are in a mature state, and that the migrated LCs were sometimes activated with cytokines whereas the digested LCs were not (55).

Antimicrobial Genes Upregulated in Activated LCs and in LCs Compared to Other Cell Types

We examined the transcriptomes of LCs activated *in vitro* by cytokines or microbes. We identified eight genes that encode proteins with direct antimicrobial activity by mining the two transcriptomes of TNF-activated migratory LCs (Transcriptomes 4 and 7), this was the greatest number in any of the comparisons performed (**Supplementary Table S2**). There were six genes encoding chemokines that were upregulated in migratory LCs after stimulation with TNF: *CCL1, CCL2, CCL17, CCL19, CCL20*, and *CXCL2*. In addition, we detected two other genes, *ADM* and *IL26* in LCs stimulated with TNF (**Figure 1**). Of the eight total genes, *CCL2*, *CCL19* and *ADM* were detected in both transcriptomes of TNF treated LCs. We did not identify any genes encoding peptides with direct antimicrobial genes upregulated in LCs stimulated with live mosquito-derived third-stage larvae (L3) of *B. malayi*, which is consistent with the previous finding that the live mosquito-derived third-stage larvae (L3) fails to activate LCs compared to known activators (50). By analyzing the comparisons of LCs to other cell types, we identified 16 antimicrobial genes, of which only *ADM* was identified in the transcriptomes of TNF treated LCs.

We found nine studies in which the LC transcriptome was compared to other DC subtypes, including dermal DCs, peripheral blood DCs and cytokine-derived DCs, as well as to macrophage subpopulations. The nomenclature used to define DC subpopulations has evolved with changing technologies, such that different studies use different markers to define subpopulations. Dermal DCs have been identified based on the expression of various cell surface markers including $XCR1^+$, $CD141^+$, $CD1c^+$, $CD1a^+$ and $CD14^+$ (3, 21, 47, 56–58), which may vary according to the method of isolation, digestion vs. migration (55). The analysis of DC subpopulations in human blood by single cell RNA sequencing has led to a revised gene-based classification (59). In reporting the comparison of transcriptomes in LCs to other cell types, we have maintained the nomenclature in the original citation.

In comparing LCs to other DC and myeloid cell types, *CCL22* was the most frequently detected gene, expressed in seven of the nine studies and in eight separate comparisons (**Figure 2**). *CXCL14* was detected as upregulated in six instances in three LCs transcriptomes (**Figure 3**). *B2M* was identified in the transcriptomes of LCs compared to other cell types in three different instances (**Supplementary Figure S1**). *GAPDH* was more highly expressed in LCs in two different transcriptomes (**Supplementary Figure S2**). *CCL27*, *DEFB1, FURIN, LEAP2, SNCA*, and *S100A7* were each identified as preferentially expressed in LCs in two instances but always in a single LC transcriptome as compared to other cell types (**Supplementary Table S3**). *HMGN2* was preferentially expressed in LCs compared to $CD141^+$ and $CD141^-CD14^-$ dermal DCs in one transcriptome (**Supplementary Figure S3**). *SAA2, FAM3A*, and

TABLE 1 | Identification of genes encoding peptides with antimicrobial activity in LCs in transcriptome studies.

Genes	Multiple transcriptomes			Identified in the literature in non-transcriptome studies	References	Total instances identified
	Number of transcriptome studies	Number of transcriptome comparisons	Comparisons			
CCL22	6	7	LCs vs pDCs (T2, T8), LCs vs CD11c+ dermal DCs (T4), LCs vs dermal MΦ (T5), LCs vs CD14+ dermal DCs (T6), LCs vs CD14+ CD1c- monocyte-derived MΦ (T9) and LCs vs monocyte-derived CD14+CD1c +DCs (T9)	1	[Ross et al. (51)]	8
CXCL14	3	6	LCs vs CD1c+ mDCs (T1 and T2), LCs vs pDCS (T2), LCs vs Dermal langerin- cDC2 (T9), LCs vs CD14+ CD1c-monocytederived MΦ (T9) and LCs vs monocyte- derived CD14+CD1c+DCs (T9)	0	N/A	6
ADM	3	4	LCs vs CD1c+ mDCs (T2), LCs vs pDCS (T2), LCs 2h vs 0h (T4, T7)	0	N/A	4
CCL20	2	4	LCs vs moDCs (T1), LCs vs blood CD1c+ mDCs (T1), LCs at 2h vs 0h (T7), LCs 24h vs 0h (T7)	0	N/A	4
B2M	2	3	LCs vs CD1c+ mDCs (T2), LCs vs CD141+ dermal DCs (T6), LCs vs CD14+ dermal DCs (T6)	0	N/A	3
CCL17	1	2	LCs 24h vs 0h (T4), LCs 8h vs 0h (T4)	1	[Alferink et al. (52)]	3
CCL19	2	3	LCs 8h vs 0h (T4), LCs 24h vs 0h (T4, T7)	0	N/A	3
CXCL2	2	2	LCs vs blood $CD1c^+$ mDCs (T1), LCs 2h vs 0h (T7)	1	[Heufler et al. (53)]	3
CCL1	1	1	LCs 24h vs 0h (T4)	1	[Schaerli et al. (54)]	2
CCL2	2	2	LCs 24h vs 0h (T4 and T7)	0	N/A	2
CCL27	1	2	LCs vs moDCs (T1), LCs vs blood CD1c+ mDCs (T1), LCs 24h vs 0h, LCs 8h vs 0h (T4)	0	N/A	2
DEFB1	1	2	LCs vs moDCs (T1), LCs vs blood CD1c+ mDCs (T1)	0	N/A	2
FURIN	1	2	LCs vs pDCs (T8), LCs vs MΦ (T8)	0	N/A	2
GAPDH	2	2	LCs vs pDCs (T2 and T8)	0	N/A	2
HMGN2	1	2	LCs vs CD141+ Dermal DCs (T6), LCs vs CD141-CD14- DCs (T6)	0	N/A	2
LEAP2	1	2	LCs vs Dermal CD14+ CD1c+ DCs (T9), LCs vs Dermal Langerin+ cDC2 (T9)	0	N/A	2
S1007A	1	2	LCs vs moDCs (T1), LCs vs blood CD1c+ mDCs (T1)	0	N/A	2
SNCA	1	2	LCs vs moDCs (T1), LCs vs blood CD1c+ mDCs (T1)	0	N/A	2

By mining publicly available data in GEO DataSets, we were able to identify 23 genes encoding antimicrobial peptides that are more strongly expressed in LCs vs. other DC subtypes and/or in LCs activated with cytokines vs. LCs with no activation. N/A, Not applicable.

RARRES2 were identified as upregulated in LCs in one instance each. Heat maps showing the expression of each gene in the different transcriptome comparisons are shown in **Supplementary Figures 4–6**.

Antimicrobial Genes in LCs Identified in the Literature

We found corroborating evidence in the literature that four of the 23 direct antimicrobial genes were expressed in LCs. These included the *CCL17*-encoded peptide in cytokine activated LCs (52), *CXCL2* mRNA in freshly isolated LCs (53), *CCL22* mRNA during maturation of LCs (51), and the *CCL1*-encoded peptide in epidermal LCs *in situ* (54). We found reports indicating expression of eight genes encoding directly antimicrobial peptides and/or the antimicrobial proteins themselves in activated LCs that were not detected in any of transcriptomes. These include *CXCL9, CXCL10*, *CXCL11* (60), *POMC* (61) and *NPY* (62) mRNAs, as well as *CAMP*, *DEFB4* (33) and *DEFB103* (63, 64) encoded antimicrobial peptides (**Supplementary Table S4**). Thus, a total of 31 antimicrobial genes/proteins were identified in LCs from analysis of LCs transcriptomes and published studies.

Cross-Validation of Antimicrobial Genes

Overall, we found that ten of the 23 antimicrobial genes identified in the LC transcriptomes were cross-validated in at least two separate studies in the nine LC transcriptomes and/or four additional published studies. Six of the ten antimicrobial genes were cross validated by detection in two separate LC transcriptomes each, in each instance comparing LCs to the same other DC or myeloid cell type. *CXCL14* was upregulated in LCs vs. blood CD1c+ DCs (Transcriptomes 1 and 2), *CCL22* and GAPDH in LCs vs pDCs (Transcriptomes 2 and T8), and *B2M* in LCs compared to different DC populations in Transcriptomes 2 and 6. *CCL2* and *CCL19* were each upregulated in LCs treated with TNF for 24 hours vs 0 hours (Transcriptomes 4 and 7). *ADM* was upregulated in LCs treated with TNF for 2 hours vs 0 hours (Transcriptomes 4 and 7) and was also more strongly expressed in LCs vs blood CD1c+ DCs. *CCL22* and *CXCL2* expression was greater in LCs compared to other cell types in seven and two different transcriptomes, respectively, and validated by reverse transcriptase-polymerase chain reaction in additional studies (51, 53).

We also examined which antimicrobial genes were differentially expressed in LCs vs keratinocytes (KCs). We

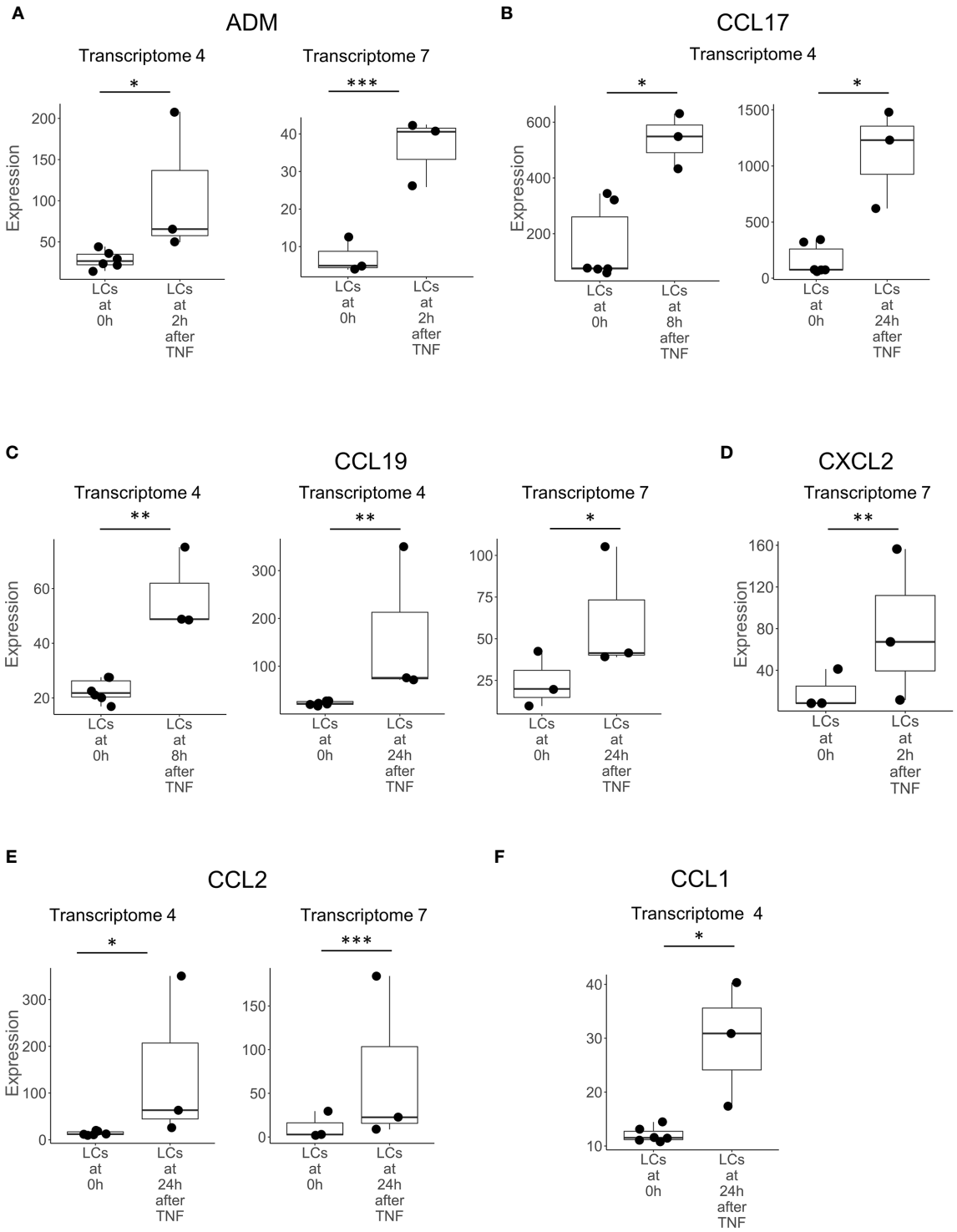

FIGURE 1 | Genes upregulated in LCs after activation with TNF. Boxplots showing the expression of **(A)** *ADM*, **(B)** *CCL17*, **(C)** *CCL19*, **(D)** *CXCL2*, **(E)** *CCL2*, and **(F)** *CCL1*, encoding antimicrobial peptides in LCs prior to (0h) and at various time points following activation with TNF in transcriptomes 4 and 7. Genes shown above were identified in at least two instances, either in multiple transcriptomes experiments or in one transcriptome experiment but also identified in LCs in non-transcriptome experiments in the literature. *$p < 0.05$, **$p < 0.01$, ***$p < 0.001$.

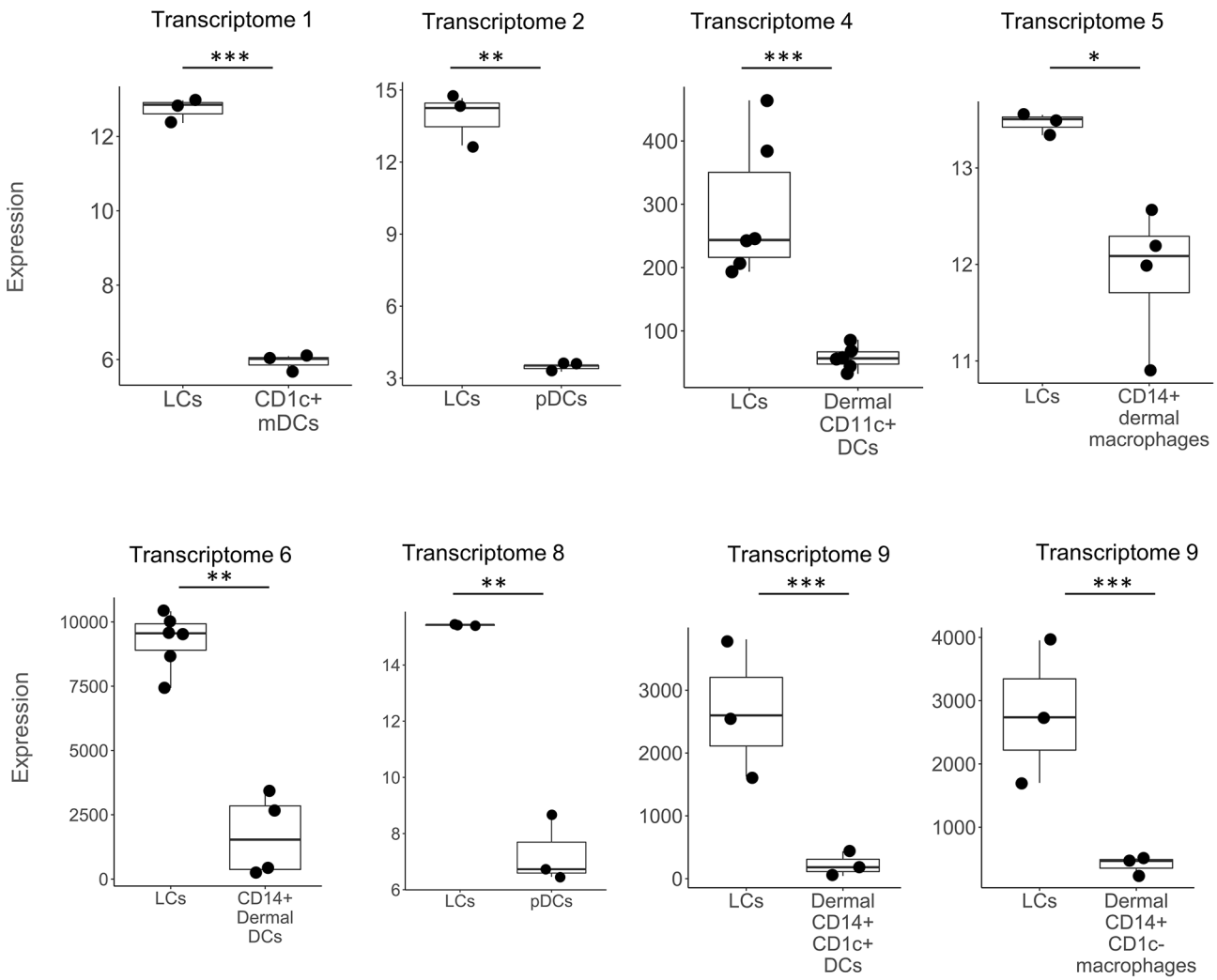

FIGURE 2 | *CCL22* expression in LCs vs other DC subtypes. *CCL22* was preferentially expressed in LCs vs other DC types in 7 out of the 9 transcriptomes in a total of 8 instances. *CCL22* was the most frequently detected gene in transcriptomes and was also previously reported in LCs in non-transcriptome experiments in the literature. *p < 0.05, **p < 0.01, ***p < 0.001.

surveyed GEO DataSets for datasets containing both LCs and KCs using the key terms "Langerhans AND keratinocytes" and found two datasets (GSE168167 and GSE72104), both data sets containing LCs (n=3) and KCs (n=2) although our original criteria required n≥3 for each cell type. We found the expression of *CCL22* was greater in LCs than KCs for both datasets, showing a 6.4- and 3.9-fold change. In one dataset (GSE72104), *CCL17* expression was 4.3-fold greater in LCs than KCs and was identified in transcriptome 4 as being upregulated in LCs by TNF at 8 and 24 hours and validated at the protein level in a reporter mouse (*CCL17*) (52). *CCL1* was identified in a single LC transcriptome upregulated by TNF after 24 hours and the protein validated by immunohistochemistry (*CCL1*) (54).

Using Ingenuity Pathways Analysis, we investigated the canonical pathways in LCs compared to other cell types, focusing on the three "Noah's ark like" instances in which LCs were compared to the identical cell type in two transcriptomic studies. Thus, there were two studies each comparing LCs to pDCs, blood CD1c+ DCs and $CD14^+$ dermal DCs. From the top 100 canonical pathways in each comparison, we identified one pathway present in all six comparisons and 23 in 5/6 comparisons (**Supplementary Table S7**), noting that there were fewer genes and hence pathways identified in LCs vs. CD14+ dermal DCs from Transcriptome 5. Overall, 21/23 pathways were identified as "signaling" pathways, including RANK, CD40, CXCR4, IL6 and IL8 signaling, consistent with the known functional properties of LCs.

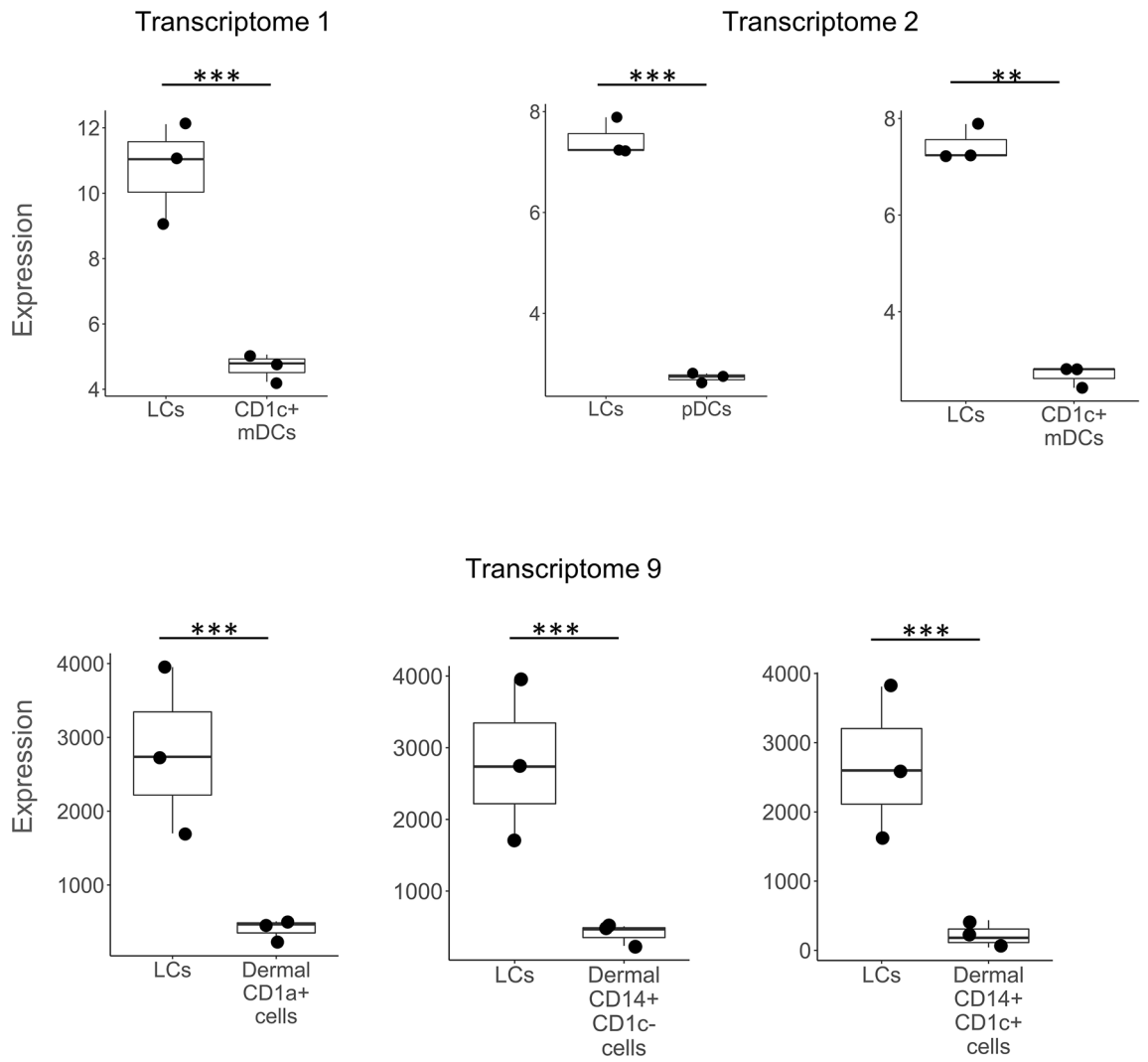

FIGURE 3 | *CXCL14* expression in LCs vs other DC subtypes. *CXCL14* was preferentially expressed in LCs vs other DC types in 3 out of the 9 transcriptomes in a total of 6 different instances. **p < 0.01, ***p < 0.001.

Upstream Regulator Analysis of Genes Encoding Antimicrobial Proteins in LCs

We used Ingenuity Pathways Analysis and its knowledge database to identify the predicted upstream regulators of the 31 antimicrobial genes identified in LCs. Of the genes that encode cytokines, the top upstream regulator was *IL1B*, ($p = 7.07 \times 10^{-18}$) (**Figure 4**). The top 5 upstream regulator genes encode IL-1β, IFN-γ and TNF, all have been reported to induce one or more of the 30 LC antimicrobial genes *in vitro* (52). *TNF* was identified as the upstream regulator of 20 antimicrobial genes, followed by *IFNG* as the upstream regulator of 19 antimicrobial genes and *IL1B* as the upstream regulator of 18 antimicrobial genes. Together, the three cytokine genes were identified as upstream regulators for 25 of the 31 antimicrobial genes (**Figure 5**). In addition, we examined the target genes for other top upstream regulators that are known to contribute to the pathogenesis of skin disease: IL-10 (n=14 downstream genes), IL-22 (n=10), IL-13 (n=9), IL-17A (n=9). Thus, the antimicrobial gene response would likely be influenced by the local cytokine environment.

Of the 20 genes predicted to be induced by TNF, we detected nine genes, *ADM, CXCL2, CCL17, CCL27, IL26, CCL19, CCL2,*

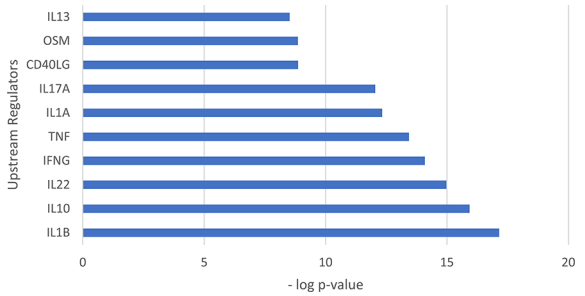

FIGURE 4 | Upstream regulation of genes encoding antimicrobial peptides identified in LCs. Bar graph showing the top 10 upstream regulators ranked by p value. The top upstream regulator was *IL1B* ($p= 7.07x10^{-18}$).

CCL20 and *CCL1*, that were also upregulated in the transcriptomes of TNF-treated LCs. Of these, CCL17 protein has been validated to be induced by TNF *in vitro* (52). Although the Ingenuity pathways analysis did not predict TNF as an upstream regulator of *CXCL10*, TNF induced LCs to secrete CXCL10 *in vitro* (65).

Ingenuity pathways analysis identified IL1B as the upstream regulator for 18 of the 31 antimicrobial genes we identified in LC transcriptomes and/or the literature. For one these genes, the IL-1 family member, IL-1α, induces *CCL17* encoded peptide in LCs (52). was validated to induce CCL17 peptide (Alferink et al., 2003). The addition of IFN-γ to LCs leads to the induction of *CAMP* and *DEFB4* encoded peptides (33), as well as *CXCL9, CXCL10*, and *CXCL11* mRNAs (60).

Overall, we identified 31 antimicrobial genes in LCs, of which eight genes were induced by activation with TNF in transcriptomes, 16 additional genes by comparison of LCs to other cell types, of which all but one gene were unique, and eight additional genes were identified in LCs in publications. Of the 31 genes, 12 genes belonged to the chemokine superfamily and making it the largest family of antimicrobial genes identified in LCs. Additionally, according to the Antimicrobial Peptide Database (APD) (35), of the 31 antimicrobial genes identified in LCs, 29 encode proteins that are antibacterial. Of the 29 genes, 23 encode peptides with activity against gram-positive bacillus *Staphylococcus aureus*, which is the leading cause of skin and soft tissue infections (66–68) (**Supplementary Table S6**). A total of 18 of the 31 genes encode proteins that are antifungal, six are antiviral, and five are antiparasitic (**Supplementary Table S5**).

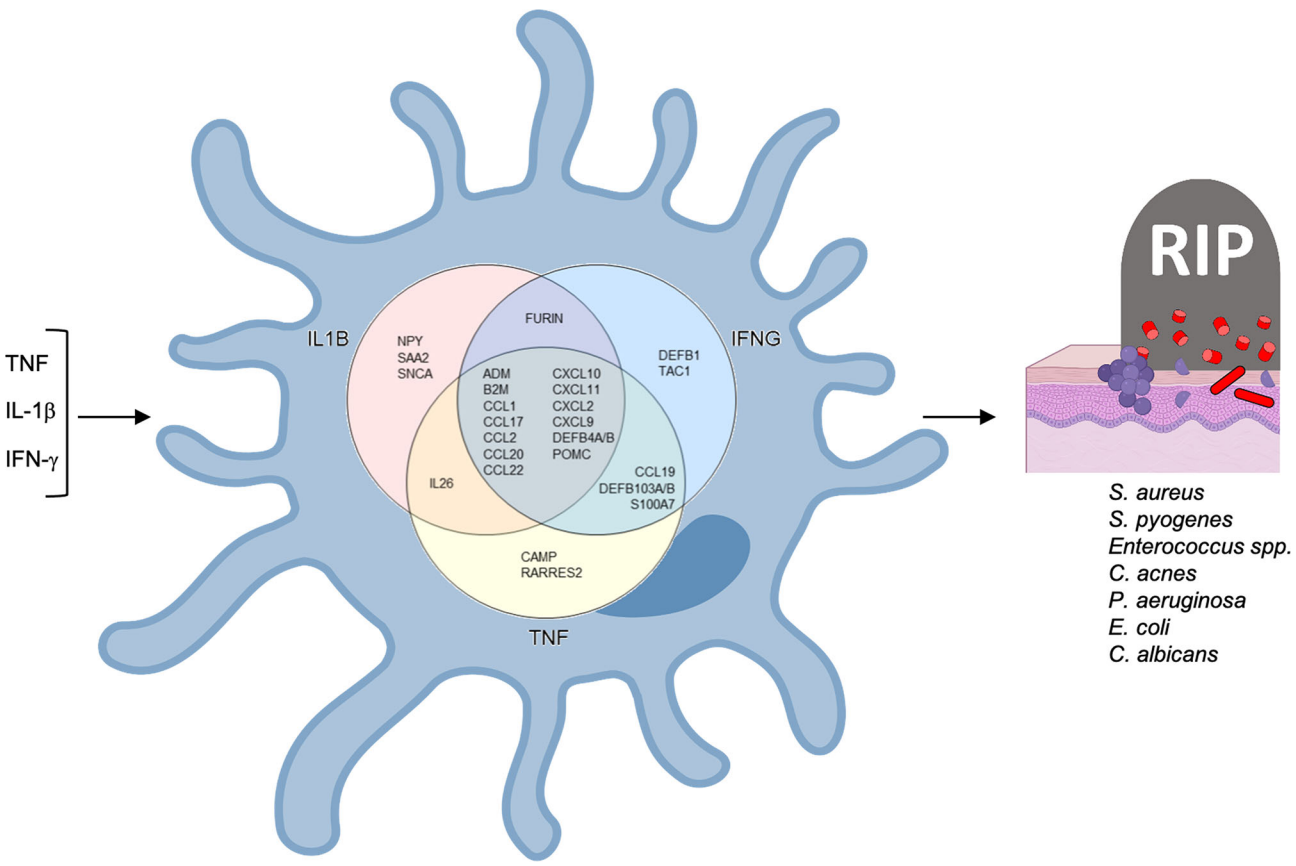

FIGURE 5 | Antimicrobial network induced by *TNF, IFNG* and *IL1B* in LCs. *TNF* and *IFNG* were each identified as upstream regulators of 19 antimicrobial genes and *IL1B* as the upstream regulator of 18 antimicrobial genes.

DISCUSSION

The localization of LCs to the epidermis provides a first line of defense for the innate immune system to defend the host against microbial pathogens invading the skin. Surprisingly, few pathways have been identified by which LCs mediate antimicrobial responses against viruses (31, 32), bacteria, and fungi (33). Here, in order to gain insight into the breadth of mechanisms by which LCs are equipped to mount an antimicrobial response, we searched publicly available databases for LC transcriptomes and also reviewed the literature to identify genes which encode proteins with direct antimicrobial activity against cutaneous pathogens. Overall, we identified 31 genes encoding proteins with direct antimicrobial activity, ten of which were identified in at least two different experiments, thus representing a core set of genes that comprise the LC antimicrobial gene program. Seven of these ten antimicrobial genes encode chemokines, *CCL1, CCL17, CCL19, CCL2, CCL22, CXCL14* and *CXCL2*, which mediate both antimicrobial and inflammatory responses. *CCL22* was identified in seven of nine transcriptomes in eight total comparisons, as well as validated in cultured LCs by PCR (51). As such, LCs are armed with an antimicrobial gene program to combat microbial pathogens.

Chemokines were the largest family of antimicrobial genes identified in LCs, accounting for 12 of the 31 genes, including seven of the ten genes that were cross-validated in at least two studies. Of the 12 genes, seven belonged to the chemokine family with a "CC" structure and five to the family with the "CXC" structure. Chemokines are pro-inflammatory, such that as part of host defense against microbial pathogens their trigger the migration of immune cells to the site of infection (69). However, many chemokines have a dual function, as they possess direct microbicidal activity (36, 37, 39, 70). Of the chemokines, *CCL22* was the most frequently detected antimicrobial gene, expressed in six different LC transcriptomes when compared to other cell types. *CCL22* was also previously identified in mature LCs cocultured with keratinocytes (51). CCL22 is one of the natural ligands for CCR4, along with CCL17 and CCL2. Both *CCL17* and *CCL22* were also upregulated in TNF treated LCs, with CCL17 protein induced in LCs by TNF *in vitro* (52). CCR4 is highly expressed by skin-infiltrating lymphocytes (71) and is involved in skin homing (72–74) of Th2 T cells, Th17 cells, Th22 cells and Tregs (75–79). LCs, by expression of *CCL22, CCL17*, and *CCL2* have the potential to recruit a range of functional $CCR4^+$ T cell subpopulations to the site of disease.

Three of the top five upstream regulators of the 31 antimicrobial genes detected in LCs, *TNF*, *IL1B* and *IFNG*, have been corroborated by *in vitro* studies in which the cytokine was directly added to LCs. In the two data series in which TNF was added to activate migratory LCs *in vitro*, eight antimicrobial genes were identified (24, 49), all consistent with the TNF-downstream genes in the Ingenuity knowledge database. TNF is known to induce the maturation and migration of LCs (19, 80), increasing the number of LCs (65), and induce the expression of inflammatory genes in LCs (49, 65, 81).

Of the eight TNF inducible genes in migrating LCs, six encode chemokines, *CCL1, CCL2, CCL17, CCL19* and *CCL20*, which along with *IL26* were only detected in the transcriptomes of TNF activated LCs but not in LCs compared to transcriptomes of other myeloid cell types. Three of these antimicrobial genes have been corroborated in published papers; CCL1 protein has been identified in epidermal LCs *in situ* (54), CCL17 protein in IL-1α or TNF-activated LCs *in vivo* in mice (52) and *CXCL2* mRNA in freshly isolated murine LC cells (53). In addition to TNF, other inflammatory stimuli have been reported to induce the expression of genes in LCs encoding directly antimicrobial peptides. *CAMP* and *DEFB4* encoded peptides are induced in LCs by IFN-γ (33). *CXCL9, CXCL10*, and *CXCL11* mRNAs are induced in LCs by stimuli including IFN-γ, LPS, and poly I:C (32, 60). *NPY* mRNA expression in LCs is enhanced by GM-CSF and LPS (62). In addition, LCs have been shown to express *POMC* mRNA upon activation (61). Therefore, the activation and/or maturation of LCs triggers expression of multiple antimicrobial genes.

By comparing the expression of antimicrobial genes in LCs to other cell types, we identified 23 genes that arm LCs with the capacity to combat cutaneous pathogens and eight additional genes described in the literature to be expressed by LCs. Of these 31 genes, 23 genes encode peptides with activity against gram-positive bacillus *Staphylococcus aureus*, which is the leading cause of skin and soft tissue infections (66–68). LC expression of CAMP and DEFB4 results in an antimicrobial activity against the cutaneous pathogens including *M. leprae, S. aureus, Streptococcus pyogenes* and *Candida albicans* (33). In addition, LC have been previously shown to mediate an antiviral activity (32, 82, 83), although the mechanisms involved are not clear.

We previously found that the antimicrobial activity of LCs leads to killing and subsequent processing of microbial antigens facilitating antigen presentation to T cells (33). Some of the antimicrobial peptides expressed by migratory LCs have been shown to be pro-inflammatory, such as CCL22 and CCL17, which both act as a chemoattractant for CCR4-expressing T cells promoting LC:T cell interaction (84). Thus, the ability of LCs, in particular migratory LCs, to upregulate antimicrobial peptides links the innate and adaptive immune response, defending the host against cutaneous pathogens. There are at least two possible contributions of antimicrobial gene expression in migrating LCs.

We found that ten of the antimicrobial genes expressed in LCs were cross-validated by various methodologies, identifying a core set of genes by which LCs can contribute to host defense, that provide a basis for further functional studies. Any one antimicrobial gene may be sufficient to mediate an antimicrobial response, given our published data that IFN-γ upregulation of CAMP was required for antimicrobial activity in LCs (33). This was demonstrated by knockdown of the *CAMP* gene and the use of neutralizing monoclonal antibodies to IFN-γ (33). These strategies provide a strategy to determine whether the upregulation of multiple antimicrobial genes by cytokines and cell surface receptors such as Toll-like receptor ligands leads to a more potent antimicrobial response. It should be possible to identify key LC pathways that could be leveraged by immune

therapy augmenting LC antimicrobial responses to combat cutaneous infection.

DATA AVAILABILITY STATEMENT

The original contributions presented in the study are included in the article/**Supplementary Material**. Further inquiries can be directed to the corresponding author.

AUTHOR CONTRIBUTIONS

Conceptualization: AO and RM. Data curation: AH and JR. Formal analysis: AO, RM, RT, FM, and EK. Funding acquisition: RM. Investigation: AO and RM. Methodology: AO and RM. Project administration: AO and RM. Resources: RM, FM, and MP. Software: FM and MP. Supervision: RM. Validation: EK. Visualization: AO and RM. Writing—original draft preparation: AO and RM. Writing—review and editing: AO, RM, AH, RT, FM, and BA. All authors contributed to the article and approved the submitted version.

FUNDING

NIH grants R01 AI022553 (RLM, MP), R01 AR040312 (RLM, MP), R01 AR073252 (RLM, MP), R01 AR074302 (RLM, MP), NHMRCIdeas Grant APP1181482 (AH), 5R21EB024767-02 (EK), 1R01AR075959-01 (EK) and 1R01CA245277-01A1 (EK).

SUPPLEMENTARY MATERIAL

The Supplementary Material for this article can be found online at: https://www.frontiersin.org/articles/10.3389/fimmu.2021.695373/full#supplementary-material

REFERENCES

1. Banchereau J, Steinman RM. Dendritic Cells and the Control of Immunity. *Nature* (1998) 392:245–52. doi: 10.1038/32588
2. Klechevsky E, Banchereau J. Human Dendritic Cells Subsets as Targets and Vectors for Therapy. *Ann N Y Acad Sci* (2013) 1284:24–30. doi: 10.1111/nyas.12113
3. Klechevsky E, Morita R, Liu M, Cao Y, Coquery S, Thompson-Snipes L, et al. Functional Specializations of Human Epidermal Langerhans Cells and CD14 + Dermal Dendritic Cells. *Immunity* (2008) 29(3):497–510. doi: 10.1016/j.immuni.2008.07.013
4. Banchereau J, Zurawski S, Thompson-Snipes L, Blanck JP, Clayton S, Munk A, et al. Immunoglobulin-Like Transcript Receptors on Human Dermal CD14+ Dendritic Cells Act as a CD8-Antagonist to Control Cytotoxic T Cell Priming. *Proc Natl Acad Sci USA* (2012) 109(46):18885–90. doi: 10.1073/pnas.1205785109
5. Ueno H, Klechevsky E, Morita R, Aspord C, Cao T, Matsui T, et al. Dendritic Cell Subsets in Health and Disease. *Immunol Rev* (2007) 219:118–42. doi: 10.1111/j.1600-065X.2007.00551.x
6. Korenfeld D, Gorvel L, Munk A, Man J, Schaffer A, Tung T, et al. A Type of Human Skin Dendritic Cell Marked by CD5 Is Associated With the Development of Inflammatory Skin Disease. *JCI Insight* (2017) 2(18). doi: 10.1172/jci.insight.96101
7. Bertram KM, Botting RA, Baharlou H, Rhodes JW, Rana H, Graham JD, et al. Identification of HIV Transmitting CD11c(+) Human Epidermal Dendritic Cells. *Nat Commun* (2019) 10(1):2759. doi: 10.1038/s41467-019-10697-w
8. Valladeau J, Ravel O, Dezutter-Dambuyant C, Moore K, Kleijmeer M, Liu Y, et al. Langerin, a Novel C-Type Lectin Specific to Langerhans Cells, is an Endocytic Receptor That Induces the Formation of Birbeck Granules. *Immunity* (2000) 12(1):71–81. doi: 10.1016/s1074-7613(00)80160-0
9. Fithian E, Kung P, Goldstein G, Rubenfeld M, Fenoglio C, Edelson R. Reactivity of Langerhans Cells With Hybridoma Antibody. *Proc Natl Acad Sci USA* (1981) 78(4):2541–4. doi: 10.1073/pnas.78.4.2541
10. Kubo A, Nagao K, Yokouchi M, Sasaki H, Amagai M. External Antigen Uptake by Langerhans Cells With Reorganization of Epidermal Tight Junction Barriers. *J Exp Med* (2009) 206(13):2937–46. doi: 10.1084/jem.20091527
11. Osorio F, Reis e Sousa C. Myeloid C-Type Lectin Receptors in Pathogen Recognition and Host Defense. *Immunity* (2011) 34(5):651–64. doi: 10.1016/j.immuni.2011.05.001
12. de Jong MA, Geijtenbeek TB. Langerhans Cells in Innate Defense Against Pathogens. *Trends Immunol* (2010) 31(12):452–9. doi: 10.1016/j.it.2010.08.002
13. Nasr N, Lai J, Botting RA, Mercier SK, Harman AN, Kim M, et al. Inhibition of Two Temporal Phases of HIV-1 Transfer From Primary Langerhans Cells to T Cells: The Role of Langerin. *J Immunol* (2014) 193(5):2554–64. doi: 10.4049/jimmunol.1400630
14. Kashem SW, Haniffa M, Kaplan DH. Antigen-Presenting Cells in the Skin. *Annu Rev Immunol* (2017) 35(1):469–99. doi: 10.1146/annurev-immunol-051116-052215
15. Klechevsky E. Functional Diversity of Human Dendritic Cells. *Adv Exp Med Biol* (2015) 850:43–54. doi: 10.1007/978-3-319-15774-0_4
16. Merad M, Ginhoux F, Collin M. Origin, Homeostasis and Function of Langerhans Cells and Other Langerin-Expressing Dendritic Cells. *Nat Rev Immunol* (2008) 8(12):935–47. doi: 10.1038/nri2455
17. Larsen CP, Steinman RM, Witmer-Pack M, Hankins DF, Morris PJ, Austyn JM. Migration and Maturation of Langerhans Cells in Skin Transplants and Explants. *J Exp Med* (1990) 172(5):1483–93. doi: 10.1084/jem.172.5.1483
18. Harman AN, Wilkinson J, Bye CR, Bosnjak L, Stern JL, Nicholle M, et al. HIV Induces Maturation of Monocyte-Derived Dendritic Cells and Langerhans Cells. *J Immunol* (2006) 177(10):7103–13. doi: 10.4049/jimmunol.177.10.7103
19. Kimber I, Cumberbatch M. Stimulation of Langerhans Cell Migration by Tumor Necrosis Factor Alpha (TNF-Alpha). *J Invest Dermatol* (1992) 99 (5):48s–50s. doi: 10.1111/1523-1747.ep12668986
20. Wang B, Amerio P, Sauder DN. Role of Cytokines in Epidermal Langerhans Cell Migration. *J Leukoc Biol* (1999) 66(1):33–9. doi: 10.1002/jlb.66.1.33
21. Artyomov MN, Munk A, Gorvel L, Korenfeld D, Cella M, Tung T, et al. Modular Expression Analysis Reveals Functional Conservation Between Human Langerhans Cells and Mouse Cross-Priming Dendritic Cells. *J Exp Med* (2015) 212(5):743–57. doi: 10.1084/jem.20131675
22. Wu X, Briseño CG, Durai V, Albring JC, Haldar M, Bagadia P, et al. Mafb Lineage Tracing to Distinguish Macrophages From Other Immune Lineages Reveals Dual Identity of Langerhans Cells. *J Exp Med* (2016) 213(12):2553–65. doi: 10.1084/jem.20160600
23. Banchereau J, Thompson-Snipes L, Zurawski S, Blanck J-P, Cao Y, Clayton S, et al. The Differential Production of Cytokines by Human Langerhans Cells and Dermal CD14(+) DCs Controls CTL Priming. *Blood* (2012) 119 (24):5742–9. doi: 10.1182/blood-2011-08-371245
24. Sirvent S, Vallejo AF, Davies J, Clayton K, Wu Z, Woo J, et al. Genomic Programming of IRF4-Expressing Human Langerhans Cells. *Nat Commun* (2020) 11(1):313. doi: 10.1038/s41467-019-14125-x
25. Balin SJ, Pellegrini M, Klechevsky E, Won ST, Weiss DI, Choi AW, et al. Human Antimicrobial Cytotoxic T Lymphocytes, Defined by NK Receptors and Antimicrobial Proteins, Kill Intracellular Bacteria. *Sci Immunol* (2018) 3 (26). doi: 10.1126/sciimmunol.aat7668

26. Penel-Sotirakis K, Simonazzi E, Peguet-Navarro J, Rozieres A. Differential Capacity of Human Skin Dendritic Cells to Polarize CD4+ T Cells Into IL-17, IL-21 and IL-22 Producing Cells. *PloS One* (2012) 7(11):e45680. doi: 10.1371/journal.pone.0045680
27. Fujita H, Nograles KE, Kikuchi T, Gonzalez J, Carucci JA, Krueger JG. Human Langerhans Cells Induce Distinct IL-22-Producing CD4+ T Cells Lacking IL-17 Production. *Proc Natl Acad Sci USA* (2009) 106(51):21795–800. doi: 10.1073/pnas.0911472106
28. Porcelli S, Brenner MB, Greenstein JL, Balk SP, Terhorst C, Bleicher PA. Recognition of Cluster of Differentiation 1 Antigens by Human CD4-CD8-Cytolytic T Lymphocytes. *Nature* (1989) 341:447–50. doi: 10.1038/341447a0
29. de Jong A, Cheng TY, Huang S, Gras S, Birkinshaw RW, Kasmar AG, et al. CD1a-Autoreactive T Cells Recognize Natural Skin Oils That Function as Headless Antigens. *Nat Immunol* (2014) 15(2):177–85. doi: 10.1038/ni.2790
30. Hunger RE, Sieling PA, Ochoa MT, Sugaya M, Burdick AE, Rea TH, et al. Langerhans Cells Utilize CD1a and Langerin to Efficiently Present Nonpeptide Antigens to T Cells. *J Clin Invest* (2004) 113(5):701–8. doi: 10.1172/jci19655
31. van der Vlist M, Geijtenbeek TB. Langerin Functions as an Antiviral Receptor on Langerhans Cells. *Immunol Cell Biol* (2010) 88(4):410–5. doi: 10.1038/icb.2010.32
32. Renn CN, Sanchez DJ, Ochoa MT, Legaspi AJ, Oh CK, Liu PT, et al. TLR Activation of Langerhans Cell-Like Dendritic Cells Triggers an Antiviral Immune Response. *J Immunol* (2006) 177(1):298–305. doi: 10.4049/jimmunol.177.1.298
33. Dang AT, Teles RM, Liu PT, Choi A, Legaspi A, Sarno EN, et al. Autophagy Links Antimicrobial Activity With Antigen Presentation in Langerhans Cells. *JCI Insight* (2019) 4(8):e126955. doi: 10.1172/jci.insight.126955
34. Edgar R, Domrachev M, Lash AE. Gene Expression Omnibus: NCBI Gene Expression and Hybridization Array Data Repository. *Nucleic Acids Res* (2002) 30(1):207–10. doi: 10.1093/nar/30.1.207
35. Wang G, Li X, Wang Z. APD3: The Antimicrobial Peptide Database as a Tool for Research and Education. *Nucleic Acids Res* (2016) 44(D1):D1087–93. doi: 10.1093/nar/gkv1278
36. Hoover DM, Boulegue C, Yang D, Oppenheim JJ, Tucker K, Lu W, et al. The Structure of Human Macrophage Inflammatory Protein-3alpha/CCL20. Linking Antimicrobial and CC Chemokine Receptor-6-Binding Activities With Human Beta-Defensins. *J Biol Chem* (2002) 277(40):37647–54. doi: 10.1074/jbc.M203907200
37. Kotarsky K, Sitnik KM, Stenstad H, Kotarsky H, Schmidtchen A, Koslowski M, et al. A Novel Role for Constitutively Expressed Epithelial-Derived Chemokines as Antibacterial Peptides in the Intestinal Mucosa. *Mucosal Immunol* (2010) 3(1):40–8. doi: 10.1038/mi.2009.115
38. Krijgsveld J, Zaat SA, Meeldijk J, van Veelen PA, Fang G, Poolman B, et al. Thrombocidins, Microbicidal Proteins From Human Blood Platelets, are C-Terminal Deletion Products of CXC Chemokines. *J Biol Chem* (2000) 275(27):20374–81. doi: 10.1074/jbc.275.27.20374
39. Burkhardt AM, Tai KP, Flores-Guiterrez JP, Vilches-Cisneros N, Kamdar K, Barbosa-Quintana O, et al. CXCL17 is a Mucosal Chemokine Elevated in Idiopathic Pulmonary Fibrosis That Exhibits Broad Antimicrobial Activity. *J Immunol* (2012) 188(12):6399–406. doi: 10.4049/jimmunol.1102903
40. Strbo N, Pastar I, Romero L, Chen V, Vujanac M, Sawaya AP, et al. Single Cell Analyses Reveal Specific Distribution of Anti-Bacterial Molecule Perforin-2 in Human Skin and its Modulation by Wounding and Staphylococcus Aureus Infection. *Exp Dermatol* (2019) 28(3):225–32. doi: 10.1111/exd.13870
41. Dhiman R, Venkatasubramanian S, Paidipally P, Barnes PF, Tvinnereim A, Vankayalapati R. Interleukin 22 Inhibits Intracellular Growth of Mycobacterium Tuberculosis by Enhancing Calgranulin A Expression. *J Infect Dis* (2014) 209(4):578–87. doi: 10.1093/infdis/jit495
42. Steinbakk M, Naess-Andresen CF, Lingaas E, Dale I, Brandtzaeg P, Fagerhol MK. Antimicrobial Actions of Calcium Binding Leucocyte L1 Protein, Calprotectin. *Lancet* (1990) 336(8718):763–5. doi: 10.1016/0140-6736(90)93237-j
43. Oliveros JC. *Venny 2.1.0*. (2007).
44. Széles L, Póliska S, Nagy G, Szatmari I, Szanto A, Pap A, et al. Research Resource: Transcriptome Profiling of Genes Regulated by RXR and its Permissive and Nonpermissive Partners in Differentiating Monocyte-Derived Dendritic Cells. *Mol Endocrinol* (2010) 24(11):2218–31. doi: 10.1210/me.2010-0215
45. Hutter C, Kauer M, Simonitsch-Klupp I, Jug G, Schwentner R, Leitner J, et al. Notch is Active in Langerhans Cell Histiocytosis and Confers Pathognomonic Features on Dendritic Cells. *Blood* (2012) 120(26):5199–208. doi: 10.1182/blood-2012-02-410241
46. Lim KPH, Milne P, Poidinger M, Duan K, Lin H, McGovern N, et al. Circulating CD1c+ Myeloid Dendritic Cells Are Potential Precursors to LCH Lesion CD1a+CD207+ Cells. *Blood Adv* (2020) 4(1):87–99. doi: 10.1182/bloodadvances.2019000488
47. McGovern N, Schlitzer A, Gunawan M, Jardine L, Shin A , Poyner E, et al. Human Dermal $CD14^+$ Cells are a Transient Population of Monocyte-Derived Macrophages. *Immunity* (2014) 41(3):465–77. doi: 10.1016/j.immuni.2014.08.006
48. Rhodes JW, Botting RA, Bertram KM, Rana H, Baharlou H, Longmuir-Vine EE, et al. Identification of HIV-Transmitting Sub-Epithelial Mononuclear Phagocytes in Human Anogenital and Colorectal Tissues. *bioRxiv* (2020). doi: 10.1101/2020.05.26.117408. 2020.05.26.117408.
49. Polak ME, Thirdborough SM, Ung CY, Elliott T, Healy E, Freeman TC, et al. Distinct Molecular Signature of Human Skin Langerhans Cells Denotes Critical Differences in Cutaneous Dendritic Cell Immune Regulation. *J Invest Dermatol* (2014) 134(3):695–703. doi: 10.1038/jid.2013.375
50. Boyd A, Bennuru S, Wang Y, Sanprasert V, Law M, Chaussabel D, et al. Quiescent Innate Response to Infective Filariae by Human Langerhans Cells Suggests a Strategy of Immune Evasion. *Infect Immun* (2013) 81(5):1420–9. doi: 10.1128/iai.01301-12
51. Ross R, Ross XL, Ghadially H, Lahr T, Schwing J, Knop J, et al. Mouse Langerhans Cells Differentially Express an Activated T Cell-Attracting CC Chemokine. *J Invest Dermatol* (1999) 113(6):991–8. doi: 10.1046/j.1523-1747.1999.00803.x
52. Alferink J, Lieberam I, Reindl W, Behrens A, Weiss S, Hüser N, et al. Compartmentalized Production of CCL17 *In Vivo*: Strong Inducibility in Peripheral Dendritic Cells Contrasts Selective Absence From the Spleen. *J Exp Med* (2003) 197(5):585–99. doi: 10.1084/jem.20021859
53. Heufler C, Topar G, Koch F, Trockenbacher B, Kämpgen E, Romani N, et al. Cytokine Gene Expression in Murine Epidermal Cell Suspensions: Interleukin 1 Beta and Macrophage Inflammatory Protein 1 Alpha are Selectively Expressed in Langerhans Cells But Are Differentially Regulated in Culture. *J Exp Med* (1992) 176(4):1221–6. doi: 10.1084/jem.176.4.1221
54. Schaerli P, Ebert L, Willimann K, Blaser A, Roos RS, Loetscher P, et al. A Skin-Selective Homing Mechanism for Human Immune Surveillance T Cells. *J Exp Med* (2004) 199(9):1265–75. doi: 10.1084/jem.20032177
55. Botting RA, Bertram KM, Baharlou H, Sandgren KJ, Fletcher J, Rhodes JW, et al. Phenotypic and Functional Consequences of Different Isolation Protocols on Skin Mononuclear Phagocytes. *J Leukoc Biol* (2017) 101(6):1393–403. doi: 10.1189/jlb.4A1116-496R
56. Nestle FO, Zheng XG, Thompson CB, Turka LA, Nickoloff BJ. Characterization of Dermal Dendritic Cells Obtained From Normal Human Skin Reveals Phenotypic and Functionally Distinctive Subsets. *J Immunol* (1993) 151:6535–45.
57. Zaba LC, Fuentes-Duculan J, Steinman RM, Krueger JG, Lowes MA. Normal Human Dermis Contains Distinct Populations of CD11c+BDCA-1+ Dendritic Cells and CD163+FXIIIA+ Macrophages. *J Clin Invest* (2007) 117(9):2517–25. doi: 10.1172/JCI32282
58. Lenz A, Heine M, Schuler G, Romani N. Human and Murine Dermis Contain Dendritic Cells. Isolation by Means of a Novel Method and Phenotypical and Functional Characterization. *J Clin Invest* (1993) 92:2587–96. doi: 10.1172/JCI116873
59. Villani AC, Satija R, Reynolds G, Sarkizova S, Shekhar K, Fletcher J, et al. Single-Cell RNA-Seq Reveals New Types of Human Blood Dendritic Cells, Monocytes, and Progenitors. *Science* (2017) 356(6335). doi: 10.1126/science.aah4573
60. Fujita H, Asahina A, Sugaya M, Nakamura K, Gao P, Fujiwara H, et al. Differential Production of Th1- and Th2-Type Chemokines by Mouse Langerhans Cells and Splenic Dendritic Cells. *J Invest Dermatol* (2005) 124(2):343–50. doi: 10.1111/j.0022-202X.2004.23607.x
61. Luger TA, Scholzen T, Grabbe S. The Role of Alpha-Melanocyte-Stimulating Hormone in Cutaneous Biology. *J Investig Dermatol Symp Proc* (1997) 2(1):87–93. doi: 10.1038/jidsymp.1997.17

62. Lambert RW, Campton K, Ding W, Ozawa H, Granstein RD. Langerhans Cell Expression of Neuropeptide Y and Peptide YY. *Neuropeptides* (2002) 36 (4):246–51. doi: 10.1016/s0143-4179(02)00020-3
63. Lu Q, Samaranayake LP, Darveau RP, Jin L. Expression of Human Beta-Defensin-3 in Gingival Epithelia. *J Periodontal Res* (2005) 40(6):474–81. doi: 10.1111/j.1600-0765.2005.00827.x
64. Pilkington SM, Dearman RJ, Kimber I, Griffiths CEM. Langerhans Cells Express Human β-Defensin 3: Relevance for Immunity During Skin Ageing. *Br J Dermatol* (2018) 179(5):1170–1. doi: 10.1111/bjd.16770
65. Berthier-Vergnes O, Bermond F, Flacher V, Massacrier C, Schmitt D, Péguet-Navarro J. TNF-Alpha Enhances Phenotypic and Functional Maturation of Human Epidermal Langerhans Cells and Induces IL-12 P40 and IP-10/CXCL-10 Production. *FEBS Lett* (2005) 579(17):3660–8. doi: 10.1016/j.febslet.2005.04.087
66. Moet GJ, Jones RN, Biedenbach DJ, Stilwell MG, Fritsche TR. Contemporary Causes of Skin and Soft Tissue Infections in North America, Latin America, and Europe: Report From the SENTRY Antimicrobial Surveillance Program (1998-2004). *Diagn Microbiol Infect Dis* (2007) 57(1):7–13. doi: 10.1016/j.diagmicrobio.2006.05.009
67. Ray GT, Suaya JA, Baxter R. Incidence, Microbiology, and Patient Characteristics of Skin and Soft-Tissue Infections in a U.S. Population: A Retrospective Population-Based Study. *BMC Infect Dis* (2013) 13:252. doi: 10.1186/1471-2334-13-252
68. Rennie RP, Jones RN, Mutnick AH. Occurrence and Antimicrobial Susceptibility Patterns of Pathogens Isolated From Skin and Soft Tissue Infections: Report From the SENTRY Antimicrobial Surveillance Program (United States and Canada, 2000). *Diagn Microbiol Infect Dis* (2003) 45 (4):287–93. doi: 10.1016/s0732-8893(02)00543-6
69. Lukacs NW. Role of Chemokines in the Pathogenesis of Asthma. *Nat Rev Immunol* (2001) 1(2):108–16. doi: 10.1038/35100503
70. Yang D, Chen Q, Hoover DM, Staley P, Tucker KD, Lubkowski J, et al. Many Chemokines Including CCL20/MIP-3alpha Display Antimicrobial Activity. *J Leukoc Biol* (2003) 74(3):448–55. doi: 10.1189/jlb.0103024
71. Kunkel EJ, Boisvert J, Murphy K, Vierra MA, Genovese MC, Wardlaw AJ, et al. Expression of the Chemokine Receptors CCR4, CCR5, and CXCR3 by Human Tissue-Infiltrating Lymphocytes. *Am J Pathol* (2002) 160(1):347–55. doi: 10.1016/s0002-9440(10)64378-7
72. Campbell JJ, Haraldsen G, Pan J, Rottman J, Qin S, Ponath P, et al. The Chemokine Receptor CCR4 in Vascular Recognition by Cutaneous But Not Intestinal Memory T Cells. *Nature* (1999) 400(6746):776–80. doi: 10.1038/23495
73. Reiss Y, Proudfoot AE, Power CA, Campbell JJ, Butcher EC. CC Chemokine Receptor (CCR)4 and the CCR10 Ligand Cutaneous T Cell-Attracting Chemokine (CTACK) in Lymphocyte Trafficking to Inflamed Skin. *J Exp Med* (2001) 194(10):1541–7. doi: 10.1084/jem.194.10.1541
74. Imai T, Baba M, Nishimura M, Kakizaki M, Takagi S, Yoshie O. The T Cell-Directed CC Chemokine TARC Is a Highly Specific Biological Ligand for CC Chemokine Receptor 4. *J Biol Chem* (1997) 272(23):15036–42. doi: 10.1074/jbc.272.23.15036
75. O'Leary NA, Wright MW, Brister JR, Ciufo S, Haddad D, McVeigh R, et al. Reference Sequence (RefSeq) Database at NCBI: Current Status, Taxonomic Expansion, and Functional Annotation. *Nucleic Acids Res* (2016) 44(D1): D733–45. doi: 10.1093/nar/gkv1189
76. Ghadially H, Ross XL, Kerst C, Dong J, Reske-Kunz AB, Ross R. Differential Regulation of CCL22 Gene Expression in Murine Dendritic Cells and B Cells. *J Immunol* (2005) 174(9):5620–9. doi: 10.4049/jimmunol.174.9.5620
77. Acosta-Rodriguez EV, Rivino L, Geginat J, Jarrossay D, Gattorno M, Lanzavecchia A, et al. Surface Phenotype and Antigenic Specificity of Human Interleukin 17-Producing T Helper Memory Cells. *Nat Immunol* (2007) 8(6):639–46. doi: 10.1038/ni1467
78. Sallusto F, Lanzavecchia A. Heterogeneity of CD4+ Memory T Cells: Functional Modules for Tailored Immunity. *Eur J Immunol* (2009) 39 (8):2076–82. doi: 10.1002/eji.200939722
79. Lindestam Arlehamn CS, Gerasimova A, Mele F, Henderson R, Swann J, Greenbaum JA, et al. Memory T Cells in Latent Mycobacterium Tuberculosis Infection Are Directed Against Three Antigenic Islands and Largely Contained in a CXCR3+CCR6+ Th1 Subset. *PloS Pathog* (2013) 9(1): e1003130. doi: 10.1371/journal.ppat.1003130
80. Ratzinger G, Baggers J, de Cos MA, Yuan J, Dao T, Reagan JL, et al. Mature Human Langerhans Cells Derived From CD34+ Hematopoietic Progenitors Stimulate Greater Cytolytic T Lymphocyte Activity in the Absence of Bioactive IL-12p70, by Either Single Peptide Presentation or Cross-Priming, Than do Dermal-Interstitial or Monocyte-Derived Dendritic Cells. *J Immunol* (2004) 173(4):2780–91. doi: 10.4049/jimmunol.173.4.2780
81. Polak ME, Newell L, Taraban VY, Pickard C, Healy E, Friedmann PS, et al. CD70-CD27 Interaction Augments CD8+ T-Cell Activation by Human Epidermal Langerhans Cells. *J Invest Dermatol* (2012) 132(6):1636–44. doi: 10.1038/jid.2012.26
82. de Witte L, Nabatov A, Pion M, Fluitsma D, de Jong MA, de Gruijl T, et al. Langerin Is a Natural Barrier to HIV-1 Transmission by Langerhans Cells. *Nat Med* (2007) 13(3):367–71. doi: 10.1038/nm1541
83. Ribeiro CM, Sarrami-Forooshani R, Setiawan LC, Zijlstra-Willems EM, van Hamme JL, Tigchelaar W, et al. Receptor Usage Dictates HIV-1 Restriction by Human TRIM5α in Dendritic Cell Subsets. *Nature* (2016) 540(7633):448–52. doi: 10.1038/nature20567
84. Tang HL, Cyster JG. Chemokine Up-Regulation and Activated T Cell Attraction by Maturing Dendritic Cells. *Science* (1999) 284(5415):819–22. doi: 10.1126/science.284.5415.819

Conflict of Interest: The authors declare that the research was conducted in the absence of any commercial or financial relationships that could be construed as a potential conflict of interest.

Publisher's Note: All claims expressed in this article are solely those of the authors and do not necessarily represent those of their affiliated organizations, or those of the publisher, the editors and the reviewers. Any product that may be evaluated in this article, or claim that may be made by its manufacturer, is not guaranteed or endorsed by the publisher.

frontiers in Microbiology

ORIGINAL RESEARCH
published: 30 August 2021
doi: 10.3389/fmicb.2021.728429

Differential Early *in vivo* Dynamics and Functionality of Recruited Polymorphonuclear Neutrophils After Infection by Planktonic or Biofilm *Staphylococcus aureus*

*Aizat Iman Abdul Hamid[1], Andréa Cara[2], Alan Diot[2], Frédéric Laurent[2], Jérôme Josse[2] and Pascale Gueirard[1]**

[1] Laboratoire Microorganismes: Génome et Environnement, CNRS UMR 6023, Université Clermont Auvergne, Clermont-Ferrand, France, [2] Centre International de Recherche et Infectiologie, Inserm U1111, CNRS UMR 5308, École Normale Supérieure de Lyon, Université Claude Bernard Lyon 1, Lyon, France

Staphylococcus aureus is a human pathogen known for its capacity to shift between the planktonic and biofilm lifestyles. *In vivo*, the antimicrobial immune response is characterized by the recruitment of inflammatory phagocytes, namely polymorphonuclear neutrophils (PMNs) and monocytes/macrophages. Immune responses to planktonic bacteria have been extensively studied, but many questions remain about how biofilms can modulate inflammatory responses and cause recurrent infections in live vertebrates. Thus, the use of biologically sound experimental models is essential to study the specific immune signatures elicited by biofilms. Here, a mouse ear pinna model of infection was used to compare early innate immune responses toward *S. aureus* planktonic or biofilm bacteria. Flow cytometry and cytokine assays were carried out to study the inflammatory responses in infected tissues. These data were complemented with intravital confocal imaging analyses, allowing the real-time observation of the dynamic interactions between EGFP + phagocytes and bacteria in the ear pinna tissue of LysM-EGFP transgenic mice. Both bacterial forms induced an early and considerable recruitment of phagocytes in the ear tissue, associated with a predominantly pro-inflammatory cytokine profile. The inflammatory response was mostly composed of PMNs in the skin and the auricular lymph node. However, the kinetics of PMN recruitment were different between the 2 forms in the first 2 days post-infection (pi). Two hours pi, biofilm inocula recruited more PMNs than planktonic bacteria, but with decreased motility parameters and capacity to emit pseudopods. Inversely, biofilm inocula recruited less PMNs 2 days pi, but with an "over-activated" status, illustrated by an increased phagocytic activity, CD11b level of expression and ROS production. Thus, the mouse ear pinna model allowed us to reveal specific differences in the dynamics of recruitment and functional properties of phagocytes against biofilms. These differences would influence the specific adaptive immune responses to biofilms elicited in the lymphoid tissues.

Keywords: *Staphylococcus aureus*, biofilm, innate immunity, polymorphonuclear neutrophils, macrophages, murine model, intravital imaging

OPEN ACCESS

Edited by:
Fabienne Tacchini-Cottier, University of Lausanne, Switzerland

Reviewed by:
Meredith Crane, Brown University, United States
Guillaume Tabouret, Institut National de Recherche Pour l'Agriculture, l'Alimentation et l'Environnement (INRAE), France

****Correspondence:***
Pascale Gueirard
pascale.gueirard@uca.fr

Specialty section:
This article was submitted to Microbial Immunology, a section of the journal Frontiers in Microbiology

Received: *21 June 2021*
Accepted: *05 August 2021*
Published: *30 August 2021*

Citation:
Abdul Hamid AI, Cara A, Diot A, Laurent F, Josse J and Gueirard P (2021) Differential Early in vivo Dynamics and Functionality of Recruited Polymorphonuclear Neutrophils After Infection by Planktonic or Biofilm Staphylococcus aureus. Front. Microbiol. 12:728429. doi: 10.3389/fmicb.2021.728429

INTRODUCTION

Staphylococcus aureus (*S. aureus*) is a Gram-positive commensal bacterium that is also a leading cause of various invasive infections from soft skin tissue colonization to infections on implanted medical devices such as prosthetic joints. The wide range of staphylococcal virulence factors coupled with the apparition of community and hospital associated methicillin-resistant *S. aureus* (MRSA) strains have made infections by this bacterial species a particularly difficult therapeutic challenge (Turner et al., 2019; de Vor et al., 2020; Pidwill et al., 2021). Furthermore, the intrinsic capacity of *S. aureus* to adapt to its environment contributes toward its survival inside host tissues. An example of this type of adaptation is the capacity to form biofilms which are, contrary to the free-floating planktonic form of growth, microbial communities encased in a self-produced matrix composed of extracellular DNA (eDNA), proteins and polysaccharides (Moormeier and Bayles, 2017). According to the US Center for Disease Control, approximately 65% of human infections involve biofilms, with *S. aureus* accounting for up to 50% of pathogens isolated from prosthetic joint infections (Costerton, 2001; Ricciardi et al., 2018). Moreover, biofilms are often implicated in recurrent infections due to their increased tolerance toward antimicrobial treatments and even host immune attacks (Bjarnsholt, 2013).

Typically, polymorphonuclear neutrophils (PMNs) and monocytes/macrophages (MOs/MΦs) are rapidly recruited to infected tissue by microbe derived signals like formylated peptides or chemokines such as chemokine ligand 1 (CXCL1) and monocyte chemotactic protein-1 (MCP-1) (Capucetti et al., 2020; de Vor et al., 2020; Pidwill et al., 2021). These innate immune cells subsequently realize phagocytosis and efficiently kill planktonic bacteria through various effector mechanisms, including acidification of phagolysosomes and release of neutrophil extracellular traps (NETs) (de Vor et al., 2020; Pidwill et al., 2021). However, the transition to the biofilm lifestyle not only modifies the spatial distribution of *S. aureus* in colonized tissues, but is also accompanied by a shift in virulence mechanisms, both factors contributing toward the immunosuppressive nature of biofilms and thus to a recalcitrance toward elimination by innate immune phagocytes (Horn and Kielian, 2020; de Vor et al., 2020; Pidwill et al., 2021). *In vitro*, MΦs at the surface of *S. aureus* biofilms were mostly viable and retained a round morphology. However, the majority of cells that successfully penetrated biofilms were not viable, illustrating the protective barrier role that biofilms play in immune evasion (Thurlow et al., 2011; Gries et al., 2020a). Recently, most of the insights into the immune evasion mechanisms elicited by staphylococcal biofilms have been gained from *in vivo* models of skin/abscess infection or from biofilm infections on implanted medical devices (Horn and Kielian, 2020; Pidwill et al., 2021). These models have highlighted anti-inflammatory responses elicited by *S. aureus* biofilms due in part to the polarization of recruited MΦs toward an M2 anti-inflammatory phenotype, and also to the recruitment of an immature population of myeloid cells known as myeloid-derived suppressor cells (MDSCs) which were present as early as day 3 in infected knee joint tissue (Thurlow et al., 2011; Heim et al., 2018). Inversely, adoptive transfer of M1 MΦs, preactivated by IFN-γ or TNF-α and *S. aureus*–derived peptidoglycan, to the infectious tissue surrounding a biofilm inoculated catheter ameliorated immune responses and biofilm clearance (Hanke et al., 2013).

Even though PMNs are key cells in the *S. aureus* innate immune responses, little is known about the specific *in vivo* interactions between PMNs and biofilms. Indeed, while many *in vitro* studies have analyzed the effects of the various virulence factors of *S. aureus* biofilms, from the expression of PMN-killing toxins to NET degradation (de Vor et al., 2020), most *in vivo* knowledge has been restricted to FACS analyses of PMN recruitment toward infected tissue. Furthermore, most models studying innate immune responses toward *S. aureus* biofilms do not include comparisons with planktonic bacteria.

Thus, the early inflammatory responses toward both forms of *S. aureus* were characterized in a previously developed mouse soft skin tissue infection model. In these works, either *S. aureus* planktonic or biofilm bacteria were intradermally inoculated into the mouse ear pinna, which allowed the study of their effects on immune cell dynamics using intravital confocal microscopy (Forestier et al., 2017; Abdul Hamid et al., 2020; Sauvat et al., 2020). The use of this type of imaging in the context of biofilm infections has rarely been done but has allowed new insights into the study of immune responses from a cellular dynamic perspective (Gries et al., 2020b). Here, classic immunology techniques were coupled with intravital confocal imaging to rigorously compare inflammatory responses and phagocyte behavior in response to either the planktonic or biofilm form of *S. aureus*. Results show that early immune responses were globally similar at the tissue and cytokine levels but were significantly changed when analyzing cellular dynamics and specific interactions with bacteria. These data were coherent with modifications in the functional properties of phagocytes recruited toward the cutaneous infection site.

MATERIALS AND METHODS

Mice and Ethics Statement

C57BL/6J WT mice (6–16-week-old males and females) were purchased from Charles River Laboratories. LysM-EGFP transgenic mice (6–16-week-old males and females) were obtained from the bacteria-cell interactions unit of the Pasteur Institute (Paris, France). Mice were bred in the animal care facility at Clermont Auvergne University (Clermont-Ferrand, France). All experiments were approved by the local Ethics Committee on Animal Experimentation (Auvergne C2E2A, Clermont-Ferrand, France, agreement number: 1,725) and were carried out in accordance with the applicable guidelines and regulations. All mice were provided an appropriate environment including shelter in cages, a comfortable resting area, sufficient space (not more than 5 animals per cage) and ready access to fresh water and food to maintain full health and vigor. Animal welfare was observed daily to ensure optimal conditions and treatment which avoid suffering. Littermates destined to be inoculated were housed in separate cages with access to the

same facilities previously stated. The anesthetic used during experiments was chosen to promote deep anesthesia. During and after anesthesia, mice were kept warm in order to prevent any risks related to hypothermia. Euthanasia was performed by cervical dislocation on the anesthetized animal at the end of the infection period.

SH1000 mCherry and GFP-Tagged *Staphylococcus aureus* Strain Construction

The *S. aureus* SH1000 strain was chosen for its capacity to produce high quantities of biofilm *in vitro* (Tasse et al., 2018), and used in all the experiments presented in this work. As described previously, the SH1000 strain possess a functional *agr* system (Herbert et al., 2010). The *S. aureus* SH1000 GFP-tagged fluorescent strain (named GFP-SH1000) was constructed after insertion of the pCN47-GFP plasmid (Charpentier et al., 2004) by electroporation into the SH1000 strain (O'Neill, 2010), as described previously (Schenk and Laddaga, 1992). The GFP-SH1000 strain was then selected onto Luria-Bertani (LB) agar containing erythromycin (10 μg/mL). Clones were grown overnight with shaking in Trypticase Soy broth (TSB) containing erythromycin (10 μg/mL) and stored at –80°C in the same medium with 15% glycerol. Fluorescence was detected in bacterial suspensions by fluorescence microscopy. The *S. aureus* SH1000 mCherry-tagged fluorescent strain (named mCherry-SH1000) was constructed in the same way with the pCN47-mCherry plasmid.

Reagents and Monoclonal Antibodies

The reagents used in this study were as follows: collagenase, Type IV (Gibco), Deoxyribonuclease I from bovine pancreas (Sigma-Aldrich), EDTA (Invitrogen), Erythromycin (Sigma-Aldrich), Gentamicin (Sigma-Aldrich), LB agar (Condalab), Liberase^{TM} Research Grade (Roche), Pierce protease inhibitor (Thermo Fisher Scientific), PBS (Dutscher), RPMI 1640 w/stable glutamine (Dutscher), and TSB (BD Bacto). Antibodies and dyes from Miltenyi Biotec include: anti-mouse CD3ε (clone 17A2), CD335 (clone REA815), CD19 (clone REA749), CD45 (clone REA737), CD11b (clone REA592), Ly6G (clone REA526), Ly6C (clone REA796), Viobility 405/452 fixable dye, REA Control-APC (clone REA 293), REA Control-FITC (clone REA 293), REA Control-PE-Vio 770 (clone REA 293), REA Control- APC-Vio 770 (clone REA 293), REA Control- APC-VioBlue (clone REA 293), and REA Control- APC-VioGreen (clone REA 293).

Bacterial Growth Conditions and Inocula Preparation

WT (non-fluorescent), GFP and mCherry-SH1000 strains were used in all the experiments performed. WT planktonic bacterial cultures were prepared from an aliquot of frozen bacteria in 5 mL of TSB and placed overnight at 37°C with agitation under aerobic conditions. Culture media of fluorescent strains were supplemented with erythromycin (10 μg/mL).

Planktonic inocula were prepared by first homogenizing overnight cultures and then determining bacterial concentration (CFU/mL), deduced by measuring the optical density at 600 nm ($OD_{600\ nm}$) and multiplying it by the known titer ($CFU/OD_{600\ nm}$) of the strain. The corresponding volume of overnight culture containing 5×10^6 CFUs was withdrawn and centrifuged at 3,000 × g for 5 min. The pellet was resuspended in 3.8 μL of PBS (Phosphate-Buffered Saline) which was used as inocula.

Biofilm inocula were prepared by adjusting an overnight culture to $OD_{600\ nm} = 1 \pm 0.05$ in TSB. The suspension was then diluted 1:100 and deposited in at least two flat-bottomed-wells in a 24-well cell culture plate (1 mL per well) before being placed in a humidity chamber at 37°C for 24 h without agitation. After the incubation period, the cell culture plate was overturned to eliminate excess media. Biofilms formed at the bottom of the wells were then steam-washed for 40 min as described previously (Tasse et al., 2018) and recovered by flushing and scraping the bottom of the well in 200 μL of PBS. This suspension was transferred to the second steam-washed well to recover biofilms, using the same recovery technique to obtain a final concentration of 5×10^6 CFUs/3.8 μL of PBS. A small aliquot of the resulting suspension, 3.8 μL, was destined as inocula.

Bacterial CFUs in the injected inocula were confirmed by serial 10-fold dilutions on LB agar plates, containing erythromycin (10 μg/mL) for fluorescent strains, incubated overnight at 37°C. Before plating, biofilm inocula were first vortexed for 30 s, sonicated for 10 min (Thermo Fisher Scientific, 80 W, 37 kHz) and then vortexed again for a further 30 s. Average titrations of planktonic and biofilm inocula were $3.55 \times 10^6 \pm 1.58 \times 10^6$ CFUs/3.8 μL and $4.81 \times 10^6 \pm 4.58 \times 10^5$ CFUs/3.8 μL, respectively, with no significant difference between the values (results not shown).

Control inocula corresponded to a small volume of PBS, 3.8 μL.

Micro-Injection of Biofilm and Planktonic Inocula Into Mice

Mice were anesthetized by intraperitoneal injection of a ketamine (100 mg/kg) and xylazine (5 mg/kg) mixture. Planktonic or biofilm inocula or PBS were micro-injected intradermally into the mouse ear pinna, as previously described (Mac-Daniel et al., 2016). Briefly, the ventral side of the mouse ear pinna was affixed under a stereomicroscope using clear tape. A 10 μL NanoFil syringe (World Precision Instruments) fitted to a 34-gauge beveled needle was then loaded with either 3.8 μL of planktonic or biofilm bacteria (containing 5×10^6 CFUs) or PBS. Inocula were delivered into the ear tissue by inserting the needle beneath the epidermis on the dorsal side of the ear, and injecting the loaded suspension. A characteristic papule was observable at the injection site, evidence of an intradermal injection.

Bacterial Burden in Ear Skin Tissue and Draining Lymph Nodes

The SH1000 WT strain was used for bacterial burden analysis. At 2 h pi, mice were euthanized, and the ear pinna tissue and auricular dLNs of infected and control mice were harvested using sterile scissors and weighed. Samples were kept on ice whenever possible throughout the duration of the experiment. Ear tissue

and dLNs were first placed in 500 μL of sterile physiological water per ear or dLN, in individual tubes. Ear tissue were then washed in a bath of ethanol and then rinsed in two consecutive baths of distilled water before being dissected into small pieces and placed in a hemolysis tube containing 500 μL of sterile PBS. Draining lymph nodes were washed in two baths of distilled water and directly placed in a hemolysis tube containing 500 μL of sterile PBS. Ears and dLNs were homogenized using a PRO 200 handheld tissue homogenizer (PRO Scientific). Serial 10-fold dilutions were performed on tissue homogenates and plated on LB agar plates to enumerate viable *S. aureus* per milligram of tissue. Ear tissues and dLNs from mice inoculated with biofilm bacteria were vortexed and sonicated as described above before serial dilution and plating. Experiments were repeated from day 1 to day 7 pi and at 10 days pi.

Evaluation of Ear Swelling

Ear swelling measurements were carried out on mice inoculated with SH1000 WT strain. Mice destined to be euthanized were first anesthetized by intraperitoneal injection of a ketamine and xylazine mixture. Ear thickness measurements were carried out in triplicate by the same experimenter using an engineer's micrometer (Powerfix Profi Digital Caliper). Care was taken to measure only the outer two-thirds of the ear pinna and to not overly compress the swollen ear tissue between measurements. Due to the development of tissue necrosis at the later stages of infection, this parameter was only measured during the first 48 h pi.

Inflammation Scoring

Upon mice euthanasia, photos were taken of the ear pinna tissue and then examined in a blinded fashion. Inflammation was scored on the basis of erythema (redness due to capillary swelling) ranging between 0 and 2. Ear tissue not presenting any signs of erythema were assigned a score of 0, while ears with any observable redness were scored between 1 and 2. The former corresponded to the presence of mild erythema over a small area of the ear tissue, while the latter referred to intense redness occupying a larger surface area on the skin.

Multiplex Cytokine Assay

An aliquot from ear pinnae tissue and dLN homogenates generated during bacterial load experiments were centrifuged for 10 min at 10,000 × g at 4°C. Supernatants were stored with 1X Pierce protease inhibitor (Thermo Fisher Scientific) at −80°C until ready for analysis. Samples destined to a multiplex cytokine assay were first thawed on ice and centrifuged a second time for 10 min at 10,000 × g at 4°C. Right and left ear pinna tissue and dLNs from the same mouse were pooled before analysis. The cytokines tested in supernatants included murine IFN-γ, IL-12 p70, TNF-α, IL-17A, IL-6, IL-10, IL-1β, CXCL1, and CXCL9, and were analyzed using multiplex fluorescent bead arrays from Biorad on a BioPlex 200 Luminex system (BioRad), according to manufacturer's directions. Concentrations were expressed per mg of total protein previously established by Bradford assay (Bio-Rad).

Intravital Imaging Acquisition by Confocal Microscopy

Time-Lapse Video Acquisition

Two to five hours after inoculation of either planktonic or biofilm mCherry-SH1000 bacteria into the ear tissue of LysM-EGFP transgenic mice, mice were anesthetized to observe the recruitment of EGFP + fluorescent immune cells at the injection sites (intra vital imaging). Video time-lapse acquisition was carried out as previously described (Abdul Hamid et al., 2020). Briefly, the inner side of the ear pinna was flattened on a glass slide and imaged on the ZEISS Spinning Disk Cell Observer (SD) (Carl Zeiss Microscopy) confocal microscope. Acquisition was performed with 10X (dry), 20X (dry), and 40X (oil) objectives for periods of 20–30 min. Ear tissues of control mice were inoculated with PBS and imaged at the same time points.

Mosaic Acquisition

Infected ears were also imaged on the ZEISS LSM 800 (LSM 800) (Carl Zeiss Microscopy), 3–5 h after inoculation, as previously described (Abdul Hamid et al., 2020). Briefly, multiple fields of observation covering the entirety of the ear tissue surface were imaged with a 10X (dry) objective in order to reconstruct an image of the ear. EGFP fluorescence signal was detected in six Z-stacks while the bright-field signal was only detected on a central stack. Acquisition was repeated 24 and 48 h pi, with imaging sessions typically lasting 30–40 min. Ear tissues of control mice injected with PBS were also imaged with the same protocol.

In vivo Confocal Image Analysis

SD Image and Video Analysis

Time-lapse videos at 20X and 40X were analyzed with Imaris software, as previously described (Abdul Hamid et al., 2020). Briefly, tracks were generated and attributed to each immune cell in the observation field using the "Spots" tool. Three different parameters of immune cell dynamics were then extracted: average speed, straightness and displacement. All cells in time-lapse videos where bacteria were visible were analyzed. For cell perimeter analysis, EGFP + immune cells destined to be measured were first selected from 40X time-lapse videos where bacteria were visible using the ZEN 3D image viewer. Only cells with clearly delimited borders present between the first and last stacks were chosen. ROIs were then drawn on Z-projected images prior to perimeter measurements using ImageJ software.

Mosaic Analysis

Images acquired on the ZEISS LSM 800 confocal were stitched together using ZEN software to reconstruct an entire image of the ear tissue at each time point. The images shown represent the Z-projected maximal intensity signal of a reconstituted image of the ear tissue for the EGFP channel. Images were then analyzed as previously described (Abdul Hamid et al., 2020). Briefly, a Region Of Interest (ROI) was drawn manually around the EGFP fluorescent zone of the 48-h image to obtain the sum of EGFP fluorescence intensities of each pixel in the ROI. The same ROI was applied to the other images of the same time point image and

the ratio of the sum of intensities of EGFP fluorescence to the area of the ROI was then calculated for both time points.

Lymph Node and Ear Cell Preparation for Flow Cytometry Analysis

The GFP-SH1000 fluorescent strain was used for flow cytometry analyses. At 2, 24, and 48 h pi, mice were euthanized, and the ear tissue and dLNs of infected and control mice were harvested using sterile scissors and weighed. Samples were kept on ice whenever possible throughout the duration of the experiment. Left and right ear pinna leaflets were first dissociated before being completely submerged in 5 mL of RPMI 1640 medium containing 1 mM HEPES, 400 U/mL collagenase IV and 50 μg/mL DNase I from bovine pancreas and placed at 37°C for 1 h. Left and right LNs were digested in the same type of medium but only for 15 min. After 15 min of incubation, ear pinna tissue was dissected into small pieces to facilitate digestion. Tissues were then ground on a 70-μm cell strainer to obtain single-cell suspensions before being centrifuged at 300 × g for 10 min at 4°C. Cell pellets were suspended in 500 μL of PBS containing 1% SVF and 1 mM Ethylenediaminetetraacetic acid (EDTA). Cells were then counted and labeled according to manufacturer's directions, using the following markers: Viobility Fixable Dye, CD3ε, CD19, CD335, CD45, CD11b, Ly6G, and Ly6C. To define inflammatory cell populations recruited to these tissues, live single cells were gated to exclude any debris, dead cells or doublets. T lymphocytes, B lymphocytes, NK cells, and dead cells (DUMP channel) were excluded from live single cells, respectively, on the basis of the CD3ε, CD19, CD335, and Viobility 405/452 fixable dye specific markers. Live myeloid populations ($CD45^+CD11b^+$) were subdivided into PMNs ($Ly6G^+Ly6C^+$) and MO/MΦ ($Ly6G^-Ly6C^{hi}$). Samples were run on a BD LSR II (BD Biosciences), and data were analyzed with FlowLogic version 7.2.

Ex vivo Intracellular Bacteria Analysis

The mCherry-SH1000 fluorescent strain was used for *ex vivo* intracellular bacteria analyses. At 2, 24 and 48 h pi, infected mice were euthanized, and the ear pinna tissue were harvested using sterile scissors and weighed. Samples were kept on ice whenever possible throughout the duration of the experiment. Left and right ear pinnae leaflets were first dissociated before being completely submerged in 700 μL of PBS containing Liberase™ Research Grade (Roche), diluted 2:7, and placed at 37°C for 1 h with agitation. Fifteen mL of cold PBS were added to each tube and tissues were then ground on a 40-μm cell strainer to obtain single-cell suspensions that were then centrifuged at 1200 × g for 5 min at 4°C. Cell pellets were suspended in 1 mL of PBS containing 5% SVF. Cell suspensions resulting from 2 infected mice per bacterial form were pooled for 24- and 48-h time points. $CD11b^+$ cells were isolated using CD11b microbeads mouse/human magnetic cell separation (Miltenyi Biotec) according to manufacturer's directions.

To assess the quantity of intracellular bacteria, a portion of sorted skin cells were centrifuged at 300 × g for 10 min at 4°C, and resuspended in 1 mL of room temperature RPMI 1640 medium containing 100 μg/mL gentamycin. Cells were incubated for 1 h at 37°C, CO_2 5% before being centrifuged again at 300 × g for 10 min at 4°C. Cells were then lysed by resuspending pellets in 500 μL of cold ultrapure water, followed by vigorous shaking for 1 min. Serial 10-fold dilutions were performed on the resulting suspension and plated on LB agar plates to enumerate viable *S. aureus* per 10^6 CD11b + cells.

To characterize the distribution of intracellular bacteria, another portion of sorted skin cells were adhered to glass slides by centrifugation (800 rpm for 5 min, Thermo Shandon Cytospin 3 Centrifuge) and were fixed with 4% PFA prior to MGG staining. Glass slides were then examined by bright field microscopy (Axio Imager 2, Zeiss) and intracellular bacteria were counted in at least 100 $CD11b^+$ cells per condition, per time point.

Neutrophil NADPH Oxidase Assay

The SH1000 WT strain was used for Neutrophil NADPH oxidase analysis. Single cell suspensions were obtained 48 h pi from mouse ear pinna tissue, as described in the flow cytometry analysis section. NADPH oxidase quantity was assessed, as described previously (Borbón et al., 2019). Briefly, cells were labeled using the following markers: CD45, CD11b, and Ly6G and then incubated for 15 min at 37°C, 5% CO_2 in PBS containing 10 μM of dihydrorhodamine 123 (DHR) (Sigma-Aldrich) with or without 100 ng/mL of phorbol myristate acetate (PMA) (Sigma-Aldrich). Samples were run on a BD LSR II (BD Biosciences), and data were analyzed with FlowLogic version 7.2.

Statistical Analysis

Data generated were analyzed with Prism 5 software (GraphPad Software, Inc.) and a non-parametric Mann-Whitney one-tailed or two-tailed statistical test. $p \leq 0.05$ was considered statistically significant (symbols: * ≤ 0.05).

RESULTS

Comparable Bacterial Load and Inflammatory Responses in the Mouse Ear Pinna After the Micro-Injection of Either the Planktonic or Biofilm Form of *Staphylococcus aureus*

Calibrated *S. aureus* inocula were prepared and microinjected into the mouse ear pinna tissue. Bacterial load was first measured in the cutaneous ear tissue and the auricular draining lymph node (auricular dLN) following inoculation of WT C57BL/6J mice with 5 × 10^6 CFUs of non-fluorescent planktonic or biofilm *S. aureus*. CFUs were enumerated, starting from 2 h post-infection (h pi) until day 7 pi, and then after 10 days. Bacterial load quantification showed that viable planktonic and biofilm bacteria were detected in both cutaneous ear tissue and dLNs at 2 h pi (**Figures 1A,B**), and were continuously present throughout the infection period. In the ear pinna tissue, bacterial loads were mostly similar and stable throughout the

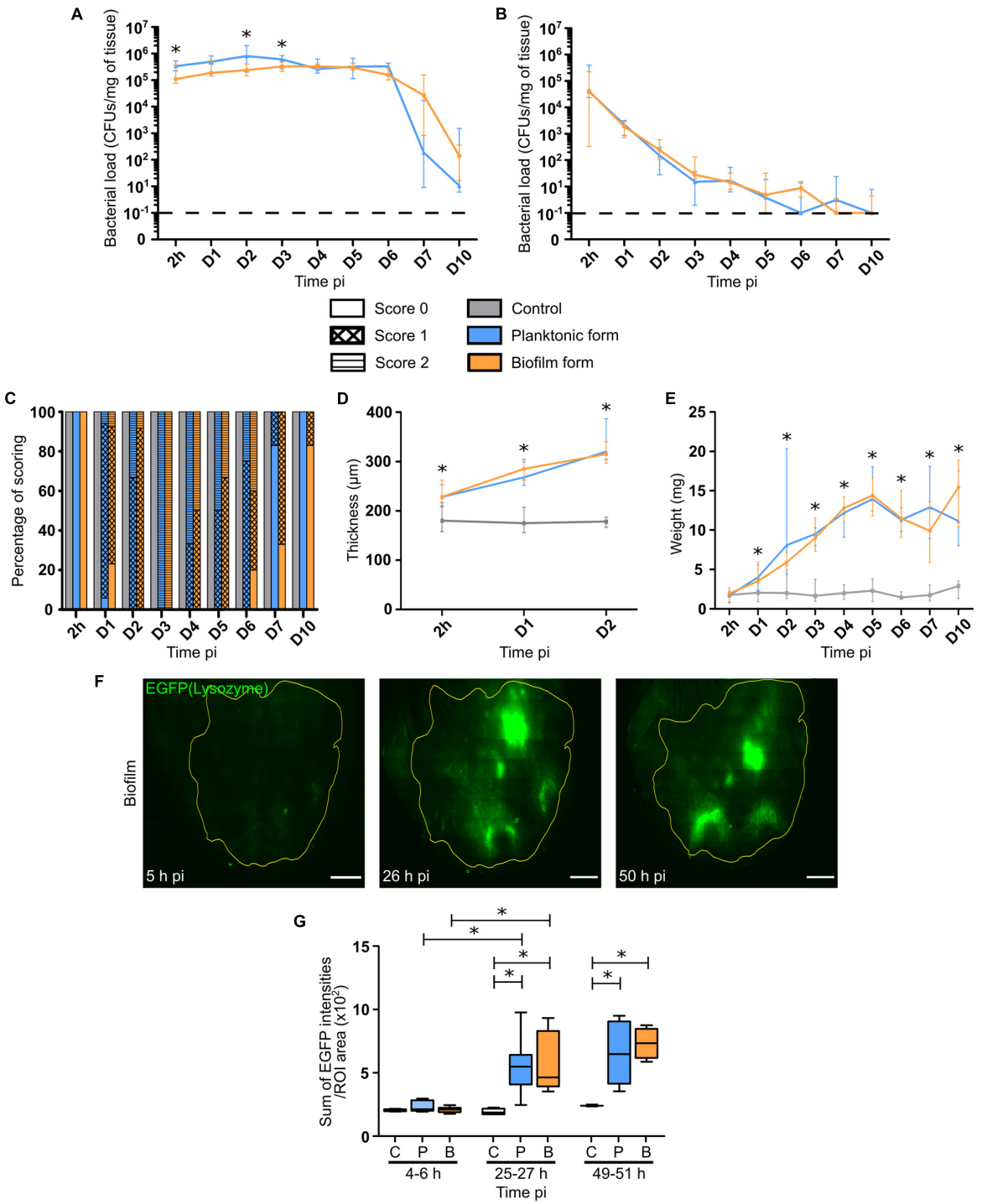

FIGURE 1 | Bacterial load and inflammatory responses in *S. aureus* infected tissue. **(A,B)** Bacterial load quantification, expressed in CFUs/mg of tissue, from 2 h pi to day 7 pi, and at day 10 pi in the ear pinnae **(A)** and dLNs **(B)** of WT C57BL/6J mice following micro-injection of PBS (C) or WT SH1000 planktonic (P) or biofilm (B) bacteria. Dotted line represents the limit of detection (median ± IQR, number of ear pinnae: N_C = 8–10 ear pinnae, N_P = 10–12 ear pinnae, N_{BF} = 11–12 ear pinnae, from 3 different experiments, Mann-Whitney two-tailed test, $*p < 0.05$). **(C)** Evaluation of ear pinnae inflammation from 2 h pi to day 7 pi, and at day 10 pi for the 3 groups of mice, by scoring based on erythema. Results expressed as percentage of each score (Number of mice: N_C = 6–10 mice, N_P = 4–17 mice, N_{BF} = 5–13 mice, from 3 different experiments). **(D)** Ear pinna thickness measurements from 2 h pi to day 2 pi for the 3 groups of mice (median ± IQR, number of ear pinnae: N_C = 4–7 ear pinnae, N_P = 6–8 ear pinnae, N_{BF} = 6–7 ear pinnae, from 3 different experiments, Mann-Whitney two-tailed test, $*p < 0.05$). **(E)** dLN weight measurements from 2 h pi to day 7 pi, and at day 10 pi for the 3 groups of mice (median ± IQR, number of dLNs: N_C = 8–10 dLNs, N_P = 10–12 dLNs, N_{BF} = 11–12 dLNs, from 3 different experiments, Mann-Whitney two-tailed test, $*p < 0.05$). **(F)** Reconstituted confocal images of LysM-EGFP transgenic mouse ear pinna tissue

(Continued)

FIGURE 1 | Continued
following micro-injection of mCherry-SH1000 biofilm bacteria. Images correspond to the maximal projection intensities of the EGFP signal, and the yellow line indicates the ROI where the "Sum of EGFP fluorescence intensities" was measured. Scale bar: 2 mm. One representative image is shown from at least 3 independent experiments. **(G)** Ratio of the sum of EGFP fluorescence intensities to ROI areas (median ± IQR, number of ear pinnae tissues: N_C = 4, N_P = 5–8, N_{BF} = 4–9, from at least 3 different experiments, Mann-Whitney two-tailed test, $*p < 0.05$).

first 6 days of infection for both forms of bacteria, with the first signs of bacterial clearance appearing at day 7. Although this sharp decrease seemed more pronounced in mice inoculated with planktonic bacteria, no significant difference was observed between the two forms. At day 10 pi, a lower bacterial load was detected in both groups of infected mice, as compared to day 7 pi, but was once again comparable between the two forms. In the dLNs, bacteria were present throughout all the infection period, with similar infection kinetics. This was in line with the maintenance of bacteria in the cutaneous tissue previously observed. Indeed, CFUs were detected even at day 10 pi in the dLN in 3/10 and 3/12 samples for planktonic and biofilm bacteria, respectively. At this time point, the bacterial load was low in most of the samples and often below the detection threshold.

Certain macroscopic parameters of inflammation related to the presence of bacteria in the target tissues (ear pinnae, dLNs) were then analyzed, including redness and swelling (thickness) of ear pinna tissue and dLN weight. In control mice, no redness was observed throughout the experimental period (**Figure 1C**). The first signs of redness (**Supplementary Figure 1**) appeared 24 h pi within the infected group of mice (**Figure 1C**), where most samples had a score of 1. Redness then peaked at day 3 pi within both infected groups, and then slowly decreased to give way to tissue necrosis from day 2 pi, with a peak at day 10 pi. Interestingly, the presence of redness in the cutaneous ear tissue lasted longer in the biofilm group of mice than in the planktonic group. The ear tissue swelling was further analyzed in the first 2 days of infection. Ear thickness was significantly increased as early as 2 h pi, as compared to control mice. Values continued to increase until the second day of infection with no observable difference between the two infected groups of mice (**Figure 1D**). Lastly, the weight of dLNs significantly and constantly increased after infection, as compared to control mice, starting from day 1 pi until the end of the infection period. Again, no observable difference was observed between the two infected groups of mice (**Figure 1E**).

To follow the evolution of early inflammatory responses in the skin, a semi-quantitative measure of EGFP positive (EGFP +) phagocyte recruitment in the ear pinna tissue was realized as previously described (Abdul Hamid et al., 2020; **Figure 1F** and **Supplementary Figure 2**). The ratio of the sum of EGFP fluorescence intensities to ROI area (**Figure 1G**), measured from 2 to 48 h pi, showed that both bacterial forms did not induce a significant increase in EGFP + cell recruitment at early time points (4–6 h pi), as compared to control mice. However, after 25 and 49 h pi, a significant increase of the ratio was observed in both groups of challenged mice, as compared to control mice. In infected mice, a significant increase of cell recruitment was observed between 4–6 and 25–27 h pi, but not between 25–27 and 49–51 h pi, meaning that the peak of cell recruitment was on day 1.

Taken together, these data show that global inflammatory responses are comparable in the target tissues after micro-injection of both bacterial forms.

Comparable Early Cytokine and Chemokine Profiles in the Mouse Ear Pinna and the Auricular Draining Lymph Node After the Micro-Injection of Either the Planktonic or Biofilm Form of *Staphylococcus aureus*

In a second set of experiments, cytokine and chemokine profiles were analyzed in ear tissue and dLN homogenates during the first few days of infection (24–72 h pi).

The chemokines analyzed were CXCL1/KC (**Figures 2A,B**) and CXCL9/MIG (**Figures 2C,D**), both responsible for the recruitment of phagocytes, namely PMNs and MOs/MΦs. Significantly higher levels of these chemokines were detected from 24 to 72 h pi in both target tissues, with higher concentrations measured in the skin than in the dLNs of infected mice. Globally, no difference was observed between the two bacterial forms, except after 72 h in the dLN where CXCL9 were comparable to those in controls.

The chemokine response was associated with a pro-inflammatory cytokine production by recruited innate immune cells. Pro-inflammatory cytokines IL-1β (**Figures 2E,F**) and IL-6 (**Supplementary Figures 3A,B**) were significantly increased in both target tissues, again with higher concentrations measured in the skin than in the dLNs of infected mice, and at all-time points analyzed. A larger quantity of TNF-α was also detected in the ear pinnae of infected mice, as compared to controls at 24 and 72 h pi (**Supplementary Figure 3C**). However, this increase was only observed at 24 h pi in the dLNs (**Supplementary Figure 3D**). Interestingly, IFNγ concentrations were comparable in control and infected mice in cutaneous ear tissue at 24 and 72 h pi (**Supplementary Figure 3E**), but were significantly increased at both time points in dLNs of infected mice, as compared to those of control mice (**Supplementary Figure 3F**). The last pro-inflammatory cytokine analyzed was IL-17 (**Supplementary Figures 3G,H**), largely produced by Th17 cells and capable of upregulating the expression of certain proinflammatory mediators such as IL-1β and IL-6 in MΦs. As seen previously for IL-6, significantly higher levels of IL-17 were detected in both target tissues of infected mice, as compared to controls at 24 and 72 h pi.

Finally, concentrations of the anti-inflammatory cytokine IL-10 (**Figures 2G,H**) were significantly increased in the ear pinnae tissue of infected mice, as compared to control mice at 24 and

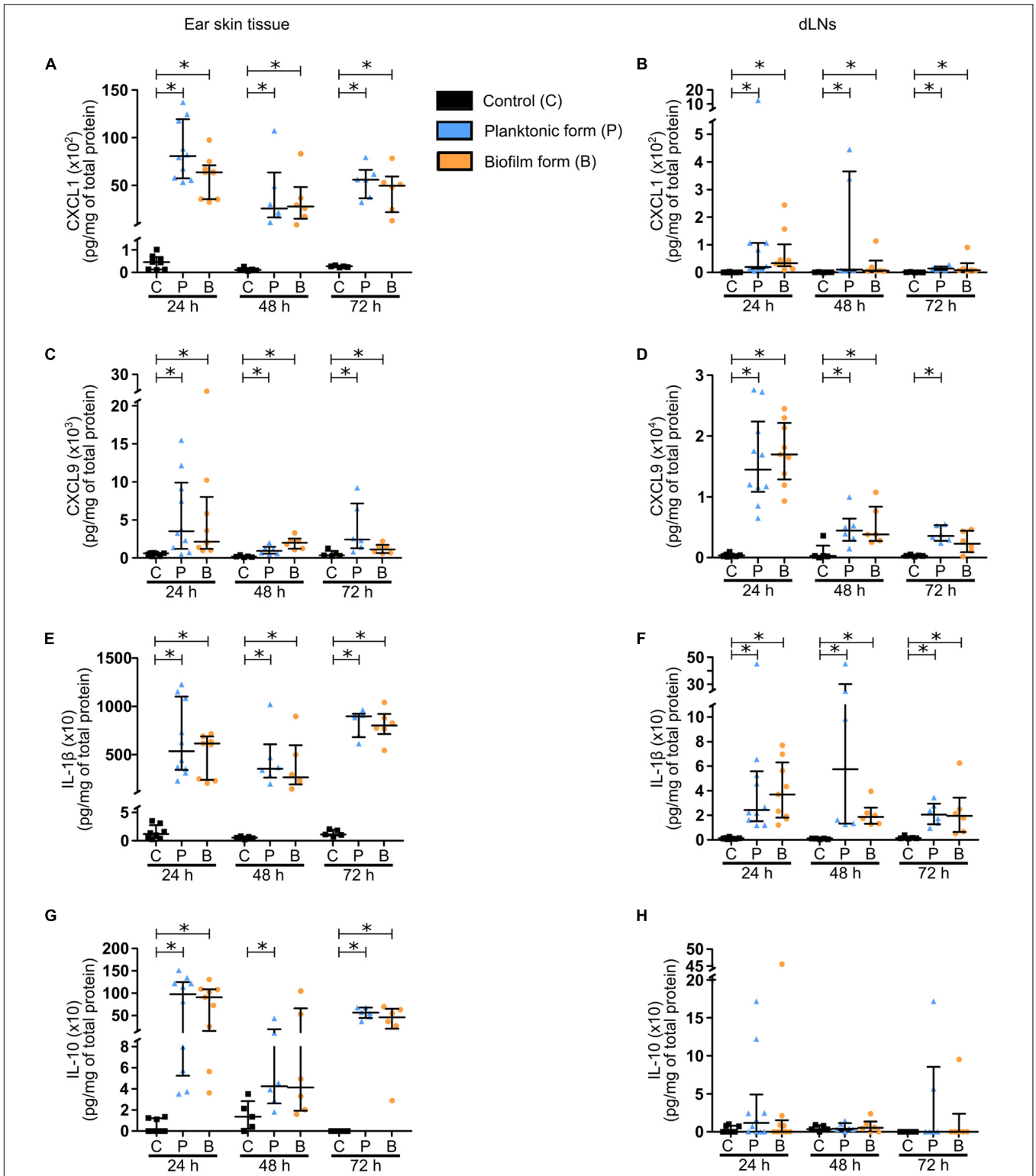

FIGURE 2 | Chemokine and cytokine production in *S. aureus* infected tissue. **(A–H)** Chemokine **(A–D)** and cytokine **(E–H)** levels, expressed in pg/mg of total protein, analyzed by Bioplex in the supernatants of ear pinna tissues **(A,C,E,G)** and dLNs **(B,D,F,H)** homogenates at 24, 48, and 72 h pi (median ± IQR, number of mice: N_C = 5–8, N_P = 6–10, N_{BF} = 6–9, from at least 3 different experiments, Mann-Whitney two-tailed test, $*p < 0.05$).

72 h pi, while only being significantly increased after inoculation of planktonic bacteria at 48 h pi.

Altogether, these results reveal early pro-inflammatory and anti-inflammatory responses in both target tissues at the molecular level, with IL-1β, IL-10, and CXCL1 being majorly produced in the cutaneous ear tissue, and CXCL9 largely detected in the dLN. These responses were globally comparable for both bacterial forms.

Differential Early Dynamics of Recruited Phagocytes in the Mouse Ear Pinna After the Microinjection of Either the Planktonic or Biofilm Form of *Staphylococcus aureus*

The very early dynamics of inflammatory responses observed in the skin were further analyzed by using an intravital confocal imaging approach, as previously described (Abdul Hamid et al., 2020). The first goal was to reproduce our previous results described for the *S. aureus* LYO-S2 clinical strain with the SH1000 laboratory strain in terms of cell recruitment and behavior of recruited cells after biofilm infection. Briefly, 5×10^6 CFUs of planktonic or biofilm mCherry-SH1000 were intradermally inoculated in the ear pinna tissue of LysM-EGFP transgenic mice. Time-lapse videos of cutaneous injection sites were then acquired during the first few hours following infection (from 2 to 5 h pi).

Using this laboratory strain, we observed a considerable influx of EGFP + phagocytes at injection sites, as early as 2 h pi for both bacterial forms. Cells recruited in response to the planktonic form were capable of invading the injection sites and creating bacteria cell interaction zones (**Figure 3A**, **Supplementary Figures 4A,B**, and **Supplementary Movie 1**). In contrast, cells that were recruited toward biofilm injection sites behaved differently, as previously described (Abdul Hamid et al., 2020). Indeed, EGFP + innate immune cells were arrested at the periphery of biofilm injection sites, with only few cells capable of penetrating the biofilm (**Figure 3B**, **Supplementary Figures 4C,D**, and **Supplementary Movie 2**).

The motility parameters (average speed, trajectory straightness, displacement) of recruited EGFP + phagocytes both in contact or not with bacteria at the injection site were also studied using Imaris software, as previously described (Abdul Hamid et al., 2020). SH1000 biofilms impacted cell motility similarly to previous observations, with a significant decrease in average speed and straightness of cells recruited toward biofilm bacteria, as compared to the planktonic form (**Figures 3C,D**). This means that cells were more heavily arrested and had a non-linear trajectory in biofilm-inoculated sites, as compared to planktonic-inoculated sites. The displacement of cell trajectories, representing the straight-line distance of the cell from the first timepoint to the last, was also analyzed in both infected conditions (**Figure 3E**). A significant decrease of this parameter was detected following biofilm inoculation, as compared to planktonic condition. This result was coherent with the decrease in straightness of cell trajectories observed with biofilm inocula.

Interestingly, observations made during intravital confocal microscopy experiments revealed that cells in contact with biofilms behaved differently from those in contact with planktonic bacteria, with a diminished capacity to emit pseudopods and retaining a round morphology (**Figures 3F,G** and **Supplementary Figures 4E–H**). Quantitative data were obtained by measuring the perimeter of EGFP + phagocytes in contact with either bacterial form with ImageJ software. Using this methodology, a significant decrease of cell perimeter in the presence of the biofilm inoculum was observed, as compared to planktonic inocula (**Figure 3H**). This result obtained *in vivo* was coherent with observations made *in vitro*, where PMNs in contact with *Pseudomonas aeruginosa* biofilms conserved their round shape (Jesaitis et al., 2003).

Differential Kinetics of Polymorphonuclear Neutrophil Recruitment After the Micro-Injection of Either the Planktonic or Biofilm Form of *Staphylococcus aureus*

To further understand the early inflammatory responses to the biofilm inocula, imaging data were complemented by flow cytometry analysis of the phenotype of recruited inflammatory cells in the cutaneous ear tissue and the dLNs. Here, ear pinna tissue of WT C57BL/6J mice were inoculated with either PBS or 5×10^6 CFUs of GFP fluorescent *S. aureus* planktonic or biofilm bacteria. After 2, 24, and 48 h, organs were harvested, digested to obtain a single cell suspension, labeled for specific membrane markers of innate inflammatory cells, and then analyzed by flow cytometry. Myeloid populations ($CD45^+CD11b^+$) were identified among live single cells and further subdivided into PMNs ($Ly6G^+Ly6C^+$) and MO/MΦ ($Ly6G^-Ly6C^{hi}$) (**Figure 4A** and **Supplementary Figure 5**).

Total cell counts prior to labeling showed a significant recruitment of cells to the cutaneous ear tissue as soon as 2 h pi in infected mice, as compared to control mice, which continued until 48 h pi (**Supplementary Figure 6A**). However, absolute values of myeloid cells in the ear pinna tissue of infected mice were only significantly increased after 24 and 48 h, as compared to control mice (**Figure 4B**). These data correlate with the previous measures of overall tissue inflammation in LysM-EGFP transgenic mice (**Figure 1G**). Interestingly, a decrease in the number of myeloid cells recruited in the ear tissue was observed 48 h following biofilm inoculation, as compared to the planktonic condition.

When looking further at the phenotype of recruited myeloid cells, a significantly higher percentage of PMNs was present in infected cutaneous ear tissue compared to controls, from 2 to 48 h pi (**Figure 4C**). However, PMN cell numbers revealed that this increase was significant only after 24 h in the planktonic group of mice, and from 2 h pi in biofilm infected mice (**Figure 4D**). Indeed, biofilms recruited more PMNs than controls at 2 h pi, with only a trend to increase when compared to mice infected with planktonic bacteria ($p = 0.0673$). Similar to their parent population ($CD45^+CD11b^+$ cells), biofilms recruited a significantly lower number of PMNs at 48 h pi, as compared to planktonic inoculated sites.

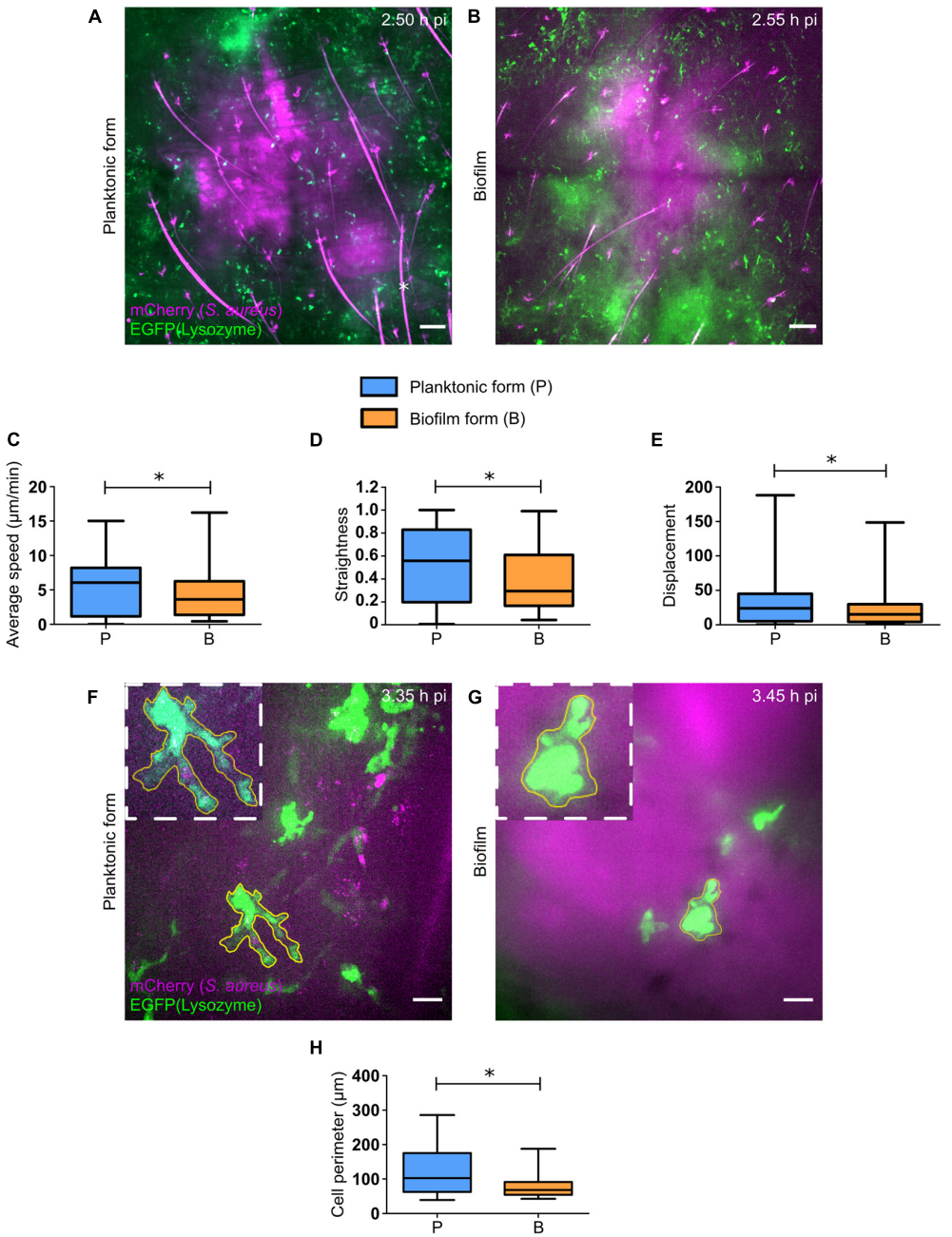

FIGURE 3 | Early dynamics of recruited EGFP + cells in the skin of *S. aureus* infected tissue. **(A,B)** Live confocal imaging, using X10 objectives, in the ear pinna tissue of LysM-EGFP transgenic mice following micro-injection of mCherry-SH1000 planktonic **(A)** or biofilm **(B)** bacteria. Average projections of green (EGFP + innate immune cells) and magenta (mCherry-SH1000) fluorescence, acquired at 2.50 h pi **(A)** and 2.55 h pi **(B)**, show immune cells recruited toward the injection site. Asterisk: autofluorescent hair (also in magenta). Scale bar: 100 µm. One representative experiment is shown for each group of mice from at least 9 independent experiments. **(C–E)** Quantification of EGFP + innate immune cell average speed **(C)**, straightness **(D)**, and displacement **(E)**, from X20 time-lapse acquisitions of infected mice (median ± minimum and maximum values, number of cells: N_P = 209, N_{BF} = 126, from at least 3 different experiments, Mann-Whitney two-tailed test, $*p < 0.05$). **(F,G)** Live confocal imaging, using X40 objectives, in the ear pinna tissue of LysM-EGFP transgenic mice following micro-injection of mCherry-SH1000 planktonic **(F)** or biofilm **(G)** bacteria. Maximum projections of green (EGFP + innate immune cells) and magenta (mCherry bacteria) fluorescence, acquired at 3.35 h pi **(F)** and 3.45 h pi **(G)**, show immune cells interacting with bacteria. The yellow line indicates the ROI where cell perimeter was measured. Scale bar: 15 µm. One representative experiment is shown for each group of mice from at least 9 independent experiments. **(H)** Measure of EGFP + innate immune cell perimeter, from maximum projection time-lapse acquisitions of infected mice (median ± minimum and maximum values, number of cells: N_P = 19, N_{BF} = 25, from 4 different experiments, Mann-Whitney one-tailed test, $*p < 0.05$).

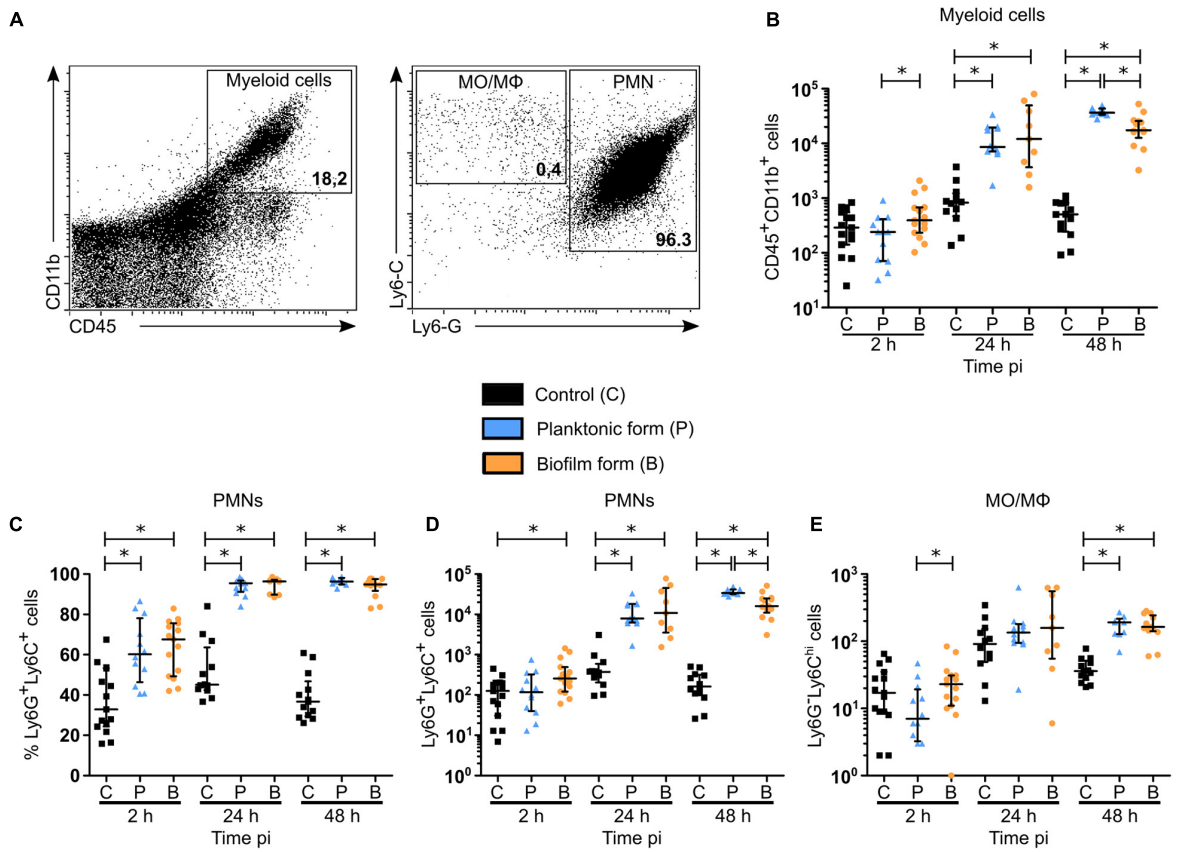

FIGURE 4 | Myeloid cell recruitment in the skin of *S. aureus* infected tissue. **(A)** Flow cytometric analysis showing the gating strategy of myeloid cells ($CD45^+CD11b^+$, left plot—upper right region), PMNs ($Ly6G^+Ly6C^+$, right plot—right most region), MOs/MΦs ($Ly6G^-Ly6C^{hi}$, right plot—upper left). Representative dot plots and percentages of cells gated are shown from planktonic infected WT C57BL/6J mice at 48 h pi. **(B)** Total number of myeloid cells among live cells in ear pinna tissue of control and planktonic or biofilm infected mice from 2 h pi to day 2 pi (median ± IQR, number of mice: N_C = 12–15, N_P = 9–12, N_{BF} = 9–15, from at least 3 different experiments, Mann-Whitney two-tailed test, $^*p < 0.05$). **(C–E)** Percentages **(C)** and total numbers **(D,E)** of PMNs **(C,D)** and MOs/MΦs **(E)** among myeloid cells in ear pinnae of control and planktonic or biofilm infected mice, from 2 h pi to day 2 pi (median ± IQR, number of mice: N_C = 12–15, N_P = 9–12, N_{BF} = 9–15, from at least 3 different experiments, Mann-Whitney two-tailed test, $^*p < 0.05$).

Altogether, **Figures 4C,D** illustrate that the majority of myeloid cells, and thus EGFP + phagocytes recruited to the cutaneous ear tissue after biofilm injection were PMNs. Their recruitment kinetics were different at 2 and 48 h pi, when compared to planktonic bacteria.

For MO/MΦ, a significant recruitment was detected in ear pinna tissue for both bacterial forms only after 48 h, as compared to control mice, but in a much lower proportion compared to PMNs (**Figure 4E**).

In dLNs, total cell counts were significantly increased only after 48 h with planktonic bacteria, as compared to controls, while only a trend to increase was detected in the biofilm group of mice ($p = 0.069$) (**Supplementary Figure 6B**). As shown previously in the cutaneous ear tissue, a significant increase in the percentage of PMNs was observed at 2 and 24 h pi in biofilm infected mice, as compared to control mice (**Figure 5A**). Additionally, a decrease in the percentage of these cells among their parent population was observed after 48 h, as compared to the planktonic condition. Thus, recruitment kinetics of PMNs in the dLN were similar to those in the cutaneous ear tissue (**Figure 5B**). Interestingly, bacteria inoculation induced a significant increase in both percentage and MO/MΦ cell numbers in the dLN at 24 and 48 h pi, a result which was not observed in the cutaneous ear tissue (**Figures 4E, 5B,C**). In contrast to PMNs, the percentage of MO/MΦ in the dLN was higher after 48 h following biofilm inoculation, as compared to the planktonic condition (**Figures 5A,C**).

Taken globally, these results show that PMNs comprise the majority of cells recruited during the early stages of anti-biofilm inflammatory responses. However, their recruitment seemed to be specifically impacted by biofilms.

Staphylococcus aureus Biofilm Bacteria Inoculated Into the Mouse Ear Pinna Mostly Interact With Polymorphonuclear Neutrophils

Imaging data presented in **Figure 3** illustrate qualitative differences in the interaction between EGFP + innate immune cells and either planktonic or biofilm bacteria at cutaneous

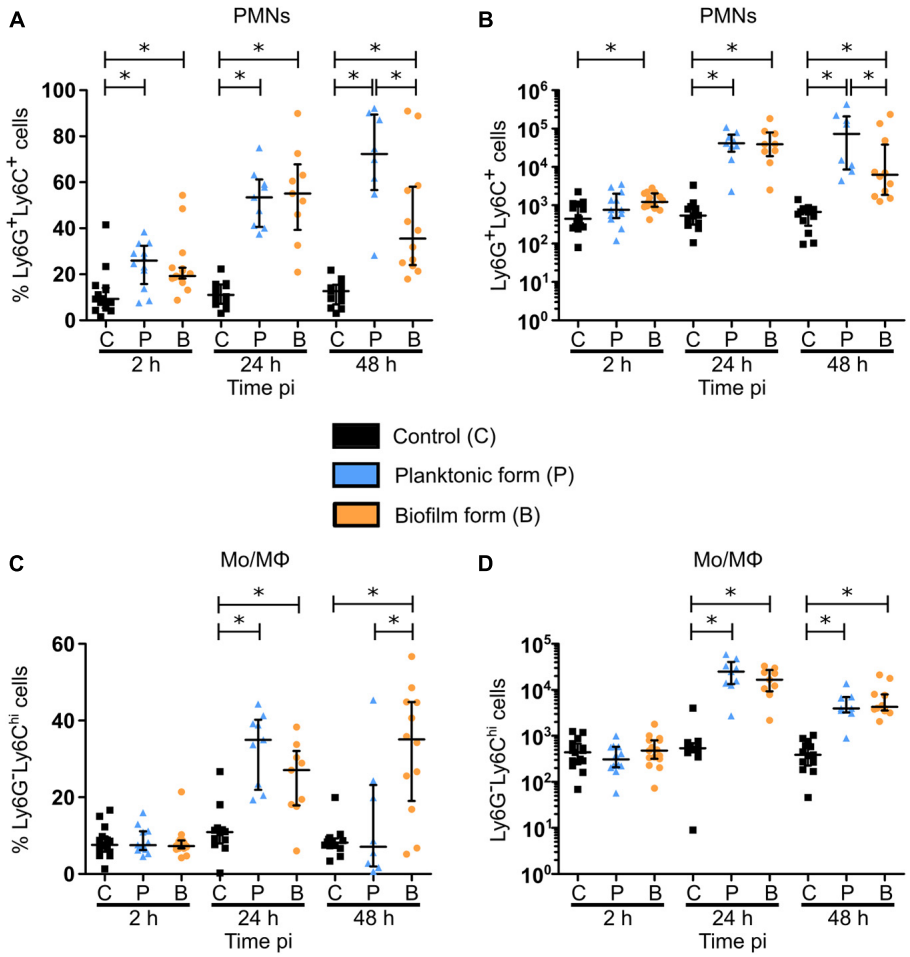

FIGURE 5 | Myeloid cell recruitment in the auricular draining lymph nodes of *S. aureus* infected mice. **(A–D)** Percentages **(A,C)** and total numbers **(B,D)** of PMNs **(A,B)** and MOs/MΦs **(C,D)** among myeloid cells in dLNs of control and planktonic or biofilm infected mice, from 2 h pi to day 2 pi (median ± IQR, number of mice: N_C = 12–15, N_P = 8–12, N_{BF} = 9–15, from at least 3 different experiments, Mann-Whitney two-tailed test, *$p < 0.05$).

injection sites. Thus, in complementary experiments, bacterial association with recruited inflammatory cells, and more specifically PMNs, was quantified in the cutaneous ear tissue by flow cytometry. To do this, ear pinnae of WT C57BL/6J mice were inoculated with either PBS or 5×10^6 CFUs of planktonic or biofilm GFP-SH1000, and the proportion of recruited inflammatory cells associated to bacteria was quantified at 2, 24, and 48 h pi (**Figure 6A**). To verify the specificity of bacterial association, we measured the median fluorescence intensity (MFI) of the GFP signal in PMN and MO/MΦ subpopulations and compared them to the MFIs of controls (**Supplementary Figures 6C,D**). **Supplementary Figures 6E,F** show that although GFP autofluorescent cells were detected in ear tissues of control mice, a significant GFP specific signal was associated to recruited phagocytes in the ear tissues of infected mice (**Supplementary Figures 6C–F**).

Bacterial association was observed in myeloid cell populations ($CD45^+CD11b^+$) as early as 2 h pi (**Figure 6B**), which corroborates observations made by intravital imaging (**Figure 3**). The proportion of bacteria associated cells increased significantly for both bacterial forms at 24 and 48 h pi, as compared to PBS inoculated control mice. Interestingly, a decrease in biofilm association was observed at 48 h pi, as compared to planktonic bacteria. Recruited PMNs followed the same kinetics of bacterial association as myeloid cells (**Figure 6C** and **Supplementary Figure 6E**), with the same significant decrease observed after 48 h for the biofilm inoculum. These data were coherent with the decrease of myeloid cells and PMN numbers observed at this time point (**Figures 4B,D**). Bacteria associated to MOs/MΦs were detected in a significantly increased proportion at 24 and 48 h pi (**Figure 6D** and **Supplementary Figure 6F**), but in a much smaller proportion, as compared to PMNs. Furthermore, the percentage of PMNs associated to bacteria was continuously higher than those observed in MO/MΦ at all three time points analyzed.

Taken together, these data suggest that PMNs represent key cells in the interactions with biofilm bacteria at the cutaneous injection site.

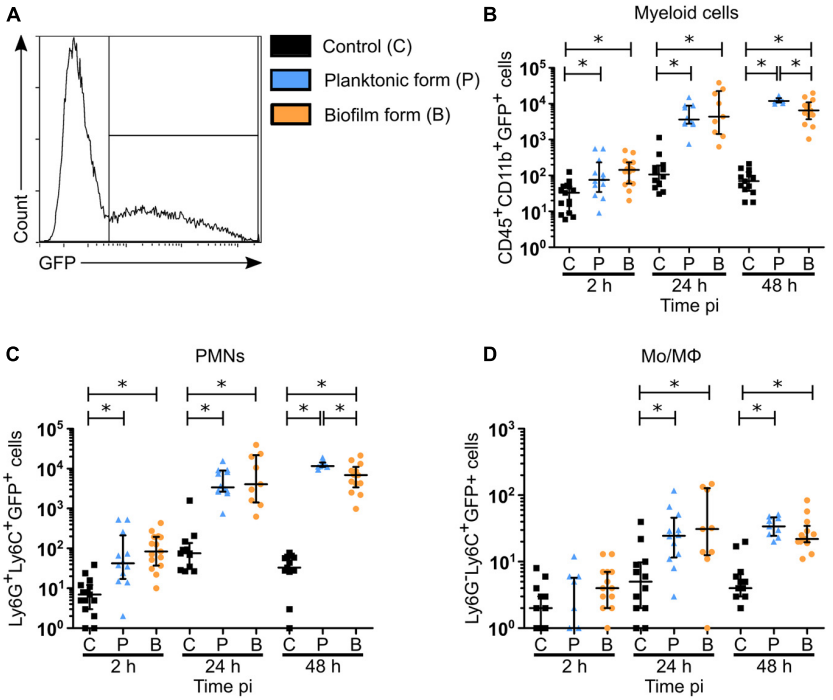

FIGURE 6 | Biofilm bacteria associated myeloid cells in the skin of *S. aureus* infected mice. **(A)** Flow cytometric analysis showing the gating strategy to analyze GFP-SH1000 associated cells among myeloid cells ($CD45^+CD11b^+GFP^+$), PMNs ($Ly6G^+Ly6C^+GFP^+$), and MOs/MΦs ($Ly6G^-Ly6C^{hi}GFP^+$). Representative histogram is shown from planktonic infected WT C57BL/6J mice at 48 h pi. **(B–D)** Total number of bacteria associated myeloid cells **(B)**, PMNs **(C)**, and MOs/MΦs **(D)** in ear pinna tissue of control and planktonic or biofilm infected mice, from 2 h pi to day 2 pi (median ± IQR, number of mice: N_C = 12–15, N_P = 9–12, N_{BF} = 9–15, from at least 3 different experiments, Mann-Whitney two-tailed test, $^*p < 0.05$).

Differential Functional Properties of Recruited Polymorphonuclear Neutrophil in the Mouse Ear Pinna After the Micro-Injection of Either the Planktonic or Biofilm Form of *Staphylococcus aureus*

Figures 4–6 illustrated that PMNs consist of the majority of inflammatory cells recruited to both the cutaneous ear tissue and the dLN, and are greatly associated to biofilms at the cutaneous injection site. In complementary experiments, their functional properties were studied in the ear pinna tissue of WT C57BL/6J mice, after inoculation of either PBS or *S. aureus* planktonic or biofilm bacteria.

In the first set of experiments, activation of myeloid cells and PMNs was assessed at 2, 24, and 48 h pi, based on their expression of the activation marker integrin receptor CD11b (**Figures 7A,B**). For both populations studied, an increased expression of CD11b was observed at 24 and 48 h pi, as compared to control mice, with a significant increase following biofilm inoculation at 48 h pi, as compared to the planktonic group. Interestingly, an initial significant increase in CD11b expression was shown 2 h pi in PMN populations only after planktonic bacteria inoculation.

In a second set of experiments, phagocytic activity of PMNs and MO/MΦ was analyzed 24 and 48 h pi. Intracellular bacteria were counted inside $CD11b^+$ cells purified from cutaneous infected tissues and subsequently stained using the May Grünwald-Giemsa (MGG) staining (**Figure 7C** and **Supplementary Figures 7A,B**). This analysis revealed that the proportion of PMNs harboring intracellular bacteria was significantly increased at 48 h pi when biofilms were inoculated, as compared to planktonic bacteria (**Figure 7D**). Further analyses showed that the proportion of PMNs harboring 5 or more intracellular bacteria was significantly increased in biofilm infected mice compared to the planktonic condition after 24 h. This seemed to continue at 48 h pi where a trend to increase was observed in the same group of cells. Conversely, the proportion of PMNs not harboring any intracellular bacteria was significantly increased 48 h pi after planktonic bacteria inoculation (**Figure 7E**), illustrating differential phagocytosis capacities of PMNs in response to the planktonic or biofilm inocula.

For MO/MΦ, the proportion of intracellular bacteria was comparable for both bacterial forms at both 24 and 48 h pi (**Supplementary Figure 7C**). However, as seen previously for PMNs, the proportion of these cells harboring 5 or more intracellular bacteria was also significantly increased after 24 h for biofilm inocula (**Supplementary Figure 7D**).

The viability of intracellular bacteria counted on MGG stained slides was also verified (**Supplementary Figure 7E**). To do this, CD11b + cells were purified from ear skin tissue of infected

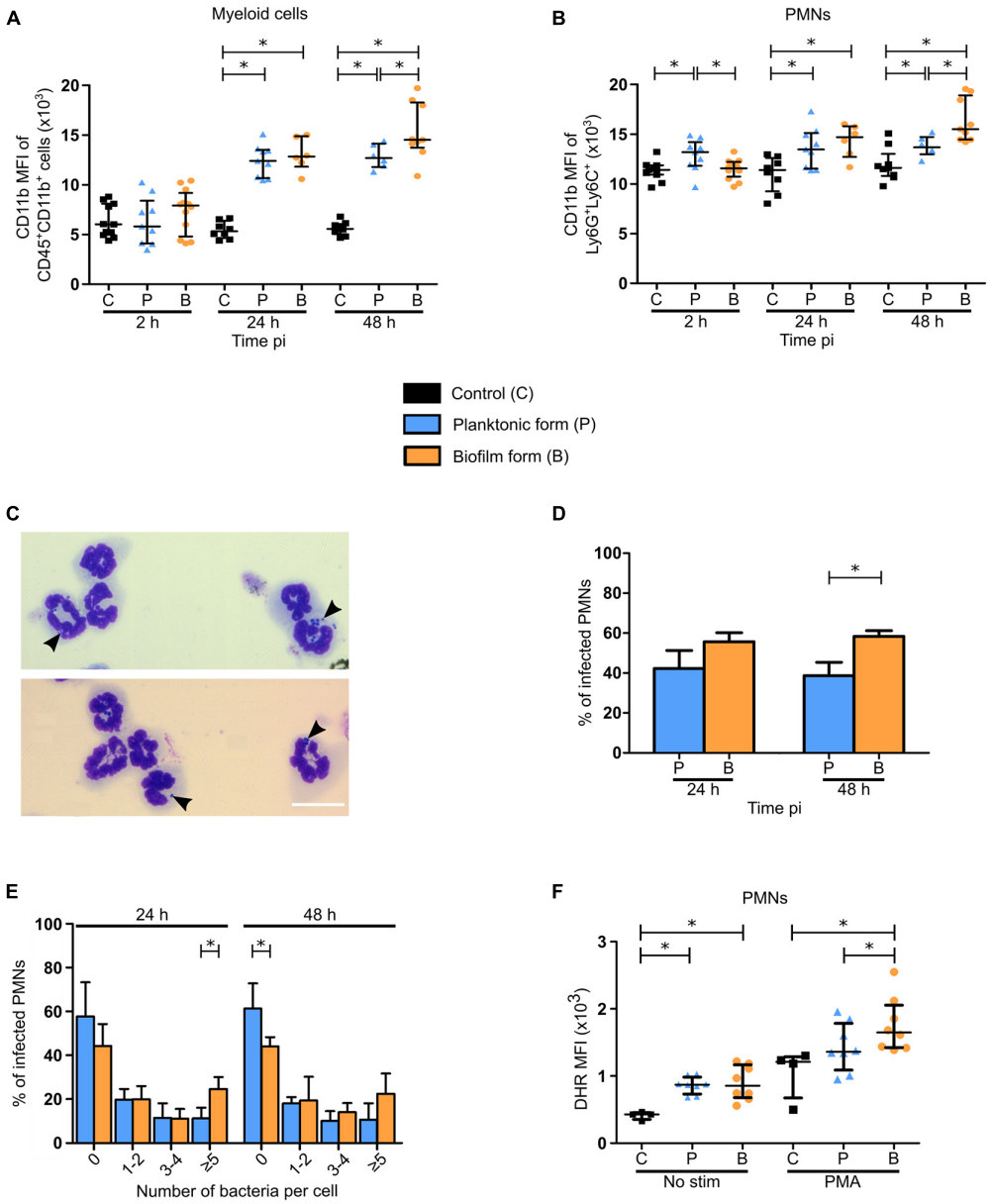

FIGURE 7 | Functional properties of neutrophils recruited in the ear pinna tissue of *S. aureus* infected mice. **(A,B)** APC-Cy7 conjugated CD11b antibody MFI of myeloid cells ($CD45^+CD11b^+$) **(A)** and PMNs ($Ly6G^+Ly6C^+$) **(B)** in ear pinna tissue of control and planktonic or biofilm infected mice, from 2 h pi to day 2 pi (median ± IQR, number of mice: N_C = 8–11, N_P = 6–9, N_{BF} = 6–12, from at least 3 different experiments, Mann-Whitney two-tailed test, $^*p < 0.05$). **(C)** Transmitted light images of $CD11b^+$ cells, following isolation from ear pinna tissue onto glass slides and MGG staining, show neutrophils harboring intracellular bacteria. Representative images are shown from planktonic infected WT C57BL/6J mice at 24 h pi. **(D)** Percentage of PMNs containing intracellular bacteria assessed at 24 and 48 h pi (mean ± SEM, number of cells: N_P = 223–238, N_{BF} = 232–338, from at least 3 different experiments, Mann-Whitney one-tailed test, $^*p < 0.05$). **(E)** Percentage of PMNs containing 0, 1–2, 3–4, or 5 or more intracellular bacteria assessed at 24 and 48 h pi (mean ± SEM, number of cells: N_P = 223–238, N_{BF} = 232–338, from at least 3 different experiments, Mann-Whitney one-tailed test, $^*p < 0.05$). **(F)** DHR MFI of PMNs, in the ear pinna tissue of control and planktonic or biofilm infected mice at day 2 pi, stimulated or not with PMA *ex vivo* in the presence of DHR, to assess NADPH oxidase activity (median ± IQR, number of mice: N_C = 4, $N_{P/BF}$ = 8, from at least 3 different experiments, Mann-Whitney one-tailed test, $^*p < 0.05$).

mice and treated with gentamycin. Cells were then lysed, and bacteria were enumerated following plating on agar plates. Results indicate the presence of viable intracellular planktonic and biofilm bacteria inside these cells (mainly PMNs and MOs/MΦs) at 24 and 48 h pi, in similar proportions.

Figures 4C,D illustrate that PMN recruitment was significantly decreased in response to biofilms after 48 h, as compared to planktonic inocula. However, the increased expression of the CD11b surface marker and of phagocytosis capacity of PMNs observed at this time-point supposed that

they were more activated in this context. To test this hypothesis, flow cytometry analysis was performed to assess DHR oxidation by Reactive Oxygen Species (ROS), reflective of NADPH oxidase activity generated in recruited PMNs in response to PMA (**Figure 7F**). When not in the presence of this soluble agent, DHR MFI was comparable between the two bacterial forms, despite being significantly increased compared to controls. PMA-stimulated PMNs from infected ear pinnae also presented a higher DHR MFI than controls, with an increased production of ROS after biofilm inoculation, as compared to planktonic bacteria.

Taken together, these results illustrated differential functional properties in recruited PMNs at 48 h pi following biofilm inoculation.

DISCUSSION

PMNs and MΦ have been largely described as key effector cells in the inflammatory responses during *S. aureus* infections (de Vor et al., 2020; Pidwill et al., 2021). Certain *in vivo* models have also shown that biofilms induce anti-inflammatory responses as early as day 3 or day 5 pi (Heim et al., 2015, 2018). As the infection outcome is conditioned in the first few days following host-bacteria contact, we sought out to highlight the very early impacts of *S. aureus* biofilms on the main cellular components of innate immune responses, meaning phagocytes. To do this, we compared inflammatory responses elicited by either planktonic or biofilm bacteria at different levels of the organism, in a mouse ear pinna model of infection. In this report, we demonstrated globally similar responses at the tissue and cytokine level, but found different cellular responses, including cell behavior, recruitment, and certain functional properties.

At the tissue level, we first observed a globally similar evolution of bacterial load between the two forms of *S. aureus*, contradicting a previous study that compared the fate of non-biofilm and biofilm inocula in mice. Thurlow and collaborators showed a better bacterial clearance of non-biofilm bacteria in skin abscess as early as day 3 compared to catheter grown biofilms implanted sub-cutaneously (Thurlow et al., 2011). They assigned this to the presence of the catheter, which could impede access of leukocytes toward the site of infection. In contrast, in the ear pinna model used in this work, biofilm inocula were accessible to host innate immune cells as no abiotic support was used. One possible reason for the comparable bacterial load observed in the ear pinna tissue could be the *in vivo* transition of planktonic bacteria to the biofilm lifestyle, representing a possible limit of the model. Several days are nevertheless probably necessary for this transition, even if the precise timing of this event to occur *in vivo* is currently unknown. In the clinical setting, *S. aureus* is prevalent in early prosthetic infections, which become manifest within 1 month following surgery (Arciola et al., 2018). To identify a possible planktonic to biofilm transition in the ear pinna, biofilm matrix components could be labeled *in vivo* by using specific fluorescent probes several days pi (Sauvat et al., 2020). Genes upregulated during biofilm formation could also be identified by transcriptomic analysis from planktonic-infected ear tissues, as previously carried out *in vitro* by Resch et al. (2005).

An observable inflammatory response was characterized by the apparition of redness and tissue swelling of the ear pinna tissue of infected mice, which was coherent with the presence of a high dose of bacteria in the first few days of infection. These results were further corroborated by the semi-quantitative measure of EGFP + phagocyte recruitment in the ear pinna tissue, and observations of bacterial injection sites showing a considerable recruitment of leukocytes for both bacterial forms. *S. aureus* is known to produce toxins and enzymes, such as leukocidins and coagulase, that are able to induce cell death by apoptosis, necroptosis, and also pyroptosis (Soe et al., 2021). This was coherent with ear pinna tissue necrosis observed as early as day 3. However, the exact proportion of each cell death pathway is yet to be studied.

We further determined the chemokine and cytokine profile in both cutaneous ear tissue and dLNs after *S. aureus* infection. In the ear tissue, we found large proportions of the PMN chemoattractant CXCL1 which has been shown previously to be notably secreted by keratinocytes in response to *S. aureus* (Olaru and Jensen, 2010). This would partially explain the significant increase in EGFP + immune cells observed at 24 h pi. High amounts of CXCL9/MIG, a Th1 cell-recruiting chemokine, were also found in infected mice. Globally, we found a robust pro-inflammatory cytokine response comparable between bacterial forms in both infected tissues, due to the presence of IL-1β, IL-6, and TNF-α. In line with these data, the presence of IL-17 may indicate that infected mice also mount a Th17 response, which is coherent with a previous study implicating IL-17 in establishing an effective antimicrobial response by γδ T cells (Cho et al., 2010). At early time points, IL-17 could also be produced by innate lymphoid cells in the skin and the dLNs (Cua and Tato, 2010). The absence of IFNγ production in infected mice could be explained by the early time points and/or by the presence of IL-10 in the infectious milieu, as the two are negatively correlated (Saraiva and O'Garra, 2010). Biofilms have indeed been shown to skew host immune responses toward an anti-inflammatory phenotype, in part *via* IL-10 secretion by M2 polarized MΦs and recruited MDSCs (Thurlow et al., 2011; Heim et al., 2018). In this study, the presence of IL-10 was comparable in both planktonic and biofilm infected ear tissues. In a previous study (Heim et al., 2020), *S. aureus* bacteria derived lactate was shown to inhibit HDAC11 in MΦs and MDSCs, which led to an increase in histone 3 acetylation at the IL-10 promoter, thus enhancing its expression. This discovery was, however, demonstrated in a biofilm prosthetic joint infection model, without comparison with planktonic bacteria. This anti-inflammatory response may be dependent on bacterial concentration, as IL-10 was not significantly increased in auricular dLNs of infected mice. Depending on the strain used, the inocula doses and the target tissues analyzed, some discrepancies may be observed between the inflammatory and anti-inflammatory chemokines and cytokines measured in different *in vivo* models. In all cases, host immune responses to *S. aureus* biofilm infection may be modulated by quorum sensing

or metabolically dampened bacteria induced by host immune responses (Yamada and Kielian, 2018).

The use of intravital confocal imaging to further decorticate very early inflammatory responses allowed us to highlight differences in cellular behavior. First, we validated the previously observed "biofilm" phenotype that leukocytes present at the injection site, with cells arrested at the periphery of the biofilm and modified motility parameters of recruited cells (Abdul Hamid et al., 2020; Sauvat et al., 2020). This means that the protective barrier role that biofilms exert are common between these two *S. aureus* strains, and probably among all biofilm-producing strains. The two strains used in our previous works were both MSSAs, but a "biofilm" phenotype has also been described for the MRSA strain USA300 (Thurlow et al., 2011; Gries et al., 2020b). The use of biofilms grown over longer periods (3 or 4 days) in the latter experiments compared to those used in this report further suggest a common immune evasion mechanism conserved throughout biofilm maturation. Furthermore, the fate of phagocytes capable of penetrating *S. aureus* biofilms have been explored *in vitro*. For example, Bhattacharya et al. (2020) showed that biofilms provoked NET formation in penetrating PMNs *via* the activity of Panton-Valentine Leukocidins and γ-hemolysin AB. Otherwise, Thurlow et al. (2011) showed that MΦs closer to the base of biofilms were not viable, while those on the surface were intact. In the ear pinna model, the "biofilm" phenotype also extended to a difference in migration properties, namely average speed, displacement, and trajectory straightness between the two bacterial forms. Indeed, EGFP + phagocytes possessed decreased values for all three motility parameters stated previously in the presence of biofilms, meaning that cells moved at a slower rate, were more restrained and were not recruited directly toward biofilms. This could be partly explained by the inability of phagocytes to bind to bacterial components embedded in the extracellular matrix or by the expression of chemotaxis inhibitory protein of *Staphylococcus* (CHIPS) (de Vor et al., 2020). Observing bacteria-cell interactions using higher magnification objectives allowed us to show for the first time *in vivo* that phagocytes interacting with biofilms were less capable of emitting pseudopods (illustrated by the decrease in cell perimeter) in the first hours after bacteria inoculation. Previously, Jesaitis et al. (2003) have shown a comparable phenomenon *in vitro* with PMNs and *Pseudomonas aeruginosa* biofilms. In these experiments, PMNs were immobilized on the surface of biofilms, while conserving a rounded morphology, a characteristic of unstimulated phagocytes. Unfortunately, the dynamics of $EGFP^+$ cells could not be further analyzed by intravital imaging due to ear tissue swelling and necrosis starting at 24 h pi. In line with these results, we found that the expression of the activation marker CD11b in PMNs (Kinhult et al., 2003) of biofilm-infected mice was similar to that of controls at 2 h pi, while it was upregulated in cells in the presence of planktonic bacteria.

Complementing these findings with FACS analysis allowed us to quantify the proportion of phagocytic cells recruited to both ear and dLN tissue over the first few days, and also to evaluate phagocytosis efficacy of recruited cells. Our results show that the majority of EGFP + cells that were observed in the cutaneous injection sites as early as 2 h pi were PMNs. After 24 h and onward, PMNs comprised the main bulk of the myeloid cell response, suggesting an important role played by these cells in the *S. aureus* early immune responses. Interestingly, at 2 h pi, increased PMN numbers were only observed in response to biofilms alluding to biofilm specific properties that favor PMN recruitment. In the Gram-negative bacterium *Pseudomonas aeruginosa*, the quorum sensing molecule N-acylhomoserine lactone acted as a strong PMN chemoattractant (Holm and Vikström, 2014). Recruitment continued at 24 and 48 h pi, coherent with the high levels of CXCL1 found in ear skin tissue at these time points.

In the dLN, kinetics of PMN recruitment were mostly similar to those observed in the ear tissue, except for a significant difference between both infected conditions in PMN percentage after 48 h. The recruitment of PMNs over the course of time was coherent with the large quantity of CXCL1 found in the skin and the dLN. As almost the same number of cells could be observed in both tissues despite the gap in CXCL1 concentration observed in the dLN, this suggests the implication of other homing mechanisms toward dLN. Moreover, the decrease in PMN numbers in the dLN of biofilm infected mice at 48 h pi, as compared to the planktonic condition, seemed more pronounced than in the ear tissue.

MO/MΦ arrived at the injection site after PMNs, but only after 48 h, and always in a smaller proportion compared to PMNs. Indeed, an initial increase in MO/MΦ numbers in biofilm mice compared to planktonic mice was observed at 2 h pi, but the two were however comparable to controls. Moreover, MO/MΦ were also recruited in control mice between 2 and 24 h pi, which could be reflective of their non-specific recruitment after skin trauma due to intradermal injection of PBS.

The numbers of recruited MO/MΦ were almost comparable to those of PMNs in the dLN, which coincides with the large quantity of CXCL9 predominant at 24 h pi. This chemokine has been previously shown to induce MΦ migration and activation in a apical periodontitis mouse model (Hasegawa et al., 2021). Resch et al. (2005) described the upregulation of polysaccharide intercellular adhesins, staphylococcal secretory antigen and staphyloxanthin during biofilm formation, as compared to planktonic growth. The recruited MOs/MΦs are antigen presenting cells that will migrate to the cutaneous dLN. Their mobilization from the skin and probably also from the blood circulation is clearly detected in the auricular dLN from 24 h pi. They will present antigens to naïve T cells, therefore playing a key role in inducing specific adaptive immune responses to biofilms. These responses need to be further explored.

In further experiments, the functional properties of PMNs recruited at the cutaneous injection sites were analyzed, as they were the major player in inflammatory responses mounted against *S. aureus* in this model.

CD11b is a β2 integrin that is found on the cell surface and also PMN granules. Following activation, intracellular pools of CD11b are translocated to the cell surface where they form heterodimers with CD18 capable of interacting with fibrinogen and inactivated

complement component 3 (iC3b) (Solovjov et al., 2005). The latter is implicated in opsonization, thus increasing phagocytosis effectiveness in PMNs with higher levels of CD11b. PMNs in contact with biofilms did not overexpress the CD11b surface marker at the beginning of the infection period. This could be due to the physical barrier represented by biofilms which could limit PMN access to bacteria. However, higher levels of CD11b were detected 48 h pi despite the PMNs decreased numbers observed at this later time point. This difference between the two inocula after 48 h could be due to the presence of matrix components in the biofilm inoculum, representing a multiplicity of additional antigens that are absent in the planktonic inoculum. Furthermore, a proportion of biofilm bacteria could be lysed after phagocytosis and matrix components could be released at the cutaneous injection sites. Namely, Phenol Soluble Modulins are biofilm matrix proteins well known as immunomodulators (Richardson et al., 2018). They also have been shown to fix to PMN formyl peptide receptors inducing their recruitment. The activation of this PMN receptor has been shown to induce chemotaxis, ROS production, degranulation, cytokine expression, and phagocytosis (Cheung et al., 2014; Dorward et al., 2015).

Analysis of bacterial association to immune cells showed that PMNs were the predominant immune cell interacting with inoculated *S. aureus* throughout the first few days of infection. Inversely, MO/MΦ were less likely to interact with bacteria, as they were detected in lesser proportions (number and percentage) compared to PMNs at each time-point. In just 2 h, PMNs present at the injection site were able to interact with planktonic and biofilm bacteria, corroborating intravital imaging observations. In response to large aggregates of bacteria and phagocytosis failure, PMNs release NETs composed of chromatin and antimicrobial peptides which subsequently trap and degrade bacteria (Branzk et al., 2014). Furthermore, this process causes cell membrane rupture and thus cell death although certain studies have shown that some PMNs conserve membrane integrity after NET release (non-lytic NETosis) and continue to phagocytose bacteria (Bhattacharya et al., 2020). The proportion of cells undergoing this type of NETosis in the ear pinna model is yet to be examined.

Phagocytic capacity of recruited PMNs was further studied. Phagocytosis of biofilm bacteria was increased at 48 h pi, as compared to planktonic bacteria, while it was comparable for both bacterial forms 24 h pi. In line with these results, a higher proportion of PMNs containing bacterial aggregates of 5 or more at 24 h pi was also observed in MO/MΦ. This could be explained by the spatial distribution of bacteria that are more compact in biofilms, allowing greater entry into cells during phagocytosis. Planktonic and biofilm bacteria that were observed intracellularly (in PMNs and MO/MΦ) were shown to be viable, and at comparable levels between the two forms. This proves the *in vivo* ability of *S. aureus* to maintain intracellularly inside phagocytes. Indeed, to combat degradation, *S. aureus* produce a variety of enzymes ranging from extracellular adherence protein that inhibit PMN serine protease (Stapels et al., 2014) to catalase and superoxide dismutase that prevent the oxidation effects of ROS (Painter et al., 2015). However, the exact *in vivo* contribution of persisting bacteria or of new phagocytosed bacteria to the proportion of detected intracellular bacteria in the ear tissue is not known.

A previous study suggested that PMN accumulation in *S. aureus* infected skin tissue was attributed to blood stream recruitment of mature PMNs, prolonged survival of recruited PMNs and local proliferation/maturation of c-kit$^+$ progenitor cells into mature PMNs (Kim et al., 2011). These progenitor cells were also capable of differentiating into MDSCs. The latter were initially described as having an important role in cancer where they promote an immunosuppressive microenvironment *via* the secretion of IL-10 and TGFβ or high levels of ROS, which have been associated with T-cell deactivation. They also have been identified in *S. aureus* biofilm prosthetic joint infections where they contribute toward anti-inflammatory responses (Heim et al., 2014). In the described mouse models, MDSCs were identified based on the co-expression of surface markers CD11b, Ly6G, and Ly6C. The selection of our PMN population was based on the same markers. In this report, even if PMN numbers were decreased after 48 h of biofilm infection as compared to the planktonic condition, these cells globally expressed higher levels of CD11b, had an increased production of ROS, and an increased phagocytic capacity. These results illustrate a potential PMN "over-activated" status in response to biofilms after 48 h. Further experiments are required to identify the specific phenotype of the different PMN subsets induced by *S. aureus* biofilms at this time point and their possible MDSC nature.

Taken globally, at early time points (2 h), we observed an initial increase in PMN numbers associated with CD11b expression levels comparable to controls, and a decreased capacity to penetrate biofilms and to emit pseudopods. At later time points (48 h), we observed a decrease in PMN numbers with a potential "over-activated" status associated with increased CD11b expression levels, ROS production and phagocytic capacity. In these conditions, we could have expected a higher and lower biofilm bacterial load after 2 and 48 h, respectively. Surprisingly, no differences in CFU numbers were observed with the planktonic condition in all experiments performed, suggesting a more complex mechanism of bacterial survival at play involving other immune or non-immune cell populations. Namely, Natural Killer cells that are recruited to *S. aureus* skin infections have been reported to secrete IL-17, subsequently activating keratinocytes to produce pro-inflammatory cytokines, chemokines and adhesion molecules that mediate neutrophil recruitment (Krishna and Miller, 2012). In any case, this comparative study where immune responses and bacterial loads were followed over time has never been carried out, and thus gives new insights into the understanding of innate immune responses directed toward *S. aureus* biofilms.

In conclusion, the ear pinna model allowed us to obtain a global picture of the early dynamics of immune responses against both forms of *S. aureus* at different levels of the organism. By performing a direct comparison of innate immune responses between planktonic and biofilm bacteria in the cutaneous tissue and dLN, we provide evidence that biofilms elicit specific immune signatures regarding PMN kinetics of recruitment and functional properties at very early time points.

DATA AVAILABILITY STATEMENT

The raw data supporting the conclusions of this article will be made available by the authors, without undue reservation.

ETHICS STATEMENT

The animal study was reviewed and approved by the Ethics Committee on Animal Experimentation (Auvergne C2E2A, Clermont-Ferrand, France) Agreement number: 1,725.

AUTHOR CONTRIBUTIONS

AA, AC, AD, JJ, FL, and PG conceived and designed the experiments. AA analyzed the data. AA, AC, AD, and PG performed experiments. AA, AC, AD, JJ, and PG participated in the provision of materials for experiments. PG supervised, managed, and coordinated responsibility for the research activity. AA and PG verified the overall replication and reproducibility of results, visualized, and wrote the manuscript. All authors contributed to the article and approved the submitted version.

FUNDING

PG obtained funding for this work by the Auvergne-Rhône-Alpes (AURA) region (Pack Ambition Recherche 2017-IMMUNOFILM-Staph project). The funders had no role in study design, data collection and analysis, decision to publish, or preparation of the manuscript.

ACKNOWLEDGMENTS

We wish to thank Ivo Boneca (Bacteria-Cell Interactions Unit, Pasteur Institute, Paris, France) for the LysM-EGFP transgenic mouse line, Caroline Vachias and Pierre Pouchin (Clermont Imagerie Confocal: CLIC, GReD, Clermont Auvergne University) for their help with setting up confocal microscopy acquisition parameters and subsequent image analysis and processing, Christelle Blavignac (Centre d'Imagerie Cellulaire Santé: CICS, Clermont Auvergne University) for helping us with flow cytometry parameters and data analysis, Tessa Amblard and Julie Durif for cytokine assays, Abdullah Azaz, Laurence Olivier-Nakusi and Sarah Chateauneuf for their preliminary results and setting up the mouse ear pinna model, as well as Elisabeth Billard for manuscript revision and helpful discussions, and Abdelkrim Alloui for ensuring mouse care and housing.

SUPPLEMENTARY MATERIAL

The Supplementary Material for this article can be found online at: https://www.frontiersin.org/articles/10.3389/fmicb.2021.728429/full#supplementary-material

Supplementary Figure 1 | Representative images illustrating the different levels of scoring used to assess ear pinna tissue inflammation. Images of C57BL/6J mice ear pinnae showing erythema (black empty arrowheads) at different time points following infection by *S. aureus*.

Supplementary Figure 2 | Mosaic acquisition of LysM-EGFP transgenic mice ear pinna tissue. Reconstituted confocal images of LysM-EGFP transgenic mice ear pinna tissue following micro-injection of PBS **(A)** or mCherry-SH1000 planktonic bacteria **(B)**. Images correspond to the maximal projection intensities of the EGFP signal, and the yellow line indicates the ROI where the "Sum of EGFP fluorescence intensities" was measured. Scale bar: 2 mm. One representative experiment is shown for each group of mice from at least 3 independent experiments.

Supplementary Figure 3 | Cytokine production in the ear pinna tissue and dLNs of control and planktonic or biofilm infected mice. **(A–H)** Cytokine levels, expressed in pg/mg of total protein, were analyzed by Bioplex in the supernatants of ear pinna tissue **(A,C,E,G)** and dLN **(B,D,F,H)** homogenates at 24 and 72 h pi (median ± IQR, number of mice: $N_C = 5$, $N_{P/BF} = 6$, from at least 3 different experiments, Mann-Whitney two-tailed test, $^*p < 0.05$).

Supplementary Figure 4 | Representative images of EGFP + immune cell recruitment to either *S. aureus* planktonic or biofilm bacteria. **(A–D)** Live confocal imaging, using X10 objectives, in the ear pinna tissue of LysM-EGFP transgenic mice following micro-injection of mCherry-SH1000 planktonic **(A,B)** or biofilm **(C,D)** bacteria. Representative average projections of green (EGFP + innate immune cells) and magenta (bacteria) fluorescence, acquired at 2.10 h pi **(A)**, 3.30 h pi **(B)**, 2.10 h pi **(C)**, and 3.30 h pi **(D)**, show immune cells recruited toward the injection site. Asterisk: autofluorescent hair (also in magenta). Scale bar: 100 μm. **(E–H)** Live confocal imaging, using X40 objectives, in the ear pinna tissue of LysM-EGFP transgenic mice following micro-injection of mCherry-SH1000 planktonic **(E,F)** or biofilm **(G,H)** bacteria. Maximum projections of green (innate immune cells) and magenta (bacteria) fluorescence, acquired at 4.20 h pi **(E)**, 3.25 h pi **(F)**, 3.25 h pi **(G)**, and 2.30 h pi **(H)** show immune cells in the injection area. The yellow line indicates the ROI where cell perimeter was measured. Asterisk: autofluorescent hair (also in magenta). Scale bar: 15 μm. One representative experiment is shown for each group of mice from at least 9 independent experiments.

Supplementary Figure 5 | Flow cytometry gating strategy for myeloid cells populations isolated from the ear tissue and dLN. Representative dot plots showing the gating strategy to analyze myeloid cell populations in the skin and dLN following inoculation. Representative dot plots and percentages of cells gated are shown from planktonic infected WT C57BL/6J mice at 24 h pi.

Supplementary Figure 6 | Immune cell counts and percentage of bacteria associated immune cells. **(A,B)** Total number of live cells recruited to ear pinna tissue **(A)** and dLNs **(B)** of control and planktonic or biofilm infected mice from 2 h pi to day 2 pi (median ± IQR, number of mice: $N_C = 12–15$, $N_P = 9–12$, $N_{BF} = 9–15$, from at least 3 different experiments, Mann-Whitney two-tailed test, $^*p < 0.05$). **(C,D)** GFP median fluorescence intensity of PMNs **(C)** and MOs/MΦs **(D)** associated to GFP-SH1000 in the ear pinna tissues of control and planktonic or biofilm infected mice from 2 to 48 h pi (median ± IQR, number of mice: $N_C = 12–15$, $N_P = 9–12$, $N_{BF} = 9–15$, from at least 3 different experiments, Mann-Whitney one-tailed test, $^*p < 0.05$). **(E,F)** Percentage of bacteria associated PMNs **(E)** and MOs/MΦs **(F)** in ear pinna tissue of control and planktonic or biofilm infected mice from 2 h pi to day 2 pi (median ± IQR, number of mice: $N_C = 12–15$, $N_P = 9–12$, $N_{BF} = 9–15$, from at least 3 different experiments, Mann-Whitney two-tailed test, $^*p < 0.05$).

Supplementary Figure 7 | Phagocytosis of *S. aureus* planktonic or biofilm bacteria by $CD11b^+$ myeloid cells in the ear pinna tissue. **(A,B)** Transmitted light images of $CD11b^+$ cells, following isolation from ear pinna tissue onto glass slides and MGG staining, show PMNs **(A,B)** and MOs/MΦs **(B)** harboring intracellular bacteria (black arrowheads). Representative images are shown from planktonic infected WT C57BL/6J mice at 24 h pi **(A)** and 48 h pi **(B)**. **(C)** Percentage of MOs/MΦs containing intracellular bacteria assessed at 24 and 48 h pi (mean ± SEM, number of cells: $N_P = 223–238$, $N_{BF} = 232–338$, from at least 3 different experiments, Mann-Whitney one-tailed test, $^*p < 0.05$). **(D)** Percentage of MOs/MΦs containing 0, 1–2, 3–4, or 5 or more intracellular bacteria assessed at 24 and 48 h pi (mean ± SEM, number of cells: $N_P = 223–238$, $N_{BF} = 232–338$, from at least 3 different experiments, Mann-Whitney one-tailed test, $^*p < 0.05$).

(E) Quantification of intracellular bacteria, expressed in CFUs/10^6 cells, in CD11b + cells isolated from ear pinna tissue of planktonic or biofilm infected mice, at 24 and 48 h pi (median ± IQR, number of mice: N_P = 5, N_{BF} = 3–4, from at least 3 different experiments, Mann-Whitney one-tailed test, $^*p < 0.05$).

Supplementary Movie 1 | EGFP + innate immune cells are recruited toward a planktonic injection site. *In vivo* confocal time-lapse imaging of immune cell migration in LysM-EGFP transgenic mice ear tissue injected with planktonic bacteria from 2.50 to 3.10 hpi. Average projections of time-lapse images. Z-stacks collected 72.98 s apart. Scale bar: 100 μm.

Supplementary Movie 2 | EGFP + innate immune cells are recruited toward a biofilm injection site. *In vivo* confocal time-lapse imaging of immune cell migration in LysM-EGFP transgenic mice ear tissue injected with planktonic bacteria from 2.55 to 3.25 hpi. Average projections of time-lapse images. Z-stacks collected 106.55 s apart. Scale bar: 100 μm.

REFERENCES

Abdul Hamid, A. I., Nakusi, L., Givskov, M., Chang, Y.-T., Marquès, C., and Gueirard, P. (2020). A mouse ear skin model to study the dynamics of innate immune responses against *Staphylococcus aureus* biofilms. *BMC Microbiol.* 20:22. doi: 10.1186/s12866-019-1635-z

Arciola, C. R., Campoccia, D., and Montanaro, L. (2018). Implant infections: adhesion, biofilm formation and immune evasion. *Nat. Rev. Microbiol.* 16, 397–409. doi: 10.1038/s41579-018-0019-y

Bhattacharya, M., Berends, E. T. M., Zheng, X., Hill, P. J., Chan, R., Torres, V. J., et al. (2020). Leukocidins and the nuclease nuc prevent neutrophil-mediated killing of *Staphylococcus aureus* biofilms. *Infect. Immun.* 88, e00372-20. doi: 10.1128/IAI.00372-20

Bjarnsholt, T. (2013). The role of bacterial biofilms in chronic infections. *APMIS Suppl.* 121, 1–51. doi: 10.1111/apm.12099

Borbón, T. Y., Scorza, B. M., Clay, G. M., de Queiroz, F. L. N., Sariol, A. J., Bowen, J. L., et al. (2019). Coinfection with Leishmania major and *Staphylococcus aureus* enhances the pathologic responses to both microbes through a pathway involving IL-17A. *PLoS Negl. Trop. Dis.* 13:e0007247. doi: 10.1371/journal.pntd.0007247

Branzk, N., Lubojemska, A., Hardison, S. E., Wang, Q., Gutierrez, M. G., Brown, G. D., et al. (2014). Neutrophils sense microbe size and selectively release neutrophil extracellular traps in response to large pathogens. *Nat. Immunol.* 15, 1017–1025. doi: 10.1038/ni.2987

Capucetti, A., Albano, F., and Bonecchi, R. (2020). Multiple roles for chemokines in neutrophil biology. *Front. Immunol.* 11:1259. doi: 10.3389/fimmu.2020.01259

Charpentier, E., Anton, A. I., Barry, P., Alfonso, B., Fang, Y., and Novick, R. P. (2004). Novel cassette-based shuttle vector system for gram-positive bacteria. *Appl. Environ. Microbiol.* 70, 6076–6085. doi: 10.1128/AEM.70.10.6076-6085.2004

Cheung, G. Y. C., Joo, H.-S., Chatterjee, S. S., and Otto, M. (2014). Phenol-soluble modulins – critical determinants of staphylococcal virulence. *FEMS Microbiol. Rev.* 38, 698–719. doi: 10.1111/1574-6976.12057

Cho, J. S., Pietras, E. M., Garcia, N. C., Ramos, R. I., Farzam, D. M., Monroe, H. R., et al. (2010). IL-17 is essential for host defense against cutaneous *Staphylococcus aureus* infection in mice. *J. Clin. Invest.* 120, 1762–1773. doi: 10.1172/JCI40891

Costerton, J. W. (2001). Cystic fibrosis pathogenesis and the role of biofilms in persistent infection. *Trends Microbiol.* 9, 50–52. doi: 10.1016/S0966-842X(00)01918-1

Cua, D. J., and Tato, C. M. (2010). Innate IL-17-producing cells: the sentinels of the immune system. *Nat. Rev. Immunol.* 10, 479–489. doi: 10.1038/nri2800

de Vor, L., Rooijakkers, S. H. M., and van Strijp, J. A. G. (2020). Staphylococci evade the innate immune response by disarming neutrophils and forming biofilms. *FEBS Lett.* 594, 2556–2569. doi: 10.1002/1873-3468.13767

Dorward, D. A., Lucas, C. D., Chapman, G. B., Haslett, C., Dhaliwal, K., and Rossi, A. G. (2015). The role of formylated peptides and formyl peptide receptor 1 in governing neutrophil function during acute inflammation. *Am. J. Pathol.* 185, 1172–1184. doi: 10.1016/j.ajpath.2015.01.020

Forestier, C., Billard, E., Milon, G., and Gueirard, P. (2017). Unveiling and characterizing early bilateral interactions between biofilm and the mouse innate immune system. *Front. Microbiol.* 8:2309. doi: 10.3389/fmicb.2017.02309

Gries, C. M., Biddle, T., Bose, J. L., Kielian, T., and Lo, D. D. (2020a). *Staphylococcus aureus* fibronectin binding protein a mediates biofilm development and infection. *Infect. Immun.* 88, e00859-19. doi: 10.1128/IAI.00859-19

Gries, C. M., Rivas, Z., Chen, J., and Lo, D. D. (2020b). Intravital multiphoton examination of implant-associated *Staphylococcus aureus* biofilm infection. *Front. Cell. Infect. Microbiol.* 10:574092. doi: 10.3389/fcimb.2020.574092

Hanke, M. L., Heim, C. E., Angle, A., Sanderson, S. D., and Kielian, T. (2013). Targeting macrophage activation for the prevention and treatment of *Staphylococcus aureus* biofilm infections. *J. Immunol.* 190, 2159–2168. doi: 10.4049/jimmunol.1202348

Hasegawa, T., Venkata Suresh, V., Yahata, Y., Nakano, M., Suzuki, S., Suzuki, S., et al. (2021). Inhibition of the CXCL9-CXCR3 axis suppresses the progression of experimental apical periodontitis by blocking macrophage migration and activation. *Sci. Rep.* 11:2613. doi: 10.1038/s41598-021-82167-7

Heim, C. E., Bosch, M. E., Yamada, K. J., Aldrich, A. L., Chaudhari, S. S., Klinkebiel, D., et al. (2020). Lactate production by *Staphylococcus aureus* biofilm inhibits HDAC11 to reprogram the host immune response during persistent infection. *Nat. Microbiol.* 5, 1271–1284. doi: 10.1038/s41564-020-0756-3

Heim, C. E., Vidlak, D., and Kielian, T. (2015). Interleukin-10 production by myeloid-derived suppressor cells contributes to bacterial persistence during *Staphylococcus aureus* orthopedic biofilm infection. *J. Leukoc. Biol.* 98, 1003–1013. doi: 10.1189/jlb.4VMA0315-125RR

Heim, C. E., Vidlak, D., Scherr, T. D., Kozel, J. A., Holzapfel, M., Muirhead, D. E., et al. (2014). Myeloid-derived suppressor cells (MDSCs) contribute to S. aureus orthopedic biofilm infection. *J. Immunol.* 192, 3778–3792. doi: 10.4049/jimmunol.1303408

Heim, C. E., West, S. C., Ali, H., and Kielian, T. (2018). Heterogeneity of Ly6G+ Ly6C+ Myeloid-Derived suppressor cell infiltrates during *Staphylococcus aureus* biofilm infection. *Infect. Immun.* 86, e00684-18. doi: 10.1128/IAI.00684-18

Herbert, S., Ziebandt, A.-K., Ohlsen, K., Schäfer, T., Hecker, M., Albrecht, D., et al. (2010). Repair of global regulators in *Staphylococcus aureus* 8325 and comparative analysis with other clinical isolates. *Infect. Immun.* 78, 2877–2889. doi: 10.1128/IAI.00088-10

Holm, A., and Vikström, E. (2014). Quorum sensing communication between bacteria and human cells: signals, targets, and functions. *Front. Plant Sci.* 5:309. doi: 10.3389/fpls.2014.00309

Horn, C. M., and Kielian, T. (2020). Crosstalk between *Staphylococcus aureus* and innate immunity: focus on immunometabolism. *Front. Immunol.* 11:621750. doi: 10.3389/fimmu.2020.621750

Jesaitis, A. J., Franklin, M. J., Berglund, D., Sasaki, M., Lord, C. I., Bleazard, J. B., et al. (2003). Compromised host defense on *Pseudomonas aeruginosa* biofilms: characterization of neutrophil and biofilm interactions. *J. Immunol.* 171, 4329–4339. doi: 10.4049/jimmunol.171.8.4329

Kim, M.-H., Granick, J. L., Kwok, C., Walker, N. J., Borjesson, D. L., Curry, F.-R. E., et al. (2011). Neutrophil survival and c-kit+-progenitor proliferation in *Staphylococcus aureus*–infected skin wounds promote resolution. *Blood* 117, 3343–3352. doi: 10.1182/blood-2010-07-296970

Kinhult, J., Egesten, A., Benson, M., Uddman, R., and Cardell, L. O. (2003). Increased expression of surface activation markers on neutrophils following migration into the nasal lumen. *Clin. Exp. Allergy* 33, 1141–1146. doi: 10.1046/j.1365-2222.2003.01682.x

Krishna, S., and Miller, L. S. (2012). Innate and adaptive immune responses against *Staphylococcus aureus* skin infections. *Semin. Immunopathol.* 34, 261–280. doi: 10.1007/s00281-011-0292-6

Mac-Daniel, L., Buckwalter, M. R., Gueirard, P., and Ménard, R. (2016). Myeloid cell isolation from mouse skin and draining lymph node following intradermal immunization with live attenuated plasmodium sporozoites. *J. Vis. Exp.* 2016:53796. doi: 10.3791/53796

Moormeier, D. E., and Bayles, K. W. (2017). *Staphylococcus aureus* biofilm: a complex developmental organism. *Mol. Microbiol.* 104, 365–376. doi: 10.1111/mmi.13634

O'Neill, A. J. (2010). *Staphylococcus aureus* SH1000 and 8325-4: comparative genome sequences of key laboratory strains in staphylococcal research. *Lett. Appl. Microbiol.* 51, 358–361. doi: 10.1111/j.1472-765X.2010.02885.x

Olaru, F., and Jensen, L. E. (2010). *Staphylococcus aureus* stimulates neutrophil targeting chemokine expression in keratinocytes through an autocrine IL-1α signaling loop. *J. Invest. Dermatol.* 130, 1866–1876. doi: 10.1038/jid.2010.37

Painter, K. L., Strange, E., Parkhill, J., Bamford, K. B., Armstrong-James, D., and Edwards, A. M. (2015). *Staphylococcus aureus* adapts to oxidative stress by producing H2O2-resistant small-colony variants via the SOS response. *Infect. Immun.* 83, 1830–1844. doi: 10.1128/IAI.03016-14

Pidwill, G. R., Gibson, J. F., Cole, J., Renshaw, S. A., and Foster, S. J. (2021). The role of macrophages in *Staphylococcus aureus* infection. *Front. Immunol.* 11:620339. doi: 10.3389/fimmu.2020.620339

Resch, A., Rosenstein, R., Nerz, C., and Götz, F. (2005). Differential gene expression profiling of *Staphylococcus aureus* cultivated under biofilm and planktonic conditions. *Appl. Environ. Microbiol.* 71, 2663–2676. doi: 10.1128/AEM.71.5.2663-2676.2005

Ricciardi, B. F., Muthukrishnan, G., Masters, E., Ninomiya, M., Lee, C. C., and Schwarz, E. M. (2018). *Staphylococcus aureus* evasion of host immunity in the setting of prosthetic joint infection: biofilm and beyond. *Curr. Rev. Musculoskelet. Med.* 11, 389–400. doi: 10.1007/s12178-018-9501-4

Richardson, J. R., Armbruster, N. S., Günter, M., Henes, J., and Autenrieth, S. E. (2018). *Staphylococcus aureus* PSM peptides modulate human monocyte-derived dendritic cells to prime regulatory T cells. *Front. Immunol.* 9:2603. doi: 10.3389/fimmu.2018.02603

Saraiva, M., and O'Garra, A. (2010). The regulation of IL-10 production by immune cells. *Nat. Rev. Immunol.* 10, 170–181. doi: 10.1038/nri2711

Sauvat, L., Hamid, A. I. A., Blavignac, C., Josse, J., Lesens, O., and Gueirard, P. (2020). Biofilm-coated microbeads and the mouse ear skin: an innovative model for analysing anti-biofilm immune response in vivo. *PLoS One* 15:e0243500. doi: 10.1371/journal.pone.0243500

Schenk, S., and Laddaga, R. A. (1992). Improved method for electroporation of *Staphylococcus aureus*. *FEMS Microbiol. Lett.* 73, 133–138. doi: 10.1016/0378-1097(92)90596-g

Soe, Y. M., Bedoui, S., Stinear, T. P., and Hachani, A. (2021). Intracellular Staphylococcus aureus and host cell death pathways. *Cell. Microbiol.* 23:e13317. doi: 10.1111/cmi.13317

Solovjov, D. A., Pluskota, E., and Plow, E. F. (2005). Distinct roles for the α and β subunits in the functions of integrin αMβ2*. *J. Biol. Chem.* 280, 1336–1345. doi: 10.1074/jbc.M406968200

Stapels, D. A. C., Ramyar, K. X., Bischoff, M., von Köckritz-Blickwede, M., Milder, F. J., Ruyken, M., et al. (2014). *Staphylococcus aureus* secretes a unique class of neutrophil serine protease inhibitors. *Proc. Natl. Acad. Sci. U.S.A.* 111, 13187–13192. doi: 10.1073/pnas.1407616111

Tasse, J., Cara, A., Saglio, M., Villet, R., and Laurent, F. (2018). A steam-based method to investigate biofilm. *Sci. Rep.* 8:13040. doi: 10.1038/s41598-018-31437-y

Thurlow, L. R., Hanke, M. L., Fritz, T., Angle, A., Aldrich, A., Williams, S. H., et al. (2011). *Staphylococcus aureus* biofilms prevent macrophage phagocytosis and attenuate inflammation in vivo. *J. Immunol.* 186, 6585–6596. doi: 10.4049/jimmunol.1002794

Turner, N. A., Sharma-Kuinkel, B. K., Maskarinec, S. A., Eichenberger, E. M., Shah, P. P., Carugati, M., et al. (2019). Methicillin-resistant *Staphylococcus aureus*: an overview of basic and clinical research. *Nat. Rev. Microbiol.* 17, 203–218. doi: 10.1038/s41579-018-0147-4

Yamada, K. J., and Kielian, T. (2018). Biofilm-Leukocyte cross-talk: impact on immune polarization and immunometabolism. *J. Innate Immun.* 11, 280–288. doi: 10.1159/000492680

Conflict of Interest: The authors declare that the research was conducted in the absence of any commercial or financial relationships that could be construed as a potential conflict of interest.

Publisher's Note: All claims expressed in this article are solely those of the authors and do not necessarily represent those of their affiliated organizations, or those of the publisher, the editors and the reviewers. Any product that may be evaluated in this article, or claim that may be made by its manufacturer, is not guaranteed or endorsed by the publisher.

Advantages of publishing in Frontiers

OPEN ACCESS
Articles are free to read for greatest visibility and readership

FAST PUBLICATION
Around 90 days from submission to decision

HIGH QUALITY PEER-REVIEW
Rigorous, collaborative, and constructive peer-review

TRANSPARENT PEER-REVIEW
Editors and reviewers acknowledged by name on published articles

Frontiers
Avenue du Tribunal-Fédéral 34
1005 Lausanne | Switzerland

Visit us: www.frontiersin.org
Contact us: frontiersin.org/about/contact

REPRODUCIBILITY OF RESEARCH
Support open data and methods to enhance research reproducibility

DIGITAL PUBLISHING
Articles designed for optimal readership across devices

FOLLOW US
@frontiersin

IMPACT METRICS
Advanced article metrics track visibility across digital media

EXTENSIVE PROMOTION
Marketing and promotion of impactful research

LOOP RESEARCH NETWORK
Our network increases your article's readership